frontiers | Research Topics

Clinical and basic research of radiotherapy for esophageal cancer

Edited by
Li Jiancheng, Tao Li, Kuaile Zhao, Chi Lin and Feng-Ming Kong

Published in
Frontiers in Oncology

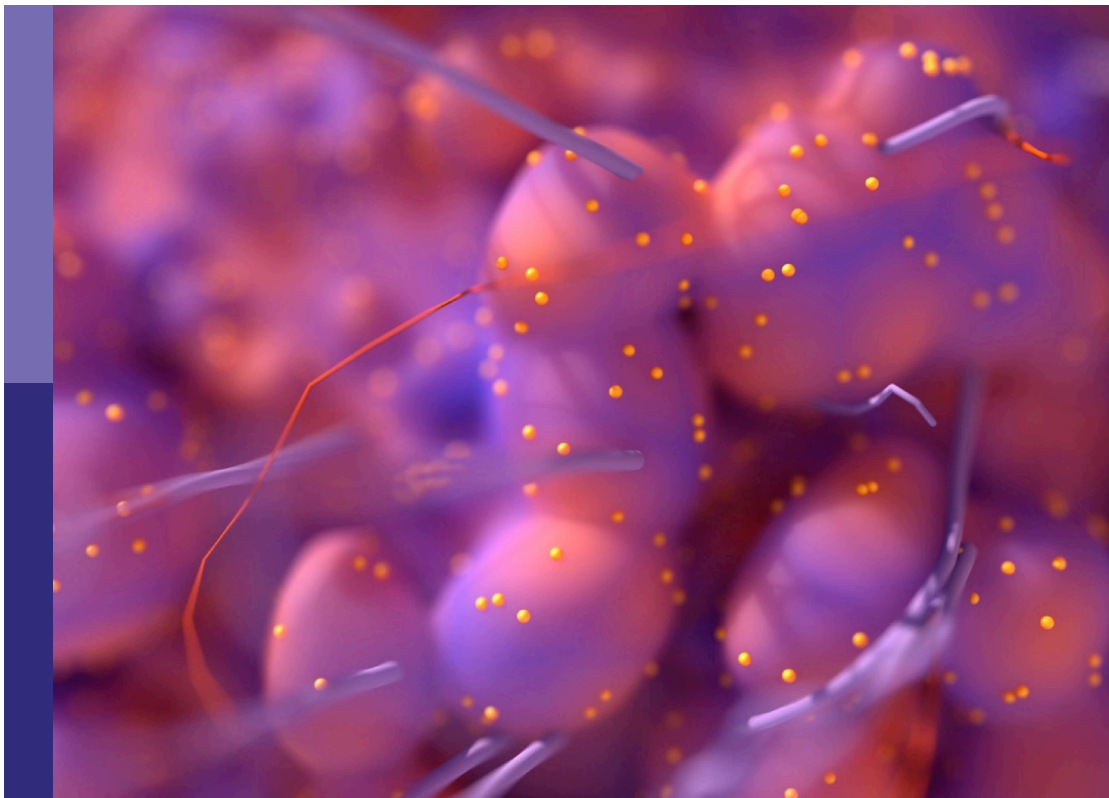

ISSN 1664-8714
ISBN 978-2-8325-4053-4
DOI 10.3389/978-2-8325-4053-4

About Frontiers

Frontiers is more than just an open access publisher of scholarly articles: it is a pioneering approach to the world of academia, radically improving the way scholarly research is managed. The grand vision of Frontiers is a world where all people have an equal opportunity to seek, share and generate knowledge. Frontiers provides immediate and permanent online open access to all its publications, but this alone is not enough to realize our grand goals.

Frontiers journal series

The Frontiers journal series is a multi-tier and interdisciplinary set of open-access, online journals, promising a paradigm shift from the current review, selection and dissemination processes in academic publishing. All Frontiers journals are driven by researchers for researchers; therefore, they constitute a service to the scholarly community. At the same time, the *Frontiers journal series* operates on a revolutionary invention, the tiered publishing system, initially addressing specific communities of scholars, and gradually climbing up to broader public understanding, thus serving the interests of the lay society, too.

Dedication to quality

Each Frontiers article is a landmark of the highest quality, thanks to genuinely collaborative interactions between authors and review editors, who include some of the world's best academicians. Research must be certified by peers before entering a stream of knowledge that may eventually reach the public - and shape society; therefore, Frontiers only applies the most rigorous and unbiased reviews. Frontiers revolutionizes research publishing by freely delivering the most outstanding research, evaluated with no bias from both the academic and social point of view. By applying the most advanced information technologies, Frontiers is catapulting scholarly publishing into a new generation.

What are Frontiers Research Topics?

Frontiers Research Topics are very popular trademarks of the *Frontiers journals series*: they are collections of at least ten articles, all centered on a particular subject. With their unique mix of varied contributions from Original Research to Review Articles, Frontiers Research Topics unify the most influential researchers, the latest key findings and historical advances in a hot research area.

Find out more on how to host your own Frontiers Research Topic or contribute to one as an author by contacting the Frontiers editorial office: frontiersin.org/about/contact

Clinical and basic research of radiotherapy for esophageal cancer

Topic editors

Li Jiancheng — Fujian Medical University, Fujian Cancer Hospital, China
Tao Li — Sichuan Cancer Hospital, China
Kuaile Zhao — Fudan University, China
Chi Lin — University of Nebraska Medical Center, United States
Feng-Ming Kong — The University of Hong Kong, SAR China

Citation

Jiancheng, L., Li, T., Zhao, K., Lin, C., Kong, F.-M., eds. (2023). *Clinical and basic research of radiotherapy for esophageal cancer*. Lausanne: Frontiers Media SA. doi: 10.3389/978-2-8325-4053-4

Table of contents

frontiers in Oncology

ORIGINAL RESEARCH
published: 25 February 2022
doi: 10.3389/fonc.2022.839516

Effects of Enteral Nutrition on Patients With Oesophageal Carcinoma Treated With Concurrent Chemoradiotherapy: A Prospective, Multicentre, Randomised, Controlled Study

Jiahua Lyu[1], Anhui Shi[2], Tao Li[1], Jie Li[3], Ren Zhao[4], Shuchai Zhu[5], Jianhua Wang[6], Ligang Xing[7], Daoke Yang[8], Conghua Xie[9], Liangfang Shen[10], Hailin Zhang[1], Guangying Zhu[2], Jing Wang[3], Wenyan Pan[4], Fang Li[1], Jinyi Lang[1] and Hanping Shi[11]*

[1] Sichuan Cancer Hospital, School of Medicine, University of Electronic Science and Technology of China, Chengdu, China, [2] Department of Radiotherapy, Peking University Cancer Hospital, Beijing, China, [3] Department of Radiotherapy, Shanxi Provincial Cancer Hospital, Taiyuan, China, [4] Department of Radiotherapy, General Hospital of Ningxia Medical University, Yinchuan, China, [5] Department of Radiotherapy, Fourth Hospital of Hebei Medical University, Shijiazhuang, China, [6] Department of Radiotherapy, Henan Provincial Cancer Hospital, Zhengzhou, China, [7] Department of Radiotherapy, Shandong Cancer Hospital, Shandong University, Jinan, China, [8] Department of Radiotherapy, First Affiliated Hospital of Zhengzhou University, Zhengzhou, China, [9] Department of Oncology, Zhongnan Hospital, Wuhan University, Wuhan, China, [10] Department of Oncology, Xiangya Hospital, Central South University, Changsha, China, [11] Department of Gastrointestinal Surgery/Clinical Nutrition, Beijing Shijitan Hospital, Capital Medical University, Beijing, China

OPEN ACCESS

Edited by:
Xi Yang,
Fudan University, China

Reviewed by:
Zhenzhou Yang,
Chongqing Medical University, China
Naseer Ahmed,
CancerCare Manitoba, Canada

***Correspondence:**
Tao Li
litaoxmf@126.com

Specialty section:
This article was submitted to Radiation Oncology, a section of the journal Frontiers in Oncology

Received: *20 December 2021*
Accepted: *31 January 2022*
Published: *25 February 2022*

Citation:
Lyu J, Shi A, Li T, Li J, Zhao R, Zhu S, Wang J, Xing L, Yang D, Xie C, Shen L, Zhang H, Zhu G, Wang J, Pan W, Li F, Lang J and Shi H (2022) Effects of Enteral Nutrition on Patients With Oesophageal Carcinoma Treated With Concurrent Chemoradiotherapy: A Prospective, Multicentre, Randomised, Controlled Study. Front. Oncol. 12:839516. doi: 10.3389/fonc.2022.839516

Background: The oesophageal carcinoma patients show high incidence of malnutrition, which negatively affects their therapy outcome. Moreover, benefits of enteral nutrition remain to be studied in details in these patients. Therefore, we set to assess the effects of enteral nutrition on the nutritional status, treatment toxicities and survival in the oesophageal carcinoma patients treated with concurrent chemoradiotherapy (CCRT).

Materials and Methods: Eligible patients were randomly assigned to either the experimental or control group. The patients in the experimental group were treated with a whole-course enteral nutrition management, while the control group were provided a unsystematic nutrition without setting intake goals for energy and protein. The primary endpoint was a change in body weight, while the secondary endpoints included nutrition-related haematological indicators, toxicities, completion rate of treatment and survival.

Results: A total of 222 patients were randomised to either the experimental (n=148) or control (n=74) group. Patients in the experimental group showed significantly less decrease in body weight, serum albumin and haemoglobin levels, a lower incidence rates of grade ≥3 myelosuppression and infection, and a higher completion rate of CCRT than those in the control group. While analyses of the 2 and 3 year overall survival (OS) and progression-free survival (PFS) did not reveal differences between these groups, we observed a significantly higher OS at 1 year (83.6% vs. 70.0%). In the subgroup analysis, patients with patient-generated subjective global assessment (PG-SGA)=C were likely to have better OS and PFS with enteral nutrition.

Conclusions: In EC patients treated with CCRT, enteral nutrition conferred positive effects on the nutritional status, treatment toxicities and prognosis, which mandate its inclusion in clinical practice.

Clinical Trial Registration: This prospective trial has been registered with www.clinicaltrials.gov as NCT02399306.

Keywords: oesophageal carcinoma, enteral nutrition, chemoradiotherapy, nutritional status, prognosis

INTRODUCTION

Oesophageal cancer (EC) is a malignant tumour with a high incidence rate and more than 570000 cases are newly diagnosed worldwide every year (1). In China, the incidence rate of oesophageal cancer ranks fifth in men and ninth in women (2). Chemoradiotherapy is an important intervention for patients with oesophageal cancer (3).

The incidence of weight loss and malnutrition is high in patients with oesophageal cancer due to dysphagia, painful swallowing, alterations in metabolism, and adverse effects of radiotherapy and chemotherapy. Moreover, oesophageal carcinoma often ranks first in the incidence of malnutrition as 60–85% patients show different degrees of malnutrition (4–6). Furthermore, malnutrition not only reduces sensitivity to chemoradiotherapy, clinical outcomes and quality of life, but also increases treatment toxicity and hospital stays (7–9).

The European Society for Parenteral and Enteral Nutrition have suggested the importance of nutritional interventions in cancer patients (10). Moreover, recent studies have indicated that nutritional treatment can improve the nutritional status, treatment tolerability and quality of life, and decrease the treatment toxicity and duration of hospital stay in patients with esophageal cancer (11, 12).

However, well-designed, large-scale, and multicentre randomised studies need to be conducted. Additionally, previous studies have entirely focused on studying the effects of enteral nutrition in improving the body weight or other nutritional indicators, and only few studies have addressed the long-term analysis of patient survival. Therefore, the controversies pertaining the survival benefits of nutritional therapy remain to be studied.

The present study has its genesis in the discussion about a possibility of the beneficial effect of enteral nutrition on patients with esophageal cancer (EC). This is the first, prospective, multicentre, randomised, controlled clinical study in China and abroad, where the effect of enteral nutrition was evaluated in patients with EC undergoing chemoradiotherapy. The aim of the study was to evaluate the effects of enteral nutrition on nutritional status and treatment toxicities. Additionally, we performed a long-term follow-up of patients post-discharge to evaluate whether the administration of enteral nutrition can influence the survival.

MATERIALS AND METHODS

Eligibility Criteria

Patients were recruited based on the following inclusion criteria: (1) histologically confirmed, stage II–III oesophageal carcinoma; (2) adequate digestive and absorption functions; (3) 18 years ≤ age ≤ 75 years; (4) the patient-generated subjective global assessment (PG-SGA) scores ≥ 2 points; (5) Karnofsky performance status (KPS) scores ≥ 70 points; (6) adequate haematological, renal, hepatic and pulmonary functions (defined as, absolute neutrophil count ≥ 1500 cells/mm^3, a platelet count ≥ 100000 cells/mm^3, haemoglobin levels ≥ 9.0 g/dL, bilirubin levels ≤ 1.5 times the upper limit of the institutional normal range, transaminase levels ≤ 3 times the upper normal limit and serum creatinine levels ≤ 2.0 mg/dL); and (7) no signs of perforation.

Further, the exclusion criteria were: (1) the intestinal functions severely impaired or patients intolerant to enteral nutrition; (2) incapable of oral feeding and insertion of nutrition tube or unwilling to accept the insertion of nutrition tube; (3) no malnutrition or nutritional risk; (4) severe malnutrition (weight loss > 10% or serum albumin [ALB] < 30 g/L or BMI < 18.5 kg/m^2 or haemoglobin < 90 g/L) before the treatment; (5) serious heart, lung, liver and kidney diseases; (6) mental disease or severe cognitive disorder.

All participants provided written informed consent before participating in the study. The study protocol was approved by the Ethics Committee of our hospitals. Research was conducted in accordance with the 1964 Declaration of Helsinki and its later amendments.

Randomisation

Eligible patients were randomly assigned (2:1) to either the experimental or control group. Randomisation was performed centrally using computer-generated randomisation lists.

Chemoradiotherapy

Patients in both groups received concurrent chemoradiotherapy. All of the patients were treated with intensity-modulated radiotherapy (IMRT) using a linear accelerator with 6-MV X-rays *via* external beam radiation. The total dose prescribed to 95% volume PTV-GTV was 60–66Gy/30–33 times and PTV-CTV 46–50Gy/23–25 times. Chemotherapy consisted of docetaxel and cisplatin was administered every 21–28 days. The average chemotherapy cycles of the experimental group were 2.5 ± 1.2, while that of the control group were 2.3 ± 1.0, with no significant difference (p=0.125).

Nutritional Intervention

The patients in the experimental group were administered a whole-course enteral nutrition management. The basic process is as follows: (1) nutritional risk screening with NRS-2002, nutritional assessment with PG-SGA; (2) enteral nutrition with

oral nutritional supplement (ONS, Nutrison produced by Nutricia) or tube feeding based on the results of nutrition assessment, dietary investigation, degree of dysphagia; (3) timely evaluation of the treatment effect and adjustment of the nutritional program according to the dynamic changes of the nutritional status and adverse effect of patients; (4) quality control of the whole-course nutrition. The enteral nutrition was conducted by a nutrition support team (NST), which included clinicians, nutritionists, pharmacologists and nutrition nurses. The intake goals for energy and protein were set as 30–35 kcal/kg/d and 1.5–2.0g/kg/d, respectively. Doctors and nurses recorded and checked the patients' energy and protein intake every day and ensured nutrition quality control, such that each patient received sufficient nutrients.

Whereas, the control group was treated with unsystematic nutrition based on the general eating conditions, hematologic test and treatment toxicities but not the nutritional assessment and dietary investigation, without considering the intake goals and nutrition quality control.

Endpoints

The primary endpoint of the study was the change in body weight which was measured every week. Body weight change after the treatment = body weight evaluated within 1 week after treatment - body weight before the start of treatment. The secondary endpoints included: a) changes in haemoglobin and serum albumin levels, which were defined as haemoglobin and serum albumin levels evaluated within 1 week after treatment - haemoglobin and serum albumin levels before the start of treatment, monitored every week and at least every two weeks, respectively; b) side effects of radiotherapy and chemotherapy, which were evaluated according to the Radiation Therapy Oncology Group criteria and the National Cancer Institute Common Terminology Criteria for Adverse Events (version 3.0); c) infection rate, which was defined as patients with the use of antimicrobials; d) treatment completion rate; e) survival, including progression-free survival (PFS) and overall survival (OS).

Follow-Up

All patients were followed up every 3 months within the first 3 years after treatment completion by outpatient clinic, telephone, WeChat, etc. After the third year, follow-up was performed every 6 months until 5 years after treatment completion. Contrast computed tomography of the chest, ultrasonography of the neck and abdomen, contrast esophagography and whole-body bone ECT scan were scheduled during follow-up. Additional diagnostic investigations, such as MRI, PET-CT and fine-needle aspiration, were carried out if recurrence was suspected by these routine examinations or if complaints, such as hoarseness, renewed dysphagia, unexplained weight loss or pain, arose before the next scheduled visit.

Statistical Analyses

All statistical analyses were performed using the Statistical Package for the Social Sciences for Windows (software version 19.0; SPSS Inc., Chicago, IL, USA). Based on our preliminary experiment results, assuming a mean decrease in body weight of 0.70kg in the experimental group and 2.25 kg in the control group after treatment, a sample size of 177 patients was required (with a two-sided 5% significance level and a power of 80%). Accounting for an assumed drop-out rate of 20%, a target recruitment of 213 patients was established. Categorical variables were described by percentages and compared using the Chi-square test. Continuous variables were described by mean ± standard deviation (SD) and compared using two-sample Student's *t*-test or analysis of variance (ANOVA), when appropriate. The PFS and OS curves were derived using the Kaplan-Meier method and compared using log-rank test. Univariable and multivariable Cox proportional hazards models was used to establish the effect of enteral nutrition in subgroups. A two-sided p-value < 0.05 was considered statistically significant.

RESULTS

Baseline Characteristics of Patients

From March 2014 to June 2017, based on the established inclusion and exclusion criteria, a total of 222 esophageal squamous cell carcinomas patients from ten hospitals in China were randomised into the experimental (n=148) and control (n=74) groups. In the experimental group, 9 patients withdrew from the study, and 16 patients were lost during follow-up. A total of 10 patients in the control group withdrew from the study, and 7 patients were lost during follow-up. Therefore, in the final analysis, 123 patients in the experimental group and 57 in the control group were included. As summarised in **Table 1**, the baseline characteristics of the patients were similar in both the groups without statistical differences. A total of 27 (21.9%) patients in the experimental group had tube feeding, of which 20 patients were treated with nasogastric feeding tube and 7 patients used percutaneous endoscopic gastrostomy (PEG).

Nutritional Status, Toxicities and Treatment Completion

The early results of nutritional status and toxicities of this study have previously been published in Chinese (13). Our re-analysis suggests that the average weight loss in the experimental group after the treatment was 0.73 ± 2.78 kg, which was significantly less than that in the control group (3.47 ± 3.78 kg). Participants in the experimental group showed less decline in serum albumin levels than in the control group (3.86 ± 4.95 vs. 6.03 ± 5.22 g/L, p=0.008) and haemoglobin (10.64 ± 13.61 g/L vs. 17.67 ± 15.42 g/L, p=0.002). Incidence of grade 3/4 leukopenia (45.6% vs. 27.6%, p=0.027) and infection rate (28.1% vs. 13.0%, p=0.020) was significantly frequent in the control than in the experimental group. Patients in the experimental group experienced higher chemoradiotherapy completion rates than those in control group (96.7% vs. 87.7%, p=0.038). Further, there were no significant inter-group differences in the lymphocyte count, ≥ G2 radiation pneumonitis and radiation esophagitis ($p > 0.05$) (**Table 2**).

TABLE 1 | Characteristics of patients in experimental and control groups at baseline.

Content	Experimental group (N=123)	Control group (N=57)	p-value
Age[a]			
<60 years	39 (31.7%)	21 (36.8%)	0.502[c]
≥60 years	84 (68.3%)	36 (63.2%)	
Gender[a]			
Male	94 (76.4%)	48 (84.2%)	0.326[c]
Female	29 (23.6%)	9 (15.8%)	
Clinical stage[a]			
II	21 (17.1%)	13 (22.8%)	0.414[c]
III	102 (82.9%)	44 (77.2%)	
Tumour length[a]			
<5cm	58 (47.2%)	23 (40.4%)	0.424[c]
≥5cm	65 (52.8%)	34 (59.6%)	
Median (cm)[b]	4.95±2.00	5.22±2.20	0.416[d]
KPS score[a]			
≤80	61 (49.6%)	32 (56.1%)	0.428[c]
>90	62 (50.4%)	25 (43.9%)	
PG-SGA[a]			
B	76 (61.8%)	34 (59.6%)	0.870[c]
C	47 (38.2%)	23 (40.4%)	
Tumor location[a]			
cervical	24 (19.5%)	11 (19.3%)	
upper thoracic	63 (51.2%)	27 (47.4%)	0.316[c]
middle thoracic	34 (27.6%)	15 (26.3%)	
lower thoracic	2 (1.7%)	4 (7.0%)	
Weight (kg)[b]	58.96±8.95	58.25±9.61	0.448[d]

KPS, Karnofsky Performance Status; PG-SGA, Patient-generated Subjective Global Assessment.
[a]Categorical variables were presented by number (%).
[b]Continuous variables were presented as mean ± standard deviation.
[c]Pearson chi-square test for categorical data was used.
[d]Two independent sample t-test for numeric variables data were used.

TABLE 2 | Comparison of nutritional status, toxicities and treatment completion between the experimental and control groups.

Content	Experimental group	Control group	p-value
Weight change after the treatment (kg)[b]	-0.73±2.78	-3.47±3.78	0.000[d]
Changes in haemoglobin after the treatment (g/L)[b]	-10.64±13.61	-17.67±15.42	0.002[d]
Changes in serum albumin after the treatment (g/L)[b]	-3.86±4.95	-6.03±5.22	0.008[d]
Changes in the lymphocyte count after the treatment (10^9/L)[b]	-0.84±0.66	-0.94±0.80	0.361[d]
≥G3 leukopenia[a]	27.6%	45.6%	0.027[c]
≥G2 radiation pneumonitis[a]	27.6%	29.8%	0.859[c]
≥G2 radiation esophagitis[a]	34.1%	43.9%	0.247[c]
Incidence of infection[a]	13.0%	28.1%	0.020[c]
Treatment completion rate[a]	96.7%	87.7%	0.038[c]

[a]Categorical variables were presented as numbers (%).
[b]Continuous variables were presented as mean ± standard deviation.
[c]Pearson chi-square test for categorical data was used.
[d]Two independent sample t-test for numeric variables data were used.

Overall Survival of the Patients

The experimental and control group had a similar median OS (32.5 months vs. 26.6 months; p = 0.157). However, the OS rates in the experimental and control group were 83.6% and 70.0% at 1 year (p = 0.025), 58.9% and 52.3% at 2 years (p = 0.220), and 42.5% and 38.8% at 3 years (p = 0.323), respectively, after treatment (**Figure 1**).

The prognostic impact of enteral nutrition on OS in subgroups of EC patients with different characteristics was analysed with the Cox proportional hazards regression model (**Table 3**). Patients with tumour length ≥ 5cm or PG-SGA=C had increased probability of better OS from enteral nutrition. Moreover, in patients with tumour length ≥ 5cm, the median OS was 28.0 months and 18.9 months in the experimental and control groups, respectively (p = 0.026) (**Figure 2**). Whereas, in patients with PG-SGA qualitative evaluation=C, the median OS was 33.1 months and 21.9 months in the experimental and control groups, respectively (p = 0.020) (**Figure 3**).

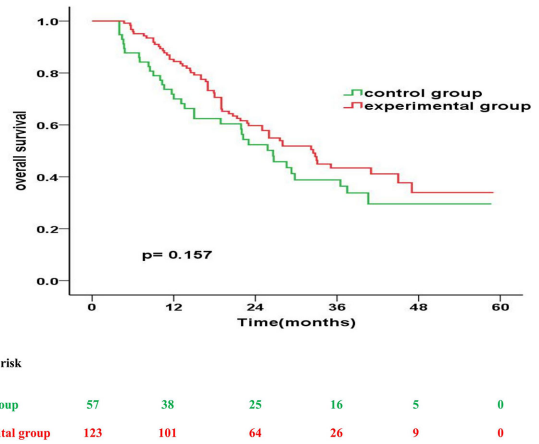

FIGURE 1 | Kaplan-Meier overall survival curves for patients in the experimental group vs. control group.

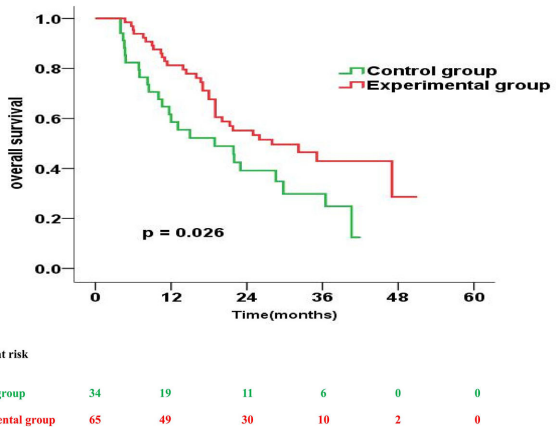

FIGURE 2 | Overall survival curves for patients with tumour length ≥ 5cm in the experimental group vs. control group.

Progression-Free Survival of the Patients

Further, the experimental and control group had a similar median PFS (22.6 months vs. 19.5 months; p = 0.489). However, the 1-year, 2-year, 3-year PFS rates were 67.8% versus 57.6% (p = 0.135), 47.5% versus 46.0% (p = 0.573) and 41.5% versus 38.4% (p = 0.648) for patients treated in the experimental and control group, respectively (**Figure 4**).

Next, we also analysed the prognostic impact of enteral nutrition on PFS in subgroups of ESCC patients with different characteristics using the Cox proportional hazards regression model (**Table 4**). Furthermore, in patients with PG-SGA qualitative evaluation=C in the experimental versus those in the control group, the median PFS was 18.3 months versus 8.6 months (p = 0.018) (**Figure 5**).

DISCUSSION

The prevalence of malnutrition is high among patients with oesophageal cancer, which negatively affects the therapy outcomes (4–6). The causes of malnutrition are complex, including psychological and mechanical reasons. Further, insufficient energy and protein intake caused by dysphagia, food avoidance, and diet change are the main mechanical reasons for malnutrition in the patients with oesophageal carcinoma (14). Therefore, in the present study, we intended to provide enteral nutrition to the patients with oesophageal cancer undergoing concurrent chemoradiothrapy (CCRT) to ensure sufficient energy and protein intake, thereby improving the nutritional status of the patients.

TABLE 3 | Prognostic impact of enteral nutrition in subgroups of EC patients with different characteristics.

Subgroup	Univariate analysis		Multivariate analysis	
	HR (95% CI)	p-value	HR (95% CI)	p-value
Tumour length				
<5cm, experimental group vs. control group	1.169 (0.587 to 2.329)	0.656	1.022 (0.499 to 2.092)	0.952
≥5cm, experimental group vs. control group	0.553 (0.325 to 0.939)	0.028	0.544 (0.318 to 0.933)	0.027
PG-SGA qualitative evaluation				
B, experimental group vs. control group	0.955 (0.545 to 1.673)	0.871	0.842 (0.469 to 1.511)	0.564
C, experimental group vs. control group	0.481 (0.256 to 0.904)	0.023	0.458 (0.236 to 0.889)	0.021
Age				
<60 years, experimental group vs. control group	0.599 (0.295 to 1.217)	0.156	0.563 (0.268 to 1.180)	0.128
≥60 years, experimental group vs. control group	0.837 (0.503 to 1.395)	0.496	0.809 (0.483 to 1.355)	0.420
KPS score				
≤80 , experimental group vs. control group	0.633 (0.367 to 1.091)	0.100	0.586 (0.330 to 1.039)	0.067
>90, experimental group vs. control group	0.881 (0.461 to 1.682)	0.701	0.887 (0.462 to 1.702)	0.718
Clinical stage				
II, experimental group vs. control group	0.564 (0.217 to 1.466)	0.240	0.459 (0.165 to 1.278)	0.136
III, experimental group vs. control group	0.790 (0.498 to 1.254)	0.318	0.812 (0.509 to 1.295)	0.381
Gender				
Male	0.840 (0.529 to 1.333)	0.458	0.808 (0.507 to 1.287)	0.369
Female	0.556 (0.221 to 1.398)	0.212	0.444 (0.164 to 1.199)	0.109

KPS, Karnofsky performance status; PG-SGA, Patient-generated Subjective Global Assessment; CI, confidence interval; HR, hazard ratio.

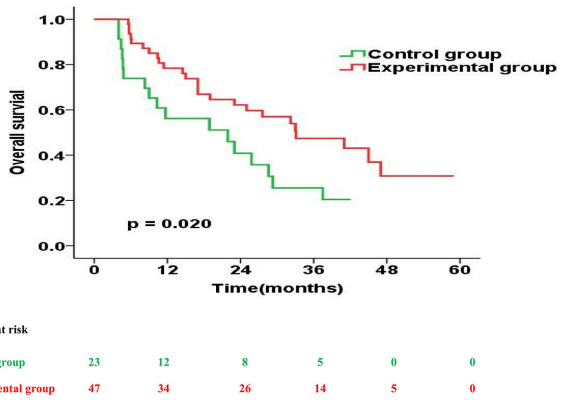

FIGURE 3 | Overall survival curves for patients with PG-SGA qualitative evaluation = C in the experimental group vs. control group.

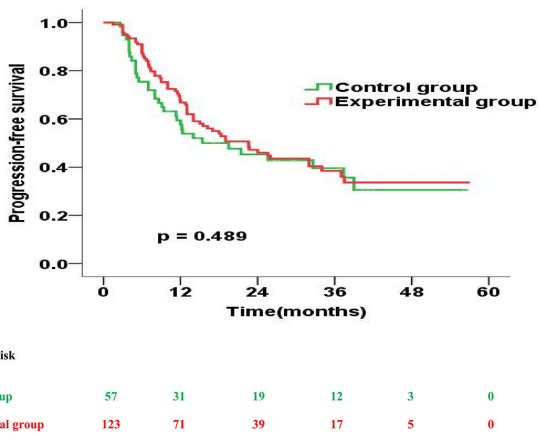

FIGURE 4 | Progression-free survival curves for patients in the experimental group vs. control group.

The change in body weight was considered as the primary endpoint since weight loss is a sensitive indicator of malnutrition, and a frequent cause of concern in patients and doctors. Moreover, a high prevalence of weight loss has been reported in oesophageal carcinoma patients at diagnosis and during the treatment (15). Additionally, Jiang et al. (6) reported 40.3% of oesophageal carcinoma patients to have ≥ 5% weight loss during radiotherapy. Furthermore, weight loss correlates with impairment of physical and psychological functions, low quality of life and poor prognosis. Therefore, maintenance of body weight in these patients is an important issue for clinicians globally.

Here, while patients in both control and experimental groups showed decrease in body weight during CCRT, those in the experimental group regained their weight after completion of treatment. Moreover, the average weight loss in the experimental group during and after CCRT was significantly less than that in the control group. The body weight alteration may be the result of an imbalance between energy intake and energy expenditure caused by reduction in food intake due to tumor obstruction, radiotherapy or chemotherapy-induced toxicities and cachexia-related high catabolism. Further, patients in the experimental group were administered a whole-course and systematic enteral nutrition, which effectively ensured their daily energy and protein needs. Thus, this strategy may be the possible explanation for better maintenance and quick recovery in body weight observed in patients in the experimental group.

Furthermore, our analysis also indicated that enteral nutrition could significantly reduce the declination in levels of serum albumin and haemoglobin, reduce the rates of grade 3/4

TABLE 4 | Progression-free survival of enteral nutrition in subgroups of oesophageal squamous cell carcinoma patients with different characteristics.

Subgroup	Univariate analysis		Multivariate analysis	
	HR (95% CI)	p-value	HR (95% CI)	p-value
Tumour length				
<5cm, experimental group vs. control group	1.530 (0.747 to 3.134)	0.245	1.630 (0.763 to 3.480)	0.207
≥5cm, experimental group vs. control group	0.604 (0.360 to 1.014)	0.091	0.637 (0.378 to 1.075)	0.091
PG-SGA qualitative evaluation				
B, experimental group vs. control group	0.765 (0.425 to 1.375)	0.370	0.730 (0.398 to 1.336)	0.307
C, experimental group vs. control group	0.493 (0.269 to 0.902)	0.022	0.527 (0.285 to 0.972)	0.040
Age				
<60 years, experimental group vs. control group	0.738 (0.386 to 1.408)	0.356	0.750 (0.384 to 1.466)	0.401
≥60 years, experimental group vs. control group	0.963 (0.559 to 1.661)	0.892	0.991 (0.567 to 1.733)	0.975
KPS score				
≤80 , experimental group vs. control group	0.785 (0.457 to 1.347)	0.380	0.812 (0.464 to 1.423)	0.468
>90, experimental group vs. control group	1.097 (0.561 to 2.145)	0.786	1.079 (0.549 to 2.121)	0.824
Clinical stage				
II, experimental group vs. control group	1.223 (0.418 to 3.583)	0.713	1.787 (0.509 to 6.267)	0.365
III, experimental group vs. control group	0.780 (0.497 to 1.223)	0.279	0.870 (0.552 to 1.373)	0.550
Gender				
Male	0.930 (0.599 to 1.444)	0.747	0.912 (0.585 to 1.423)	0.685
Female	0.892 (0.237 to 3.361)	0.866	0.748 (0.177 to 3.164)	0.693

KPS, Karnofsky performance status; PG-SGA, Patient-generated Subjective Global Assessment; CI, confidence interval; HR, hazard ratio.

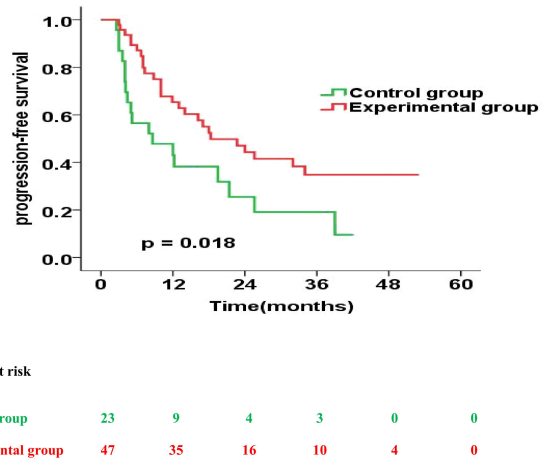

FIGURE 5 | Progression-free survival curves for patients with PG-SGA qualitative evaluation = C in the experimental group vs. control group.

leukopenia and infection, and increase the chemoradiotherapy completion rates. Moreover, similar results have been reported in other studies. For instance, Odelli C. et al. (16) showed that nutrition intervention conferred a significantly positive effect on the nutritional status and tolerance of definitive chemoradiation treatment in patients with oesophageal carcinoma. Additionally, Cong et al. (11) administered nutrition treatment with the help of an interdisciplinary nutrition support team in oesophageal carcinoma patients receiving CCRT. Their analysis suggested that nutritional therapy could help in maintaining the nutritional status, improving the compliance of CCRT, and reducing the duration of hospital stay and in-patient costs. Further, by performing a whole-course nutritional management of patients with oesophageal carcinoma undergoing CCRT, Qiu et al. (12) observed an improvement in the levels of albumin and total protein, and quality of life, while reduction in the complications of radiation oesophagitis. Taken together, our study enhances the current understanding of the effect of enteral nutrition on the nutritional status of patients with oesophageal carcinoma treated with CCRT.

Further, since requirement of nutrition to improve or maintain patient's body weight and nutritional status is unquestionable, studies are being conducted to understand whether it can improve the survival. However, it remains a controversial topic due to the limitations of related research and data analysis. Moreover, most of the clinical studies on nutritional therapy of cancer patients consider improvement in body weight and other nutritional indicators as observational end-points and only few studies have conducted long-term follow-up of patient survival. Klek S et al. (17) conducted a randomised clinical study to determine whether the post-operative use of enteral nutrition could influence survival in the patients diagnosed with stomach cancer. Their analysis suggested that the enteral nutrition group may have a low risk of mortality, especially during the first year after intervention, although, the long-term OS rates were found to be similar in both the groups ($p = 0.663$). Next, in a double-blind, randomised, controlled trial conducted by Buijs N et al. (18), the patients with head and neck cancer receiving enteral nutrition showed a significantly better OS ($p = 0.019$), disease-specific survival ($p = 0.022$) and locoregional recurrence-free survival ($p = 0.027$). However, no significant differences in the occurrence of distant metastases or second primary tumour were observed between the groups.

Further, to evaluate whether the use of enteral nutrition during hospitalization can influence the survival, we conducted a long-term follow-up after discharge of the patients, given the beneficial effect of enteral nutrition on the survival of oesophageal carcinoma patients. While we did not observe differences in survival benefit between the experimental and control groups, patients in the experimental group showed higher OS and PFS without statistical significance. Furthermore, our analysis suggested a significant survival benefit in the experimental than the control group at 1-year, but not at 2- and 3-years post treatment.

While it is expected that nutritional treatment should improve nutritional status and thus the OS of the patients, question would arise as to why enteral nutrition in our study conferred significant improvement only in the nutritional status and 1-year survival, but no survival benefit 2-years post treatment. The possible explanation for these findings may be a lack of home enteral nutrition, since malnutrition occurs not only during hospitalization, but also at home post treatment. Moreover, uncontrolled disease, oesophageal stricture and delayed side-effects of chemotherapy and radiotherapy present hurdles in the maintenance of proper nutrition in such patients. Baker ML et al. (19) observed that in patients after oesophago-gastric resection without home enteral nutrition and 3–6 months after hospital discharge, the oral intakes for energy and protein were adequate in only 55% and 77% patients, respectively, whereas 26% of the patients required rescue feeding. Moreover, as compared to baseline values, weight loss exceeding 5% (average 10.4%) was observed in 82–83% of the patients, 6-weeks post-surgery. Further, though the patients in our study received enteral nutrition during hospitalisation and their nutritional status improved during CCRT, however, they did not receive systematic and continuous nutrition monitoring, education and treatment at home. Additionally, correct nutrition concepts, good nutrition habits and standardised nutritional treatment methods appear to have gradually been ignored, forgotten or abandoned by the patients and family members post discharge from hospitalisation. Thus, the nutritional status may return to the same level in both the groups of patients. Therefore, the benefits of in-hospital enteral nutrition can only be maintained for a short duration, and the effects diminish with time as the initial decrease in risk of death in the experimental group was less and statistically insignificant.

Further, in case of oesophageal carcinoma, the importance of home nutrition is gradually gaining attention, especially in patients undergoing surgery. Several studies have shown that reasonable home nutrition therapy can improve the nutritional status, quality of life and effects of anti-tumour treatment in the

patients (19–22). Moreover, our study indirectly establishes the importance of home nutrition in patients with oesophageal carcinoma undergoing CCRT with an unexpected finding.

Additionally, we observed an interesting finding in the subgroup analysis. Although our analysis did not validate the effect of enteral nutrition on the long-term survival in all patients, the OS and PFS benefit was observed among patients with PG-SGA=C. Thus, in overall, the beneficial effect of enteral nutrition was more evident in patients with worse nutrition status, and significantly less or even doubtful in other patients. Furthermore, consistent with our study, Qiu M et al. (23) observed that in stage IV gastric cancer patients who received chemotherapy and had NRS ≥ 3, the nutrition support could help in improving the prognosis. Thus, these results suggest that the benefits of nutritional therapy may vary among different populations. Therefore, we recommend that patients should be individually stratified to determine the requirement of nutritional treatment. The PG-SGA is an adaptation of the validated nutrition assessment tool—SGA, and has been specifically developed for utility in cancer patients. It has been commonly used to assess the patient's nutritional status in clinical studies and has a significant correlation with the performance status and prognosis of patients with oesophageal carcinoma (24, 25). Moreover, the PG-SGA may be a useful reference index to determine nutritional treatment indications, although it is not the sole index. Additionally, we anticipate that this study may have important guiding significance for future research and clinical work.

CONCLUSION

In conclusion, our study showed that whole-course enteral nutrition management can be beneficial for maintaining body weight and nutritional status of patients with oesophageal carcinoma receiving CCRT, and improving their treatment tolerance and short-term prognosis (especially the patients with PG-SGA=C). Additional follow-up is required to confirm the beneficial effect of EN support in long-term survival.

DATA AVAILABILITY STATEMENT

The original contributions presented in the study are included in the article/supplementary material. Further inquiries can be directed to the corresponding author.

ETHICS STATEMENT

The studies involving human participants were reviewed and approved by Ethics Committee of Sichuan Cancer Hospital. The patients/participants provided their written informed consent to participate in this study. Written informed consent was obtained from the individual(s) for the publication of any potentially identifiable images or data included in this article.

AUTHOR CONTRIBUTIONS

TL, HS, and JHL contributed to the conception and design of the current work. TL and JHL contributed to data analyses and data interpretation. AS, JL, RZ, SZ, JHW, LX, DY, CX, LS, HZ, GZ, JW, WP, FL, and JYL substantially contributed to research conduction and data collection. All the authors have contributed to interpretation of data, and critically revised and approved the final version of this manuscript.

FUNDING

This study was funded by the Wu Jieping medical foundation (320.6750.17237).

ACKNOWLEDGMENTS

We would like to thank all the participants and their families, and the Radiologists, Pathologists, Radiation and Medical oncologists, Physicists, Physiotherapists, Dietician and Nurses from all the participating centres.

REFERENCES

1. Bray F, Ferlay J, Soerjomataram I, Siegel RL, Torre LA, Jemal A. Global Cancer Statistics 2018: GLOBOCAN Estimates of Incidence and Mortality Worldwide for 36 Cancers in 185 Countries. *CA Cancer J Clin* (2018) 68 (6):394–424. doi: 10.3322/caac.21492
2. Zheng RS, Sun KX, Zhang SW, Zeng HM, Zou XN, Chen R, et al. Report of Cancer Epidemiology in China, 2015. *Chin J Oncol* (2019) 41(1):19–28. doi: 10.12968/nuwa.2015.19.28
3. Bozzetti F, Mariani L, Lo Vullo S, Amerio ML, Biffi R, Caccialanza G, et al. The Nutritional Risk in Oncology: A Study of 1,453 Cancer Outpatients. *Support Care Cancer* (2012) 20(8):1919–28. doi: 10.1007/s00520-012-1387-x
4. Lloyd S, Chang BW. Current Strategies in Chemoradiation for Esophageal Cancer. *J Gastrointest Oncol* (2014) 5(3):156–65. doi: 10.3978/j.issn.2078-6891.2014.033
5. Song C, Cao J, Zhang F, Wang C, Guo Z, Lin Y, et al. Nutritional Risk Assessment by Scored Patient-Generated Subjective Global Assessment Associated With Demographic Characteristics in 23,904 Common Malignant Tumors Patients. *Nutr Cancer* (2019) 71(1):50–60. doi: 10.1080/01635581.2019.1566478
6. Jiang N, Zhao JZ, Chen XC, Li LY, Zhang LJ, Zhao Y. Clinical Determinants of Weight Loss in Patients With Esophageal Carcinoma During Radiotherapy: A Prospective Longitudinal View. *Asian Pac J Cancer Prev* (2014) 15(5):1943–8. doi: 10.7314/apjcp.2014.15.5.1943
7. Mak M, Bell K, Ng W, Lee M. Nutritional Status, Management and Clinical Outcomes in Patients With Esophageal and Gastro-Oesophageal Cancers: A Descriptive Study. *Nutr Diet* (2017) 74(3):229–35. doi: 10.1111/1747-0080.12306
8. Clavier JB, Antoni D, Atlani D, Ben Abdelghani M, Schumacher C, Dufour P, et al. Baseline Nutritional Status Is Prognostic Factor After Definitive Radiochemotherapy for Esophageal Cancer. *Dis Esophagus* (2014) 27 (6):560–7. doi: 10.1111/j.1442-2050.2012.01441.x
9. Miyata H, Yano M, Yasuda T, Hamano R, Yamasaki M, Hou E, et al. Randomized Study of Clinical Effect of Enteral Nutrition Support During Neoadjuvant Chemotherapy on Chemotherapy-Related Toxicity in Patients With Esophageal Cancer. *Clin Nutr* (2012) 31(3):330–6. doi: 10.1016/j.clnu.2011.11.002

10. Arends J, Bodoky G, Bozzetti F, Fearon K, Muscaritoli M, Selga G, et al. ESPEN Guidelines on Enteral Nutrition: Non-Surgical Oncology. *Clin Nutr* (2006) 25(2):245–59. doi: 10.1016/j.clnu.2006.01.020
11. Cong MH, Li SL, Cheng GW, Liu JY, Song CX, Deng YB, et al. An Interdisciplinary Nutrition Support Team Improves Clinical and Hospitalized Outcomes of Esophageal Cancer Patients With Concurrent Chemoradiotherapy. *Chin Med J* (2015) 128(22):3003–7. doi: 10.4103/0366-6999.168963
12. Qiu Y, You J, Wang K, Cao Y, Hu Y, Zhang H, et al. Effect of Whole-Course Nutrition Management on Patients With Esophageal Cancer Undergoing Concurrent Chemoradiotherapy: A Randomized Control Trial. *Nutrition* (2020) 69:110558. doi: 10.1016/j.nut.2019.110558
13. Lyu JH, Li T, Zhu GY, Li J, Zhao R, Zhu SC, et al. Influence of Enteral Nutrition on Nutritional Status, Treatment Toxicities, and Short-Term Outcomes in Esophageal Carcinoma Patients Treated With Concurrent Chemoradiotherapy: A Prospective, Multicenter, Randomized Controlled Study (NCT 02399306). *Chin J Radiat Oncol* (2018) 27(1):44–8. doi: 10.3760/cma.j.issn.1004-422
14. Miller KR, Bozeman MC. Nutrition Therapy Issues in Esophageal Cancer. *Curr Gastroenterol Rep* (2012) 14(4):356–66. doi: 10.1007/s11894-012-0272-6
15. Hill A, Kiss N, Hodgson B, Crowe TC, Walsh AD. Associations Between Nutritional Status, Weight Loss, Radiotherapy Treatment Toxicity and Treatment Outcomes in Gastrointestinal Cancer Patients. *Clin Nutr* (2011) 30(1):92–8. doi: 10.1016/j.clnu.2010.07.015
16. Odelli C, Burgess D, Bateman L, Hughes A, Ackland S, Gillies J, et al. Nutrition Support Improves Patient Outcomes, Treatment Tolerance and Admission Characteristics in Oesophageal Cancer. *Clin Oncol* (2005) 17 (8):639–45. doi: 10.1016/j.clon.2005.03.015
17. Klek S, Scislo L, Walewska E, Choruz R, Galas A. Enriched Enteral Nutrition may Improve Short-Term Survival in Stage IV Gastric Cancer Patients: A Randomized, Controlled Trial. *Nutrition* (2017) 36:46–53. doi: 10.1016/j.nut.2016.03.016
18. Buijs N, van Bokhorst-de van der Schueren MA, Langius JA, Leemans CR, Kuik DJ, Vermeulen MA, et al. Perioperative Arginine-Supplemented Nutrition in Malnourished Patients With Head and Neck Cancer Improves Long-Term Survival. *Am J Clin Nutr* (2010) 92(5):1151–6. doi: 10.3945/ajcn.2010.29532
19. Baker ML, Halliday V, Robinson P, Smith K, Bowrey DJ. Nutrient Intake and Contribution of Home Enteral Nutrition to Meeting Nutritional Requirements After Oesophagectomy and Total Gastrectomy. *Eur J Clin Nutr* (2017) 71(9):1121–8. doi: 10.1038/ejcn.2017.88
20. Donohoe CL, Healy LA, Fanning M, Doyle SL, Hugh AM, Moore J, et al. Impact of Supplemental Home Enteral Feeding Postesophagectomy on Nutrition, Body Composition, Quality of Life, and Patient Satisfaction. *Dis Esophagus* (2017) 30(9):1–9. doi: 10.1093/dote/dox063
21. Li X, Zhou J, Chu C, You Q, Zhong R, Rao Z, et al. Home Enteral Nutrition may Prevent Myelosuppression of Patients With Nasopharyngeal Carcinoma Treated by Concurrent Chemoradiotherapy. *Head Neck* (2019) 41(10):3525–34. doi: 10.1002/hed.25861
22. Ruggeri E, Giannantonio M, Agostini F, Ostan R, Pironi L, Pannuti R. Home Artificial Nutrition in Palliative Care Cancer Patients: Impact on Survival and Performance Status. *Clin Nutr* (2020) 39(11):3346–53. doi: 10.1016/j.clnu.2020.02.021
23. Qiu M, Zhou YX, Jin Y, Wang ZX, Wei XL, Han HY, et al. Nutrition Support can Bring Survival Benefit to High Nutrition Risk Gastric Cancer Patients Who Received Chemotherapy. *Support Care Cancer* (2015) 23(7):1933–9. doi: 10.1007/s00520-014-2523-6
24. Quyen TC, Angkatavanich J, Thuan TV, Xuan VV, Tuyen LD, Tu DA, et al. Nutrition Assessment and Its Relationship With Performance and Glasgow Prognostic Scores in Vietnamese Patients With Esophageal Cancer. *Asia Pac J Clin Nutr* (2017) 26(1):49–58. doi: 10.6133/apjcn.122015.02
25. Lyu J, Li T, Xie C, Li J, Xing L, Zhang X, et al. Enteral Nutrition in Esophageal Cancer Patients Treated With Radiotherapy: A Chinese Expert Consensus 2018. *Future Oncol* (2019) 15(5):517–31. doi: 10.2217/fon-2018-0697

Conflict of Interest: The authors declare that the research was conducted in the absence of any commercial or financial relationships that could be construed as a potential conflict of interest.

Publisher's Note: All claims expressed in this article are solely those of the authors and do not necessarily represent those of their affiliated organizations, or those of the publisher, the editors and the reviewers. Any product that may be evaluated in this article, or claim that may be made by its manufacturer, is not guaranteed or endorsed by the publisher.

frontiers in Oncology

ORIGINAL RESEARCH
published: 25 February 2022
doi: 10.3389/fonc.2022.814238

Is Performance of Fluorine-18-fluorodeoxyglucose Positron Emission Tomography/Computed tomography (CT) or Contrast-enhanced CT Efficient Enough to Guide the Hilar Lymph Node Staging for Patients with Esophageal Squamous Cell Carcinoma?

Li Chu[1,2,3,4†], Shuai Liu[3,5†], Tiantian Guo[1,3,4†], Liqing Zou[1,3,4], Bin Li[2,3,6], Jianjiao Ni[1,2,3,4], Xi Yang[1,2,3,4], Xiao Chu[1,2,3,4], Fei Liang[7], Yida Li[1,3,4], Yuyun Sun[3,5], Qiao Li[3,8], Fang Yin[9], Guodong Li[2,3,10] and Zhengfei Zhu[1,2,3,4*]*

[1] Department of Radiation Oncology, Fudan University Shanghai Cancer Center, Shanghai, China, [2] Institute of Thoracic Oncology, Fudan University, Shanghai, China, [3] Department of Oncology, Shanghai Medical College, Fudan University, Shanghai, China, [4] Shanghai Key Laboratory of Radiation Oncology, Shanghai, China, [5] Department of Nuclear Medicine, Fudan University Shanghai Cancer Center, Shanghai, China, [6] Department of Thoracic Surgery, Fudan University Shanghai Cancer Center, Shanghai, China, [7] Department of Biostatistics, Zhongshan Hospital, Fudan University, Shanghai, China, [8] Department of Radiology, Fudan University Shanghai Cancer Center, Shanghai, China, [9] Center for Drug Clinical Research, Shanghai University of Traditional Chinese Medicine, Shanghai, China, [10] Department of Interventional Radiology, Fudan University Shanghai Cancer Center, Shanghai, China

Introduction: We evaluated the diagnostic performance of fluorine-18-fluorodeoxyglucose (18F-FDG) positron emission tomography (PET)/computed tomography (CT) and contrast-enhanced CT in the detection of hilar lymph node metastasis (LNM) in esophageal squamous cell carcinoma (ESCC) to determine their value in guiding hilar lymph node staging and delineating radiation target volume.

Methods: Consecutive patients with ESCC who underwent both PET/CT and contrast-enhanced CT before radical lymphadenectomy and esophagectomy at our institution from September 2009 to November 2018 were enrolled. The sensitivity (SE), specificity (SP), positive predictive value (PPV), and negative predictive value (NPV) of FDG-PET/CT and contrast-enhanced CT for diagnosing hilar LNM were calculated.

Results: Of the 174 patients included, contrast-enhanced CT predicted nine positive cases, while PET/CT predicted one, and eight (4.6%) were identified as pathologically positive for their resected hilar lymph nodes. The SE, SP, PPV, and NPV of PET/CT and

OPEN ACCESS

Edited by:
Chi Lin,
University of Nebraska Medical Center, United States

Reviewed by:
Guang Han,
Hubei Cancer Hospital, China
Michael James Baine,
University of Nebraska Medical Center, United States

***Correspondence:**
Zhengfei Zhu
fuscczzf@163.com
Guodong Li
coolyyi@163.com

†These authors have contributed equally to this work and share first authorship

Specialty section:
This article was submitted to Radiation Oncology, a section of the journal Frontiers in Oncology

Received: *13 November 2021*
Accepted: *31 January 2022*
Published: *25 February 2022*

Citation:
Chu L, Liu S, Guo T, Zou L, Li B, Ni J, Yang X, Chu X, Liang F, Li Y, Sun Y, Li Q, Yin F, Li G and Zhu Z (2022) Is Performance of Fluorine-18-fluorodeoxyglucose Positron Emission Tomography/Computed tomography (CT) or Contrast-enhanced CT Efficient Enough to Guide the Hilar Lymph Node Staging for Patients with Esophageal Squamous Cell Carcinoma? Front. Oncol. 12:814238. doi: 10.3389/fonc.2022.814238

contrast-enhanced CT were 0.000, 0.994, 0.000, and 0.954; and 0.125, 0.952, 0.111, and 0.958, respectively. The specificity showed a significant difference (P=0.037). PET/CT is slightly more specific than contrast-enhanced CT.

Conclusions: PET/CT and contrast-enhanced CT may be useful tools for predicting the negativity of hilar LN status, but they are not recommended for guiding the hilar lymph node staging and the delineating of hilar LNM in radiotherapy planning of ESCC patients based on their low PPV.

Keywords: esophageal squamous cell carcinoma, PET, CT, hilar lymph node, radiotherapy

INTRODUCTION

Esophageal cancer is one of the leading causes of death from cancer (1). More than 90% of cases with esophageal carcinoma in China are esophageal squamous cell carcinoma (ESCC) (2). ESCC is a tumor type prone to lymph node metastasis (LNM), which is one of the most vital prognostic factors in ESCC patients (3, 4). Based on the operative pathology, LNM has been found to be involved in more than half of surgical patients in large-scale retrospective analyses (5, 6). However, among LN of ESCC, the incidence of hilar LNM is relatively low. In a retrospective analysis involving 1361 patients with thoracic ESCC who underwent curative esophagectomy, 52.5% (714/1361) were found to have LNM, while only 1% and 2.5% of patients experienced left and right hilar LNM, respectively (6).

Radiotherapy, which targets the primary tumor and involved LNs, has a well-established role in the management of ESCC. To delineate the target volume, reliable imaging techniques for detecting involved lymph nodes are of critical importance to ensure accurate coverage of the disease, which is also a determining factor of selecting patients with curative treatment. It is not uncommon for imaging examination to report hilar LN abnormalities in patients with ESCC in routine clinical practice. Thus, the assessment of hilar lymph node involvement in ESCC is clinically relevant, as the inclusion of hilar lymph node into the target volume can increase radiation doses to surrounding normal structures, particularly to the lungs, thereby potentially increasing the risk of normal tissue complications.

Fluorine-18-fluorodeoxyglucose Positron Emission Tomography (FDG-PET)/CT and contrast-enhanced CT are among the most common imaging modalities to evaluate the status of hilar lymph node, Unfortunately, the number of studies on their accuracy for diagnosing hilar LNM is very limited and it is very difficult to draw a solid conclusion. A recent investigation demonstrated that none of the biopsied PET/CT-positive hilar nodes (n=4) confirmed the presence of metastases, which has raised concern over the diagnostic performance of (PET)CT in the detection of hilar LNM (7). To provide further insight into this issue, we performed a retrospective study of a relatively larger cohort in patients with ESCC who underwent both FDG-PET/CT and contrast-enhanced CT before radical lymphadenectomy and esophagectomy, focusing on the diagnostic performance of FDG-PET/CT and contrast-enhanced CT for hilar lymph node.

MATERIALS AND METHODS

Patients

The database of ESCC was approved by the institutional review board of our Cancer Center for this study. From September 2009 to November 2018, a total of 1247 patients with ESCC received FDG-PET/CT and contrast-enhanced CT at our Cancer Center. Among them, 212 patients undergoing radical lymphadenectomy and esophagectomy were retrospectively analyzed. We excluded patients who underwent preoperative chemotherapy or concurrent chemoradiation before surgery (n=27), because these treatment modalities may interfere with nodal status. Patients who underwent non-radical esophageal cancer surgery and not having histopathological examination of hilar lymph node were also excluded (n=8). Additionally, there were two patients with double primary tumors, and two patients for whom there were data errors of their FDG PET/CT scans. Thus, a total of 174 patients were further evaluated and included in the study (**Figure 1**).

FDG PET/CT Procedure and Evaluation

18F-FDG was produced by cyclotron using the Explora FDG4 module at Fudan University Shanghai Cancer Center. The radiochemical purity was over 95%. All patients fasted at least 6 hours before imaging. After injecting 7.4 MBq/kg (0.2 mCi/kg) 18F-FDG, patients were kept relaxed for approximately 1 hour. Images were obtained on a Siemens biograph 16HR PET/CT scanner (Knoxville, Tennessee, USA).

The images were reviewed and manipulated in a multimodality computer platform (Syngo, Siemens, Knoxville, Tennessee, USA). Standardized uptake value (SUV) of lymph nodes = [decay-corrected activity (kBq)/tissue volume (ml)]/[injected 18F-FDG activity (kBq)/body mass (g)]. All PET/CT images were analyzed by two senior nuclear medicine physicians independently according to clinical index and image performance, and did so together for the retrospective study in which they were blinded to the pathological results. Taking the liver as a reference organ, nodes were diagnosed as "involved" *via* PET/CT if the nodes were implicated *via* CT and the relevant component exhibited FDG uptake that was greater than background.

Contrast-Enhanced CT Procedure and Evaluation

All patients underwent scanning on a Somatom Definition AS scanner (Siemens Healthcare, Erlangen, Germany). Breath-

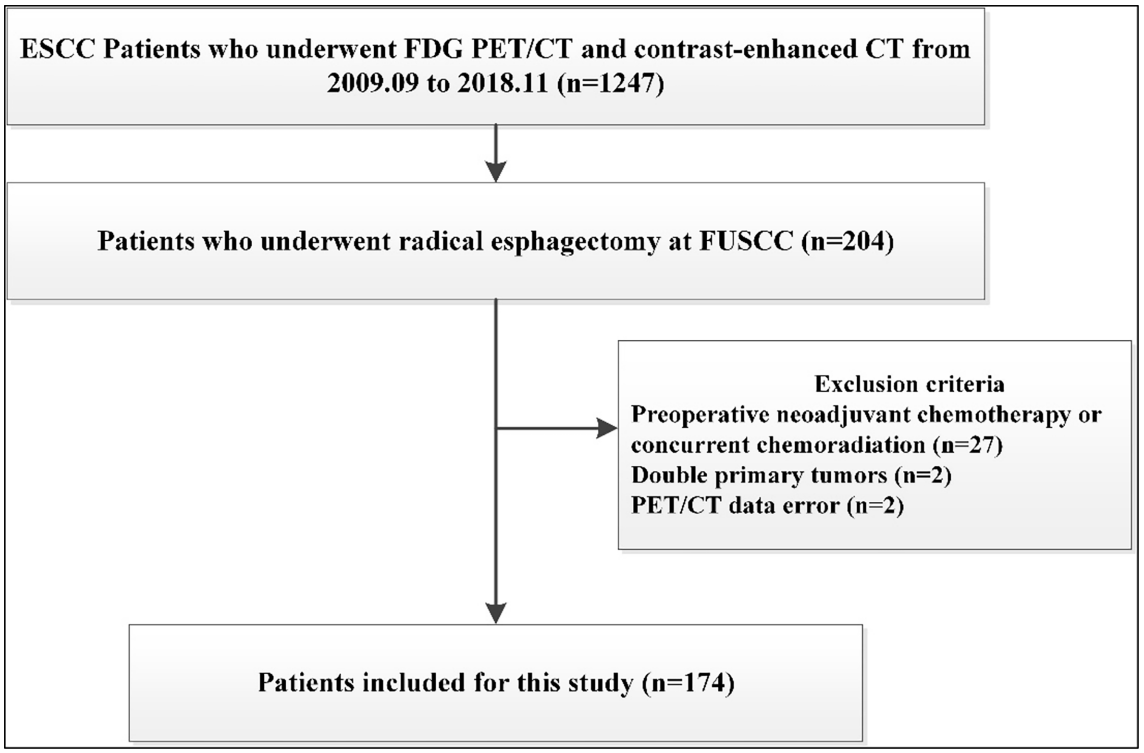

FIGURE 1 | Patient disposition chart.

hold training was performed before each examination. All patients were asked to hold their breath at the end of inspiration as long as possible. All injections were performed with an automatic power injector with which 90 ml of contrast medium (Optiray 350 mgI/ml; Mallinckrodt Medical, St. Louis, MO, USA) was injected into the antecubital vein at a rate of 4 ml/s. Contrast-enhanced images were acquired at 90 s after injection. Imaging was performed from the thoracic inlet to the middle portion of the kidneys. Scanning parameters were as follows: 120 kVp, dose modulation ACS (Brilliance-iCT), or 50–100 mA (GE HD750 and Somatom Definition AS), slice thickness 1 mm; matrix 512×512 and standard resolution algorithms.

Various CT scanning criteria have been used to define malignant involvement of lymph nodes, and there is no node size that can reliably determine the stage. In the present study, a short-axis lymph node diameter of ≥1 cm on a CT scan was chosen as the criterion for malignancy due to its wide use in clinical practice (8, 9).

Surgery and Pathology

Transthoracic esophagectomy and extensive lymph node dissection were performed by experienced thoracic surgeons. Of note, all patients received total mediastinal lymphadenectomy that included bilateral hilar lymph node dissection, and each dissected lymph node group was labelled according to a modified lymph node mapping system for esophageal cancer (10).

Statistical Analysis

Statistical Package for the Social Sciences version 25.0 (IBM Corp., Armonk, NY, USA) was used to performed statistical analysis. The sensitivity, specificity, positive predictive value, negative predictive value, and accuracy of FDG-PET/CT and contrast-enhanced CT for the assessment of hilar LNM were determined using pathological results as reference standards. Continuous data were collected as means and standard deviations, or medians and range. Classification data were collected as numbers and percentages. The Chi-square test or Fisher exact test was used to compare categorical data. Two-sided P values<0.05 were considered statistically significant.

RESULTS

Baseline Characteristics

The baseline characteristics are shown in **Table 1** according to the 7th edition of the American Joint Committee on Cancer staging. Of the 174 patients, 144 (82.8%) were men, and 30 (17.2%) were women. The median age was 63 (range: 45–79) years. The median interval between PET/CT examinations and surgery was seven days (range 1–65 days), and 10 days (range 1–65 days) between contrast-enhanced CT and surgery. A total of 5749 lymph nodes were dissected, including 210 hilar lymph nodes. The metastatic mediastinal lymph nodes were distributed in the regions of 106

TABLE 1 | Patient and tumor characteristics.

Characteristics	N = 174 (%)
Age (years)	
Median (range)	63 (45-79)
≥60	118 (67.8)
<60	56 (32.2)
Gender	
Male	144 (82.8)
Female	30 (17.2)
Alcohol intake	
Never	83 (47.7)
Ever	91 (52.3)
Smoking history	
Never	51 (29.3)
Ever	123 (70.7)
Tumor location	
Upper	11 (6.3)
Middle	111 (63.8)
Lower	52 (29.9)
Pathologic T category	
T1-2	83 (47.7)
T3-4	91 (52.3)
Pathologic N category	
N0-1	136 (78.2)
N2-3	38 (21.8)
Number of lymph node dissections*	32 (7-85)
Tumor, SUV max*	10.2 (0-33.2)
Hilar LN, SUV max*	0 (0-9.7)
Hilar LN, size (measured by CT, cm*	0.6 (0-1.3)

*Date shown as median (range).

TABLE 2 | Factors associated with hilar lymph node metastasis.

Characteristic	Patients (n)		*P*
	Hilar LNs (+)	Hilar LNs (-)	
Age			0.272[1]
<60	4	52	
≥60	4	114	
Gender			0.354[1]
Male	8	136	
Female	0	30	
Alcohol intake			0.723[1]
Ever	5	86	
Never	3	80	
Smoking history			0.440[1]
Ever	7	116	
Never	1	50	
Tumor location			0.507[1]
Upper	1	10	
Middle	7	104	
Lower	0	52	
Pathologic T category			0.282[1]
T1-2	2	81	
T3-4	6	85	
Hilar LN, size (measured by CT, cm)			1.000[1]
<1.0	6	140	
≥1.0	2	26	
Tumor, SUV max*	11.4 (6.7-15.2)	10.2 (0-33.2)	0.656[2]

*Date shown as median (range).
[1]Measured by Fisher's exact test.
[2]Measured by Student's t test.

(33.0%), 110 (20%), 108 (15.7%), 109 (13.0%), 107 (7.8%), 105 (7.0%), and 112 (3.5%). The median SUVmax for hilar lymph nodes was 0 (range: 0–9.7). The median size of the short diameter of the hilar lymph nodes examined under contrast-enhanced CT was 0.6 (range: 0–1.3) cm. Only eight (4.6%) patients were identified as positive for their resected hilar lymph nodes by pathological examination, demonstrating that hilar lymph node metastasis is a rare event in ESCC patients. As shown in **Table 2**, no clinicopathological factors could predict pathological hilar LNM.

Diagnostic Performance of PET/CT and Contrast-Enhanced CT in Hilar Lymph Node

Positive lymph nodes as determined *via* PET/CT were detected in only one patient (0.06%), but this patient did not exhibit pathological hilar LNM. Contrast-enhanced CT examination revealed nine positive cases; however, only 1 case was consistent with pathological examination. Detailed numbers of positive or negative cases of PET/CT and contrast-enhanced CT in diagnosing hilar lymph node are shown in **Table 3**.

As shown in **Table 4**, for hilar lymph node metastasis, both PET/CT and CT exhibited high specificity (99.4% and 95.2%) and negative predictive value (94.8% and 95.8%), but low sensitivity (0% and 12.5%) and positive predictive value (0% and 11.1%), suggesting that both are of limited value for this purpose. The specificity showed a significant difference (P=0.037). PET/CT is slightly more specific than contrast-enhanced CT.

DISCUSSION

Herein, we conducted a retrospective study with a relatively larger patient cohort to explore the diagnostic performance of FDG-PET/CT and contrast-enhanced CT for hilar LNM in patients with ESCC. Our results demonstrate that hilar LNM is a rare event in ESCC patients and both PET/CT and contrast-enhanced CT are of limited value for diagnosis and delineation of hilar lymph nodes in radiotherapy. The diagnostic value of PET-CT and enhanced CT in LNM of esophageal cancer has been explored by several studies (7, 11–13). The results from previous studies revealed low specificity of PET-CT or enhanced CT for detection of LNM. It is noteworthy that the eighth edition AJCC cancer staging does not consider hilar lymph nodes as regional nodes for esophageal cancer. Unique features and strengths of our study compared to previous investigations included the relatively larger patient cohort and the unique insights it offers into the clinical value of PET/CT and contrast-enhanced CT for accurate staging according to the eighth edition AJCC cancer staging system, focusing particularly on the diagnostic performance of (PET)CT and enhanced CT in the detection of hilar LNM. In our study, both PET/CT and contrast-enhanced CT exhibited high specificity (SP) and negative predictive value (NPV), but low sensitivity (SE) and positive predictive value (PPV), which is consistent with previous studies conducted for NSCLC (9, 14–16). There may be several reasons for this phenomenon. Lymph node enlargement can be caused by tumor metastasis, reactive hyperplasia, or granulomatous inflammation, and high FDG uptake is often caused by

TABLE 3 | Number of positive cases of PET/CT and contrast-enhanced CT in diagnosing hilar lymph node (n = 174).

		Pathology	
		Positive	**Negative**
PET/CT	positive	0	1
	negative	8	165
CT	positive	1	8
	negative	7	158

TABLE 4 | Diagnostic performance of PET/CT and contrast-enhanced CT in diagnosing hilar lymph node (n = 174).

	PET/CT n (95% CI)	CT n (95% CI)	*P* value[1]
Sensitivity	0.000 (0.000-0.402)	0.125 (0.007-0.533)	1.000[1]
Specificity	0.994 (0.962-1.000)	0.952 (0.904-0.977)	0.037[1]
Positive predictive value	0.000 (0.000-0.945)	0.111 (0.006-0.493)	1.000[1]
Negative predictive value	0.954 (0.908-0.978)	0.958 (0.911-0.981)	0.865[2]
Accuracy	0.948 (0.915-0.982)	0.914 (0.872-0.956)	0.290[2]

[1]*Measured by Fisher's exact test.*
[2]*Measured by Chi-square test.*

sarcoidosis, sarcoid-like reactions, or an infection. These will all cause trouble in the specificity of differential diagnosis (17). Due to the limited resolution, scatter effects, and attendant motion artifacts caused by esophageal and stomach peristalsis, PET/CT may also not be sensitive enough to detect metastases in lymph nodes.

Currently, radiation therapy is well recognized as an important part of treatment for esophageal cancer (18, 19). It is noteworthy that, given the anatomical characteristics of hilar LNM in ESCC, effective imaging of hilar LNM is critically important to guide radiotherapy treatment planning for these patients. However, based on our current research, the delineation of target volume using PET/CT or contrast-enhanced CT may lead to an unnecessarily aggressive treatment in a number of ESCC patients due to the limited positive predictive value for hilar LNM. Therefore, pathologic examination of suspicious hilar LNM by PET/CT or contrast-enhanced CT is encouraged.

There is a growing appreciation for the role of EBUS-TBNA in detecting hilar LNM. EBUS-TBNA is regarded as a safe and minimally invasive technique for sampling hilar lymph node, with an NPV of 91–99% and PPV of 92.4–100% (20–23). The utility of EBUS-TBNA for the evaluation of suspicious hilar LNM in ESCC has also been assessed by Schurink et al. They found 2.5% (21/857) patients had the positive hilar LNM at staging (11 ESCC, 10 Adenocarcinoma). Of those, 4 had successful biopsies (EBUS, CT-guided fine needle aspiration or tru-cut biopsy) and none were positive, and no recurrence of disease was seen during follow-up in these patients (7). indicating the false positive PET/CT results. However, the utility of EBUS-TBNA for the evaluation of suspicious hilar LNM in ESCC needs further investigation.

The most important limitation of this study is that there were only 8 patients in the hilar lymph node metastasis group. Thus, the diagnostic sensitivity, specificity, and positive predictive value in the CT group and PER/CT group were compared by use of Fisher's exact test. In summary, PET/CT and contrast-enhanced CT may be useful tools for predicting the negativity of hilar LN status, but they are not recommended for delineation of hilar LNM in the radiotherapy planning of ESCC patients due to their low PPV. All cases included in this study received radical operations, representing a population with relatively early-stage disease, and this may limit the generalizability. However, we found that the T stage could not predict the incidence of hilar LNM, and previous studies have shown that hilar LN recurrences are relatively low after definitive chemoradiotherapy for locally advanced ESCC (24–26). However, we think further studies regarding pathological diagnosis using minimally invasive techniques for suspected hilar LNs are warranted.

DATA AVAILABILITY STATEMENT

The raw data supporting the conclusions of this article will be made available by the authors, without undue reservation.

ETHICS STATEMENT

The studies involving human participants were reviewed and approved by the institutional review board of Fudan University Shanghai Cancer Center. Written informed consent for participation was not required for this study in accordance with the national legislation and the institutional requirements.

AUTHOR CONTRIBUTIONS

ZZ and GL designed the research. LC, SL, and TG interpreted and discussed the results. LC, SL, TG, LZ, BL, JN, XY, XC, FL, YL, YS, QL, and FY collected the data, analysed the data, wrote the manuscript. All authors read and approved the final manuscript.

FUNDING

The research was supported by National Natural Science Foundation of China (82003230, 81703024).

ACKNOWLEDGMENTS

We thank LetPub (www.letpub.com) for its linguistic assistance during the preparation of this manuscript.

REFERENCES

1. Torre LA, Bray F, Siegel RL, Ferlay J, Lortet-Tieulent J, Jemal A. Global Cancer Statistics, 2012. *CA: Cancer J Clin* (2015) 65(2):87–108. doi: 10.3322/caac.21262
2. Zhao J, He YT, Zheng RS, Zhang SW, Chen WQ. Analysis of Esophageal Cancer Time Trends in China, 1989- 2008. *Asian Pacific J Cancer Prev APJCP* (2012) 13(9):4613–7. doi: 10.7314/apjcp.2012.13.9.4613
3. Li Y, Zhao W, Ni J, Zou L, Yang X, Yu W, et al. Predicting the Value of Adjuvant Therapy in Esophageal Squamous Cell Carcinoma by Combining the Total Number of Examined Lymph Nodes With the Positive Lymph Node Ratio. *Ann Surg Oncol* (2019) 26(8):2367–74. doi: 10.1245/s10434-019-07489-3
4. Greenstein AJ, Litle VR, Swanson SJ, Divino CM, Packer S, Wisnivesky JP. Prognostic Significance of the Number of Lymph Node Metastases in Esophageal Cancer. *J Am Coll Surgeons* (2008) 206(2):239–46. doi: 10.1016/j.jamcollsurg.2007.09.003
5. Chen J, Liu S, Pan J, Zheng X, Zhu K, Zhu J, et al. The Pattern and Prevalence of Lymphatic Spread in Thoracic Oesophageal Squamous Cell Carcinoma. *Eur J Cardio-Thorac Surg Off J Eur Assoc Cardio-Thorac Surg* (2009) 36 (3):480–6. doi: 10.1016/j.ejcts.2009.03.056
6. Li B, Chen H, Xiang J, Zhang Y, Li C, Hu H, et al. Pattern of Lymphatic Spread in Thoracic Esophageal Squamous Cell Carcinoma: A Single-Institution Experience. *J Thorac Cardiovasc Surg* (2012) 144(4):778–85; discussion 85-6. doi: 10.1016/j.jtcvs.2012.07.002
7. Schurink B, Mazza E, Ruurda JP, Roeling TAP, Bleys R, van Hillegersberg R. Metastatic Incidence of (PET)CT Positive Lung Hilar and Retroperitoneal Lymph Nodes in Esophageal Cancer Patients. *Surg Oncol* (2020) 33:170–6. doi: 10.1016/j.suronc.2020.02.012
8. Silvestri GA, Gonzalez AV, Jantz MA, Margolis ML, Gould MK, Tanoue LT, et al. Methods for Staging Non-Small Cell Lung Cancer: Diagnosis and Management of Lung Cancer, 3rd Ed: American College of Chest Physicians Evidence-Based Clinical Practice Guidelines. *Chest* (2013) 143(5 Suppl):e211S–e50S. doi: 10.1378/chest.12-2355
9. Udoji TN, Phillips GS, Berkowitz EA, Berkowitz D, Ross C, Bechara RI. Mediastinal and Hilar Lymph Node Measurements. Comparison of Multidetector-Row Computed Tomography and Endobronchial Ultrasound. *Ann Am Thorac Soc* (2015) 12(6):914–20. doi: 10.1513/AnnalsATS.201312-430OC
10. Korst RJ, Rusch VW, Venkatraman E, Bains MS, Burt ME, Downey RJ, et al. Proposed Revision of the Staging Classification for Esophageal Cancer. *J Thorac Cardiovasc Surg* (1998) 115(3):660–69. doi: 10.1016/s0022-5223(98)70332-0
11. Yoon YC, Lee KS, Shim YM, Kim BT, Kim K, Kim TS. Metastasis to Regional Lymph Nodes in Patients With Esophageal Squamous Cell Carcinoma: CT Versus FDG PET for Presurgical Detection Prospective Study. *Radiology* (2003) 227(3):764–70. doi: 10.1148/radiol.2281020423
12. Tan R, Yao SZ, Huang ZQ, Li J, Li X, Tan HH, et al. Combination of FDG PET/CT and Contrast-Enhanced MSCT in Detecting Lymph Node Metastasis of Esophageal Cancer. *Asian Pacific J Cancer Prev APJCP* (2014) 15(18):7719–24. doi: 10.7314/apjcp.2014.15.18.7719
13. Yamada H, Hosokawa M, Itoh K, Takenouchi T, Kinoshita Y, Kikkawa T, et al. Diagnostic Value of ^{18}F-FDG PET/CT for Lymph Node Metastasis of Esophageal Squamous Cell Carcinoma. *Surg Today* (2014) 44(7):1258–65. doi: 10.1007/s00595-013-0725-z
14. Cerfolio RJ. Invited Commentary. *Ann Thorac Surg* (2009) 87(5):1545. doi: 10.1016/j.athoracsur.2009.03.002
15. Lee BE, Redwine J, Foster C, Abella E, Lown T, Lau D, et al. Mediastinoscopy Might Not be Necessary in Patients With Non-Small Cell Lung Cancer With Mediastinal Lymph Nodes Having a Maximum Standardized Uptake Value of Less Than 5.3. *J Thorac Cardiovasc Surg* (2008) 135(3):615–9. doi: 10.1016/j.jtcvs.2007.09.029
16. Lin WY, Hsu WH, Lin KH, Wang SJ. Role of Preoperative PET-CT in Assessing Mediastinal and Hilar Lymph Node Status in Early Stage Lung Cancer. *J Chin Med Assoc JCMA* (2012) 75(5):203–8. doi: 10.1016/j.jcma.2012.04.004
17. Takanami K, Kaneta T, Yamada T, Kinomura S, Yamada S, Fukuda H, et al. FDG PET for Esophageal Cancer Complicated by Sarcoidosis Mimicking Mediastinal and Hilar Lymph Node Metastases: Two Case Reports. *Clin Nucl Med* (2008) 33(4):258–61. doi: 10.1097/RLU.0b013e3181662fda
18. van Hagen P, Hulshof MC, van Lanschot JJ, Steyerberg EW, van Berge Henegouwen MI, Wijnhoven BP, et al. Preoperative Chemoradiotherapy for Esophageal or Junctional Cancer. *N Engl J Med* (2012) 366(22):2074–84. doi: 10.1056/NEJMoa1112088
19. Ma HF, Lv GX, Cai ZF, Zhang DH. Comparison of the Prognosis of Neoadjuvant Chemoradiotherapy Treatment With Surgery Alone in Esophageal Carcinoma: A Meta-Analysis. *OncoTargets Ther* (2018) 11:3441–7. doi: 10.2147/ott.s145063
20. Khalid U, Akram MJ, Butt FM, Ashraf MB, Khan F. Endobronchial Ultrasound Guided Transbronchial Needle Aspiration Of Mediastinal And Hilar Lymph Nodes- Five Years Of Experience At A Cancer Setting Hospital In Pakistan. *J Ayub Med College Abbottabad JAMC* (2020) 32(3):310–7.
21. Yasufuku K, Nakajima T, Waddell T, Keshavjee S, Yoshino I. Endobronchial Ultrasound-Guided Transbronchial Needle Aspiration for Differentiating N0 Versus N1 Lung Cancer. *Ann Thorac Surg* (2013) 96(5):1756–60. doi: 10.1016/j.athoracsur.2013.05.090
22. Ernst A, Eberhardt R, Krasnik M, Herth FJ. Efficacy of Endobronchial Ultrasound-Guided Transbronchial Needle Aspiration of Hilar Lymph Nodes for Diagnosing and Staging Cancer. *J Thorac Oncol* (2009) 4(8):947–50. doi: 10.1097/JTO.0b013e3181add88d
23. Yasufuku K, Pierre A, Darling G, de Perrot M, Waddell T, Johnston M, et al. A Prospective Controlled Trial of Endobronchial Ultrasound-Guided Transbronchial Needle Aspiration Compared With Mediastinoscopy for Mediastinal Lymph Node Staging of Lung Cancer. *J Thorac Cardiovasc Surg* (2011) 142(6):1393–400.e1. doi: 10.1016/j.jtcvs.2011.08.037
24. Zhou S, Zhang L, Luo L, Li Q, Shen J, Feng Z, et al. Failure Pattern of Elective Nodal Irradiation for Esophageal Squamous Cell Cancer Treated With Neoadjuvant Chemoradiotherapy. *Jpn J Clin Oncol* (2018) 48(9):815–21. doi: 10.1093/jjco/hyy099
25. Zhang X, Li M, Meng X, Kong L, Zhang Y, Wei G, et al. Involved-Field Irradiation in Definitive Chemoradiotherapy for Locally Advanced Esophageal Squamous Cell Carcinoma. *Radiat Oncol (LondEngl)* (2014) 9:64. doi: 10.1186/1748-717x-9-64
26. Sudo K, Kato K, Kuwabara H, Sasaki Y, Takahashi N, Shoji H, et al. Patterns of Relapse After Definitive Chemoradiotherapy in Stage II/III (Non-T4) Esophageal Squamous Cell Carcinoma. *Oncology* (2018) 94(1):47–54. doi: 10.1159/000480515

Conflict of Interest: The authors declare that the research was conducted in the absence of any commercial or financial relationships that could be construed as a potential conflict of interest.

Publisher's Note: All claims expressed in this article are solely those of the authors and do not necessarily represent those of their affiliated organizations, or those of the publisher, the editors and the reviewers. Any product that may be evaluated in this article, or claim that may be made by its manufacturer, is not guaranteed or endorsed by the publisher.

frontiers in Oncology

ORIGINAL RESEARCH
published: 28 February 2022
doi: 10.3389/fonc.2022.812707

Incorporation of PET Metabolic Parameters With Clinical Features Into a Predictive Model for Radiotherapy-Related Esophageal Fistula in Esophageal Squamous Cell Carcinoma

*Kaixin Li[1], XiaoLei Ni[2], Duanyu Lin[3] and Jiancheng Li[4]**

[1] Department of Radiation Oncology, Quanzhou First Hospital Affiliated to Fujian Medical University, Quanzhou, China,
[2] Department of Radiation Oncology, The First Hospital of Longyan Affiliated to Fujian Medical University, Longyan, China,
[3] Department of Nuclear Medicine, Fujian Medical University Cancer Hospital, Fujian Cancer Hospital, Fuzhou, China,
[4] Department of Radiation Oncology, Fujian Medical University Cancer Hospital, Fujian Cancer Hospital, Fuzhou, China

OPEN ACCESS

Edited by:
Alessio G. Morganti, University of Bologna, Italy

Reviewed by:
Yunlang She, Tongji University, China
Yun Chen, Fudan University, China

***Correspondence:**
Jiancheng Li
jianchengli_jack@126.com

Specialty section:
This article was submitted to Radiation Oncology, a section of the journal Frontiers in Oncology

Received: *10 November 2021*
Accepted: *24 January 2022*
Published: *28 February 2022*

Citation:
Li K, Ni X, Lin D and Li J (2022) Incorporation of PET Metabolic Parameters With Clinical Features Into a Predictive Model for Radiotherapy-Related Esophageal Fistula in Esophageal Squamous Cell Carcinoma. Front. Oncol. 12:812707. doi: 10.3389/fonc.2022.812707

Purpose: To determine whether the addition of metabolic parameters from fluorine-18-fluorodeoxyglucose positron emission tomography/computed tomography (^{18}F-FDG PET/CT) scans to clinical factors could improve risk prediction models for radiotherapy-related esophageal fistula (EF) in esophageal squamous cell carcinoma (ESCC).

Methods and Materials: Anonymized data from 185 ESCC patients (20 radiotherapy-related EF-positive cases) were collected, including pre-therapy PET/CT scans and EF status. In total, 29 clinical features and 15 metabolic parameters from PET/CT were included in the analysis, and a least absolute shrinkage and selection operator logistic regression model was used to construct a risk score (RS) system. The predictive capabilities of the models were compared using receiver operating characteristic (ROC) curves.

Results: In univariate analysis, metabolic tumor volume (MTV)_40% was a risk factor for radiotherapy (RT)-related EF, with an odds ratio (OR) of 1.036 [95% confidence interval (CI): 1.009–1.063, $p = 0.007$]. However, it was excluded from the predictive model using multivariate logistic regression. Predictive models were built based on the clinical features in the training cohort. The model included diabetes, tumor length and thickness, adjuvant chemotherapy, eosinophil count, and monocyte-to-lymphocyte ratio. The RS was defined as follows: 0.2832 – (7.1369 × diabetes) + (1.4304 × tumor length) + (2.1409 × tumor thickness) – [8.3967 × adjuvant chemotherapy (ACT)] – (28.7671 × eosinophils) + (8.2213 × MLR). The cutoff of RS was set at –1.415, with an area under the curve (AUC) of 0.977 (95% CI: 0.9536–1), a specificity of 0.929, and a sensitivity of 1. Analysis in the testing cohort showed a lower AUC of 0.795 (95% CI: 0.577–1), a specificity of 0.925, and a sensitivity of

0.714. Delong's test for two correlated ROC curves showed no significant difference between the training and testing sets (p = 0.109).

Conclusions: MTV_40% was a risk factor for RT-related EF in univariate analysis and was screened out using multivariate logistic regression. A model with clinical features can predict RT-related EF.

Keywords: esophageal squamous cell carcinoma, radiotherapy, esophageal fistula, PET/CT, metabolic parameter

1 INTRODUCTION

Esophageal cancer (EC) is the fourth most common malignancy and the leading cause of cancer-related deaths in China (1, 2). Unlike the high concentration of adenocarcinoma in North America and Europe, esophageal squamous cell carcinoma (ESCC) remains the predominant malignancy in Asia (3). Due to a lack of early screening and rapid disease progression, approximately 40%–50% of patients miss the opportunity for radical surgery, which is a mainstay treatment for localized EC. Definitive chemoradiotherapy (CRT) is the standard treatment for patients with unresectable tumors or those who refuse surgery (4). For ESCC patients without distant organ metastases, except for cervical or abdominal lymph node metastases, who were treated with radiotherapy (RT) or CRT, the median overall survival was 24.3 months (5). This value was reported to be even lower (11.0 months) in a large retrospective analysis of 221 patients with advanced ESCC who developed an esophageal fistula (EF) (6).

EF is an adverse event of ESCC that develops due to tumor progression or therapeutic intervention. As one of the most serious complications of RT for EC, the incidence of EF is 1.01%–22.1% (7–15), which is 14.6%–30.5% in T4 stage patients (16–19). The clinical application of oral meglumine diatrizoate esophagogram enables early detection of EF (20), and some salvage strategies are used such as stents or bypass surgery (21, 22). However, the prognosis of EF in patients with ESCC receiving RT remains poor. The median interval from initiation of RT to the occurrence of EF was 1.3–5.75 months (7–11, 13–19), and the median post-fistula survival time is only 3.1–3.63 months (6, 7, 13). Therefore, early prediction of radiotherapy-related EF could have a significant impact on the outcome of patients with ESCC.

Fluorine-18-fluorodeoxyglucose positron emission tomography/computed tomography (^{18}F-FDG PET/CT) has been widely used in patients with ESCC treated with RT in recent years. The impact of PET/CT on radiation treatment includes TNM staging of EC, optimization of RT planning, and therapeutic monitoring of neoadjuvant CRT (23). However, no study has yet investigated the ability of PET/CT scanning to detect or predict EF development, particularly for RT-related EF in ESCC patients.

In this study, we explored risk factors from clinical features and PET/CT metabolic parameters, built predictive models for RT-related EF in ESCC patients, and assessed the improvements in a model for EF prediction that combines metabolic and clinical factors over a model that incorporates only clinical features.

2 METHODS AND MATERIALS

2.1 Patient Eligibility

We retrospectively collected the data of consecutive patients with ESCC treated with RT who underwent ^{18}F-FDG PET/CT before treatment at our center from March 2015 to March 2021. All data were retrieved from electronic data records. The inclusion criteria were as follows: (1) squamous cell histological type, (2) treatment with RT with or without chemotherapy, (3) staging FDG PET performed before any RT or chemotherapy, (4) follow-up at least 3 months after RT or until EF was diagnosed, and (5) no EF before RT. The exclusion criteria were as follows: (1) esophageal surgery before or after RT, (2) previous thoracic RT, and (3) follow-up attrition. The institutional review board approved the retrospective analysis of routinely acquired clinical data for this study. The requirement for informed consent was waived.

2.2 Data Collection

Clinical data such as age, sex, Eastern Cooperative Oncology Group performance status (ECOG-PS), comorbidity, smoking/drinking history, nutritional status, TNM stage, tumor features as collected using imaging, inflammatory parameters, and EF status were collected. The metabolic parameters measured were as follows: maximum standardized uptake value (SUV_{max}), mean standardized uptake value (SUV_{mean}), metabolic tumor volume (MTV), total lesion glycolysis (TLG), maximum standardized uptake ratio (SUR_{max}), mean standardized uptake ratio (SUR_{mean}), and heterogeneity factor (HF). CT and barium meal images were reviewed by two experienced radiologists, and ^{18}F-FDG PET/CT images were reviewed by two experienced nuclear medicine physicians.

2.2.1 Pretreatment Evaluation

Pathological or cytological diagnosis of ESCC was confirmed by esophagoscopy. All patients were staged according to the 8th edition of the American Joint Committee on Cancer (AJCC) staging manual by endoscopic ultrasound, contrast-enhanced CT of the chest and abdomen, and ^{18}F-FDG PET/CT. The T stage was diagnosed by CT when the esophagoscope could not pass through stenotic lesions in advanced disease. T3 was defined as a primary tumor with a maximum thickness of >15 mm (24). Adjacent organ invasion was defined using computed tomography (CT) or PET/CT. For example, an aortic invasion was defined as >90° of the aorta surrounded by a tumor in more than one CT slice (25), and an airway invasion was defined as

deformities of the trachea or bronchi due to contiguous cancer. The maximum thickness and length of the tumor, and tumor location, were measured using PET/CT. Esophageal stenosis was quantified according to the narrowest transverse diameter identified using barium meal examination. Macroscopic tumor type was confirmed by esophagoscopy or barium meal examination according to the macroscopic classification of EC (26).

The inflammation-based parameters were platelet–lymphocyte ratio (PLR), neutrophil-to-lymphocyte ratio (NLR), monocyte-to-lymphocyte ratio (MLR), and systemic immune inflammation index (SII), which were calculated as follows: PLR = P/L; NLR = N/L; MLR = M/L; SII = P × N/L [neutrophil count (N), lymphocyte count (L), platelet count (P), and monocyte count (M)] (27). Since the records of body mass index (BMI) were lost in some patients, we had to use hemoglobin (Hb) and albumin (Alb) as indicators of nutritional status. Additionally, eosinophils, which are equipped to regulate tumor progression (28), were another candidate risk factor for EF in our study. The blood test data used in the analysis were obtained within 1 week before the initiation of treatment.

2.2.2 ^{18}F-FDG PET/CT Imaging and Metabolic Parameters

Pretreatment ^{18}F-FDG PET/CT was performed with a time interval of <2 weeks. All patients fasted for at least 6 h (blood glucose levels below 7.0 mml/L) before PET/CT acquisition. PET/CT images were obtained 60 min later by means of a hybrid PET/CT scanner (Gemini 64 TF, Philips Medical Systems, Best, The Netherlands) after injection of 0.10–0.15 mCi/kg of ^{18}F-FDG. Unenhanced CT was performed from the skull base to the mid-thigh with the following parameters: tube voltage, 120 kV; tube current, 100–110 mA; pitch, 0.829; and section and reconstruction thickness, 5 mm. After the CT scan, a three-dimensional model was used to obtain PET images, and the emission scan time for each bed position was 1–2 min. PET images were reconstructed with CT attenuation correction using the time-of-flight algorithm. Finally, all collected data were transferred into a Philips Extended Brilliance Workstation 3.0 (EBW 3.0, Philips) to reconstruct PET, CT, and PET/CT fusion images. The voxel size was 4 × 4 × 5 mm.

To calculate the SUV_{max}, manually defined circular regions of interest (ROIs) were drawn on the tumor. The MTV was determined either as the total volume of voxels with a threshold SUV of 40% or as 50% of the SUV_{max} in the volume of interest. The TLG was calculated as the MTV multiplied by the SUV_{mean}. The max and mean values of SUR were calculated as SUV_{max}(tumor)/SUV_{mean}(aorta) and SUV_{mean}(tumor)/SUV_{mean}(aorta) (29). To determine the HF, we first delineated the ROI with an automatic algorithm based on various SUV thresholds (e.g., 40%–80% of SUV_{max} in a 10% interval). Then, HF was calculated using linear regression analysis to identify the derivative of the volume–threshold function (30).

2.2.3 Treatment

All patients in this study were treated with concurrent CRT, sequential CRT, or RT alone, 131 patients received traditional intensity-modulated radiotherapy (*IMRT*), 41 patients received volumetric modulated arc therapy (VMAT), and 13 patients underwent helical tomotherapy (TOMO).

Each patient was placed in the supine position with a head and neck thermoplastic or body vacuum bag. A planning CT (GE Healthcare UK Ltd, Amersham Place, Little Chalfont, Buckinghamshire, England) scan was performed with 0.5-cm-thick slices from the atlas (C1) to the second lumbar vertebra (L2) level. CT images were transmitted to the planning system for delineation and planning of the target area and the endangered organ. The delineation of gross tumor volume, clinical tumor volume, and planned tumor volume, and the dose and volume constraints for normal tissues, was defined according to the standard issued by the National Comprehensive Cancer Network. The IMRT and VMAT plans were developed using the Philips Pinnacle 3 software program (Philips, Amsterdam, Netherlands), and the TOMO plans were completed in the Accuray Planning Station Version 2.1.3 (TomoHD, Accuray Inc., 1310 Chesapeake Terrace Sunnyvale, CA, USA).

All eligible patients received zero to six courses of concurrent or sequential chemotherapy. The chemotherapy regimens were based on platinum, including (A) docetaxel 75 mg/m^2 d1 or paclitaxel 135 mg/m^2 d1 + nedaplatin 75 mg/m^2 d2, cisplatin 75 mg/m^2 d2, lobaplatin 50 mg d2, or carboplatin AUC 2 d2 and (B) orally S1 40 mg/m^2 twice daily for 14 days, repeated every 3 weeks.

2.3 Definition of RT-Related EF

RT-related EF was defined as EF diagnosed by cervical and chest CT, barium or meglumine iothalamate esophagography of the esophagus after RT initiation, and before progression of the primary tumor. Data on all EFs after RT initiation were collected, regardless of the time interval from RT initiation. During RT, patients are routinely assessed every 3 weeks for 6 weeks by CT and X-ray esophagography. After RT, follow-up monitoring was performed once a month until the third month, then every 3–6 months until 2 years later, and annually thereafter. The types of EF (esophagorespiratory or esophagomediastinal) are described in the case report forms.

2.4 Statistical Analysis

The mean value comparisons of continuous variables were performed using t-tests. A chi-square test was performed to compare categorical variables. Twenty-nine clinic factors were analyzed: sex; age; ECOG-PS; smoking history; alcohol use; diabetes; macroscopic tumor type; tumor location; tumor length; maximum thickness of tumor; minimum inner diameter of tumor; TNM stage; RT fraction; RT technique; current chemotherapy; adjuvant chemotherapy (ACT); induction chemotherapy; chemotherapy regimen and circles; Hb, Alb, eosinophil, and lymphocyte counts; PLR, NLR, MLR, and SII; and 15 metabolic parameter objectives. Two multivariate prediction models were independently trained from two sets of predictors (based on clinical factors alone or based on clinical factors combined with metabolic parameters). All 185 patients were randomly divided into two cohorts in a ratio of 6:4 using

computer-generated random numbers, with 111 cases in the training dataset and 74 cases in the testing dataset. Then, the training dataset was split into primary and validation sets using cross-validation-based regularization factor selection. The least absolute shrinkage and selection operator (LASSO) logistic regression was used to construct a risk score (RS) model. Receiver operating characteristic (ROC) curve analysis was conducted to evaluate the performance of predictive models and to determine the optimal RS cutoff for separating high and low risk for EF. All analyses were performed using R software (R version 4.0.2; Tableone, glmnet package, caret package, lattice package, pROC package, plyr package, ggplot2 package, foreach package, and Matrix package).

3 RESULTS

3.1 Clinical Characteristics and Metabolism Parameters

The clinical characteristics of 185 patients are shown in **Table 1**. The median age was 63 years (range, 33–86 years). The male-to-female ratio was 4.97:1. Twenty patients (10.81%) underwent RT-related EF. Among them, eight patients experienced fistula during treatment and seven patients discontinued RT, while the other 12 developed fistula after the completion of RT. The median time of EF occurrence was 57 days (range, 5–273 days). The types of EF in this study included esophagorespiratory (three patients) and esophageal–mediastinum fistulas (17 patients). The PET/CT-based metabolism parameters are shown in **Table 2**.

Twelve of the available clinical factors and five metabolic parameters were significantly associated with RT-related EF incidence. Before logistic regression, we performed Pearson's correlation analysis and Spearman correlation analysis of the independent variables (**Figure 1**). We found that there was high collinearity among inflammation-based parameters (absolute value of correlation coefficient, ½CC½: 0.40–0.88) and metabolism-based parameters (½CC½: 0.61–0.99). We also found a significant correlation between tumor features, such as length, thickness, T stage, and metabolism parameters (½CC½: 0.40–0.76).

3.2 RS Model for Radiotherapy-Related Esophageal Fistula

To construct predictive models, we chose a penalized LASSO regression model to calculate an RS using the above 12 and 17 features, respectively. The LASSO coefficient profiles of 12 clinical features and 17 combined objectives in each model are shown in **Figures 2A, B**. Tenfold cross-validation was used to select an optimal model. We chose lambda.1se, a function in R, for model filtering, as shown in **Figures 2C, D**. Eight clinical features, including diabetes, tumor length, tumor thickness, adjuvant chemotherapy, chemotherapy circles, eosinophils, lymphocytes, and MLR, were selected to construct a clinical-factor-based predictive model. Only MTV_40% was added to construct a combined predictive model.

In univariate analysis, MTV_40% was a risk factor for RT-related EF, with an odds ratio (OR) of 1.036 [95% confidence interval (CI): 1.009–1.063, $p = 0.007$]. However, it was screened out from the predictive model using multivariate logistic regression analysis (**Table 3**). Finally, only one predictive model was generated using the training set based on the clinical factors. The function is as follows: RS = 0.2832 − (7.1369 × diabetes) + (1.4304 × tumor length) + (2.1409 × tumor thickness) − (8.3967 × ACT) − (28.7671 × eosinophils) + (8.2213 × MLR). The cutoff of RS in the training set was −1.415, with an area under the curve (AUC) of 0.977 (95% CI: 0.9536–1), a specificity of 0.929, and a sensitivity of 1 (**Figure 3A**). The cutoff of RS in the testing set was −3.067, with an AUC of 0.795 (95% CI: 0.577–1), a specificity of 0.925, and a sensitivity of 0.714 (**Figure 3B**). However, the Delong's test for two correlated ROC curves showed no significant difference between the training and testing sets ($p = 0.109$).

Assignment of involved variables were as follows: diabetes (yes = 1, no = 2), tumor length = the length of primary tumor measured on PET/CT, tumor thickness = the maximum thickness of tumor measured on PET/CT, ACT (yes = 1, no = 0), eosinophil = count number of eosinophils ($\times 10^9$/L), and MLR = monocyte-to-lymphocyte ratio.

4 DISCUSSION

EF is a severe complication in patients with ESCC treated with RT. Patients with EF experience symptoms including fever, cough, chest pain, and upper gastrointestinal bleeding. Patients may die due to sepsis or massive bleeding (31). Therefore, the prediction of radiotherapy-related EF formation is crucial before the implementation of treatment strategies. Patients who received the same dose of RT and the same intensity of chemotherapy sometimes had different outcomes of EF. This variation might be due to patient status, treatment-related factors, or tumor characteristics (12). As a functional imaging method, PET/CT can construct biological tumor volume, which could reflect cell metabolism, proliferation, hypoxia, apoptosis, and even phenotype (23). Information on tumor heterogeneity may be used to predict the occurrence of EF. Previous reports have focused on exploring the clinical risk factors of EF, while reports of metabolic parameters related to the incidence of EF are rare.

In the present study, we found that metabolic parameters, such as MTV, TLG, and HF, and diabetes, tumor length and thickness, adjuvant chemotherapy, eosinophil count, and monocyte-to-lymphocyte ratio were strongly associated with the occurrence of EF. RS models were built based on these factors.

Multiple reports have demonstrated a higher risk of radiation-induced toxicity in patients with diabetes (32, 33). However, reports on the effects of diabetes on EF are rare. Some studies tracking risk factors in EF did not show an effect of diabetes status (7, 9), while our study found that diabetes increases the risk of RT-related EF by more than seven times in ESCC.

4.1 Effect of Patient Status on Fistula Formation

In radiotherapy cases, a good nutritional status, such as appropriate BMI (10, 11) or serum cholesterol value (19),

TABLE 1 | Clinical characteristics of 185 esophageal squamous cell carcinoma patients.

Characteristics		Esophageal fistula		*p*-value
		Without (n = 165)	With (n = 20)	
Gender (n, %)	Male	137 (83)	17 (85)	1
	Female	28 (17)	3 (15)	
Age (n, %)	<70 years	118 (71.5)	14 (70)	0.887
	≥70 years	47 (28.5)	6 (30)	
ECOG PS (n, %)	1	156 (94.5)	19 (95)	1
	2	9 (5.5)	1 (5)	
Smoking history (n, %)	No	67 (40.6)	8 (40)	0.958
	Yes	98 (59.4)	12 (60)	
Alcohol use (n, %)	No	49 (29.7)	7 (35)	0.626
	Yes	116 (70.3)	13 (65)	
Diabetes (n, %)	No	14 (8.5)	5 (25)	0.038
	Yes	151 (91.5)	15 (75)	
Macroscopic tumor type (n, %)	Protruding	60 (36.4)	5 (25)	0.373
	Ulcerative and localized	9 (5.5)	0 (0)	
	Ulcerative and infiltrative	17 (10.3)	4 (20)	
	Diffusely infiltrative	79 (47.9)	11 (55)	
Tumor location (n, %)	Cervical/upper	63 (38.2)	7 (35)	0.962
	Middle	78 (47.3)	10 (50)	
	Lower	24 (14.5)	3 (15)	
Tumor length	Median (IQR)	5 (3.6, 6.6)	6.6 (4.9, 7.7)	0.025
Tumor thickness	Median (IQR)	1.5 (1.1, 1.8)	2 (1.4, 2.3)	0.007
ID_min	Median (IQR)	0.9 (0.7, 1.2)	0.8 (0.6, 1.2)	0.882
T stage (n, %)	No–T4	89 (53.9)	6 (30)	0.043
	T4	76 (46.1)	14 (70)	
N stage (n, %)	0–1	70 (42.4)	8 (40)	0.836
	2–3	95 (57.6)	12 (60)	
M stage (n, %)	0	141 (85.5)	17 (85)	1
	1	24 (14.5)	3 (15)	
Fraction dose (n, %)	≤200 cGy	70 (42.4)	10 (50)	0.518
	>200 cGy	95 (57.6)	10 (50)	
RT technique (n, %)	IMRT	116 (70.3)	15 (75)	1
	VMAT	37 (22.4)	4 (20)	
	TOMO	12 (7.3)	1 (5)	
CCT (n, %)	No	82 (49.7)	11 (55)	0.654
	Yes	83 (50.3)	9 (45)	
Chemotherapy regimen (n, %)	No	24 (14.5)	4 (20)	0.452
	S1	10 (6.1)	2 (10)	
	TP	131 (79.4)	14 (70)	
ACT (n, %)	No	63 (38.2)	17 (85)	<0.001
	Yes	102 (61.8)	3 (15)	
ICT (n, %)	No	49 (29.7)	8 (40)	0.346
	Yes	116 (70.3)	12 (60)	
Chemotherapy circles (n, %)	0	23 (13.9)	4 (20)	0.007
	1–3	65 (39.4)	14 (70)	
	4–6	77 (46.7)	2 (10)	
Eosinophil	Median (IQR)	0.1 (0.1, 0.2)	0.1 (0.1, 0.1)	0.004
Lymphocyte	Median (IQR)	1.9 (1.5, 2.3)	1.6 (1.3, 1.8)	0.007
Hemoglobin	Median (IQR)	138 (127, 147)	136.5 (128.2, 141.5)	0.7
Albumin	Median (IQR)	40.1 (37.5, 43.2)	40.9 (37.6, 42.3)	0.915
SII	Median (IQR)	580.5 (426, 864.3)	870.6 (594, 1378.3)	0.027
PLR	Median (IQR)	135 (105.6, 169.2)	161.8 (119.1, 224.6)	0.077
NLR	Median (IQR)	2.3 (1.7, 3.1)	3.4 (2.3, 5.5)	0.005
MLR	Median (IQR)	0.2 (0.2, 0.3)	0.3 (0.2, 0.5)	0.026

IQR, interquartile range; ID_min, minimum inner diameter of tumor; IMRT, intensity-modulated radiotherapy; VMAT, volumetric modulated arc therapy; TOMO, helical tomotherapy; CCT, concurrent chemotherapy; ACT, adjuvant chemotherapy; ICT, Induction chemotherapy; SII, systemic immune inflammation index; PLR, platelet-to-lymphocyte ratio; NLR, neutrophil-to-lymphocyte ratio; MLR, monocyte-to-lymphocyte ratio.

promotes wound healing and reduces the risk of EF formation. While the Hb and Alb levels were correlated with nutritional status in our study, there was no significant difference between the EF and non-EF groups. One possible explanation is the selection bias of the enrolled participants. Most patients who agree to perform PET/CT have the financial means to do so. Only 10 patients (5.4%) with poor performance status in our study had an ECOG-PS score of <1.

TABLE 2 | PET/CT-based metabolism parameters of 185 esophageal squamous cell carcinoma patients.

Parameters Median (IQR)	Esophageal fistula		*p*-value
	Without	With	
SUVmax	12.7 (9.1, 16.6)	13.2 (12.1, 16.2)	0.309
SUVmin_40%	4.9 (3.5, 6.2)	4.9 (4.6, 5.8)	0.446
SUVmean_40%	7.7 (5.2, 10.2)	8 (7, 9.5)	0.44
SUVsd_40%	1.9 (1.4, 2.5)	1.8 (1.6, 2.3)	0.837
MTV_40%	12.5 (7.2, 24.5)	24.9 (19.5, 34.4)	0.007
TLG_40%	100.4 (42.7, 215.7)	209.1 (106.7, 321.7)	0.01
SUVmin_50%	6.1 (4.4, 7.9)	6.5 (5.8, 7.2)	0.398
SUVmean_50%	8.5 (6.1, 11.1)	8.8 (7.7, 12.6)	0.304
SUVsd_50%	1.6 (1.2, 2.1)	1.6 (1.3, 2.2)	0.539
MTV_50%	9 (4.5, 17.6)	18.2 (13.4, 25.4)	0.007
TLG_50%	80.4 (29.3, 178.2)	164.9 (83.4, 259.7)	0.01
HF	3.7 (2, 6)	1.8 (1.5, 2.4)	0.004
SURmax	8.8 (6.1, 12.5)	9.4 (7.4, 12.4)	0.514
SURmean_40%	5.2 (3.6, 7.5)	5.5 (4.5, 7.5)	0.567
SURmean_50%	5.7 (4, 8.3)	6 (5, 8.5)	0.459

IQR, interquartile range; SUV, standardized uptake value; MTV, metabolic tumour volume; TLG, total lesion glycolysis; HF, heterogeneity factor; SUR, tumor-to-blood SUV ratio.

There was no significant correlation between the development of EF and tumor with ulceration or esophageal stenosis in the regression equation. This result is inconsistent with those of other studies (7–9, 12–14, 16). This finding may be due to the different assessment methods used in our study. The minimum inner diameter of the esophagus measured by barium meal examination in 117 patients was <1 cm. Since the esophagoscope could not pass through the narrowest location of the primary tumor in most cases, we had to diagnose ulceration or stenosis using radiography. We found significant differences in T4 stage, tumor length, and thickness between the groups with or without EF, which is consistent with other studies (7, 8, 11–13, 17). Finally, T4 stage was not included in the regression equation due to the correlation among these tumor characteristics.

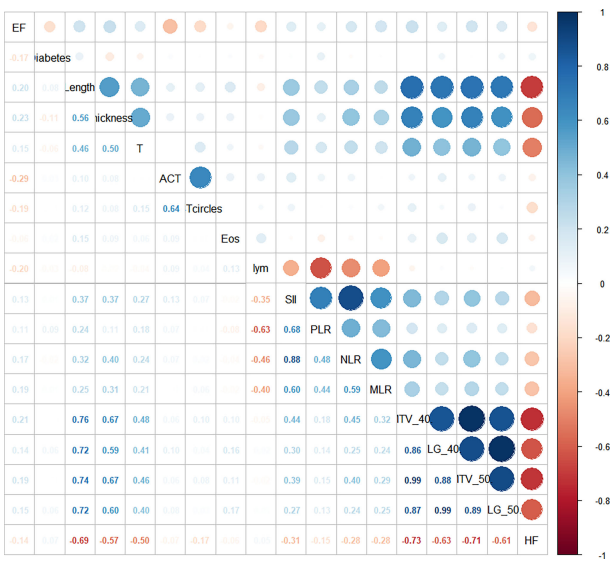

FIGURE 1 | Correlation of risk factors.

We also focused on the effects of treatment on radiotherapy-related EF. Prior studies have reported some treatment-related risk factors, including re-RT, incomplete response, and fluorouracil-based regimens (8, 11, 12, 15). In this study, we aimed to predict the occurrence of EF before treatment delivery; therefore, factors such as treatment response after treatment were not included in the analysis. We found no significant correlation between the development of EF and RT technique and dose nor between chemotherapy regimen and circles. Unexpectedly, we found that ACT could reduce the risk of EF by more than eightfold. However, this finding does not mean that ACT could avoid RT-related EF events. A reasonable explanation may be that patients who received ACT consistently showed a poor response to RT, and the EF was most related to tumor progression.

The systemic inflammatory response has been widely used to predict the prognosis of several solid tumors, and some investors have reported that the PLR is an independent predictive indicator for EC patients who receive CRT (9). In our study, the inflammatory parameters were significantly different between with and without EF groups, and we also found a significant correlation among them. Finally, only the MLR enrolled the predictive model. Additionally, an increased eosinophil count before treatment was found to be a powerful predictor of and reduced the risk of RT-related EF. Previous reports have demonstrated that eosinophils have potent capabilities to impact local immunity and tissue remodeling during homeostasis and disease (29). The protective mechanism of eosinophils in the development of EF requires further research.

To the best of our knowledge, this study is the first to investigate the relationship between PET/CT-based metabolism parameters and the development of RT-related EF. The MTV,

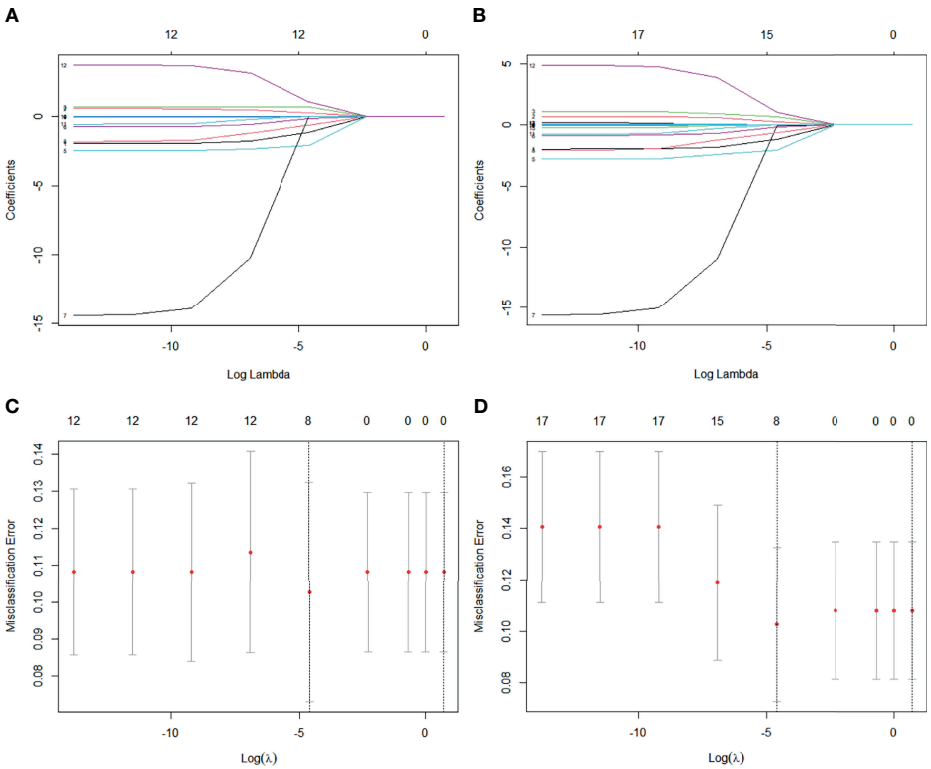

FIGURE 2 | **(A)** LASSO coefficient profiles of 12 clinical features. **(B)** LASSO coefficient profiles of 12 clinical features and five metabolism parameters. **(C)** Tenfold cross-validation for tuning parameter selection in clinical features-based LASSO model. **(D)** Tenfold cross-validation for tuning parameter selection in combined features-based LASSO model.

TABLE 3 | Multivariate analysis for the incidence of esophageal fistula.

Factors	Crude OR (95%CI)	Adj. OR (95%CI)	p (Wald's test)	p (LR-test)
Diabetes	0.1 (0.02, 0.45)	0 (0, 0.14)	0.007	<0.001
Tumor length	1.32 (1.02, 1.72)	4.18 (1.64, 10.66)	0.003	<0.001
Tumor thickness	6.13 (1.82, 20.61)	8.51 (0.81, 89.63)	0.075	0.05
ACT	0.08 (0.01, 0.61)	0 (0, 0.07)	0.004	<0.001
Eosinophil	0 (0, 1.52)	0 (0, 0.02)	0.022	0.003
MLR	13.31 (0.45, 390.03)	3,719.41 (1.68, 8,232,448.12)	0.036	0.021

OR, odds ratio; CI, confidence interval; ACT, adjuvant chemotherapy; MLR, monocyte-to-lymphocyte ratio.

TLG, and HF were different between the with and without EF groups, and there was a significant correlation among them. Only MTV_40% was selected as a risk factor to construct a predictive model after LASSO analysis and was finally screened out by multivariate logistic regression. A reasonable explanation is that MTV_40%, which is the total volume of voxels with a threshold SUV of 40% of the SUV_{max} in the volume of interest, is highly correlated with the size of the tumor. This will reduce the ability of MTV to present the heterogeneity of the tumor. Radiomics is a recent area of research in precision medicine and is based on the extraction of a large variety of features from medical images. PET radiomics may be a promising approach for predicting the development of EF instead of metabolic parameters.

The present study had several limitations. First, this was a retrospective study conducted at a single institution. Second, the sample size was small, and inherent biases were inevitable. Third, external validation of the predictive model should be performed in the future.

5 CONCLUSION

We failed to construct a predictive model for RT-related EF in ESCC patients combined with PET/CT-based metabolism parameters. However, we developed an RS model integrating patient characteristics, tumor and treatment-related factors,

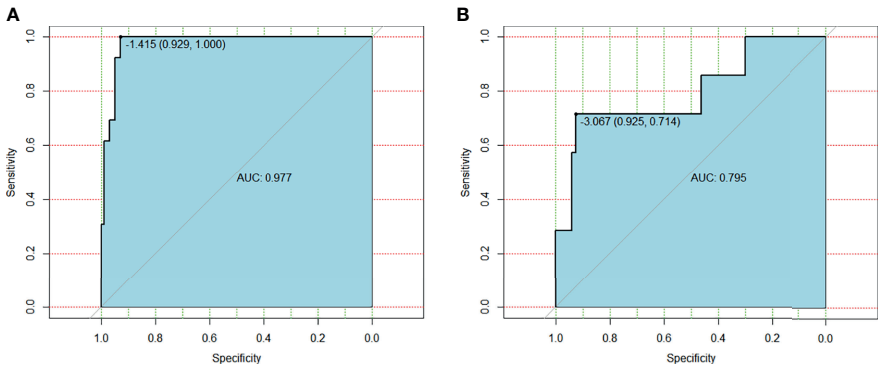

FIGURE 3 | **(A)** ROC curve for clinical features based model on training group. **(B)** ROC curve for clinical features based model on testing group.

and inflammatory parameters. This model might help to discriminate high-risk populations in clinical practice that are susceptible to RT-related EF and individualize treatment plans to prevent it.

DATA AVAILABILITY STATEMENT

The raw data supporting the conclusions of this article will be made available by the authors, without undue reservation.

ETHICS STATEMENT

The studies involving human participants were reviewed and approved by the Ethics Committee of Fujian Medical University Cancer Hospital. Written informed consent for participation was not required for this study in accordance with the national legislation and the institutional requirements.

AUTHOR CONTRIBUTIONS

KL and XN designed the study and wrote the manuscript, recruited patients, collected data, and did statistical analysis. These two authors contributed equally. JL provided idea of this research. DL extracted the PET/CT-based metabolism parameters. All authors contributed to the article and approved the submitted version.

FUNDING

This study was funded by a grant from the Quanzhou City Science & Technology Program of China (2018N049S).

SUPPLEMENTARY MATERIAL

The Supplementary Material for this article can be found online at: https://www.frontiersin.org/articles/10.3389/fonc.2022.812707/full#supplementary-material

REFERENCES

1. Sung H, Ferlay J, Siegel RL, Laversanne M, Soerjomataram I, Jemal A, et al. Global Cancer Statistics 2020: GLOBOCAN Estimates of Incidence and Mortality Worldwide for 36 Cancers in 185 Countries. *CA Cancer J Clin* (2021) 71(3):209–49. doi: 10.3322/caac.21660
2. Cao W, Chen HD, Yu YW, Li N, Chen WQ. Changing Profiles of Cancer Burden Worldwide and in China: A Secondary Analysis of the Global Cancer Statistics 2020. *Chin (Engl)* (2021) 134(7):783–91. doi: 10.1097/CCM9.0000000000001474
3. Arnold M, Soerjomataram I, Ferlay J. Global Incidence of Oesophageal Cancer by Histological Subtype in 2012. *Gut* (2015) 64(3):381–7. doi: 10.1136/gutjnl-2014-308124
4. Ajani JA, D'Amico TA, Bentrem DJ, Chao J, Corvera C, Das P, et al. Esophageal and Esophagogastric Junction Cancers, Version 2.2019, NCCN Clinical Practice Guidelines in Oncology. *J Natl Compr Canc Netw* (2019) 17:855–83. doi: 10.6004/jnccn.2019.0033
5. Zhao JJ, Zhang WC, Zhang HL, Han WM, Wang X, Li C, et al. Clinical Efficacy of Dose Escalation in 3-Dimensional Radiotherapy for Patients With Esophageal Squamous Cell Carcinoma-Multicenter Retrospective Analysis (3JECROG R-03). *Chin J Radiat Oncol* (2020) 29(11):941–7. doi: 10.3760/cma.j.cn113030-20191014-00417
6. Guan X, Liu C, Zhou TS, Ma Z, Zhang C, Wang B, et al. Survival and Prognostic Factors of Patients With Esophageal Fistula in Advanced Esophageal Squamous Cell Carcinoma. *Biosci Rep* (2020) 40:BSR20193379. doi: 10.1042/BSR20193379
7. Pao T-H, Chen Y-Y, Chang W-L, Chang JS, Chiang NJ, Lin CY, et al. Esophageal Fistula After Definitive Concurrent Chemotherapy and Intensity Modulated Radiotherapy for Esophageal Squamous Cell Carcinoma. *PloS One* (2021) 16(5):e0251811. doi: 10.1371/journal.pone.0251811
8. Hu B, Jia F, Zhou HY, Zhou T, Zhao Q, Chen Y, et al. Risk Factors Associated With Esophageal Fistula After Radiotherapy for Esophageal Squamous Cell Carcinoma. *J Cancer* (2020) 11(12):3693–700. doi: 10.7150/jca.39033
9. Han D, Zhang JJ, Zhao JJ, Lei T, Chen X, Zhang T, et al. Platelet-to-Lymphocyte Ratio is an Independent Predictor of Chemoradiotherapy-Related Esophageal Fistula in Esophageal Cancer Patients. *Ann Transl Med* (2020) 8(18):1163. doi: 10.21037/atm-20-4053
10. Watanabea S, Oginoa I, Kunisaki C, Hata M. Relationship Between Nutritional Status and Esophageal Fistula Formation After Radiotherapy for Esophageal Cancer. *Cancer Radiother* (2019) 23:222–7. doi: 10.1016/j.canrad.2018.10.005
11. Xu YY, Wang LL, He B, Li W, Wen Q, Wang S, et al. Development and Validation of a Risk Prediction Model for Radiotherapy-Related Esophageal

Fistula in Esophageal Cancer. *Radiat Oncol* (2019) 14:181. doi: 10.1186/s13014-019-1385-y
12. Zhu C, Wang HP, You YH, Nie K, Jin Y. Risk Factors for Esophageal Fistula in Esophageal Cancer Patients Treated With Radiotherapy: A Systematic Review and Meta-Analysis. *Oncol Res Treat* (2020) 43:34–40. doi: 10.1159/000503754
13. Zhang Y, Li ZJ, Zhang W, Chen W, Song Y. Risk Factors for Esophageal Fistula in Patients With Locally Advanced Esophageal Carcinoma Receiving Chemoradiotherapy. *Onco Targets Ther* (2018) 11:2311–7. doi: 10.2147/OTT.S161803
14. Tsushima T, Mizusawa J, Sudo K, Honma Y, Kato K, Igaki H, et al. Risk Factors for Esophageal Fistula Associated With Chemoradiotherapy for Locally Advanced Unresectable Esophageal Cancer: A Supplementary Analysis of JCOG0303. *Medicine* (2016) 95(20):e3699. doi: 10.1097/MD.0000000000003699
15. Chen HY, Ma XM, Ye M, Hou YL, Xie HY, Bai YR. Esophageal Perforation During or After Conformal Radiotherapy for Esophageal Carcinoma. *J Radiat Res* (2014) 55(5):940–7. doi: 10.1093/jrr/rru031
16. Chen BQ, Deng ML, Yang C, Dragomir MP, Zhao L, Bai K, et al. High Incidence of Esophageal Fistula on Patients With Clinical T4b Esophageal Squamous Cell Carcinoma Who Received Chemoradiotherapy: A Retrospective Analysis. *Radiother Oncol* (2021) 158:191–9. doi: 10.1016/j.radonc.2021.02.031
17. Taniyama TK, Tsuda T, Miyakawa K, Arai H, Doi A, Hirakawa M, et al. Analysis of Fistula Formation of T4 Esophageal Cancer Patients Treated by Chemoradiotherapy. *Esophagus* (2020) 17:67–73. doi: 10.1007/s10388-019-00691-y
18. Kawakami T, Tsushima T, Omae K, Ogawa H, Shirasu H, Kito Y, et al. Risk Factors for Esophageal Fistula in Thoracic Esophageal Squamous Cell Carcinoma Invading Adjacent Organs Treated With Definitive Chemoradiotherapy: A Monocentric Case-Control Study. *BMC Cancer* (2018) 18:573. doi: 10.1186/s12885-018-4486-3
19. Taniguchi H, Yamazaki K, Boku N, Funakoshi T, Hamauchi S, Tsushima T, et al. Risk Factors and Clinical Courses of Chemoradiation-Related Arterio-Esophageal Fistula in Esophageal Cancer Patients With Clinical Invasion of the Aorta. *Int J Clin Oncol* (2011) 16:359–65. doi: 10.1007/s10147-011-0192-8
20. Wu R, Geng LD, Zhao ZH, Liao D, He B, Hu H, et al. Clinical Application of Oral Meglumine Diatrizoate Esophagogram in Screening for Esophageal Fistula During Radiotherapy or Chemoradiotherapy for Esophageal Cancer. *Front Oncol* (2020) 10:562147. doi: 10.3389/fonc.2020.562147
21. Kim HS, Khemasuwan D, Diaz-Mendoza J, Mehta AC. Management of Tracheo-Oesophageal Fistula in Adults. *Eur Respir Rev* (2020) 29:200094. doi: 10.1183/16000617.0094-2020
22. Nakajima Y, Kawada K, Tokairin Y, Miyawaki Y, Okada T, Miyake S, et al. Retrospective Analyses of Esophageal Bypass Surgery for Patients With Esophagorespiratory Fistulas Caused by Esophageal Carcinomas. *World J Surg* (2016) 40(5):1158–64. doi: 10.1007/s00268-015-3391-z
23. Lu J, Sun XD, Yang X, Tang XY, Qin Q, Zhu HC, et al. Impact of PET/CT on Radiation Treatment in Patients With Esophageal Cancer: A Systematic Review. *Crit Rev Oncol Hemato* (2016) 107:128–37. doi: 10.1016/j.critrevonc.2016.08.015
24. Tio TL, Cohen P, Coene PP, Udding J, Den Hartog Jager FCA, Tytgat GNJ. Endosonography and Computed Tomography of Esophageal Carcinoma: Preoperative Classification Compared to the New (1987) TNM System. *Gastroenterology* (1989) 96(6):1478–86. doi: 10.1016/0016-5085(89)90515-5
25. Picus D, Balfe DM, Koehler RE, Roper CL, Owen JW. Computed Tomography in the Staging of Esophageal Carcinoma. *Radiology* (1983) 146(2):433–8. doi: 10.1148/radiology.146.2.6849089
26. Japan Esophageal Society. Japanese Classification of Esophageal Cancer, 11th Edition: Part I. *Esophagus* (2017) 14(1):1–36. doi: 10.1007/s10388-016-0551-7
27. Wang L, Wang C, Wang J, Huang X, Cheng Y. A Novel Systemic Immune-Inflammation Index Predicts Survival and Quality of Life of Patients After Curative Resection for Esophageal Squamous Cell Carcinoma. *J Cancer Res Clin Oncol* (2017) 143(10):2077–86. doi: 10.1007/s00432-017-2451-1
28. Grisaru-Tal S, Itan M, Klion AD, Munitz A. A New Dawn for Eosinophils in the Tumour Microenvironment. *Nat Rev Cancer* (2020) 20(10):594–607. doi: 10.1038/s41568-020-0283-9
29. Bütof R, Hofheinz F, Zöphel K, Stadelmann T, Schmollack J, Jentsch C, et al. Prognostic Value of Pretherapeutic Tumor-to-Blood Standardized Uptake Ratio in Patients With Esophageal Carcinoma. *J Nucl Med* (2015) 56:1150–6. doi: 10.2967/jnumed.115.155309
30. Kim SJ, Pak K, Chang S. Determination of Regional Lymph Node Status Using (18)F-FDG PET/CT Parameters in Oesophageal Cancer Patients: Comparison of SUV, Volumetric Parameters and Intratumoral Heterogeneity. *Br J Radiol* (2016) 89(1058):20150673. doi: 10.1259/bjr.20150673
31. Weaver ML, Black JH. Aortobronchial and Aortoentericfistula. *Semin Vasc Surg* (2017) 30:85–90. doi: 10.1053/j.semvascsurg.2017.10.005
32. Herold DM, Hanlon AL, Hanks GE. Diabetes Mellitus: A Predictor for Late Radiation Morbidity. *Int J Radiat Oncol Biol Phys* (1999) 43(3):475–9. doi: 10.1016/s0360-3016(98)00460-x
33. Kalman NS, Hugo GD, Mahon RN, Deng X, Mukhopadhyay ND, Weiss E. Diabetes Mellitus and Radiation Induced Lung Injury After Thoracic Stereotactic Body Radiotherapy. *Radiother Oncol* (2018) 129(2):270–6. doi: 10.1016/j.radonc.2018.08.024

Conflict of Interest: The authors declare that the research was conducted in the absence of any commercial or financial relationships that could be construed as a potential conflict of interest.

frontiers in Oncology

ORIGINAL RESEARCH
published: 24 March 2022
doi: 10.3389/fonc.2022.856402

Dosimetric Evaluation and Clinical Application of Radioactive Iodine-125 Brachytherapy Stent in the Treatment of Malignant Esophageal Obstruction

Zhe Ji[1], Qianqian Yuan[2], Lei Lin[1], Chao Xing[2], Xusheng Zhang[2], Sen Yang[2], Yuliang Jiang[1], Haitao Sun[1], Kaixian Zhang[2] and Junjie Wang[1]**

[1] Department of Radiation Oncology, Peking University Third Hospital, Beijing, China, [2] Department of Oncology, Tengzhou Central People's Hospital, Zaozhuang, China

OPEN ACCESS

Edited by:
Li Jiancheng,
Fujian Provincial Cancer Hospital, China

Reviewed by:
Konstantinos A. Mountris, University College London, United Kingdom
Xiaokun Hu, The Affiliated Hospital of Qingdao University, China
Mahdi Sadeghi, Iran University of Medical Sciences, Iran

***Correspondence:**
Kaixian Zhang
tengzhouzkx@126.com
Junjie Wang
junjiewang_edu@sina.cn

Specialty section:
This article was submitted to Radiation Oncology, a section of the journal Frontiers in Oncology

Received: *17 January 2022*
Accepted: *28 February 2022*
Published: *24 March 2022*

Citation:
Ji Z, Yuan Q, Lin L, Xing C, Zhang X, Yang S, Jiang Y, Sun H, Zhang K and Wang J (2022) Dosimetric Evaluation and Clinical Application of Radioactive Iodine-125 Brachytherapy Stent in the Treatment of Malignant Esophageal Obstruction. Front. Oncol. 12:856402. doi: 10.3389/fonc.2022.856402

Objective: To evaluate the dosimetric characteristics and the clinical application of radioactive iodine-125 brachytherapy stent (RIBS) in malignant esophageal obstruction.

Methods: The dose distribution of RIBS with different seed spacing, diameter and length was studied by treatment planning system (TPS) calculation, thermoluminescence dosimeter (TLD) measurement and Monte Carlo (MC) data fitting. And the data of esophageal cancer patients who were treat with this type of RIBS was analyzed retrospectively.

Results: Doses around the RIBS calculated by the TPS lay between those measured by the TLDs and those simulated by the MC, and the differences between the three methods were significant ($p<0.05$), the overall absolute dose differences among the three methods were small. Dose coverage at 1.5 cm from the center was comprehensive when the activity reached 0.6 mCi. Both the conformability and the uniformity of isodose lines produced by a seed spacing of 1.0 cm were superior to those produced by a seed spacing of 1.5 cm. The data of 50 patients treated with RIBS was analyzed. They were followed up until February 2020 when all of the patients died. The overall improvement rate of dysphagia after RIBS implant was 90%. Moderate and severe complications with an incidence of more than 10% were hematemesis (28%), pain (20%), and lung infection (10%). Stent restenosis occurred in 4 patients at a median interval of 108 days from the procedure. The overall incidence of fatal complications was 38% (including hematemesis, infection and asphyxia). The median survival time of patients with and without a history of radiotherapy were 3.4 months and 6 months, respectively, the difference of which was significant ($p=0.021$). No other factors affecting survival were identified. For patients with and without a history of radiotherapy, the incidences of fatal complications were 51.7% and 19%, respectively ($p=0.019$). No correlation between dose and stent restenosis was found.

Conclusion: TPS calculations are suitable for clinical applications. RIBS can effectively alleviate obstructive symptoms for patients with malignant esophageal obstruction, but the incidence of fatal complications was high, care should be taken when choosing this treatment.

Keywords: radioactive iodine-125 seed, stent, esophageal cancer, dosimetry, efficacy

INTRODUCTION

Esophageal cancer is common and accounts for 572,000 new cases and 505,000 deaths each year, ranking the 9th most common type and the 6th leading cause of death among all cancers (1). While esophageal cancer is managed mainly by surgery and chemoradiotherapy (2), it is often more important to manage the problem of obstruction among patients with severe dysphagia. However, not only it is difficult for these patients to tolerate surgery or chemoradiotherapy due to unfavorable factors, such as advanced age, poor general condition, low body mass index, and severe comorbidities, but symptoms of obstruction also cannot be rapidly alleviated because of the delayed response of tumor for chemoradiotherapy.

The application of metal stents in the treatment of malignant esophageal obstruction was first reported by Frimberger (3) in 1983. Owing to its accurate positioning and simple operation, this technique can quickly and effectively relieve symptoms of dysphagia as well as improve patients' nutritional status and quality of life, making it a standard method in treating malignant esophageal obstruction (4).

As conventional esophageal stents expand the esophagus simply by mechanical forces, they demonstrate no therapeutic effect on tumors that have caused the stenosis. In addition, due to growth of the tumor or proliferation of the granulation tissue, approximately 30–40% patients experience restenosis after stent implant (5), compromising the long-term efficacy of the stent. This issue has been resolved with the use of radioactive iodine-125 brachytherapy stent (RIBS), which can expand the esophagus while simultaneously performing brachytherapy on the tumor, thereby achieving the dual purpose of relieving dysphagia as well as eliminating cancer (6, 7). A recent randomized study showed that RIBS can prolong patient survival more effectively than conventional stents (8).

At present, there are few studies on the dosimetry of RIBS. In addition, existing studies are inconsistent regarding methods on the bundling methods and the quantity of seeds and provided little information on the prescription dose. The purpose of this study was to evaluate the dosimetric characteristics and the clinical application of RIBS in treating malignant esophageal obstruction, thereby providing references for its clinical implementation.

MATERIALS AND METHODS

RIBS Dosimetric Study

Materials

Several materials were used in this study, including a covered self-expanding esophageal stent (Micro-Tech (Nanjing) Co., Ltd., Jiangsu Province, China), and iodine-125 (I-125) seeds, type 6711_1985, with an outer diameter of 0.8 ± 0.02 mm and a length of 4.5 ± 0.2 mm (Atomic High Technology Co., Ltd., Beijing, China). The seed had an outer shell of titanium, a half-life of 59.4 days, a dose-rate constant of 0.965 cGy/(h·U), and various activities of 0.5, 0.6, 0.7, 0.8, 0.9, and 1.0 mCi. The following materials were also used: Allura Xper FD20 (Philips, Amsterdam, Netherlands), a digital subtraction angiography (DSA) system; OLYMPUS GIF-H290 (Olympus Co., Ltd., Tokyo, Japan), a gastroscope; paraffin as an analytical purity (Tianjin Basifu Chemical Co., Ltd., Tianjin, China); Brilliant Big Bore (Philips, MA, USA), a CT simulator; and a treatment planning system (TPS) (Beijing Feitianzhaoye Technology Co., Ltd., Beijing, China). Dose calculations at different distances to the radioactive source in the TPS were based on the American Association of Physicists in Medicine (AAPM) TG43 report and its updated documents (9, 10) and on thermoluminescence dosimeters (TLDs) (Beijing Institute of Chemical Defense, Beijing, China). These dosimeters were made of TLD-200 (LiF: Mg, Cu, P) square chips (3.2 cm × 3.2 cm) with a measurement range of 10 μGy to 10 Gy and a detection limit of 0.1 μGy, and a TLD reader, Harshaw 3500 (Thermo Fisher Scientific, MA, USA).

Methods

Preparation of Different Specifications of RIBS (4 Specifications)

Specification 1: length = 8.0 cm, diameter = 2.0 cm, and seed spacing = 1.0 cm; Specification 2: length = 8.0 cm, diameter = 2.0 cm, and seed spacing = 1.5 cm; Specification 3: length = 8.0 cm, diameter = 1.3 cm, and seed spacing = 1.0 cm; Specification 4: length = 12.0 cm, diameter = 2.0 cm, and seed spacing = 1.0 cm. The delivery sheath was made of polyurethane (synthesized from polytetrahydrofuran ether glycol, 4,4'-diphenylmethane diisocyanate, and 1,4-butanediol; density = 1.19 g/cm3). The RIBS was subsequently created by bundling a conventional stent with the delivery sheath containing radioactive I-125 seeds (**Figures 1A, B**).

TPS Calculations

The RIBS was vertically fixed in a cylindrical Perspex phantom (thickness = 0.8 cm, diameter = 20 cm, and height = 20 cm) filled with solid paraffin melt. Once the paraffin was cooled and solidified, the phantom was scanned using computed tomography (CT) (window width = 300 HU, window level = 15 HU, and slice thickness = 5 mm) (**Figures 1C, D**), and images were exported to the TPS. Subsequently, with the center of the stent as the origin, cumulative doses at a distance of 1.5 cm, 2.0 cm, 2.5 cm, 3.0 cm, 3.5 cm, 4.0 cm, and 5.0 cm from the origin were calculated at both 0° and 90°, the average of which was computed as the result.

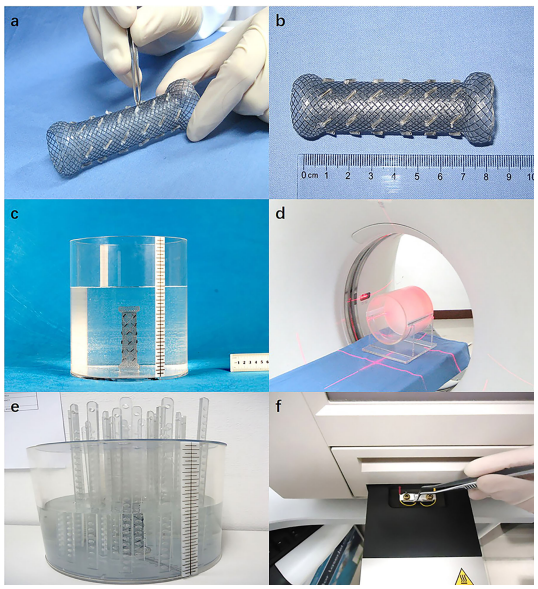

FIGURE 1 | **(A)** The periphery of the stent was bundled with a polyurethane catheter as the delivery sheath, which contains radioactive I-125 seeds; **(B)** The complete RIBS; **(C)** The RIBS was fixed in a cylindrical phantom filled with paraffin melt; **(D)** CT scan (images were exported to the TPS); **(E)** After the RIBS was fixed to the center of the cylindrical phantom and filled with distilled water, the TLD measuring rods were placed at different distances to the center of the stent; **(F)** TLD were read out 24 h after irradiation.

TLD Measurements

The RIBS was fixed in the center of the cylindrical Perspex phantom and was filled with distilled water. Subsequently, with the center of the stent as the origin, TLD measuring rods were placed at 1.5 cm, 2.0 cm, 2.5 cm, 3.0 cm, 3.5 cm, 4.0 cm, and 5.0 cm from the origin. After being irradiated for 24 h, TLDs were removed from the phantom and read out in the TLD reader (**Figures 1E, F**), with the average value at 0° and 90° calculated as the result.

Monte Carlo (MC) Simulation

An actual geometry source model was established using the MC N-Particle Transport Code (MCNP) based on the radioactive I-125 seed model (6711), so as to calculate the dose distribution of the radioactive stent in a calculation range of 1 keV to 100 keV (9, 11). In the simulations, photo-electric effect, compton scattering, rayleigh scattering and pair production were considered for photons. The energy cut-off value for photons was set to the minimum value 0.25 keV. Secondary electrons were not tracked assuming that all of their energy is deposited at the location of their generation. The number of events in each simulation was set as 1x10^8 to achieve an average statistical uncertainty less than 1%. To validate the accuracy of seed modeling and MC simulation, the dose distribution of single I-125 seed was simulated and the radial dose and anisotropy functions were calculated and compared with reference data (12, 13). The radial dose function g(r) from 0.5 to 100 mm and the 2D anisotropy functions at 5, 10, 15 and 20 mm for the polar angle $0° \leq \theta \leq 90°$ were extracted from the calculated dose distribution and found in good agreement with the relative differences being less than 2.0%. This confirms that the seed model and the MC simulation of this study are valid. The model was first placed in the center of a sphere with a radius of 10 cm and water as a medium. Subsequently, with the center of the stent as the origin, doses at a distance of 1.5 cm, 2.0 cm, 2.5 cm, 3.0 cm, 3.5 cm, 4.0 cm, and 5.0 cm from the origin were calculated at both 0° and 90°, the average of which was computed as the result.

Clinical Outcomes of RIBS in the Treatment of Esophageal Cancer

Patient Information

We retrospectively analyzed the data of patients with malignant esophageal obstruction treated with this type of RIBS from July 2014 to November 2019. The criteria of RIBS treatment were: ① Patient's age ≥ 18 years; ② Diagnosis of esophageal cancer was pathologically confirmed; ③ Patient experienced Grade 3–4 dysphagia according to the criteria proposed by the Cardiovascular and Interventional Radiological Society of Europe (CIRSE) (14), which stated that Grade 0 = normal diet, Grade 1 = soft food only, Grade 2 = semi-solids only, Grade 3 = liquids only, and Grade 4 = complete dysphagia; ④ Patient could not tolerate surgery or chemoradiotherapy due to extensive tumor growth, metastasis, or poor medical conditions; ⑤ Patient demonstrated clear consciousness as well as good compliance and was cooperative with treatment; and ⑥ Patient had a Karnofsky Performance Score (KPS) ≥ 60 and could tolerate treatment. The exclusion criteria were: ① The upper boundary of the lesion exceeded the seventh cervical vertebra; ② Patient had ulcerative esophageal cancer or esophageal fistula; ③ Patient suffered from Class II or higher bone marrow suppression and/or coagulation dysfunction; and ④ Patient had other contradictions such as severe cardiopulmonary insufficiency and liver and kidney insufficiency.

Treatment Methods

Preoperative Planning

Prior to the implant, a 5 mm enhanced CT scan of the lesion in all areas was acquired, and CT images were exported to the TPS to contour the esophageal lesions. Subsequently, a preoperative plan was created with various seed activities ranging between 0.4 and 0.8 mCi and prescriptions ranging between 60 and 80 Gy. Seeds were ordered once the total number and the activity were determined.

Production of the I-125 Seed Stent

A covered esophageal stent with a diameter of 1.8 cm or 2.0 cm was selected according to the length and stenosis of the patient's esophageal lesions. Each layer of the stent was bundled with 5–6 seeds, and the layers were separated by 1.0 cm. Seed spacing was set according to the preoperative plan to ensure that the prescription was fulfilled. Once radioactive seeds were fixed on the periphery of the stent, the internal stent was inserted into the stent pusher catheter.

Stent Implant

The patient was placed in the lateral position, anesthetized at the oropharynx with lidocaine spray, and a bite block was placed in the mouth. Subsequently, after a radiographic guide wire and a catheter were inserted through the oral cavity, contrast agents were injected in the upper and lower ends of the lesion to display the extent and the degree of stenosis. The imaging guide wire was then replaced with a super-hard and super-long guide wire, while the catheter was removed. Next, a covered stent of the right size was selected according to the extent of the lesion and implanted together with the pusher along the super-hard wire. Once its position was verified using proximal positioning, the stent was released. It was required that the upper and lower ends of the inserted stent should exceed the lesion by at least 20 mm.

Postoperative Plan Verification

At 48–72 hours after stent implantation, a 5 mm CT scan was acquired for review. After images were sent to the TPS, the esophageal lesion was contoured, and seeds were identified in the system to calculate the actual dose delivered to the tumor target (D90; i.e., the dose received by 90% of the target volume).

Outcome Indicators

Primary outcome indicators of this study included relief of patients' clinical symptoms and relevant complications. Complications were graded according to Common Terminology Criteria for Adverse Events (CTCAE) version 5.0 (15), there were five grades, as follows: mild/grade 1 (no symptoms and no treatment required), moderate/grade 2 (symptoms present and treatment required), severe/grade 3 (symptoms not controlled by drugs, and instrumentation or invasive procedure required), life-threatening/grade 4 (emergency treatment required), and death/grade 5. Secondary outcome indicators included patients' survival. Factors influencing patients' complications and survival were also investigated.

Statistical Analysis

Data analysis was performed using the SPSS 20 statistical software (IBM, Armonk, New York, USA). Measurement data were expressed as mean ± standard deviation ($\bar{X}$ ± s), while count data were expressed as absolute value and percentage (rate). Comparisons of means and rates were conducted *via* the t-test and the chi-square test, respectively. Patient's survival was calculated using the Kaplan-Meier method. Univariate analysis was performed using the log-rank test. The hazard ratio was derived *via* Cox regression. $P < 0.05$ was considered statistically significant.

RESULTS

Dosimetric Results

TPS Method

The dose around the RIBS dropped rapidly with increasing distance from the origin. According to the TPS, for stents of various specifications, the average doses (Gy) at seven different locations from the origin (1.5 cm, 2.0 cm, 2.5 cm, 3.0 cm, 3.5 cm, 4.0 cm, and 5.0 cm) were 112.3 ± 31.50, 68.0 ± 20.71, 42.5 ± 16.28, 26.8 ± 9.95, 18.4 ± 7.18, 12.7 ± 5.76, and 7.8 ± 4.95, respectively, the differences of which were statistically significant ($P < 0.001$).

It was also noted that the dose increased linearly with increasing seed activity. For the six seed activities (0.5 mCi, 0.6 mCi, 0.7 mCi, 0.8 mCi, 0.9 mCi, and 1.0 mCi) investigated in the study, the average doses (Gy) at different locations from the origin were 26.4 ± 24.99, 32.3 ± 30.01, 38.6 ± 35.81, 45.4 ± 41.69, 50.9 ± 46.06, and 57.8 ± 50.67, respectively, differences of which were statistically significant ($P < 0.001$). The average doses (Gy) at 1.5 cm from the origin were 76.8 ± 14.55, 93.0 ± 18.55, 109.5 ± 22.41, 126.8 ± 28.29, 141.3 ± 27.39, and 155.8 ± 30.23, respectively, for the different seed activities. The dose coverage at 1.5 cm from the origin was comprehensive when the seed activity reached 0.6 mCi.

In addition, it was suggested that both seed spacing and stent length demonstrated significant effects on the dosimetry. The dose of the RIBS with a seed spacing of 1.5 cm was lower than that of the RIBS with a seed spacing of 1.0 cm. For the four different specifications of RIBS (Specification 1, Specification 2, Specification 3, and Specification 4), the average doses (Gy) at different locations from the origin were 30.6 ± 28.63, 41.0 ± 41.55, 43.6 ± 40.31, and 52.3 ± 46.22, respectively, the differences of which were statistically significant ($P < 0.001$). In addition, for the RIBS with a seed spacing of 1.0 cm, it was found that both the conformability and the uniformity of its isodose lines were superior to those of the RIBS with the seed spacing of 1.5 cm, whereas the latter showed several dosimetric "cold spots" on the plan (**Figure 2**).

TLD Method

The trends of TLD measurements were consistent with that of the TPS calculations. According to TLD measurements, for stents of various specifications, the average doses at seven different locations from the origin (1.5 cm, 2.0 cm, 2.5 cm, 3.0 cm, 3.5 cm, 4.0 cm, and 5.0 cm) were 114.0 ± 34.57, 64.8 ± 21.69, 39.9 ± 16.63, 25.0 ± 10.07, 17.1 ± 7.37, 12.0 ± 6.09, and 7.2 ± 4.79, respectively, the differences of which were statistically significant ($P < 0.001$). In addition, although the dose at 1.5 cm measured by the TLD was not significantly different to that calculated by the TPS ($t = -0.807$, $P = 0.428$), at all other locations, TLD measurements were significantly lower than TPS calculations ($t = 5.588$, 4.881, 4.051, 3.358, 3.205, and 3.245, respectively, and $P < 0.001$, < 0.001, < 0.001, $= 0.003$, $= 0.004$ and $= 0.004$, respectively) (**Figure 3A**).

For the 6 seed activities (0.5 mCi, 0.6 mCi, 0.7 mCi, 0.8 mCi 0.9 mCi, and 1.0 mCi), the average doses (Gy) at different locations from the origin were 24.7 ± 24.38, 30.3 ± 29.48, 36.5 ± 34.97, 44.0 ± 41.26, 48.6 ± 45.60, and 55.8 ± 49.06, respectively, the differences of which were statistically significant ($P < 0.001$) (**Figure 3B**). Alternatively, the average doses (Gy) at 1.5 cm from the origin were 74.5 ± 17.16, 89.8 ± 20.60, 106.3 ± 23.67, 125.8 ± 24.10, 138.8 ± 28.91, and 149.3 ± 29.41, respectively. Similarly, TLD measurements were consistently lower than TPS calculations, and the differences were statistically significant ($t = 3.802$, 4.615, 6.914, 3.300, 5.243, and 2.640, respectively,

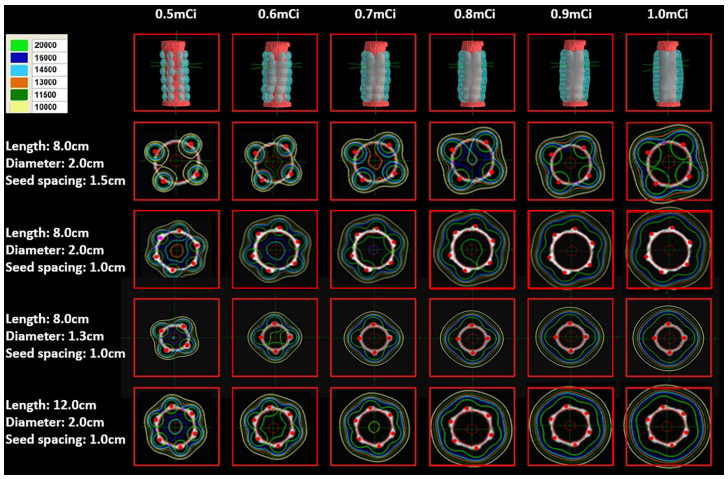

FIGURE 2 | The higher the seed activity, the higher the dose. Both the conformability and the uniformity of the isodose lines produced by a seed spacing of 1.0 cm were superior to those produced by a seed spacing of 1.5 cm, the latter also showed a few dosimetric "cold spots". The dose coverage was good with seed spacing of 1.0 cm and seed activity ≥ 0.6 mCi.

and P = 0.001, < 0.001, < 0.001, = 0.003, < 0.001, and = 0.014, respectively).

For the four different specifications of RIBS (Specification 1, Specification 2, Specification 3, and Specification 4), the average doses (Gy) at different locations from the origin were 28.2 ± 27.88, 39.1 ± 40.42, 41.8 ± 39.36, and 50.8 ± 45.62, respectively, the differences of which were statistically significant (P < 0.001). Again, all TLD measurements were significantly lower than the TPS calculations (t = 5.835, 4.782, 4.106, and 4.836, respectively, and P < 0.001).

MC Method

The trends of MC simulations were consistent with that of the TLD measurements and TPS calculations. For stents of various specifications, the average doses (Gy) at seven different locations from the origin (1.5 cm, 2.0 cm, 2.5 cm, 3.0 cm, 3.5 cm, 4.0 cm, and 5.0 cm) were 119.5 ± 35.04, 69.9 ± 20.18, 43.9 ± 16.32, 28.3 ± 10.39, 19.6 ± 6.95, 13.4 ± 5.90, and 8.0 ± 5.24, respectively, the differences of which were statistically significant (P < 0.001). Although the dose at 5.0 cm simulated by MC was not considerably different from that calculated by the TPS

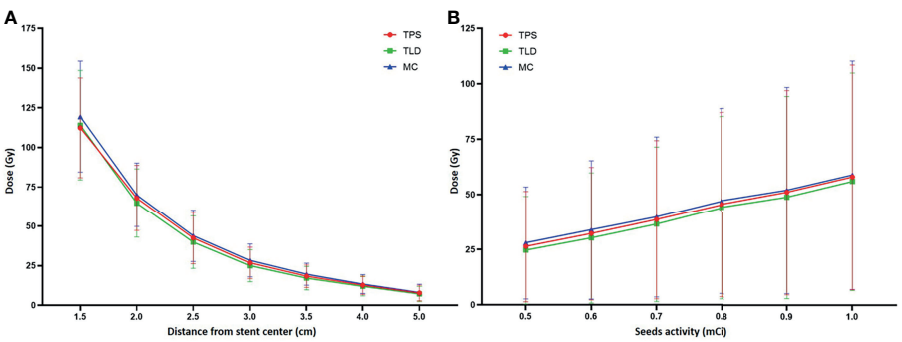

Distance from stent center	Dose (Gy) ($\bar{X}\pm s$)			P value		
	TPS	TLD	MC	TLD vs TPS	MC vs TPS	MC vs TLD
1.5cm	112.3±31.50	114.0±34.57	118.5±35.04	0.428	0.001	<0.001
2cm	68.0±20.71	64.8±21.69	68.9±20.18	<0.001	0.003	<0.001
2.5cm	42.5±16.28	39.9±16.63	43.9±16.32	<0.001	<0.001	<0.001
3cm	26.8±9.95	25.0±10.07	28.3±10.39	<0.001	0.001	<0.001
3.5cm	18.4±7.18	17.1±7.37	19.6±6.95	0.003	0.008	<0.001
4cm	12.7±5.76	12.0±6.09	13.4±5.90	0.004	<0.001	<0.001
5cm	7.8±4.95	7.2±4.79	8.0±5.24	0.004	0.07	<0.001

Seeds activity	Dose (Gy) ($\bar{X}\pm s$)			P value		
	TPS	TLD	MC	TLD vs TPS	MC vs TPS	MC vs TLD
0.5mCi	26.4±24.99	24.7±24.38	28.1±25.33	0.001	<0.001	<0.001
0.6mCi	32.3±30.01	30.3±29.48	34.0±31.34	<0.001	0.001	<0.001
0.7mCi	38.6±35.81	36.5±34.97	39.8±36.24	<0.001	<0.001	<0.001
0.8mCi	45.4±41.69	44.0±41.26	47.0±41.85	0.003	<0.001	<0.001
0.9mCi	50.9±46.06	48.6±45.60	51.8±46.50	<0.001	0.016	<0.001
1.0mCi	57.8±50.67	55.8±49.06	58.7±51.56	0.014	0.035	<0.001

FIGURE 3 | **(A)** Although the dose at 1.5 cm measured by the TLD was not significantly different from that calculated by the TPS, at all other locations, the TLD measurements were significantly lower. Alternatively, while the dose at 5.0 cm simulated by MC was not significantly different to that calculated by the TPS, all of the other MC simulation results were significantly higher. When compared to the TLD measurements, MC simulations were consistently higher with significant differences. **(B)** Dose increased linearly with increasing activity. Doses from the MC simulations were the highest, followed by TPS calculations and TLD measurements, and the differences between the three methods were significant.

(t = −1.904, P = 0.07), at all other locations, MC simulation results were significantly higher (t = −3.686, −3.347, −4.303, −3.800, −2.930, and −4.303, respectively, and P = 0.001, = 0.003, < 0.001, = 0.001, = 0.008, and < 0.001, respectively). When compared to the TLD measurements, the MC simulations were consistently higher with significant differences (t = −8.150, −6.970, −5.901, −5.584, −4.532, −5.274, and −3.984, respectively, and P < 0.001) (**Figure 3A**).

For the six seed activities (0.5 mCi, 0.6 mCi, 0.7 mCi, 0.8 mCi, 0.9 mCi, and 1.0 mCi), the average doses (Gy) at different locations from the origin were 28.1 ± 25.35, 34.0 ± 31.34, 39.8 ± 36.24, 47.0 ± 41.85, 51.8 ± 46.50, and 58.7 ± 51.56, respectively, the differences of which were statistically significant (P < 0.001) (**Figure 3B**). Alternatively, the average doses (Gy) at 1.5 cm from the origin were 78.8 ± 14.80, 96.3 ± 18.87, 111.5 ± 22.41, 129.0 ± 26.60, 142.8 ± 28.02, and 158.5 ± 30.88, respectively. The MC simulation results were consistently higher than the TPS calculations and TLD measurements, and for both comparisons, differences were statistically significant (versus TPS: t = −5.383, −3.684, −4.322, −5.717, −2.564, and −2.223, respectively, and P < 0.001, = 0.001, < 0.001, < 0.001, = 0.016, and = 0.035, respectively; versus TLD: t = −5.953, −5.653, −6.805, −6.274, −5.412, and −3.623, respectively, and P < 0.001).

For the four different specifications of RIBS (Specification 1, Specification 2, Specification 3, and Specification 4), the average doses (Gy) at different locations from the origin were 31.5 ± 29.26, 42.9 ± 41.37, 45.10 ± 41.12, and 53.5 ± 46.91, respectively, the differences of which were statistically significant (P < 0.001). All of the MC simulation results were significantly higher than TPS calculations (t = −3.315, −6.517, −4.175, and −4.577, respectively, and P = 0.002, < 0.001, < 0.001, and < 0.001, respectively). Similarly, MC simulation results were consistently higher than TLD measurements with significant differences (t = −6.779, −8.235, −5.301, and −7.213, respectively, and P < 0.001). However, the absolute dose difference between the two groups was less than 5 Gy. While the dose deviations in the high-dose area (1.5 and 2 cm from the origin) were 3.7% and 5.9%, respectively, the maximum deviation was 11.7% at 3 cm from the origin.

Clinical Results

Patient Information

A total of 50 patients were included in this study. Patients included were either ineligible or unwilling to receive radiotherapy, while stents were urgently needed to relieve their symptoms. Detailed patient information is listed in **Table 1**.

RIBS Implant

The RIBS implants were successful in the first attempt for all patients. The average operation time was approximately 15 min. Information on RIBS and related doses is listed in **Table 2**. After the implantation, patients were administered with 250 ml of hot milk to help expand the stent.

Obstruction Relief

Dysphagia was significantly improved in 90% of patients (45/50) after RIBS implant. For the 33 patients who could only eat a full-liquid diet before the procedure, 15 cases could eat soft foods, 13 cases could eat semi-liquid foods, and five remained on a liquid diet after the procedure, indicating an overall improvement rate of 85%. Alternatively, for the 17 patients with complete dysphagia before the procedure, 6 cases could eat soft foods, 9

TABLE 1 | Patients' baseline status before treatment.

General information	N (50 cases)	%
Gender		
Male	33	66.0
Female	17	34.0
Age (years old)	mean 71 (range, 52-88)	
KPS	median 70 (60-90)	
Initial stage		
III	17	34.0
IV	33	66.0
Location of lesions		
Upper-thoracic	12	24.0
Middle-thoracic	27	54.0
Lower-thoracic	7	14.0
Anastomosis	4	8.0
Disease type		
Initial treatment	19	38.0
Recurrence after treatment	24	48.0
Progress after treatment	7	14.0
History of radiotherapy		
No	21	42.0
Yes	29	58.0
Degree of obstruction		
Liquid diet	33	66.0
Complete obstruction	17	34.0
Albumin before treatment (g/L)	mean 35.1 (24.4-42.9)	
Hemoglobin before treatment (g/L)	mean 120.6 (87-201)	

cases could eat semi-solids, and 2 cases could eat liquids after the operation, indicating an overall improvement rate of 100%.

Complications

The incidences of pain, foreign body sensation, cough, nausea and vomiting, asphyxia, hematemesis, perforation, stent displacement, restenosis, and fever/pneumonia were 80%, 14%, 28%, 8%, 6%, 28%, 6%, 4%, 8%, and 6%, respectively. Stent restenosis occurred in four patients at a median interval of 108 days (31–196 days) from the procedure. No incidence of seed loss was observed. Details of the complications are shown in **Table 3**. Out of all of the patients, 3 cases suffered from asphyxia, all of which were fatal; 14 cases from hematemesis, 11 of which were fatal; 3 cases from perforation, all of which were fatal (2 cases due to hematemesis and 1 case due to lung infection); and 8 cases from fever or lung infection, 5 of which were fatal (with 1 case accompanied by perforation). Therefore, the overall incidence of fatal complications was 38% (19/50). Moderate and severe complications with an incidence of more than 10% were hematemesis (28%), pain (20%), and lung infection (10%).

Prognosis and Influencing Factors

Patients were followed up until February 2020 when all 50 patients died. The median survival was 4.4 months (95% CI: 3.4–5.4 months), and the 6-month, 12-month, and 18-month survival rates were 34%, 12%, and 2%, respectively (**Figure 4A**). A total of 6 patients survived for over 12 months, the longest of whom lived another 19.3 months after the procedure. Causes of death are listed in **Table 4**. The median survival periods of new and relapsed/uncontrolled patients were 5 months (95% CI: 2.9–9.1 months) and 3.9 months (95% CI: 2.8–4.9 months), respectively. The 18-month survival rates of the two groups were 5.3% and 3.2%, respectively, the difference of which was insignificant (P = 0.163). Alternatively, for patients with and without a previous history of radiotherapy, the median survival periods were 3.4 months (95% CIL 2.1–4.7 months) and 6 months (95% CI: 2.8–9.3 months), respectively. The 18-month survival rates of the two groups were 0% and 4.8%, respectively, which were significantly different (P = 0.021) (**Figure 4B**). Specific factors affecting patients' survival are shown in **Figure 5**.

The incidences of fatal complications in new and relapsed/uncontrolled patients were 21.1% (4/19) and 48.4% (15/31), respectively, the difference of which was close to statistical significance (chi-squared = 3.736, P = 0.053). Alternatively, for patients with and without a previous history of radiotherapy, the incidences of fatal complications were 51.7% (15/29) and 19% (4/21), respectively, the difference of which was significant (chi-squared = 5.520, P = 0.019). More specifically, for patients whose interval between radiotherapy and stent implant was < 6 months or ≥ 6 months, the incidences of upper gastrointestinal bleeding were 62.5% (5/8) and 14.3% (8/29), respectively, the difference of which was significant (chi-squared = 6.741, P = 0.019).

No correlation was found between dose and survival. For patients whose D90 < 60 Gy or ≥ 60 Gy, the median survival periods were 4.3 months (95% CI: 3.6–5.0 months) and 4.6 months (95% CI: 3.0–6.1 months), respectively, while the 18-month survival rates were 3.7% and 0%, respectively, the difference of which was insignificant (P = 0.524) (**Figure 5**). Alternatively, the incidences of fatal complications of patients whose D90 ≤ 50Gy or > 50 Gy were 18.8% (3/16) and 47.1% (16/34), respectively, the difference of which was close to statistical significance (chi-squared = 3.701, P = 0.054). Similarly, no correlation between dose and stent restenosis was found. However, all stent restenosis occurred in patients receiving ≤ 66 Gy. The incidences of stent restenosis of patients receiving ≤ 66 Gy or > 66 Gy were 14.3% (5/35) and 0% (0/15), respectively (chi-squared = 2.381, P = 0.123).

TABLE 2 | RIBS parameters.

Parameters	Median (range)
Length of stent (cm)	10 (6-12)
Diameter of stent (cm)	2 (1.8-2)
Seed spacing (cm)	1
Number of seeds per layer	6 (5-6)
Number of layers of seeds	5 (2-8)
Seeds activity (mCi)	0.6 (0.4-0.8)
Postoperative D90 (Gy)	56.7 (18.9-113.3)

TABLE 3 | Patients' complications.

Complications	N	%
Pain		
No	10	20
Mild	30	60
Moderate	7	14
Severe	3	6
Foreign body feeling		
None	43	86
Mild	6	12
Moderate	1	2
Cough		
None	36	72
Mild	11	22
Moderate	2	4
Severe	1	2
Nausea and vomiting		
None	46	92
Mild	1	2
Moderate	3	6
Asphyxia		
None	47	94
Death	3	6
Haematemesis		
None	36	72
Moderate	3	6
Death (with 2 cases of perforation)	11	22
Perforation		
None	47	94
Death	3	6
Stent displacement		
No	48	96
Yes	2	4
Restenosis		
No	46	92
Yes	4	8
Fever/pulmonary infection		
None	42	84
Mild/Moderate	3	6
Death (with 1 case of perforation)	5	10

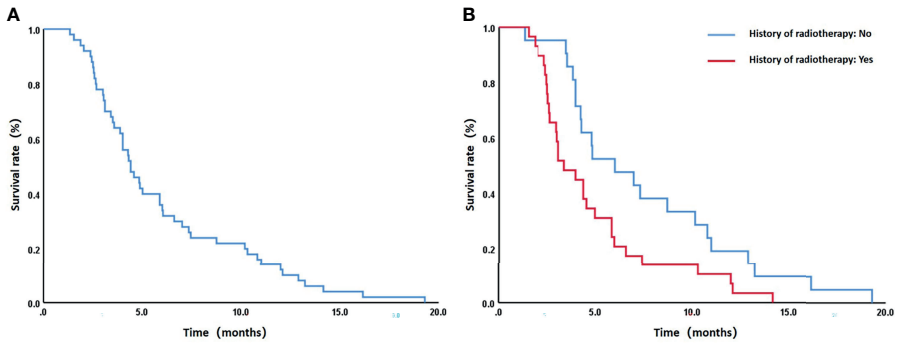

FIGURE 4 | **(A)** The overall 6-month, 12-month, and 18-month survival rates of all patients were 34%, 12%, and 2%, respectively. **(B)** For patients with and without a previous history of radiotherapy, the median survival periods were 3.4 months (95% CIL 2.1–4.7 months) and 6 months (95% CI: 2.8–9.3 months), respectively, and the 18-month survival rates were 0% and 4.8%, respectively. The difference of the latter was statistically significant (P = 0.021).

TABLE 4 | Causes of death.

Cause of death	N	%
Tumor progression/cachexia	27	54
Hemorrhage of upper digestive tract	11	22
Infection	5	10
Asphyxia	3	6
Heart failure	1	2
Unknown reason	3	6

DISCUSSIONS

Clarifying the dose distribution characteristics of RIBS and differences in doses calculated/measured by various methods can guide the clinical application of RIBS more effectively. As early as 1995, the AAPM TG-43 report established detailed I-125 dosimetry parameters and proposed evaluating methods for the dosimetry parameters of radioactive sources (9). As a random sampling statistical method, MC can simulate the transport of each incident particle in human tissue and, on this basis, calculate the three-dimensional dose deposition after irradiation with an accuracy close to that of reality (16). MC simulation has been widely applied to studies on radioactive source dosimetry owing to its ability to accurately model the physical process of radiotherapy (17–19).

In this study, dose distributions of different RIBSs were determined by a combination of TPS calculations, TLD measurements, and MC simulations. Despite the statistical differences among the three methods, the absolute dose difference was small (< 5 Gy), which was likely because of the large sample size (4 different specifications of stents and 6 seed activities) and a consistent trend. Values calculated by the TPS lay in the middle of the three methods (higher than TLD measurements but lower than MC simulations) and were less

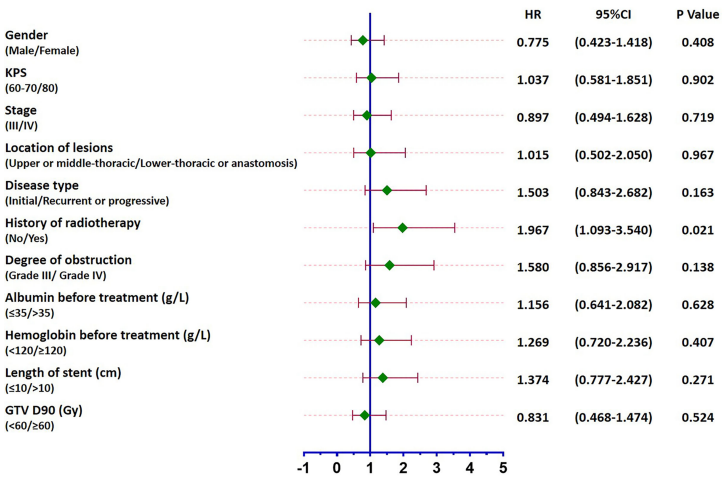

FIGURE 5 | Forest plot of factors affecting patients' survival. While a previous history of radiotherapy led to the prognosis of patients (P = 0.021), no other influencing factors were identified (P > 0.05).

than 5% different from to those simulated by MC. In contrast, TLD measurements demonstrated the largest deviation (a maximum of 11.7%), which was predominantly caused by the superposition of doses from multiple radioactive seeds and the rapid dose fall-off around the RIBS. In general, TPS calculations showed good clinical accuracy and an acceptable dose deviation. When analyzing the effects of the length, diameter, and seed spacing of the stent on dose distribution, stent length and seed spacing was seen to exert substantial effects on the dose. More specifically, the longer the stent, the higher the dose, which was again caused by superposition of doses from multiple radioactive seeds. In addition, as the isodose lines produced by a seed spacing of 1.0 cm had better conformability and uniformity, in clinical practice, it was preferred to arrange the seeds at an interval of 1.0 cm. The recommended seed activity of a single I-125 seed for the treatment of esophageal cancer was 0.4–0.8 mCi based on *in vitro* and *in vivo* experiments (20). In our study, TPS isodose lines showed multiple cold spots when the activity was in the range of 0.4–0.5 mCi, whereas higher activities could lead to an increased risk of radiotoxicity. Therefore, most RIBS treatment was performed at a seed activity of 0.6 mCi in clinical practice.

Studies have shown vastly different therapeutic effects of RIBS in treating esophageal cancer, with the median survival ranging from 4 to 11 months. On the contrary, reports on the survival of patients treated with conventional stents are more consistent, ranging from 3 to 5 months (7, 8, 21–23). In terms of the relief of dysphagia and the incidence of complications, the performance of seed stents is similar to that of conventional stents ($P > 0.05$) (8, 24). In a randomized controlled study conducted by Zhu et al. (8) that included 148 patients (73 in the RIBS group and 75 in the conventional stent group), incidences of common complications, including severe chest pain (23% versus 20%), fistula (6% versus 7%), pneumonia (15% versus 19%), bleeding (7% versu 7%), and recurrence of dysphagia (28% versus 27%), were not significantly different. In our study, patients' survival was relatively short (median survival was 4.4 months). Among all complications, the incidence of moderate to severe pain (20%), perforation (6%), and pneumonia (10%) was of a similar level, while that of bleeding was high (28%). The poor survival and the high incidence of fatal complications observed in this study were related to the fact that most patients were either relapsed/uncontrolled patients (62%) or had previously received radiotherapy (58%). In particular, patients with a previous history of radiotherapy showed low survival rates and high incidences of fatal complications. In addition, differences were statistically significant when compared these patients with those of patients without a history of radiotherapy ($P = 0.021$ and 0.019, respectively). This finding is consistent in reports by Zhu and Liu (8, 23), who listed previous history of radiotherapy as a poor prognostic factor. Since the incidence of fatal complications was substantially higher in patients with a history of radiotherapy than in those without, it was considered that the poor survival of the study mainly originated from complications. In particular, gastrointestinal bleeding is a complication that requires particular attention in patients whose interval of stent and radiotherapy was less than 6 months. Although the prognosis of patients who relapse after radiotherapy is even poorer, due to extremely limited treatment options, whether stent implant should be performed requires a joint decision made by the physician, patient, and patient's family after carefully weighing the pros and cons. This study observed a low incidence of restenosis (8%) compared to a rate of 12.3% and 13.8% reported in literatures adopting conventional stents (25, 26). This is likely because of the superior dose distribution created by the more reasonable seed arrangement in the RIBS, which plays an important role in the prevention and treatment of restenosis caused by tumor overgrowth or in-growth. Stent restenosis occurred at a median interval of 108 days (31–196 days) after RIBS implanted in our study, by comparison, the median time of restenosis of conventional metal stents was about 2-30 weeks, which was related to tumor overgrowth, stent migration, granulation hyperplasia, food bolus obstruction and so on (25, 27). This also suggests that RIBS could probably delay the occurrence of restenosis, but due to the small number of cases and large time span, further confirmation is needed. Despite the short survival of patients receiving RIBS treatment, in actual clinical practice, most patients who need stent implant are advanced or relapsed or are refractory patients who are no longer eligible for surgery or chemoradiotherapy and yet suffer from severe obstructive symptoms. Therefore, treatment should focus on relieving symptoms and improving the quality of life. For these patients, RIBS can extend their survival by 4.4 months and allow them to eat during this period, making it valuable for palliative care. However, the risk of complications associated with the technique should be fully described to patients and their families prior to the treatment.

Dosimetric analysis in this study did not discover any factors affecting patients' survival or incidence of complications. Potential indicative factors included $D90 \leq 50$ Gy or > 50 Gy, which resulted in respective incidences of fatal complications of 18.8% and 47.1% with a difference close to statistical significance ($P = 0.054$); and $D90 \leq 66$ Gy or > 66 Gy, which resulted in incidences of 14.3% and 0% ($P = 0.123$) of stent restenosis, respectively. Since existing dose evaluation methods for RIBS are still not standardized, only D90 was adopted in this study. In addition, due to large patient heterogeneity and incomplete information on patients' tumor conditions and previous radiation doses, subsequent prospective research with more appropriate indicators is required to further clarify the role of RIBS in the treatment of esophageal cancer.

The limitations of the study are as follows: ① The analysis of dosimetry was elementary, especially without considering the influence of tissue heterogeneity and esophageal cavity on dosimetry, and solutions should be developed in next research. ② Retrospective study, follow-up data may be inaccurate or bias; ③ Because the results of survival and morbidity were not prominent, the significance of dosimetric data analysis was limited; ④ Because most patients were advanced, recurrent and refractory tumors, with poor prognosis and short survival time, it was difficult to observe long-term efficacy and complications; ⑤ The study had a high incidence of complications, which may need to be further refined in terms of technology, methods and patient selection, so as to benefit patients more specifically.

CONCLUSION

Doses around the RIBS calculated by the TPS lay between those measured by the TLD and those simulated by the MC, indicating that that TPS calculations are suitable for clinical applications. In addition, the overall absolute dose differences among the three methods were small. Dose distribution was affected by seed activity, seed spacing, and stent length. Most RIBS treatment in this study was carried out with a seed spacing of 1.0 cm and a seed activity of 0.6 mCi. The application of RIBS in treating severely obstructed patients with esophageal cancer can effectively alleviate obstructive symptoms, but with a relatively a high incidence of fatal complications. Relevant research should further identify the people who can benefit from the RIBS and focus on how to improve the safety and effectiveness of RIBS in the treatment of esophageal cancer.

DATA AVAILABILITY STATEMENT

The original contributions presented in the study are included in the article/supplementary material. Further inquiries can be directed to the corresponding authors.

ETHICS STATEMENT

Ethical review and approval was not required for the study on human participants in accordance with the local legislation and institutional requirements. Written informed consent was not provided because this is a retrospective study which only analyzed the data of previously treated patients retrospectively. The patient signed the informed consent form before stent implantation, but it did not involve the informed consent form for the study.

AUTHOR CONTRIBUTIONS

Conceptualization, JW and KZ. Methodology, ZJ and JW. Software, ZJ and QY. Validation, LL, CX, and XZ. Formal analysis, ZJ and QY. Investigation, SY and YJ. Resources, LL and HS. Data curation, LL, QY, CX, and XZ. Writing—original draft preparation, ZJ and QY. Writing—review and editing, JW and KZ. Visualization, ZJ. Supervision, JW. Project administration, JW and KZ. ZJ and QY contributed equally to this work, so they are listed as co-first authors. All authors contributed to the article and approved the submitted version.

REFERENCES

1. Bray F, Ferlay J, Soerjomataram I, Siegel RL, Torre LA, Jemal A. Global Cancer Statistics 2018: GLOBOCAN Estimates of Incidence and Mortality Worldwide for 36 Cancers in 185 Countries. *CA Cancer J Clin* (2018) 68 (6):394–424. doi: 10.3322/caac.21492
2. Lordick F, Mariette C, Haustermans K, Obermannova R, Arnold D, Committee EG. Oesophageal Cancer: ESMO Clinical Practice Guidelines for Diagnosis, Treatment and Follow-Up. *Ann Oncol* (2016) 27(suppl 5):v50–7. doi: 10.1093/annonc/mdw329
3. Frimberger E. Expanding Spiral–a New Type of Prosthesis for the Palliative Treatment of Malignant Esophageal Stenoses. *Endoscopy* (1983) 15 Suppl 1:213–4. doi: 10.1055/s-2007-1021511
4. Varghese TK Jr, Hofstetter WL, Rizk NP, Low DE, Darling GE, Watson TJ, et al. The Society of Thoracic Surgeons Guidelines on the Diagnosis and Staging of Patients With Esophageal Cancer. *Ann Thorac Surg* (2013) 96 (1):346–56. doi: 10.1016/j.athoracsur.2013.02.069
5. Homs MY, Siersema PD. Stents in the GI Tract. *Expert Rev Med Devices* (2007) 4(5):741–52. doi: 10.1586/17434440.4.5.741
6. Guo JH, Teng GJ, Zhu GY, He SC, Deng G, He J. Self-Expandable Stent Loaded With 125I Seeds: Feasibility and Safety in a Rabbit Model. *Eur J Radiol* (2007) 61(2):356–61. doi: 10.1016/j.ejrad.2006.10.003
7. Guo JH, Teng GJ, Zhu GY, He SC, Fang W, Deng G, et al. Self-Expandable Esophageal Stent Loaded With 125I Seeds: Initial Experience in Patients With Advanced Esophageal Cancer. *Radiology* (2008) 247(2):574–81. doi: 10.1148/radiol.2472070999
8. Zhu H-D, Guo J-H, Mao A-W, Lv W-F, Ji J-S, Wang W-H, et al. Conventional Stents Versus Stents Loaded With 125iodine Seeds for the Treatment of Unresectable Oesophageal Cancer: A Multicentre, Randomised Phase 3 Trial. *Lancet Oncol* (2014) 15(6):612–9. doi: 10.1016/S1470-2045(14)70131-7
9. Nath R, Anderson LL, Luxton G, Weaver KA. Dosimetry of Interstitial Brachytherapy Sources: Recommendations of the AAPM Radiation Therapy Committee Task Group No. 43. American Association of Physicists in Medicine. *Med Phys* (1995) 22(2):209–34. doi: 10.1118/1.597458
10. Rivard MJ, Coursey BM, DeWerd LA, Hanson WF, Huq MS, Ibbott GS, et al. Update of AAPM Task Group No. 43 Report: A Revised AAPM Protocol for Brachytherapy Dose Calculations. *Med Phys* (2004) 31(3):633–74. doi: 10.1118/1.1646040
11. Dolan J, Lia Z, Williamson JF. Monte Carlo and Experimental Dosimetry of an 1251 Brachytherapy Seed. *Med Phys* (2006) 33(12):4675–84. doi: 10.1118/1.2388158
12. Taylor RE, Rogers DW. More Accurate Fitting of 125I and 103Pd Radial Dose Functions. *Med Phys* (2008) 35(9):4242–50. doi: 10.1118/1.2964097
13. Taylor RE, Rogers DW. An Egsnrc Monte Carlo-Calculated Database of TG-43 Parameters. *Med Phys* (2008) 35(9):4228–41. doi: 10.1118/1.2965360
14. Sabharwal T, Morales JP, Irani FG, Adam A. Quality Improvement Guidelines for Placement of Esophageal Stents. *Cardiovasc Intervent Radiol* (2005) 28 (3):284–8. doi: 10.1007/s00270-004-0344-6
15. National Cancer Institute. *Common Terminology Criteria for Adverse Events (CTCAE) Version 5.0* (2017). Available at: https://evs.nci.nih.gov/ftp1/CTCAE/CTCAE_5.0/.
16. Moutsatsos A, Pantelis E, Papagiannis P, Baltas D. Experimental Determination of the Task Group-43 Dosimetric Parameters of the New I25.S17plus (125)I Brachytherapy Source. *Brachytherapy* (2014) 13(6):618–26. doi: 10.1016/j.brachy.2014.07.001
17. Mesbahi A, Fix M, Allahverdi M, Grein E, Garaati H. Monte Carlo Calculation of Varian 2300C/D Linac Photon Beam Characteristics: A Comparison Between MCNP4C, GEANT3 and Measurements. *Appl Radiat Isotopes Including Data Instrumentation Methods Use Agric Industry Med* (2005) 62 (3):469–77. doi: 10.1016/j.apradiso.2004.07.008
18. Sadeghi M, Hamed Hosseini S. Study of the Isoaid ADVANTAGE (125)I Brachytherapy Source Dosimetric Parameters Using Monte Carlo Simulation. *Appl Radiat Isot* (2010) 68(1):211–3. doi: 10.1016/j.apradiso.2009.08.007
19. Saidi P, Sadeghi M, Shirazi A, Tenreiro C. Dosimetric Parameters of the New Design (103)Pd Brachytherapy Source Based on Monte Carlo Study. *Phys Med* (2012) 28(1):13–8. doi: 10.1016/j.ejmp.2010.12.005
20. Lv J, Cao XF, Zhu B, Ji L, An HY. ~(125)I Seed Implantation Brachytherapy for Esophageal Squamous Cell Carcinoma. *World Chin J Digestol* (2010) 18 (29):3065–71. doi: 10.11569/wcjd.v18.i29.3065
21. Zhongmin W, Xunbo H, Jun C, Gang H, Kemin C, Yu L, et al. Intraluminal Radioactive Stent Compared With Covered Stent Alone for the Treatment of Malignant Esophageal Stricture. *Cardiovasc Intervent Radiol* (2012) 35 (2):351–8. doi: 10.1007/s00270-011-0146-6

22. Dai Z, Zhou D, Hu J, Zhang L, Lin Y, Zhang J, et al. Clinical Application of Iodine-Eluting Stent in Patients With Advanced Esophageal Cancer. *Oncol Lett* (2013) 6(3):713–8. doi: 10.3892/ol.2013.1466
23. Liu N, Liu S, Xiang C, Cong N, Wang B, Zhou B, et al. Radioactive Self-Expanding Stents Give Superior Palliation in Patients With Unresectable Cancer of the Esophagus But Should be Used With Caution If They Have had Prior Radiotherapy. *Ann Thorac Surg* (2014) 98(2):521–6. doi: 10.1016/j.athoracsur.2014.04.012
24. Doosti-Irani A, Mansournia MA, Rahimi-Foroushani A, Haddad P, Holakouie-Naieni K. Complications of Stent Placement in Patients With Esophageal Cancer: A Systematic Review and Network Meta-Analysis. *PloS One* (2017) 12(10):e0184784. doi: 10.1371/journal.pone.0184784
25. Homs MY, Steyerberg EW, Kuipers EJ, van der Gaast A, Haringsma J, van Blankenstein M, et al. Causes and Treatment of Recurrent Dysphagia After Self-Expanding Metal Stent Placement for Palliation of Esophageal Carcinoma. *Endoscopy* (2004) 36(10):880–6. doi: 10.1055/s-2004-825855
26. Stewart DJ, Balamurugan R, Everitt NJ, Ravi K. Ten-Year Experience of Esophageal Self-Expanding Metal Stent Insertion at a Single Institution. *Dis Esophagus* (2013) 26(3):276–81. doi: 10.1111/j.1442-2050.2012.01364.x
27. Hirdes MM, Siersema PD, Houben MH, Weusten BL, Vleggaar FP. Stent-in-Stent Technique for Removal of Embedded Esophageal Self-Expanding Metal Stents. *Am J Gastroenterol* (2011) 106(2):286–93. doi: 10.1038/ajg.2010.394

Conflict of Interest: The authors declare that the research was conducted in the absence of any commercial or financial relationships that could be construed as a potential conflict of interest

frontiers in Oncology

ORIGINAL RESEARCH
published: 30 March 2022
doi: 10.3389/fonc.2022.811183

The Effect of Ophiopogonin C in Ameliorating Radiation-Induced Pulmonary Fibrosis in C57BL/6 Mice: An Update Study

Xiaobin Fu[1†], *Tingting Li*[1†] *and Qiwei Yao*[2*]

[1] Department of Radiation Oncology, The Second Affiliated Hospital of Fujian Medical University, Quanzhou, China,
[2] Department of Radiation Oncology, Fujian Medical University Cancer Hospital & Fujian Cancer Hospital, Fuzhou, China

Background: The aim of this study was to assess and update the protective effects and underlying mechanisms of Ophiopogonin C (OP-C), a biologically active component separated and purified from *Ophiopogon japonicus*, in ameliorating radiation-induced pulmonary fibrosis in C57BL/6 mice administered thoracic radiation.

Methods and Materials: We randomly divided 75 mice into five groups and administered a dose of 12-Gy whole thoracic radiation to establish a pulmonary fibrosis animal model. Mice were treated with OP-C or dexamethasone combined with or without cephalexin by daily gavage for 4 weeks. All mice were sacrificed after the completion of thoracic irradiation at 28 weeks. Serum levels of interleukin-6 and transforming growth factor-β1 (TGF-β1) were evaluated. Moreover, superoxide dismutase (SOD) levels in lung tissue were measured. The severity of fibrosis was evaluated using the hydroxyproline content of the lung tissue. The pathological changes in the five groups were detected by hematoxylin and eosin and Masson trichrome staining. Smooth muscle actin expression was detected using immunohistochemical staining. Matrix metalloproteinases-2 (MMP-2) and tissue inhibitors of metalloproteases-2 (TIMP-2) were examined by immunohistochemical staining of the lung sections, and semiquantitative analysis was used to calculate the expression of MMP-2 and TIMP-2.

Results: Irradiated mice treated with OP-C or DXE combined with or without cephalexin significantly reduced mortality in mice and fibrosis levels by 1) reducing the deposition of collagen and accumulation of inflammatory cells and fibroblasts, 2) downgrading levels of the promote-fibrosis cytokine TGF-β1, and 3) increasing SOD activity in the lung tissue compared with that of irradiated mice without treatment. However, there were no statistical differences in fibrosis levels among the irradiated mice treated with OP-C or DXE combined with or without cephalexin.

Conclusion: OP-C significantly ameliorates radiation-induced pulmonary fibrosis and may be a promising therapeutic strategy for this disorder.

Keywords: radiation-induced pulmonary fibrosis, C57BL/6 mice, OP-C, Chinese medicine, dexamethasone

OPEN ACCESS

Edited by:
Tao Li,
Sichuan Cancer Hospital, China

Reviewed by:
Olga Pershina,
Research Institute of Pharmacology and Regenerative Medicine named ED Goldberg (RAS), Russia
Yingming Sun,
Fujian Medical University, China

***Correspondence:**
Qiwei Yao
yaoqw1988@126.com

[†]*These authors have contributed equally to this work and share first authorship*

Specialty section:
This article was submitted to Radiation Oncology, a section of the journal Frontiers in Oncology

Received: *08 November 2021*
Accepted: *28 February 2022*
Published: *30 March 2022*

Citation:
Fu X, Li T and Yao Q (2022) The Effect of Ophiopogonin C in Ameliorating Radiation-Induced Pulmonary Fibrosis in C57BL/6 Mice: An Update Study. Front. Oncol. 12:811183. doi: 10.3389/fonc.2022.811183

BACKGROUND

The incidence of thoracic malignant tumors, such as lung, breast, and esophageal cancers, and thymoma, has been increasing annually in the past decades, and thoracic radiotherapy is the main treatment method for these cancers (1). Radiation-induced lung injury in the normal lung tissue adjacent to the tumor, which includes acute pulmonary inflammation and chronic pulmonary fibrosis, significantly affects the patients' quality of life, limits the deliverable radiation dose, interrupts radiation treatment, and can lead to death (2, 3). At present, the underlying mechanism of radiation-induced pulmonary injury is not comprehensively understood. It is generally believed that radiation disrupts alveolar epithelial cells and epithelial integrity, leading to edema and damage, which recruit inflammatory cells to release various cytokines, such as interleukin-6 (IL-6), transforming growth factor-β1 (TGF-β1), and tumor necrosis factor-α (TNF-α). A cascade of molecular events alters the microenvironment, and oxidative stress occurs immediately. Furthermore, the proliferation of fibroblasts and the deposition of collagen fibers lead to chronic pulmonary fibrosis, causing progressive fibrosis and insufficient respiratory function (4–6).

The molecular mechanism of radiation-induced pulmonary injury is complicated and unclear; therefore, there are no specific treatment methods. Conventional therapies for radiation-induced pulmonary injury include symptomatic treatment, including steroids, non-steroid anti-inflammatory medicine, antibiotics, and immunosuppressive agents. However, steroid therapy has more side effects, including moon face, high blood pressure, diabetes mellitus, osteoporosis, weakened immune system, and digestive tract ulcers. Moreover, the effects of steroid therapy are unsatisfactory.

Ophiopogonin C (OP-C) is a biologically active component separated and purified from *Ophiopogon japonicus*, which has been widely used as a traditional Chinese medicine for the treatment of inflammatory diseases for a long time. It has also been reported that OP-C plays a role in blocking tumor growth and reducing the cytotoxic effect of chemoradiotherapy (7, 8). In 2019, our group published the role of OC-P in inhibiting acute pulmonary inflammation in mice. The results of this study support the use of OP-C to inhibit radiation-induced acute pulmonary inflammation. However, the effect of OC-P in ameliorating chronic radiation-induced pulmonary fibrosis remains unclear (9). The aim of this study was to assess and update the protective effects and underlying mechanisms of OP-C in ameliorating chronic radiation-induced pulmonary fibrosis in a C57BL/6 mouse model of pulmonary fibrosis.

METHODS AND MATERIALS

Animals

Male inbred C57BL/6 mice, aged 8 weeks and weighing 18–22 g, were purchased from the SLAC Experimental Animal Center (Shanghai, China). They were housed in cages in a specific pathogen-free (SPF) graded animal care facility. Ethical approval for this study was obtained from the Fuzhou General Hospital, Fujian, China. All experimental procedures were performed under general anesthesia, which minimized the pain of the animals. The mice were allowed free access to standard mouse food and water. All mice were housed in cages in a well-controlled SPF-graded animal care facility with a 12/12-h light/dark cycle to acclimate for 7 days prior to the experiment and observed once daily for 28 weeks after whole thoracic irradiation.

Irradiation and Treatment

Mice were irradiated with 12 Gy using a medical linear accelerator (Trilogy, Varian, CA, USA) at a dose rate of 200 cGy/min. Ten mice were treated at a time using specially designed plexiglass containers to confine the radiation beam. The radiation beam was restricted to the whole thorax. For thoracic irradiation, all mice were anesthetized using 1% sodium pentobarbital (0.8 ml/100 g) intraperitoneally. Mice were observed once daily for up to 28 weeks after radiation, and the body weight and normal death of the mice were recorded. The mice that received thoracic radiation were treated with OP-C (3 mg/kg; Quanzhou Dongnan Traditional Chinese Medicine Co. Ltd., Fujian, China) (n = 15), dexamethasone ([DEX], 1,233 μg/kg; Zhejiang Asia-Pacific Pharmaceuticals Co. Ltd., Zhejiang, China) (n = 15), or DEX + cephalexin (246,600 μg/kg; Zhejiang Asia-Pacific Pharmaceuticals Co. Ltd.) (n = 15) by gavage for 4 weeks after irradiation. The radiation mice (radiation only; n = 15) received thoracic radiation and isotonic sodium chloride solution without drug treatment, but normal saline by gavage. The control group mice (n = 15) were treated with normal saline by gavage at the same volume.

Study Group

All mice (n = 75) were randomly divided into five experimental groups prior to the experiment as follows: group 1 (blank control group; received no treatment and normal saline gavage); group 2 (radiation-only group; received radiation and normal saline gavage); group 3 (OP-C group; received radiation and OP-C gavage); group 4 (DEX group; received radiation and DEX gavage); and group 5 (DEX + cephalexin group; received radiation and DEX + cephalexin gavage).

Sample Collection and Histopathology Process

After body weight measurement, all mice were sacrificed at 28 weeks after completion of whole thoracic irradiation. Blood samples were collected from cardiac puncture and kept for 1 h at 25 degrees Celsius (°C) for clotting. Serum samples were collected by centrifugation at 1,000 rpm for 15 min at 2–8°C and then stored at -70°C for further assessment of IL-6 and TGF-β1. The wet weights of both lungs were weighed and recorded. The left lungs were snap frozen with liquid nitrogen and kept at -70°C for further analysis of hydroxyproline (Hyp) and malondialdehyde (MDA) contents and superoxide dismutase (SOD) activity. The right lungs were fixed in 10% formalin solution for 24 h and embedded in paraffin for subsequent histological examination and matrix metalloproteinase-2 (MMP-2) and tissue inhibitors of metalloprotease-2 (TIMP-2) examination by immunohistochemical analyses.

Histopathological Evaluation

According to the simple method of estimating the severity of pulmonary fibrosis by the Ashcroft et al. (10) scoring system, lung sections stained by hematoxylin and eosin staining and Masson staining and combined with SMA immunohistochemical staining were evaluated. Each group received 3 slides. Each slide received four fields, and the mean value of the four fields was considered representative of the slide. Experienced pathologists in our hospital reviewed and examined the fields. The mean score of all fields was performed as the Ashcroft fibrosis score.

To assess the degree of inflammation in the five groups, the sections stained by hematoxylin and eosin were also reviewed. The pathologists evaluated the accumulation of lymphocytes and neutrophils, interstitial edema, and alveolar wall thickening and classified it into 4 grades on a scale of 0 (absent) to 3 (extensive damage) (score 0: absent, score 1: minimal damage, score 2: severe damage, score 3: extensive damage), as described previously (11).

Serum Cytokine Level Measurement

Serum levels of IL-6 and TGF-β1 were assessed by ELISA using IL-6 and TGF-β1 kits according to the manufacturer's instructions (Boster Biological Technology Co. Ltd., Wuhan, China). The optical density values were measured at 450 nm using an ELISA reader and calculated at the linear portion of the curve.

Collagen Content of Lung Measurement

The lung collagen content was measured using the Hyp assay according to the manufacturer's instructions (Nanjing Jiancheng Bioengineering Institute, Nanjing, China). Briefly, 30–100 mg of lung tissue was hydrolyzed in lysis buffer solution (approximately 1 ml) at 95°C for 20 min. Finally, the absorbance of the colored lung samples was evaluated at 550 nm.

SOD Activity Measurement in Lungs

SOD activity was measured using the xanthine oxidase method in the SOD activity assay, according to the manufacturer's instructions (Nanjing Jiancheng Bioengineering Institute).

MDA Content Measurement in Lungs

MDA is the end product of reactive oxygen species (ROS)-induced peroxidation of cell membrane lipids, which are reliable markers of oxidative stress. MDA content was measured using the thiobarbituric acid method using an MDA content kit according to the manufacturer's instructions (Nanjing Jiancheng Bioengineering Institute).

Masson Trichrome Staining

Masson staining was performed to identify the expression of collagen fibers in lung tissues. Collagen fibers were stained using the Masson staining kit according to the manufacturer's instructions (Medical Discovery Leader, Beijing, China).

Immunohistochemical Analyses

Immunohistochemical analyses were performed to identify the expression of MMP-2 and TIMP-2 in the lungs. Briefly, lung sections (5 μm) were incubated with anti-MMP-2 or anti-TIMP-2 primary antibody (1:100 dilution; Santa Cruz Biotechnology, TX, USA) at 4°C overnight. After washing with PBS three times, the sections were incubated with secondary antibodies at 25°C for 50 min and visualized using diaminobenzidine (DAKO, Glostrup, Denmark). SMA expression was also identified by immunostaining. Integrated optical density was calculated using Image-Pro Plus (Media Cybernetics, MD, USA), and the positive area was compared with the total area for semiquantitative analysis.

Statistical Analysis

Data were analyzed using SPSS version 19.0 (SPSS Inc., IL, USA). Data are expressed as mean ± standard error of mean (SEM). The differences among groups were calculated using the Kruskal–Wallis H and one-way analysis of variance (ANOVA). Statistical significance was set at $p < 0.05$.

RESULTS

OP-C Reduces Mortality in Mice

All C57BL/6 mice irradiated with a single dose of 12 Gy survived after completion of irradiation. The mice tolerated the prescribed dose well. Approximately 50% of mice died at 22–28 weeks after thoracic irradiation. The numbers of surviving mice 28 weeks after irradiation in the blank control, radiation-only, OP-C, DEX, and DEX + cephalexin groups were 13, 5, 7, 8, and 7, respectively. The mortality rates of the five groups were 86.7%, 33.3%, 46.7%, 53.3%, and 46.7%, respectively. Irradiated mice treated with OP-C had a lower mortality rate than irradiated mice without treatment. However, the mortality rate of the irradiated mice treated with OP-C was similar to that of the groups treated with DEX and DEX + cephalexin.

OP-C Reduces Collagen Deposition in Lung Tissues

To examine the effect of OP-C on histological changes and collagen deposition in lung tissue, we performed hematoxylin and eosin staining and Masson staining, and SMA was detected by immunohistochemical staining. Irradiated mice without treatment showed chronic moderate pulmonary inflammation changes, including accumulation of lymphocytes and neutrophils, markedly thickened alveolar walls, regional fibrotic foci, accumulation of fibroblasts, and deposition of collagen. Irradiated mice treated with OP-C, DEX, and DEX + cephalexin slightly reduced tissue damage, collagen deposition, and accumulation of inflammatory cells and fibroblasts (**Figure 1**).

To examine the effect of OP-C on degree of pulmonary inflammation in lung tissue, we used the inflammation scoring system, and we found that the inflammation score was significantly lower in irradiated mice treated with OP-C (7.17 ± 0.52) compared with that of irradiated mice without treatment (9.58 ± 0.58, $p < 0.001$). However, the Ashcroft score in irradiated mice treated with OP-C was not significantly different from that in mice treated with DEX (7.42 ± 0.38, p =

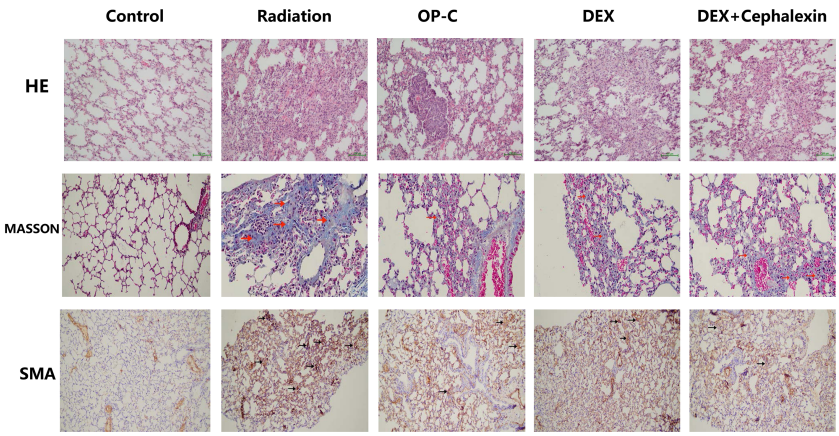

FIGURE 1 | Effects of Ophiopogonin C (OP-C) on the histological changes, including pulmonary inflammation and fibrosis, in the lung tissue at 28 weeks after whole thoracic irradiation. Photomicrographs show staining of mouse lung tissue sections with hematoxylin and eosin staining, Masson staining, and SMA detected by immunohistochemical staining in mice from the blank control, radiation-only, OP-C, dexamethasone (DEX), and DEX + cephalexin groups.

0.01) or DEX + cephalexin (p = 7.58 ± 0.52, p = 0.01; **Figure 2A**). To examine the effect of OP-C on severity of pulmonary fibrosis in lung tissue, we assessed the Ashcroft scoring system, and we found that the Ashcroft score was significantly lower in irradiated mice treated with OP-C (1.75 ± 0.25) compared with that of irradiated mice without treatment (3.75 ± 0.66, p = 0.001). However, the Ashcroft score in irradiated mice treated with OP-C was not significantly different from that in mice treated with DEX (1.58 ± 0.52, p = 0.01) or DEX + cephalexin (p = 1.83 ± 0.52, p = 0.02; **Figure 2B**).

OP-C Modulates Serum Cytokine Levels

To examine the effect of OP-C on the expression of serum cytokines, we assessed serum IL-6 and TGF-β1 levels using ELISA. No significant differences in IL-6 expression were seen in the control mice (187.15 ± 59.13 pg/ml), irradiated mice without treatment (220.05 ± 56.62 pg/ml), irradiated mice treated with OP-C (203.09 ± 41.4 pg/ml), irradiated mice treated with DEX (190.34 ± 69.66 pg/ml), and irradiated mice treated with DEX + cephalexin (201.71 ± 40.71 pg/ml, p = 0.765) (**Figure 3A**). We found that serum TGF-β1 expression was significantly lower in irradiated mice treated with OP-C (1.76 ± 0.13 ng/ml) compared with that of irradiated mice without treatment (2.15 ± 0.13 ng/ml, p = 0.046). Moreover, TGF-β1 expression was also significantly lower in irradiated mice treated with DEX (1.77 ± 0.09 ng/ml, p = 0.05) and DEX + cephalexin (1.74 ± 0.2 ng/ml, p = 0.04) compared with that of irradiated mice without treatment. However, the level of serum TGF-β1 in irradiated mice treated with OP-C was not significantly different from that in mice treated with DEX (p = 0.972) or DEX + cephalexin (p = 0.992; **Figure 3B**).

OP-C Reduces Hyp Content in the Lungs

To examine the effect of OP-C on collagen deposition, we measured the Hyp content of the left lungs. We found that the expression of Hyp content was lower in irradiated mice treated with OP-C (0.98 ± 0.14 μg/ml) than in irradiated mice without treatment (1.29 ± 0.1 μg/ml, p = 0.082); however, statistical analysis showed no significant difference. The expression of Hyp content was significantly lower in irradiated mice treated with DEX (0.91 ± 0.13 μg/ml, p = 0.008) and DEX + cephalexin (0.97 ± 0.12 μg/ml, p = 0.04) compared with that of irradiated mice without treatment. However, the level of Hyp content in irradiated mice treated with OP-C was not significantly different from that in mice treated with DEX (p = 0.425) or DEX + cephalexin (p = 0.937; **Figure 4A**).

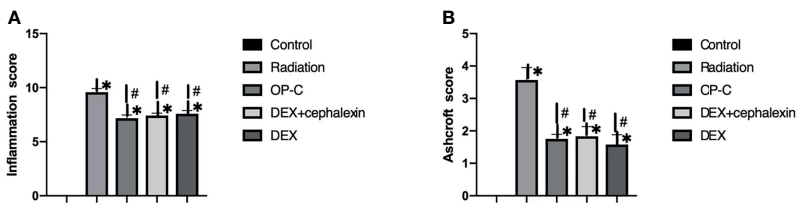

FIGURE 2 | Effects of OP-C on inflammation score **(A)** and Ashcroft score **(B)** in the lungs were measured in mice from the blank control, radiation only, OP-C, DEX, and DEX + cephalexin groups. The presented data are expressed as the mean ± SEM. *p < 0.05, compared with the control group. #p < 0.05, compared with the radiation-only group.

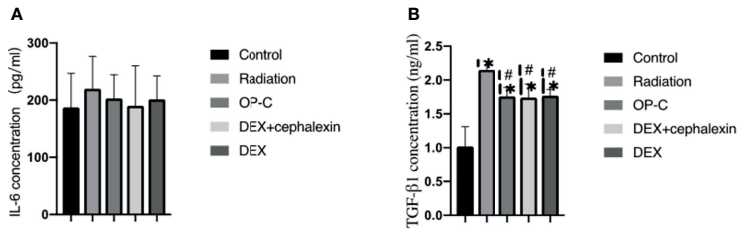

FIGURE 3 | Effects of OP-C on cytokine expression in serum. Expression of IL-6 **(A)** and TGF-β1 **(B)** in the serum were measured in mice from the blank control, radiation only, OP-C, DEX, and DEX + cephalexin groups. The presented data are expressed as the mean ± SEM. *p < 0.05, compared with the control group. #p < 0.05, compared with the radiation-only group.

OP-C Modulates SOD Activity and MDA Content in the Lungs

To examine the effect of OP-C on redox balance, we assessed the SOD activity and MDA content in the lungs. We found that SOD activity was significantly higher in irradiated mice treated with OP-C (39.98 ± 3.38 U/ml) compared with that of irradiated mice without treatment (25.57 ± 3.48 U/ml, p = 0.001). Moreover, SOD activity was significantly higher in irradiated mice treated with DEX (40.17 ± 3.78U/ml, p = 0.001) and DEX + cephalexin (39.18 ± 4.79 U/ml, p = 0.001) compared with that of irradiated mice without treatment. However, SOD activity in irradiated mice treated with OP-C was not significantly different from that in mice treated with DEX (p = 0.925) or DEX + cephalexin (p = 0.906; **Figure 4B**). No significant differences in the expression of MDA content were observed in the control mice (2.85 ± 0.82 nmol/ml), irradiated mice without treatment (3.21 ± 0.81 nmol/ml), irradiated mice treated with OP-C (2.82 ± 0.34 nmol/ml), irradiated mice treated with DEX (2.47 ± 0.65 nmol/ml), and irradiated mice treated with DEX + cephalexin (2.46 ± 0.78 nmol/ml, p = 0.377; **Figure 4C**).

OP-C Modulates MMP-2 and TIMP-2 Content in the Lungs

To examine the effect of MMP-2 and TIMP-2 content in the lungs, we performed immunohistochemical analyses and calculated the positive area by semiquantitative analysis (**Figure 5**). We found that the MMP-2 content was significantly lower in control mice (9.95 ± 2.22%) than in irradiated mice treated with OP-C (19.11 ± 2.37%, p < 0.001). However, MMP-2 expression in the irradiated mice without treatment (17.98 ± 1.62%), irradiated mice treated with OP-C (19.11 ± 2.37%), irradiated mice treated with DEX (17.33 ± 2.13%), and irradiated mice treated with DEX + cephalexin (18.84 ± 2.73%) was not significantly different (p = 0.792; **Figure 6A**). Moreover, no significant differences in the expression of TIMP-2 content were seen in the control mice (6.26 ± 1.45%), irradiated mice without treatment (7.48 ± 1.78%), irradiated mice treated with OP-C (6.76 ± 1.35%), irradiated mice treated with DEX (6.63 ± 0.94%), and irradiated mice treated with DEX + cephalexin (6.6 ± 1.27%, p = 0.794; **Figure 6B**).

DISCUSSION

In our study, we demonstrated that OP-C, a biologically active component found in *Ophiopogon japonicus*, ameliorated radiation-induced pulmonary fibrosis in C57BL/6 mice treated with a single dose of 12-Gy whole thoracic radiation. In irradiated mice, OP-C treatment significantly reduced the mortality rate, slightly alleviated lung histological tissue damage, including decreased accumulation of inflammatory cells and proliferation of fibroblasts, and inhibited collagen deposition. OP-C also regulated the levels of promote-fibrosis serum TGF-β1 and Hyp content. Moreover, we demonstrated that OP-C treatment significantly increased the activity of antioxidant enzymes in SOD. However, the levels of pulmonary fibrosis were not significantly different among the irradiated mice treated with OP-C, DEX, and DEX + cephalexin. We demonstrated that OP-C had similar protective effects to steroid therapy against radiation-induced pulmonary fibrosis. Moreover, compared with steroid therapy, no obvious adverse effects were found with OP-C treatment. Thus, OP-C may be a promising therapeutic strategy for radiation-induced pulmonary fibrosis.

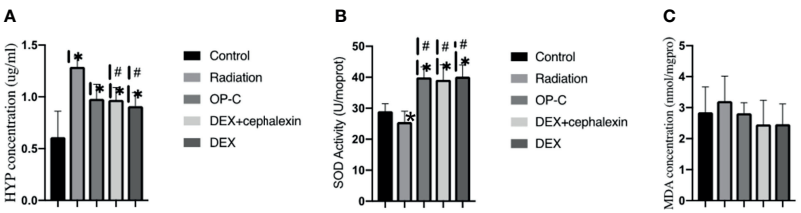

FIGURE 4 | Effects of OP-C on hydroxyproline (Hyp) contents, superoxide dismutase (SOD) activity, and malondialdehyde (MDA) contents in the lungs. Expression of Hyp **(A)**, SOD activity **(B)**, and MDA contents **(C)** in the lungs were measured in mice from the blank control, radiation-only, OP-C, DEX, and DEX + cephalexin groups. The presented data are expressed as the mean ± SEM. *p < 0.05, compared with the control group. #p < 0.05, compared with the radiation-only group.

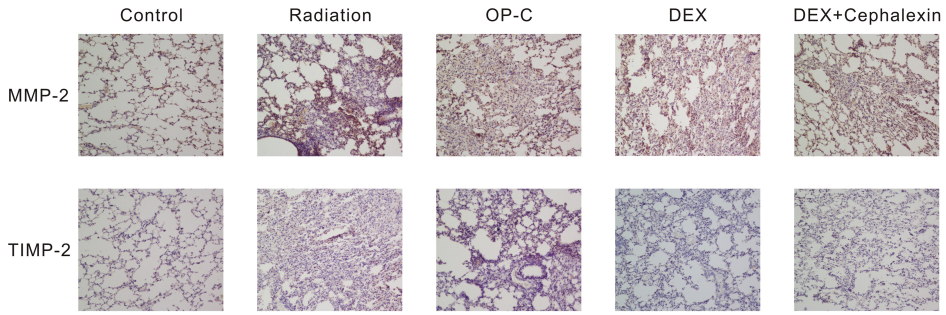

FIGURE 5 | Effects of Ophiopogonin C (OP-C) on the expression of MMP-2 and TIMP-2 changes in the lung tissue at 28 weeks after whole thoracic irradiation. Photomicrographs show staining of mouse lung tissue sections with MMP-2 and TIMP-2 detected by immunohistochemical staining in mice from the blank control, radiation-only, OP-C, dexamethasone (DEX), and DEX + cephalexin groups.

TGF-β1 is known as a promote-fibrosis cytokine, which has a direct effect on fibroblasts to promote fibroblast division and proliferation and the synthesis and deposition of extracellular matrix (ECM) proteins, and enhances the expression of relevant receptors of ECM, thereby promoting the development of pulmonary fibrosis (12–14). Previous studies have demonstrated that serum cytokine TGF-β1 could be treated as a predictive factor for pulmonary fibrosis. Rubin et al. (15) studied the relationship between serum cytokine TGF-β1 and collagen deposition in C57BL/6 mice treated with a single dose of 12.5-Gy thoracic radiation and found that there was no significant change in TGF-β1 expression at 8 weeks post-irradiation. However, TGF-β1 expression was significantly increased at 8–24 weeks post-irradiation. TGF-β1 also had a positive correlation with collagen deposition. Robb et al. (16) studied the effects of amino acid taurine in attenuating lung fibrosis in C57BL/6 mice treated with a single dose of 14-Gy thoracic radiation and found that amino acid taurine significantly decreased the serum TGF-β1 levels and Hyp content at 14 weeks post-irradiation. In our study, C57BL/6 mice received 12-Gy thoracic radiation and were treated with OP-C by gavage. The expression of serum TGF-β1 was significantly lower in irradiated mice treated with OP-C than in irradiated mice without treatment.

Hyp, which accounts for 13.4% of collagen proteins, is one of the main components of collagen proteins and is not found in other proteins. Moreover, collagen proteins are the main components of pulmonary and hepatic fibrosis. Therefore, Hyp is a sensitive predictive biomarker to determine the levels of pulmonary and hepatic fibrosis (17). Zhou et al. (18) studied the effects of lettuce glycoside B in ameliorating pulmonary fibrosis in Sprague-Dawley rats that received a single dose of 22-Gy whole thoracic radiation and found that treatment with lettuce glycoside B significantly decreased the content of Hyp in irradiated rats compared with that of irradiated rats without treatment, which is similar to reports by Hua You et al. Hua You et al. (19) studied male Sprague-Dawley rats that received a single dose of 22-Gy whole thoracic radiation and found that the irradiated rats administered the green extract epigallocatechin-3-gallate (EGCG) had a significantly decreased Hyp content 120 days post-irradiation compared with that of the irradiated rats without treatment. EGCG treatment significantly inhibited radiation-induced pulmonary fibrosis. In our study, the irradiated mice treated with OP-C had a lower Hyp content compared with that of the irradiated mice without treatment; however, the difference was not statistically significant.

Numerous studies have revealed that ROS and oxidant stress have a direct and indirect impact on radiation-induced pulmonary fibrosis. ROS immediately activate inflammatory cells, including neutrophils, monocytes, and lymphocytes, and lead to a positive feedback loop that increases the expression of oxidative enzymes and the synthesis of ROS. Thus, the balance of oxidant/antioxidant was damaged and the normal tissue damage and deposition of collagen persisted. Certain studies have demonstrated that treatment methods, including defending against and alleviating oxidative stress, could

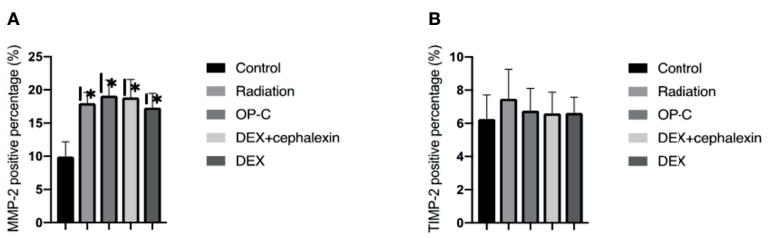

FIGURE 6 | Effects of OP-C on the expression of matrix metalloproteinases-2 (MMP-2) **(A)** and tissue inhibitors of metalloproteases-2 (TIMP-2) in the lungs **(B)**. Expressions of MMP-2 and TIMP-2 in the lungs were measured in mice from the blank control, radiation-only, OP-C, DEX, and DEX + cephalexin groups. The presented data are expressed as the mean ± SEM. *$p < 0.05$, compared with the control group. $^{\#}p < 0.05$, compared with the radiation-only group.

be a promising treatment strategy for ameliorating radiation-induced pulmonary fibrosis. SOD activity and MDA content in serum or lung tissue are crucial and sensitive biomarkers of oxidative stress and the response to oxidative stress. SOD plays a crucial role in maintaining the oxidant/antioxidant balance, which catalyzes and neutralizes the free-radical form of oxygen to generate hydrogen peroxide. MDA content reflects the levels of organic lipid peroxidation, which reveals the degree of cell membrane damage (20–22). Kang et al. (23) studied extracellular SOD-overexpressing B6C3 transgenic mice that received thoracic radiation and demonstrated that the overexpression of extracellular SOD transgenic mice significantly decreased oxidative stress and radiation-induced pulmonary injury compared with irradiated wild-type mice. SOD may be a promising treatment agent for radiation-induced pulmonary injuries. In another study by Pan et al. (24), irradiated Kunming mice received SOD-TAT, a fusion protein of the HIV-1Tat protein transduction domain and hCuZn-SOD, which significantly enhanced the pulmonary antioxidant ability and ameliorated radiation-induced pulmonary fibrosis compared with irradiated mice treated with amifostine and irradiated mice without treatment. Liu et al. (25) studied the protective effects of quercetin liposomes against radiation-induced pulmonary injury and found that irradiated C57BL/6 mice treated with quercetin liposomes had significantly increased SOD activity and decreased MDA content to protect against radiation-induced acute pneumonia and chronic pulmonary fibrosis by reducing oxidative damage compared with irradiated mice without treatment. In our study, irradiated mice treated with OP-C showed significantly increased SOD activity in the lung tissue to relieve pulmonary fibrosis by decreasing the oxidant stress compared with irradiated mice without treatment. However, no significant differences in the expression of MDA content were observed in our study.

The MMP family, a family of zinc-dependent endopeptidases, are highly homologous and possess over 20 family members. CD147, an MMP inducer, is synthesized to increase MMP expression during lung disease development. Certain studies have demonstrated that MMPs play a crucial role in degrading the ECM and remodeling structural proteins, including collagens and elastin. MMPs then restructure normal lung tissue to initiate the pathogenesis of lung diseases. The TIMP family, MMPs' endogenous inhibitors, comprise four related members, namely, TIMP-1, -2,-3, and -4, which lead to dual control to inhibit the active form and activation process of MMPs. The balance, activation, and normal expression of MMPs and TIMPs in normal lung tissue are tightly regulated to prevent harmful effects on normal lung tissue. The upregulation of MMPs and TIMPS is observed in initial lung disease development, lung tissue remodeling, and pulmonary fibrosis (26, 27). MMP-2, a critical member of MMPs, has a high affinity for collagen IV of the basement membrane to degrade type IV and remodel the pulmonary structure. Yang et al. (28) studied the effect of thoracic radiation on the MMP/TIMP system in normal lung tissue and found that thoracic radiation significantly increased the expression of MMP-2 and MMP-9 to degrade collagen IV, thereby damaging the integrity of normal lung tissue. However, the expression of TIMP-1, -2, and -3 in the lungs was not influenced by thoracic radiation. In another study by Rave-Frank et al. (29), rats received a high single-dose irradiation of 25 Gy, and it was found that the expression of MMP-2, -9, and -14, and TIMP-1, -2, and -3 significantly increased shortly after irradiation, however not at 3 months post-irradiation. Similar to this study, the expression of MMP-2 and TIMP-2 at 28 weeks post-irradiation was not significantly different among the irradiated mice without treatment, treated with OP-C, DEX, and DEX + cephalexin in our study.

This study has several limitations. First, this was a prospective study with a small sample size. A larger-scale study is required to validate these findings. Second, few blood samples were collected from C57BL/6 mice by cardiac puncture. Larger mice or rabbits are recommended for further study. Third, this study demonstrated that OP-C significantly ameliorated pulmonary fibrosis. However, the protective effects of OP-C at different doses are warranted in future studies.

CONCLUSION

Overall, the present study demonstrated that OP-C significantly ameliorates radiation-induced pulmonary fibrosis in C57BL/6 mice treated with a single dose of 12-Gy whole thoracic radiation. However, our data demonstrated that OP-C had similar protective effects on pulmonary fibrosis as steroid therapy. No obvious adverse effects were observed in the OP-C treatment. Therefore, OP-C may be a promising therapeutic strategy for this disorder.

DATA AVAILABILITY STATEMENT

The data sets generated during and/or analyzed during the current study are available from the corresponding author on reasonable request.

ETHICS STATEMENT

The animal study was reviewed and approved by The Fujian Cancer Hospital.

AUTHOR CONTRIBUTIONS

All authors listed have made a substantial, direct, and intellectual contribution to the work and approved it for publication.

FUNDING

This study was supported in part by grants from the Fujian Provincial Platform for Medical Laboratory Research and Key Laboratory for Tumor Individualized Active Immunity (Project Number: FYKFKT-2017015).

ACKNOWLEDGMENTS

The authors thank all patients who participated in the present study.

REFERENCES

1. Ferlay J, Colombet M, Soerjomataram I, Mathers C, Parkin DM, Pineros M, et al. Estimating the Global Cancer Incidence and Mortality in 2018: GLOBOCAN Sources and Methods. *Int J Cancer* (2019) 144(8):1941–53. doi: 10.1002/ijc.31937
2. Hanania AN, Mainwaring W, Ghebre YT, Hanania NA, Ludwig M. Radiation-Induced Lung Injury: Assessment and Management. *Chest* (2019) 156(1):150–62. doi: 10.1016/j.chest.2019.03.033
3. Simone CB 2nd. Thoracic Radiation Normal Tissue Injury. *Semin Radiat Oncol* (2017) 27(4):370–7. doi: 10.1016/j.semradonc.2017.04.009
4. He Y, Thummuri D, Zheng G, Okunieff P, Citrin DE, Vujaskovic Z, et al. Cellular Senescence and Radiation-Induced Pulmonary Fibrosis. *Trans Res: J Lab Clin Med* (2019) 2:20914–21. doi: 10.1016/j.trsl.2019.03.006
5. Lierova A, Jelicova M, Nemcova M, Proksova M, Pejchal J, Zarybnicka L, et al. Cytokines and Radiation-Induced Pulmonary Injuries. *J Radiat Res* (2018) 59 (6):709–53. doi: 10.1093/jrr/rry067
6. Chen Z, Wu Z, Ning W. Advances in Molecular Mechanisms and Treatment of Radiation-Induced Pulmonary Fibrosis. *Trans Oncol* (2019) 12(1):162–9. doi: 10.1016/j.tranon.2018.09.009
7. Chen MH, Chen XJ, Wang M, Lin LG, Wang YT. Ophiopogon Japonicus–A Phytochemical, Ethnomedicinal and Pharmacological Review. *J Ethnopharmacol* (2016) 181:193–213. doi: 10.1016/j.jep.2016.01.037
8. Gao GY, Ma J, Lu P, Jiang X, Chang C. Ophiopogonin B Induces the Autophagy and Apoptosis of Colon Cancer Cells by Activating JNK/c-Jun Signaling Pathway. *Biomed Pharmacother = Biomed Pharmacother* (2018) 108:1208–15. doi: 10.1016/j.biopha.2018.06.172
9. Yao QW, Wang XY, Li JC, Zhang J. Ophiopogon Japonicus Inhibits Radiation-Induced Pulmonary Inflammation in Mice. *Ann Trans Med* (2019) 7(22):622–. doi: 10.21037/atm.2019.11.01
10. Ashcroft T, Simpson JM, Timbrell V. Simple Method of Estimating Severity of Pulmonary Fibrosis on a Numerical Scale. *J Clin Pathol* (1988) 41(4):467–70. doi: 10.1136/jcp.41.4.467
11. Lee KH, Rhee KH. Radioprotective Effect of Cyclo(L-Phenylalanyl-L-Prolyl) on Irradiated Rat Lung. *J Microbiol Biotechnol* (2008) 18(2):369–76.
12. Wang S, Campbell J, Stenmark MH, Zhao J, Stanton P, Matuszak MM, et al. Plasma Levels of IL-8 and TGF-Beta1 Predict Radiation-Induced Lung Toxicity in Non-Small Cell Lung Cancer: A Validation Study. *Int J Radiat Oncol Biol Phys* (2017) 98(3):615–21. doi: 10.1016/j.ijrobp.2017.03.011
13. Wei Y, Kim TJ, Peng DH, Duan D, Gibbons DL, Yamauchi M, et al. Fibroblast-Specific Inhibition of TGF-Beta1 Signaling Attenuates Lung and Tumor Fibrosis. *J Clin Invest* (2017) 127(10):3675–88. doi: 10.1172/jci94624
14. Lee CM, Park JW, Cho WK, Zhou Y, Han B, Yoon PO, et al. Modifiers of TGF-Beta1 Effector Function as Novel Therapeutic Targets of Pulmonary Fibrosis. *Korean J Internal Med* (2014) 29(3):281–90. doi: 10.3904/kjim.2014.29.3.281
15. Rubin P, Johnston CJ, Williams JP, McDonald S, Finkelstein JN. A Perpetual Cascade of Cytokines Postirradiation Leads to Pulmonary Fibrosis. *Int J Radiat Oncol Biol Phys* (1995) 33(1):99–109. doi: 10.1016/0360-3016(95) 00095-g
16. Robb WB, Condron C, Moriarty M, Walsh TN, Bouchier-Hayes DJ. Taurine Attenuates Radiation-Induced Lung Fibrosis in C57/Bl6 Fibrosis Prone Mice. *Irish J Med Sci* (2010) 179(1):99–105. doi: 10.1007/s11845-009-0389-2
17. Srivastava AK, Khare P, Nagar HK, Raghuwanshi N, Srivastava R. Hydroxyproline: A Potential Biochemical Marker and Its Role in the Pathogenesis of Different Diseases. *Curr Protein Pept Sci* (2016) 17(6):596–602. doi: 10.2174/1389203717666151201192247
18. Zhou Y, Gao Y, Chen Y, Zheng R, Zhang W, Tan M. Effects of Lettuce Glycoside B in Ameliorating Pulmonary Fibrosis Induced by Irradiation Exposure and its Anti-Oxidative Stress Mechanism. *Cell Biochem Biophys* (2015) 71(2):971–6. doi: 10.1007/s12013-014-0295-8
19. You H, Wei L, Sun WL, Wang L, Yang ZL, Liu Y, et al. The Green Tea Extract Epigallocatechin-3-Gallate Inhibits Irradiation-Induced Pulmonary Fibrosis in Adult Rats. *Int J Mol Med* (2014) 34(1):92–102. doi: 10.3892/ijmm.2014.1745
20. Inghilleri S, Morbini P, Campo I, Zorzetto M, Oggionni T, Pozzi E, et al. Erratum to "Factors Influencing Oxidative Imbalance in Pulmonary Fibrosis: An Immunohistochemical Study". *Pulmonary Med* (2011) 2011:515608. doi: 10.1155/2011/515608
21. Inghilleri S, Morbini P, Campo I, Zorzetto M, Oggionni T, Pozzi E, et al. Factors Influencing Oxidative Imbalance in Pulmonary Fibrosis: An Immunohistochemical Study. *Pulmonary Med* (2011) 2011:421409. doi: 10.1155/2011/421409
22. Brass DM, Spencer JC, Li Z, Potts-Kant E, Reilly SM, Dunkel MK, et al. Retraction: Innate Immune Activation by Inhaled Lipopolysaccharide, Independent of Oxidative Stress, Exacerbates Silica-Induced Pulmonary Fibrosis in Mice. *PloS One* (2016) 11(5):e0155388. doi: 10.1371/journal.pone.0155388
23. Kang SK, Rabbani ZN, Folz RJ, Golson ML, Huang H, Yu D, et al. Overexpression of Extracellular Superoxide Dismutase Protects Mice From Radiation-Induced Lung Injury. *Int J Radiat Oncol Biol Phys* (2003) 57 (4):1056–66. doi: 10.1016/S0360-3016(03)01369-5
24. Pan J, Su Y, Hou X, He H, Liu S, Wu J, et al. Protective Effect of Recombinant Protein SOD-TAT on Radiation-Induced Lung Injury in Mice. *Life Sci* (2012) 91(3-4):89–93. doi: 10.1016/j.lfs.2012.06.003
25. Liu H, Xue JX, Li X, Ao R, Lu Y. Quercetin Liposomes Protect Against Radiation-Induced Pulmonary Injury in a Murine Model. *Oncol Lett* (2013) 6 (2):453–9. doi: 10.3892/ol.2013.1365
26. Hendrix AY, Kheradmand F. The Role of Matrix Metalloproteinases in Development, Repair, and Destruction of the Lungs. *Prog Mol Biol Trans Sci* (2017) 148:1–29. doi: 10.1016/bs.pmbts.2017.04.004
27. Baker AH, Edwards DR, Murphy G. Metalloproteinase Inhibitors: Biological Actions and Therapeutic Opportunities. *J Cell Sci* (2002) 115(Pt 19):3719–27. doi: 10.1242/jcs.00063
28. Yang K, Palm J, Konig J, Seeland U, Rosenkranz S, Feiden W, et al. Matrix-Metallo-Proteinases and Their Tissue Inhibitors in Radiation-Induced Lung Injury. *Int J Radiat Biol* (2007) 83(10):665–76. doi: 10.1080/09553000701558977
29. Rave-Frank M, Malik IA, Christiansen H, Naz N, Sultan S, Amanzada A, et al. Rat Model of Fractionated (2 Gy/day) 60 Gy Irradiation of the Liver: Long-Term Effects. *Radiat Environ Biophys* (2013) 52(3):321–38. doi: 10.1007/s00411-013-0468-7

Conflict of Interest: The authors declare that the research was conducted in the absence of any commercial or financial relationships that could be construed as a potential conflict of interest.

The reviewer YS declared a shared affiliation with two of the authors (XF, TL), with no collaboration to the handling editor at the time of the review.

frontiers in Oncology

ORIGINAL RESEARCH
published: 30 March 2022
doi: 10.3389/fonc.2022.824206

Chemoradiotherapy Versus Chemotherapy Alone for Advanced Esophageal Squamous Cell Carcinoma: The Role of Definitive Radiotherapy for Primary Tumor in the Metastatic Setting

*Li-Qing Li†, Qing-Guo Fu†, Wei-Dong Zhao, Yu-Dan Wang, Wan-Wan Meng and Ting-Shi Su**

Department of Radiation Oncology, Guangxi Medical University Cancer Hospital, Nanning, China

OPEN ACCESS

Edited by:
Li Jiancheng, Fujian Provincial Cancer Hospital, China

Reviewed by:
Yee Ung, University of Toronto, Canada
Yasemin Bolukbasi, Koç University Hospital, Turkey

***Correspondence:**
Ting-Shi Su
sutingshi@163.com

†These authors share first authorship

Specialty section:
This article was submitted to Radiation Oncology, a section of the journal Frontiers in Oncology

Received: *29 November 2021*
Accepted: *28 February 2022*
Published: *30 March 2022*

Citation:
Li L-Q, Fu Q-G, Zhao W-D, Wang Y-D, Meng W-W and Su T-S (2022) Chemoradiotherapy Versus Chemotherapy Alone for Advanced Esophageal Squamous Cell Carcinoma: The Role of Definitive Radiotherapy for Primary Tumor in the Metastatic Setting. Front. Oncol. 12:824206. doi: 10.3389/fonc.2022.824206

Introduction: The role of definitive radiotherapy in advanced esophageal squamous cell carcinoma (ESCC), especially in the metastatic setting, remains unclear. Therefore, we aimed to investigate the efficacy of chemoradiotherapy (CRT) versus chemotherapy (CT) alone in these selected patients.

Methods: We retrospectively evaluated 194 newly diagnosed advanced ESCC who underwent definitive CRT or CT alone, including 97 patients with locally advanced and 97 patients with distant metastatic disease. Cumulative overall survival (OS) and progression-free survival (PFS) were evaluated with a log-rank test. Propensity score matching was used to simulate random allocation. In addition, we performed subgroup analysis in the locally advanced and metastatic disease.

Results: After matching, 63 well-paired patients were selected. The adjusted median OS (12.5 vs. 7.6 months, $p = 0.002$) and PFS (9.0 vs. 4.8 months, $p = 0.0025$) in the CRT group were superior to that in the CT-alone group. Further subgroup analysis revealed that CRT conferred survival benefits to both locally advanced and metastatic cohorts. For patients with distant metastasis, median OS (12.9 vs. 9.3 months, $p = 0.029$) and PFS (9.9 vs. 4.0 months, $p = 0.0032$) in the CRT group were superior to that in the CT-alone group. In a multivariate Cox regression analysis of the entire cohort, additional definitive radiotherapy was independently associated with better OS ($p = 0.041$) and PFS ($p = 0.007$).

Conclusions: In both locally advanced and metastatic ESCC, additional definitive-dose radiotherapy was associated with improved clinical outcomes. Therefore, more consideration should be given to its application in the metastatic setting.

Keywords: esophageal squamous cell carcinoma, advanced, metastatic, chemoradiotherapy, definitive radiotherapy, survival

INTRODUCTION

Esophageal cancer (EC) is the seventh most common cancer worldwide and the sixth leading cause of cancer-related death, with approximately 572,000 patients diagnosed in 2018 (1). The prognosis of metastatic EC is inferior, with a 5-year survival rate lower than 5% (2). Definitive radiotherapy (RT) with a dose greater than or equal to 50.4 Gy to the primary tumor is the mainstay of treatment and provides effective symptomatic relief for locally advanced EC (3–5). Since the RTOG 85-01 study, radical chemoradiotherapy (CRT) with a radiation dose of 50 Gy has been established as a curative treatment paradigm for locally advanced patients without evidence of distant metastasis (6). Subsequent clinical trials have further confirmed the clinical efficacy of this combination regimen (7, 8), which is now the standard first-line regimen for patients with locally advanced EC (9, 10). However, the current guidelines generally do not recommend aggressive radiotherapy for the primary tumor in patients with metastatic EC. The latest Chinese Society of Clinical Oncology guideline recommended only system therapy for metastatic EC (11). In the Pan-Asian adapted ESMO Clinical Practice Guidelines, RT was recommended only for palliative care to relieve patients' dysphagia with metastatic EC (12). Systemic chemotherapy remains the cornerstone treatment for metastatic EC patients, with a median survival time of only 8–12 months (13–15). However, whether combined chemotherapy and aggressive radiotherapy can improve the survival of metastatic esophageal squamous cell carcinoma (ESCC) remains unclear. Therefore, in the present study, we aimed to investigate the efficacy and safety of chemotherapy-based definitive radiotherapy (≥50.4 Gy) in prolonging the survival of patients with advanced ESCC, particularly those with organ metastases.

MATERIALS AND METHODS

Study Design and Patients

We retrospectively reviewed patients with newly diagnosed advanced ESCC who received CRT or CT alone at the Guangxi Medical University Cancer Hospital between June 2010 and May 2020. The institutional ethics committee approved this study, and informed consent was waived by the board. The eligibility criteria were as follows: (1) ESCC confirmed by histology; (2) clinically confirmed advanced disease (stage IVa or IVb) according to the 8th edition AJCC staging system (16); (3) Eastern Cooperative Oncology Group (ECOG) score 0–2; (4) no history of previous thoracic radiotherapy; (5) received definitive-dose (≥50.4Gy) radiotherapy for primary tumor for the CRT cohort; and (6) received no concurrent targeted therapy or immunotherapy.

Chemotherapy and Radiotherapy Treatment

For all patients, two- or three-drug cisplatin-based chemotherapy was administrated at 3-week intervals for up to 6 cycles as first-line therapy. For patients undergoing CRT, definitive-dose radiotherapy was administrated synchronously with 2 to 3 cycles of cisplatin-based chemotherapy. Radiotherapy was performed with intensity-modulated radiotherapy using a 6-MV linear accelerator (Elekta Synergy, Stockholm, Sweden) at five fractions per week. The gross tumor volume (GTV) and metastatic lymph nodes (GTVnd) were delineated with visible lesions based on contrast-enhanced simulation CT, PET, and endoscopic evaluation results. The clinical target volume (CTV) was defined as a 0.5-cm horizontal expansion from GTV/GTVnd, a 3–5-cm craniocaudal margin from GTV, and a 0.5-cm craniocaudal margin from GTVnd. The planning target volume (PTV) was determined by adding a 0.5-cm margin to the CTV. A median total dose of 60 Gy (range, 56–66 Gy) with a median per dose of 2.0 Gy (range, 1.8–2.2 Gy) in a median fraction of 30 (range, 25–33) was prescribed to the PGTV for five consecutive days in a given week. The dose constraints for organs at risk (OARs) were as follows: (1) lung: the whole lung V20 <28%, V30 <20%, and Dmean <15–17 Gy; (2) spinal cord: Dmax <45 Gy; and (3) heart: V40 <30% and Dmean <30 Gy.

Follow-Up and Statistical Analysis

For posttreatment follow-up, enhanced CT and upper gastrointestinal endoscopy were reevaluated 1 month after treatment and every 3 months after that. Progression-free survival (PFS) was defined as the period between the date of initial treatment until disease progression or recurrence or death. Overall survival (OS) was defined as the period from initial therapy to censor or death. OS and PFS rates were evaluated using the Kaplan–Meier method with the log-rank test. Continuous variables were compared with the Student's t-test, while categorical variables were compared with Fisher's exact or Pearson's χ^2 test. We performed multivariate Cox regression analysis to identify clinical variables independently associated with PFS and OS, and factors with $p < 0.05$ in the univariate Cox regression analysis were included. Statistical analysis was undertaken using R version 4.0.2 software, and p-values <0.05 were considered statistically significant.

To minimize potential selection bias and confounders, propensity score matching (PSM) was used to control for differences in baseline characteristics. Using a caliper of width equal to 0.2 without replacement, patients in the entire cohort were matched at a 1:1 ratio to simulate random allocation. Covariates entered into the propensity model included body mass index, ECOG score, TNM stage, number of metastatic sites, absolute neutrophil count, and albumin level. All baseline covariates were balanced in the locally advanced disease and metastatic disease subgroups. Therefore, PSM was not performed in the subgroup analysis.

RESULTS

Patient Characteristics

A total of 194 patients with advanced ESCC were deemed eligible and assessed. Among them, 97 patients (50%) were locally

advanced, and 97 patients (50%) had distant metastasis. The majority of patients with distant metastasis had a low systemic tumor burden. Seventy-seven (79.4%) patients had only one metastatic site (40.2%, 16.9%, 14.3%, 14.3%, and 14.3% of these patients presented with metastasis in the non-regional lymph node, lung, liver, bone, and others, respectively), and 14 (14.4%) patients had two metastatic sites. Merely 6 (6.2%) patients had at least three or more metastatic sites. A total of 101 patients (52.1%) received CRT, and 93 patients (47.9%) received CT alone. The median cycles of chemotherapy for the entire cohort were 3 (1–6 cycles). Before propensity score matching, patients in the CT-alone group had significantly worse baseline characteristics compared to those in the CRT group, with a lower body mass index (mean 20.3 vs. 21.5 kg/m^2, p = 0.01), poorer physical performance (ECOG score 2: 8.6% vs. 0%, p = 0.011), greater tumor burden (stage IVb: 65.6% vs. 35.6%, p = 0.000, and distant metastatic sites ≥3: 6.4% vs. 0%, p = 0.001), lower absolute neutrophil count (mean 5.9 vs. 5.1 × 10^9/l, p = 0.022), and lower albumin level (mean 35.5 vs. 36.7 g/l, p = 0.047). After matching, 63 well-paired patients were selected. There were no significant differences between the CRT group and the CT-alone group in baseline characteristics after PSM, as shown in **Table 1**.

Overall Survival and Progression-Free Survival

The median follow-up time was 32.2 months. At the end date of follow-up, 136 (70.1%) patients died and 58 (29.9%) patients were right-censored. Before matching, the median OS and rates of OS at 6, 12, 24, and 60 months were superior in the CRT group to that in the CT group (12.2 months [95% CI, 9.0–15.3], 84.1%,

TABLE 1 | Patient characteristics before and after PSM in the CRT and CT alone groups.

		Before PSM			After PSM		
Factor	**Level**	**CT (n = 93)**	**CRT (n = 101)**	**p**	**CT (n = 63)**	**CRT (n = 63)**	**p**
Gender	Male	86	91	0.741	58	57	1.000
	Female	7	10		5	6	
Age (yrs, mean ± SD)		57.4 (± 0.9)	56.1 (± 0.9)	0.298	56.3 (± 1.0)	55.0 (± 1.1)	0.149
BMI (m^2/kg, mean ± SD)		20.3 (± 0.3)	21.5 (± 0.3)	0.010	20.8 (± 0.4)	21.0 (± 0.3)	0.687
ECOG	0	8	10	0.011	5	3	0.715
	1	77	91		58	60	
	2	8	0				
Smoking	No	25	38	0.149	17	23	0.339
	Yes	68	63		46	40	
Drinking	No	25	32	0.565	17	22	0.441
	Yes	68	69		46	41	
Family history	No	89	92	0.320	61	59	0.676
	Yes	4	9		2	4	
T stage	2	6	4	1.146	3	1	0.457
	3	26	18		17	14	
	4	61	79		43	48	
N stage	1	31	36	1.140	21	24	0.310
	2	40	52		30	33	
	3	22	13		12	6	
Number of metastatic sites	0	32	65	0.001	30	35	0.669
	1	48	29		28	24	
	2	7	7		5	4	
	≥3	6	0		0	0	
TNM stage	IVa	32	65	0.000	30	35	1.000
	IVb	61	36		33	28	
Tumor location	Up	20	29	0.114	11	16	0.271
	Middle	46	57		34	36	
	Down	27	14		16	11	
	Multiple lesions	2	1		2	0	
HBG (g/L, mean ± SD)		123.1 (± 1.6)	123.3 (± 1.8)	0.920	122.1 (± 1.9)	124.3 (± 2.2)	0.450
PLT (109/L, mean ± SD)		318.9 (± 11.1)	302.8 (± 8.3)	0.248	300.2 (± 12.4)	318.8 (± 12.2)	0.288
NEU (109/L, mean ± SD)		5.9 (± 0.3)	5.1 (± 0.2)	0.022	5.4 (± 0.3)	5.2 (± 0.3)	0.691
LYMPH (10^9/L, mean ± SD)		1.9 (± 0.1)	2.0 (± 0.2)	0.573	2.0 (± 0.2)	1.8 (± 0.1)	0.338
ALB (g/L, mean ± SD)		35.5 (± 0.5)	36.7 (± 0.4)	0.047	36.8 (± 0.6)	37.7 (± 0.6)	0.248
AST (U/L, mean ± SD)		17.1 (± 1.1)	17.2 (± 1.0)	0.973	18.1 (± 1.7)	17.2 (± 1.4)	0.670
ALT (U/L, mean ± SD)		25.2 (± 1.6)	22.7 (± 0.8)	0.159	26.4 (± 2.4)	22.3 (± 1.0)	0.118
Urea (mmol/L, mean ± SD)		4.8 (± 0.2)	4.7 (± 0.0)	0.786	4.7 (± 0.2)	4.5 (± 0.2)	0.517
Creatinine (μmol/L, mean ± SD)		78.3 (± 2.5)	76.9 (± 1.4)	0.630	78.1 (± 3.1)	76.1 (± 1.8)	0.589
Chemotherapy cycle	≤3	62	57	0.144	43	35	0.142
	>3	31	44		20	28	

BMI, body mass index; ECOG score, Eastern Cooperative Oncology Group; WBC, white blood cell counts; HGB, hemoglobin level; PLT, blood platelet count; NEU, absolute neutrophil count; LYMPH, absolute lymphocyte count; ALB, albumin level; ALT, alanine aminotransferase level; AST, aspartate aminotransferase level.

50.8%, 29.0%, 17.9% vs. 8.2 months [95% CI, 5.4–11.1], 66.0%, 38.3%, 9.1%, 0%, p = 0.00039, **Figure 1A**). The median PFS and rates of PFS at 6, 12, 24, and 60 months were also superior in the CRT group to that in the CT group (9.4 months [95% CI, 8.0–10.8], 69.5%, 38.1%, 19.2%, 13.1% vs. 4.7 months [95% CI, 3.5–5.9], 36.6%, 22.4%, 4.1%, 0%, $p < 0.0001$, **Figure 1B**).

Adjusting for all baseline factors also demonstrated significant differences between the CRT group and CT group in PFS and OS. The median OS and rates of OS at 6, 12, 24, and 60 months remained superior in the CRT group to that in the CT group (12.5 months [95% CI, 7.1–18.0], 85.9%, 47.4%, 23.4%, 17.3% vs. 7.6 months [95% CI, 5.4–9.8], 63.6%, 39.4%, 7.3%, 0%, p = 0.002, **Figure 2A**). The median PFS and rates of PFS at 6, 12, 24, and 60 months also remained superior in the CRT group to that in the CT group (9.0 months [95% CI, 7.6–10.5], 70.9%, 36.5%, 19.7%, 12.9% vs. 4.8 months [95% CI,4.0–5.6], 39.1%, 22.7%, 3.8%, 3.8%, p = 0.0025, **Figure 2B**).

Subgroup Analysis of Locally Advanced Disease

In patients with locally advanced ESCC, the survival outcome of the CRT group was significantly better than that of the CT group. The median OS and rates of OS at 6, 12, 24, and 60 months were superior in the CRT group to that in the CT group (10.5 months [95% CI, 7.3–13.7], 79.8%, 46.6%, 29.8%, 18.9% vs. 7.6 months [95% CI, 5.9–9.3], 65.4%, 30.3%, 4.3%, 0%, p = 0.0029, **Figure 3A**). The median PFS and rates of PFS at 6, 12, 24, and 60 months were also superior in the CRT group to that in the CT group (8.9 months [95% CI, 6.9–10.9], 65.7%, 37.3%, 22.0%, 16.0% vs. 5.4 months [95% CI, 3.8–7.0], 42.8%, 25.0%, 4.5, 0%, p = 0.0098, **Figure 3B**).

Subgroup Analysis of Metastatic Disease

CRT also conferred survival benefit to ESCC patients with distant metastasis. The median OS and rates of OS at 6, 12, 24, and 60 months were superior in the CRT group to that in the CT group (12.9 months [95% CI, 10.2–15.7], 91.4%, 58.0%, 28.1%, 17.6% vs. 9.3 months [95% CI, 5.7–13.0], 66.6%, 42.8%, 12.2%, 8.2%, p = 0.029, **Figure 4A**). The median PFS and rates of PFS at 6, 12, 24, and 60 months were also superior in the CRT group to that in the CT group (9.9 months [95% CI, 7.9–11.9], 76.5%, 39.9%, 14.7%, 9.8% vs. 4.0 months [95% CI, 2.4–5.7], 33.4%, 20.8%, 3.7%, 3.7%, p = 0.0032, **Figure 4B**).

Survival Analyses on Patients With Locally Advanced and Metastatic Disease

In the entire cohort, both OS (p = 0.75, **Supplementary Figure S1A**) and PFS (p = 0.1, **Supplementary Figure S1B**) did not differ significantly between patients with locally advanced disease and metastatic disease. Similarly, subgroup analysis based on treatment also showed no significant difference in OS (CRT subgroup: p = 0.97, **Supplementary Figure S2A**, CT-alone subgroup: p = 0.28, **Supplementary Figure S2B**) and PFS (CRT subgroup: p = 0.97, **Supplementary Figure S3A**, CT-alone subgroup: p = 0.5, **Supplementary Figure S3B**) between patients with locally advanced disease and metastatic disease.

Univariate and Multivariate Analysis for Prognostic Factors

Univariable and multivariable Cox analyses for OS and PFS of the entire cohort before PSM are shown in **Supplementary Table S1**. On multivariable analysis of the whole cohort before matching, additional RT, albumin levels, absolute neutrophil count, and chemotherapy cycle were independent prognostic factors for both OS (p = 0.041, p = 0.000, p = 0.001, and p = 0.002, respectively) and PFS (p = 0.007, p = 0.02, p = 0.02, and p = 0.000, respectively). At the same time, the N stage and number of metastatic independently predicted only PFS (p = 0.015 and p = 0.007, respectively).

Treatment Toxicities

Early toxicities that occurred in CRT and CT-alone cohorts were assessed according to the National Cancer Institute Common Toxicity Criteria for Adverse Events, version 4.0 (CTCAE 4.0) (17). The most common adverse events (grades 1–2) of the entire cohort were dysphagia, fatigue, anorexia, nausea, vomit, and hematological toxicities.

Fourteen (22.2%) patients had grade ≥3 radiation esophagitis in the matched CRT group. One (1.6%) patient developed grade 3 radiation pneumonitis 4 months after RT. One (1.6%) patient

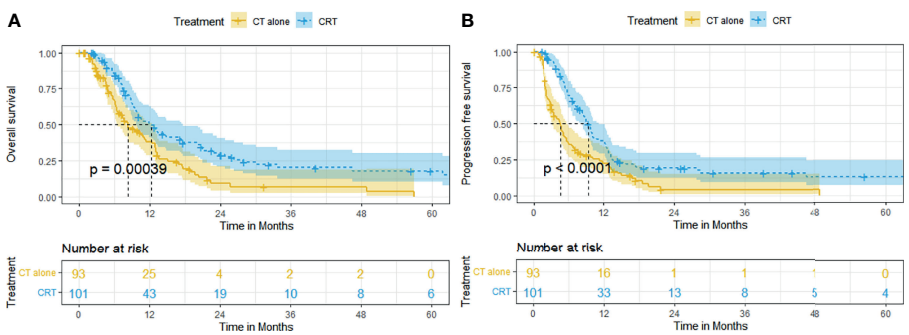

FIGURE 1 | Kaplan–Meier curves of survival in patients with advanced ESCC treated with CRT and CT before PSM: **(A)** overall survival before PSM; **(B)** progression-free survival before PSM.

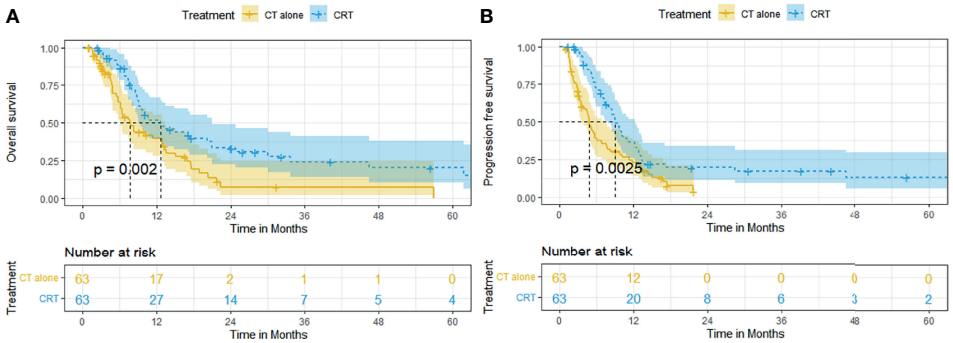

FIGURE 2 | Kaplan–Meier curves of survival in patients with advanced ESCC treated with CRT and CT after PSM: **(A)** overall survival after PSM; **(B)** progression-free survival after PSM.

developed grade 5 upper GI bleeding, and one (1.6%) patient developed grade 3 upper esophageal fistula, both at 3 months after RT. No patient experienced grade ≥3 radiation dermatitis. Twenty-three (36.5%) patients had grade ≥3 leukopenia, 21 (33.3%) had grade ≥3 neutropenia, 8 (12.7%) had grade ≥3 anemia, and 4 (6.4%) had grade ≥3 thrombocytopenia.

In the matched CT-alone group, esophageal fistula occurred in 1 (1.6%) patient after one cycle of CT. Two patients (3.2%) developed grade 3 and 5 upper gastrointestinal bleeding after 2 and 3 cycles of CT, respectively. Four (6.3%) patients had grade ≥3 leukopenia, 6 (9.5%) had grade ≥3 neutropenia, 6 (9.5%) had grade ≥3 anemia, and no patient had grade ≥3 thrombocytopenia.

Patients receiving CRT had a significantly higher incidence of grade ≥3 leukopenia (p = 0.000), neutropenia (p = 0.000), and thrombocytopenia (p = 0.006).

DISCUSSION

The current study showed that combined definitive dose RT (≥50.4) to the primary tumor with chemotherapy resulted in better OS and PFS than chemotherapy alone in advanced ESCC, even in the presence of metastatic disease, with manageable toxicities. In terms of metastatic EC, extended survival after definitive CRT has been reported by several previous studies. A prospective randomized phase 2 study demonstrated that the CRT was associated with significantly improved median PFS (9.3 vs. 4.7 months, p = 0.021) and median OS (18.3 vs. 10.2 months, p = 0.001) than CT alone (18). Moreno et al. (19) also suggested that additional RT could derive better survival compared to CT alone with extended 2- and 5-year OS of 6.4% and 2.7%, respectively (p <.001). In a large cohort of 12,683 patients with metastatic EC, Guttmann et al. (13) reported that definitive-dose (≥50.4 Gy) CRT was associated with superior survival compared to CT alone (median OS 8.3 vs. 11.3 months). As shown in **Table 2**, the clinical survival outcomes of the metastatic population in this study were highly consistent with those of previous studies (13, 18–21).

In the current study, most (93.8%) patients with metastatic disease had only one or two metastatic sites. We found no statistical difference in survival results between the locally advanced disease and metastatic disease. These results highlight that for advanced ESCC patients with low systemic tumor load, survival is most threatened by the failure of local control of the primary tumor. On the one hand, additional RT for primary tumor can effectively shrink the primary tumor and

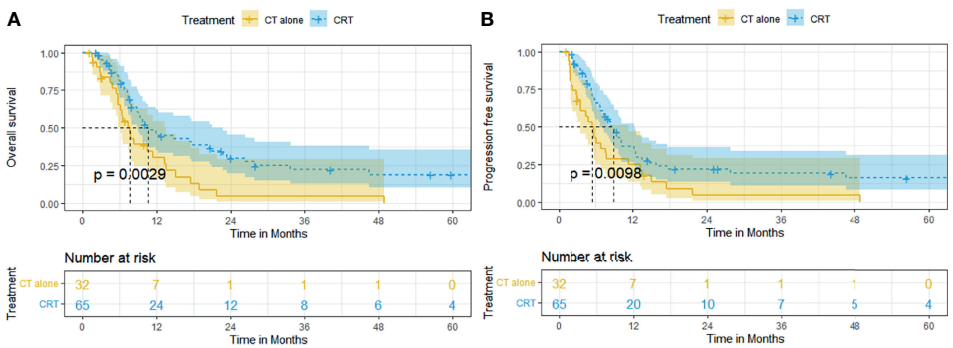

FIGURE 3 | Kaplan–Meier curves of survival in patients with locally advanced ESCC treated with CRT and CT: **(A)** overall survival; **(B)** progression-free survival.

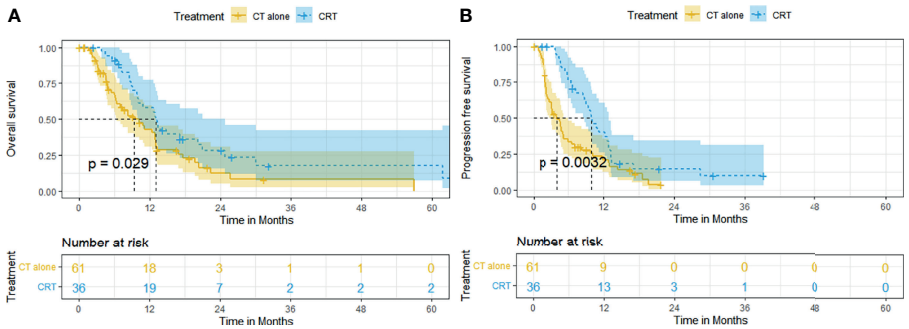

FIGURE 4 | Kaplan–Meier curves of survival in patients with metastatic ESCC treated with CRT and CT: **(A)** overall survival; **(B)** progression-free survival.

reduce dysphagia resulting from esophageal stricture. By increasing oral nutritional intake, RT may improve response rates, performance status, and long-term survival (22, 23). In the current study, multivariate analysis revealed that albumin level (p = 0.000) before treatment was an independent prognostic factor for OS, further illustrating the importance of the nutritional state for patients with advanced EC. On the other hand, aggressive RT for primary tumor can reduce life-threatening events, including airway stenosis either by external compression or by direct tumor growth into the airways, fistula, perforation, and massive bleeding. It is reported that external beam RT could provide significantly more effective relief of pain and tumor-related complications for metastatic EC compared to esophageal stent placement (5).

Based on modern radiotherapy techniques, definitive RT (≥50.4) to the primary tumor may confer more significant survival benefits than palliative RT (≤50.4 Gy) in patients with advanced EC. In the palliative setting, low-dose radiotherapy of less than 50.4 Gy is commonly used to relieve symptoms such as dysphagia, pain, and bleeding (5). However, the toxicity resulting from low-dose radiotherapy with chemotherapy may overweight the clinical benefit it confers. In a phase 3 randomized controlled trial, concurrent palliative RT (20 Gy in 5 fractions or 30 Gy in 10 fractions) did not derive additional benefit on survival for advanced EC patients with self-expanding metal stent placement (median OS: 19.7 weeks with usual care vs. 18.9 weeks with EBRT, p = 0.07) (24). Another multicenter randomized controlled trial (TROG 03.01) also indicated that palliative CRT (30–35 Gy in 10–15 fractions) failed to significantly relieve dysphagia and prolong survival (median OS: 6.9 vs. 6.7 months, p = 0.88) compared to RT alone, with increased toxicity (grade 3–4 acute toxicity: 36% vs. 16%, p = 0.0017) (25). Guttmann et al. (13) reported that compared to CT alone, definitive-dose (≥50.4 Gy) CRT was associated with superior survival (median OS 11.2 vs. 8.4 months, $p \leq 0.001$), while palliative dose (<50.4 Gy) CRT was associated with slightly inferior outcomes (median OS: 7.6 vs. 8.4 months, p = 0.004).

In the current study, patients in the definitive CRT group received a high radiation dose of 56–66 Gy, with most patients receiving radiation dose ≥60 Gy (97 in 101, 96%). The precise dose of definitive RT remains controversial. The landmark RTOG94-05 trial (26) failed to demonstrate the superiority of high-dose (64.8 Gy) over conventional-dose (50.4) concurrent CRT, providing a theoretical basis for the standard RT paradigm for EC in Europe and America (10). According to this study, high-dose RT was not able to increase survival time (median OS:

TABLE 2 | Definitive radiotherapy combined with chemotherapy versus chemotherapy alone for metastatic esophageal cancer.

Authors	Study design	Number of cases		Chemotherapy cycles	RT prescription, Gy	OS		Median PFS (m)	Median OS (m)
						1 y (%)	2 y (%)		
Li et al. (18)	Prospective	CT	30	Mean 3.6	NA	46.6	26.7	4.7	10.2
		CRT	30	Mean 3.8	Median 54.7 (range:50–61)	73.3	43.3	9.3	18.3
Guttmann et al. (13)	Retrospective	CT	7229	NA	NA	34	12	NA	8.4
		CRT	2409	NA	>50.4	47	19	NA	11.2
Moreno et al. (19)	Retrospective	CT	NA	NA	NA	NA	12.4	NA	NA
		CRT	NA	NA	40–60	NA	18.8	NA	NA
Lyu et al. (20)	Retrospective	CT	86	31.4%>2	NA	43	14	6	11
		CRT	55	36.4%>2	Median 56.4 (range: 50–66)	58	25.5	8	14
Xu et al. (21)	Retrospective	Non-RT	327	NA	NA	NA	NA	NA	6
		RT	327	NA	NA	NA	NA	NA	10
Present study	Retrospective	CT	61	Median 3	NA	42.8	12.2	4.0	9.3
		CRT	36	Median 3	Median 60 (range: 50–66)	58.0	28.1	9.9	12.9

NA, not applicable.

13.0 vs. 18.1 months, $p > 0.05$) and regional control (56% vs. 52%, $p > 0.05$), but rather it seemed to increase the toxicity and higher treatment-related mortality rate. Notably, patients with squamous cell carcinoma account for the vast majority of the participants in this trial. Differently, radiation doses above 60 Gy are more frequently adopted in Asia. Several studies proposed that high-dose concurrent CRT of ≥60Gy could improve clinical outcomes compared with standard dose (50–54 Gy) in EC (27, 28), especially ESCC. A pooled analysis reported that in cisplatin-based definitive concurrent CRT, high-dose RT (≥60 Gy) was associated with significantly higher local regional recurrent rates (22% vs. 30%, p = 0.01) and distant failure rates (13% vs. 25%, $p < 0.000$) compared with conventional-dose RT (50–54 Gy) in ESCC patients (27). However, according to the ARTDECO study, an increase in RT dose to 61.6 Gy did not result in better local control over 50.4 Gy for both adenocarcinoma and squamous cell carcinoma (29). The optimal radiation dose of definitive CRT for EC merits further investigation, especially in a metastatic setting.

Safety findings in the current study were consistent with the known safety profile of CRT and CT alone (30–32). Significantly higher incidences of grade ≥3 hematological toxicities were observed in patients treated with CRT. What is more, additional definitive RT has led to severe radiation-related toxicities such as radiation esophagitis in certain patients, but with an acceptable incidence rate (14/63, 22.3%). Advancement of modern RT techniques, such as intensity-modulated RT (IMRT), volume modulated arc therapy (VMAT), and image-guided RT (IGRT), has improved the safety of definitive RT with precise radiation delivery while reducing the dose to organ at risk. Therefore, standard CRT may be a better option in well-selected metastatic ESCC patients who are in good general condition and had low burden of distant metastases. It should be considered after patients are fully informed of the risk benefits.

In the rapid development of immunotherapeutic strategies, local radiotherapy may play a more significant role in metastatic EC. Anti-programmed death 1 (PD-1)/programmed death ligand-1 (PD-L1) therapies are currently the research hotspot and have demonstrated durable antitumor activity in patients with advanced EC (32–34). According to the recently published ESCORT-1st randomized clinical trial, camrelizumab combined with chemotherapy significantly improved OS (15.3 vs. 12.0 months, $p = 0.001$) and PFS (6.9 vs. 5.6 months, $p <; 0.001$) compared with chemotherapy alone as first-line treatment in patients with advanced ESCC (14). As previously demonstrated in various cancers (such as non-small cell lung cancer (NSCLC) and metastatic melanoma), the combination of radiotherapy and immune checkpoint inhibitors could promote systemic antitumor immunity and abscopal effect (35, 36). This novel approach also represents an effective therapeutic option in advanced EC, and pertinent clinical trials are currently ongoing (37). A phase 3 study (KEYNOTE-975) of definitive CRT plus pembrolizumab in advanced EC is now in the recruiting phase (NCT04210115). The dual primary endpoints are OS and event-free survival, which is highly anticipated (38).

The present study had several limitations. Firstly, propensity score matching was used to reduce selection bias in this study. However, this led to the selection of patients and thereby decreased the sample size. Secondly, due to the retrospective nature of this study, data on quality of life were not available to us. Thirdly, we did not consider the changes in objective factors during the long-term period, such as increased applications of PET-CT, radiotherapy techniques, and chemotherapy regimens.

In conclusion, additional definitive-dose radiotherapy was associated with improved clinical outcomes in locally advanced and metastatic ESCC. Therefore, more consideration should be given to its application in the metastatic setting.

DATA AVAILABILITY STATEMENT

The original contributions presented in the study are included in the article/**Supplementary Material**. Further inquiries can be directed to the corresponding author.

ETHICS STATEMENT

The studies involving human participants were reviewed and approved by the Institutional Ethics Committee of Guangxi Medical University Cancer Hospital. The ethics committee waived the requirement of written informed consent for participation.

AUTHOR CONTRIBUTIONS

Data curation: L-QL, Y-DW, and W-DZ, W-WM. Formal analysis: L-QL and Q-GF. Writing—original draft: L-QL and Q-GF. Writing—review and editing: T-SS. Funding acquisition: T-SS. All authors contributed to the article and approved the submitted version.

FUNDING

This research was supported in part by the Guangxi Natural Science Foundation (CN) (2020GXNSFAA297171), China International Medical Foundation-Tumor Precise Radiotherapy Spark Program (2019-N-11-01), Guangxi Medical University Training Program for Distinguished Young Scholars, and Guangxi BaGui Scholars' Special Fund.

SUPPLEMENTARY MATERIAL

The Supplementary Material for this article can be found online at: https://www.frontiersin.org/articles/10.3389/fonc.2022.824206/full#supplementary-material

REFERENCES

1. Bray F, Ferlay J, Soerjomataram I, Siegel RL, Torre LA, Jemal A. Global Cancer Statistics 2018: GLOBOCAN Estimates of Incidence and Mortality Worldwide for 36 Cancers in 185 Countries. *CA Cancer J Clin* (2018) 68 (6):394–424. doi: 10.3322/caac.21492
2. Tanaka T, Fujita H, Matono S, Nagano T, Nishimura K, Murata K, et al. Outcomes of Multimodality Therapy for Stage IVB Esophageal Cancer With Distant Organ Metastasis (M1-Org). *Dis Esophagus* (2010) 23(8):646–51. doi: 10.1111/j.1442-2050.2010.01069.x
3. Jeene PM, Vermeulen BD, Rozema T, Braam PM, Lips I, Muller K, et al. Short-Course External Beam Radiotherapy Versus Brachytherapy for Palliation of Dysphagia in Esophageal Cancer: A Matched Comparison of Two Prospective Trials. *J Thorac Oncol* (2020) 15(8):1361–8. doi: 10.1016/j.jtho.2020.04.032
4. Deressa BT, Tigeneh W, Bogale N, Buwenge M, Morganti AG, Farina E. Short-Course 2-Dimensional Radiation Therapy in the Palliative Treatment of Esophageal Cancer in a Developing Country: A Phase II Study (Sharon Project). *Int J Radiat Oncol Biol Phys* (2020) 106(1):67–72. doi: 10.1016/j.ijrobp.2019.10.004
5. Martin EJ, Bruggeman AR, Nalawade VV, Sarkar RR, Qiao EM, Rose BS, et al. Palliative Radiotherapy Versus Esophageal Stent Placement in the Management of Patients With Metastatic Esophageal Cancer. *J Natl Compr Canc Netw* (2020) 18(5):569–74. doi: 10.6004/jnccn.2019.7524
6. Cooper JS, Guo MD, Herskovic A, Macdonald JS, Martenson JA Jr, Al-Sarraf M, et al. Chemoradiotherapy of Locally Advanced Esophageal Cancer: Long-Term Follow-Up of a Prospective Randomized Trial (RTOG 85-01). Radiation Therapy Oncology Group. *JAMA* (1999) 281(17):1623–7. doi: 10.1001/jama.281.17.1623
7. Stahl M, Wilke H, Lehmann N, Stuschke M. Long-Term Results of a Phase III Study Investigating Chemoradiation With and Without Surgery in Locally Advanced Squamous Cell Carcinoma (LA-SCC) of the Esophagus. *J Clin Oncol* (2008) 26(15):431–6. doi: 10.1200/jco.2008.26.15_suppl.4530
8. Bedenne L, Michel P, Bouché O, Milan C, Binquet C. Chemoradiation Followed by Surgery Compared With Chemoradiation Alone in Squamous Cancer of the Esophagus: FFCD 9102. *J Clin Oncol* (2007) 25(10):1160–8. doi: 10.1200/JCO.2005.04.7118
9. Shah MA, Kennedy EB, Catenacci DV, Deighton DC, Goodman KA, Malhotra NK, et al. Treatment of Locally Advanced Esophageal Carcinoma: ASCO Guideline. *J Clin Oncol* (2020) 38(23):2677–94. doi: 10.1200/JCO.20.00866
10. Ajani JA, D'Amico TA, Bentrem DJ, Chao J, Corvera C, Das P, et al. Esophageal and Esophagogastric Junction Cancers, Version 2.2019, NCCN Clinical Practice Guidelines in Oncology. *J Natl Compr Canc Netw* (2019) 17 (7):855–83. doi: 10.6004/jnccn.2019.0033
11. Chen K, Fan Q, Fang W, Fu J, Han Y, Hu B, et al. *Guidelines of Chinese Society of Chinical Oncology(CSCO):Esophageal Cancer*. Available at: http://meeting.csco.org.cn/MUser/M/1?returnurl=http://www.csco.org.cn/cn/index.aspx.
12. Muro K, Lordick F, Tsushima T, Pentheroudakis G, Baba E, Lu Z, et al. Pan-Asian Adapted ESMO Clinical Practice Guidelines for the Management of Patients With Metastatic Oesophageal Cancer: A JSMO-ESMO Initiative Endorsed by CSCO, KSMO, MOS, SSO and TOS. *Ann Oncol* (2019) 30 (1):34–43. doi: 10.1093/annonc/mdy498
13. Guttmann DM, Mitra N, Bekelman J, Metz JM, Plastaras J, Feng W, et al. Improved Overall Survival With Aggressive Primary Tumor Radiotherapy for Patients With Metastatic Esophageal Cancer. *J Thorac Oncol* (2017) 12 (7):1131–42. doi: 10.1016/j.jtho.2017.03.026
14. Luo H, Lu J, Bai Y, Mao T, Wang J, Fan Q, et al. Effect of Camrelizumab vs Placebo Added to Chemotherapy on Survival and Progression-Free Survival in Patients With Advanced or Metastatic Esophageal Squamous Cell Carcinoma: The ESCORT-1st Randomized Clinical Trial. *JAMA* (2021) 326 (10):916–25. doi: 10.1001/jama.2021.12836
15. Forde PM, Kelly RJ. Chemotherapeutic and Targeted Strategies for Locally Advanced and Metastatic Esophageal Cancer. *J Thorac Oncol* (2013) 8(6):673–84. doi: 10.1097/JTO.0b013e31828b5172
16. Rice TW, Ishwaran H, Blackstone EH, Hofstetter WL, Kelsen DP, Apperson-Hansen C, et al. Recommendations for Clinical Staging (cTNM) of Cancer of the Esophagus and Esophagogastric Junction for the 8th Edition AJCC/UICC Staging Manuals. *Dis Esophagus* (2016) 29(8):913–9. doi: 10.1111/dote.12540
17. National Cancer Institute. Common Terminology Criteria for Adverse Events (CTCAE) Version 4.0. *US Department of Health and Human Services* (2009) no. 09-5410. Available at: https://evs.nci.nih.gov/ftp1/CTCAE/CTCAE_4.03/CTCAE_4.03_2010-06-1_QuickReference_5x7.pdf.
18. Li T, Lv J, Li F, Diao P, Wang J, Li C, et al. Prospective Randomized Phase 2 Study of Concurrent Chemoradiation Therapy (CCRT) Versus Chemotherapy Alone in Stage IV Esophageal Squamous Cell Carcinoma (ESCC). *Int J Radiat Oncol Biol Phys* (2016) 96(2):4050. doi: 10.1016/j.ijrobp.2016.06.020
19. Moreno AC, Zhang N, Giordano S, Komaki RU, Liao Z, Nguyen QN, et al. Comparative Effectiveness of Chemotherapy Alone Versus Chemotherapy and Radiation Therapy for Patients With Stage IV Esophageal Cancer. *Int J Radiat Oncol Biol Phys* (2017) 99(2):E172–E3. doi: 10.1016/j.ijrobp.2017.06.1014
20. Lyu J, Li T, Wang Q, Li F, Diao P, Liu L, et al. Outcomes of Concurrent Chemoradiotherapy Versus Chemotherapy Alone for Stage IV Esophageal Squamous Cell Carcinoma: A Retrospective Controlled Study. *Radiat Oncol* (2018) 13(1):233. doi: 10.1186/s13014-018-1183-y
21. Xu J, Lu D, Zhang L, Li J, Sun G. Palliative Resection or Radiation of Primary Tumor Prolonged Survival for Metastatic Esophageal Cancer. *Cancer Med* (2019) 8(17):7253–64. doi: 10.1002/cam4.2609
22. Mendes J, Alves P, Amaral TF. Comparison of Nutritional Status Assessment Parameters in Predicting Length of Hospital Stay in Cancer Patients. *Clin Nutr* (2014) 33(3):466–70. doi: 10.1016/j.clnu.2013.06.016
23. Cotogni P, Pedrazzoli P, De Waele E, Aprile G, Farina G, Stragliotto S, et al. Nutritional Therapy in Cancer Patients Receiving Chemoradiotherapy: Should We Need Stronger Recommendations to Act for Improving Outcomes? *J Cancer* (2019) 10(18):4318–25. doi: 10.7150/jca.31611
24. Adamson D, Byrne A, Porter C, Blazeby J, Griffiths G, Nelson A, et al. Palliative Radiotherapy After Oesophageal Cancer Stenting (ROCS): A Multicentre, Open-Label, Phase 3 Randomised Controlled Trial. *Lancet Gastroenterol Hepatol* (2021) 6(4):292–303. doi: 10.1016/S2468-1253(21)00004-2
25. Penniment MG, De Ieso PB, Harvey JA, Stephens S, Au HJ, O'Callaghan CJ, et al. Palliative Chemoradiotherapy Versus Radiotherapy Alone for Dysphagia in Advanced Oesophageal Cancer: A Multicentre Randomised Controlled Trial (TROG 03.01). *Lancet Gastroenterol Hepatol* (2018) 3(2):114–24. doi: 10.1016/S2468-1253(17)30363-1
26. Minsky BD, Pajak TF, Ginsberg RJ, Pisansky TM, Martenson J, Komaki R, et al. INT 0123 (Radiation Therapy Oncology Group 94-05) Phase III Trial of Combined-Modality Therapy for Esophageal Cancer: High-Dose Versus Standard-Dose Radiation Therapy. *J Clin Oncol* (2002) 20(5):1167–74. doi: 10.1200/JCO.2002.20.5.1167
27. Song T, Liang X, Fang M, Wu S. High-Dose Versus Conventional-Dose Irradiation in Cisplatin-Based Definitive Concurrent Chemoradiotherapy for Esophageal Cancer: A Systematic Review and Pooled Analysis. *Expert Rev Anticancer Ther* (2015) 15(10):1157–69. doi: 10.1586/14737140.2015.1074041
28. Luo HS, Huang HC, Lin LX. Effect of Modern High-Dose Versus Standard-Dose Radiation in Definitive Concurrent Chemo-Radiotherapy on Outcome of Esophageal Squamous Cell Cancer: A Meta-Analysis. *Radiat Oncol* (2019) 14(1):178. doi: 10.1186/s13014-019-1386-x
29. Hulshof M, Geijsen ED, Rozema T, Oppedijk V, Buijsen J, Neelis KJ, et al. Randomized Study on Dose Escalation in Definitive Chemoradiation for Patients With Locally Advanced Esophageal Cancer (ARTDECO Study). *J Clin Oncol* (2021) 39(25):2816–24. doi: 10.1200/JCO.20.03697
30. Hironaka S, Komori A, Machida R, Ito Y, Takeuchi H, Ogawa G, et al. The Association of Primary Tumor Site With Acute Adverse Event and Efficacy of Definitive Chemoradiotherapy for Cstage II/III Esophageal Cancer: An Exploratory Analysis of JCOG0909. *Esophagus* (2020) 17(4):417–24. doi: 10.1007/s10388-020-00741-w
31. Song T, Zhang X, Fang M, Zhao R, Wu S. Long-Term Results of Definitive Concurrent Chemoradiotherapy Using Paclitaxel Plus Oxaliplatin in Unresectable Locally Advanced Esophageal Cancer: A Prospective Phase II Trial. *Cancer Med* (2016) 5(12):3371–7. doi: 10.1002/cam4.897
32. Kojima T, Shah MA, Muro K, Francois E, Adenis A, Hsu CH, et al. Randomized Phase III KEYNOTE-181 Study of Pembrolizumab Versus Chemotherapy in Advanced Esophageal Cancer. *J Clin Oncol* (2020) 38 (35):4138–48. doi: 10.1200/JCO.20.01888

33. Kato K, Shah MA, Enzinger P, Bennouna J, Shen L, Adenis A, et al. KEYNOTE-590: Phase III Study of First-Line Chemotherapy With or Without Pembrolizumab for Advanced Esophageal Cancer. *Future Oncol* (2019) 15(10):1057–66. doi: 10.2217/fon-2018-0609
34. Doi T, Piha-Paul SA, Jalal SI, Saraf S, Lunceford J, Koshiji M, et al. Safety and Antitumor Activity of the Anti-Programmed Death-1 Antibody Pembrolizumab in Patients With Advanced Esophageal Carcinoma. *J Clin Oncol* (2018) 36(1):61–7. doi: 10.1200/JCO.2017.74.9846
35. Liu Y, Dong Y, Kong L, Shi F, Zhu H, Yu J. Abscopal Effect of Radiotherapy Combined With Immune Checkpoint Inhibitors. *J Hematol Oncol* (2018) 11 (1):104. doi: 10.1186/s13045-018-0647-8
36. Grassberger C, Ellsworth SG, Wilks MQ, Keane FK, Loeffler JS. Assessing the Interactions Between Radiotherapy and Antitumour Immunity. *Nat Rev Clin Oncol* (2019) 16(12):729–45. doi: 10.1038/s41571-019-0238-9
37. Sardaro A, Ferrari C, Carbonara R, Altini C, Lavelli V, Rubini G. Synergism Between Immunotherapy and Radiotherapy in Esophageal Cancer: An Overview of Current Knowledge and Future Perspectives. *Cancer Biother Radiopharm* (2021) 36(2):123–32. doi: 10.1089/cbr.2020.3643
38. Shah MA, Bennouna J, Doi T, Shen L, Kato K, Adenis A, et al. KEYNOTE-975 Study Design: A Phase III Study of Definitive Chemoradiotherapy Plus Pembrolizumab in Patients With Esophageal Carcinoma. *Future Oncol* (2021) 17(10):1143–53. doi: 10.2217/fon-2020-0969

Conflict of Interest: The authors declare that the research was conducted in the absence of any commercial or financial relationships that could be construed as a potential conflict of interest.

frontiers | Frontiers in Oncology

ORIGINAL RESEARCH
published: 01 April 2022
doi: 10.3389/fonc.2022.831506

NRAGE Confers Radiation Resistance in 2D and 3D Cell Culture and Poor Outcome in Patients With Esophageal Squamous Cell Carcinoma

Huandi Zhou[1,2†], Guohui Wang[1†], Zhiqing Xiao[1†], Yu Yang[1], Zhesen Tian[1], Chen Gao[1], Xuetao Han[1], Wei Sun[1], Liubing Hou[1,2], Junling Liu[1] and Xiaoying Xue[1]*

[1] Department of Radiotherapy, Second Hospital of Hebei Medical University, Shijiazhuang, China, [2] Department of Central Laboratory, Second Hospital of Hebei Medical University, Shijiazhuang, China

OPEN ACCESS

Edited by:
Li Jiancheng,
Fujian Provincial Cancer Hospital, China

Reviewed by:
Youliang Wang,
Beijing Institute of Technology, China
Suna Zhou,
Wenzhou Medical University, China

***Correspondence:**
Xiaoying Xue
xxy6412@163.com

[†]*These authors have contributed equally to this work and share first authorship*

Specialty section:
This article was submitted to Radiation Oncology, a section of the journal Frontiers in Oncology

Received: *08 December 2021*
Accepted: *28 February 2022*
Published: *01 April 2022*

Citation:
Zhou H, Wang G, Xiao Z, Yang Y, Tian Z, Gao C, Han X, Sun W, Hou L, Liu J and Xue X (2022) NRAGE Confers Radiation Resistance in 2D and 3D Cell Culture and Poor Outcome in Patients With Esophageal Squamous Cell Carcinoma. Front. Oncol. 12:831506. doi: 10.3389/fonc.2022.831506

Objective: The purpose of the study is to explore the mechanism of NRAGE enhancing radioresistance of esophageal squamous cell carcinoma (ESCC) in 2D and 3D levels.

Methods: Stably NRAGE-overexpressed ESCC cells and 3D-printing models for ESCC cells were established. Then, cellular malignancy indexes, such as cell morphology, proliferation, radioresistance, motility, apoptosis, cell cycle, and proteins of the Wnt/β-catenin pathway, were compared between radioresistant and its parental cells in 2D and 3D levels. Additionally, 44 paraffin ESCC specimens with radical radiotherapy were selected to examine NRAGE and β-catenin protein expression and analyze the clinical correlation.

Results: Experiments in 2D culture showed that morphology of the Eca109/NRAGE cells was more irregular, elongated spindle-shaped and disappeared polarity. It obtained faster growth ability, stronger resistance to irradiation, enhanced motility, reduced apoptosis ratio and cell cycle rearrangement. Moreover, Western blot results showed β-catenin, p-Gsk-3β and CyclinD1 expressions were induced, while p-β-catenin and Gsk-3β expressions decreased in Eca109/NRAGE cells. Experiments in the 3D-printing model showed Eca109/NRAGE cell-laden 3D scaffolds had the advantage on growth and spheroiding according to the brightfield observation, scanning electron microscopy and Ki-67 IHC staining, and higher expression at the β-catenin protein. Clinical analysis showed that NRAGE expression was higher in tumor tissues than in control tissues of ESCC patients from the Public DataBase. Compared with radiotherapy effective group, both NRAGE total and nuclear and β-catenin nuclear expressions were significantly upregulated from ESCC specimens in invalid group. Further analysis showed a positive and linear correlation between NRAGE nuclear and β-catenin nuclear expressions. Additionally, results from univariate and multivariate analyses revealed NRAGE nuclear expression could serve as a risk factor for ESCC patients receiving radical radiotherapy.

Conclusion: ESCC cells with NRAGE nuclear accumulation demonstrated greater radioresistance, which may be related to the activation of the Wnt/β-catenin signaling pathway. It indicated that NRAGE nuclear expression was a potential biomarker for monitoring radiotherapeutic response.

Keywords: esophageal squamous cell carcinoma, radioresistance, NRAGE, 3D bio-printing, Wnt/β-catenin

INTRODUCTION

Esophageal cancer (EC), arising from esophageal epithelial cells, is an epidemic malignancy with conspicuous geographic distribution worldwide. It is fairly well known that China is one of the regions with a high incidence rate of esophageal squamous cell carcinoma (ESCC), which has an enormous burden and is a major histological subtype accounting for 95% of ECs in China (1–4). Statistically, the 5-year overall survival (OS) rate for ESCC is approximately 9–27.1%. Even worse, patients will have poorer prognosis if diagnosed with locally advanced ESCC (5, 6). Radiotherapy (RT) is one of the main treatment methods for ESCC, especially for inoperable and locally advanced ESCC, on which RT plays a crucial role (7). Although the prognosis of patients with ESCC receiving radical RT has dramatically improved recently, owing to better RT technology, the 5-year survival rate of ESCC treated with RT is suboptimal (8). However, the response of ESCC to irradiation (IR) is limited so that numerous patients with ESCC cannot benefit from RT due to radioresistance, which is a major hurdle for successful treatment (9–11). Undoubtedly, exploring molecular markers, which may regulate ESCC radioresistance, to improve clinical outcomes is of primary concern in increasing survival of patients with ESCC.

NRAGE, a neurotrophin-receptor-interacting melanoma antigen-encoding gene homolog, also known as MAGED1 or Dlxin-1, was discovered as a new member of the melanoma antigen family and encodes a cancer-related protein (12, 13). Given its diverse cellular functions, NRAGE is deemed to be greatly crucial in cancer development and progression. Current researchers reported that there were complex and apparently controversial functions on different progression, metastasis, and invasion of tumors (14, 15). Initially, NRAGE was reported as a cancer suppressor gene, which promotes cell apoptosis *via* binding to p75 neurotrophin receptor (P75NTR) (16, 17), Che-1 (18), XIAP-TAK1-TAB1 (19), and UNC5H1 (20) and inhibits proliferation (21) and angiogenesis (22). Contradictorily, functions such as pro-apoptotic gene and growth promotion were slowly discovered (12–14, 23–26). Kodera et al. (25) found that increased NRAGE expression affects the malignant phenotype of hepatocellular carcinoma (HCC) *via* its interaction with apoptosis antagonizing transcription factor (AATF). Zou et al. (24) proved that NRAGE may be a potential biomarker for HCC early diagnosis due to its ability of distinguishing HCC from benign liver disease. Yang et al. (26) reported that an aberrant NRAGE expression in both mRNA and protein levels in ESCC tissues was detected and could induce DNA-damaging chemoresistance by regulating homologous recombination repair.

Originally, our previous studies indicated that NRAGE was significantly overexpressed in the nucleus of ESCC cells with radioresistance (23) and knockdown NRAGE has significantly enhanced radiosensitivity in established radioresistant ESCC cells (14). Scantily, there were only instantaneous intervention at constructed radioresistant EC cells cultured in the 2D level and no correlation with OS of ESCC. Surprisingly, the 3D culture system has a unique superiority in more similar tumor cell growth microenvironment than the 2D *in vitro* system and more short research cycles than the 2D *in vivo* system. This study aimed to confirm the tumor promotor function of NRAGE in ESCC and mechanism that it can accelerate cell growth and survival and induce radioresistance in 2D and 3D culture levels and confer poor prognosis in the clinical setting.

METHODS

Patient Characteristics

All 44 patients who were clinically and histopathologically diagnosed with primary ESCC based on the WHO criteria, received radical RT through conventional fractionated RT by 6MV X-ray linear accelerator at the Second Hospital of Hebei Medical University from January 2010 to December 2015. The curative effects in the 44 patients were determined 1–3 months later after RT referred to the evaluation standard of esophageal barium swallow. The tissue specimens of the patients were collected, fixed in 4% formalin, and embedded in paraffin. The informed consent of the patients was obtained, and the study was approved by the Ethics Committee of the Second Hospital of Hebei Medical University (No. 20160275). Patient baseline characteristics are shown in **Table S2**.

3D Bioprinting of E and E/N Cells

Before printing, the 3D printed workstation (Regenovo Bio-Architect® WS, Hangzhou, China) was sterilized by 75% v/v ethanol and irradiated under UV for 30 min. E and E/N cells (5×10^6) were suspended in 0.2 ml culture medium, followed by the addition of 3 ml of a gelatin–sodium alginate blend (10% gelatin and 3% sodium alginate). Gelatin and sodium alginate were purchased from Sigma (St. Louis, MO, USA). The temperature of 3D-printed platform was set at 8°C measuring $10 \times 10 \times 1.4$ mm in size. After printing, the hydrogels were soaked in 3% calcium chloride for 3 min for a crosslink reaction. Subsequently, the 3D bioprinted scaffolds were incubated at 37°C with 5% CO_2.

Live/Dead Staining

The survival rate of newly printed 3D structure E and E/N cells was detected by fluorescent live/dead viability assay kit (KeyGen Biotech, Co., Ltd., Nanjing, China) according to the instructions of the manufacturer. 3D cell-laden constructs were immersed in 1 ml PBS containing 8 μM PI (red, staining dead cells) and 2 μM calcein AM (green, staining living cells) under the conditions of protection from light at room temperature reaction for 15 min and then washed with PBS. Stained cells were imaged using an inverted fluorescence phase contrast microscope (Zeiss, Germany). Live/dead cells were counted in five random fields at ×100 magnification for each sample. The cell death rate was calculated as follows: ratio of cell survival = number of living cells/(number living cells + dead cells) × 100%.

AlamarBlue

E and E/N cell proliferation in 3D bioprinted hydrogels were tested using an alamarBlue™ cell viability reagent (Invitrogen, USA). 3D-printed scaffolds were washed with PBS, and 500 μl of alamarBlue working solution (alamarBlue: medium = 1:9) was added to each well of a 24-well plate. Then, the 24-well plate was incubated at 37°C and 5% CO2 for 2 h. Then, each 100 μl of working solution was transferred to a 96-well plate, and the absorbances at electron fixation solution at 570 and 600 nm on a multi-function microporous plate detector (bioTek Synergy H1, USA). The scaffolds were cultured for 19–21 days, and the OD values at 570 and 600 nm were detected every 2 days. The cell proliferation ratio calculation was as follows: reduction rate (%) = (A570 − A600 × R) × 100%; R = ($A570_{control}$ − $A'570_{control}$)/($A600_{control}$ − $A'600_{control}$); $A570_{control}$ and $A600_{control}$, the OD values at 570 and 600 nm of cell-free alamarBlue working solution; $A'570_{control}$ and $A'600_{control}$, the OD values at 570 and 600 nm of cell-free medium.

Scanning Electron Microscopy (SEM) Analysis

The 3D-printed scaffolds at 7 and 14 days were fixed with 2.5% glutaraldehyde (Solarbio, Beijing, China) for the night at room temperature and washed three times with PBS for 15 min. The samples were soaked in a series of ethanol solutions (30, 50, 70, 80, 90, 95, and 100%) for 15 min in each solution for dehydration. Subsequently, the scaffolds were dried in the ventilated kitchen. Then, the constructs were coated with platinum (5 nm thickness) and imaged with an Ultra-55 SEM (Zeiss, Germany).

Cell Culture, Plasmids and Stable Transfection, Realtime PCR, Western Blot Analysis, CCK-8 Assay, IR and Clonogenic Assay, Wound Healing Assay, Transwell Invasion Assay, Flow Cytometry Analysis, γ-H2AX Immunofluorescence Staining, Histology and Immunohistochemistry (IHC)

Experimental analyses were conducted as described previously (14, 27) and detailed in the **Supplementary Materials and Methods**.

Statistical Analysis

In vitro experiments were analyzed by unpaired two-sided Student's t-test, Welch's t-test, one-way analysis of variance (ANOVA) or two-way ANOVA. The total and nuclear protein expression of NRAGE and β-catenin in ESCC tissues were analyzed by Mann–Whitney U test. Survival curves were plotted using the Kaplan–Meier method and compared using the log-rank (Mantel–Cox) test. These statistical analyses were conducted by GraphPad Prism 8.0 software. Clinicopathological characteristics of patients with EC following radical RT were analyzed using the chi-squared test. The correlation between NRAGE or β-catenin and clinicopathological features of patients was analyzed using Spearman analysis. The linear correlation between NRAGE nuclear protein and β-catenin nuclear protein were analyzed using the Mantel–Haenszel chi-squared test. Survival data were evaluated using univariate log-rank test and multivariate Cox regression analyses. These data were analyzed using SPSS 25 statistical software (SPSS Inc., Chicago, IL, USA). A P-value <0.05 was considered statistically significant.

RESULTS

Overexpression of NRAGE Induces Radioresistance of ESCC Cells in 2D Culture

Our previous studies indicated that NRAGE was upregulated in ESCC radioresistant cells and extremely likely to be a RT-related critical factor (14, 23, 28). Inadequately, there was lack of direct evidence to confirm the effect of NRAGE on resistance-promoting to IR. To verify the association between NRAGE and ESCC radioresistance, the expression of NRAGE in three types of ESCC cells, TE13, Kyse170, and Eca109, were compared (**Figures 1A, B**). Moreover, Eca109 cells with the least NRAGE expression was selected to stably overexpress NRAGE (**Figures 1C, D**). First, compared with Eca109-vector cells (indicated below as E), we aimed to identify the cellular changes resulting from expression of NRAGE in Eca109 cells (indicated below as E/N). It was visibly different in morphological distinction with more irregular, elongated spindle-shaped cells, and disappearance of polarity (**Figure 1E**). Additionally, cell proliferation and radiosensitivity were tested through CCK-8 and clone formation assay. E/N cell exhibits its super growth ability and radiation-hardened effect (**Figures 1F–H**). Before exposure to IR, both E and E/N cells showed vigorous multiplication without difference during the first 4 days. From the fifth day, E/N cells displayed enhanced proliferation ability. However, in the IR group, the significant difference between them was observed early at the fourth day (E *vs* EN, 0Gy: p_{5d} <0.0001, p_{6d} <0.0001, p_{7d} <0.0001; 2 Gy: p_{4d} = 0.0277, p_{5d} <0.0001, p_{6d} <0.0001, p_{7d} <0.0001; 5 Gy: p_{4d} <0.0001, p_{5d} <0.0001, p_{6d} <0.0001, p_{7d} <0.0001; **Figure 1F**). Moreover, E and E/N cells were exposed to different doses of radiation for colony formation. E/N cells showed relatively higher colony survival rates (p = 0.0429) and increased radiobiological parameter, SF2 (E vs EN = 0.518 vs 0.636), D0 (E vs EN =

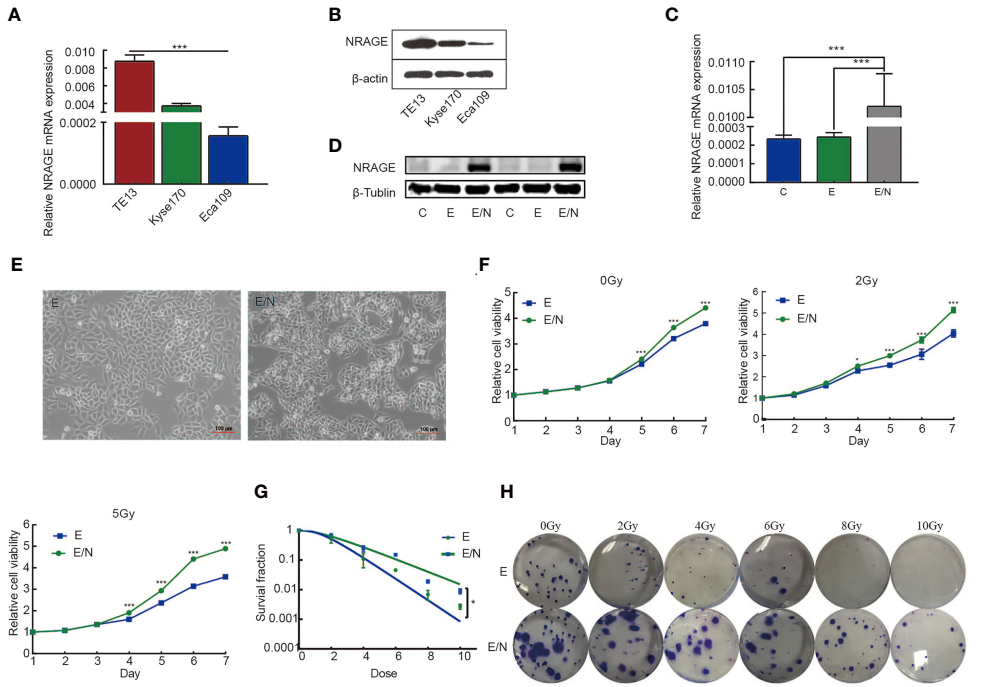

FIGURE 1 | Overexpression of NRAGE enhanced the proliferation and radioresistance of ESCC cells in 2D culture. **(A)** Quantification and analysis of NRAGE mRNA in different ESCC cell lines. **(B)** NRAGE protein levels were analyzed using western blotting in different ESCC cell lines. **(C, D)** Realtime PCR and Western blot assays to determine the overexpression efficiency of transduced Eca109 cells (C: Eca109; E: Eca109-vector; E/N: Eca109-NRAGE); **(E)** cellular morphology compared between E and E/N cells; **(F)** growth curve was detected by CCK8 analysis upon NRAGE stable transfection followed by different irradiation doses with 0, 2 or 5 Gy; **(G)** Dose–response curves were fitted according to the multi-target, single-hit model and analyzed using GraphPad Prism 8.0 software. **(H)** Representative images of colony formation of E and E/N cells after exposure to radiation. All data represented as means ± SD. *$p < 0.05$ vs. E; ***$p < 0.001$ vs. E.

1.201 vs 2.020), and Dq (E *vs* EN = 1.492 *vs* 1.530), under a series of doses of 0, 2, 4, 6, 8, and 10 Gy (**Table S1**; **Figures 1G, H**). These results suggest that NRAGE overexpression induces radioresistance of ESCC cells in 2D culture.

Overexpression of NRAGE Regulates Cell Migration, Invasion, Cell Cycle Progression and Apoptosis After IR in 2D Culture

To further define the mechanism of NRAGE in ESCC radioresistance, cell migration, invasion, cell cycle progression, and apoptosis in E/N cells were analyzed in addition to the detection of proliferation. Wound healing assays were performed in E and E/N cells with or without 5 Gy X-ray radiation and then imaged at 12 and 24 h. Results showed that ESCC cells with upregulated NRAGE had significantly faster migration ratio than E cells, especially after IR (**Figures 2A, B**). Transwell assays also showed that the number of invasion cells through the membrane regardless of the presence of IR was significantly larger in E/N cells (**Figures 2C, D**). It revealed that NRAGE may enhance invasion and migration of ESCC cells after IR led to more resistive effect to IR. Cell apoptosis assays showed that the rate of spontaneous apoptosis in E/N cells was significantly decreased (E vs E/N, 7.99% ± 0.50% vs 4.16% ± 0.15%, $p = 0.0057$). After RT, E/N cells had lower apoptosis than E cells (E vs E/N, 24.29% ± 1.12% vs 34.63% ± 1.83%, $p < 0.0001$) (**Figures 2E, F**). Furthermore, we analyzed the cell cycle progression of E and E/N cells with or without 5 Gy IR (**Figures 2G, H**). It was found that, before IR exposure, NRAGE overexpression was associated with an increased percentage of cells in the S phase (33.23 ± 1.78 vs 25.69 ± 1.70, $p = 0.01$), the most radioresistant cell stage, and a lower ratio in the most radiosensitive cell stage G2/M (18.87 ± 0.46 vs 27.91 ± 0.81, $p = 0.0018$). After treatment with 5 Gy IR, cell cycle distributions were rearranged to a greater extent with more arrested cells in the S phase (26.46 ± 5.61 vs 16.27 ± 2.71, $p = 0.0005$) and G0/G1 phase (45.50 ± 4.95 vs 35.21 ± 0.96, $p = 0.0004$) and downregulated cells in the G2/M phase (28.04 ± 0.67 vs 48.52 ± 1.77, $p < 0.0001$). These revealed that NRAGE overexpression could reduce cell apoptosis and change cell cycle division of ESCC, affecting cellular radioresistance.

NRAGE Overexpression Activates Canonical Wnt Signaling Pathway in ESCC Cells With 2D Culture

Previous studies indicated that NRAGE had a potential association with β-catenin in the formation of radioresistance in ESCC (14), so we detected protein expression in canonical Wnt signaling

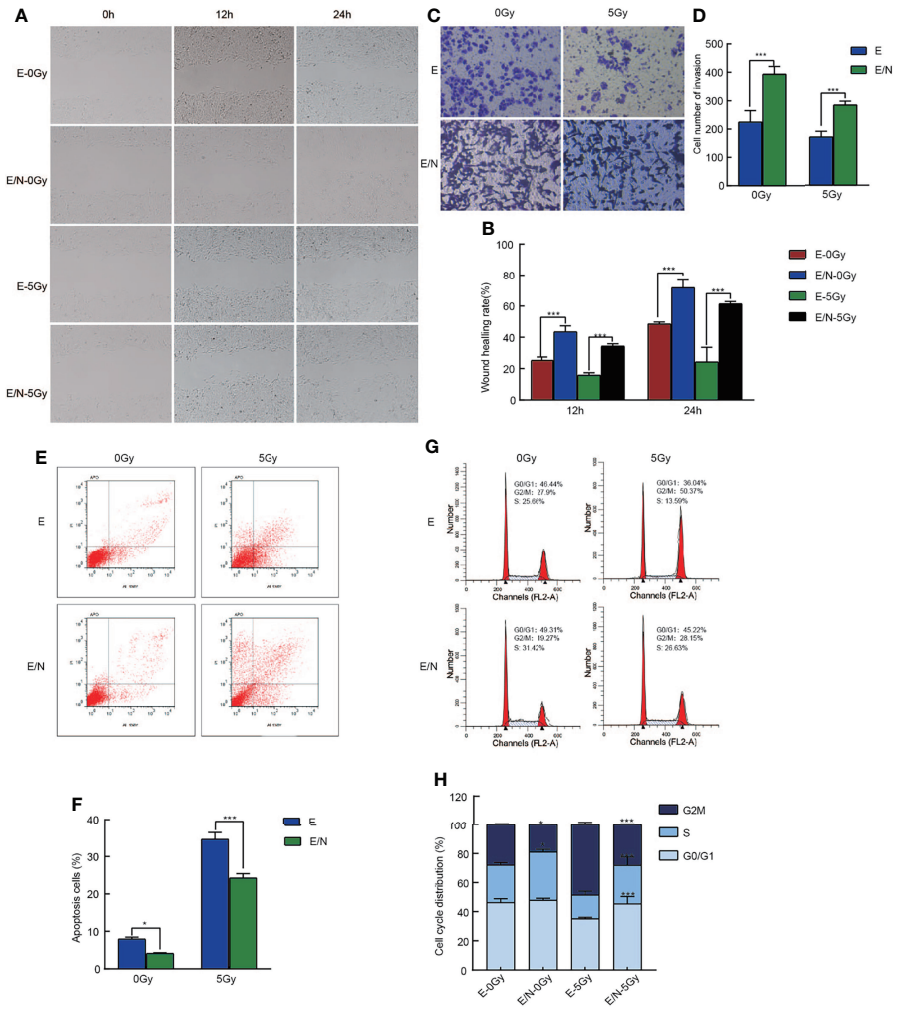

FIGURE 2 | Overexpression of NRAGE inhibits cell migration, invasion, cell cycle progression and apoptosis after IR in 2D culture. **(A)** Wound Healing assay was applied to test the migration ability of E and E/N with or without 5 Gy irradiation (magnification: ×200); **(B)** Quantitative assessment of wound-healing rate at the different times (12 and 24 h); **(C)** Matrigel invasion assay was applied to compare E and E/N cells for invasion ability with or without 5 Gy irradiation (magnification: ×200); **(D)** Quantitative assessment of the number of invasion cells. *P < 0.05 vs. E; **P < 0.01 vs. E; ***P < 0.005 vs. E; **(E)** Annexin V-FITC/PI staining was applied to test the apoptotic rates of E and E/N cells with or without 5 Gy IR by flow cytometry; **(F)** Quantitative assessment of the apoptotic rates; **(G)** Propidium iodide stain was applied to test cell cycle of E and E/N cells with or without 5 Gy IR by flow cytometric; **(H)** Cell cycle distributions were analyzed using GraphPad Prism 8.0 software; All data represented as means ± SD. *p < 0.05 vs. E; ***p < 0.001 vs. E.

pathway, namely, β-catenin, phosphorylation of β-catenin (p-β-catenin), Gsk-3β, phosphorylation of Gsk-3β (p-Gsk-3β), and CyclinD1. Compared with E, an increase in β-catenin (p= *0.037*) level, followed by increased trend of p-Gsk-3β levels (p = *0.917*), led to the increased expression of cyclin D1 (p = 0.023), a targeting gene of β-catenin in E/N cells, while downregulation of p-β-catenin (p = 0.037) and Gsk-3β (p = *0.049*) was detected (**Figures 3A, B**). To further investigate the role of the Wnt/β-catenin signaling pathway in radioresistance of ESCC regulated by NRAGE, FH535 (HY-15721, MCE, USA), a reversible inhibitor of the Wnt pathway, was used. After treated with FH535, E/N cells were tested the radioresistance and proliferation by clonogenic and cck-8 assay. The results showed that E/N cell treated with inhibitor had significant decline on both colony survival (E/N vs E/N-inhibitor: p = 0.0139; E/N-NC vs E/N-inhibitor, p = 0.0442, **Figures 3C, D**) and proliferation rates (**Figures 3E, F**). In addition, γ-H2AX Immunofluorescence experiment exhibited that E/N cells with FH535 had a remarkable higher formation of γ-H2AX foci after irradiation than both E/N and E/N-NC cells at 0.5 h (E/N vs E/N-inhibitor, 22.33 ± 3.06 vs 42 ± 3.60, p <0.0001; E/N-NC vs E/N-inhibitor, 24.67 ± 2.52 vs 42 ± 3.60, p = 0.0003), 2 h (E/N vs E/N-inhibitor, 30.67 ± 4.51 vs 56 ± 4.00, p <0.0001; E/N-NC vs E/N-inhibitor, 32.33 ± 3.79 vs 56 ± 4.00, p <0.0001), 6 h (E/N vs E/N-inhibitor, 6.83 ± 1.61 vs 19.67 ± 3.06, p = 0.003; E/N-NC vs E/N-inhibitor, 6.33 ± 1.53 vs 19.67 ± 3.06, p = 0.0023) (**Figures 3G, H**). Western blot results demonstrated that CyclinD1 (E/N vs E/N-inhibitor, p = 0.001; E/N-NC vs E/N-inhibitor, p <0.001), β-catenin (E/N vs E/N-inhibitor, p = 0.008;

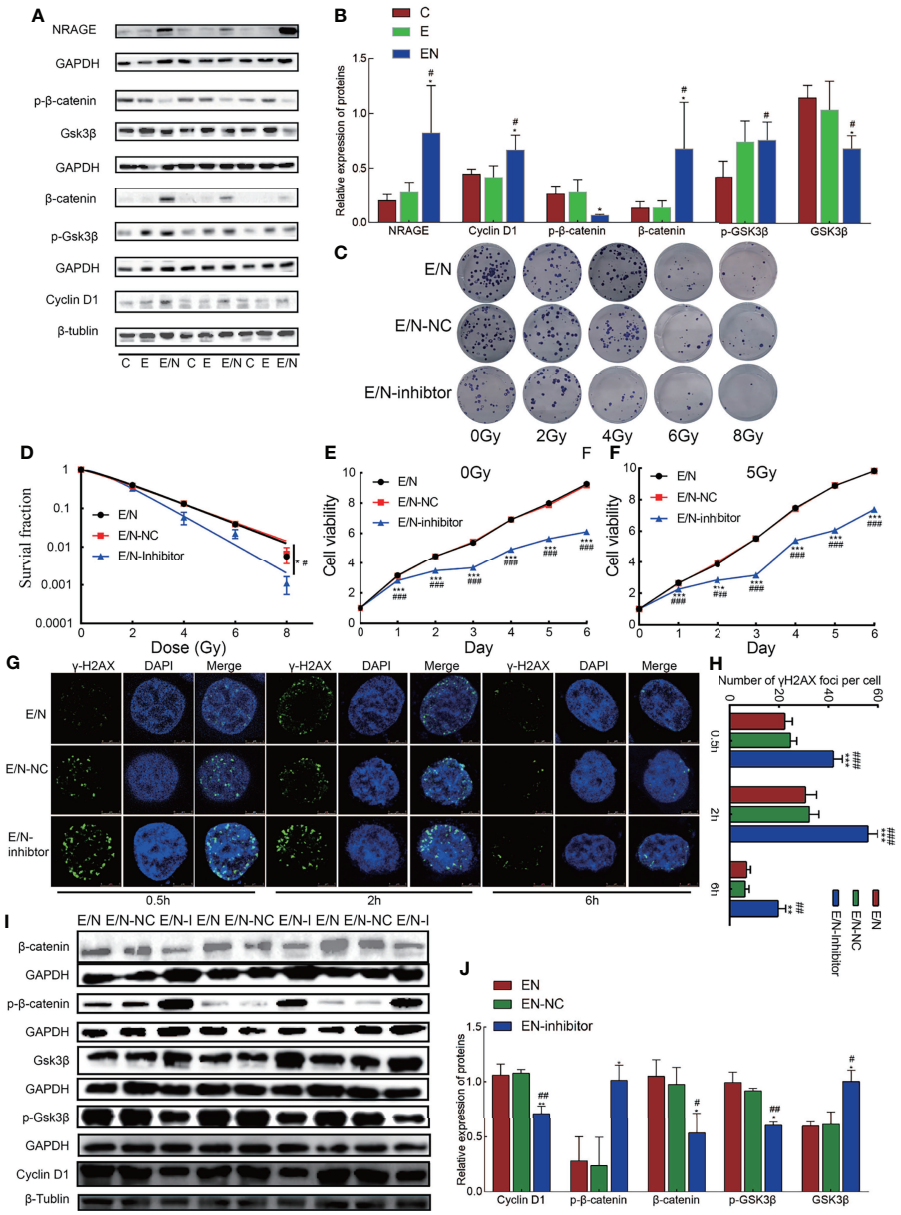

FIGURE 3 | Overexpression of NRAGE activates canonical Wnt signaling pathways in ESCC cells with 2D culture. **(A)** The expression of Wnt/β-catenin signaling pathway-related proteins was determined using western blotting. **(B)** Quantitative assessment of related proteins in Wnt/β-catenin signaling pathway. All data represented as means ± SD. $^{*}p < 0.05$ vs. E; $^{**}p < 0.01$ vs. E; $^{***}p < 0.001$ vs. E, $^{\#}p < 0.05$ vs. C; $^{\#\#}p < 0.01$ vs. C; $^{\#\#\#}p < 0.001$ vs. C. **(C)** Representative images of colony formation of E/N cells after exposure to radiation with or without FH535. **(D)** Dose–response curves were fitted according to the multi-target, single-hit model and analyzed using GraphPad Prism 8.0 software. **(E, F)** growth curve was detected by CCK-8 analysis in EN cells with or without FH535 by different irradiation doses with 0 and 5 Gy. **(G, H)** The formation of γ-H2AX foci at 0.5, 2, 6 after 5 Gy irradiation in EN cells with or without FH535. **(I, J)** Western blotting analysis the expression of Wnt/β-catenin signaling pathway-related proteins with or without FH535. All data represented as means ± SD. $^{*}p < 0.05$ vs. EN; $^{**}p < 0.01$ vs. EN; $^{\#}p < 0.05$ vs. EN-NC; $^{\#\#}p < 0.01$ vs. EN-NC.

E/N-NC vs E/N-inhibitor, $p = 0.015$) and p-Gsk-3β (E/N vs E/N-inhibitor, $p = 0.030$; E/N-NC vs E/N-inhibitor, $p = 0.008$) decreased, while p-β-catenin (E/N vs E/N-inhibitor, $p = 0.074$; E/N-NC vs E/N-inhibitor, $p = 0.025$) and Gsk-3β (E/N vs E/N-inhibitor, $p = 0.037$; E/N-NC vs E/N-inhibitor, $p = 0.031$) slightly increased after FH535 treatment (**Figures 3I, J**) in E/N cells. These data indicated that after NRAGE overexpression, the canonical Wnt signaling pathway was overall activated, which may be a switch-induced radioresistance. Also, the inhibitor of Wnt/β-catenin signaling pathway, FH535, could reverse the enhanced radioresistance induced by NRAGE overexpression.

3D Bioprinted ESCC Cell-Laden System Cultured *In Vitro*

To the best of our knowledge, there is considerable difference on the cancer cell morphology genetic profile and tumoral heterogeneity in 2D cultures. To focus more on the tumor cell growth environment and microenvironment *in vitro*, we selected culture cells in the 3D bioprinting system to identify the function of NRAGE in radioresistance of ESCC cells. A gelatin–alginate blend (10% gelatin and 3% sodium alginate) was used as the 3D bioprinted material. Hydrogel seeded with E and E/N cells were extruded at variable pressure (0.31 MPa), needle type (cylindrical), and needle diameter (340 μm) to study cell characteristics directly after printing. Extruded gelatin–alginate blend was stained with live/dead dye and imaged (**Figures 4A, B**). Most cells remained viable (green), and only a small number of dead cells (red) were observed. Subsequently, the result of the analyses showed that dead or live cells were counted to quantify cell survival at >80% and E/N cell-laden 3D-scaffolds exhibited stronger survivability. After printing, images were obtained, followed by crosslinking in 3% $CaCl_2$ and incubation at 37°C to allow the gelatin to leach out. The cell-laden 3D-scaffolds had a grid-like structure arranged in multiple layers, and cells were uniformly distributed in porous scaffolds with tight order, exhibiting good cytocompatibility (**Figure 4C**). At the first week, the printed scaffolds did not display obvious proliferation. Then, the cell growth rate accelerated slowly over time. After 3 weeks, cells began to grow into spheroids and pushed the surrounding hydrogels aside to occupy a larger space. Especially for E/N cell-laden hydrogels, the phenomena were highlighted. It was extremely biomimetic to the solid tumor growth *in vivo*. SEM observations revealed the spheroids bulged out over the scaffolds surface, and the trace of cells squeezed the surrounding hydrogel, which showed that E/N cell-laden scaffolds were apt to spheroiding. It was also suggested that E/N cells in the 3D group have a significantly higher secretion of growth hormone than E cells, and the difference gradually became pronounced over time (**Figure 4E**). After culture for 7 days, as shown in HE staining, individual cells scattered in printed scaffolds were observed (**Figure 4F**). During the culture period, natural gelatin began to degrade gradually *via* hydrolysis in the culture medium and then provided space for cells proliferating in clusters at 14 and 21 days. Furthermore, more and larger cell clusters were observed in E/N cell-laden 3D scaffolds.

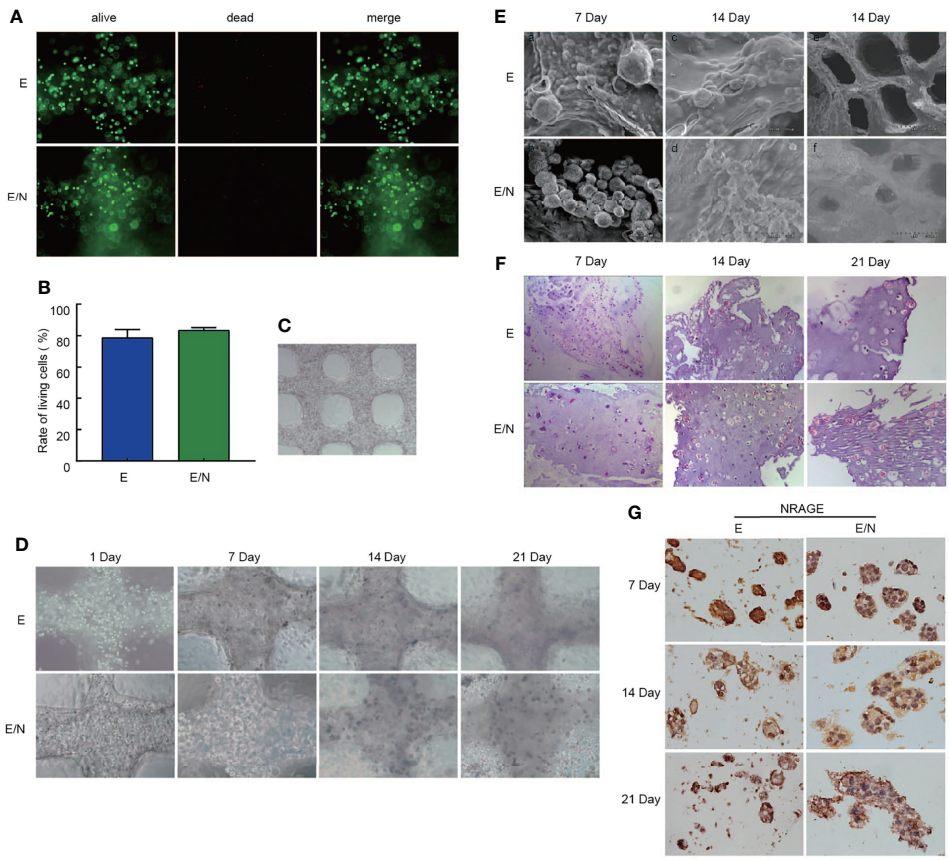

FIGURE 4 | 3D bioprinted ESCC cell-laden system cultured *in vitro*. **(A)** Live/dead staining for cell viability after printing, where live cells are stained in green and dead cells in red. **(B)** Cell viability of E and E/N cells after printing. **(C)** 3D bioprinted E and E/N cells at day 1 of culturing. **(D)** optical microscopy images. **(E)** SEM images. **(F)** Hematoxylin–eosin staining: 3D bioprinted E and E/N cells cultured *in vitro* for 7, 14, and 21 d **(G)** Immunohistochemistry of 3D bioprinted E and E/N cells: NRAGE expression at 7, 14, and 21 d in culture. Scale bars: **(A, D, F)** 100 μm; **(C)** 200 μm; **(E)** a–d 50 μm, e–f 500 μm; **(G)** 50 μm.

Figure 4G shows that both positive expressions of NRAGE were observed at E-3D and E/N-3D cells, while NRAGE in E/N cells in the 3D culture system had a distinct positive staining in nuclear cells with larger cluster. These results implied that cells with NRAGE overexpression in the 3D culture system are more suitable for survival and cloud growth, which hinted that ESCC cells with NRAGE overexpression exerted greater adaptability to survive and multiply.

NRAGE Overexpression Enhanced the Proliferation and Radioresistance of ESCC Cells in 3D Bioprinted Hydrogels

The obvious advancement and characteristic of the 3D-printed model showed more similar growth environment and microenvironment *in vivo*. To identify the effect of NRAGE overexpression in ESCC cells cultured in the 3D-printed model on proliferation of tumor cells, alamarBlue assays were selected to compare cell viability between 3D-printed and 2D groups. As shown in **Figure 5A**, regardless of the culture condition (2D or 3D), E/N cells had considerably higher survival percentages than E cells. More interestingly, there was a faster proliferation rate in E/N cells in the 2D group in the first 20 days, whereas the 3D-printed group showed a significantly higher proliferation rate of cells after 20 days. Similarly, an apparent trend that E cells in the 3D-printed group would proliferate faster than those in the 2D group after 21 days was observed (**Figure 5A**). Moreover, the difference in responses to IR between E and E/N cells in the 3D-printed model was identified by alamarBlue assays after 5 Gy IR. Evidently, E/N-3D cells had an absolute dominance of survival on resistance to IR compared with E-3D cells (**Figure 5B**). Deeply, the protein expression of Ki-67, a marker for cell proliferation activity, between E-3D and E/N-3D cells with or without 5 Gy IR, was evaluated by IHC, and both of them had a positive expression in relative individual cells scattered in hydrogel at 7 days. However, after 14 days, more positive staining in larger clusters in E/N-3D cells appeared. Furthermore, this different trend was also found after 5 Gy IR (**Figure 5C**). To verify whether the β-catenin expression change in ESCC cells with NRAGE overexpression was consistent from 2D to 3D groups, IHC staining was performed. Similarly, in the first 7 days, both E-3D and E/N-3D cells had a higher β-catenin expression levels with larger cell clusters. After culture for 14 days, larger E/N-3D cell clusters were stained positively by β-catenin antibody compared with those in E cells. Unsurprisingly, there was a more obvious distinction between groups after 5 Gy IR (**Figure 5D**). The results confirmed further that accelerated NRAGE expression in ESCC cells activate β-catenin expression to regulate radiosensitivity.

NRAGE is Upregulated in Patient Samples With EC Following Radical RT and Correlated With Poor Prognosis

We analyzed NRAGE expression in public database, and found that it was upregulated both in ESCA samples (182 cases) compared with adjacent normal tissue samples (286 cases) (p <0.05) (match TCGA normal and GTEx data, http://gepia.cancer-pku.cn/) and in ESCC samples compared with paired Paracancerous tissue from the GSE20347 dataset (p = 0.0001, https://www.ncbi.nlm.nih.gov/geo/) (**Figure 6A**). Additionally, to thoroughly explore the role of NRAGE on radioresistance of ESCC and relationship with β-catenin, we further analyzed the expression of NRAGE and β-catenin in a total of 44 paraffin-embedded, ESCC tumor tissues receiving definitive RT (**Table S2**). As shown in **Figure 6B**, the 1-, 3-, and 5-year overall survival rates of 44 patients were 69, 36, and 21%, respectively (**Figure 6B**). According to the evaluation criteria of RT curative effect, 36 patients were classified in the efficacy group (complete response, CR, 26 patients, and partial response, PR, 9 patients) and 8 patients were classified in the inefficacy group (No response, NR, 8 cases) (**Figures 6D–F**). There were statistically significant differences between the two groups in the 1-, 3-, and 5-year OS rates: 81, 45, and 26% for the efficacy group and only 15% of 1-year OS rate in the inefficacy group were achieved (p = *0.0001*) (**Figure 6C**). Compared to the inefficacy group in which NRAGE and β-catenin were expressed at low levels (**Figures 6G, I**), NRAGE and β-catenin were overexpressed, especially for positive nuclear expression, in efficacy group specimens (**Figures 6H, J**). According to the analysis of the relationship between staining score and short-term effect of RT, NRAGE protein expression was dramatically upregulated in the NR group tumor tissues compared with the efficacy group (CR + PR)(P = 0.015) (**Figure 6K**). Unsurprisingly, more NRAGE nuclear protein expression were detected in NR group (p = 0.0021) (**Figure 6L**). Additionally, there was higher β-catenin total protein expression in the NR group than in the efficacy group (p = 0.081) (**Figure 6M**). However, the difference in β-catenin nuclear protein expression between the two groups was significant (p = 0.0037) (**Figure 6N**).

Routinely, we analyzed the association between NRAGE total/nuclear protein or β-catenin total/nuclear protein expressions and clinicopathological features of 44 patients with ESCC by Spearman analysis. It was revealed that the expression of NRAGE total protein, especially for NRAGE nuclear protein, was strongly associated with curative efficacy (p = 0.0023, p = 0.006). However, regardless of NRAGE total protein or NRAGE nuclear protein, there was no association with age (p = 0.656, p = 0.277), gender (p = 0.734, p = 0.277), clinical stage (p = 0.932, p = 0.759), tumor size (p = 0.121, p = 0.488), LNM (p = 0.153, p = 0.148), synchronous chemotherapy (p = 0.906, p = 0.862), and events (p = 0.135, p = 0.528) (**Table 1**). As shown in **Table 1**, no correlation between β-catenin expression and age (p = 0.288, p = 0.231), sex (p = 1.000, p = 0.358), clinical stage (p = 0.824, p = 0.986), tumor size (p = 0.168, p = 0.263), LNM (p = 0.221, p = 0.587), synchronous chemotherapy (p = 0.099, p = 0.459), and events (p = 0.754, p = 0.296) was found. A significant correlation could not be found between β-catenin total protein expression and clinicopathological features (p = 0.143), but a strong association between β-catenin nuclear protein expression and curative efficacy was observed (p = 0.006). Kaplan–Meier survival curves exhibited no association between OS in definitive RT and NRAGE or β-catenin total protein expression (**Figures 6O, Q**, p = 0.198, p = 0.504), but a strong positive NRAGE nuclear protein

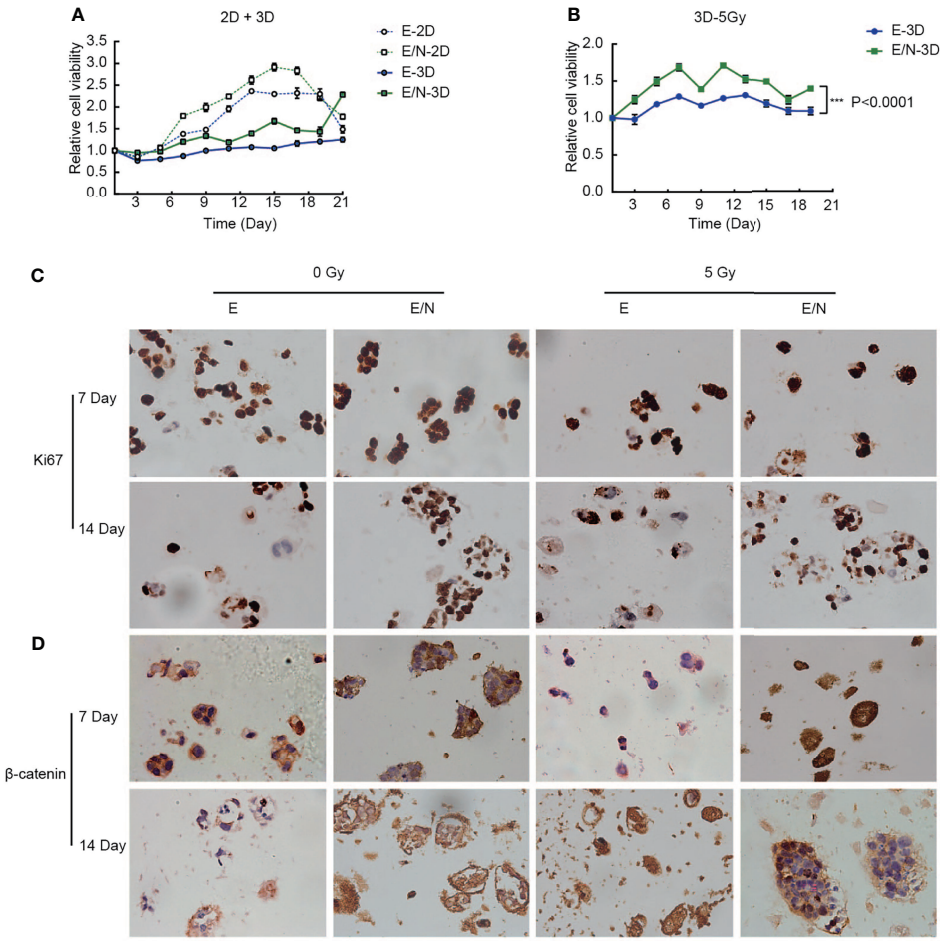

FIGURE 5 | Overexpression of NRAGE enhanced the proliferation and radioresistance of ESCC cells in 3D bioprinted hydrogels. **(A)** Comparing cell proliferation between E and E/N in 2D and 3D by alamarBlue assays; **(B)** Cell proliferation was tested by immunohistochemistry of 3D bioprinted E and E/N cells: Ki-67 expression at 7,14 d in culture with or without IR; **(C)** cell viability between E and E/N in 3D after 5 Gy IR by alamarBlue assays; **(D)** Immunohistochemistry of 3D bioprinted E and E/N cells: β-catenin expression at 7, 14, and 21 d in culture with or without IR. Scale bars: **(B, D)** 50 μm, all data represented as means ± SD. ***$p < 0.001$ vs. E.

expression was significantly shorter than those with positive and weak positive NRAGE expression (**Figure 6P**, p <0.0001). Additionally, there was a correlated trend between β-catenin nuclear protein expression and OS (**Figure 6R**, p = 0.081). Moreover, we analyzed the association between NRAGE and β-catenin nuclear protein expressions and found their linear correlation trend (cor = 0.291, p = 0.055) (**Table S3**). These results indicate that NRAGE expression, especially NRAGE nuclear expression, in patients with ESCC receiving radical RT was correlated with poor survival and may be linked to heightened β-catenin nuclear accumulation. Furthermore, univariate, and multivariate analyses were used to determine whether NRAGE could be a risk factor in patients with ESCC receiving radical RT. Log-rank test in the univariate analysis showed that synchronous chemotherapy (p = 0.037), curative efficacy (p = 0.000), and strong positive NRAGE nuclear protein expression (p = 0.000) were associated with a significantly increased risk of death in patients with ESCC receiving radical RT (**Table 2**). Multivariate Cox regression analysis revealed that NRAGE nuclear protein could be a factor for predicting poor survival when it has strong positive expression (HR = 14.536, p = 0.000). Synchronously, clinical stage (HR = 2.995, p = 0.024) and synchronous chemotherapy (HR = 0.354, p = 0.019) were included as factors (**Table 2**). Collectively, all these indicated that NRAGE overexpression occurred during nuclear translocation after IR and stimulated β-catenin expression in the cytoplasm to increase the nuclear localization of β-catenin, which activated the Wnt/β-catenin signaling pathway and then induced the radioresistance in ESCC. A flowchart of the possible mechanism is shown in **Figure 6S**.

DISCUSSION

EC is one of the most common primary malignancies with high mortality, and mainly in ESCC in China. RT is one of the

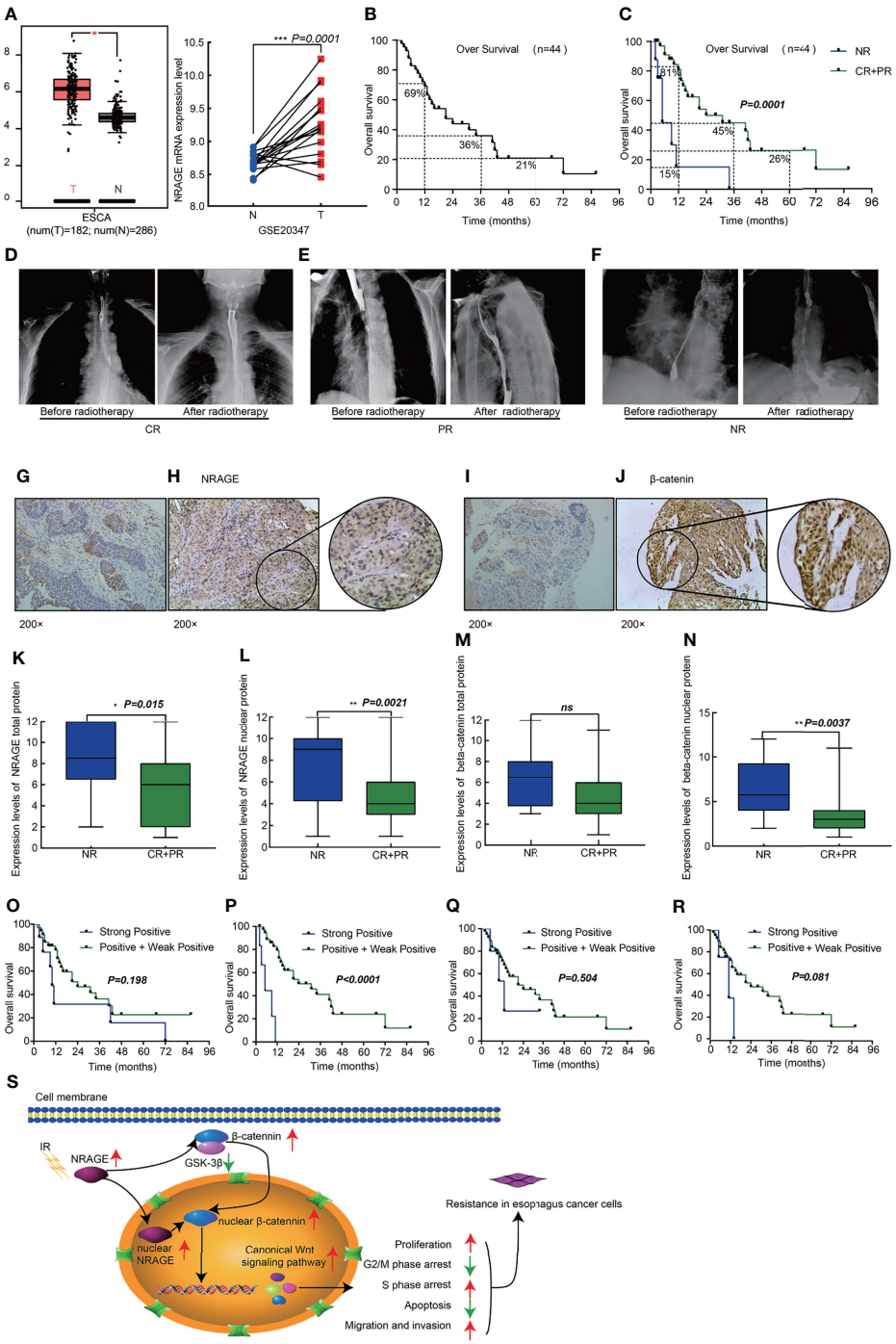

FIGURE 6 | High expression nuclear NRAGE in patient samples with ESCC following radical radiotherapy correlates with poor survival. **(A)** NRAGE Expression in esophageal cancer tissues and normal control esophageal tissues from the TCGA (left, ESCA) and the GSE20347 (Right, ESCC) data; **(B)** Kaplan–Meier overall survival curves for all 44 patients with esophagus cancer; **(C)** Kaplan–Meier overall survival curves for all 44 patients with esophagus cancer stratified by NR and CR + PR; **(D–F)** Images of radiotherapeutic short-term effects, CR **(D)**, PR **(E)**, NR **(F)**; **(G, H)** Representative images of NRAGE negative **(G)** and positive **(H)** expression; **(I, J)** Representative images of β-catenin negative **(I)** and positive **(J)** expression; **(K, L)** Comparison of NRAGE total **(K)** and nuclear **(L)** protein expression between NR group and CR + PR group; **(M, N)** Comparison of β-catenin total **(M)** and nuclear **(N)** protein expression between NR group and CR + PR group; **(O, P)** Kaplan–Meier overall survival curves for all 44 patients with esophagus cancer stratified by strong positive and weak positive+positive expression of NRAGE total **(O)** and nuclear **(P)** protein; **(Q, R)** Kaplan–Meier overall survival curves for all 44 patients with esophagus cancer stratified by strong positive and weak positive + positive expression of β-catenin total **(Q)** and nuclear **(R)** protein; **(S)** Schematic illustration depicting the NRAGE associations with cancer proliferation, apoptosis, cell cycle and invasive migration that induce resistance to radiation. *$p < 0.05$; **$p < 0.01$; ***$p < 0.001$; ns, no significance.

TABLE 1 | Spearman analysis of correlation among NRAGE, β-catenin and clinicopathological features.

Variables	Group	NRAGE expression		NRAGE nuclear expression		β-catenin expression		β-catenin nuclear expression	
		Spearman correlation	*P*-value	Spearman correlation	*P*-value	Spearman correlation	*P*-value	Spearman correlation	*P*-value
Age (y)	≥60 <60	−0.069	0.656	−0.168	0.277	−0.164	0.288	0.184	0.231
Gender	Male Female	0.053	0.734	0.168	0.277	0.000	1.000	0.142	0.358
Clinical Stage	I–II III–IV	−0.013	0.932	0.048	0.759	−0.034	0.824	−0.003	0.986
Tumor size	≥5 cm <5 cm	−0.237	0.121	−0.107	0.488	−0.212	0.168	−0.172	0.263
lymph nodes metastasis (LNM)	Yes No	−0.219	0.153	−0.222	0.148	−0.188	0.221	0.084	0.587
Synchronous chemotherapy	Yes No	0.018	0.906	−0.027	0.862	0.252	0.099	−0.115	0.459
Curative efficacy	effectivity inefficacy	−0.342	***0.023***	−0.405	***0.006***	−0.225	0.143	−0.41	**0.006**
Events	Censored Dead	0.229	0.135	0.098	0.528	0.049	0.754	0.161	0.296

The italic font and bold values represents there was a significance.

TABLE 2 | Univariate and Multivariate analysis of various prognostic parameters in patients with ESCC following Radical radiotherapy.

Univariate analysis					Multivariate analysis			
Variable	**OS (m)**		**Log Rank χ^2**	***P*-value**	**Variable**	**HR**	**95% CI**	***P*-value**
	Median (95% CI)							
Age (y)			1.314	0.252	**clinical stage**	2.995	(1.154–7.775)	0.024
≥60	15	(5.734–24.266)						
<60	34	(7.584–60.416)						
Gender			0.895	0.344	**Synchronous chemotherapy**	0.354	(0.149–0.843)	0.019
Male	16	(0–42.659)						
Female	21	(8.291–33.709)						
Clinical Stage			3.222	0.073	**Expression of NRAGE nuclear**	14.536	(3.847–54.928)	0.000
I–II	31	(6.170–55.830)						
III–IV	15	(8.452–21.548)						
Tumor size			0.145	0.704				
≥5 cm	21	(10.280–31.720)						
<5 cm	16	(0–49.001)						
lymph nodes metastasis (LNM)			0.001	0.973				
Yes	21	(6.566–35.434)						
No	34	(1.442–66.558)						
Synchronous chemotherapy			4.366	***0.037***				
Yes	41	(13.456–68.544)						
No	14	(9.020–18.980)						
Curative efficacy			14.831	***0.000***				
effectivity	24	(7.702–40.298)						
inefficacy	5	(2.540–7.460)						
Expression of NRAGE			1.660	0.198				
Weak positive + Positive	24	(8.038–39.962)						
Strongly positive	10	(7.690–12.310)						
Expression of NRAGE nuclear			23.831	***0.000***				
Weak positive + Positive	34	(14.792–47.208)						
Strongly positive	5	(1.080–8.920)						
Expression of β-catenin								
Weak positive + Positive	21	(4.322–37.678)	0.446	0.504				
Strongly positive	13	(6.363–19.637)						
Expression of β-catenin nuclear			3.040	0.081				
Weak positive + Positive	24	(6.734–41.266)						
Strongly positive	11	(2.018–19.982)						

The italic font and bold values represents there was a significance.

primary therapeutic modalities in patients with ESCC. The existence of radioresistance is a major limit to achieve long-term survival in ESCC, which has been linked to an increased likelihood of recurrence and distant metastasis (29–32).

NRAGE has complicated and contradictory functions. It encodes an 86-KDa protein and is a member of the Type II MAGE family, comprising 778 amino acids (aa), of which the MAGE homology domain is common for MAGE family members and the interspersed repeat domain (IRD) is relatively unique to NRAGE for no homology to any public specific protein. These features imply that there are both uniform and specific characteristics of NRAGE compared with other members of the MAGE family (33–36). Growing evidence confirmed that NRAGE functions as a transcriptional regulator mediating multiple signaling pathways from apoptosis (16, 18–20), cell differentiation (37–39), cell cycle distribution (26), cell adhesion (40), and angiogenesis (22). In contrast, NRAGE could promote cell apoptosis through interaction with P75NTR (16), Che-1 (18), XIAP-TAK1-TAB1 (19), and UNC5H1 (20). However, Kumar et al. (41) initially found the anti-apoptosis role of NRAGE, in which NRAGE had carried out anoikis resistance after it transferred into the nucleus and coacted with TBX2. Moreover, NRAGE also exerted cell differentiation functions through activating the transcriptional function of Dlx5 (37), downregulating TrkA (38), and been reducing by Praja1 (39). Furthermore, as an important adaptor, NRAGE could interact with PCNA to promote anti-apoptosis, accelerate cell growth, and change cell cycle distribution (26). Additionally, NRAGE could regulate cell adhesion by participating in epithelial–mesenchymal transformation (EMT) activity (40) and angiogenesis by interfering with HIF-1-dependent gene expression (22). Mitsuro et al. (35) reported NRAGE's carcinogenic role that is the knockdown of NRAGE could reduce proliferation, migration, and invasion in gastric cancer cells, which was positively correlated with AATF. Generally, the above mentioned studies indicate that NRAGE, as a molecular bridge, exerts complex and contradictory functions as either an inhibitor or promoter depending on different cell types.

Innovatively, our team provided a new insight for NRAGE into the ability of pro-radioresistance that NRAGE was unexpectedly overexpressed in radioresistant ESCC cells based on gene microarray analysis and experiment verification. It was shown that NRAGE had a growing trend following enhanced IR dose and time (23). Another study of our team determined whether NRAGE subcellular localization alteration led to radioresistance and may be related to the occurrence of EMT in ESCC (40). Subsequently, our study verified that NRAGE was upregulated in constructed radioresistant cells from ESCC cells TE13 and Eca109 and participated in the information of radioresistance in ESCC (14). Clinical sample detection revealed that there was high expression of NRAGE in patients with ESCC in the invalid group based on short-term efficacy evaluation treated with definitive RT. Inadequately, the abovementioned contents were obtained in 2D level, and the interference measure for NRAGE was transitory RNA interference (RNAi). In addition, the relationship between NRAGE expression and OS of the patients was not analyzed. The evidence that NRAGE overexpression was related to poor prognosis of patients with ESCC treated by radical RT was relatively weak.

In this study, we selected Eca109 cells to artificially stably overexpress NRAGE, in which NRAGE expression was at a related lower level compared with those in TE13 and Kyse170 cells (**Figures 1A–D**). After interference, accelerated growth speed, degressive apoptosis rate, more malignant migration and invasion, and redistributed cell cycle led to the accumulation of IR resistance in Eca109 cells with NRAGE overexpression (**Figures 1F–H**, **2A–H**). Moreover, the experiments in the cell level on the mechanism of NRAGE involved in radioresistance in ESCC cells were performed at both 2D and 3D levels. It is a truism that 3D printing technology has high precision and fast building speed, which can not only improve and more fully simulate the natural microenvironment *in vivo* but also shorten the research cycle compared with the mouse model (42–45). In the 3D system, we printed the 3D E-cells and E/N cell models using a gelatin–alginate blend (10% gelatin and 3% sodium alginate). Through observing model morphology by brightfield and SEM, the 3D E/N cell model showed more powerful spheroiding capacity (**Figures 4D, E**). From the results of HE staining, alamarBlue detection, and ki-67 IHC staining, more strong proliferation ability and resistance to IR were apparent (**Figures 4F**, **5A–C**). As for the mechanism of NRAGE participating in the information of radioresistance in ESCC cells, the Western blot analysis results on the total and phosphorylated β-catenin protein and total and phosphorylated Gsk-3β protein and β-catenin IHC stain results of 3D-cells scaffolds demonstrated that NRAGE may trigger β-catenin nuclear protein accumulation and then activate the canonical Wnt signaling pathways to motivate cancer-promoting activities (**Figures 3A, B**). Additionally, after treated with FH535 in E/N cells, the canonical Wnt signaling pathways genes Cyclin D1, β-catenin, and p-Gsk-3β were downregulated specifically, while p-β-catenin and Gsk-3β were upregulated, indicating the inhibition of the Wnt/β-catenin pathway (**Figures 3I, J**). Subsequently, we tested whether FH535 could reverse the radioresistance and proliferation by a colony forming assay and CCK-8 analysis. The conjecture was proved following decreased colony survival and proliferation rates in FH535 treated group (**Figures 3C–F**). Furthermore, the increase formation of γ-H2AX foci, a sensitive indicator of DNA repair, in E/N cells after added FH535, indicates poorer DNA damage repair ability. Altogether, it was suggested that FH535 could potentially act as a radiosensitizer for E/N cells.

β-catenin, a core member of the canonical Wnt signaling pathway, was strongly linked to EC progression, metastasis, and invasion (46–49). In off state of canonical Wnt signaling pathways, β-catenin is mainly expressed at the cytoplasm, and Gsk-3β inhibits tumor growth by degrading β-catenin. However, in the on state, Gsk-3β was inactivated through phosphorylation, and then β-catenin is accumulated in the cytoplasm so as to increase the nuclear localization of β-catenin, activating downstream target genes and modulating the behavior of

tumor cells. Prominently, numerous investigations showed a close-knit relationship between radioresistance and β-catenin in EC (14, 50–56). Che et al. (53) used fractionate IR to acquire radioresistant EC cells Eca109R50Gy and tested the aberrant expression of β-catenin. When treated with a COX-2 inhibitor, downregulation of β-catenin and enhanced radiosensitivity were observed. In 2014, Su et al. screened three mircroRNAs (mir-301a, mir-131, and mir-18b) based on human miRNA microarray results reserved on Public DataBase on radioresistant ESCC cell line KYSE-150R and its parental KYSE-150 and subsequent real-time qPCR verification. Target gene prediction revealed that wnt1 was a potential target gene of mir-301a and overexpressed in KYSE-150R (54). Their subsequent study confirmed that microRNA−301a could increase the radiosensitivity and restrain the migration of ESCC cells with radioresistance through affecting canonical Wnt signaling pathways (50). Another study of the team showed EMT phenotypes and acquisition of radioresistance in EC cells were related to activation of the canonical Wnt signaling pathway. Moreover, a type of this pathway inhibitor, FH535, can reverse the abovementioned phenomenon (51). Previously, our team presented the correlation between NRAGE and β-catenin only in the cell level (14). Unfortunately, many studies were short of clinical relevance.

Profoundly, in the present study, with further analysis, we found the close-knit pertinence between NRAGE and β-catenin in the clinical setting, in which NRAGE protein expression level, especially for NRAGE nuclear protein, was negatively correlated to short-term efficacy and long-term survival of patients with ESCC receiving radical RT (**Tables 1**, **2**). Meanwhile, a positive correlation trend between NRAGE and β-catenin nuclear expression were also observed using the Spearman analysis (**Table S3**). Comprehensively, the current results confirmed that IR may cause the upregulation of NRAGE, which could accumulate NRAGE to promote nuclear translocation, and triggered β-catenin nuclear accumulation to induce proliferation and anti-proptosis of the ESCC cells, enhance invasiveness and migration capability and cell cycle rearrangement, and promote decreased radiosensitivity (**Figure 6S**).

CONCLUSION

Collectively, our study verified the NRAGE, with anti-oncogene and oncogene contradictory roles, was regarded as an oncogene due to the functions that accelerated proliferation, anti-apoptosis effect, more malignant migration and invasion, and accumulation of IR resistance by triggering Wnt/β-catenin signaling pathway in ESCC cells in 2D and 3D levels. Not only that, clinical correlation analysis also demonstrated that NRAGE, specifically for NRAGE nuclear protein, was a risk factor in patients with ESCC treated by definitive RT and had a positive relationship with β-catenin nuclear protein expression. As a putative oncogene, NRAGE may have the potential to serve as a novel predictive biomarker for tumor progression and target of molecular therapy.

DATA AVAILABILITY STATEMENT

The original contributions presented in the study are included in the article/**Supplementary Material**. Further inquiries can be directed to the corresponding author.

ETHICS STATEMENT

The studies involving human participants were reviewed and approved by the Ethics Committee of the Second Hospital of Hebei Medical University. The patients/participants provided their written informed consent to participate in this study. Written informed consent was obtained from the individual(s) for the publication of any potentially identifiable images or data included in this article.

AUTHOR CONTRIBUTIONS

HZ and GW is attributed for the study design, data analysis, and manuscript writing. ZX established cell lines, tissue collection, and evaluation of radiotherapy efficacy. ZX, YY, and ZT helped interpreting the data. CG, XH, WS, and LH prepared all the figures. JL, HZ, and GW edited all the tables. XX is attributed for the experiment conduction. All authors listed have made a substantial, direct, and intellectual contribution to the work and approved it for publication.

FUNDING

This work is supported by a grant from the Natural Science Foundation of Hebei Province (No. H2019206182).

SUPPLEMENTARY MATERIAL

The Supplementary Material for this article can be found online at: https://www.frontiersin.org/articles/10.3389/fonc.2022.831506/full#supplementary-material

REFERENCES

1. Chen W, Li H, Ren J, Zheng R, Shi J, Li J, et al. Selection of High-Risk Individuals for Esophageal Cancer Screening: A Prediction Model of Esophageal Squamous Cell Carcinoma Based on a Multicenter Screening Cohort in Rural China. *Int J Cancer* (2021) 148:329–39. doi: 10.1002/ijc.33208
2. He Q, Li J, Dong F, Cai C, Zou X. LKB1 Promotes Radioresistance in Esophageal Cancer Cells Exposed to Radiation, by Suppression of Apoptosis and Activation of Autophagy *via* the AMPK Pathway. *Mol Med Rep* (2017) 16:2205–10. doi: 10.3892/mmr.2017.6852
3. Strizova Z, Snajdauf M, Stakheev D, Taborska P, Vachtenheim JJr, Biskup J, et al. The Paratumoral Immune Cell Signature Reveals the Potential for the

Implementation of Immunotherapy in Esophageal Carcinoma Patients. *J Cancer Res Clin Oncol* (2020) 146(8):1979–92. doi: 10.1007/s00432-020-03258-y
4. Zhou W, Wu J, Liu X, Ni M, Meng Z, Liu S, et al. Identification of Crucial Genes Correlated With Esophageal Cancer by Integrated High-Throughput Data Analysis. *Med (Baltimore)* (2020) 99:e20340. doi: 10.1097/MD.0000000000020340
5. Mallet R, Modzelewski R, Lequesne J, Mihailescu S, Decazes P, Auvray H, et al. Prognostic Value of Sarcopenia in Patients Treated by Radiochemotherapy for Locally Advanced Oesophageal Cancer. *Radiat Oncol* (2020) 15:116. doi: 10.1186/s13014-020-01545-z
6. Wang Y, Lyu Z, Qin Y, Wang X, Sun L, Zhang Y, et al. FOXO1 Promotes Tumor Progression by Increased M2 Macrophage Infiltration in Esophageal Squamous Cell Carcinoma. *Theranostics* (2020) 10:11535–48. doi: 10.7150/thno.45261
7. Er P, Qian D, Zhang W, Zhang B, Wei H, Zhang T, et al. The Expression of PDGF-BB Predicts Curative Effect in Locally Advanced Esophageal Squamous Cell Carcinoma Treated by Radiotherapy. *Aging (Albany NY)* (2020) 12:6586–99. doi: 10.18632/aging.102993
8. Wang Z, Zhang J, Li M, Kong L, Yu J. The Expression of P-P62 and Nuclear Nrf2 in Esophageal Squamous Cell Carcinoma and Association With Radioresistance. *Thorac Cancer* (2020) 11:130–9. doi: 10.1111/1759-7714.13252
9. Yang L, Zhang X, Hou Q, Huang M, Zhang H, Jiang Z, et al. Single-Cell RNA-Seq of Esophageal Squamous Cell Carcinoma Cell Line With Fractionated Irradiation Reveals Radioresistant Gene Expression Patterns. *BMC Genomics* (2019) 20:611. doi: 10.1186/s12864-019-5970-0
10. Chen H, Yao X, Di X, Zhang Y, Zhu H, Liu S, et al. MiR-450a-5p Inhibits Autophagy and Enhances Radiosensitivity by Targeting Dual-Specificity Phosphatase 10 in Esophageal Squamous Cell Carcinoma. *Cancer Lett* (2020) 483:114–26. doi: 10.1016/j.canlet.2020.01.037
11. Zhou S, Liu S, Lin C, Li Y, Ye L, Wu X, et al. TRIB3 Confers Radiotherapy Resistance in Esophageal Squamous Cell Carcinoma by Stabilizing TAZ. *Oncogene* (2020) 39:3710–25. doi: 10.1038/s41388-020-1245-0
12. Yang Q, Pan Q, Li C, Xu Y, Wen C, Sun F. NRAGE is Involved in Homologous Recombination Repair to Resist the DNA-Damaging Chemotherapy and Composes a Ternary Complex With RNF8-BARD1 to Promote Cell Survival in Squamous Esophageal Tumorigenesis. *Cell Death Differ* (2016) 23:1406–16. doi: 10.1038/cdd.2016.29
13. Liu L, Cui Z, Zhang J, Wang J, Gu S, Ma J, et al. Knockdown of NRAGE Impairs Homologous Recombination Repair and Sensitizes Hepatoblastoma Cells to Ionizing Radiation. *Cancer Biother Radiopharm* (2020) 35:41–9. doi: 10.1089/cbr.2019.2968
14. Zhou H, Zhang G, Xue X, Yang Y, Yang Y, Chang X, et al. Identification of Novel NRAGE Involved in the Radioresistance of Esophageal Cancer Cells. *Tumour Biol* (2016) 37:8741–52. doi: 10.1007/s13277-015-4747-6
15. Zhang G, Zhou H, Xue X. Complex Roles of NRAGE on Tumor. *Tumour Biol* (2016) 37:11535–40. doi: 10.1007/s13277-016-5084-0
16. Salehi AH, Roux PP, Kubu CJ, Zeindler C, Bhakar A, Tannis LL, et al. NRAGE, a Novel MAGE Protein, Interacts With the P75 Neurotrophin Receptor and Facilitates Nerve Growth Factor-Dependent Apoptosis. *Neuron* (2000) 27:279–88. doi: 10.1016/s0896-6273(00)00036-2
17. Qin T, Yuan Z, Yu J, Fu X, Deng X, Fu Q, et al. Saikosaponin-D Impedes Hippocampal Neurogenesis and Causes Cognitive Deficits by Inhibiting the Survival of Neural Stem/Progenitor Cells *via* Neurotrophin Receptor Signaling in Mice. *Clin Transl Med* (2020) 10:e243. doi: 10.1002/ctm2.243
18. Di Certo MG, Corbi N, Bruno T, Iezzi S, De Nicola F, Desantis A, et al. NRAGE Associates With the Anti-Apoptotic Factor Che-1 and Regulates its Degradation to Induce Cell Death. *J Cell Sci* (2007) 120:1852–8. doi: 10.1242/jcs.03454
19. Rochira JA, Matluk NN, Adams TL, Karaczyn AA, Oxburgh L, Hess ST, et al. A Small Peptide Modeled After the NRAGE Repeat Domain Inhibits XIAP-TAB1-TAK1 Signaling for NF-κb Activation and Apoptosis in P19 Cells. *PloS One* (2011) 6:e20659. doi: 10.1371/journal.pone.0020659
20. Williams ME, Strickland P, Watanabe K, Hinck L. UNC5H1 Induces Apoptosis *via* its Juxtamembrane Region Through an Interaction With NRAGE. *J Biol Chem* (2003) 278:17483–90. doi: 10.1074/jbc.M300415200
21. Du Q, Zhang Y, Tian XX, Li Y, Fang WG. MAGE-D1 Inhibits Proliferation, Migration and Invasion of Human Breast Cancer Cells. *Oncol Rep* (2009) 22:659–65. doi: 10.3892/or_00000486
22. Shen WG, Xue QY, Zhu J, Hu BS, Zhang Y, Wu YD, et al. Inhibition of Adenovirus-Mediated Human MAGE-D1 on Angiogenesis *In Vitro* and *In Vivo*. *Mol Cell Biochem* (2007) 300:89–99. doi: 10.1007/s11010-006-9373-6
23. Xue XY, Liu ZH, Jing FM, Li YG, Liu HZ, Gao XS. Relationship Between NRAGE and the Radioresistance of Esophageal Carcinoma Cell Line TE13R120. *Chin J Cancer* (2010) 29:900–6. doi: 10.5732/cjc.010.10141
24. Zou W, Cui J, Ren Z, Leng Y. NRAGE is a Potential Diagnostic Biomarker of Hepatocellular Carcinoma. *Med (Baltimore)* (2018) 97:e13411. doi: 10.1097/MD.0000000000013411
25. Shimizu D, Kanda M, Sugimoto H, Sueoka S, Takami H, Ezaka K, et al. NRAGE Promotes the Malignant Phenotype of Hepatocellular Carcinoma. *Oncol Lett* (2016) 11:1847–54. doi: 10.3892/ol.2016.4120
26. Yang Q, Ou C, Liu M, Xiao W, Wen C, Sun F. NRAGE Promotes Cell Proliferation by Stabilizing PCNA in a Ubiquitin-Proteasome Pathway in Esophageal Carcinomas. *Carcinogenesis* (2014) 35:1643–51. doi: 10.1093/carcin/bgu084
27. Miao R, Luo H, Zhou H, Li G, Bu D, Yang X, et al. Identification of Prognostic Biomarkers in Hepatitis B Virus-Related Hepatocellular Carcinoma and Stratification by Integrative Multi-Omics Analysis. *J Hepatol* (2014) 61:840–9. doi: 10.1016/j.jhep.2014.05.025
28. Ping Z, Zhou ZG, Gao XS. Isolation and Characterization of Radioresistant Human Esophageal Cancer Cells and the Differential Gene Expression by cDNA Microarray Analysis. *Chin J Radiol Med Prot* (2006) 26(6):566–70. doi: 10.3760/cma.j.issn.0254-5098.2006.06.007
29. Malhotra A, Sharma U, Puhan S, Chandra Bandari N, Kharb A, Arifa PP, et al. Stabilization of miRNAs in Esophageal Cancer Contributes to Radioresistance and Limits Efficacy of Therapy. *Biochimie* (2019) 156:148–57. doi: 10.1016/j.biochi.2018.10.006
30. Liu J, Xue N, Guo Y, Niu K, Gao L, Zhang S, et al. CircRNA_100367 Regulated the Radiation Sensitivity of Esophageal Squamous Cell Carcinomas Through miR-217/Wnt3 Pathway. *Aging (Albany NY)* (2019) 11:12412–27. doi: 10.18632/aging.102580
31. Li M, Fan L, Han D, Yu Z, Ma J, Liu Y, et al. Ribosomal S6 Protein Kinase 4 Promotes Radioresistance in Esophageal Squamous Cell Carcinoma. *J Clin Invest* (2020) 130(8):4301–19. doi: 10.1172/JCI134930
32. Zhang H, Si J, Yue J, Ma S. The Mechanisms and Reversal Strategies of Tumor Radioresistance in Esophageal Squamous Cell Carcinoma. *J Cancer Res Clin Oncol* (2021) 147:1275–86. doi: 10.1007/s00432-020-03493-3
33. Zhou Y, Huang N, Wu J, Zhen N, Li N, Li Y, et al. Silencing of NRAGE Induces Autophagy *via* AMPK/Ulk1/Atg13 Signaling Pathway in NSCLC Cells. *Tumour Biol* (2017) 39:1010428317709676. doi: 10.1177/1010428317709676
34. Jiang X, Jiang X, Yang Z. NRAGE Confers Poor Prognosis and Promotes Proliferation, Invasion, and Chemoresistance in Gastric Cancer. *Gene* (2018) 668:114–20. doi: 10.1016/j.gene.2018.05.060
35. Kanda M, Shimizu D, Fujii T, Tanaka H, Tanaka Y, Ezaka K, et al. Neurotrophin Receptor-Interacting Melanoma Antigen-Encoding Gene Homolog is Associated With Malignant Phenotype of Gastric Cancer. *Ann Surg Oncol* (2016) 23:532–9. doi: 10.1245/s10434-016-5375-0
36. Liu H, Zhang X, Yang Q, Zhu X, Chen F, Yue J, et al. Knockout of NRAGE Promotes Autophagy-Related Gene Expression and the Periodontitis Process in Mice. *Oral Dis* (2021) 27:589–99. doi: 10.1111/odi.13575
37. Masuda Y, Sasaki A, Shibuya H, Ueno N, Ikeda K, Watanabe K. Dlxin-1, a Novel Protein That Binds Dlx5 and Regulates its Transcriptional Function. *J Biol Chem* (2001) 276:5331–8. doi: 10.1074/jbc.M008590200
38. Feng Z, Li K, Liu M, Wen C. NRAGE is a Negative Regulator of Nerve Growth Factor-Stimulated Neurite Outgrowth in PC12 Cells Mediated Through TrkA-ERK Signaling. *J Neurosci Res* (2010) 88:1822–8. doi: 10.1002/jnr.22340
39. Teuber J, Mueller B, Fukabori R, Lang D, Albrecht A, Stork O. The Ubiquitin Ligase Praja1 Reduces NRAGE Expression and Inhibits Neuronal Differentiation of PC12 Cells. *PloS One* (2013) 8:e63067. doi: 10.1371/journal.pone.0063067
40. Chang X, Xue X, Zhang Y, Zhang G, Zhou H, Yang Y, et al. The Role of NRAGE Subcellular Location and Epithelial-Mesenchymal Transition on Radiation Resistance of Esophageal Carcinoma Cell. *J Cancer Res Ther* (2018) 14:46–51. doi: 10.4103/jcrt.JCRT_687_17
41. Kumar S, Park SH, Cieply B, Schupp J, Killiam E, Zhang F, et al. A Pathway for the Control of Anoikis Sensitivity by E-Cadherin and Epithelial-to-

Mesenchymal Transition. *Mol Cell Biol* (2011) 31:4036–51. doi: 10.1128/MCB.01342-10
42. Shafiee A. 3D Printed Scaffolds for Cancer Precision Medicine. *Tissue Eng Part A* (2020) 26(5–6):305–17. doi: 10.1089/ten.TEA.2019.0278
43. Fazili Z, Ward A, Walton K, Blunt L, Asare-Addo K. Design and Development of a Novel Fused Filament Fabrication (FFF) 3D Printed Diffusion Cell With UV Imaging Capabilities to Characterise Permeation in Pharmaceutical Formulations. *Eur J Pharm Biopharm* (2020) 152:202–09. doi: 10.1016/j.ejpb.2020.05.013
44. Gordy CL, Sandefur CI, Lacara T, Harris FR, Ramirez MV. Building the Lac Operon: A Guided-Inquiry Activity Using 3d-Printed Models. *J Microbiol Biol Educ* (2020) 21(1):21.1.28. doi: 10.1128/jmbe.v21i1.2091
45. Bahcecioglu G, Basara G, Ellis BW, Ren X, Zorlutuna P. Breast Cancer Models: Engineering the Tumor Microenvironment. *Acta Biomater* (2020) 106:1–21. doi: 10.1016/j.actbio.2020.02.006
46. Cao W, Lee H, Wu W, Zaman A, McCorkle S, Yan M, et al. Multi-Faceted Epigenetic Dysregulation of Gene Expression Promotes Esophageal Squamous Cell Carcinoma. *Nat Commun* (2020) 11:3675. doi: 10.1038/s41467-020-17227-z
47. Wall JA, Klempner SJ, Arend RC. The Anti-DKK1 Antibody DKN-01 as an Immunomodulatory Combination Partner for the Treatment of Cancer. *Expert Opin Investig Drugs* (2020) 29(7):639–44. doi: 10.1080/13543784.2020.1769065
48. Wang W, He S, Zhang R, Peng J, Guo D, Zhang J, et al. ALDH1A1 Maintains the Cancer Stem-Like Cells Properties of Esophageal Squamous Cell Carcinoma by Activating the AKT Signal Pathway and Interacting With β-Catenin. *BioMed Pharmacother* (2020) 125:109940. doi: 10.1016/j.biopha.2020.109940
49. Pan X, Ma L, Wang J. The Clinicopathological Significance and Prognostic Value of β-Catenin Ser45-Phosphorylation Expression in Esophageal Squamous Cell Carcinoma. *Int J Clin Exp Pathol* (2019) 12:3507–13.
50. Su H, Wu Y, Fang Y, Shen L, Fei Z, Xie C, et al. MicroRNA–301a Targets WNT1 to Suppress Cell Proliferation and Migration and Enhance Radiosensitivity in Esophageal Cancer Cells. *Oncol Rep* (2019) 41:599–607. doi: 10.3892/or.2018.6799
51. Su H, Jin X, Zhang X, Zhao L, Lin B, Li L, et al. FH535 Increases the Radiosensitivity and Reverses Epithelial-to-Mesenchymal Transition of Radioresistant Esophageal Cancer Cell Line KYSE-150r. *J Transl Med* (2015) 13:104. doi: 10.1186/s12967-015-0464-6
52. Li WF, Zhang L, Li HY, Zheng SS, Zhao L. WISP-1 Contributes to Fractionated Irradiation-Induced Radioresistance in Esophageal Carcinoma Cell Lines and Mice. *PloS One* (2014) 9:e94751. doi: 10.1371/journal.pone.0094751
53. Che SM, Zhang XZ, Liu XL, Chen X, Hou L. The Radiosensitization Effect of NS398 on Esophageal Cancer Stem Cell-Like Radioresistant Cells. *Dis Esophagus* (2011) 24:265–73. doi: 10.1111/j.1442-2050.2010.01138.x
54. Su H, Jin X, Zhang X, Xue S, Deng X, Shen L, et al. Identification of microRNAs Involved in the Radioresistance of Esophageal Cancer Cells. *Cell Biol Int* (2014) 38:318–25. doi: 10.1002/cbin.10202
55. Li HZ, Gao XS, Xiong W, Zhao J, Zhang H, Zhou DM. Identification of Differentially Expressed Genes Related to Radioresistance of Human Esophageal Cancer Cells. *Chin J Cancer* (2010) 29:882–8. doi: 10.5732/cjc.010.10148
56. Zhang X, Komaki R, Wang L, Fang B, Chang JY. Treatment of Radioresistant Stem-Like Esophageal Cancer Cells by an Apoptotic Gene-Armed, Telomerase-Specific Oncolytic Adenovirus. *Clin Cancer Res* (2008) 14:2813–23. doi: 10.1158/1078-0432.CCR-07-1528

Conflict of Interest: The authors declare that the research was conducted in the absence of any commercial or financial relationships that could be construed as a potential conflict of interest.

Publisher's Note: All claims expressed in this article are solely those of the authors and do not necessarily represent those of their affiliated organizations, or those of the publisher, the editors and the reviewers. Any product that may be evaluated in this article, or claim that may be made by its manufacturer, is not guaranteed or endorsed by the publisher.

frontiers | Frontiers in Oncology

ORIGINAL RESEARCH
published: 01 April 2022
doi: 10.3389/fonc.2022.817413

Inter-Observer and Intra-Observer Variability in Gross Tumor Volume Delineation of Primary Esophageal Carcinomas Based on Different Combinations of Diagnostic Multimodal Images

Fengxiang Li[1†], Yankang Li[1†], Xue Wang[2], Yingjie Zhang[1], Xijun Liu[1], Shanshan Liu[1], Wei Wang[1], Jinzhi Wang[1], Yanluan Guo[1], Min Xu[1] and Jianbin Li[1*]*

[1] Department of Radiation Oncology, Shandong Cancer Hospital and Institute, Shandong First Medical University and Shandong Academy of Medical Sciences, Jinan, China, [2] Department of Radiation Oncology, Linyi Cancer Hospital, Linyi, China

Background and Purpose: This study aimed to investigate inter-/intra-observer delineation variability in GTVs of primary esophageal carcinomas (ECs) based on planning CT with reference to different combinations of diagnostic multimodal images from endoscopy/EUS, esophagography and FDG-PET/CT.

Materials and Methods: Fifty patients with pathologically proven thoracic EC who underwent diagnostic multimodal images before concurrent chemoradiotherapy were enrolled. Five radiation oncologist independently delineated the GTVs based on planning CT only (GTV_C), CT combined with endoscopy/EUS (GTV_{CE}), CT combined with endoscopy/EUS and esophagography (X-ray) (GTV_{CEX}), and CT combined with endoscopy/EUS, esophagography, and FDG-PET/CT (GTV_{CEXP}). The intra-/inter-observer variability in the volume, longitudinal length, generalized CI (CI_{gen}), and position of the GTVs were assessed.

Results: The intra-/inter-observer variability in the volume and longitudinal length of the GTVs showed no significant differences ($p>0.05$). The mean intra-observer CI_{gen} values for all observers was 0.73 ± 0.15. The mean inter-observer CI_{gen} values for the four multimodal image combinations was 0.67 ± 0.11. The inter-observer CI_{gen} for the four combined images was the largest, showing significant differences with those for the other three combinations. The intra-observer CI_{gen} among different observers and inter-observer CI_{gen} among different combinations of multimodal images showed significant differences ($p<0.001$). The intra-observer CI_{gen} for the senior radiotherapists was larger than that for the junior radiotherapists ($p<0.001$).

Edited by:
Tao Li,
Sichuan Cancer Hospital, China

Reviewed by:
Signe Friesland,
Karolinska University Hospital, Sweden
Diane Schott,
University of Nebraska Medical Center, United States

***Correspondence:**
Fengxiang Li
lifengxiangli@aliyun.com
Jianbin Li
lijianbin@msn.com

†These authors share first authorship

Specialty section:
This article was submitted to Radiation Oncology, a section of the journal Frontiers in Oncology

Received: *18 November 2021*
Accepted: *28 February 2022*
Published: *01 April 2022*

Citation:
Li F, Li Y, Wang X, Zhang Y, Liu X, Liu S, Wang W, Wang J, Guo Y, Xu M and Li J (2022) Inter-Observer and Intra-Observer Variability in Gross Tumor Volume Delineation of Primary Esophageal Carcinomas Based on Different Combinations of Diagnostic Multimodal Images. Front. Oncol. 12:817413. doi: 10.3389/fonc.2022.817413

Conclusion: For radiation oncologists with advanced medical imaging training and clinical experience, using diagnostic multimodal images from endoscopy/EUS, esophagography, and FDG-PET/CT could reduce the intra-/inter-observer variability and increase the accuracy of target delineation in primary esophageal carcinomas.

Keywords: esophageal carcinoma, diagnostic multimodal images, target delineation, intra-observer variability, inter-observer variability

HIGHLIGHTS

- There is large variability in target volume delineation for esophageal carcinoma.
- Evaluation of inter-/intra-observer delineation variability based on diagnostic multimodal imaging.
- Multimodal diagnostic image combinations can reduce the intra-/inter-observer variability and increase delineation accuracy.

INTRODUCTION

Esophageal carcinoma is the seventh most commonly diagnosed cancer and the third leading cause of cancer deaths worldwide in 2018 (1). Preoperative and definitive chemoradiation therapies have played a key role in the treatment of esophageal carcinoma (2–5). The proportion of residual esophageal carcinoma after chemoradiation is significantly correlated with locoregional and distant failure (6–9). Reliable delineation of the target gross tumor volume (GTV) is required for accurate radiation dose delivery and successful radiation therapy (10, 11). There is generally large variability in the target volume delineation for esophageal carcinoma, which might be primarily derived from the geometric uncertainties of different images and inherent variability among different observers based on the studies on other malignancies (12, 13).

Conventional three-dimensional CT (3DCT) has been the workhorse modality used to delineate the esophageal tumor target volume. However, it is difficult to determine the proximal and distal extension of tumors and differentiate the layers of the esophageal wall (14–16). An esophagography has shown a higher accuracy in assessing the tumor length (59% of cases, compared with 32% with CT), with tumor morphology influencing the accuracy (14–16). Although endoscopy and endoscopic ultrasonography (EUS) might present the tumor length more accurately (17, 18), it is difficult to transform the imaging to radiotherapy (RT) planning (19). Fluorine-18 fluorodeoxyglucose positron emission tomography/computed tomography (18F-FDG-PET/CT) has proved useful for diagnosing and staging esophageal carcinoma. However, there is limited evidence supporting the validity of FDG-PET/CT for target volume delineation (20, 21). The false-positive FDG uptake in areas of inflammation reduces the specificity of tumor extent visualization (22). Therefore, the combination of multimodal images is critical for determining the GTV of esophageal cancer (EC) accurately. Several studies have focused on the inter-observer variability of target volume delineation in FDG-PET/CT compared with pure CT imaging (10, 23). As CT imaging has proved indispensable for the visualization/detection of esophageal tumors, the use of multimodality imaging including esophagography, endoscopy/EUS and FDG-PET/CT for target volume delineation has not received sufficient attention.

In general, patients scheduled to receive radiotherapy or chemoradiotherapy undergo diagnostic multimodal imaging including enhanced CT, endoscopy/EUS, esophagography, or FDG-PET/CT. In clinical practice, radiation oncologists generally delineate the target volumes based on the planning CT images, with reference to various preexisting diagnostic images. However, the outcome of using different combinations of diagnostic multimodal images on the inter-observer and intra-observer delineation variability remains unclear. The purpose of this study was to investigate the inter-observer and intra-observer delineation variability in the GTVs of primary esophageal tumors with reference to different combinations of multimodal images from endoscopy/EUS, esophagography, and FDG-PET/CT. This study indicated the influence of the addition of different multimodal images on the GTVs delineation variability, which may contribute to making clinical decision on acquire different multimodal images.

MATERIALS AND METHODS

Patient Selection and Characteristics

This study was approved by the institutional research ethics board and informed consent has been obtained from the participants involved. Fifty-one patients with pathologically proven thoracic EC who had undergone preoperative or definitive concurrent chemoradiotherapy between May 2015 and June 2017 at the institutional hospital were enrolled. Among the selected patients, there were seventeen cases each of upper, middle, and lower EC. One patient with lower EC was excluded due to the lack of PET-CT imaging data. All patients underwent a diagnostic imaging examination that included an endoscopy/EUS, esophagography, and FDG-PET/CT before receiving chemoradiotherapy. The average time for acquiring the diagnostic images was within the two-week period before chemoradiotherapy. **Table 1** presents the patient characteristics.

Multimodal Imaging

Endoscopy/EUS examination: All patients underwent diagnostic endoscopy examinations using an electronic gastroscope

TABLE 1 | Patient's characteristics.

Characteristics	Number
Sex, n (%)	
M	40 (80%)
F	10 (20%)
Age, median, y (range)	63 (44-88)
Tumor histology, n (%)	
Squamous cell carcinoma	50 (100%)
SUV_{max}, mean, median, y (range)	17.1, 15.2 (2.8~49.5)
TNM* stage, n (%)	
$T_2N_{0-2}M_0$	4 (8%)
$T_3N_{1-3}M_{0-1}$	34 (68%)
$T_{4a}N_{0-2}M_{0-1}$	12 (24%)
Tumor location, n (%)	
Upper	17 (34%)
Mid-	17 (34%)
Distal	16 (32%)

(Olympus GIF-Q260J) before treatment. Seven patients did not undergo EUS examinations due to esophageal stenosis. The ultrasonic probe (Olympus EVIS EUS EU-ME2) was inserted into the patient's esophagus along the track of the biopsy forceps to detect the depth of tumor infiltration in the esophageal wall and the extent of proximal and distal tumor infiltration. The distances from the proximal and distal ends of the tumor to the incisors were recorded.

Esophagography (X-ray) image acquisition: Esophagography was performed before treatment using a digital radiography machine (Siemens Luminos dRT Max). All barium examinations were performed under fasting conditions, followed by a standard protocol (drinking 200 ml of diluted barium, in the upright, supine, and prone positions, with and without the gas powder).

PET/CT image acquisition: The PET-CT scan was performed within the two-week period prior to the planning CT scan as a part of the routine diagnostic management for EC. An 18F-FDG PET/CT scan of the chest was performed with an integrated PET/CT system (Philips Gemini TF Big Bore). The PET images were reconstructed with the CT-derived attenuation correction using an ordered subset expectation maximization algorithm with post-reconstruction Gaussian filtering, with a full width at half maximum of 5 mm.

Planning CT image acquisition: During the simulation, all patients were immobilized using a thermoplastic mask in the supine position with the arms placed along the side of the body. Each patient underwent an enhanced planning CT scan of the thoracic region on a 16-slice CT scanner (Philips Brilliance Bores CT) under free-breathing conditions. The planning CT images were reconstructed using a thickness of 3 mm and subsequently transferred to an Eclipse treatment planning system (Varian Eclipse 11).

Target Volume Delineation

A treatment planning system (Eclipse; Varian Medical Systems, Inc., Palo Alto, CA, USA) was used to contour the GTVs of the primary EC. The visualization parameter for delineation included the mediastinal window set to +40/400 HU. Before contouring, some clinical information such as the physical examination, pathological findings, and diagnostic CT image data were made available to the observers, while they were blind to the diagnostic endoscopy/EUS, esophagography, and FDG-PET/CT data. If the positive lymph nodes could not be separated from the primary tumor visually, they were delineated together with the primary tumor.

Five radiation oncologists (observers), who were blind to the diagnostic endoscopy/EUS, esophagography, and FDG-PET/CT patient data, were asked to independently delineate the GTVs with reference to different combinations of the multimodal images, including planning CT only (GTV_C), CT combined with endoscopy/EUS (GTV_{CE}), CT combined with endoscopy/EUS and esophagogram (X-ray) (GTV_{CEX}), and CT combined with endoscopy/EUS, esophagogram, and FDG-PET/CT (GTV_{CEXP}) (**Figure 1**). All observers were blind to the contours delineated by the other oncologists and their own former/previous contours. Observers 1 and 2 with clinical experience within five years were regarded as junior observers, while observers 3, 4, and 5 with more than ten years of clinical experience were regarded as senior observers. All contours were delineated in about two years. A delay of at least two months existed between each contouring of the tumor to eliminating a recall of the previous contouring for observers 1, 2, 3, and 5. The time interval for observer 4 was only one month, as the former observer 4 dropped out of the delineation process due to parturition.

Inter-/Intra-Observer Variability Analysis

Inter-/intra-observer variability in the volume, longitudinal length, generalized conformity index (CI_{gen}), and position of the GTVs was assessed. The intra-observer variability can be generally regarded as the variability of the same observer when re-contouring a single case. However, in this study, it is defined as the variability of the contours on the four multimodal imaging/image combinations for one observer (23).

The mean volume and longitudinal length of the GTVs based on different multimodal imaging combinations for different observers were calculated. The inter-observer variability in the volume and longitudinal length on different multimodal imaging, combinations and the intra-observer variability for different observers were measured. The tumor length was measured using CT, endoscopy/EUS (43 cases), esophagography, and FDG-PET/CT, with the difference between the tumor length and corresponding longitudinal length of the GTVs subsequently evaluated.

Conformity index (CI) was defined as the ratio of the common volume to encompassing volume (13, 24). The generalized CI (CI_{gen}) was used to assess the overall consistency of all volume combinations delineated by different observers on the same imaging-modality combination, and that delineated by the same observer on different imaging-modality combinations. The formula is given by (13, 25):

$$CI_{gen} = \frac{\sum_{pairsij} \left| A_i \cap A_j \right|}{\sum_{pairsij} A_i \cup A_j}$$

CI_{gen} is a good parameter for revealing the difference in the volumes delineated based on the size, shape, and location (10, 23).

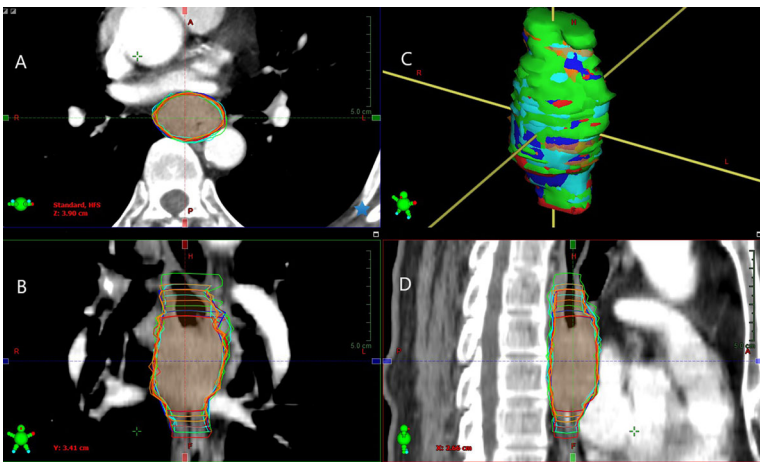

FIGURE 1 | Example of GTVs delineated based on different combinations of multimodal images by observer 1 (green segment), observer 2 (red segment), observer 3 (blue segment), observer 4 (orange segment), and observer 5 (cyan segment) in tansversal **(A)**, frontal **(B)**, surface **(C)**, and sagittal **(D)** planes for one patient (Patient 5). Inter-/intra-observer variability in the volume and longitudinal length on different combinations of multimodal images exhibiting significant differences.

The use of CI_{gen} tends to decrease the bias in the number of delineations (13). The lower is the CI_{gen} value for the same imaging-modality combination, the greater is the inter-observer variability. Similarly, a lower CI_{gen} for the same observer suggests a greater intra-observer variability.

In addition, the x (right-left), y (anterior-posterior), and z (superior-inferior) axes of the center of mass (COM) of the volume were measured. The centroid shifts between the different volumes were then obtained. Finally, the three dimensional (3D) centroid shifts were calculated using the followed equation (24, 26):

$$3D\ centroid\ shifts = \sqrt{\Delta x^2 + \Delta y^2 + \Delta z^2}$$

Statistical Analysis

Statistical analysis was performed using the SPSS software package (SPSS 25.0). All the data had an approximately normal distribution. The one-way ANOVA test was applied to detect the inter-/intra-observer variability in the volume, longitudinal length, CI_{gen}, and position of the GTVs among different observers and different multimodal imaging combinations. The paired *t*-test was used to compare the volume, longitudinal length, CI_{gen}, and position of the GTVs between two observers or two multimodal imaging combinations. A $P<0.05$ was considered significant.

RESULTS

GTV Volume

Table 2 shows the primary GTV delineated based on four different multimodal imaging combinations for each observer. No significant inter-observer differences in the volume were observed for GTV_C, GTV_{CE}, GTV_{CEX}, or GTV_{CEXP} (p= 0.904, 0.987, 0.984, and 0.97, respectively). The intra-observer variability in the volume of the GTVs derived from four different multimodal imaging combinations for observers 1–5 also showed no significant differences (p= 0.926, 0.997, 0.908, 0.943, and 0.99, respectively). However, the paired comparisons indicated significant differences in the GTV volume between observers 1 and 2, observers 1 and 4, and observers 3 and 4 (t= 3.154, 6.368, and 3.342, p= 0.002, <0.001, and 0.001, respectively). Approximate statistical differences in the GTV volume were found between observers 1 and 3, and observers 2 and 4 (t= 3.342 and 1.869, p= 0.061 and 0.063, respectively).

Esophageal Tumor Length

Table 3 shows the mean tumor lengths measured by CT, endoscopy/EUS, esophagography, and FDG-PET/CT. No significant differences were found between any two image-based tumor lengths. **Table 3** presents the mean longitudinal lengths measured by the five observers corresponding to GTV_C, GTV_{CE}, GTV_{CEX}, and GTV_{CEXP}. The mean longitudinal length for GTV_{CEXP} was larger than the tumor length measured by FDG-PET/CT (p=0.0035). The intra-observer variability in the longitudinal length of the GTVs based on four multimodal imaging combinations for observers 1–5 showed no significant differences (p= 0.751, 0.794, 0.115, 0.962, and 0.753, respectively). **Table 2** shows the tumor lengths measured based on the four different multimodal imaging combinations for each observer. No significant inter-observer differences in the longitudinal length were recorded for GTV_C, GTV_{CE}, GTV_{CEX}, and GTV_{CEXP} (p= 0.286, 0.503, 0.997, and 0.749, respectively). The two-related-samples tests indicated significant differences in the longitudinal lengths of the four GTVs between observers 1 and 2 (t=2.776, p=0.006), observers 1 and 5 (t=1.98, p=0.049), observers 3 and 2 (t=−3.166, p=0.002), and observers 3 and 5 (t=2.992, p=0.003).

TABLE 2 | The volume and longitudinal length of GTVs based on different combinations of multimodal imaging for different observers.

Parameter		Observer 1	Observer 2	Observer 3	Observer 4	Observer 5	Mean±SD
GTV_C	Volume(cm^3)	37.57 ± 26.68	33.78 ± 27.42	36.42 ± 26.91	33.48 ± 28.07	33.28 ± 26.87	34.91 ± 27.19
	Length(mm)	5.7 ± 2.6	5.3 ± 2.5	6.3 ± 2.5	5.7 ± 2.6	5.3 ± 2.3	5.7 ± 2.5
GTV_{CE}	Volume(cm^3)	34.06 ± 25.90	34.47 ± 26.65	36.33 ± 27.10	32.68 ± 25.79	35.13 ± 27.50	34.68 ± 26.82
	Length(mm)	5.7± 2.5	5.4 ± 2.2	6.3 ± 2.4	5.8 ± 2.4	5.7 ± 2.3	5.8 ± 2.4
GTV_{CEX}	Volume(cm^3)	35.43 ± 25.79	35.00 ± 26.40	33.57 ± 26.68	34.50 ± 26.84	35.03 ± 28.37	34.34 ± 26.81
	Length(mm)	5.6 ± 2.2	5.6 ± 2.2	5.5 ± 2.3	5.6 ± 2.2	5.6 ± 2.5	5.6 ± 2.3
GTV_{CEXP}	Volume(cm^3)	36.30 ± 27.41	34.17 ± 26.19	33.48 ± 27.13	33.28 ± 26.67	36.73 ± 28.27	35.04 ± 27.17
	Length(mm)	6.1± 2.5	5.7 ± 2.2	5.5 ± 2.3	5.8 ± 2.4	5.8 ± 2.3	5.8 ± 2.3
Mean ± SD	Volume(cm^3)	35.84 ± 26.45	34.36 ± 26.67	34.95 ± 27.20	33.52 ± 26.91	35.04 ± 27.75	34.37 ± 27.29
	Length(mm)	5.8 ± 2.4	5.5 ± 2.3	5.9 ± 2.4	5.7 ± 2.4	5.6 ± 2.4	5.7 ± 2.4

Gross target volumes (GTV) delineated on planning CT only (GTV_C), CT combined with endoscopy/EUS (GTV_{CE}), CT combined with endoscopy/EUS and esophagography (X-ray) (GTV_{CEX}), and CT combined with endoscopy/EUS, esophagography, and FDG-PET/CT (GTV_{CEXP}).

Generalized CI (CI_{gen})

Table 4 lists the mean CI_{gen} values for the four GTVs derived from different multimodal imaging combinations (mean intra-observer CI_{gen}) for each observer. The mean intra-observer CI_{gen} values for all observers was 0.73 ± 0.15. The mean intra-observer CI_{gen} was the largest for observer 4, exhibiting significant differences with that for the other observers. The mean intra-observer CI_{gen} for observer 1 was the lowest, exhibiting significant differences with that for observers 3, 4, and 5. The mean intra-observer CI_{gen} among different observers was statistically significant (F=32.493, p<0.001). **Table 5** lists the mean CI_{gen} values for the five GTVs derived from different observers (mean inter-observer CI_{gen}) for each multimodal imaging combination. The mean inter-observer CI_{gen} values for the four multimodal imaging combinations was 0.67 ± 0.11. The mean inter-observer CI_{gen} was the largest for the fourth multimodal imaging combination, which exhibited significant differences with that for the other three combinations. The mean inter-observer CI_{gen} among the different multimodal imaging combinations showed a significant difference (F=6.872, p<0.001).

Three-Dimensional (3D) Centroid Shifts

Table 4 lists the mean 3D centroid shifts of the four GTVs derived from different multimodal imaging combinations (mean intra-observer 3D centroid shifts) for each observer. The mean intra-observer 3D centroid shifts for all observers was 3.67 ± 4.62 mm. The mean intra-observer 3D centroid shifts for observer 4 showed significant differences compared with the other observers. The mean intra-observer 3D centroid shifts among different observers was significant (F=3.898, p=0.004). **Table 5** presents the 3D centroid shifts of the five GTVs derived from different observers (mean inter-observer 3D centroid shifts) for each multimodal imaging combination. The mean inter-observer 3D centroid shifts for all four multimodal imaging combinations was 3.81 ± 4.7 mm. The mean inter-observer 3D centroid shifts among the different multimodal imaging combinations showed no significant difference (F=0.327, p=0.806).

DISCUSSION

Uncertainties in volume delineation for esophageal carcinomas is a well-recognized potential cause of treatment failure in radiotherapy (27, 28). Minimizing the inter-/intra-observer delineation variability in volume delineation is regarded as an effective alternative method to define the GTV accurately (29, 30), since the gold standard of a pathological reference volume is rarely attainable (31, 32). The significance of quantifying the degree of variability or uncertainty in volume delineation is that the resulting impact on dosimetry and clinical outcomes (29, 30).

Accurate target delineation for esophageal cancer is often restricted by the poor discriminative value of current imaging modalities (23), particularly CT, and the inability to relate diagnostic endoscopy/EUS, esophagography, or FDG-PET/CT information to the panning CT images (13–17, 23). However, reasonable pretreatment staging assessments are essential to determine a rational treatment strategy. In each patient with newly diagnosed esophageal cancer, the acquired diagnostic imaging information should identify the feasibility of delineating the GTVs of the primary based on the planning CT

TABLE 3 | Comparison the tumor length measured by CT, endoscopy/EUS, esophagography, and FDG-PET/CT with the mean longitudinal length measured by five observers for GTV_C, GTV_{CE}, GTV_{CEX}, and GTV_{CEXP}.

Imaging modality		CT	Endoscopy/EUS	Esophagography	PET-CT
Tumor length(cm)		5.5 ± 2.2	5.1 ± 2.0	5.3 ± 2.0	5.4 ± 2.2
Target volume		GTV_C	GTV_{CE}	GTV_{CEX}	GTV_{CEXP}
Longitudinal length(cm)		5.7 ± 2.5	5.8 ± 2.4	5.6 ± 2.3	5.8 ± 2.3
Paired comparison	t-value	-0.704	-1.759	-1.272	-2.172
	p-value	0.485	0.086	0.209	0.035

Gross target volumes (GTV) delineated on planning CT only (GTV_C), CT combined with endoscopy/EUS (GTV_{CE}), CT combined with endoscopy/EUS and esophagography (X-ray) (GTV_{CEX}), and CT combined with endoscopy/EUS, esophagography, and FDG-PET/CT (GTV_{CEXP}).

TABLE 4 | The CI_{gen} values and 3D centroid shifts (Mean ± SD) of the four GTVs derived from different combinations of multimodal imaging for each observer.

Parameter	Observer 1	Observer 2	Observer 3	Observer 4	Observer 5
CI_{gen}	0.68 ± 0.12	0.69 ± 0.14	0.75 ± 0.15	0.80 ± 0.15	0.74 ± 0.17
Paired t-test	0.173 (vs Obs2)	–	–	–	–
(p value)	<0.001 (vs Obs3)	<0.001 (vs Obs3)	–	–	–
	<0.001 (vs Obs4)	<0.001 (vs Obs4)	<0.001 (vs Obs4)	–	–
	<0.001 (vs Obs5)	<0.001 (vs Obs5)	0.264 (vs Obs5)	<0.001 (vs Obs5)	–
CI (G_C, G_{CEXP})	0.66 ± 0.12	0.70 ± 0.18	0.75 ± 0.13	0.78 ± 0.17	0.73 ± 0.18
CI (G_C, G_{CE})	0.69 ± 0.15	0.68 ± 0.14	0.77 ± 0.15	0.84 ± 0.15	0.78 ± 0.17
Paired t-test t	-1.718	1.247	-0.848	-2.592	-2.666
(p value)	0.092	0.218	0.4	0.013	0.01
3D shifts(mm)	3.69 ± 4.47	4.34 ± 4.24	3.84 ±3.93	2.85 ± 4.24	3.65 ± 6.19
Paired t-test	0.023 (vs Obs2)	–	–	–	–
(p value)	0.572 (vs Obs3)	0.077 (vs Obs3)	–	–	–
	0.005 (vs Obs4)	<0.001 (vs Obs4)	0.001 (vs Obs4)	–	–
	0.911 (vs Obs5)	0.084 (vs Obs5)	0.59 (vs Obs5)	0.039 (vs Obs5)	–

Gross target volumes (GTV) delineated on planning CT only (G_C), CT combined with endoscopy/EUS (G_{CE}), and CT combined with endoscopy/EUS, esophagography, and FDG-PET/CT (G_{CEXP}). The CI between G_C and G_{CEXP} [CI (G_C, G_{CEXP})], the CI between G_C and G_{CE} [CI (G_C, G_{CE})].

TABLE 5 | The CI_{gen} values and 3D centroid shifts (Mean ± SD) of the five GTVs delineated by different observers based on each combinations of multimodal imaging.

Parameter	GTV_C	GTV_{CE}	GTV_{CEX}	GTV_{CEXP}
CI_{gen}	0.66 ± 0.13	0.66 ± 0.12	0.67 ± 11	0.69 ± 0.10
Paired t-test	0.443 (vs G_{CE})	–	–	–
(p value)	<0.088 (vs G_{CEX})	0.269 (vs G_{CEX})	–	–
	<0.001 (vs G_{CEXP})	<0.001 (vs G_{CEXP})	<0.001 (vs G_{CEXP})	–
3D shifts (mm)	3.78 ± 4.04	3.78 ± 3.79	3.98 ± 5.03	3.68 ± 5.94
Paired t-test	0.981 (vs G_{CE})	–	–	–
(p value)	0.463 (vs G_{CEX})	0.463 (vs G_{CEX})	–	–
	0.762 (vs G_{CEXP})	0.744 (vs G_{CEXP})	0.218 (vs G_{CEXP})	–

Gross target volumes (GTV) delineated on planning CT only (GTV_C), CT combined with endoscopy/EUS (GTV_{CE}), CT combined with endoscopy/EUS and esophagography (X-ray) (GTV_{CEX}), and CT combined with endoscopy/EUS, esophagography, and FDG-PET/CT (GTV_{CEXP}).

image with reference to the above-mentioned information. In this study, the geometric features of the GTVs derived from different observers and different planning CT image combinations were compared with the diagnostic imaging information. Furthermore, the value of the different planning CT image combinations in conjunction with diagnostic imaging information was evaluated for tumor delineation in esophageal carcinoma.

The results of this study showed no statistically significant inter-observer differences in the esophageal volume estimation based on different combinations of the CT, endoscopy/EUS, esophagography, and FDG-PET/CT data (**Table 2**). For a particular multimodal imaging combination, different observers reported similar estimates for the GTV based on a similar knowledge of multimodal imaging. Moreover, for each observer, the volumes of the four GTVs delineated on different multimodal imaging combinations showed no significant differences. This indicates that the GTV volume assessments on different multimodal imaging combinations did not transform/change for the same observer. The data presented here is similar to the results reported in other literature (33, 34). However, Choi et al. (13) reported that the number of observers and number of observations made might affect the level of significance. In this study, many significant differences were observed in the GTV volume between different observers in the pairwise comparisons. Therefore, inter-observer variation in the target delineation could not be revealed/identified by merely comparing the volumes of the GTVs.

Similar to the observed variability in the volumes of the GTVs, the inter-observer and intra-observer variability in the longitudinal length showed no statistically significant differences (**Table 3**). However, some significant differences between different observers were identified in the pairwise comparisons. The main reason behind these differences might be a different understanding of the procedure of determining the tumor length on multimodal imaging by different observers. Radiation oncologists have always found the procedure to determine the proximal and distal extension of esophageal carcinoma based on different images challenging. Conventional images from CT, endoscopy/EUS, and esophagography, and MRI or FDG-PET/CT have their share of advantages and limitations for determining the tumor length (14–17, 22, 35, 36). It is critical to familiarize radiation oncologists with these advantages and limitations before selecting the different image combinations. In this study, the tumor length determined by the multimodal images tended to be larger than that measured by a single image. In particular, the longitudinal length of GTV_{CEXP} was significantly larger than the tumor length measured by FDG-PET/CT. Therefore, the use of the multimodal images to determine the target length contributes to reducing the

limitation of a single image, and improving the accuracy of target delineation; however, this is based on the precondition that the observers develop a good knowledge of the features of the multimodal images *via* unified training.

The CI_{gen} values for GTV_C, GTV_{CE}, GTV_{CEX}, and GTV_{CEXP} for each observer represent the intra-observer variations, which include the random and inherent variations derived from different multimodal imaging combinations for the same observer. Here, the mean CI_{gen} for intra-observer variability (0.73) was larger than that for inter-observer variability (0.67). This indicates that the intra-observer variability in delineating esophageal tumors was lower than the inter-observer variability, which shows agreement with the results reported in other studies (33, 34). Machiels et al. (33) reported the mean CI_{gen} values for intra-observer delineation variability and inter-observer variability in ten patients without endoscopically implanted fiducial markers versus those with markers to be 0.54 versus 0.68 and 0.68 versus 0.75, respectively. Vollenbrock et al. (34) reported the mean CI_{gen} over six patients as 0.68 on FDG-PET/CT, 0.66 on T_2w-MRI, and 0.68 on T_2w+DW(diffusion-weighted)-MRI. Compared with the above studies, fifty patients with upper, middle, and lower thoracic esophageal carcinoma were enrolled in this study. Moreover, different multimodal imaging combinations, including CT, endoscopy/EUS, esophagography, and FDG-PET/CT, were employed to eliminate any bias from a single imaging technique.

In addition, the CT is a basic image (GTV_C). CT combined with endoscopy/EUS is a simple combination(GTV_{CE}), while CT combined with endoscopy/EUS, esophagography, and FDG-PET/CT (GTV_{CEXP}) is regarded as an effective alternative method to define the GTV accurately (**Table 5**). Therefore, The CI between GTV_C and GTV_{CEXP}, was significantly less than the CI between GTV_C and GTV_{CE} for all observers (t= -3.018, p = 0.003), which suggested that a comprehensive combination of multimodal images was more conducive to influence the target delineation compared a simple combination.

In the ANOVA analysis, the intra-observer CI_{gen} for the GTVs derived from different multimodal imaging combinations among the five observers was statistically significant (p<0.001). The intra-observer CI_{gen} for the senior radiation oncologists (observers 3, 4, and 5) was larger than that for the junior radiation oncologists (observers 1 and 2). An optimum intra-observer CI_{gen} was obtained for the senior radiotherapist who spent minimal time delineating the GTVs (observer 4) (**Table 4**). The senior radiotherapists, who were generally familiar with the multimodal imaging features for distinguishing the tumors from the normal structures and the location subject to relapse, might not be easily affected when only a single imaging modality is used/available for target contouring (37, 38). In addition, the shorter repeating delineation intervals did not eliminate the record of previous delineations, which might have improved the consistency of the target delineation. This suggests that background knowledge in medical imaging, clinical experience, and repeating delineation intervals might affect the intra-observer variability of the target CI_{gen}. Strengthening the target delineation and medical imaging knowledge training contributes to improve the accuracy of target delineation for EC.

While the inter-observer CI_{gen} calculated for the different multimodal imaging combinations did not increase for the combined CT and endoscopy/EUS data, as compared with CT only, CI_{gen} tended to increase for the combined CT and endoscopy/EUS and esophagography information (p=0.088). Furthermore, the addition of FDG-PET/CT to the endoscopy/EUS, and esophagography data significantly improved the inter-observer CI_{gen}. The use of multimodal imaging, including CT, endoscopy/EUS, esophagography, and FDG-PET/CT, for target delineation reduced the inter-observer variability.

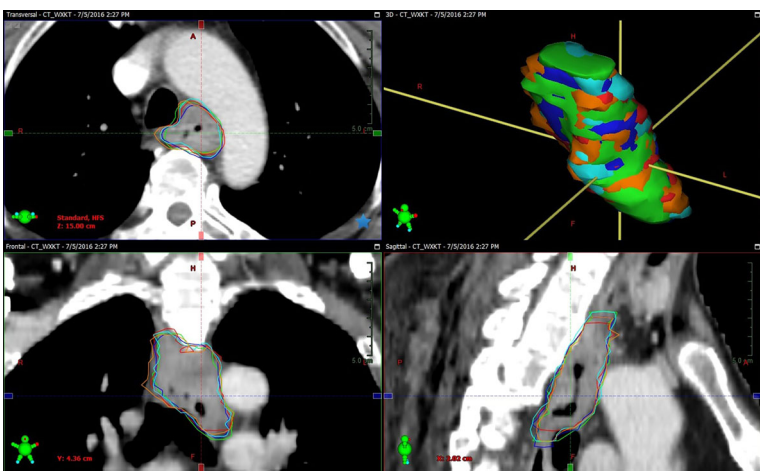

FIGURE 2 | Example of GTVs delineated based on CT combined with endoscopy/EUS, esophagogram, and FDG-PET/CT (GTV_{CEXP}) by observer 1 (green segment), observer 2 (red segment), observer 3 (blue segment), observer 4 (orange segment), and observer 5 (cyan segment) in tansversal, frontal, surface, and sagittal planes for one patient (Patient 10). The volume and longitudinal length of GTV_{CEXP} delineated on CT combined with endoscopy/EUS, esophagogram, and FDG-PET/CT exhibiting a good consistency.

Figure 2 showed example of GTVs delineated based on CT combined with endoscopy/EUS, esophagogram, and FDG-PET/CT (GTV_{CEXP}) by five oncologists, and the volume and longitudinal length of GTV_{CEXP} exhibited a good consistency. The effect of FDG-PET/CT on the intra- and inter-observer variability of target volume delineation in patients with gastro-esophageal cancer remains controversial. Vesprini et al. (39) reported that the combined use of FDG-PET/CT based on CT for GTV delineation significantly decreased both intra- and inter-observer variability, while Schreurs et al. (40) did not find PET/CT to have a significant effect on the inter-observer variability. Therefore, besides FDG-PET/CT, the additional use of endoscopy/EUS and esophagography for target delineation might prove beneficial in reducing the inter-observer variability. Recent studies have shown that the use of endoscopically implanted fiducial markers and MRI might reduce the variability of target volume delineation (33, 34). The use of multimodal imaging has proved increasingly valuable in improving the accuracy of target definition in esophageal carcinoma.

The target conformity index (CI) is mainly influenced by positional and morphological difference of targets. Here, the intra-observer variability in the 3D centroid shifts of the GTVs among different observers showed a significant difference. In the case of no significant variability in the volume of the GTVs, the intra-observer variability in the position could have mainly contributed to the statistical significance in the CI_{gen} value. The intra-observer variability in the shape also tends to affect the intra-observer CI_{gen}. The inter-observer variability in the 3D centroid shifts and volume of the GTVs showed no significant differences, suggesting that the inter-observer variability in the shape had a critical influence on the inter-observer CI_{gen}. Thus, this study indirectly implies that using different multimodal image combinations might transform/change different observers' visual perception of tumors. In addition, we found the 3D centroid shifts were 3-4mm either between the observers themselves or between the observers. Therefore, whether it is necessary to expand an extra margin to include this error is a clinical problem and deserves further thinking.

CONCLUSION

In conclusion, for radiation oncologists with advanced medical imaging training and clinical experience, the use of diagnostic multimodal images from endoscopy/EUS, esophagography, and FDG-PET/CT for target delineation based on planning CT reduced the intra- and inter-observer variability and increased the accuracy of target delineation in primary thoracic esophageal carcinomas. The use of the combination of multimodal images would reduce uncertainties in volume delineation for esophageal carcinomas, and potentially increase the success rate of radiotherapy. We also found the inter/intra observer variability in the 3D centroid shifts of GTVs were about 3-4mm, whether it is necessary to expand an extra margin to include this error deserves further thinking.

DATA AVAILABILITY STATEMENT

The original contributions presented in the study are included in the article/supplementary material. Further inquiries can be directed to the corresponding authors.

ETHICS STATEMENT

The studies involving human participants were reviewed and approved by Shandong Cancer Hospital and Institute. The patients/participants provided their written informed consent to participate in this study.

AUTHOR CONTRIBUTIONS

FL and YL contributed to the study design, the patient enrollment, the data statistics and analysis, and writing the manuscript. JL participated in the study design. XW contributed to the patient enrollment. YZ, XL, SL, JW, and MX contributed to the delineation. WW and YG made important contributions in collecting the data and revising the content. All authors contributed to the article and approved the submitted version.

FUNDING

This work was supported by Shandong Cancer Hospital and Institute, China. National Natural Science Foundation of China (817732870); Beijing Medical Award Foundation (YXJL-2020-0785-0616); Taishan Scholars Program of Shandong Province (NO.ts 20190982); Wu Jieping Medical Foundation (320.6750.2021-02-79).

REFERENCES

1. Bray F, Ferlay J, Soerjomataram I, Siegel RL, Torre LA, Jemal A. Global Cancer Statistics 2018: GLOBOCAN Estimates of Incidence and Mortality Worldwide for 36 Cancers in 185 Countries. *CA Cancer J Clin* (2018) 68:394–424. doi: 10.3322/caac.21492
2. Sjoquist KM, Burmeister BH, Smithers BM, Zalcberg JR, Simes RJ, Barbour A, et al. Survival After Neoadjuvant Chemotherapy or Chemoradiotherapy for Resectable Oesophageal Carcinoma: An Updated Meta-Analysis. *Lancet Oncol* (2011) 12(7):681–92. doi: 10.1016/S1470-2045(11)70142-5
3. Shapiro J, van Lanschot JJB, Hulshof MCCM, van Hagen P, van Berge Henegouwen MI, Wijnhoven BPL, et al. Neoadjuvant Chemoradiotherapy Plus Surgery Versus Surgery Alone for Oesophageal or Junctional Cancer (CROSS): Long-Term Results of a Randomised Controlled Trial. *Lancet Oncol* (2015) 16(9):1090–8. doi: 10.1016/S1470-2045(15)00040-6

4. Lagergren J, Smyth E, Cunningham D, Lagergren P. Oesophageal Cancer. *Lancet* (2017) 390(10110):2383–96. doi: 10.1016/S0140-6736(17)31462-9
5. Cooper JS, Guo MD, Herskovic A, Macdonald JS, Martenson JA Jr, Al-Sarraf M, et al. Chemoradiotherapy of Locally Advanced Esophageal Cancer: Long-Term Follow-Up of a Prospective Randomized Trial (RTOG 85-01). *JAMA* (1999) 281(17):1623–7. doi: 10.1001/jama.281.17.1623
6. Rohatgi PR, Swisher SG, Correa AM, Wu TT, Liao Z, Komaki R, et al. Failure Patterns Correlate With the Proportion of Residual Carcinoma After Preoperative Chemoradiotherapy for Carcinoma of the Esophagus. *Cancer* (2005) 104(7):1349–55. doi: 10.1002/cncr.21346
7. Welsh J, Settle SH, Amini A, Xiao L, Suzuki A, Hayashi Y, et al. Failure Patterns in Patients With Esophageal Cancer Treated With Definitive Chemoradiation. *Cancer* (2012) 118(10):2632–40. doi: 10.1002/cncr.26586
8. Amini A, Ajani J, Komaki R, Allen PK, Minsky BD, Blum M, et al. Factors Associated With Local-Regional Failure After Definitive Chemoradiation for Locally Advanced Esophageal Cancer. *Ann Surg Oncol* (2014) 21(1):306–14. doi: 10.1245/s10434-013-3303-0
9. Xi M, Yang Y, Zhang L, Yang H, Merrell KW, Hallemeier CL, et al. Multi-Institutional Analysis of Recurrence and Survival After Neoadjuvant Chemoradiotherapy of Esophageal Cancer: Impact of Histology on Recurrence Patterns and Outcomes. *Ann Surg* (2019) 269(4):663–70. doi: 10.1097/SLA.0000000000002670
10. Nowee ME, Voncken FEM, Kotte ANTJ, Goense L, van Rossum PSN, van Lier ALHMW, et al. Dutch National Platform for Radiotherapy of Gastrointestinal Tumours (LPRGE) Group. Gross Tumour Delineation on Computed Tomography and Positron Emission Tomography-Computed Tomography in Oesophageal Cancer: A Nationwide Study. *Clin Transl Radiat Oncol* (2018) 14:33–9. doi: 10.1016/j.ctro.2018.10.003
11. Muijs C, Smit J, Karrenbeld A, Beukema J, Mul V, van Dam G, et al. Residual Tumor After Neoadjuvant Chemoradiation Outside the Radiation Therapy Target Volume: A New Prognostic Factor for Survival in Esophageal Cancer. *Int J Radiat Oncol Biol Phys* (2014) 88(4):845–52. doi: 10.1016/j.ijrobp.2013.11.009
12. Steenbakkers RJ, Duppen JC, Fitton I, Deurloo KE, Zijp LJ, Comans EF, et al. Reduction of Observer Variation Using Matched CT-PET for Lung Cancer Delineation: A Three-Dimensional Analysis. *Int J Radiat Oncol Biol Phys* (2006) 64(2):435–48. doi: 10.1016/j.ijrobp.2005.06.034
13. Choi HJ, Kim YS, Lee SH, Lee YS, Park G, Jung JH, et al. Inter- and Intra-Observer Variability in Contouring of the Prostate Gland on Planning Computed Tomography and Cone Beam Computed Tomography. *Acta Oncol* (2011) 50(4):539–46. doi: 10.3109/0284186X.2011.562916
14. Pollard JM, Wen Z, Sadagopan R, Wang J, Ibbott GS. The Future of Image-Guided Radiotherapy Will be MR Guided. *Br J Radiol* (2017) 90:20160667. doi: 10.1259/bjr.20160667
15. Drudi FM, Trippa F, Cascone F, Righi A, Iascone C, Ricci P, et al. Esophagogram and CT vs Endoscopic and Surgical Specimens in the Diagnosis of Esophagealcarcinoma. *Radiol Med* (2002) 103(4):344–52.
16. Encaoua J, Abgral R, Leleu C, El Kabbaj O, Caradec P, Bourhis D, et al. Radiotherapy Volume Delineation Based on (^{18}F)-Fluorodeoxyglucose Positron Emission Tomographyfor Locally Advanced or Inoperable Oesophageal Cancer. *Cancer Radiother* (2017) 21(4):267–75. doi: 10.1016/j.canrad.2016.12.004
17. Caputo FM, Buquicchio GL. Esophageal Cancer Staging: The Role of Radiology. *Rays* (2005) 30(4):309–14.
18. Wang B, Liu C, Lin C, Hsu PK, Hsu WH, Wu YC, et al. Endoscopic Tumor Length Is an Independent Prognostic Factor in Esophageal Squamous Cell Carcinoma. *Ann Surg Oncol* (2012) 19:2149–58. doi: 10.1245/s10434-012-2273-y
19. Gao XS, Qiao X, Wu F, Cao L, Meng X, Dong Z, et al. Pathological Analysis of Clinical Target Volume Margin for Radiotherapy in Patients With Esophageal and Gastroesophageal Junction Carcinoma. *Int J Radiat Oncol Biol Phys* (2007) 67:389–96. doi: 10.1016/j.ijrobp.2006.09.015
20. Muijs CT, Beukema JC, Pruim J, Mul VE, Groen H, Plukker JT, et al. A Systematic Review on the Role of FDG-PET/CT in Tumour Delineation and Radiotherapy Planning in Patients With Esophageal Cancer. *Radiother Oncol* (2010) 97(2):165–71. doi: 10.1016/j.radonc.2010.04.024
21. Thomas L, Lapa C, Bundschuh RA, Polat B, Sonke JJ, Guckenberger M, et al. Tumour Delineation in Oesophageal Cancer – A Prospective Study of Delineation in PET and CT With and Without Endoscopically Placed Clip Markers. *Radiother Oncol* (2015) 116:269–75. doi: 10.1016/j.radonc.2015.07.007
22. Metser U. Even-Sapir E Increased (18)F-Flfluorodeoxyglucose Uptake in Benign, Nonphysiologic Lesions Found on Whole-Body Positron Emission Tomography/Computed Tomography (PET/CT): Accumulated Data From Four Years of Experience With PET/Ct. *Semin Nucl Med* (2007) 37:206–22. doi: 10.1053/j.semnuclmed.2007.01.001
23. Louie AV, Rodrigues G, Olsthoorn J, Palma D, Yu E, Yaremko B, et al. Inter-Observer and Intra-Observer Reliability for Lung Cancer Target Volume Delineation in the 4D-CT Era. *Radiother Oncol* (2010) 95(2):166–71. doi: 10.1016/j.radonc.2009.12.028
24. Li FX, Li JB, Zhang YJ, Xu M, Shang D, Fan T, et al. Geometrical Differences in Gross Target Volumes Between 3DCT and 4DCT Imaging in Radiotherapy for Non-Small-Cell Lung Cancer. *J Radiat Res* (2013) 54(5):950–6. doi: 10.1093/jrr/rrt017
25. Kouwenhoven E, Giezen M, Struikmans H. Measuring the Similarity of Target Volume Delineations Independent of the Number of Observers. *Phys Med Biol* (2009) 54:2863 – 73. doi: 10.1088/0031-9155/54/9/018
26. Li FX, Li JB, Zhang YJ, Liu TH, Tian SY, Xu M, et al. Comparison of the Planning Target Volume Based on Three-Dimensional CT and Four-Dimensional CT Images of Non-Small-Cell Lung Cancer. *Radiother Oncol* (2011) 99(2):176–80. doi: 10.1016/j.radonc.2011.03.015
27. Thomas M, Mortensen HR, Hoffmann L, Møller DS, Troost EGC, Muijs CT, et al. Proposal for the Delineation of Neoadjuvant Target Volumes in Oesophageal Cancer. *Radiother Oncol* (2021) 156:102–12. doi: 10.1016/j.radonc.2020.11.032
28. Chang X, Deng W, Wang X, Zhou Z, Yang J, Guo W, et al. Interobserver Variability in Target Volume Delineation in Definitive Radiotherapy for Thoracic Esophageal Cancer: A Multi-Center Study From China. *Radiat Oncol* (2021) 16(1):102. doi: 10.1186/s13014-020-01691-4
29. Vinod SK, Jameson MG, Min M, Holloway LC. Uncertainties in Volume Delineation in Radiation Oncology: A Systematic Review and Recommendations for Future Studies. *Radiother Oncol* (2016) 121(2):169–79. doi: 10.1016/j.radonc.2016.09.009
30. Weiss E, Hess CF. The Impact of Gross Tumor Volume (GTV) and Clinical Target Volume (CTV) Definition on the Total Accuracy in Radiotherapy Theoretical Aspects and Practical Experiences. *Strahlenther Onkol* (2003) 179(1):21–30. doi: 10.1007/s00066-003-0976-5
31. Daisne JF, Duprez T, Weynand B, Lonneux M, Hamoir M, Reychler H, et al. Tumor Volume in Pharyngolaryngeal Squamous Cell Carcinoma: Comparison at CT, MR Imaging, and FDG PET and Validation With Surgical Specimen. *Radiology* (2004) 233:93–100. doi: 10.1148/radiol.2331030660
32. Wanet M, Lee JA, Weynand B, De Bast M, Poncelet A, Lacroix V, et al. Gradient-Based Delineation of the Primary GTV on FDG-PET in Nonsmall Cell Lung Cancer: A Comparison With Thresholdbased Approaches, CT and Surgical Specimens. *Radiother Oncol* (2011) 98:117–25. doi: 10.1016/j.radonc.2010.10.006
33. Machiels M, Jin P, van Hooft JE, Gurney-Champion OJ, Jelvehgaran P, Geijsen ED, et al. Reduced Inter-Observer and Intra-Observer Delineation Variation in Esophageal Cancer Radiotherapy by Use of Fiducial Markers. *Acta Oncol* (2019) 58(6):943–50. doi: 10.1080/0284186X.2019.1588991
34. Vollenbrock SE, Nowee ME, Voncken FEM, Kotte ANTJ, Goense L, van Rossum PSN, et al. Gross Tumor Delineation in Esophageal Cancer on MRI Compared With 18f-FDG-PET/Ct. *Adv Radiat Oncol* (2019) 4(4):596–604. doi: 10.1016/j.adro.2019.04.004
35. Hou DL, Shi GF, Gao XS, Asaumi J, Li XY, Liu H, et al. Improved Longitudinal Length Accuracy of Gross Tumor Volume Delineation With Diffusion Weightedmagnetic Resonance Imaging for Esophageal Squamous Cell Carcinoma. *Radiat Oncol* (2013) 8:169. doi: 10.1186/1748-717X-8-169
36. Machiels M, van Montfoort ML, Thuijs NB, Henegouwen MIVB, Hulshof MCCM. PO-0812: Pathological Validation of Endoscopically Placed Fiducials

on Tumor Borders in Esophageal Cancer. *Radiother Oncol* (2019) 133:S423–S24. doi: 10.1016/S0167-8140(19)31232-0
37. Van de Steene J, Linthout N, de Mey J, Vinh-Hung V, Claassens C, Noppen M, et al. Definition of Gross Tumor Volume in Lung Cancer: Inter-Observer Variability. *Radiother Oncol* (2002) 62(1):37–49. doi: 10.1016/S0167-8140(01)00453-4
38. Schimek-Jasch T, Troost EG, Rücker G, Prokic V, Avlar M, Duncker-Rohr V, et al. A Teaching Intervention in a Contouring Dummy Run Improved Target Volume Delineation in Locally Advanced Non-Small Cell Lung Cancer: Reducing the Interobserver Variability in Multicentre Clinical Studies. *Strahlenther Onkol* (2015) 191(6):525–33. doi: 10.1007/s00066-015-0812-8
39. Schreurs LM, Busz DM, Paardekooper GM, Beukema JC, Jager PL, van der Jagt EJ, et al. Impact of 18- Flfluorodeoxyglucose Positron Emission Tomography on Computed Tomography Defifined Target Volumes in Radiation Treatment Planning of Esophageal Cancer: Reduction in Geographic Misses With Equal Inter-Observer Variability. *Dis Esophagus* (2010) 23(6):493–501. doi: 10.1111/j.1442-2050.2009.01044.x
40. Vesprini D, Ung Y, Dinniwell R, Breen S, Cheung F, Grabarz D, et al. Improving Observer Variability in Target Delineation for Gastro-Oesophageal Cancer – The Role of (18F)Flfluoro-2-Deoxy-Dglucose Positron Emission Tomography/Computed Tomography. *Clin Oncol (R Coll Radiol)* (2008) 20:631–8. doi: 10.1016/j.clon.2008.06.004

Conflict of Interest: The authors declare that the research was conducted in the absence of any commercial or financial relationships that could be construed as a potential conflict of interest.

Publisher's Note: All claims expressed in this article are solely those of the authors and do not necessarily represent those of their affiliated organizations, or those of the publisher, the editors and the reviewers. Any product that may be evaluated in this article, or claim that may be made by its manufacturer, is not guaranteed or endorsed by the publisher.

frontiers | Frontiers in Oncology

ORIGINAL RESEARCH
published: 05 April 2022
doi: 10.3389/fonc.2022.839765

Long-Term Results of a Phase 2 Study of Definitive Chemoradiation Therapy Using S-1 for Esophageal Squamous Cell Carcinoma Patients Who Were Elderly or With Serious Comorbidities

Yun Chen[1,2,3], *Zhengfei Zhu*[1,2,3], *Weixin Zhao*[1,2,3], *Qi Liu*[1,2,3], *Junhua Zhang*[1,2,3], *Jiaying Deng*[1,2,3], *Dashan Ai*[1,2,3], *Saiquan Lu*[1,2,3], *Liuqing Jiang*[1,2,4], *Ihsuan Tseng*[1,2,3], *Huixun Jia*[5,6] *and Kuaile Zhao*[1,2,3]*

[1] Department of Radiation Oncology, Fudan University Shanghai Cancer Center, Shanghai, China, [2] Department of Oncology, Shanghai Medical College, Fudan University, Shanghai, China, [3] Shanghai Key Laboratory of Radiation Oncology, Shanghai, China, [4] Department of Radiation Oncology, Fujian Medical University Union Hospital, Fuzhou, China, [5] Clinical Statistics Center, Fudan University Shanghai Cancer Center, Shanghai, China, [6] Department of Ophthalmology, Shanghai General Hospital, Shanghai, China

OPEN ACCESS

Edited by:
Li Jiancheng,
Fujian Provincial Cancer Hospital, China

Reviewed by:
Naseer Ahmed,
CancerCare Manitoba, Canada
Xue Wu,
Geneseeq Technology Inc., Canada

***Correspondence:**
Kuaile Zhao
kuaile_z@fudan.edu.cn

Specialty section:
This article was submitted to Radiation Oncology, a section of the journal Frontiers in Oncology

Received: *20 December 2021*
Accepted: *07 March 2022*
Published: *05 April 2022*

Citation:
Chen Y, Zhu Z, Zhao W, Liu Q, Zhang J, Deng J, Ai D, Lu S, Jiang L, Tseng I, Jia H and Zhao K (2022) Long-Term Results of a Phase 2 Study of Definitive Chemoradiation Therapy Using S-1 for Esophageal Squamous Cell Carcinoma Patients Who Were Elderly or With Serious Comorbidities. Front. Oncol. 12:839765. doi: 10.3389/fonc.2022.839765

Background: The optimal evidence-based management for the subsets of locally advanced esophageal squamous cell carcinoma (ESCC) patients who rejected or were intolerant to intravenous chemotherapy due to old age or serious comorbidities is currently lacking. This study aimed to assess the safety and local control rate (LCR) of S-1 (tegafur–gimeracil–oteracil potassium) combined with radiotherapy in these subsets of ESCC patients.

Methods: Locally advanced ESCC patients who rejected or were intolerant to intravenous chemotherapy due to age >75 years or serious comorbidities were enrolled in a prospective, single-arm, phase 2 trial. The patients were treated with definitive concurrent chemoradiotherapy with S-1, which was administered orally twice daily for 28 days. The radiotherapy dose was 61.2 Gy delivered in 34 fractions. The primary end-point was the 3-year LCR.

Results: One hundred five ESCC patients were recruited between March 2013 and October 2015. At the median follow-up of 73.1 months (IQR 65.5–81.4 months), 3-year LCR was 61.1%, and 1, 3, and 5-year overall survival was 77.9, 42.3, and 24.8% respectively. For safety analysis, ≥grade 3 acute adverse events included thrombocytopenia (6.7%), leukopenia (2.9%), anemia (1.0%), anorexia (1.0%), fatigue

(10.5%), hiccup (1.0%), pneumonitis (4.8%), and esophagitis (3.8%). Two patients (1.9%) died of late esophageal hemorrhage, and one patient (1.0%) died of late radiation-induced pneumonitis.

Conclusion: S-1 is a promising regimen in concurrent chemoradiotherapy with low toxicity and a favorable LCR in ESCC patients who rejected or were intolerant to intravenous chemotherapy due to old age or serious comorbidities.

Clinical Trial Registration: ClinicalTrials.gov, NCT01831531.

Keywords: esophageal squamous cell carcinoma, S-1, definitive chemoradiotherapy, elderly, serious comorbidities

INTRODUCTION

Esophageal cancer (EC) is the 4th most common cause of cancer deaths in China (1). The RTOG85-01 trial established the efficacy of definitive concurrent chemoradiotherapy (dCRT), which can significantly improve survival compared with radiotherapy (RT) alone (2). All patients in the RT alone arm died of cancer by 3 years. Since then, dCRT has become the standard treatment for inoperable locally advanced EC patients, and RT alone should only be reserved for palliation or for patients who are medically unable to receive chemotherapy. However, there is indeed a group of EC patients who rejected or were intolerant to intravenous chemotherapy due to old age or serious comorbidities. The management of these patients is a therapeutic challenge. Searching an alternative effective chemotherapy agent with moderate treatment related toxicities seems to be a promising strategy for these patients.

S-1 is an oral chemotherapy agent of fluoropyrimidine, consisting of tegafur, gimeracil, and oteracil potassium, and has been proven to be noninferior in efficacy to infusional fluorouracil in gastric cancer (3). In addition, the S-1-based regimen showed a good safety profile with lower incidence of grade 3/4 neutropenia (OR = 0.33) than the 5-fluorouracil based regimen in advanced gastric cancer (4). Moderate toxicities and promising response rates were also observed in EC patients treated with concurrent chemoradiotherapy with an S-1 based regimen (5, 6). Therefore, S-1 combined with definitive RT may be an optimal option for locally advanced EC patients who rejected or were intolerant to intravenous chemotherapy due to old age or serious comorbidities.

In this phase 2 clinical trial (ESO-Shanghai 7), we aimed to verify the safety and efficacy of definitive RT combined with S-1 alone in locally advanced esophageal squamous cell carcinoma (ESCC) patients who rejected or were intolerant to intravenous chemotherapy due to old age or serious comorbidities. We hypothesized that S-1 combined with radiotherapy had low toxicity and improves local control in these ESCC patients.

Abbreviations: AEs, adverse events; BSA, body surface area; CTV, clinical target volume; dCRT, definitive concurrent chemoradiotherapy; EC, Esophageal cancer; ECOG, Eastern Cooperative Oncology Group; ESCC, esophageal squamous cell carcinoma; FUSCC, Fudan University Shanghai Cancer Center; GTV, gross tumor volume; OS, overall survival; PTV, planning target volume; RT, radiotherapy; ULN, upper limit of normal.

MATERIALS AND METHODS

Study Design

This single arm phase 2 clinical trial was performed at the Fudan University Shanghai Cancer Center (FUSCC). Eligible patients were histologically confirmed diagnosis of ESCC, stage IIa to IVa, and were previously untreated. They rejected or were intolerant to intravenous chemotherapy due to old age (more than 75 years), or serious comorbidities (namely, severe cardiovascular diseases, sequelae of cerebral infarction, uncontrolled diabetes, etc.). Other inclusion criteria were an Eastern Cooperative Oncology Group (ECOG) performance status of 0 to 2, a life expectancy of at least 3 months, adequate organ function (hemoglobin ≥9 g/dl, white blood count $\geq 3 \times 10^9$/L, neutrophil count $\geq 1.5 \times 10^9$/L, platelet count $\geq 70 \times 10^9$/L, aspartate transaminase and alanine aminotransferase <2.5 × upper limit of normal (ULN), total bilirubin <1.5× ULN, and creatinine <1.5× ULN), and the use of an effective contraceptive for adults to prevent pregnancy. The major exclusion criteria were: complete esophageal obstruction, distant metastatic disease, drug addiction, alcoholism or AIDS, and other concomitant cancers. For the full inclusion and exclusion criteria, see **Appendix 1**.

Treatment

S-1 was given orally as described from days 1 to 28 at the beginning of the first fraction of radiotherapy. The dose of S-1 was calculated according to body surface area (BSA) (<1.6 m^2: 40 mg bid and ≥1.6 m^2: 50 mg bid). A powder form of S-1 would be administered if patients could not swallow the oral capsule. If patients had hematologic toxic effects of grade 4 or nonhematologic toxic effects of more than grade 3, their daily dose was reduced, from 100 to 80 mg or from 80 to 60 mg.

A total dose of 61.2 Gy was prescribed at the isocenter delivered by 6 MV photons in 34 fractions of 1.8 Gy (five fractions per week, one fraction per day). Intensity modulated radiotherapy based on a CT simulation planning system with a 5 mm thickness scan slice throughout the entire neck and thorax was required. Involved-field irradiation was used in this study. The gross tumor volume (GTV) was defined as visible esophageal tumor and metastatic lymph nodes based on the imaging of endoscopic ultrasound, esophageal radiography, or CT scan (whichever was larger). The criteria for metastatic lymph nodes were as follows: pathologic confirmation or short axis of ≥10 mm

in the mediastinum or cervix, or short axis of ≥5 mm in the tracheoesophageal groove, or histologically proven as metastatic by puncture. The clinical target volume (CTV) included the GTV manually extended by 30 mm in the superior–inferior direction for potential submucosal invasions. Metastasis lymph nodes had no CTV. A further 1 cm expansion added to the CTV in all directions was applied to account for technical uncertainties, which defined the planning target volume (PTV). The field next to the spinal cord could be slightly changed in order to reduce the exposure of the spinal cord. The criteria of dose distribution were as follows: 95% of the PTV to receive ≥99% of the prescribed dose, 99% of the PTV to receive ≥95% of the prescribed dose, $<2cm^3$ of the PTV to receive ≥120% of the prescribed dose, and $<1\ cm^3$ of the PTV to receive ≥110% of the prescribed dose. Highest and lowest point dose inside PTV were recorded. Normal organ dose restrictions were defined as follows: spinal cord: the highest point dose has to be less than 45 Gy; lung: The volume of lung (PTV excluded) receiving 20 Gy has to be equal to or less than 30% of the total lung volume, and the mean lung dose has to be equal to or less than 15 Gy at the same time; and heart: the mean dose has to be less than 40 Gy.

Outcomes

The primary endpoints of this trial included the 3-year local control rate (included the primary esophageal tumor and regional lymph node failure) and the number and grade of participants with adverse events (AEs). The secondary endpoint was the overall survival (OS). We defined OS as the time between the start of the study treatment (Day 1) and death from any cause or the last follow-up for patients alive at the end of the study. We defined locoregional failure as either failure within the primary esophageal tumor or the area of regional lymph node and distant failure as failure in distant organ or non-regional lymph node area.

Statistical Analysis

As a retrospective study done by our team showing a 3-year local control rate of 46% in ESCC patients aged ≥70 years treated with radiotherapy alone (7), we designed this phase 2 study to see if radiotherapy concurrent with S-1 regimen could achieve a 3-year local control rate of 60%. Assuming a type I error rate of 0.05 and a type II error rate of 0.20, 103 assessable patients were needed to provide a statistically significant difference between 46 and 60% with 80% power. Adjusting this figure by 2% to account for patient ineligibility or loss, a total sample size of 105 will be needed for the study. We used the Kaplan–Meier method and log-rank tests to estimate the local control rate and OS. Cox regression was used to estimate the hazard ratios. Data were analyzed with SPSS version 19.0 (SPSS Inc., Chicago, IL, USA).

RESULTS

From March 2013 to October 2015, a total of 105 patients with ESCC were enrolled in the Fudan University Shanghai Cancer Center (**Figure 1**). The baseline and tumor characteristics of the enrolled patients are listed in **Table 1**. The median age was 77 years (IQR 72–80). Seven (6.7%) patients who were initially staged as stage IVa were upstaged to IVb due to the incorrect staging for supraclavicular lymph node metastasis after staging review. Two patients were initially staged as stage IIa were downstage to I due to reevaluation by endoscopic ultrasound. The median tumor lengths of the patients enrolled were 5.3 cm (IQR 3.8–6.5). Details of serious comorbidities of patients enrolled are listed in **Table A.1**.

Sixty-eight (64.8%) patients completed the full treatment, namely, 93 (88.6%) patients completed the full radiotherapy prescribed and 70 (66.7%) patients completed the full-prescribed dose of S-1. The details of the treatment compliance are shown in

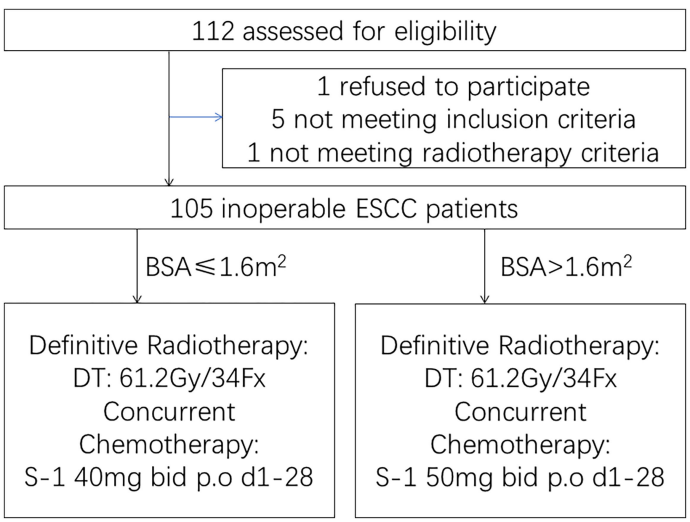

FIGURE 1 | Trial profile. One hundred five inoperable esophageal squamous cell carcinoma patients who were aged >75 years or rejected or were intolerant to intravenous chemotherapy due to serious medical comorbidities were enrolled.

TABLE 1 | Characteristic parameters of enrolled patients.

Characteristics	No. of patients (N = 105, %)
Sex	
Male	81 (77.1)
Female	24 (22.9)
Age, years	
>85	3 (2.9)
81–85	19 (18.1)
76–80	41 (39.0)
71–75	19 (18.1)
≤70	23 (21.9)
Smoking history	
Never	45 (42.9)
Former or current	60 (57.1)
Drinking history	
Never	55 (52.4)
Former or current	50 (47.6)
Stage (AJCC 6th)	
I*	2 (1.9)
IIa	34 (32.4)
IIb	10 (9.5)
III	47 (44.8)
IVa	5 (4.8)
IVb*	7 (6.7)
Site	
Cervical	7 (6.7)
Upper	28 (26.7)
Middle	61 (58.1)
Lower	9 (8.6)
Tumor length, cm#	5.3 ± 2.2
≤7	88 (83.5)
>7	17 (16.2)
ECOG	
0	29 (27.6)
1	51 (48.6)
2	25 (23.8)
BSA	
≤1.6 m^2	28 (26.7)
>1.6 m^2	77 (73.3)
Subgroups of patients enrolled	
Aged >75 years without serious comorbidities	47 (44.8)
Aged >75 years with serious comorbidities	16 (15.2)
Aged ≤75 with serious comorbidities	35 (33.3)
Aged ≤75 refusal	7 (6.7)

AJCC, American Joint Committee on Cancer; ECOG, Eastern Cooperative Oncology Group performance status; BSA, body surface area.

**Two patients had incorrect T staging and the stage was changed from IIa to I after reevaluation by endoscopic ultrasound. Seven patients had incorrect staging for supraclavicular lymph node metastasis, and the stage was changed from IVa to IVb after staging review.*

#*Data are mean ± SD with available data.*

Table A.2. Treatment delay and cessation were mainly due to treatment-induced toxicities. One hundred one (96.2%a patients received at least 50 Gy radiotherapy.

At the data cutoff date (October 31, 2020), the median follow-up of the surviving patients was 73.1 months (IQR 65.5–81.4 months). Two patients were lost to follow-up. Twenty-three (21.9%) patients were alive without local disease progression. The 1, 3, and 5-year local control rates were 77.8, 61.1, and 58.1%, respectively (**Figure 2A**). Twenty-three (21.9%) were alive without metastasis. The patterns of treatment failure are shown in **Table 2**. Eighty-one (77.1%) patients suffered deaths at the time of analysis, namely, 59 patients who died of tumor progression and 22 patients who died of other causes. The median survival was 26.1 months. The 1, 3, and 5-year OS rates were 77.9, 42.3, and 24.8%, respectively (**Figure 2B**). Moreover, the differences in terms of OS between the patients aged >75 years and patients aged ≤75 years, and between the patients with serious comorbidities and patients without serious comorbidities were not significant (**Figure A.1**).

Since all patients received at least one dose of S-1, the safety population was equal to the intention-to-treat population. All ≥grade 2 side effects and grade 1 side effects that occurred in more than 10% of the patients reported during treatment are shown in **Table 3**. Seventy (66.7%) patients had ≥grade 2 acute side effects from the treatment, most of which were related to leukopenia and radiation-induced esophagitis. Twenty-six (24.8%) patients had grade 3 or above adverse events, namely, anemia, leukopenia, thrombocytopenia, anorexia, hiccups, fatigue, radiation-induced pneumonitis, and esophagitis. Two patients (1.9%) died of late esophageal hemorrhage, and one patient (1.0%) died of late radiation-induced pneumonitis.

DISCUSSION

Definitive concurrent chemoradiotherapy is the standard treatment for inoperable esophageal cancer patients. The RTOG 85-01 trial showed that EC patients treated with cisplatin plus fluorouracil concurrent with radiotherapy had significantly better overall survival than those treated with radiotherapy alone (2). Likewise, our previous ESO-Shanghai 1 trial, enrolling ESCC patients aged 18–75 without serious medical comorbidities, showed a promising 3-year OS in both dCRT with cisplatin plus fluorouracil (51.8%) and dCRT with paclitaxel plus fluorouracil (55.4%) (8). However, the optimal evidence-based management for the EC patients who rejected or were intolerant to intravenous chemotherapy due to old age or serious comorbidities is currently lacking. The long-term results of this prospective phase 2 trial showed a promising local control and a low incidence of side effects of dCRT with S-1 alone when treating this group of ESCC patients. The 3-year local control rate in this trial was comparable with that of the ESO-Shanghai 1 trial (61% vs. 62.2%) and the incidence of ≥grade 3 acute AEs was much lower (24.8% vs. 50.2%) (8).

With global aging, it is very important to understand the treatment of geriatric cancer patients. However, most of clinical trials excluded elderly patients because of the high risk of treatment-related morbidity and mortality, limited life expectancy, and functional status. The treatment effects of this age group were underrepresentation with paucity of data (9, 10). Chemotherapy concurrently combined with radiotherapy is often considered to be too toxic for most elderly EC patients. Jingu et al. showed concurrent chemotherapy with radiotherapy for esophageal cancer in patients aged 80 years or older did not have a significant OS benefit but led to significantly more severe late toxicities than RT alone (11). Likewise, Xu et al. compared patients ≥80 years with esophageal cancer treated with

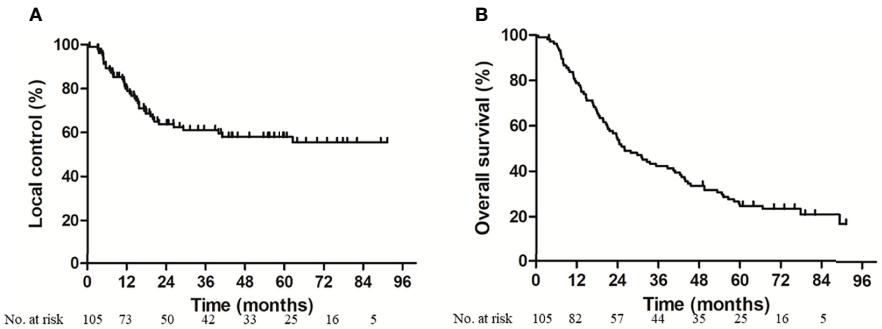

FIGURE 2 | Local control **(A)** and overall survival **(B)** for enrolled patients. At the median follow-up of 73.1 months, 3-year local control rate and overall survival was 61.1 and 42.3% respectively.

conventional dCRT with 2 younger patient cohorts (65–79 years and <65 years) treated with dCRT by propensity score matching and showed that the elderly cohort exhibited statistically significant evidence of an increased rate of severe radiation pneumonitis (12). Several studies have suggested that dCRT improves overall survival in elderly patients only in locally advanced stage compared with RT alone (13, 14). Since elderly patients have unique issues, namely, life expectancy, comorbidities, and the risk of treatment-induced morbidity, chemoradiotherapy requires careful consideration and should be carefully selected in elderly EC patients (10).

Single agent or doublet agents, such as docetaxel, nedaplatin/5-fluorouracil, and cisplatin/capecitabine, have been combined with radiotherapy for treating with elderly EC patients in several studies and have achieved promising survival results (15–18). However, for elderly EC patients, compared with double-agent-based dCRT, single-agent-based dCRT was considered to have a lower incidence of treatment side effects and comparable OS (19, 20). The long-term results of a retrospective analysis of elderly ESCC patients treated with S-1 concurrent with radiotherapy showed satisfactory survival outcomes and tolerable toxicities (21). Furthermore, several prospective trials also showed mild toxicity and satisfactory efficacy in elderly ESCC patients treated with S-1 concurrent with radiotherapy (22–24). In our prospective trial, S-1 concurrent with definitive radiotherapy was well tolerated in either elderly patients or patients with serious comorbidities. The incidence of ≥grade 3 toxicities in each side effect was less than 10%, which was comparable to previous studies with single S1 and much lower than that with doublet agents in dCRT in elderly ESCC patients (21–25). The median survival time in present trial was favorable (26.1 months) and comparable to previous similar studies (22.6–25.7 months) (21–24).

A phase 2 trial using a single agent of platinum concurrent with radiotherapy of 50 Gy in 30 elderly EC patients and showed mediocre mid-term efficacy with a 3-year OS of only 22.2%, and nine patients died from local failure. They suggested that the therapeutic ratio or locoregional control might be improved by increasing the radiotherapy dose or by testing new radiosensitizer agents (26). In this phase 2 trial, we used a radiotherapy dosage of 61.2 Gy according to the treatment guidelines of radiotherapy for Chinese esophageal carcinoma and achieved a promising 3-year local control rate (61.1%) and OS (1, 3, and 5-year OS of 77.9, 42.3, and 24.8%, respectively) (27). Our results were comparable to the long-term results of a retrospective study treating elderly ESCC patients with S-1 concurrent with radiation doses of 54.0–60.0 Gy (21). The 1, 3, and 5-year OS in that study were 70.6, 41.8, and 25.9% respectively.

It is known that comorbidities have an independent prognostic effect on cancer patients (28). However, few studies have focused on comorbidities in the treatment decision of EC patients. Patients with serious comorbidities, such as chronic diseases of the cardiovascular, pulmonary, and hepatic systems, are usually excluded from clinical trials. In this phase 2 trial, the enrollment included this group of ESCC patients, and promising

TABLE 2 | Pattern of treatment failure.

Characteristics	No. of patients (N = 105, %)
Live without treatment failure	22 (21.0)
Failure	83 (79.0)
– Locoregional only	29 (27.6)
– Distant only	22 (21.0)
– Locoregional and distant	10 (9.5)
– Died of other cause	22 (21.0)
– Second primary tumor	8 (7.6)
– Toxicity-induced death	3 (2.9)
– Comorbidities	11 (10.5)
Locoregional failure time	
– Within 1 year	20 (19.0)
– Within 2 years	14 (13.3)
– Within 3 years	5 (4.8)
Locoregional failure subgroup	
Tumor stage	
– I–II	15/46 (14.3)
– III–IV	24/59 (40.7)
Age	
– >75	27/63 (42.9)
– ≤75	12/42 (28.6)

TABLE 3 | Side effects of patients enrolled.

Side effects*	No. of patients (N = 105, %)				
	Grade 1	Grade 2	Grade 3	Grade 4	Grade 5
Acute side effects					
Anemia	54 (51.4)	2 (1.9)	1 (1.0)	0	0
Leukopenia	43 (41.0)	26 (24.8)	2 (1.9)	1 (1.0)	–
Thrombocytopenia	27 (25.7)	10 (9.5)	6 (5.7)	1 (1.0)	–
Anorexia	27 (25.7)	7 (6.7)	1 (1.0)	0	0
Nausea	17 (16.2)	11 (10.5)	0	–	–
Vomiting	6 (5.7)	5 (4.8)	0	0	0
Fatigue	24 (22.9)	9 (8.6)	11 (10.5)	–	–
Fever	6 (5.7)	3 (2.9)	0	0	0
Hiccups	5 (4.8)	0	1 (1.0)	–	–
Cardiac disorders	8 (7.6)	0	0	0	0
Radiation-induced dermatitis	6 (5.7)	1 (1.0)	0	0	0
Radiation-induced esophagitis	57 (54.3)	17 (16.2)	4 (3.8)	0	0
Radiation-induced pneumonitis	33 (31.4)	19 (18.1)	4 (3.8)	1 (1.0)	0
Late side effects					
Cardiac	0	0	0	0	0
Radiation-induced esophagitis	1 (1.0)	5 (4.8)	0 (0.0)	0 (0.0)	2 (1.9)[#]
Radiation-induced pneumonitis	18 (17.1)	0 (0.0)	0 (0.0)	0 (0.0)	1 (1.0)

**All ≥Grade 2 side effects and Grade 1 side effects that occurred in more than 10% of patients reported during treatment.*
[#]Patients died of esophageal hemorrhage without clear evidence of progression.

local control and good tolerance of S-1 concurrent with definitive RT with low treatment toxicities were observed. However, we did observe that a high percentage of patients (13.3%) died of nononcologic causes, which is undoubtedly related to the aging and serious comorbidities pretreatment.

Our study had several limitations. First, we did not set the control group of radiotherapy alone, and a randomized controlled study would be ideal for the comparison. A randomized phase 3 trial comparing simultaneous integrated boost radiotherapy with or without S-1 is ongoing (29). Another limitation is that we did not assess the quality of life of patients enrolled, which may offer more comprehensive knowledge of the safety results of S-1 concurrent with radiotherapy when treating ESCC patients who were elderly or had serious comorbidities.

CONCLUSION

In summary, the long-term results of this phase 2 trial demonstrated that S-1 concurrent with radiotherapy was well tolerated in ESCC patients who rejected or were intolerant to intravenous chemotherapy due to old age or serious comorbidities. The promising 3-year local control rate suggests that this approach was effective and merits randomized phase 3 trial evaluation.

AUTHOR'S NOTE

Parts of this manuscript were previously presented in 2016 ASTRO meeting and 2019 ASTRO meeting, respectively.

DATA AVAILABILITY STATEMENT

The original contributions presented in the study are included in the article/**Supplementary Material**. Further inquiries can be directed to the corresponding author.

ETHICS STATEMENT

The studies involving human participants were reviewed and approved by the Ethical Committee of Fudan University Shanghai Cancer Center. The patients/participants provided their written informed consent to participate in this study.

FUNDING

This trial was supported by the National Natural Science Foundation of China (grant 81703160).

SUPPLEMENTARY MATERIAL

The Supplementary Material for this article can be found online at: https://www.frontiersin.org/articles/10.3389/fonc.2022.839765/full#supplementary-material

Supplementary Figure 1 | Overall survival for subgroups of patients enrolled. No significant difference in overall survival was observed neither between the patients aged >75 years and patients aged ≤75 years **(A)**, nor between the patients with serious comorbidities and patients without serious comorbidities **(B)**.

REFERENCES

1. Chen W, Zheng R, Baade PD, Zhang S, Zeng H, Bray F, et al. Cancer Statistics in China, 2015. *CA Cancer J Clin* (2016) 66(2):115–32. doi: 10.3322/caac.21338
2. Cooper JS, Guo MD, Herskovic A, Macdonald JS, Martenson JA Jr, Al-Sarraf M, et al. Chemoradiotherapy of Locally Advanced Esophageal Cancer: Long-Term Follow-Up of a Prospective Randomized Trial (RTOG 85-01). *Radiat Ther Oncol Group JAMA* (1999) 281(17):1623–7. doi: 10.1001/jama.281.17.1623
3. Boku N, Yamamoto S, Fukuda H, Shirao K, Doi T, Sawaki A, et al. Fluorouracil Versus Combination of Irinotecan Plus Cisplatin Versus S-1 in Metastatic Gastric Cancer: A Randomised Phase 3 Study. *Lancet Oncol* (2009) 10(11):1063–9. doi: 10.1016/S1470-2045(09)70259-1
4. Huang J, Cao Y, Wu L, Liao C, He Y, Gao F. S-1-Based Therapy Versus 5-FU-Based Therapy in Advanced Gastric Cancer: A Meta-Analysis. *Med Oncol* (2011) 28(4):1004–11. doi: 10.1007/s12032-010-9594-0
5. Cho SH, Shim HJ, Lee SR, Ahn JS, Yang DH, Kim YK, et al. Concurrent Chemoradiotherapy With S-1 and Cisplatin in Advanced Esophageal Cancer. *Dis Esophagus* (2008) 21(8):697–703. doi: 10.1111/j.1442-2050.2008.00837.x
6. Iwase H, Shimada M, Tsuzuki T, Hirashima N, Okeya M, Hibino Y, et al. Concurrent Chemoradiotherapy With a Novel Fluoropyrimidine, S-1, and Cisplatin for Locally Advanced Esophageal Cancer: Long-Term Results of a Phase II Trial. *Oncology* (2013) 84(6):342–9. doi: 10.1159/000348383
7. Lv B, Chen Y, Li Y, Zhu H, Zhao K. Outcomes and Clinical Prognostic Factors for Elderly Patients With Esophageal Squamous Cell Carcinoma Treated After Definitive Radio(Chemo)Therapy. *China Oncol* (2015) 25(3):217–21. doi: 10.3969/j.issn.1007-3639.2015.03.012
8. Chen Y, Ye J, Zhu Z, Zhao W, Zhou J, Wu C, et al. Comparing Paclitaxel Plus Fluorouracil Versus Cisplatin Plus Fluorouracil in Chemoradiotherapy for Locally Advanced Esophageal Squamous Cell Cancer: A Randomized, Multicenter, Phase III Clinical Trial. *J Clin Oncol* (2019) 37(20):1695–703. doi: 10.1200/JCO.18.02122
9. Scher KS, Hurria A. Under-Representation of Older Adults in Cancer Registration Trials: Known Problem, Little Progress. *J Clin Oncol* (2012) 30(17):2036–8. doi: 10.1200/JCO.2012.41.6727
10. Won E, Ilson DH. Management of Localized Esophageal Cancer in the Older Patient. *Oncologist* (2014) 19(4):367–74. doi: 10.1634/theoncologist.2013-0178
11. Jingu K, Takahashi N, Murakami Y, Ishikawa K, Itasaka S, Takahashi T, et al. Is Concurrent Chemotherapy With Radiotherapy for Esophageal Cancer Beneficial in Patients Aged 80 Years or Older? *Anticancer Res* (2019) 39(8):4279–83. doi: 10.21873/anticanres.13592
12. Xu C, Xi M, Moreno A, Shiraishi Y, Hobbs BP, Huang M, et al. Definitive Chemoradiation Therapy for Esophageal Cancer in the Elderly: Clinical Outcomes for Patients Exceeding 80 Years Old. *Int J Radiat Oncol Biol Phys* (2017) 98(4):811–9. doi: 10.1016/j.ijrobp.2017.02.097
13. Chen M, Liu X, Han C, Wang X, Zhao Y, Pang Q, et al. Does Chemoradiotherapy Benefit Elderly Patients With Esophageal Squamous Cell Cancer? A Propensity-Score Matched Analysis on Multicenter Data (3JECROG R-03a). *BMC Cancer* (2020) 20(1):36. doi: 10.1186/s12885-019-6461-z
14. Jingu K, Numasaki H, Toh Y, Nemoto K, Uno T, Doki Y, et al. Chemoradiotherapy and Radiotherapy Alone in Patients With Esophageal Cancer Aged 80 Years or Older Based on the Comprehensive Registry of Esophageal Cancer in Japan. *Esophagus* (2020) 17(3):223–9. doi: 10.1007/s10388-020-00725-w
15. Kawamoto T, Shikama N, Oshima M, Kosugi Y, Tsurumaru M, Sasai K. Safety of Radiotherapy With Concurrent Docetaxel in Older Patients With Esophageal Cancer. *J Geriatr Oncol* (2020) 11(4):675–9. doi: 10.1016/j.jgo.2019.08.009
16. Watanabe A, Katada C, Komori S, Moriya H, Yamashita K, Harada H, et al. Feasibility of Definitive Chemoradiation Therapy With Nedaplatin and 5-Fluorouracil in Elderly Patients With Esophageal Squamous Cell Carcinoma: A Retrospective Study. *Adv Radiat Oncol* (2018) 3(3):305–13. doi: 10.1016/j.adro.2018.02.010
17. Tougeron D, Di Fiore F, Thureau S, Berbera N, Iwanicki-Caron I, Hamidou H, et al. Safety and Outcome of Definitive Chemoradiotherapy in Elderly Patients With Oesophageal Cancer. *Br J Cancer* (2008) 99(10):1586–92. doi: 10.1038/sj.bjc.6604749
18. Chen F, Luo H, Xing L, Liang N, Xie J, Zhang J. Feasibility and Efficiency of Concurrent Chemoradiotherapy With Capecitabine and Cisplatin Versus Radiotherapy Alone for Elderly Patients With Locally Advanced Esophageal Squamous Cell Carcinoma: Experience of Two Centers. *Thorac Cancer* (2018) 9(1):59–65. doi: 10.1111/1759-7714.12536
19. Huang C, Zhu Y, Li Q, Zhang W, Liu H, Zhang W, et al. Feasibility and Efficiency of Concurrent Chemoradiotherapy With a Single Agent or Double Agents vs Radiotherapy Alone for Elderly Patients With Esophageal Squamous Cell Carcinoma: Experience of Two Centers. *Cancer Med* (2019) 8(1):28–39. doi: 10.1111/1759-7714.12536
20. Zhao L, Zhou Y, Pan H, Yin Y, Chai G, Mu Y, et al. Radiotherapy Alone or Concurrent Chemoradiation for Esophageal Squamous Cell Carcinoma in Elderly Patients. *J Cancer* (2017) 8(16):3242–50. doi: 10.7150/jca.20835
21. Lv S, Fang M, Yang J, Zhan W, Jia Y, Xu H, et al. Long-Term Results of Definitive Concurrent Chemoradiotherapy Using S-1 in the Treatment of Geriatric Patients With Esophageal Cancer. *Onco Targets Ther* (2016) 9:5389–97. doi: 10.2147/OTT.S107668
22. Ji Y, Du X, Tian Y, Sheng L, Cheng L, Chen Y, et al. A Phase II Study of S-1 With Concurrent Radiotherapy in Elderly Patients With Esophageal Cancer. *Oncotarget* (2017) 8(47):83022–9. doi: 10.18632/oncotarget.20938
23. Wang X, Ge X, Wang X, Zhang W, Zhou H, Lin Yu, et al. S-1-Based Chemoradiotherapy Followed by Consolidation Chemotherapy With S-1 in Elderly Patients With Esophageal Squamous Cell Carcinoma: A Multicenter Phase II Trial. *Front Oncol* (2020) 10:1499:1499. doi: 10.3389/fonc.2020.01499
24. Ji Y, Du X, Zhu W, Yang Y, Ma J, Zhang Li, et al. Efficacy of Concurrent Chemoradiotherapy With S-1 vs Radiotherapy Alone for Older Patients With Esophageal Cancer: A Multicenter Randomized Phase 3 Clinical Trial. *JAMA Oncol* (2021) 7(10):1459–66. doi: 10.1001/jamaoncol.2021.2705
25. Huang C, Huang D, Zhu Y, Xie G, Wang H, Shi J, et al. Comparison of a Concurrent Fluorouracil-Based Regimen and a Taxane-Based Regimen Combined With Radiotherapy in Elderly Patients With Esophageal Squamous Cell Carcinoma. *Transl Oncol* (2020) 13(3):100736. doi: 10.1016/j.tranon.2019.12.008
26. Servagi-Vernat S, Crehange G, Roullet B, Guimas V, Maingon P, Puyraveau M, et al. Phase II Study of a Platinum-Based Adapted Chemotherapy Regimen Combined With Radiotherapy in Patients 75 Years and Older With Esophageal Cancer. *Drugs Aging* (2015) 32(6):487–93. doi: 10.1007/s40266-015-0275-8
27. Esophageal Carcinoma Cooperative Group of Radiation Oncology Society of Chinese Medical A. Treatment Guideline of Radiotherapy for Chinese Esophageal Carcinoma (Draft). *Chin J Cancer* (2010) 29(10):855–9. doi: 10.5732/cjc.010.10250
28. Janssen-Heijnen ML, Houterman S, Lemmens VE, Louwman MW, Maas HA, Coebergh JW. Prognostic Impact of Increasing Age and Co-Morbidity in Cancer Patients: A Population-Based Approach. *Crit Rev Oncol Hematol* (2005) 55(3):231–40. doi: 10.1016/j.critrevonc.2005.04.008
29. Li C, Wang X, Wang X, Han C, Wang P, Pang Q, et al. A Multicenter Phase III Study Comparing Simultaneous Integrated Boost (SIB) Radiotherapy Concurrent and Consolidated With S-1 Versus SIB Alone in Elderly Patients With Esophageal and Esophagogastric Cancer - the 3JECROG P-01 Study Protocol. *BMC Cancer* (2019) 19(1):397. doi: 10.1186/s12885-019-5544-1

Conflict of Interest: The authors declare that the research was conducted in the absence of any commercial or financial relationships that could be construed as a potential conflict of interest.

frontiers | Frontiers in Oncology

ORIGINAL RESEARCH
published: 08 April 2022
doi: 10.3389/fonc.2022.878851

Toripalimab in Combination With Induction Chemotherapy and Subsequent Chemoradiation as First-Line Treatment in Patients With Advanced/Metastatic Esophageal Carcinoma: Protocol for a Single-Arm, Prospective, Open-Label, Phase II Clinical Trial (TR-EAT)

Lei Wu, Yi Wang, Baisen Li, Gang Wan, Long Liang, Tao Li, Jinyi Lang and Qifeng Wang**

Radiation Oncology Key Laboratory of Sichuan Province, Department of Radiation Oncology, Sichuan Cancer Hospital & Institute, Sichuan Cancer Center, School of Medicine, University of Electronic Science and Technology of China, Chengdu, China

Immune checkpoint inhibitor therapy combined with chemotherapy is safe and effective in treating advanced esophageal carcinoma; however, some patients still experience tumor progression and/or metastasis. Whether the addition of radiotherapy to immunotherapy combined with chemotherapy improves the prognosis of patients with advanced/metastatic esophageal carcinoma needs to be investigated. In the present study, we developed a protocol for our clinical trial indicating that toripalimab combined with induction chemotherapy followed by chemoradiotherapy can safely prolong survival in patients with stage IV esophageal carcinoma. This open-label, single-arm, phase II trial will include patients with unresectable stage IV esophageal squamous cell carcinoma who have not received prior systemic therapy. The patients will be treated with two cycles of toripalimab (240 mg, 1 day before chemotherapy, Q3W) combined with induction chemotherapy (paclitaxel, 135–175 mg/m^2 + carboplatin, area under the curve = 4–6, day 1, intravenous, Q3W). Thereafter, they will undergo two cycles of the aforementioned treatment with concurrent radiotherapy (30–50 Gy in 15–25 fractions), followed by toripalimab (240 mg, day 1, Q3W) for 1 year. The primary outcome measure will be progression-free survival; the secondary outcome measures will include the objective response rate, disease control rate, duration of remission, 1- and 2-year overall survival rates, safety and tolerability, and changes in health-related quality of life. The study protocol was approved by the Ethics Committee of Sichuan Cancer Hospital (SCCHEC-02-2021-021). The trial is underway in accordance with the Declaration of Helsinki.

OPEN ACCESS

Edited by:
Ira Ida Skvortsova, Innsbruck Medical University, Austria

Reviewed by:
Yirui Zhai, Chinese Academy of Medical Sciences and Peking Union Medical College, China
Wencheng Zhang, Tianjin Medical University Cancer Institute and Hospital, China
Lei Deng, Chinese Academy of Medical Sciences and Peking Union Medical College, China
Yaping Xu, Tongji University, China

***Correspondence:**
Qifeng Wang
littlecancer@163.com
Jinyi Lang
langjy610@sichuancancer.org

Specialty section:
This article was submitted to Radiation Oncology, a section of the journal Frontiers in Oncology

Received: *18 February 2022*
Accepted: *18 March 2022*
Published: *08 April 2022*

Citation:
Wu L, Wang Y, Li B, Wan G, Liang L, Li T, Lang J and Wang Q (2022) Toripalimab in Combination With Induction Chemotherapy and Subsequent Chemoradiation as First-Line Treatment in Patients With Advanced/Metastatic Esophageal Carcinoma: Protocol for a Single-Arm, Prospective, Open-Label, Phase II Clinical Trial (TR-EAT). Front. Oncol. 12:878851. doi: 10.3389/fonc.2022.878851

Clinical Trial Registration: http://www.chictr.org.cn/showproj.aspx?proj=126830, identifier ChiCTR2100046715.

Keywords: advanced/metastatic esophageal carcinoma, PD-L1 blockade, concurrent chemoradiotherapy, clinical protocol, toripalimab

INTRODUCTION

Esophageal carcinoma is a potentially life-threatening malignant disease with a poor prognosis (1). Among the malignant tumors in China, the prevalence of esophageal carcinoma ranks sixth, and its mortality ranks fourth (2). Squamous cell carcinomas form a majority of esophageal cancers in China; most patients with these carcinomas are diagnosed at an advanced stage.

For advanced esophageal cancer, immunotherapy combined with chemotherapy has become the standard treatment recommended by the guidelines. In the phase III trial of pabolizumab or placebo combined with first-line chemotherapy for advanced esophageal cancer (keynote-590) (3), the median overall survival (OS) in the immunotherapy combined with chemotherapy group was more than 12 months, and the efficacy exceeded that of the previous standard first-line chemotherapy. Another phase III clinical study (ESCORT-1ST) showed that carilizumab combined with chemotherapy can significantly prolong the median survival (mOS, 15.3 months vs. 12.0 months) and median progression free survival (mPFS, 6.9 months vs 5.6 months) of patients with advanced esophageal squamous cell carcinoma (ESCC) and has good safety (4).

Despite the combination of immunotherapy and chemotherapy, the prognosis of advanced esophageal cancer is still unsatisfactory. Radiotherapy is a crucial treatment method for patients with advanced esophageal cancer. Theoretically, radiotherapy has a good local tumor control effect, and the improvement of the local control rate is helpful in alleviating symptoms and prolonging survival. Therefore, some studies have tried to add radiotherapy to the first-line treatment of advanced esophageal cancer. Suzuki et al. (5) treated 32 patients with stage IVB esophageal cancer with palliative radiotherapy at an external dose of 30–60 Gy. After treatment, dysphagia in 73% of patients was relieved. Li et al. (6) conducted a retrospective study of 82 patients with heterochronic, oligometastatic esophageal cancer; patients were divided into radiotherapy and non-radiotherapy groups. The median OS of the radiotherapy group (RT) and non-radiotherapy group (NRT) were 14 months and 7 months, respectively. Multivariate analysis showed that treatment mode (RT vs NRT) was an independent prognostic factor for patients with oligometastatic esophageal cancer. In these studies, radiotherapy only was used for local palliative treatment. Whether radiotherapy can achieve a better therapeutic effect in combination with immunotherapy and chemotherapy is an urgent research topic (7–9) However, there are no reports on the combination of radiation with chemoimmotherapy in advanced esophageal cancer.

Although radiotherapy combined with chemotherapy may have benefits, its mechanism of action raises safety concerns because radiotherapy- and immunotherapy-related toxic and side effects might overlap. In addition, the optimal target range, dose fraction schemes, total radiation dose, and timing of incorporation of radiation into the treatment region are unknown. To address this question, we will conduct a single-arm phase II study involving 30 patients with unresectable advanced ESCC. Patients will initially receive a combination of programmed cell death protein 1 (PD-1) inhibitor (toripalimab) therapy and induction chemotherapy, followed by immunotherapy and concurrent chemoradiotherapy (cCRT); eventually, they will be treated with toripalimab as maintenance therapy. Through this trial, we aim to provide preliminary evidence regarding the feasibility of this combination regimen as a first-line treatment option for patients with advanced ESCC.

The main objective of this study is to evaluate the efficacy and safety of triple therapy involving toripalimab in combination with induction chemotherapy followed by chemoradiation in patients with primary stage IV ESCC.

METHODS

Study Design

This is an open-label, single-arm, single-center phase II clinical trial. Patients with locally advanced or distant metastatic ESCC who have not received prior systemic therapy, including those with primary stage IV ESCC with multiple lymph node metastases (N3) and distant oligometastases (M1; the American Joint Committee on Cancer, 8th edition), will be enrolled (10).

Patient and Public Involvement

Patients and the general public were not involved in the design, recruitment, and implementation of the study. We have no plans of informing the results of this study to the included patients. However, the results will be disseminated to the applicants in the form of a published article as requested.

Key Eligibility Criteria

Eligible patients should present histologically confirmed, untreated ESCC considered unresectable (locally advanced or metastatic). In addition, these patients are required to have an Eastern Cooperative Oncology Group performance status (ECOG PS) of 0 to 1, normal organ function, no history of active autoimmune disease, and no history of immune checkpoint inhibitor (ICI) or chemotherapy treatment. Key inclusion and exclusion criteria are listed in **Table 1**.

Withdrawal Criteria

Patients will be withdrawn from this study for the following reasons: (1) patients with disease progression, according to

TABLE 1 | Key eligibility criteria for this trial.

Inclusion criteria	Exclusion criteria
Age from 18 to 75 years	Active or untreated CNS metastases, as determined using CT or MRI during screening and prior radiographic assessments
Pathologically confirmed unresectable esophageal squamous cell carcinoma	The site or number of tumor metastases has exceeded the range for oligometastasis
Multiple lymph node metastases (N3) and/or distant oligometastasis (M1)[†]	Uncontrolled cancer-related pain
At least 1 measurable lesion according to RECIST v1.1	Uncontrolled pleural effusion, pericardial effusion, or ascites requiring recurrent drainage procedures (once monthly or more frequently)
ECOG PS 0–1	Uncontrolled or symptomatic hypercalcemia
Life expectancy ≥ 6 months	Bone metastases of the multi-segmental vertebral body, ilium, and other sites
Suited for concurrent radiochemotherapy	Patients with the tendency to exhibit a complete obstruction under endoscopy that requires interventional therapy or surgery for relief of the obstruction
Suited for toripalimab treatment	Stent implanted in the esophagus or trachea
No autoimmune disease	High risk of hemorrhage or perforations due to tumor invasion in adjacent organs (aorta or trachea), or the presence of a fistula
No previous anti-cancer systematic treatment	Severe malnutrition (PG-SGA ≥ 9)
Adequate organ function in accordance with the following:	Allergy to any component of toripalimab, paclitaxel/nab -paclitaxel, or carboplatin
• absolute neutrophil count ≥ 1.5×10^9/L	History of or comorbid bleeding disease
• hemoglobin ≥ 9 g/dL	Pregnancy or lactation (women)
• platelet count ≥ 100×10^9/L	Severe insufficiency of heart, lungs, liver, or kidneys
• serum albumin ≥ 2.8 g/dL	Disease of the hematopoietic or immune system, or cachexia
• white blood cell count ≥ 4.0×10^9/L	Participation in another interventional clinical study at the same time
• total bilirubin ≤ 1.5 ULN; ALT, AST ≤ 1.5 UILN	
• serum creatinine ≤ 1.5 ULN	
• endogenous creatinine clearance rate ≥ 50 mL/min (Cockcroft–Gault formula)	
• blood urea nitrogen within the normal range	
• normal thyroid function	

[†]*Oligometastasis was defined as ≤5 metastatic lesions in ≤3 metastatic organs. Abbreviations: CNS, central nervous system; CT, computed tomography; MRI, magnetic resonance imaging; RECIST, Response Evaluation Criteria in Solid Tumours; ECOG PS, Eastern Cooperative Oncology Group performance status; PG-SGA, Patient-Generated Subjective Global Assessment; ULN, upper limit of normal; UILN, upper international limit of normal; ALT, alanine transaminase; AST, aspartate transaminase.*

Response Evaluation Criteria In Solid Tumors (RECIST) 1.1; (2) patients who experience any unacceptable treatment-related adverse events and cannot continue the study after being evaluated by the study physician; (3) patients that may significantly affect the evaluation of clinical status, for example if they are non-compliant with the research plan, received other treatment, etc.; (4) patients with diseases requiring interruption of treprizumab treatment, such as an allergy, sudden onset of other diseases, and accidents and injuries not related to the disease; and (5) patients exercising their right to withdraw from the trial at any time and for any reason.

Screening

Patients will be screened within 2 weeks prior to treatment commencement to assess their tolerance to the treatment. Comprehensive information on potentially eligible patients will be collected and recorded during this period. The screening process will include obtaining written informed consent, collection of demographic information and medical history, physical examination, evaluation of ECOG PS score and vital signs, clinical testing (chemistry, hematology, and coagulation), examination of liver and kidney function, and cardiac analyses. Tumor information will be obtained *via* imaging evaluation [computed tomography (CT) or magnetic resonance imaging (MRI)], fibroscopy, esophagoscopy, or positron emission tomography/CT. Eventually, the inclusion and exclusion criteria will be reviewed to make a final judgment regarding each patient's eligibility.

Interventions

Eligible patients will receive two cycles of immunotherapy [toripalimab (240 mg), intravenously infused on the day before chemotherapy] in combination with standard chemotherapy [paclitaxel (135–175 mg/m^2), day 1 (d1); intravenously infused + carboplatin, area under the curve (AUC) = 4–6, day 1, intravenously infused] every 3–4 weeks. Thereafter, the patients will undergo two cycles of the aforementioned treatment, with concurrent radiotherapy *via* an involved-field irradiation (IFI) technique, thereby targeting only the primary esophageal foci and metastatic lymph nodes, rather than attempting regional prophylactic irradiation of the lymph node drainage area. Stereotactic body radiation therapy (SBRT) may be preferred for some patients with oligometastatic lesions in the bones, lungs, and liver. Eventually, toripalimab monotherapy (240 mg, intravenously infused) will be administered as the maintenance treatment every 3 weeks after the completion of radiotherapy for a maximum period of 1 year. Moreover, the patients will sign an informed consent form to indicate that they understand the purpose and method of the study and will voluntarily cooperate with the trial process; furthermore, they will follow the treatment regimen until progressive disease (PD) or intolerable adverse events (AEs) occur. If AEs of grade 3 occur, the treatment will be suspended,

and the AEs will be aggressively managed until the patient's condition returns to normal or until the AEs have been reduced to grade 1 or 2. The chemotherapy dose may be reduced in the second treatment cycle at the discretion of the investigator. In addition, the medical safety team will review all the safety information during this clinical study. The flow chart of the study is illustrated in **Figure 1**.

Patients will be allowed to withdraw from the study owing to PD or intolerable toxicity as well as upon patient or investigator request. Toripalimab injections may be continued if, in the judgment of the investigator, the treatment remains clinically beneficial for patients with imaging-confirmed PD according to RECIST 1.1. Patients who complete the study treatment will be followed up for survival.

Follow-up

Patients will undergo tumor assessments at baseline (screening period) and every 6 weeks (± 7 days) for the first 12 months after treatment initiation. Patients will be followed up once every 3 months in the first two years, once every 6 months in the third to fifth year, and once a year thereafter. The electronic case report form will be used for data collection and data management. Follow-up examinations will include contrast-enhanced CT scans of the neck, chest, and abdomen, esophagoscopy, abdominal color Doppler ultrasonography, and laboratory analysis of tumor markers in the blood. **Table 2** provides details of the schedule of enrollment, interventions, and assessments.

Outcome Measures

The primary outcome of this study is progression-free survival (PFS) among the patients, whereas the secondary outcomes include the objective response rate (ORR), disease control rate (DCR), duration of response (DOR), 1- and 2-year OS rates, patient-reported health-related quality of life, and safety and tolerability of the treatment.

Moreover, we will investigate the potential predictive and prognostic biomarkers, including programmed death-ligand 1 (PD-L1) expression in archived and/or fresh tumor tissue and blood samples obtained before and/or after the completion of the study treatment and/or at the time of PD *via* next-generation sequencing and multicolor immunohistochemical assays. Thereafter, we will assess the relationships between biomarkers, including PD-L1, circulating tumor DNA (ctDNA), and cytokines as well as the therapeutic effect of combination treatment. Furthermore, we aim to investigate the immune microenvironment, immune-related gene expression, and immune-related factors, as well as their associations with disease status and treatment response.

Safety Assessment

Safety will be assessed based on the observation and documentation of AEs and serious AEs of any grade (according to NCI-CTCAE 5.0) during treatment, laboratory analyses, electrocardiography, physical examination, and ECOG PS scores. Investigators will be responsible for the appropriate measurement of AEs and the determination of causal relationships between AEs and the study drugs.

Statistical Analysis

All patients who receive the experimental drugs at least once and have had at least one safety evaluation will be included in the Safety Set (SS) analysis. According to the principle of intention-to-treat (ITT) analysis, the full analysis set (FAS) will include data from the last observation of all the cases that had used drugs at least once and were followed up at least once; the entire

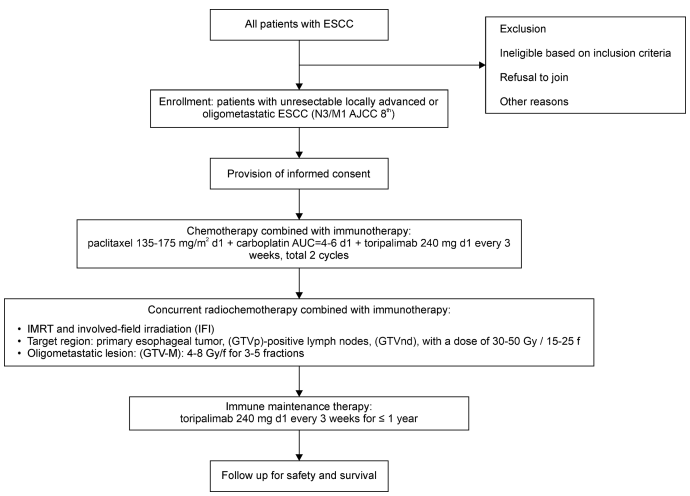

FIGURE 1 | Flowchart of the phase II study. ESCC, esophageal squamous cell carcinoma; AJCC, American Joint Committee on Cancer; d1, day 1; AUC, area under the curve, IMRT, intensity-modulated radiation therapy; GTV-M, gross tumor volume of the primary metastatic lesions; GTV_{nd}, gross tumor volume of lymph nodes; GTV_p, primary gross tumor volume.

TABLE 2 | Flowchart of enrollment, interventions, and assessments.

Study Phase Therapy	Screening	Treatment visit I+C cycle 1	Treatment visit I+C cycle 2	Treatment visit I+C+R cycle 3	Treatment visit I+C+R cycle 4	Treatment Visit End of RT	Treatment Visit Immunotherapy	Follow up visit Follow up
Timepoint	-d14–d0	d1 (w1d1)	d22 (w4d1)	d43 (w7d1)	d85 (w10d1)	w11–w12	w13–w52	
Procedures Visit No	1	2	3	4	5	6	7	8
Informed Consent	X							
Inclusion/Exclusion Criteria	X							
Medical History	X							
Prior cancer therapy	X							
ECOG PS	X	X	X	X	X	X	X	X
Physical Examination	X	X	X	X	X	X	X	X
Vital Signs	X	X	X	X	X			
Weight	X	X	X	X	X	X	X	X
Symptom/Adverse Event Assessment	X	X	X	X	X	X	X	X
Concomitant Medication	X	X	X	X	X	X	X	X
Laboratory tests	X	X	X	X	X	X	X	X
Esophagoscopy	X						X	X
Fibroscopy	X							
Imaging (CT/MRI)	X			X		X	X	X
ECT	X							
Pulmonary function	X							
ECG	X	X	X	X	X	X	X	X
Doppler echocardiography	X			X		X	X	
Histology assessment	X							
QoL-Questionnaires	X			X		X	X	
Exploratory biomarker blood draw	X			X		X		
Survival status							X	X
Review of subsequent therapy							X	X

CT, computed tomography; MRI, magnetic resonance imaging; ECOG PS, Eastern Cooperative Oncology Group performance status; I, immunotherapy; C, chemotherapy; R/RT, radiotherapy; ECG, electrocardiograph; ECT, emission computed tomography; QoL-Questionnaires, quality of life-questionnaires.

treatment process cannot be observed until the final results. The FAS data set will be used for fall-out analysis, equilibrium analysis of basic indicators, analysis of the main efficacy indicators, and analysis of safety indicators. The per protocol set (PPS) analysis is a statistical analysis of case data that can meet all the prescribed requirements in accordance with the protocol. This analysis method does not include cases that violate the trial protocol, such as cases lost on follow-up or where patients used prohibited drugs. In this study, the SPSS22.0 software will be used for statistical analysis. Quantitative data satisfies the requirements of normal distribution using the mean ± standard deviation and meets the requirements expressed by median (P25, P75). Qualitative data will be expressed as percentage (%), and a confidence level of 95% will be used for confidential intervals. The Kaplan–Meier method will be used to estimate survival rates and median survival time and to draw the survival curve. The Log-Rank test will be used to compare the survival rate. A Cox regression model will be established to estimate the hazard ratio (HR) between different parting spaces. A two-sided test will be conducted for all statistical tests, and $P<0.05$ will indicate that the differences were significant.

Sample Size Calculation

Based on the literature, the mPFS of pabolizumab combined with cisplatin and 5-fluorouracil as the first-line treatment of unresectable locally advanced or metastatic esophageal cancer was 6.3 months (3). Our preliminary work showed that the mPFS of toripalimab in combination with induction chemotherapy and subsequent chemoradiation in the treatment of primary stage IV ESCC was 12.0 months or more. We hypothesized that the mPFS of our trial can reach 12 months. The type I error rate is 5%, and the power is 80%. The sample size calculated by PASS 22.0 was 25 cases (or a minimum of 25 patients). In consideration of a 20% drop-out rate, the final sample size is set at 30 cases.

Data Collection, Management, and Monitoring

The final patient data should be collected according to the study protocol, including electronic Case Report Form (eCRF) and external data (such as laboratory data), which will be saved by the study sponsor at the end of the study. In the collection of data in eCRF, the instructions in the filling guidance of eCRF should be followed. The researcher is ultimately responsible for collecting and reporting all clinical data entered into eCRF. To ensure accurate data collection, related standard procedures should be followed. The outlier, logic, inconsistency, and integrity of data will be examined. During the study, the supervisor will visit the study center, examine the protocol compliance, define the consistency between eCRF and medical records of the patient, and ensure that the study is done according to related supervision requirements.

DISCUSSION

To the best of our knowledge, the present clinical trial will be the first to examine the efficacy and safety of triple therapy involving toripalimab in combination with induction chemotherapy followed by chemoradiation in patients with primary stage IV ESCC. Recently, chemotherapy combined with immunotherapy was used as a first-line treatment for advanced esophageal cancer; however, the prognosis of advanced esophageal cancer is still poor. Therefore, more effective treatment options are needed to improve patient survival and prognosis.

Radiotherapy is an important nonsurgical option for treating esophageal cancer; cCRT has become the standard of care for treating locally advanced ESCC (11). However, for treating advanced esophageal cancer, radiotherapy is regarded as a means of palliative treatment. Advanced esophageal cancer is a broad concept, which includes patients with multiple organ metastasis and oligometastatic patients with a limited number of metastatic lesions and fewer metastatic organs. The latter is often considered to have a better prognosis. Therefore, the treatment of oligometastatic esophageal carcinoma differs from the palliative treatment of advanced esophageal cancer; the former includes more aggressive treatment modalities. For instance, radical radiotherapy with a bioequivalent dose of 10–60 Gy revealed remarkable benefit in the survival of patients with heterochronic oligometastatic esophageal cancer (6). Recent evidence suggests that ICIs act synergistically with either chemotherapy or cCRT to exert antitumor effects. Both chemotherapy and radiotherapy can upregulate PD-L1 expression by releasing cytokines and other inflammatory molecules (12, 13) and sensitizing tumors to PD-1/PD-L1-mediated therapy. In this context, chemotherapy and radiotherapy serve as synergistic therapies for immunotherapy. The removal of cancer cells *via* chemotherapy and/or radiotherapy can cause antigen release, thereby converting a less immunogenic or immunosuppressed tumor into an immunogenic tumor (14). In addition, radiotherapy can mobilize both innate and adaptive immune responses, induce tumor-specific T-cells, and establish a tumor-specific immune memory, which collectively enhances the effect of radiotherapy, improves local control, reduces metastatic spread, and prolongs OS (15).

Our previous retrospective studies (Not yet published) suggest that the treatment strategy of this study has a good therapeutic effect on patients with oligometastatic esophageal cancer. The possible advantage of this strategy is that induction therapy reduces tumor volume and tumor load by first alleviating symptoms of dysphagia and consequently improving nutrition and general physical health. Furthermore, tumor shrinkage creates favorable conditions for subsequent cCRT, which include considerably reduced target volumes for radiotherapy, alleviation of toxic side effects caused by radiotherapy, lower risk of bleeding and perforation in tumors and the gastrointestinal tract, and better protection of normal surrounding tissue. However, no standard strategies exist for synergistically combining radiotherapy with immunotherapy and chemotherapy in the treatment of advanced ESCC. Further clinical studies are required to explore the optimal target area range, segmentation mode, total dose, and time of administering radiotherapy.

There are several limitations to our study. First, the number of patients enrolled is small. Secondly, this is a single arm and single center study. We expect to have a randomized controlled study that compares the differences between the triple therapy modality with radiotherapy and the immunochemotherapy modality without radiotherapy in the future.

In summary, this clinical trial will attempt to evaluate the efficacy and safety of toripalimab in combination with induction chemotherapy and subsequent chemoradiotherapy as first-line treatment for patients with primary stage IV ESCC. We expect that the results of this phase II study will provide preliminary evidence for further evaluation of combination treatment options for patients with primary stage IV ESCC.

DATA AVAILABILITY STATEMENT

The original contributions presented in the study are included in the article/supplementary material. Further inquiries can be directed to the corresponding authors.

ETHICS STATEMENT

The studies involving human participants were reviewed and approved by Ethics Committee of Sichuan Cancer Hospital (SCCHEC-02-2021-021). The patients/participants provided their written informed consent to participate in this study.

AUTHOR CONTRIBUTIONS

JL designed the investigation and contributed to writing the paper. TL and QW participated in the administration of this study and contributed to writing the paper. JL and GW were involved in obtaining ethical approval. BL, YW, and GW provided essential assistance and gave suggestions in writing this manuscript. LW, BL, and YW performed the research and supervised the study. All authors read and approved the final manuscript.

FUNDING

This study was supported by grants from the Sichuan Science and Technology Department Key Research and Development Project Fund [2018SZ0210,2019YFS0378] and the Applied Basic Research Programs of the Science and Technology Department of Sichuan Province [2020YJ0446].

ACKNOWLEDGMENTS

We thank all participating patients and their advisors involved in this study. We also thank the patients and their family members. This clinical trial will be presented as an electronic poster at The Society for Immunotherapy of Cancer (SITC) in November 2021.

REFERENCES

1. Siegel RL, Miller KD, Jemal A. Cancer Statistics, 2018. *CA Cancer J Clin* (2018) 68:7–30. doi: 10.3322/caac.21442
2. Zheng RS, Sun KX, Zhang SW, Zeng HM, Zou XN, Chen R, et al. Report of Cancer Epidemiology in China, 2015. *Zhonghua Zhong Liu Za Zhi* (2019) 4:19–28. doi: 10.3760/cma.j.issn.0253-3766.2019.01.005
3. Sun JM, Shen L, Shah MA, Enzinger P, Adenis A, Doi T, et al. Pembrolizumab Plus Chemotherapy Versus Chemotherapy Alone for First-Line Treatment of Advanced Oesophageal Cancer (KEYNOTE-590): A Randomised, Placebo-Controlled, Phase 3 Study. *Lancet* (2021) 398:759–71. doi: 10.1016/S0140-6736(21)01234-4
4. Luo H, Lu J, Bai Y, Mao T, Wang J, Fan Q, et al. Effect of Camrelizumab vs Placebo Added to Chemotherapy on Survival and Progression-Free Survival in Patients With Advanced or Metastatic Esophageal Squamous Cell Carcinoma: The ESCORT-1st Randomized Clinical Trial. *JAMA* (2021) 326:916–25. doi: 10.1001/jama.2021.12836
5. Suzuki G, Yamazaki H, Aibe N, Masui K, Tatekawa K, Sasaki N, et al. Palliative Radiotherapy in the Local Management of Stage IVB Esophageal Cancer: Factors Affecting Swallowing and Survival. *Anticancer Res* (2017) 37:3085–92. doi: 10.21873/anticanres.11664
6. Li J, Wen Y, Xiang Z, Du H, Geng L, Yang X, et al. Radical Radiotherapy for Metachronous Oligometastasis After Initial Treatment of Esophageal Cancer. *Radiother Oncol* (2021) 154:201–6. doi: 10.1016/j.radonc.2020.09.042
7. Lee S, Ahn BC, Park SY, Kim DJ, Lee CG, Cho J, et al. A Phase II Trial of Preoperative Chemoradiotherapy and Pembrolizumab for Locally Advanced Esophageal Squamous Cell Carcinoma (ESCC). *Ann Oncol* (2019) 30(Suppl 5):v754. doi: 10.1093/annonc/mdz065.004
8. van den Ende T, de Clercq NC, van Berge Henegouwen MI, Gisbertz SS, Geijsen ED, Verhoeven RHA, et al. Neoadjuvant Chemoradiotherapy Combined With Atezolizumab for Resectable Esophageal Adenocarcinoma: A Single-Arm Phase II Feasibility Trial (PERFECT). *Clin Cancer Res* (2021) 27:3351–9. doi: 10.1158/1078-0432.CCR-20-4443
9. Liao XY, Liu CY, He JF, Wang LS, Zhang T. Combination of Checkpoint Inhibitors With Radiotherapy in Esophageal Squamous Cell Carcinoma Treatment: A Novel Strategy. *Oncol Lett* (2019) 18:5011–21. doi: 10.3892/ol.2019.10893
10. Rice TW, Ishwaran H, Ferguson MK, Blackstone EH, Goldstraw P. Cancer of the Esophagus and Esophagogastric Junction: An Eighth Edition Staging Primer. *J Thorac Oncol* (2017) 12:36–42. doi: 10.1016/j.jtho.2016.10.016
11. Ajani JA, D'Amico TA, Bentrem DJ, Chao J, Corvera C, Das P, et al. Esophageal and Esophagogastric Junction Cancers, Version 2.2019, NCCN Clinical Practice Guidelines in Oncology. *J Natl Compr Canc Netw* (2019) 17:855–83. doi: 10.6004/jnccn.2019.0033
12. Deng L, Liang H, Burnette B, Beckett M, Darga T, Weichselbaum RR, et al. Irradiation and Anti-PD-L1 Treatment Synergistically Promote Antitumor Immunity in Mice. *J Clin Invest* (2014) 124:687–95. doi: 10.1172/JCI67313
13. Zhang P, Su DM, Liang M, Fu J. Chemopreventive Agents Induce Programmed Death-1-Ligand 1 (PD-L1) Surface Expression in Breast Cancer Cells and Promote PD-L1-Mediated T Cell Apoptosis. *Mol Immunol* (2008) 45:1470–6. doi: 10.1016/j.molimm.2007.08.013
14. Vanneman M, Dranoff G. Combining Immunotherapy and Targeted Therapies in Cancer Treatment. *Nat Rev Cancer* (2012) 12:237–51. doi: 10.1038/nrc3237
15. Formenti SC, Demaria S. Combining Radiotherapy and Cancer Immunotherapy: A Paradigm Shift. *J Natl Cancer Inst* (2013) 105:256–65. doi: 10.1093/jnci/djs629

Conflict of Interest: The authors declare that the research was conducted in the absence of any commercial or financial relationships that could be construed as a potential conflict of interest. However, one drug, toripalimab, was provided for free by Shanghai Junshi Biosciences Co., Ltd., who had no direct role in the design of this protocol or in the collection, analysis, or interpretation of data.

frontiers | Frontiers in Oncology

ORIGINAL RESEARCH
published: 23 May 2022
doi: 10.3389/fonc.2022.813021

Induction Chemotherapy Followed by Chemoradiotherapy With or Without Consolidation Chemotherapy Versus Chemoradiotherapy Followed by Consolidation Chemotherapy for Esophageal Squamous Cell Carcinoma

Mingyue Xiang[1,2], *Bo Liu*[3], *Guifang Zhang*[1], *Heyi Gong*[1], *Dali Han*[1*] and *Changsheng Ma*[1*]

[1] Department of Radiation Oncology, Shandong Cancer Hospital and Institute, Shandong First Medical University and Shandong Academy of Medical Sciences, Jinan, China, [2] Department of Graduate, Shandong First Medical University and Shandong Academy of Medical Sciences, Taian, China, [3] Department of Medical Oncology, Shandong Cancer Hospital and Institute, Shandong First Medical University and Shandong Academy of Medical Sciences, Jinan, China

Objective: This study aimed to compare the efficacy and safety of induction chemotherapy followed by concurrent chemoradiotherapy (I-CCRT), induction chemotherapy followed by concurrent chemoradiotherapy and consolidation chemotherapy (I-CCRT-C), and concurrent chemoradiotherapy followed by consolidation chemotherapy (CCRT-C) for locally advanced esophageal squamous cell carcinoma (ESSC).

Patients and Methods: Patients with locally advanced ESCC who underwent definitive chemoradiotherapy with cisplatin plus fluorouracil or docetaxel from February 2012 to December 2018 were retrospectively reviewed. Kaplan–Meier curve was used to estimate survival. Efficacy was assessed using RECIST, version 1.0. Prognosis factors were identified with Cox regression analysis.

Results: Patients were treated with CCRT-C (n = 59), I-CCRT (n = 20), and I-CCRT-C (n = 48). The median follow-up duration was 73.9 months for the entire cohort. The ORR of the CCRT-C, I-CCRT, and I-CCRT-C groups was 89.8%, 70.0%, and 77.1%, respectively (p = 0.078). The median PFS in the CCRT-C, I-CCRT, and I-CCRT-C groups was 32.5, 16.1, and 27.1 months, respectively (p = 0.464). The median OS of the CCRT-C, I-CCRT, and I-CCRT-C groups was 45.9, 35.5, and 54.0 months, respectively (p = 0.788). Cox regression analysis indicated that I-CCRT-C and I-CCRT did not significantly prolong PFS and OS compared with CCRT-C ($p > 0.05$). Neutropenia grade ≥3 in CCRT-C, I-CCRT, and I-CCRT-C groups was 47.5%, 15%, and 33.3% of patients, respectively (p = 0.027).

OPEN ACCESS

Edited by:
Li Jiancheng,
Fujian Provincial Cancer Hospital, China

Reviewed by:
Chai Hong Rim,
Korea University, South Korea
Wencheng Zhang,
Tianjin Medical University Cancer Institute and Hospital, China

***Correspondence:**
Dali Han
dalihan_sdch@163.com
Changsheng Ma
machangsheng_2000@126.com

Specialty section:
This article was submitted to Radiation Oncology, a section of the journal Frontiers in Oncology

Received: *11 November 2021*
Accepted: *21 April 2022*
Published: *23 May 2022*

Citation:
Xiang M, Liu B, Zhang G, Gong H, Han D and Ma C (2022) Induction Chemotherapy Followed by Chemoradiotherapy With or Without Consolidation Chemotherapy Versus Chemoradiotherapy Followed by Consolidation Chemotherapy for Esophageal Squamous Cell Carcinoma. Front. Oncol. 12:813021. doi: 10.3389/fonc.2022.813021

Conclusions: I-CCRT and I-CCRT-C using cisplatin plus fluorouracil or docetaxel regimen are not superior to CCRT-C in survival but seem to have less severe neutropenia than CCRT-C. Further randomized controlled studies are warranted.

Keywords: esophageal squamous cell carcinoma, induction chemotherapy, concurrent chemoradiotherapy, consolidation chemotherapy, survival

INTRODUCTION

Based on GLOBOCAN estimates, in 2018, esophageal cancer (EC) was the seventh most common cancer with approximately 572,000 newly diagnosed patients. It was also the sixth most common cause of cancer-related deaths, with 509,000 patient deaths (1). In China, EC is the third most diagnosed cancer with the fourth highest mortality rate (2). Unlike in western countries, esophageal squamous cell carcinoma (ESCC) is a predominant histopathological subtype of EC in China, comprising more than 90% of EC cases with a higher locoregional recurrence rate than adenocarcinoma (3).

Endoscopic resection is recommended as the standard option for intramucosal ESCC due to preservation of esophageal function and encouraging outcome (4). Surgical resection with neoadjuvant or adjuvant chemoradiotherapy is an important radical medical procedure for patients with resectable ESCC (5, 6). Unfortunately, half of ESCC patients are diagnosed at the locally advanced, unresectable stage associated with worsened prognosis (7). Even if medically fit for surgery, some patients with ESCC tend to receive radical chemoradiotherapy for the preservation of esophageal function.

Definitive chemoradiotherapy currently remains a treatment option for these patients who can to tolerate chemoradiation. Definitive chemoradiotherapy treatment options for ESCC include concurrent chemoradiotherapy (CCRT) (8), concurrent chemoradiotherapy followed by consolidation chemotherapy (CCRT-C) (9–11), induction chemotherapy followed by concurrent chemoradiotherapy (I-CCRT) (12, 13), and sequential chemoradiotherapy (SCRT) (14). Studies have demonstrated that CCRT confers a survival benefit for locally advanced ESCC compared with SCRT (14, 15). Therefore, CCRT and CCRT-C are recommended as the standard treatments for locally advanced unresectable ESCC (16). However, the outcome for ESCC patients receiving definitive CCRT remains poor, with 5-year overall survival (OS) rate of less than 20% (17).

Theoretically, adding induction chemotherapy before definitive CCRT has the potential to eradicate micrometastases, shrink tumor volume, and improve outcome (18), even reducing the radio-induced injury. A phase II study showed that I-CCRT with cisplatin-irinotecan is well-tolerated with a clinical complete response rate of 58.1% for EC (19). A retrospective study suggested that I-CCRT is superior to CCRT in OS and progress-free survival (PFS) for ESCC (18). However, the outcome and safety among I-CCRT, I-CCRT-C, and CCRT-C for patients with locally advanced ESCC has not been established.

Here, we conducted a retrospective study to compare the efficacy and safety of CCRT-C, I-CCRT, and I-CCRT-C with the chemotherapy regimen of cisplatin plus fluorouracil (PF) or docetaxel (DP) in locally advanced ESSC patients.

PATIENTS AND METHODS

Data of ESCC patients who received definitive CCRT-C, I-CCRT, and I-CCRT-C using the regimen of PF or DP were retrieved from our Medical Record System between February 2012 and December 2018 and analyzed. Variables included gender, age, Eastern Cooperative Oncology Group performance status (ECOG PS), serum levels of Cyfra 21-1 and carcinoembryonic antigen (CEA), tumor location, tumor length, T stage, N stage, M stage, differentiation, radiation technology, radiation dose, chemotherapy regimen, chemotherapy cycle, and treatment options. The inclusion criteria were as follows: age ≥18, ECOG PS ≤2, histopathologically confirmed squamous cell carcinoma, cT3-4N0M0/cT1-4N+M0 or cM1 (positive nonregional lymph nodes and irradiated during radiotherapy) in accordance with AJCC 7th edition, treated by 3DCRT/IMRT with radiation total doses ≥50 Gy using conventional fractionated radiotherapy, chemotherapy cycles ≥4, chemotherapy with PF or DP, no previous treatment, and no surgery after definitive chemoradiation. The exclusion criteria were as follows: underwent tumor resection before or after definitive chemoradiotherapy and changed chemotherapy regimens during definitive chemoradiotherapy. This study was approved by the ethics committee of our institute according to the Declaration of Helsinki. Patient informed consent was waived due to the nature of the retrospective study.

Treatment Strategy

Concurrent chemoradiotherapy followed by chemotherapy included 1 to 6 cycles of chemotherapy after concurrent chemoradiotherapy (CCRT-C group). Induction chemotherapy followed by concurrent chemotherapy was defined as 1 to 6 cycles of chemotherapy delivered prior to concurrent chemoradiotherapy (I-CCRT group). Induction chemotherapy followed by concurrent chemoradiotherapy and consolidation chemotherapy included 1 to 4 cycles of chemotherapy followed by concurrent chemoradiotherapy and another 1 to 4 cycles of chemotherapy (I-CCRT-C group).

The chemotherapy regimens included the following: (i) cisplatin (60–80 mg/m^2 on day 1) and docetaxel (60 mg/m^2 on day 1); and (ii) cisplatin (75–100 mg/m^2 on day 1) and fluorouracil (750–1,000 mg/m^2 CIV 96 h on day 1). Chemotherapy was performed every 3 or 4 weeks, and the dosage was adjusted if necessary.

Patients lay on the examination bed of a big core CT fixed with a vacuum cushion. The radiotherapy was delivered using

the 3DCRT or IMRT techniques. The plan was designed by Varian Eclipse or Pinnacle treatment planning system (TPS) with a 6-MV X-ray using 5, 7, or 9 coplanar radiated fields with elective or involved filed irradiation. The beam numbers and radiation directions were manually adjusted to optimize the plan. The gross tumor volume (GTV) was defined as the visible primary tumor (GTVp) and metastatic lymph nodes (GTVnd) detected by contrast-enhanced CT, PET/CT, and endoscopy. The clinical target volume of the primary tumor (CTVp) was defined as a 3.0-cm margin from the GTVp in up-down directions and a 0.5–0.6-cm margin in the posteroanterior and right–left directions. The clinical target volume of metastatic lymph nodes (CTVnd) was defined as a 0.5–0.6-cm margin from the GTVnd. The planning target volume (PTV) was generated from the CTVp and CTVnd with a 5-mm extended margin. The total radiation dose was delivered ≥50 Gy at 1.8 or 2 Gy per fraction, given once per day, 5 fractions per week. The PTV was covered with 95% of the prescription isodose line, and the volume receiving 104.5% of the prescription was limited to 5%. Dose-volume histograms (DVHs) were used to optimize target coverage and normal tissue sparing. The dose limitation for organs at risk (OARs) was defined as previously reported (20).

Response Evaluation

The efficacy was evaluated by the Response Evaluation Criteria in Solid Tumors Version 1.0. PFS was defined as the period from the start of the anticancer treatment to the time of the first diagnostic progression or death or last follow-up. OS was defined from the start of the initial antitumor treatment to the date of death from any cause, regardless of disease status or last follow-up. The Common Terminology Criteria for Adverse Events Version 4.0 (CTCAE 4.0) was used to evaluate acute toxicities including leukocytopenia, neutropenia, anemia, thrombocytopenia, transaminase, bilirubinemia, and nausea/vomiting. Patients were followed up every 1 to 3 months after completion of chemotherapy for the first 2 years and every 6 to 12 months thereafter.

Statistical Analyses

The Chi-square test or Fischer's exact test was used to compare the difference for categorical variables. One-way ANOVA was used for continuous variables. A p-value reaching <0.05 was further compared using the rcompanion package for categorical variables or the LSD test for continuous variables. Survival was calculated using the Kaplan–Meier curve and compared by the log-rank test. Univariable and multivariable Cox regression analyses were used to identify the independent prognostic factors. Statistical analyses were performed using SPSS version 26 (IBM Corporation, USA) or R-3.6.3. The survival figure was delineated using GraphPad Prism 7.0 (GraphPad Software, USA). A p-value <0.05 was considered statistically significant.

RESULTS

Patient Characteristics

A total of 127 patients treated with definitive chemoradiotherapy from February 2012 to December 2018 were analyzed in this study. Patients (59 of 127) were treated with CCRT-C, 20 with I-CCRT, and 48 with I-CCRT-C. The median tumor length in the CCRT-C, I-CCRT, and I-CCRT-C groups was 4.8, 4.6, and 5.7 cm, respectively (p = 0.031). *Post hoc* multiple comparisons showed that the I-CCRT-C group had longer primary tumors than CCRT-C (p = 0.023) and I-CCRT (p = 0.031). There were no significant difference in tumor length between CCRT-C and I-CCRT (p = 0.608). In the CCRT-C, I-CCRT, and I-CCRT-C groups, 49.2%, 75.0%, and 75.0% patients received the chemotherapy regimen of DP, respectively (p = 0.011). The CCRT-C group had more patients who received DP compared with I-CCRT-C (p = 0.034). There was no significant difference in the chemotherapy regimen between CCRT-C and I-CCRT (p = 0.120). The I-CCRT group also had a similar chemotherapy regimen to I-CCRT-C (p = 1.000). In total, 78.0%, 75.0%, and 31.3% were treated with 4 or 5 chemotherapy cycles in the CCRT-C, I-CCRT, and I-CCRT-C groups, respectively (p = 0). The I-CCRT-C group had fewer chemotherapy cycles than the CCRT-C (p = 0) and I-CCRT groups (p = 0.004). Meanwhile, the I-CCRT and I-CCRT groups had similar chemotherapy cycles. There were no significant differences in gender, age, ECOG PS, CEA, Cyfra 21-1, differentiation, T stage, N stage, M stage, radiation technology, and radiation dose among groups (p > 0.05). Detailed patient characteristics are summarized in **Table 1**.

Efficacy

The treatment response rate of CCRT-C, I-CCRT, and I-CCRT-C is summarized in **Table 2**. The objective response rate (ORR) in the CCRT-C, I-CCRT, and I-CCRT-C groups was 89.8%, 70.0%, and 77.1%, respectively (p = 0.078). The disease control rate (DCR) was 93.2%, 75.0%, and 100%, respectively (p = 0.009). I-CCRT-C had significantly higher DCR than I-CCRT (P = 0.006). However, CCRT-C had comparable DCR with I-CCRT (p = 0.106) and I-CCRT-C (p = 0.185).

Survival

The latest follow-up was in March 2021. The median follow-up duration was 73.9 months for the entire cohort. The Kaplan–Meier survival curves are shown in **Figure 1**. The median PFS in the CCRT-C, I-CCRT, and I-CCRT-C groups was 32.5 (95% confidence interval (CI): 20.3, 44.7), 16.1 (95% CI: 0, 47.0), and 27.1 (95% CI: 14.2, 40.0) months, respectively (p = 0.464) (**Figure 1A**). The median OS of the CCRT-C, I-CCRT, and I-CCRT-C groups was 45.9 (95% CI: 29.0, 62.8), 35.5 (95% CI: 1.4, 69.5), and 54.0 (95% CI: 38.5, 69.5) months, respectively (p = 0.788) (**Figure 1B**).

Prognostic Factors

The univariate and multivariate Cox regression analyses of prognostic factors for PFS are shown in **Table 3**. In the univariable Cox regression analysis, age, ECOG PS, CYFRA 21-1, tumor differentiation, and M stage were potential prognostic factors for PFS. In the multivariable model using the Enter method, ECOG PS 1 [HR: 1.62 (95% CI: 1.01–2.61), p = 0.045], middle or poor differentiation (HR: 2.30 (95% CI:

TABLE 1 | Characteristics of patients [*n* (%)].

Covariant	CCRT-C (*n* = 59)	I-CCRT (*n* = 20)	I-CCRT-C (*n* = 48)	*p*-value
Gender				0.101
Male	45 (76.3)	17 (85.0)	44 (91.7)	
Female	14 (23.7)	3 (15.0)	4 (8.3)	
Age (year)	59.2 ± 7.6	59.9 ± 6.2	61.8 ± 7.6	0.193
ECOG PS				0.231
0	35 (59.3)	9 (45.0)	21 (43.8)	
1	24 (40.7)	11 (55.0)	27 (56.2)	
Tumor location				0.218
Cervical or upper	37 (62.7)	11 (55.0)	22 (45.8)	
Middle or lower	22 (37.3)	9 (45.0)	26 (54.2)	
Tumor length (cm)	4.8 ± 1.9	4.6 ± 1.4	5.7 ± 2.4	0.031
CEA (ng/ml)				0.185
<3.4	43 (72.9)	18 (90.0)	40 (83.3)	
≥3.4	16 (27.1)	2 (10.0)	8 (16.7)	
Cyfra 21-1 (ng/ml)				0.089
<3.3	45 (78.0)	16 (80.0)	29 (60.4)	
≥3.3	13 (22.0)	4 (20.0)	19 (39.4)	
Differentiation				0.157
High	26 (44.1)	8 (40.0)	29 (60.4)	
Poor-middle	33 (55.9)	12 (60)	19 (39.6)	
T stage				0.363
T1–2	4 (6.8)	3 (15.0)	7 (14.6)	
T3–4	55 (93.2)	14 (85.0)	41 (85.4)	
N stage				0.162
N0	14 (23.7)	1 (5.0)	8 (16.7)	
N+	45 (76.3)	19 (95.0)	40 (83.3)	
M stage				0.230
M0	52 (88.1)	15 (75.0)	37 (77.1)	
M1	7 (11.9)	5 (25.0)	11 (22.9)	
Technology				0.927
3DCRT	20 (33.9)	7 (35.0)	18 (37.5)	
IMRT	39 (66.1)	13 (65.0)	30 (62.5)	
Dose (Gy)				0.075
<60	23 (39.0)	4 (20.0)	10 (20.8)	
≥60	36 (61.0)	16 (80.0)	38 (79.2)	
Regimen				0.011
DP	29 (49.2)	15 (75.0)	36 (75.0)	
PF	30 (50.8)	5 (25.0)	12 (25.0)	
Cycles				0
4–5	46 (78.0)	15 (75.0)	15 (31.3)	
6–8	13 (22.0)	5 (25.0)	33 (68.7)	

TABLE 2 | The treatment response rates among groups [*n* (%)].

Response	CCRT-C	I-CCRT	I-CCRT-C
Complete response	8 (13.6)	1 (5.0)	2 (4.2)
Partial response	45 (76.3)	13 (65.0)	35 (72.9)
Stable disease	2 (3.4)	1 (5.0)	11 (22.9)
Progression disease	4 (6.8)	5 (25.0)	0 (0)

1.47–3.60), $p = 0$), and M1 stage [HR: 1.72 (95% CI: 1.02–2.90), $p = 0.44$] were also associated with shorter PFS.

Univariate and multivariate Cox regression analyses predicting OS are summarized in **Table 4**. The results indicated that age, ECOG PS, CYFRA 21-1, differentiation, and M stage were possible OS predictive factors. In the multivariable analysis, middle or poor differentiation [HR: 2.47 (95% CI: 1.51–4.03), $p = 0$] and M1 stage [HR: 1.98 (95% CI: 1.12–3.49), $p = 0.019$] were the independent adverse predictors for OS.

Adverse Events

A summary of adverse events related to definitive chemoradiotherapy is provided in **Table 5**. Overall, these treatment strategies were relatively well tolerated. Hematological and gastrointestinal toxicities were the most common. Neutropenia grade ≥3 was observed in 47.5% of the CCRT-C group, 15% of the I-CCRT group, and 33.3% of the I-CCRT-C group ($p = 0.027$). *Post hoc* comparison demonstrated that the CCRT-C group had a higher incidence of severe neutropenia than

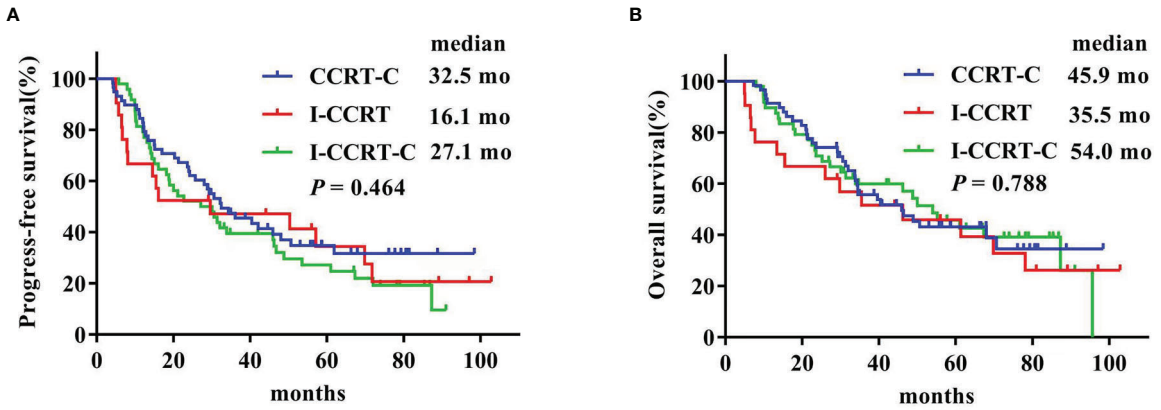

FIGURE 1 | Kaplan–Meier curves of progress-free survival **(A)** and overall survival **(B)**.

TABLE 3 | Univariate and multivariate Cox regression of prognostic factors for PFS.

Covariant	Univariate Cox regression		Multivariate Cox regression	
	HR (95% CI)	*p*-value	HR (95% CI)	*p*-value
Gender female vs. male	0.77 (0.42, 1.38)	0.375		
Age	1.03 (1.00, 1.06)	0.032	1.03 (0.99, 1.06)	0.102
ECOG PS 1 vs. 0	2.09 (1.37, 3.18)	0.001	1.62 (1.01, 2.61)	0.045
CEA ≥3.4 vs. <3.4	0.91 (0.54, 1.54)	0.726		
Cyfra 21-1 ≥3.3 vs. <3.3	1.57 (1.01, 2.42)	0.045	1.38 (0.88, 2.16)	0.165
Tumor location				
Middle/lower vs. cervical/upper	1.25 (0.83, 1.90)	0.288		
Differentiation				
Middle or poor vs. high	2.26 (1.48, 3.45)	0	2.30 (1.47, 3.60)	0
Tumor length	0.97 (0.87, 1.07)	0.512		
T stage T3–4 vs. T1–2	1.75 (0.81, 3.78)	0.156		
N stage N+ vs. N0	1.30 (0.75, 2.28)	0.348		
M stage M1 vs. M0	1.73 (1.03, 2.92)	0.038	1.72 (1.02, 2.90)	0.044
Technology IMRT vs. 3DCRT	0.92 (0.60, 1.41)	0.687		
Dose ≥60 vs. <60 Gy	1.06 (0.67, 1.70)	0.792		
Regimen PF vs. TP	1.30 (0.85, 1.99)	0.219		
Cycles 6–8 vs. 4–5	1.36 (0.90, 2.07)	0.142		
Treatment options				
I-CCRT vs. CCRT-C	1.26 (0.69, 2.31)	0.449		
I-CCRT-C vs. CCRT-C	1.32 (0.84, 2.07)	0.234		

the I-CCRT group ($p = 0.021$). However, the I-CCRT-C group had comparable severe neutropenia with the CCRT-C ($p = 0.201$) and I-CCRT ($p = 0.215$) groups. There were no significant differences in leukopenia, anemia, thrombocytopenia, radiation esophagitis, radiation pneumonitis, cardiac disorders, nausea or vomiting, and esophageal mediastinal or esophagotracheal fistula among the groups. There were no treatment-related deaths.

DISCUSSION

To the best of our knowledge, our study is the first to report the outcomes and safety of definitive chemoradiotherapy with CCRT-C, I-CCRT, and I-CCRT-C in patients with advanced ESCC. Our findings suggested that I-CCRT and I-CCRT-C are not superior to CCRT-C in survival for patients with advanced ESCC, based on the chemotherapy regimen of DP and PF, whereas I-CCRT had less grade ≥3 neutropenia than CCRT-C. Based on the results, I-CCRT or I-CCRT-C has the potential to be a standard treatment option for locally advanced ESCC.

According to the NCCN Guidelines for Esophageal Cancer 2021 v1, the preferred definitive chemoradiotherapy for nonsurgical EC was either CCRT or CCRT-C. However, several studies suggested that the addition of induction chemotherapy prior to CCRT in locally advanced ESCC was feasible (**Table 6**). A multicenter phase II FFCD trial (19) reported that induction chemotherapy with cisplatin and irinotecan followed by CCRT without surgery for stages I–III EC resulted in CR of 58.1% and 1- and 2-year OS of 62.8% and 27.9%, respectively. Watkins et al. (21) reported that induction cisplatin and irinotecan followed by

TABLE 4 | Univariate and multivariate Cox regression in predicting OS.

Covariant	Univariate Cox regression		Multivariate Cox regression	
	HR (95% CI)	*p*-value	HR (95% CI)	*p*-value
Gender female vs. male	0.68 (0.35, 1.32)	0.258		
Age	1.03 (1.00, 1.06)	0.077	1.03 (0.99, 1.06)	0.146
ECOG PS 1 vs. 0	2.10 (1.32, 3.34)	0.002	1.62 (0.97, 2.71)	0.065
CEA ≥3.4 vs. <3.4	1.04 (0.59, 1.83)	0.899		
Cyfra 21-1 ≥3.3 vs. <3.3	1.59 (0.98, 2.60)	0.062	1.46 (0.89, 2.40)	0.138
Tumor location				
Middle/lower vs. cervical/upper	1.31 (0.83, 2.06)	0.244		
Tumor length	1.00 (0.90, 1.12)	0.948		
Differentiation				
Middle or poor vs. high	2.49 (1.55, 4.00)	0	2.47 (1.51, 4.03)	0
T stage T3–4 vs. T1–2	1.55 (0.67, 3.57)	0.303		
N stage N+ vs. N0	1.44 (0.77, 2.68)	0.251		
M stage M1 vs. M0	1.83 (1.05, 3.19)	0.033	1.98 (1.12, 3.49)	0.019
Technology IMRT vs. 3DCRT	0.96 (0.60, 1.53)	0.848		
Dose ≥60 vs. <60 Gy	1.06 (0.63, 1.76)	0.839		
Regimen PF vs. TP	1.45 (0.92, 2.29)	0.115		
Cycles 6–8 vs. 4–5	1.26 (0.80, 1.98)	0.324		
Treatment options				
I-CCRT vs. CCRT-C	1.24 (0.66, 2.33)	0.509		
I-CCRT-C vs. CCRT-C	1.02 (0.61, 1.68)	0.950		

TABLE 5 | Adverse events related to definitive chemoradiotherapy [*n* (%)].

Grade	CCRT-C	I-CCRT	I-CCRT-C	*p*-value
Hematological				
Leukopenia				0.412
0–2	35 (59.3)	14 (70.0)	34 (70.8)	
3–4	24 (40.7)	6 (30.0)	14 (29.2)	
Neutropenia				0.027
0–2	31 (52.5)	17 (85.0)	32 (66.7)	
3–4	28 (47.5)	3 (15.0)	16 (33.3)	
Thrombocytopenia				0.488
0–2	51 (86.4)	18 (90.0)	45 (93.8)	
3–4	8 (13.6)	2 (10.0)	3 (6.2)	
Anemia				0.157
0–1	59 (100.0)	19 (95.0)	48 (100.0)	
2–4	0 (0)	1 (5.0)	0 (0)	
Nonhematological				
Radiation esophagitis				0.381
0–2	49 (83.1)	18 (90.0)	44 (91.7)	
3–4	10 (16.9)	2 (10.0)	4 (8.3)	
Radiation pneumonitis				0.858
0–2	57 (96.6)	19 (95.0)	45 (93.8)	
3–4	2 (3.4)	1 (5.0)	3 (6.2)	
Cardiac disorders				0.752
No	53 (89.8)	18 (90.0)	41 (85.4)	
Yes	6 (10.2)	2 (10.0)	7 (14.6)	
Nausea or vomiting				0.058
0–1	27 (45.8)	11 (55.0)	33 (68.8)	
2–3	32 (54.2)	9 (45.0)	15 (31.2)	
Fistula				0.753
No	53 (89.8)	18 (90.0)	45 (93.8)	
Yes	6 (10.2)	2 (10.0)	3 (6.2)	

concurrent cisplatin, irinotecan, and radiotherapy for locally advanced esophageal cancer is tolerable with a 2-year OS of 42% and 2-year PFS of 9.2%. A prospective, multicenter phase I/II study (16) reported that induction chemotherapy with docetaxel, cisplatin, and fluorouracil followed by CCRT was tolerable, with a CR of 39.4%, the median PFS of 12.2 months, and the median OS of 26.0 months in unresectable locally advanced ESCC. Another phase I/II study (22) found that induction chemotherapy with

TABLE 6 | Published literatures of definitive I-CCRT for ESCC.

Author	Number of patients	Regimen	Response	Outcome	Severe neutropenia [*n* (%)]
Michel et al. (19)	43	Cisplatin/irinotecan	CR 58.1% PR NA	1-year OS 62.8% 2-year OS 27.9%	NA
Watkins et al. (21)	53	Cisplatin/irinotecan	NA	2-year OS 42% 2-year PFS 9.2%	13 (28%)
Satake et al. (16)	33	Docetaxel/cisplatin/5-Fu	CR 39.4% PR 33.3%	mPFS 12.2 months mOS 26.0 months 3-year OS 40.4%	24 (72%)
Pöttgen et al. (22)	16	Irinotecan/folinic acid/5-Fu/ cisplatin	CR 56% PR NA	1-year OS 77% 2-year OS 53% 3-year OS 41% 5-year OS 29%	10 (62%)
Luo et al. (18)	85	Docetaxel/cisplatin	CR+PR50.6% (after induction therapy)	mOS 26.0 months 3-year OS 30.6%	33 (38.8%)

NA, non-available.

irinotecan, folinic acid, 5-fluorouracil, and cisplatin followed by concurrent chemoradiation with cisplatin and irinotecan was tolerable, with clinical CR, 1-year OS and local regional PFS of 56%, 77%, and 59%. In addition, Luo et al. (18) reported that I-CCRT had significantly longer OS compared with CCRT (26.0 vs. 22.0 months). However, whether the outcome and safety of I-CCRT or I-CCRT-C are superior to CCRT-C has not been established.

Our findings suggested that the I-CCRT and I-CCRT-C groups had similar ORR to that of the CCRT-C group (70.0% vs. 77.1% vs. 89.8%). Previous reports showed that patient with ESCC receiving I-CCRT resulted in an ORR of 72.7% (16), similar to the present study. Our study also found that I-CCRT-C had a significantly higher DCR than I-CCRT, indicating that adding chemotherapy after I-CCRT might improve the DCR.

Our findings showed that the I-CCRT and I-CCRT-C groups had similar PFS (median, 16.1 vs. 27.1 vs. 32.5 months) and OS (35.5 vs. 54.0 vs. 45.9) with that of the CCRT-C group, which is superior to that of the PRODIGE5/ACCORD17 trial (median PFS, 9.7 months in the FOLFOX group and 9.4 months in the fluorouracil and cisplatin group) with CCRT-C. The reason likely was that the radiation dose of the present study was different from the PRODIGE5/ACCORD17 trial. A larger meta-analysis (23) reported that CCRT with doses of ≥60 Gy for ESCC patients might improve locoregional control and survival compared with the standard-dose CCRT. More than half of the patients received the prescribed total dose of ≥60 Gy, whereas the PRODIGE5/ACCORD17 trial used the standard dose radiation (50 Gy) with a conventional fraction. A phase II randomized controlled trial (24) demonstrated that CCRT with the DP regimen had similar treatment responses (ORR, 84.4% in the DP group and 87.3% in the PF group), PFS (1- and 2-year PFS, 77.4% and 55.0% for the PF group and 78.8% and 69.4% for the DP group), and OS (the 1- and 2-year OS, 93.7% and 86.2% for the PF group and 87.3% and 69.1% for the DP group) with those using CCRT with the PF regimen as a first-line treatment for patients with ESCC. Additionally, our study also suggested that the chemotherapy regimen was not associated with PFS and OS in the Cox regression analysis.

Several prospective or retrospective studies reported that the incidence of grade ≥3 neutropenia ranged from 2.6% to 41% in EC patients who received I-CCRT with a two-drug regimen. A randomized phase II study suggested that the incidence of grades 3–4 neutropenia of preoperative I-CCRT using oxaliplatin/capecitabine or carboplatin/paclitaxel for resectable esophageal adenocarcinoma was 2.6% (1/38) and 21.4% [9/42] ($p = 0.011$) (25). Another randomized phase II trial demonstrated that the incidence of grade 3 or 4 neutropenia of I-CCRT and CCRT alone with DP in ESCC was 18.2% and 7.3%, respectively ($p = 0.151$) (26). There were no significant differences in rates of other grades 3–5 hematological adverse events between groups were observed (26). Simoni et al. (13) reported that the rate of neutropenia (grade ≥3) of I-CCRT as an intensive neoadjuvant protocol for patients with EC was 22.7% (27/119). A matched case–control study (18) reported that the rates of grade ≥3 neutropenia of I-CCRT and CCRT with DP in the treatment of ESCC were 32.9% ($n = 28$) and 23.5% ($n = 20$) ($p = 0.173$), respectively. Additionally, more toxicity would be observed when using triple drugs during I-CCRT. A prospective, multicenter phase I/II study reported that the incidence of severe neutropenia in I-CCRT with a triple-drug of docetaxel, cisplatin, and fluorouracil in unresectable locally advanced EC was 72% ($n = 33$) (16). Another small sample study showed that I-CCRT (induction chemotherapy with irinotecan, folinic acid, and 5-fuorouracil weekly and cisplatin every 2 weeks followed by CCRT with cisplatin and irinotecan) for ESCC had more serious neutropenia (62%). Our study demonstrated that the neutropenia grade ≥3 was observed in 15% of the I-CCRT group, whereas 47.5% of the CCRT-C group and 33.3% of the I-CCRT-C group ($p = 0.027$). Zhu et al. (24) reported that definitive CCRT with a DP regimen was associated with more severe hematological toxicities than with PF regimen, including neutropenia. In the present study, the I-CCRT group was associated with less severe neutropenia than that of the CCRT-C group, which used fewer DP regimen and chemotherapy cycles. Taken together, we inferred that I-CCRT had a lower incidence of severe neutropenia than CCRT-C. We interpreted that the induction chemotherapy before CCRT might have the

potential to shrink tumor volume, leading to less radiation volume, which could result in less neutropenia.

However, several limitations also existed in the present study, which require mentioning. First, this was a retrospective study, which could have had an influence on the quality of the data and the selection of patients. Second, there were a relatively small number of patients among groups, especially in the I-CCRT group. Third, the basic characteristics of patients, including tumor length, chemotherapy regimen, and chemotherapy, were unbalanced among groups. However, these factors did not significantly affect the PFS and OS in Cox regression analysis, thus having a limited effect in the present study.

CONCLUSIONS

Our study suggested that I-CCRT and I-CCRT-C using cisplatin plus fluorouracil or docetaxel regimens are not superior to CCRT-C in ORR, PFS, and OS for locally advanced ESCC. I-CCRT or I-CCRT-C seems to have less severe neutropenia than CCRT-C. I-CCRT and I-CCRT-C have the potential to be treatment options for selective locally advanced ESCC patients. Prospective, randomized controlled studies are warranted to verify the presented results.

DATA AVAILABILITY STATEMENT

The original data are available if requested. Further inquiries can be directed to the corresponding authors.

ETHICS STATEMENT

This study was approved by the Ethics Committee of Shandong Cancer Hospital and Institute according to the Declaration of Helsinki. Patient informed consent was waived due to the nature of the retrospective study.

AUTHOR CONTRIBUTIONS

MX and BL: drafted, conceived, and designed the manuscript. GZ, HG, and DH: contributed to acquiring, analyzing, and interpreting data. CM: contributed to acquiring data and enhancing its intellectual content. All authors read and approved the final manuscript.

FUNDING

This work is supported by National Nature Science Foundation of China (81800156, 81974467), Shandong Province Key R&D Program (2018GSF118031), and Natural Science Foundation of Shandong Province (ZR2019MH136, ZR2017BH024).

ACKNOWLEDGMENTS

The authors would like to thank the editor and reviewers for their insightful suggestions, which helped improve the manuscript.

REFERENCES

1. Bray F, Ferlay J, Soerjomataram I, Siegel RL, Torre LA, Jemal A. Global Cancer Statistics 2018: GLOBOCAN Estimates of Incidence and Mortality Worldwide for 36 Cancers in 185 Countries. *CA* (2018) 68(6):394–424. doi: 10.3322/caac.21492
2. Chen W, Zheng R, Baade PD, Zhang S, Zeng H, Bray F, et al. Cancer Statistics in China, 2015. *CA Cancer J Clin* (2016) 66(2):115–32. doi: 10.3322/caac.21338
3. Chen H, Zhou L, Yang Y, Yang L, Chen L. Clinical Effect of Radiotherapy Combined With Chemotherapy for Non-Surgical Treatment of the Esophageal Squamous Cell Carcinoma. *Med Sci monitor* (2018) 24:4183–91. doi: 10.12659/MSM.910326
4. Semenkovich TR, Hudson JL, Subramanian M, Mullady DK, Meyers BF, Puri V, et al. Trends in Treatment of T1N0 Esophageal Cancer. *Ann Surg* (2019) 270(3):434–43. doi: 10.1097/SLA.0000000000003466
5. Yang H, Liu H, Chen Y, Zhu C, Fang W, Yu Z, et al. Neoadjuvant Chemoradiotherapy Followed by Surgery Versus Surgery Alone for Locally Advanced Squamous Cell Carcinoma of the Esophagus (NEOCRTEC5010): A Phase III Multicenter, Randomized, Open-Label Clinical Trial. *J Clin Oncol* (2018) 36(27):2796–803. doi: 10.1200/JCO.2018.79.1483
6. Fuchs CS, Niedzwiecki D, Mamon HJ, Tepper JE, Ye X, Swanson RS, et al. Adjuvant Chemoradiotherapy With Epirubicin, Cisplatin, and Fluorouracil Compared With Adjuvant Chemoradiotherapy With Fluorouracil and Leucovorin After Curative Resection of Gastric Cancer: Results From CALGB 80101 (Alliance). *J Clin Oncol* (2017) 35(32):3671–77. doi: 10.1200/JCO.2017.74.2130
7. Wang X, Liu X, Li D, Wang X, Huang W, Li B. Concurrent Selective Lymph Node Radiotherapy and S-1 Plus Cisplatin for Esophageal Squamous Cell Carcinoma: A Phase II Study. *Ann Surg Oncol* (2019) 26(6):1886–92. doi: 10.1245/s10434-019-07264-4
8. Owens R, Cox C, Gomberg S, Pan S, Radhakrishna G, Parikh S, et al. Outcome of Weekly Carboplatin-Paclitaxel-Based Definitive Chemoradiation in Oesophageal Cancer in Patients Not Considered to be Suitable for Platinum-Fluoropyrimidine-Based Treatment: A Multicentre, Retrospective Review. *Clin Oncol (Royal Coll Radiologists (Great Britain))* (2020) 32(2):121–30. doi: 10.1016/j.clon.2019.09.058
9. Wang X, Ge X, Wang X, Zhang W, Zhou H, Lin Y, et al. S-1-Based Chemoradiotherapy Followed by Consolidation Chemotherapy With S-1 in Elderly Patients With Esophageal Squamous Cell Carcinoma: A Multicenter Phase II Trial. *Front Oncol* (2020) 10:1499. doi: 10.3389/fonc.2020.01499
10. Gao LR, Wang X, Han W, Deng W, Li C, Wang X, et al. A Multicenter Prospective Phase III Clinical Randomized Study of Simultaneous Integrated Boost Intensity-Modulated Radiotherapy With or Without Concurrent Chemotherapy in Patients With Esophageal Cancer: 3JECROG P-02 Study Protocol. *BMC Cancer* (2020) 20(1):901. doi: 10.1186/s12885-020-07387-y
11. Fan XW, Wang HB, Mao JF, Li L, Wu KL. Sequential Boost of Intensity-Modulated Radiotherapy With Chemotherapy for Inoperable Esophageal Squamous Cell Carcinoma: A Prospective Phase II Study. *Cancer Med* (2020) 9(8):2812–19. doi: 10.1002/cam4.2933
12. Miyata H, Yamasaki M, Takiguchi S, Nakajima K, Fujiwara Y, Konishi K, et al. Prognostic Value of Endoscopic Biopsy Findings After Induction Chemoradiotherapy With and Without Surgery for Esophageal Cancer. *Ann Surg* (2011) 253(2):279–84. doi: 10.1097/SLA.0b013e318206824f
13. Simoni N, Pavarana M, Micera R, Weindelmayer J, Mengardo V, Rossi G, et al. Long-Term Outcomes of Induction Chemotherapy Followed by Chemo-Radiotherapy as Intensive Neoadjuvant Protocol in Patients With Esophageal Cancer. *Cancers* (2020) 12(12):1–14. doi: 10.3390/cancers 12123614
14. Yao B, Tan B, Wang C, Song Q, Wang J, Guan S, et al. Comparison of Definitive Chemoradiotherapy in Locally Advanced Esophageal Squamous

Cell Carcinoma. *Ann Surg Oncol* (2016) 23(7):2367–72. doi: 10.1245/s10434-016-5154-y
15. Xing L, Liang Y, Zhang J, Wu P, Xu D, Liu F, et al. Definitive Chemoradiotherapy With Capecitabine and Cisplatin for Elder Patients With Locally Advanced Squamous Cell Esophageal Cancer. *J Cancer Res Clin Oncol* (2014) 140(5):867–72. doi: 10.1007/s00432-014-1615-5
16. Satake H, Tahara M, Mochizuki S, Kato K, Hara H, Yokota T, et al. A Prospective, Multicenter Phase I/II Study of Induction Chemotherapy With Docetaxel, Cisplatin and Fluorouracil (DCF) Followed by Chemoradiotherapy in Patients With Unresectable Locally Advanced Esophageal Carcinoma. *Cancer Chemother Pharmacol* (2016) 78(1):91–9. doi: 10.1007/s00280-016-3062-2
17. Liao Z, Cox JD, Komaki R. Radiochemotherapy of Esophageal Cancer. *J Thorac Oncol* (2007) 2(6):553–68. doi: 10.1097/01.JTO.0000275339.62831.5e
18. Luo LL, Xi M, Yang YD, Li QQ, Zhao L, Zhang P, et al. Comparative Outcomes of Induction Chemotherapy Followed By Definitive Chemoradiotherapy Versus Chemoradiotherapy Alone In Esophageal Squamous Cell Carcinoma. *J Cancer* (2017) 8(17):3441–47. doi: 10.7150/jca.21131
19. Michel P, Adenis A, Di Fiore F, Boucher E, Galais MP, Dahan L, et al. Induction Cisplatin-Irinotecan Followed by Concurrent Cisplatin-Irinotecan and Radiotherapy Without Surgery in Oesophageal Cancer: Multicenter Phase II FFCD Trial. *Br J Cancer* (2006) 95(6):705–9. doi: 10.1038/sj.bjc.6603328
20. Qin Q, Ge X, Wang X, Wang L, Li C, Chen J, et al. Stage III Esophageal Squamous Cell Carcinoma Patients With Three-Dimensional Conformal or Intensity-Modulated Radiotherapy: A Multicenter Retrospective Study. *Front Oncol* (2020) 10:580450. doi: 10.3389/fonc.2020.580450
21. Watkins JM, Zauls AJ, Kearney PL, Shirai K, Ruppert BN, Harper JL, et al. Toxicity, Response Rates and Survival Outcomes of Induction Cisplatin and Irinotecan Followed by Concurrent Cisplatin, Irinotecan and Radiotherapy for Locally Advanced Esophageal Cancer. *Jpn J Clin Oncol* (2011) 41(3):334–42. doi: 10.1093/jjco/hyq208
22. Pöttgen C, Gkika E, Stahl M, Abu Jawad J, Gauler T, Kasper S, et al. Dose-Escalated Radiotherapy With PET/CT Based Treatment Planning in Combination With Induction and Concurrent Chemotherapy in Locally Advanced (Ut3/T4) Squamous Cell Cancer of the Esophagus: Mature Results of a Phase I/II Trial. *Radiat Oncol (London England)* (2021) 16 (1):59. doi: 10.1186/s13014-021-01788-4
23. Xiao L, Czito BG, Pang Q, Hui Z, Jing S, Shan B, et al. Do Higher Radiation Doses With Concurrent Chemotherapy in the Definitive Treatment of Esophageal Cancer Improve Outcomes? A Meta-Analysis and Systematic Review. *J Cancer* (2020) 11(15):4605–13. doi: 10.7150/jca.44447
24. Zhu Y, Zhang W, Li Q, Li Q, Qiu B, Liu H, et al. A Phase II Randomized Controlled Trial: Definitive Concurrent Chemoradiotherapy With Docetaxel Plus Cisplatin Versus 5-Fluorouracil Plus Cisplatin in Patients With Oesophageal Squamous Cell Carcinoma. *J Cancer* (2017) 8(18):3657–66. doi: 10.7150/jca.20053
25. Mukherjee S, Hurt CN, Gwynne S, Sebag-Montefiore D, Radhakrishna G, Gollins S, et al. NEOSCOPE: A Randomised Phase II Study of Induction Chemotherapy Followed by Oxaliplatin/Capecitabine or Carboplatin/Paclitaxel Based Pre-Operative Chemoradiation for Resectable Oesophageal Adenocarcinoma. *Eur J Cancer (Oxford Engl 1990)* (2017) 74:38–46. doi: 10.1016/j.ejca.2016.11.031
26. Liu S, Luo L, Zhao L, Zhu Y, Liu H, Li Q, et al. Induction Chemotherapy Followed by Definitive Chemoradiotherapy Versus Chemoradiotherapy Alone in Esophageal Squamous Cell Carcinoma: A Randomized Phase II Trial. *Nat Commun* (2021) 12(1):4014. doi: 10.1038/s41467-021-24288-1

Conflict of Interest: The authors declare that the research was conducted in the absence of any commercial or financial relationships that could be construed as a potential conflict of interest.

Publisher's Note: All claims expressed in this article are solely those of the authors and do not necessarily represent those of their affiliated organizations, or those of the publisher, the editors and the reviewers. Any product that may be evaluated in this article, or claim that may be made by its manufacturer, is not guaranteed or endorsed by the publisher.

frontiers | Frontiers in Oncology

ORIGINAL RESEARCH
published: 07 June 2022
doi: 10.3389/fonc.2022.898383

Gross Tumor Volume Predicts Survival and Pathological Complete Response of Locally Advanced Esophageal Cancer After Neoadjuvant Chemoradiotherapy

Rong Wang†, *Xiaomei Zhou*†, *Tongxin Liu*, *Shuimiao Lin*, *Yanxia Wang*, *Xiaogang Deng* and *Wei Wang**

Department of Radiation Oncology, Nanfang Hospital, Southern Medical University, Guangzhou, China

OPEN ACCESS

Edited by:
Li Jiancheng, Fujian Provincial Cancer Hospital, China

Reviewed by:
Keiichi Jingu, Tohoku University, Japan
Mengzhong Liu, Sun Yat-sen University Cancer Center (SYSUCC), China

***Correspondence:**
Wei Wang
wangwei9500@hotmail.com

†*These authors have contributed equally to this work and share first authorship*

Specialty section:
This article was submitted to Radiation Oncology, a section of the journal Frontiers in Oncology

Received: *17 March 2022*
Accepted: *09 May 2022*
Published: *07 June 2022*

Citation:
Wang R, Zhou X, Liu T, Lin S, Wang Y, Deng X and Wang W (2022) Gross Tumor Volume Predicts Survival and Pathological Complete Response of Locally Advanced Esophageal Cancer After Neoadjuvant Chemoradiotherapy. Front. Oncol. 12:898383. doi: 10.3389/fonc.2022.898383

Background: Neoadjuvant chemoradiotherapy (neo-CRT) plus surgery has greatly improved the prognosis of locally advanced esophageal cancer (EC) patients. But which factors may influence the pathological tumor response and long-term survival remains unclear. The purpose of this study was to identify the prognostic biomarkers of locally advanced EC patients receiving neo-CRT.

Methods: We reviewed the data of 72 patients with cT2-4N0-3M0 EC who underwent neo-CRT at our hospital. The patients received intensity-modulated radiation therapy with a total radiation dose of 41.4–60.0 Gy. Most patients received platinum + paclitaxel-based combination regimens every three weeks for 2–4 cycles. The recorded data included age, sex, smoking history, alcohol use, histology, tumor location, clinical TNM stage, tumor length, gross tumor volume (GTV), GTV of primary tumor (GTVp), GTV of lymph nodes (GTVn), radiation dose, and number of chemotherapy cycles. Overall survival (OS), progression-free survival (PFS), and pathological complete response (pCR) were analyzed.

Results: The 3-year OS and PFS rates of these patients who underwent neo-CRT were 51.14% and 43.28%, respectively. In the univariate analyses, smoking history, clinical stage, GTV, GTVp, and GTVn were significantly associated with OS, whereas alcohol use, GTV, GTVp, and GTVn were significantly associated with PFS. Furthermore, in the multivariate analysis, GTV was an independent prognostic predictor of OS (hazard ratio (HR): 14.14, 95% confidence interval (CI): 3.747–53.33, $P < 0.0001$) and PFS (HR: 6.090,

95% CI: 2.398–15.47, $P < 0.0001$). In addition, GTV < 60.50 cm^3 compared to > 60.50 cm^3 was significantly associated with higher pCR rate (59.3% and 27.8%, respectively, $P = 0.038$). High dose (> 50 Gy) and increased number of chemotherapy cycles (≥ 3) didn't improve the OS or PFS in patients with GTV > 60.50 cm^3.

Conclusion: GTV was an independent prognostic factor of long-term survival in EC patients, which may be because GTV is associated with histological response to neo-CRT. Additionally, patients with GTV > 60.50 cm^3 didn't benefit from increased radiation dose or increased number of chemotherapy cycles.

Keywords: esophageal cancer (EC), neoadjuvant chemoradiotherapy, gross tumor volume (GTV), pathological complete response (PCR), survival analysis

INTRODUCTION

Esophageal cancer (EC) is the seventh most frequently diagnosed cancer and the sixth leading cause of cancer-related death worldwide (1). In particular, Asia has a high prevalence of EC, accounting for over 50% of the global morbidity and mortality (2); more than 90% of EC patients have esophageal squamous cell carcinoma. Based on the results of the CROSS (3) and NEOCRTEC5010 (4) studies, neoadjuvant chemoradiotherapy (neo-CRT) followed by surgery is recommended by the National Comprehensive Cancer Network, European Society for Medical Oncology, and Chinese Society of Clinical Oncology guidelines as the standard treatment modality for patients with non-metastatic thoracic EC (5, 6). Neo-CRT and surgery significantly improved the 5-year survival rate of EC patients compared to those undergoing surgery alone (7). However, the clinical application of neo-CRT has certain limitations. First, the clinical outcomes of neo-CRT vary between studies and the pathological complete response (pCR) rates range from 28% to 43.2% (3, 4, 8, 9). Second, compared to EC patients who underwent surgery alone, those receiving neo-CRT experienced more adverse events and might get disease progression due to delay in surgery. Therefore, it is imperative to identify patients who are likely to benefit from neo-CRT, to improve the efficacy of neo-CRT and establish appropriate treatment strategies.

The prognostic predictors of EC patients receiving neo-CRT are unclear. Previous studies have reported TNM stage (4, 10, 11), lymphatic invasion (12, 13), tumor grade (14), and age (15) as independent predictors of long-term survival of EC patients. However, EC patients with the same TNM stage may have different outcomes. Additionally, maximal esophageal wall thickness (16–18) and tumor length (19, 20) were reported to be associated with survival, suggesting that tumor burden may be a prognostic factor for EC patients. However, esophageal wall thickness and tumor length only provide one-dimensional information, which do not accurately reflect the tumor burden. In light of this, gross tumor volume (GTV) is easy to determine based on the target delineation system, provides information regarding tumor thickness and length, and may be an accurate prognostic factor for EC patients.

In this study, we collected data on the aforementioned factors, including GTV as a comprehensive tumor burden marker, to identify prognostic factors for survival in EC patients.

Abbreviations: EC, esophageal cancer; neo-CRT, neoadjuvant chemoradiotherapy; GTV, gross tumor volume; GTVp, gross tumor volume of primary tumor; GTVn, gross tumor volume of lymph nodes; OS, overall survival; PFS, progression-free survival; pCR, pathological complete response; HR, hazard ratio; CI, confidence interval; CT, computed tomography; ^{18}F-FDG PET/CT, ^{18}F-fluorodeoxyglucose-positron emission tomography/computed tomography.

METHODS

Patients

This single-center, retrospective study of the outcomes of EC after neoadjuvant therapy was approved by the Research Ethics Committee of Nanfang Hospital, Southern Medical University. Between January 2017 and October 2020, 481 EC patients received radiotherapy at our institution. We excluded 403 patients who did not receive neo-CRT and 6 patients without complete medical records. Thus, 72 patients with clinical stages of cT2-4N0-3M0 were enrolled in the study. All patients were aged ≥ 18 with histologically confirmed EC with no distant metastasis who received neoadjuvant chemoradiotherapy and had complete survival and treatment information. Patients with distant metastasis or death within 1 month after surgery were excluded.

We retrospectively collected the clinical characteristics of patients, including age, sex, smoking history, alcohol use, histological type, tumor location, TNM stage, tumor length, GTV, GTV of primary tumor (GTVp), GTV of lymph nodes (GTVn), radiation dose and number of chemotherapy cycles. Tumor location was determined by endoscopy. A tumor 15 to 20 cm away from the superior incisor was considered as cervical, whereas tumors 20 to 25 cm, 25 to 30 cm, and 30 to 40 cm were considered upper thoracic, middle thoracic, and lower thoracic, respectively. The stage of EC was determined based on the eighth edition of the American Joint Committee of Cancer TNM staging system for EC. Pathologic responses to neo-CRT were determined by two pathologists using the criteria developed by the American Joint Committee of Cancer and College of American Pathologists, which are defined as follows: grade 0 (complete response), no viable cancer cells; grade 1 (moderate response), single or small groups of cancer cells; grade 2

(minimal response), residual cancer outgrown by fibrosis; and grade 3 (poor response), minimal or no tumor kill, extensive residual cancer.

Protocol of Neoadjuvant Chemoradiotherapy

All patients received external beam radiation, using intensity-modulated radiation therapy, which was delivered using megavoltage equipment with photon energies of 6–8 MV. Before radiotherapy, the patients underwent contrast-enhanced computed tomography (CT) simulation at 3-mm slice thickness in the supine position with immobilization for stereotactic treatment. We determined the GTVp using the borders of the increased esophageal wall thickness on CT scan, hypermetabolic lesions on 18F-fluorodeoxyglucose-positron emission tomography/computed tomography PET-CT (18F-FDG PET/CT), and the tumor location on endoscopy and endoscopic ultrasound. GTVn was defined by the enlarged regional lymph nodes, i.e., lymph nodes with short diameter ≥ 1 cm (paraesophageal or tracheoesophageal groove ≥ 5 mm) on CT or endoscopic ultrasound, or lymph nodes with high standardized uptake value (except for inflammatory lymph nodes) on 18F-FDG PET/CT. The GTV consisted of GTVp and GTVn. Then, the GTV, GTVp, and GTVn were calculated in cubic centimeters using the Varian Eclipse system. The clinical target volume (CTV) included a 3 cm craniocaudal and a 0.5–0.8 cm radial margin around the GTVp, and a 1-cm craniocaudal and a 0.5–0.8 cm radial margin around the GTVn, which included the area of subclinical involvement. The planning gross target volume (PGTV) was determined by including an area of 0.5 cm around the GTV in all directions for tumor motion and set-up variations. The planning clinical target volume (PCTV) was determined by including an area of 0.5 cm around the CTV in all directions. The prescription dose for the PCTV was 41.4–50 Gy at 1.8–2 Gy per fraction over 4–5 weeks. The prescription dose for the PGTV was 41.4–60 Gy at 1.8–2 Gy per fraction over 4–6 weeks. All plan were optimized such as D95 (DV is the absorbed dose in V% of the volume) ≥ the prescription dose and D1cc ≤ 115% of the prescription dose. The normal tissue-dose constraints included Dmax < 45 Gy for spinal cord, V30 < 45% for heart, V20 < 25% for lungs, Dmax < 45 Gy for intestines, and V30 < 30% for liver. During radiotherapy, chemotherapy was administered with either paclitaxel and platinum every three weeks, or fluoropyrimidine and platinum every four weeks for 2–4 cycles. The median time from the last day of neoadjuvant chemoradiotherapy to surgery is 42 days (range 21–91).

Surgery

In the present study, an open or thoracoscopic transthoracic esophagectomy was performed in all patients. McKeown procedure, including a right-sided thoracotomy, laparotomy and cervical incision, was usually used for tumors in the middle and upper thoracic esophagus. Ivor Lewis procedure including a right-sided thoracotomy and laparotomy, or Sweet procedure including a left-sided thoracotomy was usually used for tumors in the lower thoracic esophagus. Lymph node dissections were performed according to the tumor location.

Follow Up

Patients were regularly followed up in the outpatient clinic or using telephone interviews. Clinical evaluations included a CT scan of the neck-, thorax-, and abdomen, performed every 3 to 6 months. An endoscopic examination and bone scan were performed to detect recurrence and metastasis when necessary. The patients were followed up until death. Overall survival (OS) was defined as the interval from the date of neoadjuvant chemoradiotherapy to the date of cancer-related death or last follow-up. Progression-free survival (PFS) was calculated from the date of neoadjuvant chemoradiotherapy until disease progression or death. Patients who were still alive or lost to follow-up were treated as censored data for the analysis of survival rates.

Statistical Analysis

The statistical analyses were performed using SPSS software (version 23.0; IBM Corp., Armonk, NY, USA) and GraphPad Prism 8.0 software (GraphPad, La Jolla, CA, USA). Categorical variables were presented as numbers and percentages, and groups were compared using the χ^2 test. Furthermore, continuous variables were expressed as means and standard deviations, and means were compared using the Student's t test. Time-dependent receiver operating characteristic curve analysis was used to identify the optimal cut-off values of GTV, GTVp, GTVn and tumor length for predicting the 1-year OS, as well as to compare their predictive capacity. The survival time distribution was evaluated using the Kaplan-Meier method, and the log-rank test was used for comparisons. A multivariate Cox proportional-hazard regression model was used to identify independent prognostic markers. A two-tailed $P < 0.05$ was considered statistically significant.

RESULTS

Clinical Features and Treatment Information

To identify the prognostic factors for EC patients receiving neo-CRT, we reviewed the clinical information of 72 patients fulfilling the study's eligibility criteria between 2017 and 2020 (**Figure 1**). The collected information included age, sex, smoking history, alcohol use, histology, tumor location, T stage, N stage, clinical stage, tumor length, GTV, GTVp, GTVn, radiation dose, and number of chemotherapy cycles. As shown in **Table 1**, a majority of patients were males (80.6%) with esophageal squamous cell carcinoma (95.8%), and nearly half had a history of smoking (59.7%) and alcohol use (48.6%). More than half of the cancers were located in the middle (44.4%) and lower (33.3%) esophagus, and the most common stages were T3 (76.4%) and N2 (40.3%). Most patients had locally advanced EC, i.e., stage III (56.9%) and IV (26.4%). In this study, concurrent chemoradiotherapy was used as neoadjuvant treatment. The most common radiotherapy dose for GTV was 50 Gy with a fractionated dose of 2 Gy (69.4%). Platinum + paclitaxel-based combination regimens were used in a large proportion of patients (88.9%), administered every three weeks for 2–4 cycles.

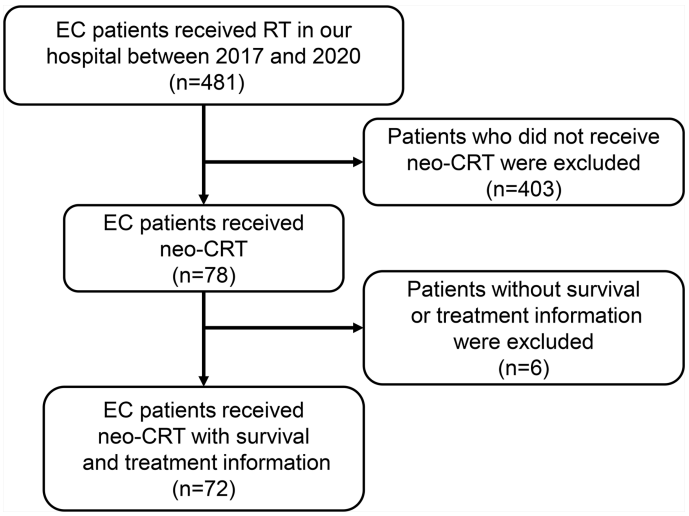

FIGURE 1 | Flowchart of patient inclusion. EC, esophageal cancer; RT, radiotherapy; neo-CRT, neoadjuvant chemoradiotherapy.

Additionally, we also summarized the information regarding tumor burden, including GTV (mean: 79.21 cm^3), GTVp (mean: 55.87 cm^3), GTVn (mean: 14.51 cm^3), and tumor length (mean: 6.57cm). Using the receiver operating characteristic analysis method, we determined the optimal cut-off values to be 60.50 cm^3, 41.45 cm^3, 9.40 cm^3 and 5.95 cm for GTV, GTVp, GTVn, and tumor length, respectively (**Supplementary Figure 1**). Then, patients were divided into two groups based on the optimal cut-off values for further analysis.

Univariate and Multivariate Analyses of OS and PFS

All patients were followed up for a median period of 20 months (range 3-47). The 3-year OS rate was 51.14% (95% confidence interval (CI): 33.30–66.43%) (**Figure 2A**) and the 3-year PFS rate was 43.28% (95% CI: 28.85–56.88%) (**Figure 2B**), similar to the CROSS study, in which the 3-year OS rate of the chemoradiotherapy–surgery group was 58% (3). Currently, the TNM staging system is the most widely used tool for predicting the prognosis of EC patients. However, we found that the clinical stage was significantly associated with OS (**Figure 2C**), but not PFS (**Figure 2D**). In addition, neither the T stage (**Figures 2E, F**) nor the N stage (**Figures 2G, H**) was associated with OS or PFS, suggesting the need to identify other prognostic factors.

The univariate analysis (**Figures 3A, B**) was performed using the abovementioned clinical features. Age, sex, location, T stage, N stage, tumor length, radiation dose and the number of chemotherapy cycles were not associated with OS or PFS. Smoking history (P = 0.0249) and clinical stage (P = 0.0170) were associated with OS, whereas alcohol use (P = 0.0193) was associated with PFS. Surprisingly, GTV, GTVp, and GTVn were significantly associated with both OS and PFS, with the largest survival difference for GTV. Multivariate Cox regression analysis showed that GTV was an independent prognostic factor for OS

TABLE 1 | Patients and treatment characteristics.

Variables	Study Cohort (n = 72) *
Age (yr)†	59.92 ± 7.99
Males	58 (80.6)
Smoking	43 (59.7)
Alcohol use	35 (48.6)
Histology	
SCC	69 (95.8)
Others	3 (4.2)
Location	
Upper thoracic	15 (20.8)
Middle thoracic	32 (44.4)
Lower thoracic	24 (33.3)
Others	1 (1.4)
T stage	
T2	4 (5.5)
T3	55 (76.4)
T4	12 (16.7)
Unknown	1 (1.4)
N stage	
N0	9 (12.5)
N1	23 (31.9)
N2	29 (40.3)
N3	9 (12.5)
Unknown	2 (2.8)
Clinical stage	
II	9 (12.5)
III	41 (56.9)
IVA	19 (26.4)
Unknown	3 (4.2)
Tumor length (cm)†	6.57 ± 2.48
GTV (cm^3)†	79.21 ± 70.08
GTVp (cm^3)†	55.87 ± 35.92
GTVn (cm^3)†	14.51 ± 17.95
Radiation dose	
> 50 Gy	10 (13.9)
50 Gy	50 (69.4)
< 50 Gy	12 (16.7)
Chemotherapy regimen	

(Continued)

TABLE 1 | Continued

Variables	Study Cohort (n = 72) *
Paclitaxel + platinum	64 (88.9)
Fluoropyrimidine + platinum	8 (11.1)
Chemotherapy cycles	
≥ 3	23 (31.9)
< 3	49 (68.1)

SCC, squamous cell carcinoma; GTV, gross tumor volume; GTVp, GTV of primary tumor; GTVn, GTV of lymph nodes.

**Except where indicated, data are numbers of patients (%).*

†Data are mean ± standard deviation.

[hazard ratio (HR): 14.14, 95% CI: 3.747–53.33, $P < 0.0001$] and PFS (HR: 6.090, 95% CI: 2.398–15.47, $P < 0.0001$) in EC patients receiving neoadjuvant therapy (**Figures 3A, B**). Furthermore, as shown in **Figures 3C, D**, patients with GTV > 60.50 cm^3 had shorter OS (HR: 7.570, 95% CI: 3.012–19.02, $P < 0.0001$) and PFS (HR: 4.936, 95% CI: 2.254–10.81, $P < 0.0001$) than those with GTV > 60.50 cm^3.

Prognostic Value of GTV

We evaluated the prognostic value of GTV in patients receiving neo-CRT with the same clinical stage. In stage III patients, GTV > 60.50 cm^3 was associated with shorter OS (HR: 7.867, 95% CI: 1.670–37.07, $P = 0.0020$) and PFS (HR: 6.663, 95% CI: 2.098–21.16, $P < 0.0001$) (**Figures 4A, B**). These finding confirmed the independent prognostic value of GTV. To determine the basis of the relationship between GTV and prognosis, we explored the relationship between GTV and pCR rate after neo-CRT. The results showed that patients with GTV < 60.50 cm^3 had higher pCR rate than those with GTV > 60.50 cm^3 (59.3% and 27.8%, respectively, $P = 0.038$) and earlier post-neoadjuvant pathological stage after neoadjuvant therapy (**Figures 4C, D**). Moreover, even in patients achieving pCR (**Figures 4E, F**), GTV > 60.50 cm^3 was associated with shorter OS and PFS. Similar results were found in patients with stages II and III (**Figures 5A, B**) or ypStage I (**Figures 5C, D**) after neoadjuvant treatment and surgery. Therefore, GTV is an important prognostic marker in EC patients.

Survival Analysis Combining GTV and Treatment Information

Finally, we combined GTV and treatment information for comprehensive analysis. Similarly, it was showed in **Figure 6** that patients with GTV > 60.50 cm^3 had poorer OS and PFS than those with GTV < 60.50 cm^3. Whereas, we found that increasing the radiation dose (**Figures 6A, B**) and the number of chemotherapy cycles (**Figures 6C, D**) did not improve OS and PFS, neither in EC patients with GTV > 60.50 cm^3 nor < 60.50 cm^3. In addition, for EC patients with GTV > 60.50 cm^3, increased number of chemotherapy cycles (≥ 3) did not influence the pCR rate and downstaging rate after neo-CRT (**Supplementary Figure 2**). These results suggested that EC patients could not benefit from additional chemoradiotherapy. It is necessary to explore new treatment options to improve the prognosis of EC patients, especially those with GTV > 60.50 cm^3.

DISCUSSION

The CROSS study suggested that neoadjuvant chemoradiotherapy is the preferred treatment for locally advanced EC patients (3). In the present study, an optimal cut-off GTV value of 60.50 cm^3 was an independent prognostic factor for EC patients undergoing neo-CRT. Similar results were observed in patients with the same TNM stage, suggesting that the GTV may add valuable information to the TNM staging system. Furthermore, we found that patients with GTV < 60.50 cm^3 had a better prognosis probably due to higher pCR rate. Patients with GTV > 60.50 cm^3 did not benefit from increased radiation dose or increased number of chemotherapy cycles.

Pre-chemoradiotherapy maximal esophageal wall thickness on CT scan (odds ratio: 2.002, 95% CI: 1.075–3.728, $P = 0.029$) and tumor length (HR: 1.30, 95% CI: 1.21-1.40, $P < 0.001$) were independently associated with long-term survival (16, 21). Our results showed that large GTV correlated with poor OS (HR: 14.14, 95% CI: 3.747–53.33, $P < 0.0001$) and poor PFS (HR: 6.090, 95% CI: 2.398–15.47, $P < 0.0001$). GTV, as a three-

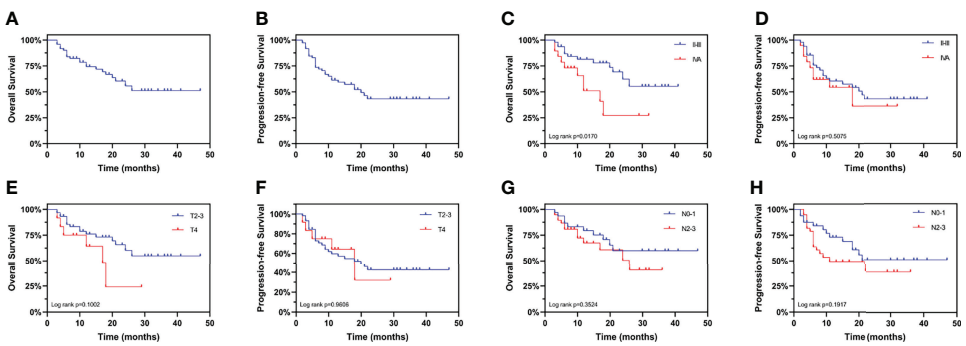

FIGURE 2 | Kaplan-Meier curves for overall survival and progression-free survival stratified by clinical TNM stage. Curves are shown for overall survival in esophageal cancer patients **(A)** overall, **(C)** stratified by clinical stage, **(E)** stratified by clinical T stage, and **(G)** stratified by clinical N stage. Curves are shown for progression-free survival in esophageal cancer patients **(B)** overall, **(D)** stratified by clinical stage, **(F)** stratified by clinical T stage, and **(H)** stratified by clinical N stage.

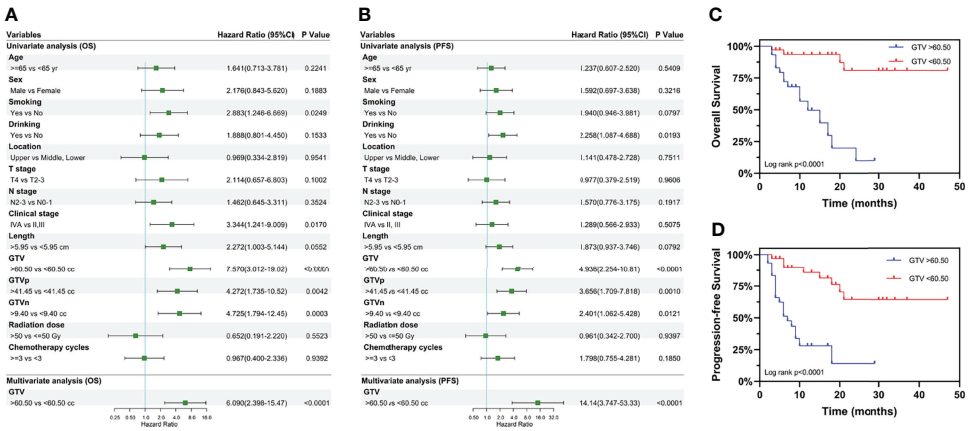

FIGURE 3 | Univariate and multivariate analyses of overall survival and progression-free survival. Results of the univariate and multivariate analyses of the GTV effect on **(A)** overall survival and **(B)** progression-free survival. Kaplan-Meier curves for overall survival **(C)** and progression-free survival **(D)** stratified by GTV. Hazard ratios and 95% confidence intervals for death in the group with GTV > 60.50 cc, compared to the group with GTV < 60.50 cc. GTV, gross tumor volume; GTVp, gross tumor volume of primary; GTVn, gross tumor volume of lymph nodes; HR, hazard ratio; CI, confidence interval; cc, cubic centimeters.

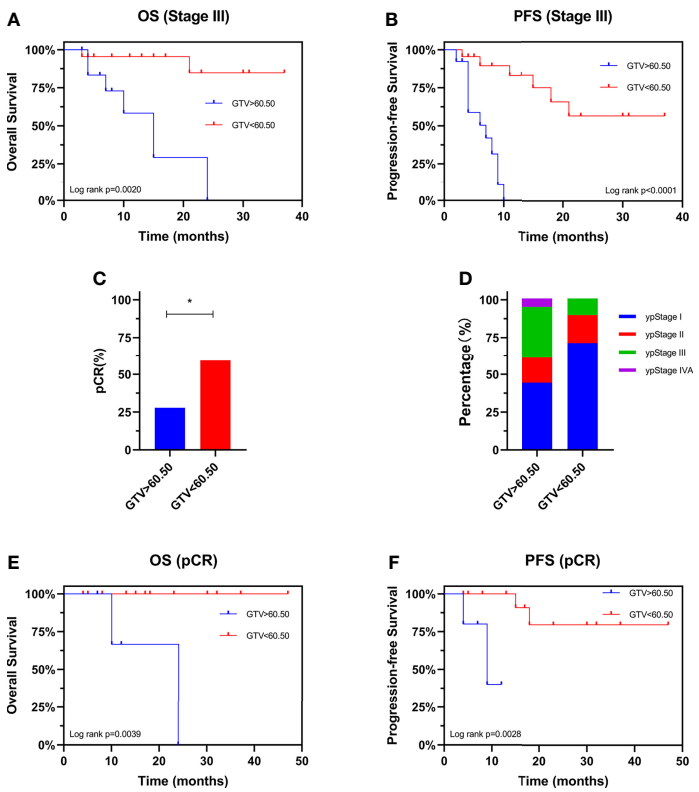

FIGURE 4 | Prognostic value of GTV. Kaplan-Meier curves are shown for overall survival **(A)** and progression-free survival **(B)** stratified by GTV in patients with stage III disease. Pathological complete response rate **(C)** and ypStage **(D)** after neoadjuvant therapy stratified by GTV. Kaplan-Meier curves are shown for overall survival **(E)** and progression-free survival **(F)** stratified by GTV in patients achieving pCR. *$P < 0.05$ by $\chi 2$ test. GTV, gross tumor volume; pCR, pathological complete response; ypStage, post-neoadjuvant pathological stage.

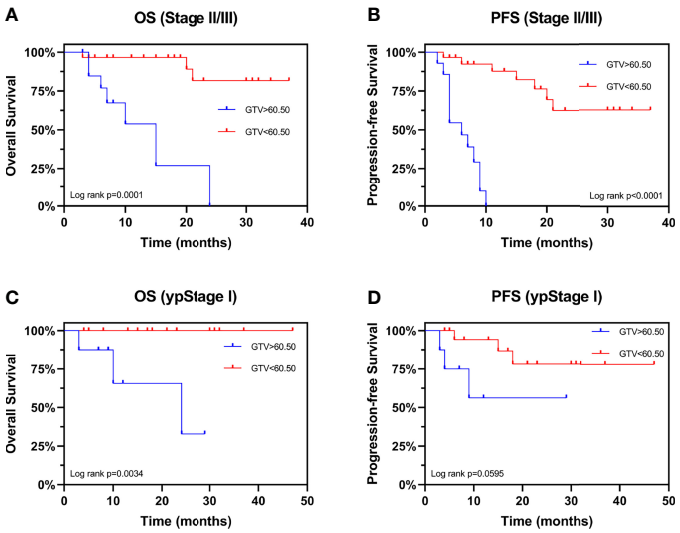

FIGURE 5 | Kaplan-Meier Curves for overall survival and progression-free survival stratified by GTV. Curves are shown for overall survival stratified by GTV in patients with **(A)** stages II and III and **(C)** ypStage I Curves are shown for progression-free survival stratified by GTV in patients with **(B)** stages II and III and **(D)** ypStage I. GTV, gross tumor volume; ypStage, post-neoadjuvant pathological stage.

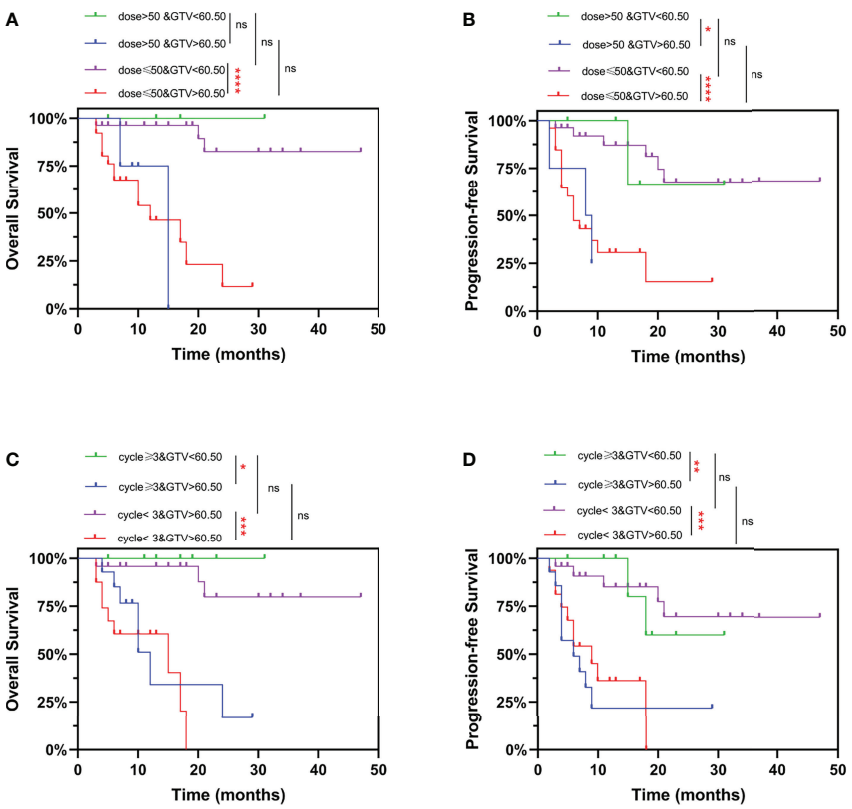

FIGURE 6 | Kaplan-Meier curves for overall survival and progression-free survival stratified by GTV and radiation dose/number of chemotherapy cycles. Curves are shown for overall survival stratified by GTV and **(A)** prescription dose, or **(C)** number of chemotherapy cycles. Curves are shown for progression-free survival stratified by GTV and **(B)** prescription dose, or **(D)** number of chemotherapy cycles. ns, $P > 0.05$, *$P < 0.05$, **$P < 0.01$, ***$P < 0.001$, ****$P < 0.0001$ by log-rank test. GTV, gross tumor volume.

dimensional factor, may be a better prognostic marker for EC patients than one-dimension factors. In the present study, the pCR rate of patients with GTV < 60.50 cm^3 was 59.3%, which was significantly higher than the 49% in esophageal squamous cell carcinoma patients in the CROSS study (3). It has been reported that pCR after neo-CRT was associated with a better prognosis (22–24). Our results indicated that GTV may affect the prognosis by influencing the pCR rate.

The National Comprehensive Cancer Network guideline recommends a radiation dose of 41.4–50.4 Gy for neo-CRT, which remains controversial. Many studies have investigated the relationship between radiation dose and survival. Semenkovich et al. (25) suggested that high-dose radiation (> 50.4 Gy) did not improve tumor response, whereas Buckstein et al. (26) found no OS benefit to using doses > 41.4 Gy in neo-CRT for surgically resected EC patients. The ARTDECO study concluded absence of benefit to dose escalation in a phase III randomized setting, which is a topic of recent interest (27). Similarly, our study showed that the increase in radiation dose (> 50 Gy) and the number of chemotherapy cycles (≥ 3) may not improve the prognosis of patients with large GTV. EC patients could not benefit from additional chemoradiotherapy. Therefore, it is necessary to explore new treatment options, such as combinations with immune or targeted drugs, to improve the prognosis of EC patients, especially those with GTV > 60.50 cm^3.

The present study revealed that large GTV leads to poor pCR rate and survival. This was one of the few studies to demonstrate the association between GTV and histological response to neo-CRT in locally advanced EC patients. However, limitations inherent in retrospective analyses also applied to our study. This was a retrospective study performed at a single institution; therefore, the results should be verified by prospective clinical studies. Makino et al. (28) reported that metabolic tumor volume change measured by 18F-FDG PET/CT before and after neoadjuvant chemotherapy predicted both long-term survival and histological response to preoperative chemotherapy in locally advanced EC patients. Therefore, tumor volume change may be a better marker for response to neo-CRT. Our study failed to explore the value of GTV change in predicting response to neo-CRT in EC patients because of the difficulty in determining GTV after radiotherapy. Finally, GTV could affect the prognosis of EC patients, but whether this was based on different biological backgrounds remains unclear. Further studies are needed to explore the biological mechanisms underlying the association of GTV and prognosis, which may provide new therapeutic targets for EC patients with large GTV.

CONCLUSION

This study highlighted the important role of GTV in predicting long-term survival and histological response to neo-CRT. Patients with GTV > 60.50 cm^3 did not benefit from increased radiation dose or increased number of chemotherapy cycles.

DATA AVAILABILITY STATEMENT

The original contributions presented in the study are included in the article/**Supplementary Material**. Further inquiries can be directed to the corresponding author.

ETHICS STATEMENT

The studies involving human participants were reviewed and approved by the Research Ethics Committee of Nanfang Hospital, Southern Medical University. Written informed consent for patients was not required for this study in accordance with the national legislation and the institutional requirements.

AUTHOR CONTRIBUTIONS

All authors read and approved the final manuscript prior to submission. WW and RW are responsible for the conception and design of the study. RW and XZ are responsible for analysis and interpretation of data. XZ are responsible for drafting the article and revising it. TL, SL, YW, and XD are responsible for acquisition of data. All authors contributed to the article and approved the submitted version.

FUNDING

This work was supported by the National Natural Science Foundation of China (grant number 82172642), the Outstanding Youths Development Scheme of Nanfang Hospital, Southern Medical University (grant number 2021J007), the GuangDong Basic and Applied Basic Research Foundation (grant number 2019A1515110931), and the President Foundation of Nanfang Hospital, Southern Medical University (grant number 2019L001).

ACKNOWLEDGMENTS

We would like to express our sincere thanks to Department of Radiation Oncology, Nanfang Hospital and Southern Medical University. We thank LetPub (www.letpub.com) for its linguistic assistance during the preparation of this manuscript.

SUPPLEMENTARY MATERIAL

The Supplementary Material for this article can be found online at: https://www.frontiersin.org/articles/10.3389/fonc.2022.898383/full#supplementary-material

REFERENCES

1. Bray F, Ferlay J, Soerjomataram I, Siegel RL, Torre LA, Jemal A. Global Cancer Statistics 2018: Globocan Estimates of Incidence and Mortality Worldwide for 36 Cancers in 185 Countries. *CA Cancer J Clin* (2018) 68 (6):394–424. doi: 10.3322/caac.21492
2. Chen W, Zheng R, Baade PD, Zhang S, Zeng H, Bray F, et al. Cancer Statistics in China, 2015. *CA Cancer J Clin* (2016) 66(2):115–32. doi: 10.3322/caac.21338

3. van Hagen P, Hulshof MC, van Lanschot JJ, Steyerberg EW, van Berge Henegouwen MI, Wijnhoven BP, et al. Preoperative Chemoradiotherapy for Esophageal or Junctional Cancer. *N Engl J Med* (2012) 366(22):2074–84. doi: 10.1056/NEJMoa1112088
4. Yang H, Liu H, Chen Y, Zhu C, Fang W, Yu Z, et al. Neoadjuvant Chemoradiotherapy Followed by Surgery Versus Surgery Alone for Locally Advanced Squamous Cell Carcinoma of the Esophagus (Neocrtec5010): A Phase Iii Multicenter, Randomized, Open-Label Clinical Trial. *J Clin Oncol* (2018) 36(27):2796–803. doi: 10.1200/JCO.2018.79.1483
5. Ajani JA, D'Amico TA, Bentrem DJ, Chao J, Corvera C, Das P, et al. Esophageal and Esophagogastric Junction Cancers, Version 2.2019, Nccn Clinical Practice Guidelines in Oncology. *J Natl Compr Canc Netw* (2019) 17 (7):855–83. doi: 10.6004/jnccn.2019.0033
6. Lordick F, Mariette C, Haustermans K, Obermannova R, Arnold D, Committee EG. Oesophageal Cancer: Esmo Clinical Practice Guidelines for Diagnosis, Treatment and Follow-Up. *Ann Oncol* (2016) 27(suppl 5):v50–v7. doi: 10.1093/annonc/mdw329
7. Herskovic A, Russell W, Liptay M, Fidler MJ, Al-Sarraf M. Esophageal Carcinoma Advances in Treatment Results for Locally Advanced Disease: Review. *Ann Oncol* (2012) 23(5):1095–103. doi: 10.1093/annonc/mdr433
8. Leichman LP, Goldman BH, Bohanes PO, Lenz HJ, Thomas CR, Billingsley KG, et al. S0356: A Phase Ii Clinical and Prospective Molecular Trial With Oxaliplatin, Fluorouracil, and External-Beam Radiation Therapy Before Surgery for Patients With Esophageal Adenocarcinoma. *J Clin Oncol* (2011) 29(34):4555–60. doi: 10.1200/JCO.2011.36.7490
9. Tepper J, Krasna MJ, Niedzwiecki D, Hollis D, Reed CE, Goldberg R, et al. Phase Iii Trial of Trimodality Therapy With Cisplatin, Fluorouracil, Radiotherapy, and Surgery Compared With Surgery Alone for Esophageal Cancer: Calgb 9781. *J Clin Oncol* (2008) 26(7):1086–92. doi: 10.1200/JCO.2007.12.9593
10. Okadome K, Baba Y, Yagi T, Kiyozumi Y, Ishimoto T, Iwatsuki M, et al. Prognostic Nutritional Index, Tumor-Infiltrating Lymphocytes, and Prognosis in Patients With Esophageal Cancer. *Ann Surg* (2020) 271 (4):693–700. doi: 10.1097/SLA.0000000000002985
11. Eloubeidi MA, Desmond R, Arguedas MR, Reed CE, Wilcox CM. Prognostic Factors for the Survival of Patients With Esophageal Carcinoma in the U.S.: The Importance of Tumor Length and Lymph Node Status. *Cancer* (2002) 95 (7):1434–43. doi: 10.1002/cncr.10868
12. von Rahden BHA, Stein HJ, Feith M, Becker K, Siewert JR. Lymphatic Vessel Invasion as a Prognostic Factor in Patients With Primary Resected Adenocarcinomas of the Esophagogastric Junction. *J Clin Oncol* (2005) 23 (4):874–9. doi: 10.1200/Jco.2005.12.151
13. Wayman J, Bennett MK, Raimes SA, Griffin SM. The Pattern of Recurrence of Adenocarcinoma of the Oesophago-Gastric Junction. *Br J Cancer* (2002) 86 (8):1223–9. doi: 10.1038/sj.bjc.6600252
14. Situ DR, Wang JY, Lin P, Long H, Zhang LJ, Rong TH, et al. Do Tumor Location and Grade Affect Survival in Pt2n0m0 Esophageal Squamous Cell Carcinoma? *J Thorac Cardiovasc Surg* (2013) 146(1):45–51. doi: 10.1016/j.jtcvs.2013.01.034
15. Farrow NE, Raman V, Jawitz OK, Voigt SL, Tong BC, Harpole DHJr., et al. Impact of Age on Surgical Outcomes for Locally Advanced Esophageal Cancer. *Ann Thorac Surg* (2021) 111(3):996–1003. doi: 10.1016/j.athoracsur.2020.06.055
16. Li SH, Rau KM, Lu HI, Wang YM, Tien WY, Liang JL, et al. Pre-Treatment Maximal Oesophageal Wall Thickness Is Independently Associated With Response to Chemoradiotherapy in Patients With T3-4 Oesophageal Squamous Cell Carcinoma. *Eur J Cardio-Thoracic Surg* (2012) 42(6):958–64. doi: 10.1093/ejcts/ezs136
17. Jost C, Binek J, Schuller JC, Bauerfeind P, Metzger U, Werth B, et al. Endosonographic Radial Tumor Thickness After Neoadjuvant Chemoradiation Therapy to Predict Response and Survival in Patients With Locally Advanced Esophageal Cancer: A Prospective Multicenter Phase Ll Study by the Swiss Group for Clinical Cancer Research (Sakk 75/02). *Gastrointest Endosc* (2010) 71(7):1114–21. doi: 10.1016/j.gie.2009.12.015
18. Wu Y, Li J. Change in Maximal Esophageal Wall Thickness Provides Prediction of Survival and Recurrence in Patients With Esophageal Squamous Cell Carcinoma After Neoadjuvant Chemoradiotherapy and Surgery. *Cancer Manag Res* (2021) 13:2433–45. doi: 10.2147/CMAR.S295646
19. Gaur P, Sepesi B, Hofstetter WL, Correa AM, Bhutani MS, Watson TJ, et al. Endoscopic Esophageal Tumor Length: A Prognostic Factor for Patients With Esophageal Cancer. *Cancer* (2011) 117(1):63–9. doi: 10.1002/cncr.25373
20. Wang BY, Goan YG, Hsu PK, Hsu WH, Wu YC. Tumor Length as a Prognostic Factor in Esophageal Squamous Cell Carcinoma. *Ann Thorac Surg* (2011) 91(3):887–93. doi: 10.1016/j.athoracsur.2010.11.011
21. Wang ZY, Jiang YZ, Xiao W, Xue XB, Zhang XW, Zhang L. Prognostic Impact of Tumor Length in Esophageal Cancer: A Systematic Review and Meta-Analysis. *BMC Cancer* (2021) 21(1):988. doi: 10.1186/s12885-021-08728-1
22. Berger AC, Farma J, Scott WJ, Freedman G, Weiner L, Cheng JD, et al. Complete Response to Neoadjuvant Chemoradiotherapy in Esophageal Carcinoma Is Associated With Significantly Improved Survival. *J Clin Oncol* (2005) 23(19):4330–7. doi: 10.1200/Jco.2005.05.017
23. Li Z, Shan F, Wang Y, Zhang Y, Zhang L, Li S, et al. Correlation of Pathological Complete Response With Survival After Neoadjuvant Chemotherapy in Gastric or Gastroesophageal Junction Cancer Treated With Radical Surgery: A Meta-Analysis. *PloS One* (2018) 13(1):e0189294. doi: 10.1371/journal.pone.0189294
24. Al-Kaabi A, van der Post RS, van der Werf LR, Wijnhoven BPL, Rosman C, Hulshof M, et al. Impact of Pathological Tumor Response After Cross Neoadjuvant Chemoradiotherapy Followed by Surgery on Long-Term Outcome of Esophageal Cancer: A Population-Based Study. *Acta Oncol* (2021) 60(4):497–504. doi: 10.1080/0284186X.2020.1870246
25. Semenkovich TR, Samson PP, Hudson JL, Subramanian M, Meyers BF, Kozower BD, et al. Induction Radiation Therapy for Esophageal Cancer: Does Dose Affect Outcomes? *Ann Thorac Surg* (2019) 107(3):903–11. doi: 10.1016/j.athoracsur.2018.09.064
26. Buckstein M, Rhome R, Ru M, Moshier E. Neoadjuvant Chemoradiation Radiation Dose Levels for Surgically Resectable Esophageal Cancer: Predictors of Use and Outcomes. *Dis Esophagus* (2018) 31(5):1–8. doi: 10.1093/dote/dox148
27. Hulshof M, Geijsen ED, Rozema T, Oppedijk V, Buijsen J, Neelis KJ, et al. Randomized Study on Dose Escalation in Definitive Chemoradiation for Patients With Locally Advanced Esophageal Cancer (Artdeco Study). *J Clin Oncol* (2021) 39(25):2816–24. doi: 10.1200/JCO.20.03697
28. Makino T, Yamasaki M, Tanaka K, Masuike Y, Tatsumi M, Motoori M, et al. Metabolic Tumor Volume Change Predicts Long-Term Survival and Histological Response to Preoperative Chemotherapy in Locally Advanced Esophageal Cancer. *Ann Surg* (2019) 270(6):1090–5. doi: 10.1097/Sla.0000000000002808

Conflict of Interest: The authors declare that the research was conducted in the absence of any commercial or financial relationships that could be construed as a potential conflict of interest.

frontiers | Frontiers in Oncology

ORIGINAL RESEARCH
published: 10 June 2022
doi: 10.3389/fonc.2022.810898

Neoadjuvant Immune Checkpoint Inhibitors Plus Chemotherapy in Locally Advanced Esophageal Squamous Cell Carcinoma: Perioperative and Survival Outcomes

Xiao Ma[1,2†], Weixin Zhao[2,3†], Bin Li[1,2], Yongfu Yu[4], Yuan Ma[5], Mathew Thomas[6], Yawei Zhang[1,2], Jiaqing Xiang[1,2] and Yiliang Zhang[1,2*]*

[1] Department of Thoracic Surgery, Fudan University Shanghai Cancer Center, Institute of Thoracic Oncology, Fudan University, Shanghai, China, [2] Department of Oncology, Shanghai Medical College, Fudan University, Shanghai, China, [3] Department of Radiation Oncology, Fudan University Shanghai Cancer Center, Shanghai Key Laboratory of Radiation Oncology, Shanghai, China, [4] Department of Biostatistics, The Key Laboratory of Public Health Safety of Ministry of Education, School of Public Health, Fudan University, Shanghai, China, [5] Chinese Institute for Brain Research, Beijing, China, [6] Department of Cardiothoracic Surgery, Mayo Clinic, Jacksonville, FL, United States

Background: Immune checkpoint inhibitors (ICI) improve survival in patients with late-stage esophageal squamous cell carcinoma (ESCC) but have not been fully evaluated in locally advanced ESCC.

Method: We retrospectively assessed outcomes of consecutive, treatment-naïve locally advanced ESCC (stage III or IVA) adults treated with neoadjuvant ICI plus chemotherapy followed by surgery, who refused or lacked access to radiotherapy, with regards to surgery feasibility, pathological response, and relapse-free survival (RFS).

Results: We uneventfully treated 34 patients with the combined regimen in 2020. None reported grade III or higher toxic effects. All underwent surgery as planned: 32 received complete (R0) resections and 2 had microscopically positive margins (R1). Tumor downstaging occurred in 33 (97.1%) patients and 11 (32.4%) had pathologically complete response of the primary lesion. Median postoperative length of stay was 12 days (interquartile range: 11 to 17). All patients resumed a semi-liquid diet on discharge. The 90-day postoperative morbidity rate was 20.6% (7/34) with no mortalities. The 1-year RFS was 77.8% [95% CI, 64.2-94.2].

Conclusion: Neoadjuvant ICI plus chemotherapy was safe and resulted in significant downstaging, rendering inoperable tumors operable, relieving symptoms of dysphagia and prolonging survival for locally advanced ESCC patients who refused or lacked access to radiotherapy.

Keywords: esophageal squamous cell carcinoma, neoadjuvant therapy, immune checkpoint inhibitor, esophagectomy, perioperative outcomes, survival outcomes

OPEN ACCESS

Edited by:
Chi Lin,
University of Nebraska Medical Center, United States

Reviewed by:
Yunlang She,
Tongji University, China
Prasenjit Das,
All India Institute of Medical Sciences, India

****Correspondence:***
Yiliang Zhang
zhang_yiliang@outlook.com
Jiaqing Xiang
j.q.xiang@hotmail.com

†These authors have contributed equally to this work

Specialty section:
This article was submitted to Radiation Oncology, a section of the journal Frontiers in Oncology

Received: *08 November 2021*
Accepted: *28 April 2022*
Published: *10 June 2022*

Citation:
Ma X, Zhao W, Li B, Yu Y, Ma Y, Thomas M, Zhang Y, Xiang J and Zhang Y (2022) Neoadjuvant Immune Checkpoint Inhibitors Plus Chemotherapy in Locally Advanced Esophageal Squamous Cell Carcinoma: Perioperative and Survival Outcomes. Front. Oncol. 12:810898. doi: 10.3389/fonc.2022.810898

INTRODUCTION

Esophageal cancer is the sixth most common cause of cancer-related death worldwide and is therefore a major global health challenge (1). Esophageal squamous cell carcinoma (ESCC) is the main histologic type in East Asian and Middle Eastern countries. At the time of their first diagnosis, 40-50% of ESCC present as locally advanced esophageal cancer that invades local structures or involves regional lymph nodes but without distant metastases (2, 3). Surgery is recognized as the definitive treatment for this cancer, but the prognosis is poor with esophagectomy alone, mostly due to relapse of residual disease (4, 5). Neoadjuvant chemoradiotherapy followed by surgery, has shown promising survival benefit and been recommended as the standard management for resectable ESCC patients (6–9). However, radiotherapy has been reported to have a high risk of side effects that could preclude the planned surgical procedure (10–13). Moreover, it is not always available due to the lack of access to radiotherapy worldwide, especially in many low- and middle-income countries (14).

Compared to the standard strategy of preoperative chemoradiotherapy, the current neoadjuvant chemotherapy regimen without radiotherapy has significantly low disease-control rate and inferior histopathologic outcomes for locally advanced ESCC (12). Therefore, it is imperative to develop novel alternative treatment options for those who refuse or lack of access to radiotherapy. Immune checkpoint inhibitors (ICI), including both pembrolizumab and camrelizumab, combined with chemotherapy have recently been reported to be safe and effective in patients with late-stage ESCC (15, 16). One ICI, nivolumab, improved relapse-free survival (RFS) when used as adjuvant therapy in stage II/III resected esophageal cancer (17). This study was aimed to explore the preliminary outcomes of neoadjuvant ICI plus chemotherapy followed by surgery for patients with treatment-naïve, locally advanced ESCC.

PATIENTS AND METHODS

Study Design

We performed this retrospective analysis of prospective collected data at a single medical institute. From January 1st, 2020 to December 31st, 2020, data of consecutive ESCC patients were prospectively collected in Fudan University Shanghai Cancer Center (FUSCC). The Institutional Review Board of FUSCC approved this study. All the patients provided written informed consents.

Abbreviations: AJCC, American Joint Committee on Cancer; CI, Confidential interval; CT, Computed tomography; CTCAE, Common Terminology Criteria for Adverse Events; ECOG, Eastern Cooperative Oncology Group; ESCC, Esophageal squamous cell carcinoma; EUS, Endoscopic ultrasound; FUSCC, Fudan University Shanghai Cancer Center; HR, Hazard ratio; ICI, Immune checkpoint inhibitors; pCR, pathologic complete response; PET, Positron emission tomography; RECIST, Response Evaluation Criteria in Solid Tumors; RFS, Relapse-free survival; TNM, Tumor Nodes Metastases; TRG, Tumor regression grade.

Patient Eligibility

All patients underwent baseline tumor staging, including contrast-enhanced computed tomography (CT) of the chest and upper abdomen, ultrasound of the neck, and endoscopic ultrasound (EUS) of upper digestive tract with biopsy if necessary. Positron emission tomography (PET)/CT was suggested for those patients who could afford it as it was not covered by the common healthcare insurance yet (18–20).

Eligible patients were between 18 and 75 years of age, and had treatment-naïve ESCC located in the middle and lower thoracic esophagus and clinically staged as T3 to T4aN1 to N3 with no evidence of distant metastasis (M0) according to the American Joint Committee on Cancer (AJCC) 8th staging system (21). All the patients had an Eastern Cooperative Oncology Group (ECOG) performance status score of 0 or 1, adequate cardiopulmonary function, and no surgical contradictions. Key exclusion criteria were signs of esophageal perforation, immunodeficiency, ongoing systemic immunosuppressive therapy, active autoimmune or infectious disease, and clinically significant concurrent cancers.

Treatment Protocol

The patients received two doses of intravenous pembrolizumab or camrelizumab (both at a dose of 200 mg every 3 weeks) plus chemotherapy with paclitaxel (260 mg/m^2 every 3 weeks) and cisplatin (75 mg/m^2 every 3 weeks) for 2 cycles. Surgery was planned to be performed within 14 weeks after the last dose if the patients met the following surgical criteria: 1) the tumor was considered to completely resectable upon evaluation of the multidisciplinary team; 2) the patient had the physiological conditions for upper gastrointestinal reconstruction after esophagectomy; 3) there's no contraindications to general anesthesia; 4) the patient refused radiation therapy. The primary end points were surgery feasibility rate, including the proportion of patients able to undergo surgery after neoadjuvant therapy, completeness of resection, and 90-day post-operative morbidity and mortality rates. The secondary end points were pathologic response and RFS rates. Drug toxicities were assessed according to the Common Terminology Criteria for Adverse Events (CTCAE v5.0). Changes in tumor size were evaluated according to Response Evaluation Criteria in Solid Tumors (RECIST), version 1.1. Surgical procedures of esophagectomy and lymph node dissection were conducted according to FUSCC institutional standards (22–25). The complications were specified and evaluated based on the International Consensus on Standardization of Data Collection for Complications Associated with Esophagectomy (26) and the Clavien-Dindo classification of surgical complications (27).

Pathological Assessment

Surgical specimens were assessed and staged according to the AJCC 8th criteria for evaluating tumor size, invasion depth, resection margin, and affected lymph nodes, for the percentage of residual viable tumor that was identified on routine hematoxylin and eosin staining (21). Pathologic response was evaluated and classified using the internationally recognized standards of tumor regression grade (TRG) system, based on two

parameters of histomorphologic tumor regression and lymph node status (ypN) (28). Those with no evidence of vital residual tumor cells in both primary tumor and lymph nodes were considered to have pathological complete response (pCR).

Statistical Analysis

The patients were characterized by demographic and clinicopathologic variables. Differences in patient features were evaluated using chi-square tests for categorical variables and Wilcoxon rank-sum tests for continuous variables. All statistical analyses were two-sided, with $p < 0.05$ indicative of statistical significance, and performed using SPSS (version 22.0 IBM Corporation, Armonk, NY) and R 4.0.3 software (R Foundation for Statistical Computing, Vienna, Austria).

RESULTS

Patient Characteristics

Thirty-four patients underwent treatment with the combined protocol during the 1-year study period (**Table 1**). They had either stage III (41.2%) or IVA (58.8%) ESCC and received two cycles of chemotherapy plus pembrolizumab (n=20) or camrelizumab (n=14). The median age of these patients was 61 years (range: 47-74). The majority of the cohort consisted of males (91.2%) and smokers (59%). Nearly half of the patients (47.1%) were documented to have a history of alcohol addiction. On initial evaluation by the thoracic surgeons, all patients were considered to have tumors that could not be completely resected.

TABLE 1 | Baseline demographics and clinical characteristics.

Variables (%)	All Patients (N=34)	Pembrolizumab (N=20)	Camrelizumab (N=14)
Sex			
Female	3 (8.8%)	0	3 (21.4%)
Male	31 (91.2%)	20 (100%)	11 (78.6%)
Age			
Median (range)	61 (47-74)	60.5 (47-74)	63 (55-68)
ECOG			
0	25 (73.5%)	15 (75%)	10 (71.4%)
1	9 (26.5%)	5 (25%)	4 (28.6%)
BMI, kg/m^2			
Median (range)	22.2 (14.7-29.8)	21.6 (14.7-26.0)	22.4 (17.5-29.8)
Smoking	20 (59%)	14 (70%)	6 (43%)
Alcohol addiction	16 (47.1)	12 (60%)	4 (28.5%)
Tumor location			
Middle	25 (73.5%)	13 (65%)	12 (85.7%)
Lower	9 (26.5%)	7 (35%)	2 (14.3%)
Clinical T stage			
cT3	26 (76.5%)	15 (75%)	11 (78.6%)
cT4a	8 (23.5%)	5 (25%)	3 (25%)
Clinical N stage			
cN2	16 (47%)	9 (45%)	7 (50%)
cN3	18 (53%)	11 (55%)	7 (50%)
Clinical stage			
III	14 (41.2)	8 (40%)	6 (43%)
IVA	20 (58.8)	12 (60%)	8 (57%)
Grade			
G1	1 (3%)	1 (5%)	0
G2	13 (38.2%)	9 (45%)	4 (28.6%)
G3	9 (26.5%)	4 (20%)	5 (35.7%)
GX	11 (32.3%)	6 (30%)	5 (35.7%)

Safety and Feasibility

Therapy-related adverse events of any grade during the neoadjuvant regimen occurred in 58.8% (20/34) patients, but none were grade III or higher. The most common adverse incidents were grade 1 digestive tract-associated side effects (8/34), such as nausea, vomiting and diarrhea. Another adverse event of high incidence was reactive capillary endothelial proliferation (7/34; grade 1 in 6 patients and grade 2 in one patient), which was commonly associated with camrelizumab (16). The median interval between the administration of the second dose and surgery was 5 weeks (range 4-8 weeks), and there were no therapy-related surgical delays. FUSCC multidisciplinary team for thoracic cancer evaluated the medical data of each patient including the symptoms, endoscopic and radiological findings. All patients showed partial response (PR) or stable disease (SD) and underwent surgery with intent to curative treatment; 16 (47%) received esophagectomy with 2-field lymphadenectomy whereas 18 (53%) had 3-field lymphadenectomy. Regarding the anastomotic site, half of the patients underwent intra-thoracic anastomosis and half cervical procedure. The average operating time was 211 ± 47 min, and the intraoperative blood loss was 144 ± 126 ml. There were 7 (20.6%) patients who experienced postoperative complications, which were all below grade IIIa according to Clavien-Dindo classification. No patients died within 90 days after surgery. All patients resumed a semi-liquid diet at the time of discharge which relieved their chief complaint of dysphagia noted at the initial clinic visit. (**Tables 2**, **3**).

Radiologic and Pathologic Response

Representative radiologic responses after two preoperative doses of ICI plus chemotherapy are shown in **Figure 1**. The evaluation and comparison of the radiographic results before and after the neoadjuvant therapy were described previously (29). Surgical pathology revealed 32 (94.1%) patients had complete resection (R0) of the primary tumor and the local lymph nodes, while 2 (5.9%) had macroscopic negative resection but positive circumferential margins microscopically (R1) on the resected esophagus. The median number of resected lymph nodes for each patient was 30 (interquartile range (IQR): 25 to 38). Based on the 8th AJCC system for clinical and pathologic staging, all patients were down-staged after neoadjuvant therapy; 28 (82.3%) patients had significant tumor (T) shrinkage, and 27 (79.4%) had nodal (N) downstaging. Tumor regression grade (TRG) I, II, III and IV, defined by two parameters of histomorphologic tumor regression and lymph node status (ypN) (28), were observed in 23.5%, 8.8%, 20.6% and 47.1% of patients, respectively. Complete pathologic response of the primary tumor site (ypT0) was seen in 11 (32.4%) patients, but 3 of them had residual cancer cells in the resected lymph nodes (**Table 3** and **Supplementary Table**).

TABLE 2 | Adverse events during neoadjuvant immune checkpoint inhibitors plus chemotherapy and postoperative complications.

Events (%)	All patients (N=34, %)	Grade	Pembrolizumab (N=20)	Camrelizumab (N=14)
All events during neoadjuvant therapy	20 (58.8%)	/	6 (30%)	14 (100%)
Nausea/vomiting/diarrhea	8	I	4	4
Reactive capillary endothelial proliferation	7	I/II	0	7
Fatigue	3	I	1	2
Leukopenia	2	I	1	1
All postoperative complications	7 (20.6%)	/	5 (25%)	2 (14.3%)
Anastomotic leak	3	II	2	1
Pneumonia	2	II	2	0
hoarseness	1	I	1	0
Subcutaneous emphysema	1	I	0	1
90-day Postoperative mortality	0	/	0	0

Drugs toxicity was assessed and graded according to the Common Terminology Criteria for Adverse Events (CTCAE v5.0). Postoperative complications were evaluated by the Clavien-Dindo classification.

TABLE 3 | Surgery, pathologic response and survival outcomes.

Variables (%)	All Patients (N=34)	Pembrolizumab (N=20)	Camrelizumab (N=14)
Operative duration, mean (SD), min	211 (47)	204 (40)	222 (55)
Estimated blood loss, mean (SD), mL	144 (126)	144 (126)	144 (127)
Postoperative hospital stay, median (IQR), day	12 (11-17)	13 (11-23)	12 (10-13)
Completeness of Resection			
R0	32 (94.1%)	19 (95%)	13 (92.9%)
R1	2 (5.9%)	1 (5%)	1 (7.1%)
Lymph nodes resected, median (IQR), No	30 (25-38)	31 (25-37)	27 (23-37)
Complete response of primary tumor	11 (32.4%)	6 (30%)	5 (35.7%)
TRG1	8 (23.4)	4 (20)	4 (28.6)
TRG			
1	8 (23.5%)	4 (20%)	4 (28.6%)
2	3 (8.8%)	2 (10%)	1 (7.1%)
3	7 (20.6)	5 (25%)	2 (14.3%)
4	16 (47.1%)	9 (45%)	7 (50%)
ypT			
0	11 (32.4%)	6 (30%)	5 (35.7%)
1	6 (17.6%)	5 (25%)	1 (7.2%)
2	5 (14.7%)	3 (15%)	2 (14.2%)
3	12 (35.3%)	6 (30)	6 (42.9%)
ypN+	19 (55.9%)	11 (55%)	8 (57%)
ypStage			
I	13 (38.2%)	7 (35%)	6 (42.9%)
II	2 (5.9%)	5 2(10%)	0
III	12 (35.3%)	6 (30%)	6 (42.9)
IV	7 (20.6%)	5 (25%)	2 (14.2%)
1-year relapse events	7 (20.6%)	5 (25%)	2 (14.2%)
1-year RFS,% (95%CI)	77.8 (64.2-94.2)	72.7 (54.5-97)	85.7 (69.2-100)

IQR, interquartile range; pCR, pathological complete response; defined as no evidence of residual viable tumor cells in the resected primary tumor and lymph nodes. TRG, tumor regression grade, based on two parameters of histomorphologic tumor regression and lymph node status (ypN) (28). RFS, relapse-free survival.

Survival Outcomes

The median follow-up time was 9.5 months (IQR: 8.5 to 11 months. 7 patients had documented disease recurrence, of whom 3 developed supraclavicular lymph node metastases and 4 distant spread, including bone, brain and liver involvement. At the time of their most recent follow up, no deaths occurred as a result of esophageal cancer; one patient died while undergoing treatment for primary kidney cancer. For the entire cohort, the 1-year RFS was 77.8% (95% confidential interval (CI) 64.2% to 94.2%) (**Figure 2**). No significant difference in survival was observed between the 2 ICI drugs of pembrolizumab and camrelizumab. Overall survival data were not mature (**Table 3**).

DISCUSSION

Our study shows that two cycles of preoperative ICI plus chemotherapy were well tolerated in locally-advanced ESCC patients, without therapy-related surgical delays. Furthermore, the preoperative regimen provided significant disease downstaging, turning unresectable ESCC into completely resectable tumors. More importantly, our data showed the introduction of preoperative ICI drugs did not increase the surgical difficulty or the postoperative complication, including treatment-related mortality. On the short-term follow-up, our study cohort demonstrated favorable 1-year RFS without any

FIGURE 1 | Cases of radiological responses after neoadjuvant immune checkpoint inhibitors and chemotherapy. **(A)** This shows the radiological images of a 67-year-old male (patient 1) with a stage IVA ESCC before and after neoadjuvant treatment. This patient achieved pathological regression of 100% for esophageal lesion with no residual lymph node metastasis according to postoperative specimen **(B)** This shows the images of a 68-year-old female (patient 2), who had a stage IVA ESCC before neoadjuvant treatment. This patient had 100% pathological regression of the primary tumor but had residual metastatic lymph nodes.

deaths from the late-stage disease. Therefore, this preoperative strategy allowed locally advanced ESCC that were unlikely to be surgical candidates at the first diagnosis to be completely removed eventually, without the need for radiotherapy. In this way, the novel treatment method could relieve dysphagia symptom of these patients, but also potentially extend their long-term survival.

Several clinical trials are currently evaluating the neoadjuvant role of ICI combined with chemoradiotherapy for esophageal cancer (NCT03604991, NCT03087864, NCT03044613, NCT02844075 and NCT03792347), some of which have reported preliminary outcomes confirming the high degree of safety and feasibility of the treatment strategy (30). Our previous work demonstrated that the use of neoadjuvant ICI plus chemotherapy could achieve a rate of over 40% of major pathologic response (MPR) in ESCC, without increasing the complication rates during the therapy and surgery (29).

Our study also brings special attention to a particular dilemma regarding treatment response. We noted that in 8.8% (3/34) of

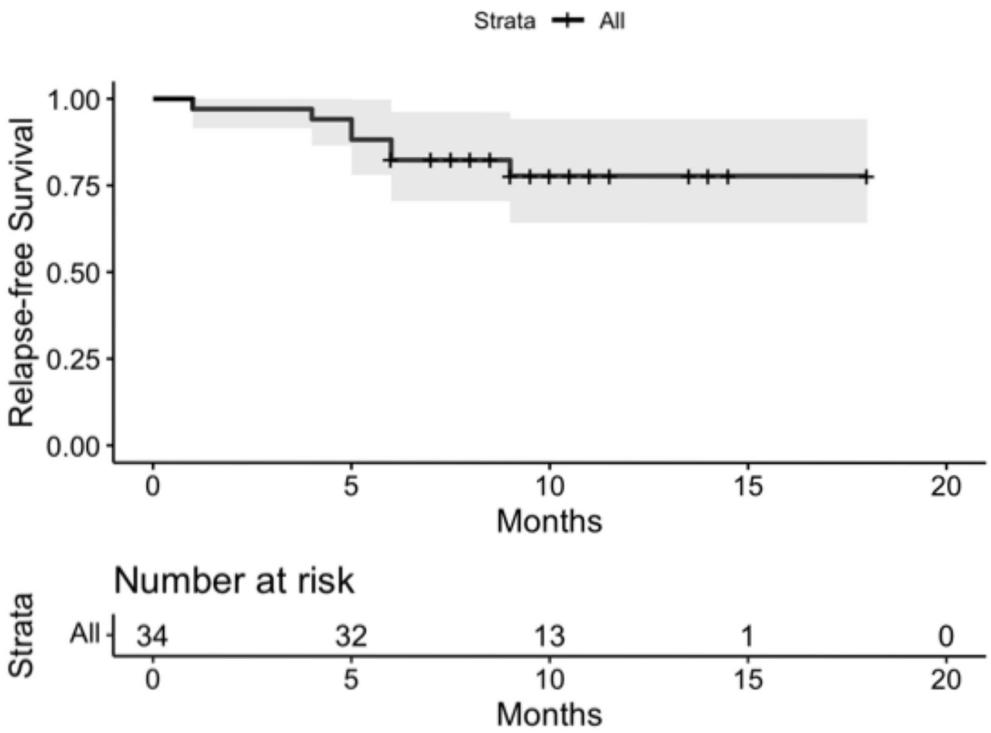

FIGURE 2 | For the entire cohort, the 1-year Relapse-free survival (RFS) was 77.8% (95% confidential interval (CI) 64.2% to 94.2%).

patients, although the primary site had pCR following neoadjuvant therapy, persistent disease was still present within involved lymph nodes. A similar observation has also been made by other investigators. PALACE-1 which is a phase II multicenter study aiming to evaluate preoperative pembrolizumab combined with chemoradiotherapy for resectable ESCC recently published its preliminary results, showing 11% (2/18) achieved pCR in primary tumor, however, had residual cancer cells in resected lymph nodes (30). The management of these patients with persistent nodal disease has opened up a new challenge for oncologists. It is unclear whether there is any benefit for adjuvant therapy using the original regimen after complete resection of ESCC. On the one hand, these patients who harbored residual cancer cells in the lymph nodes showed definite pathologic proof that their tumor was well responsive to ICI plus chemotherapy. On the other, current guidelines suggest that there is no proven benefit of adjuvant therapy for ESCC (3, 31). CheckMate 577 (17), a global, randomized, double-blind, placebo-controlled phase 3 trial to evaluate adjuvant therapy with ICI in esophageal or gastroesophageal junction cancer, reported that among patients who underwent resection after neoadjuvant chemoradiotherapy, RFS was significantly longer with nivolumab adjuvant therapy compared to placebo therapy. It should be noted that the majority (71%) of CheckMate 577 participants had adenocarcinoma and only 29% ESCC. We anticipate that studies focusing on the ICI adjuvant therapy for ESCC patients will provide more data, and could possibly result in new guidelines.

Our study has certain limitations that should be addressed. First, although this study may have the largest sample size of ESCC patients receiving neoadjuvant ICI plus chemotherapy followed by surgery to date, it is likely that some sort of selection bias was present due to the nature of monocentric series in a single institution. The inclusion of a validation cohort would have strengthened the findings of the study. Second, the study population was limited to East Asians, thereby raising concerns about the generalizability of our results, since disease spectra as well as biological and pathologic characteristics may differ among ethnic groups. Third, this is a retrospective single-armed study, and the results should be further validated by multi-institutional prospective randomized-controlled trials. Encouragingly, there are several ongoing prospective clinical trials which will provide more evidence in this area.

In summary, neoadjuvant ICI plus chemotherapy was safe for those patients with locally advanced ESCC who refused or lacked access to radiotherapy. This treatment regimen provided significant tumor downstaging rendering inoperable tumors operable, relieving symptoms of dysphagia and prolonging survival.

DATA AVAILABILITY STATEMENT

The original contributions presented in the study are included in the article/**Supplementary Material**. Further inquiries can be directed to the corresponding authors.

AUTHOR CONTRIBUTIONS

JX and YiZ conceptualized and designed the study; XM and WZ collected data, follow-up, wrote the manuscript; BL, YY and YM performed data cleansing and statistical analysis; BL, YaZ, JX and YiZ participated in the surgery and perioperative management. MT and YiZ established the clinical management protocols and edited the manuscript. All authors have reviewed, discussed, and approved the manuscript.

FUNDING

This work is supported by Shanghai Pujiang Program (2020PJD014).

SUPPLEMENTARY MATERIAL

The Supplementary Material for this article can be found online at: https://www.frontiersin.org/articles/10.3389/fonc.2022.810898/full#supplementary-material

REFERENCES

1. Smyth EC, Lagergren J, Fitzgerald RC, Lordick F, Shah MA, Lagergren P, et al. Oesophageal Cancer. *Nat Rev Dis Primers* (2017) 3:17048. doi: 10.1038/nrdp.2017.48
2. Zhang S, Sun K, Zheng R, Zeng H, Wang S, Chen R, et al. Cancer Incidence and Mortality in China, 2015. *J Natl Cancer Center* (2020) 1(1):2–11. doi: 10.1016/j.jncc.2020.12.001
3. Shah MA, Kennedy EB, Catenacci DV, Deighton DC, Goodman KA, Malhotra NK, et al. Treatment of Locally Advanced Esophageal Carcinoma: ASCO Guideline. *J Clin Oncol* (2020) 38:2677–94. doi: 10.1200/JCO.20.00866
4. Leng X, He W, Yang H, Chen Y, Zhu C, Fang W, et al. Prognostic Impact of Postoperative Lymph Node Metastases After Neoadjuvant Chemoradiotherapy for Locally Advanced Squamous Cell Carcinoma of Esophagus: From the Results of NEOCRTEC5010, a Randomized Multicenter Study. *Ann Surg* (2019) 274(6):e1022–29. doi: 10.1097/SLA.0000000000003727
5. Wan T, Zhang XF, Liang C, Liao CW, Li JY, Zhou YM, et al. The Prognostic Value of a Pathologic Complete Response After Neoadjuvant Therapy for Digestive Cancer: Systematic Review and Meta-Analysis of 21 Studies. *Ann Surg Oncol* (2019) 26:1412–20. doi: 10.1245/s10434-018-07147-0
6. Eyck BM, van Lanschot JJB, Hulshof M, Wilk BJ, Shapiro J, Hagen P, et al. Ten-Year Outcome of Neoadjuvant Chemoradiotherapy Plus Surgery for Esophageal Cancer: The Randomized Controlled CROSS Trial. *J Clin Oncol* (2021) 39:1995–2004. doi: 10.1200/JCO.20.03614
7. Yang H, Liu H, Chen Y, Zhu C, Fang W, Yu Z, et al. Neoadjuvant Chemoradiotherapy Followed by Surgery Versus Surgery Alone for Locally Advanced Squamous Cell Carcinoma of the Esophagus (NEOCRTEC5010): A Phase III Multicenter, Randomized, Open-Label Clinical Trial. *J Clin Oncol* (2018) 36:2796–803. doi: 10.1200/JCO.2018.79.1483
8. van Hagen P, Hulshof MC, van Lanschot JJ, Steyerberg EW, van Berge Henegouwen MI, Wijnhoven BPL, et al. Preoperative Chemoradiotherapy for Esophageal or Junctional Cancer. *N Engl J Med* (2012) 366:2074–84. doi: 10.1056/NEJMoa1112088
9. Sjoquist KM, Burmeister BH, Smithers BM, Zalcberg JR, Simes RJ, Barbour A, et al. Survival After Neoadjuvant Chemotherapy or Chemoradiotherapy for Resectable Oesophageal Carcinoma: An Updated Meta-Analysis. *Lancet Oncol* (2011) 12:681–92. doi: 10.1016/S1470-2045(11)70142-5
10. Kumagai K, Rouvelas I, Tsai JA, Mariosa D, Klevebro F, Lindblad M, et al. Meta-Analysis of Postoperative Morbidity and Perioperative Mortality in Patients Receiving Neoadjuvant Chemotherapy or Chemoradiotherapy for Resectable Oesophageal and Gastro-Oesophageal Junctional Cancers. *Br J Surg* (2014) 101:321–38. doi: 10.1002/bjs.9418
11. Bosch DJ, Muijs CT, Mul VE, beukema JC, Hospers GAP, Burgerhof JGM, et al. Impact of Neoadjuvant Chemoradiotherapy on Postoperative Course After Curative-Intent Transthoracic Esophagectomy in Esophageal Cancer Patients. *Ann Surg Oncol* (2014) 21:605–11. doi: 10.1245/s10434-013-3316-8
12. Wang H, Tang H, Fang Y, Tan L, Yin J, Shen Y, et al. Morbidity and Mortality of Patients Who Underwent Minimally Invasive Esophagectomy After Neoadjuvant Chemoradiotherapy vs Neoadjuvant Chemotherapy for Locally Advanced Esophageal Squamous Cell Carcinoma: A Randomized Clinical Trial. *JAMA Surg* (2021) 156(5):444–51. doi: 10.1001/jamasurg.2021.0133
13. Klevebro F, Elliott JA, Slaman A, Vermeulen BD, Kamiya S, Rosman C, et al. Cardiorespiratory Comorbidity and Postoperative Complications Following Esophagectomy: A European Multicenter Cohort Study. *Ann Surg Oncol* (2019) 26:2864–73. doi: 10.1245/s10434-019-07478-6
14. Gospodarowicz M. Global Access to Radiotherapy-Work in Progress. *JCO Glob Oncol* (2021) 7:144–5. doi: 10.1200/GO.20.00562
15. Kojima T, Shah MA, Muro K, Francois E, Adenis A, Hsu CH, et al. Randomized Phase III KEYNOTE-181 Study of Pembrolizumab Versus Chemotherapy in Advanced Esophageal Cancer. *J Clin Oncol* (2020) 38:4138–48. doi: 10.1200/JCO.20.01888
16. Huang J, Xu J, Chen Y, Zhuang W, Zhang Y, Chen Z, et al. Camrelizumab Versus Investigator's Choice of Chemotherapy as Second-Line Therapy for Advanced or Metastatic Oesophageal Squamous Cell Carcinoma (ESCORT): A Multicentre, Randomised, Open-Label, Phase 3 Study. *Lancet Oncol* (2020) 21:832–42. doi: 10.1016/S1470-2045(20)30110-8
17. Kelly RJ, Ajani JA, Kuzdzal J, Zander T, Cutsem EV, Piessen G, et al. Adjuvant Nivolumab in Resected Esophageal or Gastroesophageal Junction Cancer. *N Engl J Med* (2021) 384:1191–203. doi: 10.1056/NEJMoa2032125
18. Choi J, Kim SG, Kim JS, Jung HC, Song IS. Comparison of Endoscopic Ultrasonography (EUS), Positron Emission Tomography (PET), and Computed Tomography (CT) in the Preoperative Locoregional Staging of Resectable Esophageal Cancer. *Surg Endosc* (2010) 24:1380–6. doi: 10.1007/s00464-009-0783-x
19. Nishimaki T, Tanaka O, Ando N, Ide H, Watanabe H, Shinoda M, et al. Evaluation of the Accuracy of Preoperative Staging in Thoracic Esophageal Cancer. *Ann Thorac Surg* (1999) 68:2059–64. doi: 10.1016/S0003-4975(99)01171-6
20. Li B, Li N, Liu S, Li Y, Qian B, Zhang Y, et al. Does [18F] Fluorodeoxyglucose-Positron Emission Tomography/Computed Tomography Have a Role in Cervical Nodal Staging for Esophageal Squamous Cell Carcinoma? *J Thorac Cardiovasc Surg* (2020) 160:544–50. doi: 10.1016/j.jtcvs.2019.11.046
21. Rice TW, Ishwaran H, Ferguson MK, Blackstone EH, Goldstraw P. Cancer of the Esophagus and Esophagogastric Junction: An Eighth Edition Staging Primer. *J Thorac Oncol* (2017) 12:36–42. doi: 10.1016/j.jtho.2016.10.016
22. Li B, Zhang Y, Miao L, Ma L, Luo X, Zhang Y, et al. Esophagectomy With Three-Field Versus Two-Field Lymphadenectomy for Middle and Lower Thoracic Esophageal Cancer: Long-Term Outcomes of a Randomized Clinical Trial. *J Thorac Oncol* (2021) 16:310–7. doi: 10.1016/j.jtho.2020.10.157
23. Li B, Hu H, Zhang Y, Zhang J, Miao L, Ma L, et al. Three-Field Versus Two-Field Lymphadenectomy in Transthoracic Oesophagectomy for Oesophageal Squamous Cell Carcinoma: Short-Term Outcomes of a Randomized Clinical Trial. *Br J Surg* (2020) 107:647–54. doi: 10.1002/bjs.11497
24. Li B, Hu H, Zhang Y, Zhang J, Miao L, Ma L, et al. Extended Right Thoracic Approach Compared With Limited Left Thoracic Approach for Patients With Middle and Lower Esophageal Squamous Cell Carcinoma: Three-Year Survival of a Prospective, Randomized, Open-Label Trial. *Ann Surg* (2018) 267:826–32. doi: 10.1097/SLA.0000000000002280
25. Li B, Xiang J, Zhang Y, Li H, Zhang J, Sun Y, et al. Comparison of Ivor-Lewis vs Sweet Esophagectomy for Esophageal Squamous Cell Carcinoma: A Randomized Clinical Trial. *JAMA Surg* (2015) 150:292–8. doi: 10.1001/jamasurg.2014.2877
26. Low DE, Alderson D, Cecconello I, Chang AC, Darling GE, D'Journo XB, et al. International Consensus on Standardization of Data Collection for Complications Associated With Esophagectomy: Esophagectomy

Complications Consensus Group (ECCG). *Ann Surg* (2015) 262:286–94. doi: 10.1097/SLA.0000000000001098
27. Clavien PA, Barkun J, de Oliveira ML, Vauthey JN, Dindo D, Schulick RD, et al. The Clavien-Dindo Classification of Surgical Complications: Five-Year Experience. *Ann Surg* (2009) 250:187–96. doi: 10.1097/SLA.0b013e3181b13ca2
28. Schneider PM, Baldus SE, Metzger R, Kocher M, Bongartz R, Bollschweiler E, et al. Histomorphologic Tumor Regression and Lymph Node Metastases Determine Prognosis Following Neoadjuvant Radiochemotherapy for Esophageal Cancer: Implications for Response Classification. *Ann Surg* (2005) 242:684–92. doi: 10.1097/01.sla.0000186170.38348.7b
29. Wu Z, Zheng Q, Chen H, Xiang J, Hu H, Li H, et al. Efficacy and Safety of Neoadjuvant Chemotherapy and Immunotherapy in Locally Resectable Advanced Esophageal Squamous Cell Carcinoma. *J Thorac Dis* (2021) 13:3518–28. doi: 10.21037/jtd-21-340
30. Li C, Zhao S, Zheng Y, Han Y, Chen X, Cheng Z, et al. Preoperative Pembrolizumab Combined With Chemoradiotherapy for Oesophageal Squamous Cell Carcinoma (PALACE-1). *Eur J Cancer* (2021) 144:232–41. doi: 10.1016/j.ejca.2020.11.039
31. Ajani JA, D'Amico TA, Bentrem DJ, Chao J, Corvera C, Das P, et al. Esophageal and Esophagogastric Junction Cancers, Version 2.2019, NCCN Clinical Practice Guidelines in Oncology. *J Natl Compr Canc Netw* (2019) 17:855–83. doi: 10.6004/jnccn.2019.0033

Conflict of Interest: Author MT was employed by Mayo Clinic.

The remaining authors declare that the research was conducted in the absence of any commercial or financial relationships that could be construed as a potential conflict of interest.

Publisher's Note: All claims expressed in this article are solely those of the authors and do not necessarily represent those of their affiliated organizations, or those of the publisher, the editors and the reviewers. Any product that may be evaluated in this article, or claim that may be made by its manufacturer, is not guaranteed or endorsed by the publisher.

frontiers | Frontiers in Oncology

ORIGINAL RESEARCH
published: 11 July 2022
doi: 10.3389/fonc.2022.857881

Comparison of Recurrence Patterns and Salvage Treatments After Definitive Radiotherapy for cT1a and cT1bN0M0 Esophageal Cancer

Terufumi Kawamoto[1]*, *Naoto Shikama*[1], *Shinji Mine*[2] and *Keisuke Sasai*[1]

[1] Department of Radiation Oncology, Graduate School of Medicine, Juntendo University, Tokyo, Japan, [2] Department of Esophageal and Gastroenterological Surgery, Graduate School of Medicine, Juntendo University, Tokyo, Japan

Background: Definitive radiotherapy (RT) for stage I esophageal cancer was reported to result in noninferior overall survival (OS) compared with surgery. However, only a few detailed reports of recurrence patterns and subsequent salvage treatments have been published. This study aimed to compare recurrence patterns and subsequent salvage treatments after definitive RT or chemoradiotherapy (CRT) between cT1a and cT1bN0M0 esophageal cancer (EC).

Methods: Patients with cT1a or cT1bN0M0 esophageal squamous cell carcinoma who received definitive RT or CRT were included. Survival outcomes, recurrence patterns, and salvage treatments were evaluated.

Results: In total, 40 patients with EC receiving RT or CRT were divided into two groups for evaluation: cT1a (20 patients) and cT1b (20 patients) groups. The 3-year OS rates were 83% and 65% (p = 0.06) and the 3-year progression-free survival rates were 68% and 44% (p = 0.15) in the cT1a and cT1b groups, respectively. Among those in the cT1a group, six had local recurrence and two had metachronous recurrence. Seven patients underwent salvage endoscopic submucosal dissection and one patient received argon plasma coagulation treatment. Among those in the cT1b group, six had local recurrence, one had regional recurrence, and one had both. Of these, one underwent salvage endoscopic submucosal dissection, one received photodynamic therapy, three underwent surgery, one received RT, and two received the best supportive care. Compared with the cT1b group, the cT1a group had a higher proportion of patients who underwent endoscopic treatments (p = 0.007). After the endoscopic treatments, no recurrences were observed in both groups.

Conclusions: Regional recurrence and distant metastasis were not observed in the cT1a group. A higher proportion of patients in the cT1a group received salvage endoscopic treatments, and their OS tended to be favorable.

Keywords: superficial esophageal cancer, chemoradiotherapy, salvage therapy, patterns of failure, carcinoma

OPEN ACCESS

Edited by:
Yusuke Sato,
Akita University, Japan

Reviewed by:
Giovanni Capovilla,
Johannes Gutenberg University Mainz, Germany
Po-Kuei Hsu,
Taipei Veterans General Hospital, Taiwan

***Correspondence:**
Terufumi Kawamoto
t-kawamoto@juntendo.ac.jp

Specialty section:
This article was submitted to Radiation Oncology, a section of the journal Frontiers in Oncology

Received: *19 January 2022*
Accepted: *20 June 2022*
Published: *11 July 2022*

Citation:
Kawamoto T, Shikama N, Mine S and Sasai K (2022) Comparison of Recurrence Patterns and Salvage Treatments After Definitive Radiotherapy for cT1a and cT1bN0M0 Esophageal Cancer. Front. Oncol. 12:857881. doi: 10.3389/fonc.2022.857881

INTRODUCTION

Esophageal cancer (EC) is the eighth most common cancer and the sixth leading cause of cancer-associated death globally (1). Owing to improvements in diagnostic measures, the number of patients diagnosedwith superficial EC has been increasing. According to the Comprehensive Registry of Esophageal Cancer in Japan, the incidence rate of clinical stage I cancer among all cancer cases increased from 23.1% in 1999 to 38.6% in 2013 (2).

Endoscopic resection is generally indicated for patients with tumors invading the cT1a-epithelium (EP)/lamina propria mucosa (LPM). For patients with tumors invading the cT1a-muscularis mucosa (MM), endoscopic resection or esophagectomy is the main treatment (3). However, in clinical practice, radiotherapy (RT) is often chosen as an alternative for patients with T1a EC depending on comorbidities, tumor localization, and extensive extension. For patients with tumors invading the cT1b-submucosa (SM), esophagectomy is the main treatment (3, 4). Recently, the outcomes of chemoradiotherapy (CRT) showed a noninferior trend compared with surgery in terms of overall survival (OS) in patients with cT1bN0M0 EC (5). However, elderly patients and those medically unsuitable for surgery were excluded or underrepresented in this trial, thus questioning the generalizability of the results for these populations. In recent years, favorable RT results have been reported for elderly patients and those medically unsuitable for surgery, including cT1a and cT1b EC (6–8). Moreover, only a few detailed reports discussed the patterns of recurrence and subsequent salvage treatments in these cases.Thus, this study aimed to compare the recurrence patterns and subsequent salvage treatments after definitive RT or CRT between cT1a and cT1b EC.

METHODS

Study Population

This retrospective study protocol was reviewed and approved by the Juntendo Hospital review board (approval number: H20-0391). Informed consent was obtained *via* an opt-out method on the hospital's website. This study was conducted in accordance with the Declaration of Helsinki.

We reviewed the medical records, RT treatment plans, and diagnostic images of patients with EC in the Juntendo Hospital between January 2009 and December 2020. Eligibility criteria were as follows: (i) presence of pathologically proven esophageal squamous cell carcinoma; (ii) presence of Eastern Cooperative Oncology Group performance status (ECOG PS) (9) scores of 0–2; (iii) presence of cT1a or cT1bN0M0 cancer based on the *UICC-TNM Classification, Eighth Edition* (10); and (iv) medically unsuitable for endoscopic resection and surgery or desire to receive RT. Patients who previously underwent endoscopic resection or other surgery and received RT or chemotherapy for EC were excluded. The same study population in T1a EC has been described previously (11). EC was diagnosed comprehensively based on the findings of upper gastrointestinal endoscopy, computed tomography (CT), and physical examination. Magnifying endoscopy and endoscopic ultrasonography were used for the clinical diagnostic differentiation of T1a-EP, LPM, T1a-MM, and T1b-SM1-3 EC (3). Comorbidities were estimated using the Charlson comorbidity index (CCI) based on 12 disease comorbidity categories (from 1 to 6 according to the relative risk of 1-year mortality) (12, 13). Any other active cancer was counted as two points.

Treatment

External beam RT was administered using 6- or 10-MV X-rays of a linear accelerator. The daily fractional size of RT was 1.8–2.0 Gy based on the International Commission on Radiation Units and Measurements point; it was administered 5 days per week, with a total dose of 59.4–66 Gy. Either elective nodal irradiation (ENI), including the bilateral supraclavicular and mediastinal lymph node regions, or involved-field irradiation covering the primary tumor with a margin of 2–4 cm was used. Three-dimensional conformal RT was performed for all the patients. We used 2–4 fields to avoid the spinal cord. Among patients who received two-field irradiation, the beam direction was changed after irradiation with 40–41.4 Gy. ENI tended to be used in patients with normal respiratory and cardiac functions.

Chemotherapy was combined with RT in all patients except those with poor general conditions. The chemotherapy regimen consisted of either 5-fluorouracil (5 FU; 700 mg/m^2 on days 1–4 every 4 weeks) plus cisplatin (CDDP; 70 mg/m^2 on day 1 every 4 weeks) or docetaxel (DOC; 10 mg/m^2 on day 1 per week). The 5-FU plus CDDP regimen tended to be used in patients with normal renal function, whereas DOC therapy tended to be used in older patients and those with deteriorating renal function. After treatment completion, the patients were followed up at 1- to 3-month intervals for the first 2 years and at 4- to 6-month intervals thereafter. Follow-up evaluations included history taking and physical examination, blood test, upper gastrointestinal endoscopy, and CT.

Outcomes

The initial response was measured using the Response Evaluation Criteria in Solid Tumors guideline (version 1.1) (14) and based on endoscopy findings for the primary tumor according to the modified criteria of the 10th edition of the Japanese Classification of Esophageal Cancer established by the Japanese Society for Esophageal Disease. Complete response (CR) was defined as the disappearance of the primary tumor and the absence of irregular erosive, ulcerative, or elevated lesions as observed during endoscopy and/or the absence of malignant cells in biopsy specimens (15). Progressive disease (PD) was defined as distinct tumor growth or progression in esophageal stenosis compared with that at pretreatment. Incomplete response/stable disease (IR/SD) was defined as a response not meeting CR or PD. Radiological imaging studies, upper gastrointestinal endoscopy, and medical records of physical examinations were used to identify the recurrence sites. The presence of lesions outside the primary site was defined as metachronous recurrence, at the primary site was defined as local recurrence, and involvement of regional lymph nodes was defined as regional recurrence. Salvage treatments after the recurrence were also assessed. Toxicity was assessed and documented following the National Cancer Institute Common

Terminology Criteria for Adverse Events version 5.0 (12, 15, 16). Toxicities were defined as acute and late if they occurred within and >3 months post-treatment, respectively.

Statistical Analyses

The Mann–Whitney U test and Fisher's exact test were used for assessing quantitative and qualitative data, respectively, and compare patient characteristics and toxicities between groups. OS, disease-specific survival (DSS), and progression-free survival (PFS) rates from the start of treatment were measured using the Kaplan–Meier method, and survival estimates were compared using the log-rank test. Death from any cause was defined as an event for calculating the OS rate, esophageal cancer-related death was defined as an event for calculating the DSS, and disease progression at any site or death from any cause was defined as an event for calculating PFS. All statistical analyses were performed using the EZR version 1.54 (17), and statistical significance was set at $p < 0.05$ (two-sided).

RESULTS

Patients and Tumor Characteristics

Between January 2009 and December 2020, 75 patients with cT1a or cT1bN0M0 EC received definitive RT or CRT. Among them, 35 previously underwent endoscopic resection, and the remaining 20 in the cT1a and cT1b groups each received definitive RT or CRT as an alternative to endoscopic resection or surgery. The patient and tumor characteristics did not differ in patients between the two groups (**Table 1**).

The reasons for the patients' unsuitability for endoscopic resection were tumor metastasis along the entire circumference of the tumor in 15 and 10 patients and widespread progression of the cancer in 6 and 6 patients (including duplicates) in the cT1a and cT1b groups, respectively. The reasons for patients' unsuitability for surgery included comorbidities in 12 and 7 patients, double cancer in 5 and 7 patients, and desire to receive RT for esophageal conservation in 7 and 6 patients (including duplicates) in the cT1a and cT1b groups, respectively. The comorbidities were atrial fibrillation requiring anticoagulation in 6 and 2 patients, renal failure requiring dialysis in 4 and 0 patients, unstable angina requiring antiplatelet therapy in 2 and 3 patients, severe chronic obstructive pulmonary disease in 2 and 1 patients, chronic rheumatoid arthritis in 0 and 1 patients, hemophilia in 0 and 1 patients, and severe Parkinson's disease in 1 and 1 patients (including duplicates) in the cT1a and cT1b groups, respectively. The median follow-up period was 67 (range, 13–131 months) and 29 (range, 13–83 months) for 14 and 11 survivors in the cT1a and cT1b groups, respectively. Among the 14 and 11 survivors in the cT1a and cT1b groups, 3 and 4 patients were lost to follow-up, respectively.

Initial Response and Survivals

At the initial treatment, 20 and 16 patients achieved CR in the cT1a and cT1b groups, respectively. Four patients achieved IR/SD in the cT1b group. The 3-year OS rates were 83% and 63% ($p = 0.06$), the 3-year DSS rates were 100% and 80% ($p = 0.06$), and the 3-year PFS rates were 68% and 44% ($p = 0.15$) in the cT1a and cT1b groups, respectively (**Figure 1**). Among the six patients in the cT1a group, three died of other cancers and the other three died of other causes, including chronic obstructive pulmonary disease (one patient) and aspiration pneumonia attributable to cerebral infarction (two patients). Out of nine patients in the cT1b group, three died of EC, two of other cancers, and four of other causes, including heart failure, radiation pneumonitis, bleeding after salvage surgery, and natural death due to unknown cause (one patient each).

Toxicity

Table 2 shows toxicities associated with RT or CRT. Grade 3 acute esophagitis was observed in 2 and 4 patients, grade 3 acute pneumonia in 1 and 0 patients, grade 3 white blood cell decrease in 1 and 1 patients, and grade 3 anemia in 0 and 2 patients in the cT1a and cT1b groups, respectively. Grade 4 esophagitis, grade 4 white blood cell decrease, grade 4 platelet count decrease, and grade 5 late pneumonitis were observed in 1 patient each in the T1b group.

Recurrence Patterns and Salvage Treatments

Table 3 summarizes the cases with recurrence. Recurrence occurred in eight patients each from both cT1a and cT1b groups. Among those in the cT1a group, six had local recurrence and two had metachronous recurrence. Metachronous recurrence was observed outside the radiation field in two patients. After identifying recurrence, seven patients underwent salvage endoscopic submucosal dissection (ESD), whereas one received argon plasma coagulation (APC). Among those in the cT1b group, six had local recurrence, one had regional recurrence, and one had both. Regional recurrence was observed outside (one patient) and within (one patient) the field of prophylactic irradiation. After identifying recurrence, among the patients with local recurrence, one underwent salvage ESD, one received photodynamic therapy (PDT), two underwent surgery for long craniocaudal tumor length and SM invasion, and two received the best supportive care for the onset of cerebral infarction and worsening hemophilia, respectively. Further, one patient with regional recurrence received RT and one with local and regional recurrence underwent surgery. Compared with the cT1b group, the cT1a group had a higher proportion of patients who underwent endoscopic treatments ($p = 0.007$). After endoscopic treatments, no recurrences were observed in both groups. After those in the cT1b group underwent salvage surgery, one patient died a month later owing to bleeding secondary to the surgery, one died 18 months later owing to liver metastasis, and one died 48 months later owing to heart failure, the original complication.

DISCUSSION

The present study was designed to clarify differences in the recurrence patterns and subsequent salvage treatments of

TABLE 1 | Patient and tumor characteristics.

Patient and tumor characteristics	cT1a group	cT1b group	p-value
Median age no.(range)	70 (41–82)	70 (52–86)	0.45
Sex no.(%)			0.13
Male	13 (65)	19 (95)	
Female	7 (35)	1 (5)	
ECOG PS no.(%)			0.75
0	6 (30)	10 (50)	
1	13 (65)	9 (45)	
2	1 (5)	1 (5)	
Location of primary tumor no.(%)			0.82
Cervix	1 (5)	3 (15)	
Upper thorax	0	1 (5)	
Middle thorax	15 (75)	13 (65)	
Lower thorax	3 (15)	2 (10)	
Abdomen	1 (5)	1 (5)	
Invasion depth no.(%)			
EP	0	–	
LPM	11 (55)	–	
MM	9 (45)	–	
SM1	–	8 (40)	
SM2	–	6 (30)	
SM3	–	6 (30)	
Median tumor craniocaudal length, cm (range)	6 (2–12)	6 (2–17)	0.88
Tumor craniocaudal length (cm)			1
< 5	5 (25)	6 (30)	
5–10	9 (45)	8 (40)	
≥ 10	6 (30)	6 (30)	
Tumor circumference no.(%)			0.055
< 1/3	0	2 (10)	
1/3–< 2/3	1 (5)	6 (30)	
2/3–< entire	4 (20)	2 (10)	
Entire	15 (75)	10 (50)	
Charlson comorbidity index no.(%)			0.42
0	5 (25)	8 (40)	
1	4 (20)	0	
2	6 (30)	7 (35)	
3	1 (5)	1 (5)	
4	3 (15)	3 (15)	
5	1 (5)	1 (5)	
Concurrent chemotherapy no.(%)			0.086
None	8 (40)	2 (10)	
DOC	11 (55)	14 (70)	
FP	1 (5)	4 (20)	
Total radiation dose no.(%)			0.49
59.4 Gy	0	1 (5)	
60 Gy	18 (90)	19 (95)	
66 Gy	2 (10)	0	
Radiation Field no.(%)			0.75
ENI	10 (50)	8 (40)	
IFI	10 (50)	12 (60)	

DOC, docetaxel; ECOG PS, Eastern Cooperative Oncology Group performance status; ENI, elective nodal irradiation; EP, epithelium; FP, 5-fluorouracil and cisplatin; IFI, involved-field irradiation; LPM, lamina propria mucosa; MM, muscularis mucosa; SM, submucosa.

definitive RT or CRT between cT1a and cT1b EC. All patients in the cT1a group received salvage endoscopic treatments, whereas two patients in the cT1b group received salvage endoscopic treatments.

Table 4 presents data of previous studies that examined the efficacy of RT for stage I EC (18–23). The local and metachronous recurrence rate in patients with cT1a EC (0%–29%) was relatively lower than that in patients with cT1b EC (23%–38%). The local and metachronous recurrence rate in our study was slightly high compared with the rates reported in previous studies. This might be associated with a longer tumor craniocaudal length in our study than that in previous studies. Previous studies reported that a long tumor craniocaudal length was a prognostic factor for local recurrence of superficial EC, consistent with our findings (19, 21). The regional recurrence and distant metastasis rates were 6%–12% and 1%–6% in those with cT1b EC, respectively, whereas neither of them were observed in those with cT1a EC, except in one previous study (22). The regional recurrence rate in our study was similar to the rates reported previously. A previous study reported regional metastasis rates of 0%, 9%–15%, and 41%–44% at the time of surgery among patients with EP/LPM, MM/SM1, and SM2/SM3

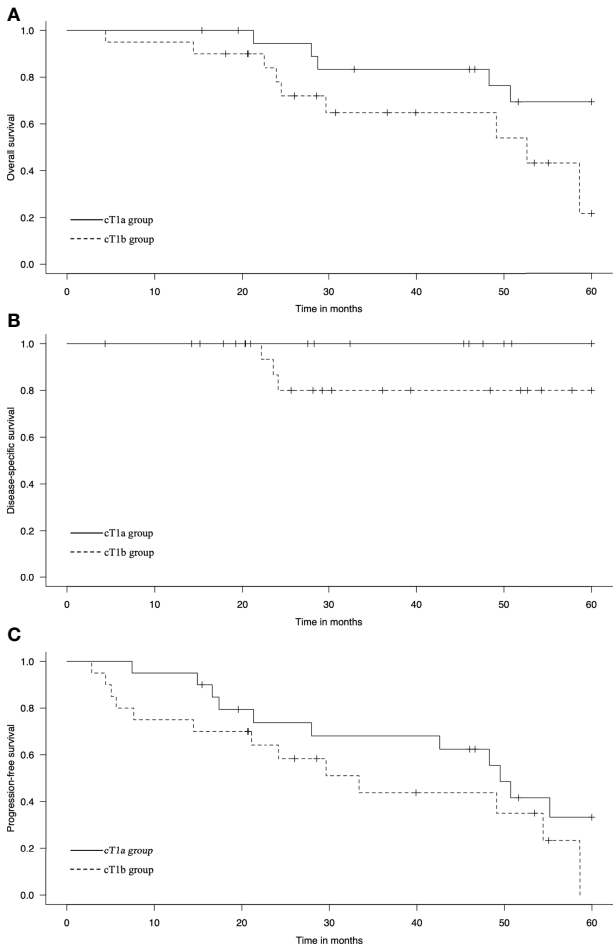

FIGURE 1 | Kaplan–Meier estimates of **(A)** overall survival, **(B)** disease-specific survival, and **(C)** progression-free survival in the cT1a and cT1b groups.

EC, respectively (24). In the cT1b group, the lower rate of regional recurrence after RT compared with that of regional metastasis at the time of surgery suggested that potential lymph node metastasis was suppressed by ENI and concurrent chemotherapy.

When there is a local residual or recurrent lesion after definitive RT or CRT, salvage surgery or endoscopic treatment may allow long-term survival. In case of medically unsuitable for salvage surgery or endoscopic treatment, patients are indicated

TABLE 2 | Treatment toxicities.

		cT1a group			cT1b group		
		Grade 1-2 no. (%)	**Grade 3 no. (%)**	**Grade 4-5 no. (%)**	**Grade 1-2 no. (%)**	**Grade 3 no. (%)**	**Grade 4-5 no. (%)**
Acute toxicity	Malaise	5 (25)	–	–	5 (25)	–	–
	Esophagitis	17 (85)	2 (10)	–	15 (75)	4 (20)	1 (5)
	Dermatitis	1 (5)	–	–	4 (20)	–	–
	Pneumonitis	–	1 (5)	–	1 (5)	–	–
	White blood cell decreased	9 (45)	1 (5)	–	8 (40)	1 (5)	1 (5)
	Anemia	4 (20)	–	–	9 (45)	2 (10)	–
	Platelet count decreased	4 (20)	–	–	9 (45)	–	1 (5)
Late toxicity	Dysphasia	2 (10)	–	–	1 (5)	–	–
	Pleural effusion	4 (20)	–	–	1 (5)	–	–
	Pericardial effusion	7 (35)	–	–	5 (25)	–	–
	Pneumonitis	3 (15)	–	–	3 (15)	–	1 (5)
	Hypothyroidism	3 (15)	–	–	–	–	–

TABLE 3 | Summary of recurrent cases.

Age	Sex	ECOG PS	Primay tumor location	Invasion depth	Tumor craniocaudal length (cm)	Tumor circumference	RT field	RT dose (Gy)	CRT	Months to disease recurrence	Recurrence lesions	Salvage therapy	Resected invasion depth	Resected tumor length (cm)	Tumor circumference	Sateus at last follow-up from salvage therapy
41	Male	0	Mt	MM	16	Entire	ENI	60	Yes	43	Local	ESD	EP	1.8	< 1/3	ANED 44 m
49	Female	0	Mt	MM	15	Entire	ENI	66	Yes	80	Local	ESD	EP	0.8	< 1/3	ANED 45 m
61	Male	1	Lt	LPM	10	Entire	IFI	60	Yes	15	Local	ESD	EP	1.4	< 1/3	ANED 104 m
62	Male	0	Mt	MM	3	Entire	ENI	60	Yes	17	Local	ESD	EP	0.5	< 1/3	ANED 73 m
65	Male	1	Ae	LPM	5	Entire	ENI	60	No	17	Local	ESD	EP	3	< 1/3	ANED 16 m
70	Male	1	Mt	MM	2	Entire	IFI	66	No	7	Metachronous	APC	–	–	< 1/3	DID 22 m
72	Male	1	Mt	MM	10	Entire	ENI	60	Yes	55	Local	ESD	EP	1.2	< 1/3	DID 7 m
73	Male	1	Mt	LPM	4	Entire	IFI	60	Yes	50	Metachronous	ESD	LPM	3.1	< 1/3	ANED 32 m
60	Male	0	Mt	SM2	5	Entire	IFI	60	Yes	33	Local	PDT	–	–	< 1/3	ANED 3 m
64	Male	0	Mt	SM3	6	Entire	ENI	60	Yes	54	Local	ESD	EP	0.9	< 1/3	ANED 26 m
66	Male	1	Ce	SM2	10	Entire	ENI	60	Yes	21	Locoregional	Surgery	Trachea	11	Entire	DE 1 m
66	Male	0	Mt	SM3	5	2/3	IFI	60	Yes	6	Regional	RT	–	–	–	DE 16 m
68	Male	2	Lt	SM2	6	Entire	IFI	60	Yes	5	Local	Surgery	SM2	7	Entire	DID 48 m
74	Female	1	Mt	SM2	5	Entire	ENI	60	Yes	3	Local	Surgery	SM1	7	2/3	DE 18 m
76	Male	1	Ce	SM1	8	Entire	IFI	60	Yes	24	Local	BSC	–	–	Entire	No follow-up
78	Male	1	Mt	SM1	17	Entire	IFI	59.4	Yes	8	Local	BSC	–	–	Entire	No follow-up

ANED, alive with no evidence of disease; APC, argon plasma coagulation; CRT, chemoradiotherapy; DID, died of intercurrent disease; DE, died of esophageal cancer; ECOG PS, Eastern Cooperative Oncology Group performance status; ENI, elective nodal irradiation; EP, epithelium; ESD, endoscopic submucosal dissection; IFI, involved-field irradiation; LPM, lamina propria mucosa; MM, muscularis mucosa; PDT, photodynamic therapy; RT, radiotherapy; SM, submucosa

TABLE 4 | Literature review of studies that included radiotherapy cases for cT1 aN0 M0 esophageal cancer.

Author	Year	no.	Median age (range)	Sex Male/ Female (%)	PS 0/1-2 (%)	T Stage	Tumor craniocaudal length, cm (median [range])	Median prescribed dose (Gy)	ICBT (%)	CRT (%)	Field ENI/ IFI (%)	OS rate (%)	Local and metachronous recurrence (%)	Reginal lymph node recurrence (%)	Distant metastassis (%)	Salvage treatments (%)	Salvage endscopic treatments (%)	Salvage surgery (%)
Nemoto	2001	52	68 (43–89)	85/15	NS	T1a	NS	65	63	3	0/100	62 (5y)	12	0	0		NS	
		95				T1b						42 (5y)	23	12	4			
Ishikawa	2006	18	70 (50–86)	89/11	39/61	T1a	Almost < 5 cm	60–70 (range)	33	0	100/0	100 (5y-DSS)	0	0	0	–	–	–
		50		76/24	36/64	T1b		60–73 (range)	60	0		75 (5y-DSS)	18	6	4	42	0	25
Yamada	2006	23	67 (48–83)	89/11	NS	T1a	3.6 (1–14)	59.4	83	100	100/0	85.2 (5y-DSS)	17	0	0	41	18	14
		40				T1b						70 (5y-DSS)	38	18				

(Continued)

TABLE 4 | Continued

Author	Year	no.	Median age (range)	Sex Male/ Female (%)	PS 0/1-2 (%)	T Stage	Tumor craniocaudal length, cm (median [range])	Median prescribed dose (Gy)	ICBT (%)	CRT (%)	Field ENI/ IFI (%)	OS rate (%)	Local and metachronous recurrence (%)	Reginal lymph node recurrence (%)	Distant metastassis (%)	Salvage treatments (%)	Salvage endscopic treatments (%)	Salvage surgery (%)
Kodaira	2010	24	66 (41–89)	93/7	31/69	T1a	4 (1–16)	60	27	61	0/100	82 (3y)	26	6	1	56	41	8
		71				T1b												
Murakami	2012	44	70 (43–89)	92/8	79/21	T1a	Almost < 3 cm	54	100	0	100/0	84 (5y)	29	2	0	NS	45	
		43				T1b		60	100	0	100/0	31 (5y)	30	12	2			
Suzuki	2018	3	70 (59–87)	81/19	76/24	T1a	5 (1–20)	50	0	86	19/81	NS	0	0	0	–	–	–
		18				T1b						NS	28	6	6	71	29	0
Our report	2022	20	70 (41–82)	65/35	30/70	T1a	6 (2–16)	60	0	60	50/50	83 (3y)	40	0	0	100	100	0
		20	70 (52–86)	95/5	50/50	T1b	6 (2–17)	60	0	90	40/60	65 (3y)	35	10	0	75	25	38

DSS, disease-specific survival; ECOG PS, Eastern Cooperative Oncology Group performance status; ENI, elective nodal irradiation; ICBT, intracavitary brachytherapy; IFI, involved-field irradiation; NS, not stated; OS, overall survival.
**Including submucosal cancer.*

for chemotherapy or best supportive care (25). Previous studies reported that R0 resection allowed long-term survival in salvage surgery. However, salvage surgery increased the incidence of postoperative complications and in-hospital mortality (26, 27). When a residual lesion remained confined in the MM, salvage endoscopic treatment can be performed safely (28). Salvage PDT for lesions within the SM or muscularis propria showed a high local CR rate with acceptable safety after the failure of definitive CRT (29). However, in Japan, PDT could only be performed in a few facilities, which may be the reason why the rate of salvage endoscopic treatments was low.

In our study, all patients with cT1a EC who were unsuitable for endoscopic resection as an initial treatment because of cancer metastasis along the entire circumference or a wide extent of tumor involvement could be treated with salvage ESD or APC. This can be attributed to the effect of regular follow-up with endoscopy. A previous study reported that cT1-2 and N0 stage cancers at baseline treated with salvage endoscopic resection were significant factors of good prognosis in terms of OS (30). It should be noted that local recurrence was observed in the one case more than 7 years after CRT. Thus, long regular follow-up with endoscopy and multidisciplinary treatment was considered important for the management of cT1a EC.

Among patients with cT1b EC with recurrence, <50% (including our study) could receive salvage endoscopic treatments (19–23). Local recurrences in the cT1a group had a shorter craniocaudal tumor length than the original tumor and could be treated endoscopically, whereas three patients in the cT1b group had a longer craniocaudal tumor length than the original tumor and required surgery. T1b EC may have a faster tumor growth rate than T1a EC. In the cT1b group, the invasion depth of local recurrence was deeper than the SM, except in one patient in our study. It should be noted that local and regional recurrence was observed in most cases within 2 years after CRT. Thus, frequent regular follow-up with endoscopy and CT was considered important for the management of cT1b EC compared with cT1a EC, at least within 2 years. In our study, one of three patients who underwent salvage surgery died of bleeding. In contrast, a recent study reported that salvage surgery was relatively safe (31). Among 96 patients who received RT with a total dose of 50.4 Gy, 25 underwent salvage surgery, with a 3-year survival rate of 48%. In their cohort, pulmonary complications, suture failure, and treatment-related death were observed in 4%, 12%, and 4% of patients, respectively. Nevertheless, salvage surgery after high-dose irradiation was considered to result in more complications and treatment-related deaths than conventional esophagectomy or salvage surgery after RT with a total dose of 50.4 Gy. Considering the outcomes of salvage surgery, RT with a total dose of 50.4 Gy might be an appropriate treatment for stage I EC. To establish a new treatment option, Japanese study groups are conducting a phase III clinical trial comparing CRT with a dose of 50.4 and 60 Gy for treating cT1bN0M0 EC [Japan Registry of Clinical Trials (jRCT) study number: jRCTs031200067].

The present study has several limitations associated with its retrospective design. First, the sample size was small, which

affects the statistical power. Second, the external validity might be low. Some institutions performed subtotal-to-total circumferential resection with prophylactic steroids for more than three-fourths of the circumference of the EC (32, 33). A phase III study aimed at prospectively evaluating the stenosis-preventive effect of submucosal triamcinolone injection and oral prednisolone treatment is ongoing (34). However, RT may be necessary for patients at a high risk for esophageal stricture despite treatment with prophylactic steroids.

In conclusion, regional recurrence and distant metastasis were not observed among patients in the cT1a group, whereas regional recurrence was observed among patients in the cT1b group after definitive RT or CRT. A higher proportion of patients in the cT1a group were able to receive salvage endoscopic treatments and their OS tended to be favorable compared with those in the cT1b group. Frequent regular follow-up with endoscopy and CT was considered important for the management of cT1b EC compared with cT1a EC, at least within 2 years.

DATA AVAILABILITY STATEMENT

The raw data supporting the conclusions of this article will be made available by the authors, without undue reservation.

ETHICS STATEMENT

The studies involving human participants were reviewed and approved by Juntendo Hospital review board. Written informed consent for participation was not required for this study in accordance with the national legislation and the institutional requirements.

AUTHOR CONTRIBUTIONS

TK prepared the manuscript and performed the literature search. TK reviewed and edited the manuscript. TK, NS, SM, and KS reviewed the manuscript. All authors contributed to the article and approved the submitted version.

REFERENCES

1. Di Pardo BJ, Bronson NW, Diggs BS, Thomas CRJr., Hunter JG, Dolan JP. The Global Burden of Esophageal Cancer: A Disability-Adjusted Life-Year Approach. *World J Surg* (2016) 40(2):395–401. doi: 10.1007/s00268-015-3356-2
2. Watanabe M, Tachimori Y, Oyama T, Toh Y, Matsubara H, Ueno M, et al. Comprehensive Registry of Esophageal Cancer in Japan, 2013. *Esophagus* (2021) 18(1):1–24. doi: 10.1007/s10388-020-00785-y
3. Kitagawa Y, Uno T, Oyama T, Kato K, Kato H, Kawakubo H, et al. Esophageal Cancer Practice Guidelines 2017 Edited by the Japan Esophageal Society: Part 1. *Esophagus* (2019) 16(1):1–24. doi: 10.1007/s10388-018-0641-9
4. National Comprehensive Cancer Network. NCCN Clinical Practice Guidelines in Oncology National Comprehensive Cancer Network, in: *NCCN Clinical Practice Guidelines in Oncology Esophageal and Esophagogastric Junction Cancers. Version 3* (2021). Available at: https://www.nccn.org/professionals/physician_gls/pdf/esophageal.pdf (Accessed 29 June 2021).
5. Kato K, Ito Y, Nozaki I, Daiko H, Kojima T, Yano M, et al. Parallel-Group Controlled Trial of Surgery Versus Chemoradiotherapy in Patients With Stage I Esophageal Squamous Cell Carcinoma. *Gastroenterology* (2021) 161(6):1878–86. doi: 10.1053/j.gastro.2021.08.007
6. Kawamoto T, Shikama N, Mine S, Tsurumaru M, Sasai K. Clinical Impact of Baseline Renal Function on the Safety of Radiotherapy With Concurrent Docetaxel for Esophageal Cancer in Elderly Patients. *Esophagus* (2020) 17(4):425–32. doi: 10.1007/s10388-020-00731-y
7. Kawamoto T, Shikama N, Oshima M, Kosugi Y, Tsurumaru M, Sasai K. Safety of Radiotherapy With Concurrent Docetaxel in Older Patients With Esophageal Cancer. *J Geriatr Oncol* (2020) 11(4):675–9. doi: 10.1016/j.jgo.2019.08.009
8. Takahashi N, Umezawa R, Kishida K, Yamamoto T, Ishikawa Y, Takeda K, et al. Clinical Outcomes and Prognostic Factors for Esophageal Cancer in Patients Aged 80 Years or Older Who Were Treated With Definitive Radiotherapy and Chemoradiotherapy. *Esophagus* (2022) 19(1):129–36. doi: 10.1007/s10388-021-00876-4
9. *Common Toxicity Criteria, Version2.0* (1999).
10. Brierley J, Gospodarowicz MK, Wittekind C. *TNM Classification of Malignant Tumours. Eighth.* Chichester, West Sussex, UK ; Hoboken, NJ: John Wiley & Sons, Inc (2017).
11. Kawamoto T, Shikama N, Mine S, Kosugi Y, Yamaguchi N, Oshima M, et al. Clinical Outcomes of Definitive Radiotherapy for Patients With Ct1an0m0 Esophageal Cancer Unsuitable for Endoscopic Resection and Surgery. *J Gastrointest Oncol* (2022) 13(2):454–61. doi: 10.21037/jgo-21-773
12. Quan H, Li B, Couris CM, Fushimi K, Graham P, Hider P, et al. Updating and Validating the Charlson Comorbidity Index and Score for Risk Adjustment in Hospital Discharge Abstracts Using Data From 6 Countries. *Am J Epidemiol* (2011) 173(6):676–82. doi: 10.1093/aje/kwq433
13. Charlson ME, Pompei P, Ales KL, MacKenzie CR. A New Method of Classifying Prognostic Comorbidity in Longitudinal Studies: Development and Validation. *J Chronic Dis* (1987) 40(5):373–83. doi: 10.1016/0021-9681(87)90171-8
14. Eisenhauer EA, Therasse P, Bogaerts J, Schwartz LH, Sargent D, Ford R, et al. New Response Evaluation Criteria in Solid Tumours: Revised RECIST Guideline (Version 1.1). *Eur J Cancer* (2009) 45(2):228–47. doi: 10.1016/j.ejca.2008.10.026
15. Tahara M, Ohtsu A, Hironaka S, Boku N, Ishikura S, Miyata Y, et al. Clinical Impact of Criteria for Complete Response (CR) of Primary Site to Treatment of Esophageal Cancer. *Jpn J Clin Oncol* (2005) 35(6):316–23. doi: 10.1093/jjco/hyi095
16. *National Cancer Institute: Common Terminology Criteria for Adverse Events (CTCAE) Version 5.0* . Available at: https://ctep.cancer.gov/protocolDevelopment/electronic_applications/docs/CTCAE_v5_Quick_Reference_5x7.pdf.
17. Kanda Y. Investigation of the Freely Available Easy-to-Use Software 'EZR' for Medical Statistics. *Bone Marrow Transplant* (2013) 48(3):452–8. doi: 10.1038/bmt.2012.244
18. Nemoto K, Yamada S, Hareyama M, Nagakura H, Hirokawa Y. Radiation Therapy for Superficial Esophageal Cancer: A Comparison of Radiotherapy Methods. *Int J Radiat Oncol Biol Phys* (2001) 50(3):639–44. doi: 10.1016/S0360-3016(01)01481-X
19. Ishikawa H, Sakurai H, Tamaki Y, Nonaka T, Yamakawa M, Saito Y, et al. Radiation Therapy Alone for Stage I (UICC T1N0M0) Squamous Cell Carcinoma of the Esophagus: Indications for Surgery or Combined Chemoradiotherapy. *J Gastroenterol Hepatol* (2006) 21(8):1290–6. doi: 10.1111/j.1440-1746.2006.04089.x
20. Yamada K, Murakami M, Okamoto Y, Okuno Y, Nakajima T, Kusumi F, et al. Treatment Results of Chemoradiotherapy for Clinical Stage I (T1N0M0) Esophageal Carcinoma. *Int J Radiat Oncol Biol Phys* (2006) 64(4):1106–11. doi: 10.1016/j.ijrobp.2005.10.015
21. Kodaira T, Fuwa N, Tachibana H, Nakamura T, Tomita N, Nakahara R, et al. Retrospective Analysis of Definitive Radiotherapy for Patients With Superficial Esophageal Carcinoma: Consideration of the Optimal Treatment

Method With a Focus on Late Morbidity. *Radiother Oncol* (2010) 95(2):234–9. doi: 10.1016/j.radonc.2010.01.005
22. Murakami Y, Nagata Y, Nishibuchi I, Kimura T, Kenjo M, Kaneyasu Y, et al. Long-Term Outcomes of Intraluminal Brachytherapy in Combination With External Beam Radiotherapy for Superficial Esophageal Cancer. *Int J Clin Oncol* (2012) 17(3):263–71. doi: 10.1007/s10147-011-0285-4
23. Suzuki G, Yamazaki H, Aibe N, Masui K, Shimizu D, Kimoto T, et al. Radiotherapy for T1N0M0 Esophageal Cancer: Analyses of the Predictive Factors and the Role of Endoscopic Submucosal Dissection in the Local Control. *Cancers (Basel)* (2018) 10(8):259. doi: 10.3390/cancers10080259
24. Makuuchi H. Endoscopic Mucosal Resection for Early Esophageal Cancer. *Dig Endosc* (1996) 8(3):175–9. doi: 10.1111/den.1996.8.3.175
25. Kitagawa Y, Uno T, Oyama T, Kato K, Kato H, Kawakubo H, et al. Esophageal Cancer Practice Guidelines 2017 Edited by the Japan Esophageal Society: Part 2. *Esophagus* (2019) 16(1):25–43. doi: 10.1007/s10388-018-0642-8
26. Swisher SG, Wynn P, Putnam JB, Mosheim MB, Correa AM, Komaki RR, et al. Salvage Esophagectomy for Recurrent Tumors After Definitive Chemotherapy and Radiotherapy. *J Thorac Cardiovasc Surg* (2002) 123 (1):175–83. doi: 10.1067/mtc.2002.119070
27. Tachimori Y, Kanamori N, Uemura N, Hokamura N, Igaki H, Kato H. Salvage Esophagectomy After High-Dose Chemoradiotherapy for Esophageal Squamous Cell Carcinoma. *J Thorac Cardiovasc Surg* (2009) 137(1):49–54. doi: 10.1016/j.jtcvs.2008.05.016
28. Yano T, Muto M, Hattori S, Minashi K, Onozawa M, Nihei K, et al. Long-Term Results of Salvage Endoscopic Mucosal Resection in Patients With Local Failure After Definitive Chemoradiotherapy for Esophageal Squamous Cell Carcinoma. *Endoscopy* (2008) 40(9):717–21. doi: 10.1055/s-2008-1077480
29. Yano T, Kasai H, Horimatsu T, Yoshimura K, Teramukai S, Morita S, et al. A Multicenter Phase II Study of Salvage Photodynamic Therapy Using Talaporfin Sodium (ME2906) and a Diode Laser (PNL6405EPG) for Local Failure After Chemoradiotherapy or Radiotherapy for Esophageal Cancer. *Oncotarget* (2017) 8(13):22135–44. doi: 10.18632/oncotarget.14029
30. Kondo S, Tajika M, Tanaka T, Kodaira T, Mizuno N, Hara K, et al. Prognostic Factors for Salvage Endoscopic Resection for Esophageal Squamous Cell Carcinoma After Chemoradiotherapy or Radiotherapy Alone. *Endosc Int Open* (2016) 4(8):E841–8. doi: 10.1055/s-0042-109609
31. Ito Y, takeuchi H, Ogawa G, Kato K, Onozawa M, Minashi K, et al. A Single-Arm Confirmatory Study of Definitive Chemoradiotherapy (dCRT) Including Salvage Treatment in Patients (Pts) With Clinical (C) Stage II/III Esophageal Carcinoma (EC) (Jcog0909). *J Clin Oncol* (2018) 36(15_suppl):4051–. doi: 10.1200/JCO.2018.36.15_suppl.4051
32. Yamaguchi N, Isomoto H, Nakayama T, Hayashi T, Nishiyama H, Ohnita K, et al. Usefulness of Oral Prednisolone in the Treatment of Esophageal Stricture After Endoscopic Submucosal Dissection for Superficial Esophageal Squamous Cell Carcinoma. *Gastrointest Endosc* (2011) 73 (6):1115–21. doi: 10.1016/j.gie.2011.02.005
33. Hanaoka N, Ishihara R, Takeuchi Y, Uedo N, Higashino K, Ohta T, et al. Intralesional Steroid Injection to Prevent Stricture After Endoscopic Submucosal Dissection for Esophageal Cancer: A Controlled Prospective Study. *Endoscopy* (2012) 44(11):1007–11. doi: 10.1055/s-0032-1310107
34. Mizutani T, Tanaka M, Eba J, Mizusawa J, Fukuda H, Hanaoka N, et al. A Phase III Study of Oral Steroid Administration Versus Local Steroid Injection Therapy for the Prevention of Esophageal Stricture After Endoscopic Submucosal Dissection (JCOG1217, Steroid EESD P3). *Jpn J Clin Oncol* (2015) 45(11):1087–90. doi: 10.1093/jjco/hyv120

Conflict of Interest: The authors declare that the research was conducted in the absence of any commercial or financial relationships that could be construed as a potential conflict of interest.

Publisher's Note: All claims expressed in this article are solely those of the authors and do not necessarily represent those of their affiliated organizations, or those of the publisher, the editors and the reviewers. Any product that may be evaluated in this article, or claim that may be made by its manufacturer, is not guaranteed or endorsed by the publisher.

frontiers | Frontiers in Oncology

TYPE Original Research
PUBLISHED 26 August 2022
DOI 10.3389/fonc.2022.898141

OPEN ACCESS

EDITED BY
Chi Lin,
University of Nebraska Medical Center,
United States

REVIEWED BY
Vanessa Panettieri,
The Alfred Hospital, Australia
Brendan Coutu,
University of Nebraska Medical Center,
United States

*CORRESPONDENCE
Shu-Xu Zhang
gthzsx@gzhmu.edu.cn

SPECIALTY SECTION
This article was submitted to Radiation Oncology, a section of the journal Frontiers in Oncology

RECEIVED 17 March 2022
ACCEPTED 29 July 2022
PUBLISHED 26 August 2022

CITATION
Zhou P-X, Wang R-H, Yu H, Zhang Y, Zhang G-Q and Zhang S-X (2022) Different functional lung-sparing strategies and radiotherapy techniques for patients with esophageal cancer. *Front. Oncol.* 12:898141. doi: 10.3389/fonc.2022.898141

Different functional lung-sparing strategies and radiotherapy techniques for patients with esophageal cancer

Pi-Xiao Zhou, Rui-Hao Wang, Hui Yu, Ying Zhang, Guo-Qian Zhang and Shu-Xu Zhang*

Radiotherapy Center, Affiliated Cancer Hospital and Institute of Guangzhou Medical University, Guangzhou, China

Background: Integration of 4D-CT ventilation function images into esophageal cancer radiation treatment planning aimed to assess dosimetric differences between different functional lung (FL) protection strategies and radiotherapy techniques.

Methods: A total of 15 patients with esophageal cancer who had 4D-CT scans were included. Lung ventilation function images based on Jacobian values were obtained by deformation image registration and ventilation imaging algorithm. Several different plans were designed for each patient: clinical treatment planning (non-sparing planning), the same beam distribution to FL-sparing planning, three fixed-beams FL-sparing intensity-modulated radiation therapy (IMRT) planning (5F-IMRT, 7F-IMRT, 9F-IMRT), and two FL-sparing volumetric modulated arc therapy (VMAT) planning [1F-VMAT (1-Arc), 2F-VMAT (2-Arc)]. The dosimetric parameters of the planning target volume (PTV) and organs at risk (OARs) were compared and focused on dosimetric differences in FL.

Results: The FL-sparing planning compared with the non-sparing planning significantly decreased the FL-D_{mean}, V_{5-30} and Lungs-D_{mean}, V_{10-30} (V_x: volume of receiving ≥X Gy), although it slightly compromised PTV conformability and increased Heart-V_{40} ($P< 0.05$). The 5F-IMRT had the lowest PTV-conformability index (CI) but had a lower Lungs and Heart irradiation dose compared with those of the 7F-IMRT and 9F-IMRT ($P< 0.05$). The 2F-VMAT had higher PTV-homogeneity index (HI) and reduced irradiation dose to FL, Lungs, and Heart compared to those of the 1F-VMAT planning ($P< 0.05$). The 2F-VMAT had higher PTV conformability and homogeneity and decreased FL-D_{mean}, V_{5-20} and Lungs-D_{mean}, V_{5-10} but correspondingly increased spinal cord-D_{mean} compared with those of the 5F-IMRT planning ($P< 0.05$).

Conclusion: In this study, 4D-CT ventilation function image-based FL-sparing planning for esophageal cancer can effectively reduce the dose of the FL. The

2F-VMAT planning is better than the 5F-IMRT planning in reducing the dose of FL.

KEYWORDS

esophageal cancer, four-dimensional CT (4D-CT), functional lung, intensity-modulated radiotherapy (IMRT), volumetric-modulated arc therapy (VMAT)

Introduction

Esophageal cancer (EC) is a malignant tumor originating from the mucosal epithelium of the esophagus, which is one of the common gastrointestinal malignancies and the sixth most common cancer-related cause of death globally (1). In China, the incidence of EC is relatively high, and the number of new cases and deaths each year accounts for 53.7% and 55.7% of the global total, respectively (2). Radiotherapy is one of the effective treatment options for patients with EC (1). However, radiation pneumonitis (RP) is a common and potentially fatal toxicity reaction to radiation therapy for thoracic tumors such as EC, with a G2+ RP incidence of 6%–25% (3). It may lead to pulmonary fibrosis and lung function compromise and, in severe cases, may cause death due to respiratory distress (4). It can also limit the improvement of the clinical prescription dose, which may affect the efficacy and prognosis. Although with the advancement of radiotherapy technology, intensity-modulated radiation therapy (IMRT) compared with three-dimensional conformal radiation therapy (3D-CRT) improved the target conformability and decreased the organ at risk (OAR) radiation dose. However, according to a meta-analysis, IMRT did not significantly reduce the incidence of RP in EC compared with 3D-CRT (5). Furthermore, volumetric modulated arc therapy (VMAT) is a more advanced radiotherapy technique than IMRT that can further reduce the dose of OARs (6).

Previous studies have shown that the occurrence of RP was related to the dose and volume of lung irradiation and that there was heterogeneity in the response of lung tissue to radiation in different functional states (7, 8). In addition, the functional subunits are not uniformly distributed owing to organ structure or disease (e.g., lung and liver) (9). However, conventional anatomical CT planning does not take the heterogeneity of lung function distribution into consideration, but the 3D map of functional lung (FL; high functional state) distribution identified by FL imaging can be integrated into radiotherapy planning (10). Faught et al. (11) used the normal tissue concurrent probability (NTCP) model to predict the incidence of RP in the FL-sparing planning group. The results showed that the FL-sparing planning decreased the incidence of grade 2+ and 3+ RP in lung cancer patients by 7.1% and 4.7% compared with the conventional anatomical CT planning, respectively. Moreover, the FL dose-volume parameters (e.g., functional lung mean dose (f-MLD), volume of functional lung receiving ≥ 20Gy (fV_{20})) can more accurately predict the incidence of RP than anatomical lung parameters (MLD, V_{20}) (12). Currently, several ongoing clinical trials are investigating the clinical value of using FL-sparing planning-guided radiotherapy to reduce RP (e.g., NCT02308709, NCT02843568, NCT04676828) (13, 14).

Previous functional imaging was commonly used to assess tumor heterogeneity, evaluate efficacy, and predict prognosis, and fewer studies have extended to evaluate heterogeneity of lung function distribution (15). At present, FL imaging modalities include four-dimensional computed tomography (4D-CT), dual-energy CT, magnetic resonance image (MRI), single-photon emission computed tomography (SPECT), and positron emission tomography (PET) (16). 4D-CT imaging has been routinely used in lung cancer radiotherapy workflow for respiratory motion management and individual target area delineation (ITV). It also has the advantages of high-speed scanning, higher resolution, lower cost, and the ability to acquire 3D distribution images of lung ventilation function without relying on additional functional imaging equipment and methods (17, 18). Studies have validated the accuracy of 4D-CT lung ventilation function imaging by correlating it with clinical pulmonary function test (PFT) and nuclear medicine (SPECT/CT, PET/CT) ventilation function imaging, and both results demonstrated a good correlation (18, 19). Pinder-Arabpour et al. (20) demonstrated the significant heterogeneity in the distribution of lung ventilation function in EC patients for the first time in 2019. Currently, FL imaging studies have not been applied to radiotherapy for EC separately. Therefore, this study will investigate the dosimetric value of different protection strategies and radiotherapy techniques for protecting FL based on the 4D-CT lung ventilation function image in EC patients.

Materials and methods

Patient population

Patients with EC scanned with 4D-CT and treated with radiotherapy in our hospital from 1 October 2021 to 20

February 2022 were selected for this study. Inclusion criteria were as follows: 1) The planning target volume (PTV) was located in the thoracic esophagus (including upper thoracic, middle thoracic, and lower thoracic); 2) Patients had not received previous radiotherapy to the thoracic; 3) There was no restriction on the type of radiotherapy that the patient received (neoadjuvant, adjuvant, or definitive radiotherapy). 4) 4D-CT scanning data were available.

Contrast-enhanced CT and 4D-CT scanning

All patients were immobilized in the supine position using a thermoplastic mold, and enhanced CT was performed by Brilliance Big Bore scanner (Phillips Healthcare, USA). The scanning range was from the upper edge of the first cervical vertebra (C1) or the lower edge of the seventh cervical vertebra (C7) to the upper abdomen, with the following parameters: voltage 120 kVp, current 300 mA, and slice thickness/spacing of 3–5 mm. The 4D-CT scans were performed after the enhanced CT was completed, and a marker module had been placed on the abdomen where the respiratory magnitude was most apparent (no marker was implanted). Using Varian's Real-Time Position Management (RPM) System to monitor the patient's respiratory waveform, 4D-CT scanning was performed under free breathing without any breathing control. The scanning parameters were the same as above, and the CT data were reconstructed into 10 respiratory phases using the respiratory curve after completion. The enhanced CT and 4D-CT data were then transmitted to the Pinnacle^3 (Version: 9.10, Philips Healthcare, USA) and Eclipse (Version 15.1, Varian Medical Systems, USA) treatment planning systems (TPSs), respectively.

4D-CT ventilation function imaging

Lung ventilation function images are primarily obtained through two steps. The first is deformation image registration (DIR) and the second is the ventilation imaging algorithm (VIA) (21). In this study, the end-inspiratory CT image (00%) was used as the reference image, and the end-expiratory CT image (50%) was used as a variable image for the registration and calculation. The combination of automatic and manual (removing redundant main bronchi, correcting incorrectly delineated areas, and completing lung tissue) delineation was used to generate the whole lung (Lungs) area on 00%, 50%, and average intensity projection (AIP) CT images in Eclipse. Export to 3D-Slicer software (Version 4.11.20200930, http://www.slicer.org), performing image segmentation to form the corresponding VTK files (00%.VTK, 50%.VTK). Then, the VTK files were imported into our self-developed ventilation imaging software (ZHANGShuxu 4D-CT LF, V1.0) for DIR and quantitative calculations (22, 23). Jacobian determinant of deformation was utilized to measure the corresponding lung volume changes with the two CT images (23, 24). Finally, the Jacobian data and AIP images files were imported into 3D-Slicer for visualization and quantitative analysis of lung ventilation function (Figure 1). When Jacobian = 1, it indicates no volume change in the corresponding area of two images. When Jacobian<1, the related volume shrinks compared to the reference image (24).

Target and organ at risk delineation

The tumor target area and OARs were delineated on Pinnacle^3 by an experienced radiation oncologist of our hospital according to the Chinese EC radiotherapy guidelines and the International Commission on Radiation Units and

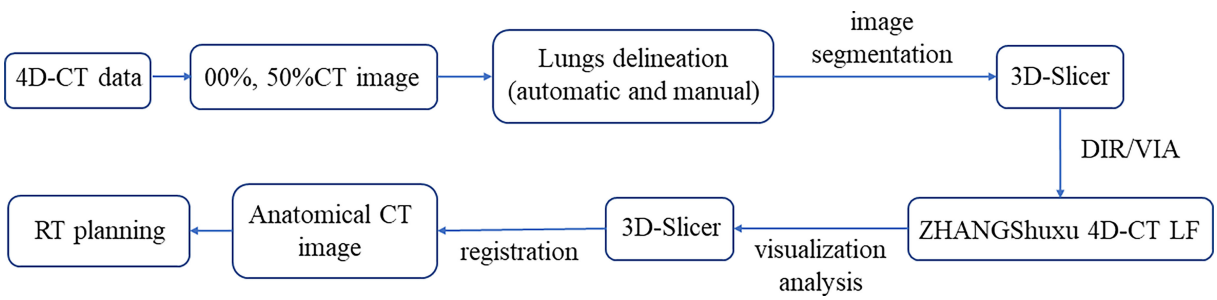

FIGURE 1
Flowchart of the functional lung obtained from 4D-CT. DIR, deformation image registration; VIA, ventilation imaging algorithm.

Measurements (ICRU) Report 62 (4, 25) and then reviewed by a senior radiation oncologist. Gross tumor target volume (GTV) was defined as the primary tumor/visible esophageal lesion (GTVp) and metastatic lymph nodes (GTVn). The clinical target volume (CTV) was defined as an 8-mm expansion of the GTV in the anterior–posterior, left–right, and superior–inferior directions. PTV is defined as CTV with 5-mm expansion in all directions. Because the esophagus is close to the Spinal cord, Heart, and surrounded by Lungs, these organs are the significant OARs. In this study, the FL is another essential OAR. Based on our prior research results, regions with a Jacobian value ≤0.8 were defined as FL (26). The 3D distribution map of the FL was exemplified in Figure 2.

Radiotherapy planning

Radiotherapy planning was designed for each patient on the Pinnacle^3 9.10, including a conventional anatomical CT treatment planning (without consideration of FL, non-sparing planning), as well as the same beam distribution FL-sparing planning, three fixed-beams FL-sparing IMRT planning [5F-IMRT (0°, 72°, 144°, 216°, 288°), 7F-IMRT (0°, 50°, 100°, 150°, 210°, 260°, 310°), 9F-IMRT (0°, 40°, 80°, 120°, 160°, 200°, 240°, 280°, 320°)], and two FL-sparing VMAT planning [1F-VMAT (1-Arc), 2F-VMAT (2-Arc)]. The non-sparing planning was accomplished through the same group of experienced physicists and radiation oncologists in consultation. The linear accelerator energy was 6 MV, and the radiation dose was 1.8–2.2 Gy/20–30 (fractions), five times a week. Prescription dose lines contain at least 95% of the PTV, and the hot spot (≤110% prescription dose) could not fall on the OARs. The FL-sparing planning for EC was consistent with the clinical treatment planning regarding prescription dose, target area dose requirements, OAR dose limitations, and weights while only requiring additional dose limitations for the FL. The PTV gave the highest priority (100%), and the FL was as low as possible under the condition that the doses of the PTV and OARs meet clinical request. The OAR dose-limitation schemes are shown in Table 1.

Planning evaluation

Dose-volume histograms (DVHs) were analyzed for the PTV and OARs. PTV evaluated its conformability index (CI) and homogeneity index (HI). CI is defined to assess the conformity of the prescribed dose distribution (27).

$$CI = \frac{V_{P,ref}}{V_P} \times \frac{V_{P,ref}}{V_{ref}}$$

$V_{P,\ ref}$, V_P, V_{ref} represented the volume of PTV surrounded by the prescription dose line, the volume of PTV, and the volume surrounded by the prescription dose line, respectively. The CI ranges from 0 to 1, and closer to 1 means better conformability of the PTV. HI was used to evaluate the uniformity of prescription dose distribution in PTV and was calculated by the following equation:

$$HI = \frac{D_{5\%}}{D_{95\%}}$$

$D_{5\%}$, $D_{95\%}$ represented the dose received 5%, 95% volume of the PTV, respectively. The closer the HI to 1, the better homogeneity of the PTV. MLD (lung mean dose), V_5 (V_x, volume of receiving dose ≥ × Gy), V_{10}, V_{20}, and V_{30} were evaluated for the whole lung, FL, and high FL, MHD (heart mean dose), V_5, V_{10}, V_{20}, V_{30}, and V_{40} for the heart, and D_{max} (maximum dose) and D_{mean} for the spinal cord.

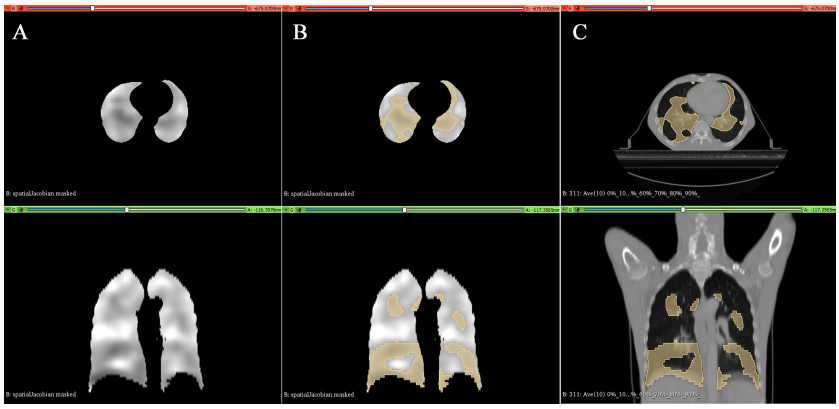

FIGURE 2
Typical lung ventilation function images generated in 3D-Slicer software. **(A)** Grayscale image containing the Jacobian value. **(B)** Defined regions of Jacobian value ≤0.8 (e.g., functional lung). **(C)** Distribution of functional lungs in the esophageal cancer patient's anatomical CT.

10.3389/fonc.2022.898141

TABLE 1 The dose-volume restrictions of organs at risk (OARs).

OARs	Restrictions
Lungs	V_5<65%, V_{20}<30%, V_{30}<20%
Heart	V_{40}<40%
Spinal cord	D_{max}<45Gy
Functional lung	V_{10}<20%, V_{20}<10%, V_{30}<5%

Statistical methods

The measurements were described by mean ± standard deviation (SD); paired t-test was conducted to compare the dose-volume parameters of PTV and OAR difference between different groups. Statistical analysis was performed with SPSS 25.0 (IBM SPSS Statistics, USA), and P< 0.05 was considered statistically significant.

Results

A total of 15 patients were included, 14 men and 1 woman, with a mean age of 57.2 years (48–68 years). The mean volume of CTV was 319.7 ± 127.4 cm^3. More than half of the patients had PTV in the upper and middle thoracic esophagus. Detailed clinical information of the patients is shown in Table 2.

TABLE 2 Detailed clinical information of the patients included in the study.

No. of patients	15
Mean age (range)	57.2 (48–68) years
Gender, n (%)	
Men	14 (93.3%)
Women	1 (6.7%)
Histology, n (%)	
Squamous cell carcinoma	13 (86.7%)
Small-cell carcinoma	2 (13.3%)
Target location (PTV), n (%)	
U+M	7 (46.7%)
M	3 (20%)
M+L	3 (20%)
L	1 (6.7%)
U+M+L	1 (6.7%)
Mean CTV (range, cm^3)	319.7 (161.7–558.3)
Mean prescription dose (PTV, range)	48.5 (36–60.2) Gy
Clinical treatment planning, n (%)	
IMRT	12 (80%)
VMAT	3 (20%)

SD, standard deviation; PTV, planning target volume; CTV, clinical target volume; U, upper thoracic; M, middle thoracic; L, lower thoracic.

Comparison of non-sparing and functional lung-sparing planning

The PTV and OAR dosimetric differences of the non-sparing planning and FL-sparing planning with consistent beam arrangement are listed in Table 3. Compared with the non-sparing planning, the FL-sparing planning has a slighter lower CI (0.662 ± 0.098 vs. 0.692 ± 0.083, P = 0.024) and a similar HI (1.144 ± 0.064 vs. 1.142 ± 0.078, P > 0.05), indicating a slightly lower conformity dose distribution to the PTV. In general, both plans maintained a good coverage of the PTV.

The dosimetric parameters of FL are also listed in Table 3, and the typical planning and dose-volume histogram for FL are shown in Figure 3. Compared with those in the non-sparing planning group, the FL-V_5, V_{10}, V_{20}, V_{30}, and D_{mean} were significantly reduced in the FL-sparing planning group (P< 0.05). The dosimetric parameters of reduction are presented as follows: 1.97% for FL-V_5 (non-sparing vs. FL-sparing: 39.68% ± 16.32% vs. 37.71% ± 14.82%, P = 0.041), 9.24% for FL-V_{10} (25.03% ± 10.24% vs. 15.79% ± 7.79%, P< 0.001), 4.81% for FL-V_{20} (11.00% ± 6.87% vs. 6.19% ± 3.72, P< 0.001), 1.28% for FL-V_{30} (4.70% ± 4.18% vs. 3.42% ± 2.49%, P = 0.033), and 1.44 Gy for FL-D_{mean} (7.38 ± 2.95 Gy vs. 5.94 ± 2.26 Gy, P< 0.001).

The dosimetric parameters for the other OARs are also presented in Table 3. According to the results, the dose limitation for one of the OARs will inevitably increase the dose to another. The D_{mean}, V_{10}, V_{20}, and V_{30} of the Lungs are significantly decreased in the FL-sparing planning, which may be caused by the dose restriction of the FL. The FL-sparing planning had a statistically significant increase in Heart-V_{40} compared to that of the non-sparing planning. However, the D_{max} and D_{mean} of the spinal cord showed no significant difference in these two plans.

Comparison of 5F-IMRT, 7F-IMRT, and 9F-IMRT planning

Different FL-sparing IMRT plannings were then investigated to evaluate their value in reducing the dose of the FL (Supplementary Table S1). Regarding the conformal and uniform dose distribution of the PTV, it was observed that 5F-IMRT had the lowest CI 5F-IMRT (five-field fixed-beam functional lung-sparing IMRT planning) vs. 7F-IMRT (seven-field fixed-beam functional lung-sparing IMRT planning)/9F-IMRT (nine-field fixed-beam functional lung-sparing IMRT planning): 0.647 vs. 0.670/0.681, P< 0.05; 7F-IMRT vs. 9F-VMAT: P > 0.05), while D_{max}, D_{mean}, and HI were not found to be statistically different between the three plans. The 5F-IMRT compared with the 7F-IMRT had lower Lungs-D_{mean}, Heart-V_5, and V_{10} (P< 0.05). The 5F-IMRT compared with the 9F-IMRT had higher FL-V_{30} but lower Heart-V_5 (P< 0.05). The 7F-IMRT compared with the 9F-IMRT had higher Lungs-D_{mean} and V_{10}

10.3389/fonc.2022.898141

TABLE 3 Dosimetric parameter comparison for PTV and OARs in different FL-sparing IMRT and VMAT planning.

OARs	Non-sparing planning	FL-sparing planning	P value
PTV			
D_{max} (Gy)	56.98 ± 8.46	58.26 ± 9.01	0.005
D_{mean} (Gy)	52.42 ± 7.98	52.60 ± 8.01	0.178
CI	0.692 ± 0.083	0.662 ± 0.098	0.024
HI	1.142 ± 0.078	1.144 ± 0.064	0.806
FL			
D_{mean} (Gy)	7.38 ± 2.95	5.94 ± 2.26	<0.001
V_5 (%)	39.68 ± 16.32	37.71 ± 14.82	0.041
V_{10} (%)	25.03 ± 10.24	15.79 ± 7.79	<0.001
V_{20} (%)	11.00 ± 6.87	6.19 ± 3.72	<0.001
V_{30} (%)	4.70 ± 4.18	3.42 ± 2.49	0.033
Lungs			
D_{mean} (Gy)	9.91 ± 2.58	9.14 ± 2.56	<0.001
V_5 (%)	50.84 ± 11.72	49.58 ± 11.82	0.117
V_{10} (%)	35.09 ± 8.11	29.70 ± 7.52	<0.001
V_{20} (%)	16.40 ± 5.86	13.82 ± 5.52	0.009
V_{30} (%)	7.45 ± 4.37	6.85 ± 3.72	0.039
Heart			
D_{mean} (Gy)	17.12 ± 10.53	17.55 ± 10.68	0.298
V_5 (%)	61.07 ± 35.27	60.96 ± 35.38	0.771
V_{10} (%)	53.46 ± 34.24	53.14 ± 34.46	0.766
V_{20} (%)	40.92 ± 29.67	40.00 ± 27.45	0.562
V_{30} (%)	22.47 ± 16.02	24.46 ± 17.11	0.078
V_{40} (%)	11.67 ± 9.91	13.57 ± 11.57	0.035
Spinal cord			
D_{max} (Gy)	38.82 ± 4.67	37.69 ± 5.87	0.600
D_{mean} (Gy)	11.99 ± 9.05	12.47 ± 9.53	0.142

Mean ± SD; P value was calculated by paired t-test. PTV, planning target volume; OARs, organs at risk; FL, functional lung; Dmax, maximum dose; Dmean, mean dose; Vx, volume of receiving = X Gy.

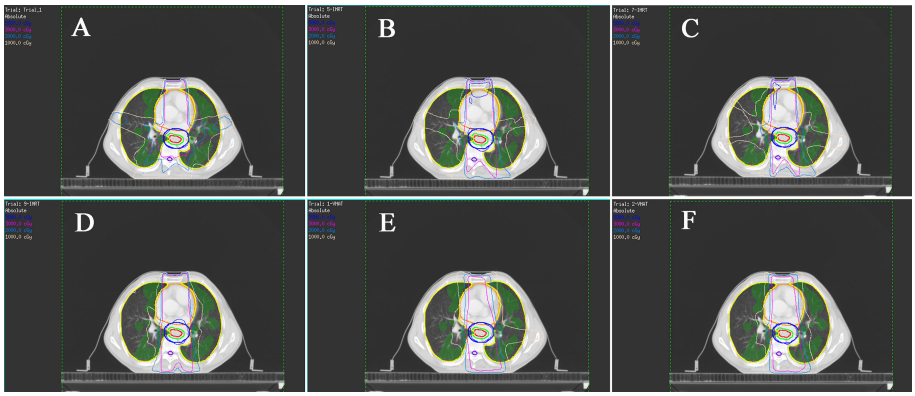

FIGURE 3
Typical isodose dose distribution map of the radiotherapy planning for esophageal cancer patients. The functional lung (FL) are green areas. **(A)** Non-sparing planning (five-field fixed-beam IMRT); **(B)** five-field fixed-beam functional lung-sparing IMRT planning (5F-IMRT); **(C)** seven-field fixed-beam FL-sparing IMRT planning (7F-IMRT); **(D)** nine-field fixed-beam FL-sparing IMRT planning (9F-IMRT); **(E)** one-arc FL-sparing VMAT planning (1F-VMAT). **(F)** two-arc FL-sparing VMAT planning (2F-VMAT)

(P< 0.05). There was no significant difference in spinal cord-D_{mean} and D_{max} between the three plans (P > 0.05).

Comparison of 1F-VMAT and 2F-VMAT planning

The differences in dose reduction for FL between the different FL-sparing VMAT planning were also explored (Supplementary Table S2). The 2F-VMAT significantly decreased the PTV-HI compared with the 1F-VMAT planning, indicating that the 2F-VMAT had higher PTV homogeneity. At the same time, D_{max}, D_{mean}, and CI of the PTV were not statistically different between the two plans (P > 0.05). The 2F-VMAT reduced FL-D_{mean}, V_{10}, Lungs-V_{10}, and Heart-V_{20} compared to the 1F-VMAT planning (P< 0.05).

Comparison of functional lung-sparing IMRT and VMAT planning

Subsequently, the dosimetric differences between different FL-sparing IMRT and VMAT planning were further analyzed (Table 4). The dosimetric differences in PTV and OARs between the 5F-IMRT and 2F-VMAT planning were selected for comparison on the premise that the PTV dose meets the clinical requirements, with a preference for low Lungs, Heart, and spinal cord irradiated doses and followed by low FL irradiated doses. The 2F-VMAT had higher target area conformability and homogeneity compared to the 5F-IMRT planning. The 2F-VMAT decreased FL-D_{mean}, V_5, V_{10}, V_{20}, and Lungs-D_{mean}, V_5, V_{10} but correspondingly increased spinal cord-D_{mean} (P< 0.05) compared with the 5F-IMRT planning. The irradiated dose of the Heart was not statistically different between the two plans (P > 0.05).

Discussion

In this study, we investigated different strategies and radiotherapy techniques for the preservation of the FL based on 4D-CT ventilation function images in patients with EC. Our results showed that the FL-sparing planning achieved better FL protection compared with the non-sparing planning while satisfying PTV dose coverage and OAR dose limitations. We also demonstrated that the 5F-IMRT had a lower Heart and Lungs irradiated dose but the lowest PTV-CI compared to the 7F-IMRT and 9F-IMRT. The 2F-VMAT had higher PTV-CI and lower Lungs, Heart, and FL dose than the 1F-VMAT. Furthermore, the 2F-VMAT achieved better FL protection compared with the 5F-IMRT.

EC is a commonly diagnosed gastrointestinal tract tumor, and different pathological types have different biological characteristics (1). Radiotherapy plays a unique role in treating EC (especially squamous cell carcinoma), but due to the anatomical location of the esophagus, it inevitably leads to radiation exposure of the lungs. Excessive radiation doses can induce the development of acute radiation pneumonia in the early stages and may progress to pulmonary fibrosis in the late stages, of which the severe cases can even be fatal (28). The risk of RP is further increased when patients combine with smoking, chronic obstructive pulmonary disease, interstitial lung disease, and concurrent chemotherapy, and there is no special treatment drug available (3, 28). Studies have shown that RP was correlated with the irradiated dose and volume of the Lungs (8). The arrival of the 3D-CRT era has improved the tumor target area conformality while reducing the OAR dose than 2D radiotherapy. IMRT is a more advanced technique than 3D-CRT and is currently the main treatment option for EC in clinical practice. However, a meta-analysis showed that although IMRT reduced the mean lung dose compared to 3D-CRT, there was no significant difference in radiation pneumonia in the two groups (5). VMAT is an advanced form of IMRT that provides a higher conformal dose distribution with less treatment time (29). The FL is a subunit with higher functionality identified by functional imaging. It has been demonstrated that the better the functional status of the area, the more sensitive it is to radiation (8). Therefore, reducing the irradiated dose to the FL is necessary by adding dose-limiting conditions and changing the direction of the beams during the radiotherapy planning design (9).

FL imaging modalities involve two aspects, one is lung ventilation function and the other is lung perfusion function. Studies have shown that FL imaging can effectively identify the differences in ventilation and perfusion of lung tissue, and radiation will reduce lung ventilation and perfusion on functional imaging images (10). The 4D-CT is one of the more convenient, high-resolution, and economically low-cost imaging modalities for pulmonary ventilation function. Yet, nuclear medicine imaging has been widely used to assess lung function for a long time, maintaining relative evaluation standards, and SPECT/CT can provide better spatial resolution and 3D anatomical information than history. So, it has been selected as a reference for assessing lung ventilation and perfusion standard (30). Brennan et al. (18) performed a correlation test between 4D-CT ventilation function metrics and PFT parameters in 98 lung cancer patients and showed a good correlation (approximately 0.7). However, PFT reflects overall lung function without distinguishing differences in lung function distribution and has limited sensitivity to early functional changes of disease. Vinogradskiy et al. (19) conducted 4D-CT ventilation and SPECT/CT ventilation function imaging scanning in 15 lung cancer patients simultaneously and showed a correlation coefficient of 0.68 between the two images. A phase 2 clinical trial showed that 4D-CT ventilation function image-guided FL-sparing planning reduced the incidence of RP to 14.9% in lung cancer patients

10.3389/fonc.2022.898141

TABLE 4 Dosimetric comparison in PTV and OARs between non-sparing (clinical treatment) planning and consistent beam directions of FL-sparing planning.

OARs	5F-IMRT	2F-VMAT	P value
PTV			
D_{max} (Gy)	58.19 ± 8.83	56.77 ± 8.75	<0.001
D_{mean} (Gy)	52.54 ± 7.99	52.43 ± 7.96	0.225
CI	0.647 ± 0.106	0.711 ± 0.113	0.002
HI	1.152 ± 0.076	1.131 ± 0.071	0.019
FL			
D_{mean} (Gy)	6.04 ± 2.32	5.64 ± 2.01	0.004
V_5 (%)	37.61 ± 14.95	34.78 ± 13.32	0.027
V_{10} (%)	16.55 ± 7.65	13.27 ± 5.99	0.002
V_{20} (%)	6.52 ± 3.76	5.99 ± 3.57	0.037
V_{30} (%)	3.61 ± 2.53	3.22 ± 2.29	0.097
Lungs			
D_{mean} (Gy)	9.18 ± 2.63	8.69 ± 2.43	0.004
V_5 (%)	50.44 ± 13.05	46.03 ± 9.80	0.002
V_{10} (%)	30.51 ± 8.82	27.07 ± 7.52	0.001
V_{20} (%)	13.71 ± 5.43	13.20 ± 5.62	0.335
V_{30} (%)	6.86 ± 3.56	6.46 ± 3.27	0.104
Heart			
D_{mean} (Gy)	17.38 ± 10.30	17.15 ± 10.34	0.302
V_5 (%)	60.88 ± 35.20	61.51 ± 35.53	0.207
V_{10} (%)	53.10 ± 34.06	53.89 ± 33.48	0.518
V_{20} (%)	38.34 ± 25.07	39.56 ± 26.96	0.277
V_{30} (%)	23.80 ± 16.08	22.59 ± 15.86	0.050
V_{40} (%)	13.61 ± 11.30	12.17 ± 10.41	0.160
Spinal cord			
D_{max} (Gy)	40.01 ± 4.04	37.52 ± 6.01	0.209
D_{mean} (Gy)	12.23 ± 9.32	13.31 ± 9.89	0.002

Mean ± SD; P value was calculated by paired t-test. PTV, planning target volume; OARs, organs at risk; FL, functional lung; Dmax, maximum dose; Dmean, mean dose; CI, conformability index; HI, homogeneity index; Vx, volume of receiving = X Gy; 5F-IMRT, five-field fixed-beam functional lung-sparing IMRT planning; 2F-VMAT, two-Arc functional lung-sparing VMAT planning.

(compared to 25% historical rate), and a phase 3 trial will be performed to validate further (31). Hence, 4D-CT ventilation function imaging integrated into radiotherapy planning is clinically valuable.

Previous studies comparing the dosimetric differences between different radiotherapy techniques in thoracic EC have shown that the 9F-IMRT does not produce lower OAR doses than the 5F-IMRT (32). This is similar to our results that the 5F-IMRT has a lower irradiated dose to the Heart and FL than the 9F-IMRT, and the PTV dose meets the clinical requirements. Gao et al. (33) compared the dosimetric differences between VMAT and IMRT techniques in EC. They found that VMAT reduced the dose of the Lungs and Heart with a similar dose distribution in the tumor target area, which was consistent with our results. FL imaging has been investigated in lung cancer radiotherapy for a long time, and a meta-analysis demonstrated that FL-sparing plans reduced the FL-D_{mean} and FL-V_{20} by 2.2Gy and 4.2%, respectively, when compared with conventional anatomical CT plans, which was also close to our results (reduced 1.4Gy and 4.8%) (10).

The optimally defined threshold for FL has not been determined so far. Most studies were defined as 90% or 70% of the maximum as FL in 4D-CT ventilation function imaging of lung cancer (10). Only Yamamoto et al. (34) utilized the definite thresholds to distinguish three different FL regions. Thus, we evaluated the dosimetric differences of FLs (definite threshold defined) under different protection strategies. Our FL dose limitations were set more strictly because the lungs were irradiated at a lower dose in EC than the lung cancer target area. However, due to the difference in the spatial relationship between FL and target area, some FL dosimetric is challenging to decrease in the FL-sparing planning design. According to our results, the 2F-VMAT is preferentially recommended to obtain better FL-sparing and a shorter treatment time (27). However, it has been reported that with the same IMRT beams, there are differences in the protection of FL with different arrangements,

and Wang et al. (23) demonstrated that five-field manually optimized beam IMRT is more protective of the FL than five-field equally spaced beam IMRT. So, manually optimizing beam IMRT may be better when VMAT is unavailable.

There are several limitations in this study. Firstly, a small sample size was included. Secondly, the optimal dose restrictions, weight, and beam arrangement for FL have not achieved widespread consensus, and there may be leeway in FL optimization. Thirdly, 4D-CT only identified the patient's ventilation function and did not measure lung perfusion function because normal lung function is the process of gas exchange in which air and blood maintain the proper proportion to ensure adequate and effective air exchange. Fourthly, this study only explored the dosimetric differences of different techniques on FL, target areas, and other OARs at the radiotherapy planning level and did not involve actual clinical application in practice, and its value needs to be verified in clinical trials in the future.

Conclusion

Our study confirms that 4D-CT ventilation function image-based FL protection planning for patients with EC can effectively reduce the FL irradiation dose without compromising target area coverage and other OAR dose limitations. In addition, among different FL protection strategies and radiation treatment techniques, the 7F/9F-IMRT has no better value than the 5F-IMRT except for higher CI, while the 2F-VMAT achieves better PTV conformity and better FL dose reduction.

Data availability statement

The original contributions presented in the study are included in the article/Supplementary Material. Further inquiries can be directed to the corresponding author.

Ethics statement

The studies involving human participants were reviewed and approved by The Ethics Committee of Affiliated Cancer Hospital and Institute of Guangzhou Medical University. The patients/participants provided their written informed consent to participate in this study. Written informed consent was obtained from the individual(s) for the publication of any potentially identifiable images or data included in this article.

Author contributions

P-XZ and S-XZ designed the study. HY and G-QZ performed 4D-CT scanning and generated functional lung ventilation images. P-XZ, YZ, and R-HW performed the design of the radiotherapy planning. P-XZ and YZ collected the data. P-XZ and S-XZ wrote and revised the manuscript. All authors contributed to the article and approved the submitted version.

Acknowledgments

This work was supported by Guangdong Medical Science and Technology Research Fund project (Grant Number: A2021283), Guangzhou Key Medical Discipline Construction Project Found, the Natural Science Foundation of Guangdong Province (No. 2021A1515011329), and the Science and Technology Plan Project of Guangzhou City-school Joint (No. 202201020121). The authors thank all the people who had participated in this study.

Conflict of interest

The authors declare that the research was conducted in the absence of any commercial or financial relationships that could be construed as a potential conflict of interest.

Publisher's note

Supplementary material

The Supplementary Material for this article can be found online at: https://www.frontiersin.org/articles/10.3389/fonc.2022.898141/full#supplementary-material

References

1. Smyth EC, Lagergren J, Fitzgerald RC, Lordick F, Shah MA, Lagergren P, et al. Oesophageal cancer. *Nat Rev Dis Primers* (2017) 3:17048. doi: 10.1038/nrdp.2017.48

2. Bray F, Ferlay J, Soerjomataram I, Siegel RL, Torre LA, Jemal A. Global cancer statistics 2018: GLOBOCAN estimates of incidence and mortality worldwide for 36 cancers in 185 countries. *CA Cancer J Clin* (2018) 68:394–424. doi: 10.3322/caac.21492

3. Du F, Qiang W, Wei W, Yingjie Z, Zhenxiang L, Jianbin L. Analysis of related factors of radiation pneumonitis after radiotherapy for thoracic segment esophageal cancer. *Chin Radiol Med Prot* (2020) 40:832–9. doi: 10.3760/cma.j.issn.0254-5098.2020.11.004

4. Branch of Radiation Oncology Physicians of Chinese Medical Doctor Association, Chinese medical association branch of radiotherapy therapy and Cancer Radiotherapy Committee of Chinese Anti-Cancer Association. Chinese Esophageal cancer radiotherapy guidelines (2020 version). *J Int Oncol* (2020) 47:641–55. doi: 10.3760/cma.j.cn371439-20201015-00095

5. Xu D, Li G, Li H, Jia F. Comparison of IMRT versus 3D-CRT in the treatment of esophagus cancer. *Med (Baltimore)* (2017) 96:e7685. doi: 10.1097/MD.0000000000007685

6. Wijsman R, Dankers F, Troost EGC, Hoffmann AL, van der Heijden EHFM, de Geus-Oei L, et al. Comparison of toxicity and outcome in advanced stage non-small cell lung cancer patients treated with intensity-modulated (chemo-) radiotherapy using IMRT or VMAT. *Radiother Oncol* (2017) 122:295–9. doi: 10.1016/j.radonc.2016.11.015

7. De Ruysscher D, Niedermann G, Burnet NG, Siva S, Lee AWM, Hegi-Johnson F. Radiotherapy toxicity. *Nat Rev Dis Primers* (2019) 5:13. doi: 10.1038/s41572-019-0064-5

8. Siva S, Hardcastle N, Kron T, Bressel M, Callahan J, MacManus MP, et al. Ventilation/Perfusion positron emission tomography–based assessment of radiation injury to lung. *Int J Radiat Oncol Biol Phys* (2015) 93:408–17. doi: 10.1016/j.ijrobp.2015.06.005

9. Partridge M, Yamamoto T, Grau C, Høyer M, Muren LP. Imaging of normal lung, liver and parotid gland function for radiotherapy. *Acta Oncol* (2010) 49:997–1011. doi: 10.3109/0284186X.2010.504735

10. Bucknell NW, Hardcastle N, Bressel M, Hofman MS, Kron T, Ball D, et al. Functional lung imaging in radiation therapy for lung cancer: A systematic review and meta-analysis. *Radiother Oncol* (2018) 129:196–208. doi: 10.1016/j.radonc.2018.07.014

11. Faught AM, Miyasaka Y, Kadoya N, Castillo R, Castillo E, Vinogradskiy Y, et al. Evaluating the toxicity reduction with computed tomographic ventilation functional avoidance radiation therapy. *Int J Radiat Oncol Biol Phys* (2017) 99:325–33. doi: 10.1016/j.ijrobp.2017.04.024

12. Farr KP, Kallehauge JF, Møller DS, Khalil AA, Kramer S, Bluhme H, et al. Inclusion of functional information from perfusion SPECT improves predictive value of dose-volume parameters in lung toxicity outcome after radiotherapy for non-small cell lung cancer: A prospective study. *Radiother Oncol* (2015) 117:9–16. doi: 10.1016/j.radonc.2015.08.005

13. Vinogradskiy Y, Rusthoven CG, Schubert L, Jones B, Faught A, Castillo R, et al. Interim analysis of a two-institution, prospective clinical trial of 4DCT-ventilation-based functional avoidance radiation therapy. *Int J Radiat Oncol Biol Phys* (2018) 102:1357–65. doi: 10.1016/j.ijrobp.2018.07.186

14. *Functional lung avoidance SPECT-guided radiation therapy of lung cancer - full text view - ClinicalTrials.gov* (2022). Available at: https://clinicaltrials.gov/ct2/show/NCT04676828.

15. Wilson JM, Partridge M, Hawkins M. The application of functional imaging techniques to personalise chemoradiotherapy in upper gastrointestinal malignancies. *Clin Oncol (R Coll Radiol)* (2014) 26:581–96. doi: 10.1016/j.clon.2014.06.009

16. Yamamoto T, Kabus S, Lorenz C, Mittra E, Hong JC, Chung M, et al. Pulmonary ventilation imaging based on 4-dimensional computed tomography: Comparison with pulmonary function tests and SPECT ventilation images. *Int J Radiat Oncol Biol Phys* (2014) 90:414–22. doi: 10.1016/j.ijrobp.2014.06.006

17. Waxweiler T, Schubert L, Diot Q, Faught A, Stuhr K, Castillo R, et al. A complete 4DCT-ventilation functional avoidance virtual trial: Developing strategies for prospective clinical trials. *J Appl Clin Med Phys* (2017) 18:144–52. doi: 10.1002/acm2.12086

18. Brennan D, Schubert L, Diot Q, Castillo R, Castillo E, Guerrero T, et al. Clinical validation of 4-dimensional computed tomography ventilation with pulmonary function test data. *Int J Radiat Oncol Biol Phys* (2015) 92:423–9. doi: 10.1016/j.ijrobp.2015.01.019

19. Vinogradskiy Y, Koo PJ, Castillo R, Castillo E, Guerrero T, Gaspar LE, et al. Comparison of 4-dimensional computed tomography ventilation with nuclear medicine ventilation-perfusion imaging: A clinical validation study. *Int J Radiat Oncol Biol Physs* (2014) 89:199–205. doi: 10.1016/j.ijrobp.2014.01.009

20. Pinder-Arabpour A, Jones B, Castillo R, Castillo E, Guerrero T, Goodman K, et al. Characterizing spatial lung function for esophageal cancer patients undergoing radiation therapy. *Int J Radiat Oncol Biol Phys* (2019) 103:738–46. doi: 10.1016/j.ijrobp.2018.10.024

21. Latifi K, Forster KM, Hoffe SE, Dilling TJ, van Elmpt W, Dekker A, et al. Dependence of ventilation image derived from 4D CT on deformable image registration and ventilation algorithms. *J Appl Clin Med Phys* (2013) 14:4247. doi: 10.1120/jacmp.v14i4.4247

22. Klein S, Staring M, Murphy K, Viergever MA, Pluim JPW. Elastix: A toolbox for intensity-based medical image registration. *IEEE T Med Imaging* (2010) 29:196–205. doi: 10.1109/TMI.2009.2035616

23. Wang R, Zhang S, Yu H, Lin S, Zhang G, Tang R, et al. Optimal beam arrangement for pulmonary ventilation image-guided intensity-modulated radiotherapy for lung cancer. *Radiat Oncol* (2014) 9:184. doi: 10.1186/1748-717X-9-184

24. Reinhardt JM, Ding K, Cao K, Christensen GE, Hoffman EA, Bodas SV. Registration-based estimates of local lung tissue expansion compared to xenon CT measures of specific ventilation. *Med Image Anal* (2008) 12:752–63. doi: 10.1016/j.media.2008.03.007

25. Yijun AN, Biao Z, Yutao Z, Liqiu HE, Kewei T, Yi Y. VMAT versus TOMO in dosimetric parameters for treatment of middle thoracic esophageal cancer. *Acad J Chin PLA Med Sch* (2018) 39:312–5. doi: 10.3969/j.issn.2095-5227.2018.04.011

26. Zhou P. *Research on protection of lung functions in patients with esophageal cancer radiotherapy based on 4D-CT ventilation images*. Guangzhou Medical University (2022).

27. Yu D, Bai Y, Feng Y, Wang L, Yun W, Li X, et al. Which bone marrow sparing strategy and radiotherapy technology is most beneficial in bone marrow-sparing intensity modulated radiation therapy for patients with cervical cancer? *Front Oncol* (2020) 10:554241. doi: 10.3389/fonc.2020.554241

28. Hanania AN, Mainwaring W, Ghebre YT, Hanania NA, Ludwig M. Radiation-induced lung injury: Assessment and management. *Chest* (2019) 156:150–62. doi: 10.1016/j.chest.2019.03.033

29. Shao Y, Chen H, Wang H, Duan Y, Feng A, Huang Y, et al. Investigation of predictors to achieve acceptable lung dose in T-shaped upper and middle esophageal cancer with IMRT and VMAT. *Front Oncol* (2021) 11:735062. doi: 10.3389/fonc.2021.735062

30. Bahig H, Campeau M, Lapointe A, Bedwani S, Roberge D, de Guise J, et al. Phase 1-2 study of dual-energy computed tomography for assessment of pulmonary function in radiation therapy planning. *Int J Radiat Oncol Biol Phys* (2017) 99:334–43. doi: 10.1016/j.ijrobp.2017.05.051

31. Vinogradskiy Y, Castillo R, Castillo E, Schubert L, Jones BL, Faught A, et al. Results of a multi-institutional phase 2 clinical trial for 4DCT-ventilation functional avoidance thoracic radiation therapy. *Int J Radiat Oncol Biol Phys* (2021) 112(4):986–95. doi: 10.1016/j.ijrobp.2021.10.147

32. Yan-li Y, Bao-sheng LI, Yong Y, Jin-hu C, Tao S, Hong-fu S. Dosimetric comparison of three-dimensional conformal radiotherapy, intensity-modulated radiotherapy and RapidArc in treatment of thoracic esophageal cancer. *Chin Radiol Med Prot* (2012) 32:65–9. doi: 10.3760/cma.j.issn.0254-5098.2012.01.016

33. Gao M, Li Q, Ning Z, Gu W, Huang J, Mu J, et al. Dosimetric comparison between step-shoot intensity-modulated radiotherapy and volumetric-modulated arc therapy for upper thoracic and cervical esophageal carcinoma. *Med Dosim* (2016) 41:131–5. doi: 10.1016/j.meddos.2015.10.007

34. Yamamoto T, Kabus S, von Berg J, Lorenz C, Keall PJ. Impact of four-dimensional computed tomography pulmonary ventilation imaging-based functional avoidance for lung cancer radiotherapy. *Int J Radiat Oncol Biol Phys* (2011) 79:279–88. doi: 10.1016/j.ijrobp.2010.02.008

frontiers | Frontiers in Oncology

TYPE Original Research
PUBLISHED 08 September 2022
DOI 10.3389/fonc.2022.936684

OPEN ACCESS

EDITED BY
Dinesh Thotala,
Washington University in St. Louis, United States

REVIEWED BY
Hsin-Hua Lee,
Kaohsiung Medical University, Taiwan
Yu-Jie Huang,
Kaohsiung Chang Gung Memorial Hospital, Taiwan

*CORRESPONDENCE
Zefen Xiao
xiaozefen@sina.com

SPECIALTY SECTION
This article was submitted to Radiation Oncology, a section of the journal Frontiers in Oncology

RECEIVED 05 May 2022
ACCEPTED 22 August 2022
PUBLISHED 08 September 2022

CITATION
Ni W, Xiao Z, Zhou Z, Chen D, Feng Q, Liang J and Lv J (2022) Severe radiation-induced lymphopenia during postoperative radiotherapy or chemoradiotherapy has poor prognosis in patients with stage IIB-III after radical esophagectomy: A *post hoc* analysis of a randomized controlled trial.
Front. Oncol. 12:936684.
doi: 10.3389/fonc.2022.936684

Severe radiation-induced lymphopenia during postoperative radiotherapy or chemoradiotherapy has poor prognosis in patients with stage IIB-III after radical esophagectomy: A *post hoc* analysis of a randomized controlled trial

Wenjie Ni[1,2], Zefen Xiao[1]*, Zongmei Zhou[1], Dongfu Chen[1], Qinfu Feng[1], Jun Liang[1] and Jima Lv[1]

[1]Department of Radiation Oncology, National Cancer Center/National Clinical Research Center for Cancer/Cancer Hospital, Chinese Academy of Medical Sciences and Peking Union Medical College, Beijing, China, [2]Department of Radiation Oncology, Beijing Shijitan Hospital, Capital Medical University, Beijing, China

Objective: To investigate whether radiation-induced lymphopenia (RIL) affects survival and identify the predictors of RIL in postoperative esophageal cancer.

Materials and methods: *Post hoc* analysis was conducted on data from 116 patients with esophageal cancer from a randomized controlled trial comparing adjuvant therapy with surgery alone. Doses of 54 Gy in 27 fractions was delivered in the postoperative radiotherapy (PORT) group and 50.4 Gy in 28 fractions combined with chemotherapy was delivered in postoperative concurrent chemoradiotherapy (POCRT) group. Blood counts were obtained before, during, and at first follow-up after treatment. Lymphopenia was graded per version 4.03 of the Common Terminology Criteria for Adverse Events. Disease-free survival (DFS) and overall survival (OS) were analyzed using the Kaplan-Meier method, and compared between groups using the log-rank test. Receiver operating characteristic curves identified thresholds for preventing grade 4 (G4) lymphopenia.

Results: Median follow-up duration was 56.0 months. During treatment, 16 patients (13.8%) had G4 lymphopenia. All cases of G4 lymphopenia occurred in

group PORT (30.2% vs 0.0%, p<0.001). Baseline absolute lymphocyte count was comparable between G1-3 and G4 patients (2.0 ± 0.8 *10^9/L vs 1.7 ± 0.5 *10^9/L; p=0.101). The 3-year DFS was significantly lower in group G4 lymphopenia than that in group G1-3 (31.3% vs 57.6%, p=0.036). The 3-year OS was comparable between both groups (50.0% vs 66.5%, p=0.095). Logistic regression analysis revealed that exposed more thoracic marrow (TM V20 ≥75%; TVB V20 ≥71%), heart (V15 ≥40%) and PTV (volume ≥507 ml) were associated with G4 lymphopenia (p<0.05).

Conclusions: G4 RIL had poor disease-free survival, which may be related to more dose exposure of thoracic marrow and heart due to larger PTV. Reasonably reducing the radiation field combined with concurrent chemotherapy, or radiation dose constraints for these normal tissues may be sufficient to decrease the incidence of G4 lymphopenia, but further prospective trials are needed to verify the results.

Clinical Trial Registration: clinicaltrials.gov, identifier NCT02279134

KEYWORDS

esophageal cancer, postoperative radiotherapy, lymphopenia, thoracic marrow, survival

Introduction

According to the Worldwide Esophageal Cancer Collaboration Investigators in 2016, about 58.7% of patients with esophageal cancer underwent surgical resection first (1). About 20% of patients with R0 resection in our hospital received postoperative radiotherapy. Especially for pathological stage III or lymph node positive esophageal cancer, it is reported that postoperative radiotherapy can significantly reduce the local regional recurrence rate and improve the survival rate (2–5). Furthermore, our research group has always devoted to the esophageal cancer clinical research after surgery alone, and has conducted many data analyses and improvement on the postoperative radiation field. Radiation therapy is an essential component of the treatment of esophageal cancer. However, it is reported that radiation may suppress host immunity, manifesting as lymphopenia (6, 7). Lymphocytes are extremely radiosensitive; therefore, relatively low doses can result in significant depletion of lymphocyte number (8). Radiation-induced lymphopenia (RIL) has been reported to adversely affect survival of patients with solid malignancies, such as glioma, lung cancer, and breast cancer (9–11). Severe lymphopenia during chemoradiotherapy is a strong predictor of poor outcomes and pathologic response rates in esophageal cancer (12–14). However, to the best of our knowledge, no study has been conducted on postoperative radiation therapy in esophageal cancer. In this study, we aimed to investigate whether RIL could affect survival, and identify the predictors of severe lymphopenia in postoperative esophageal cancer.

Materials and methods

Patients

This study was a *post hoc* analysis of data from a randomized controlled trial (NCT02279134) that was conducted from October 2014 through December 2019. The original trial recruited a total of 172 patients with esophageal cancer who had undergone radical esophagectomy. All patients were pathologically confirmed as stage IIB-III. The patients were randomly assigned to undergo surgery alone (SA group; n = 54), surgery and postoperative radiotherapy (PORT group; n = 54), or surgery and postoperative concurrent chemoradiotherapy (POCRT group; n = 64). The protocol has been described in detail elsewhere (15). Only patients who underwent PORT and POCRT were included in this study.

Laboratory data

For the present study, the absolute lymphocyte count (ALC) of patients at different time points were collected from the case report forms. The ALC values at baseline (pre-ALC; within 1 week before radiation therapy), during radiation therapy (tested once a week), and within 3 months after treatment were available. Lymphopenia was graded according to version 4.03 of the Common Terminology Criteria for Adverse Events. The nadir ALC during the course of radiation therapy was classified

as grade 0 (G0, ALC ≥ 1.0 × 10^9/L), grade 1 (G1, 0.8 ≤ ALC < 1.0 × 10^9/L), grade 2 (G2, 0.5≤ ALC < 0.8 × 10^9/L), grade 3 (G3, 0.2 ≤ ALC < 0.5 × 10^9/L), or grade 4 (G4, ALC < 0.2 × 10^9/L).

Dose-volume parameters

Thoracic marrow (TM), including sternum and thoracic vertebral body (TVB; the superior margin was 1.0 cm above the planning target volume (PTV) dose line and the inferior margin was the lower margin of T12 or PTV dose line), was contoured with the heart, lung, and spinal cord (Figure 1A). The relative volume of normal tissues at risk of receiving x Gy (V_x) along with the mean dose (D_{mean}) was calculated from the dose volume histogram.

Treatment

Postoperative concurrent chemoradiotherapy

The borders of the clinical target volume (CTV) included the superior margin, which was the cricothyroid membrane for upper-thoracic tumors or the upper margin of the first thoracic vertebral body for middle-thoracic tumors. The inferior margin was 3.0 cm below the subcarina or the lower margin of the tumor bed (only for T4 lesions), including the lower cervical, bilateral supraclavicular region, and mediastinal stations 1R/L, 2R/L, 3p, 4R/L, 7, and part of 8 (Figure 1B). The prescription dose of PTV was 50.4 Gy (1.8 Gy/28 f). Paclitaxel (135-150 mg/m^2) and cisplatin or nedaplatin (50-75 mg/m^2) were administered concurrently. Chemotherapy was repeated every 28 days for two courses in the absence of disease progression or unacceptable toxicity.

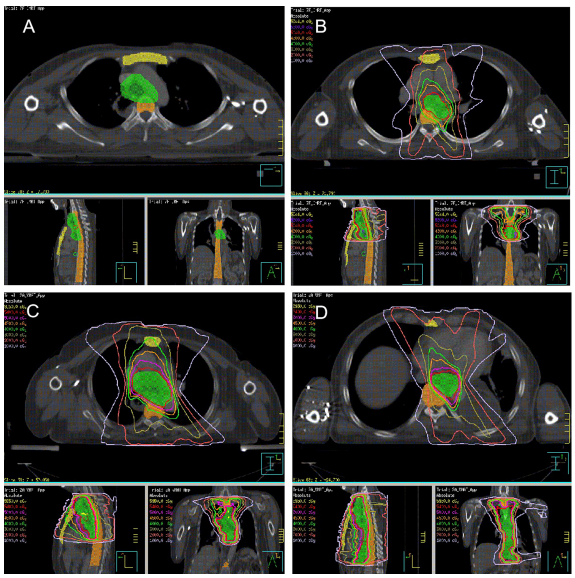

FIGURE 1
Radiation target (A. Thoracic marrow; yellow area, sternum; orange area, thoracic vertebral body; green area, PTV; **(B)** POCRT; **(C)** PORT, Upper-thoracic esophagus or Middle-thoracic esophagus with metastasis in 0 to 2 regional lymph nodes or metastasis in ≥ 3 regional lymph nodes in the mediastinum; **(D)** PORT, Lower-thoracic esophagus or middle-thoracic esophagus with metastasis in ≥ 3 regional lymph nodes distributed in two areas).

Postoperative radiotherapy

The CTV was based on tumor and positive node location during surgery and pathological examination. The PTV was generated using a uniform 0.5 cm expansion around the CTV. Contouring of the CTV for tumors in different locations has been described in detail previously (15). Figures 1C, D illustrates the radiation target. The prescription dose was 54 Gy in 27 fractions of 2.0 Gy.

Follow-up

After treatment, patients were followed up every 3 months for the first 2 years, every 6 months for the next 2 years, and once a year thereafter. Recurrence was confirmed using diagnostic imaging or histopathology.

Tumor recurrence in regional lymph nodes was defined based on the Union for International Cancer Control (7th edition) criteria. The regional lymph node groups included supraclavicular, mediastinal, and celiac area. Distant metastasis was defined as spread of tumor to distant organs or non-regional lymph nodes.

Statistical analysis

Disease-free survival (DFS) was defined as the period from surgery to date of the first recurrence or death from any cause or censorship. Overall survival (OS) was defined as the interval from surgery to death from any cause or censorship. The Kaplan–Meier method was used to calculate DFS and OS, and the log-rank was used to determine the significance of differences. Logistic regression analysis was used to identify the factors of grade 4 lymphopenia. Receiver operating characteristic (ROC) curves identified thresholds to preventing G4 lymphopenia. All statistical analyses were performed using SPSS 20.0 (IBM Corp., Armonk, NY, USA). Two-tailed p<0.05 denoted statistically significant difference.

Results

Patients characteristics

Two patients lacking complete blood count data were excluded. Therefore, a total of 116 patients were included in

TABLE 1 Comparison of patient characteristics between PORT and POCRT.

	Frequency, n (%)	PORT, n (%)	POCRT, n (%)	P
Gender				1.000
Male	104 (89.7)	48 (90.6)	56 (88.9)	
Female	12 (10.3)	5 (9.4)	7 (11.1)	
Age (mean ± SD, years)				0.326
	57.3 ± 6.3	57.9 ± 6.9	56.7 ± 5.7	
Kps				0.136
80	64 (55.2)	34 (64.2)	30 (47.6)	
90	50 (43.1)	18 (34.0)	32 (50.8)	
100	2 (1.7)	1 (1.9)	1 (1.6)	
Tumor location				0.906
Upper	6 (5.2)	3(5.7)	3 (4.8)	
Middle	49 (42.2)	21(39.6)	28 (44.4)	
Lower	61 (52.6)	29 (54.7)	32 (50.8)	
TNM stage (UICC 7th)				0.262
IIB	24 (20.7)	13 (24.5)	11 (17.5)	
IIIA	47 (40.5)	17 (32.1)	30 (47.6)	
IIIB	30 (25.9)	17 (32.1)	13 (20.6)	
IIIC	15 (12.9)	6 (11.3)	9 (14.3)	
Differentiation degree				0.221
Well	9 (7.8)	6 (11.3)	3(4.8)	
Moderate	61 (52.6)	24(45.3)	37(58.7)	
Poor	46 (39.7)	23(43.4)	23(36.5)	
Radiation modality				0.562
IMRT	74 (63.8)	32 (60.4)	42 (66.7)	
VMAT	42 (36.2)	21 (39.6)	21 (33.3)	
PTV volume (mean ± SD, ml)				<0.001
	519.5 ± 118.7	582.5 ± 109.5	464.8 ± 97.9	
Lymphopenia				<0.001
G1-3	100 (86.2)	37 (69.8)	63 (100)	
G4	16 (13.8)	16 (30.2)	0 (0)	

PORT, postoperative radiotherapy; POCRT, postoperative concurrent chemoradiotherapy; G, grade; SD, standard deviation; Kps, Karnofsky performance score; UICC, Union for International Cancer Control; IMRT, intensity-modulated radiotherapy; VAMT, volumetric modulated arc therapy; PTV, planning target volume.

the analysis. Table 1 shows the patients characteristics based on the treatment modality, 53 and 63 patients were assigned to the PORT and POCRT groups, respectively. The volume of PTV in the PORT and POCRT group were 582.5 ± 109.5 ml and 464.8 ± 97.9 ml, respectively ($p < 0.001$). Table 2 shows the demographic, tumor, and treatment characteristics between lymphopenic grades. Most of patients were male (89.7%); the average age was 57.3 years; and about half (44.8%) had a Karnofsky performance score of ≥90. Majority of patients (79.3%) had stage III disease. More patients underwent intensity-modulated radiotherapy (63.8%) rather than volumetric modulated arc therapy (36.2%). The ALC before treatment was comparable between patients in the G1-3 and G4 groups (2.0 ± 0.8 $*10^9$/L vs 1.7 ± 0.5 $*10^9$/L; p=0.101). All patients underwent different degrees of lymphopenia during treatment: G1 in 3 (2.6%) patients, G2 in 22 (19.0%) patients, G3 in 75 (64.7%) patients, and G4 in 16 (13.8%) patients. Patients with G4 lymphopenia only underwent PORT. The volume and mean dose of PTV were higher in group G4 ($p < 0.05$). All other characteristics were well balanced between the two groups.

Correlation between lymphopenia and survival

The median time of radiation therapy was 5.4 weeks. The ALC decreased gradually during treatment, and reached the nadir in the fifth week (Figure 2). The last follow-up date was January 25, 2021; the median follow-up period was 56.0 months. The median OS time was 33.2 months in group G4; however, the OS in group G1-3 was not reached. The 1-year, 3-year, and 5-year OS were 81.3%, 50.0%, and 30.0%, respectively, in the G4 group, compared with 92.0%, 66.5%, and 57.7%, respectively, in the G1-3 group (HR: 0.486, 95% CI: 0.208-1.133, p=0.095). The median DFS time was 17.4 months in group G4, but not attained in group G1-3. The 1-year, 3-year, and 5-year DFS were 62.5%, 31.3%, and 23.4%, respectively, in the G4 group, compared with

TABLE 2 Comparison of patient characteristics between lymphopenic grades.

	Frequency, n (%)	G1–3, n (%)	G4, n (%)	P
Gender				0.671
Male	104 (89.7)	90 (90.0)	14 (87.5)	
Female	12 (10.3)	10 (10.0)	2(12.5)	
Age (mean ± SD, years)				0.555
	57.3 ± 6.3	57.1 ± 6.2	58.1 ± 6.8	
Kps				0.241
80	64 (55.2)	52 (52.0)	12 (75.0)	
90	50 (43.1)	46(46.0)	4 (25.0)	
100	2 (1.7)	2(2.0)	0 (0.0)	
Tumor location				0.963
Upper	6 (5.2)	5 (5.0)	1 (6.2)	
Middle	49 (42.2)	42 (42.0)	7 (43.8)	
Lower	61 (52.6)	53 (53.0)	8 (50.0)	
TNM stage (UICC 7th)				0.610
IIB	24 (20.7)	22 (22.0)	2(12.5)	
IIIA	47 (40.5)	38 (38.0)	9(56.2)	
IIIB	30 (25.9)	27 (27.0)	3 (18.8)	
IIIC	15 (12.9)	13 (13.0)	2 (12.5)	
Differentiation degree				0.082
Well	9 (7.7)	6 (6.0)	3 (18.8)	
Moderate	61 (52.6)	56 (56.0)	5 (31.2)	
Poor	46 (39.7)	38 (38.0)	8 (50.0)	
Radiation modality				0.315
IMRT	74 (63.8)	62 (62.0)	12(75.0)	
VMAT	42 (36.2)	38 (38.0)	4 (25.0)	
PTV volume (mean ± SD, ml)				0.006
	519.5 ± 118.7	507.3 ± 119.8	594.6 ± 79.9	
PTV mean dose (mean ± SD, Gy)				0.001
	55.0 ± 2.1	54.7 ± 2.1	56.6 ± 1.7	
Concurrent chemotherapy				<0.001
Yes	63 (54.3)	63 (63.0)	0 (0.0)	
No	53 (45.7)	37 (37.0)	16 (100.0)	
Pre-ALC (mean ± SD, $*10^9$/L)				0.101
	2.0 ± 0.8	2.0 ± 0.8	1.7 ± 0.5	

G, grade; SD, standard deviation; Kps, Karnofsky performance score; UICC, Union for International Cancer Control; IMRT, intensity-modulated radiotherapy; VAMT, volumetric modulated arc therapy; PTV, planning target volume; ALC, absolute lymphocyte count.

77.0%, 57.6%, and 52.2%, respectively, in the G1-3 group (HR: 0.425, 95% CI: 0.191-0.946, p=0.036) (Figure 3).

Predictors of lymphopenia

Table 3 shows the relationship between lymphopenia during treatment and different clinical characteristics. Patients age, gender, and radiation technique were not significantly associated with the risk of G4 lymphopenia. In terms of dosimetric predictors, the radiation dose of TM, TVB, Heart, PTV, and PTV volume were all associated with higher rates of G4 lymphopenia (all p<0.05). Sternum D_{mean}, V10, and V20 were predictors of G4 lymphopenia (p<0.05).

We further explored the optimal cut-off points of the dosimetric variables significantly associated with G4 lymphopenia (TM, TVB, Heart, PTV Volume, PTV D_{mean}) using ROC curve analysis (Table 4). The ROC curves for partial important variables were available on line (Supplementary Figures 1–4).

Discussion

As we all know, the lymph node metastasis of esophageal cancer occurs early and widely, and the recurrence of lymph nodes after radical resection is the main reason, accounting for 23.8%-58% (16), especially for patients with pathological positive lymph nodes. Therefore, how to balance the effective radiation field is the focus of our research. This *post hoc* analysis is from a prospective randomized controlled trial after the third modified radiation field, which showed that postoperative adjuvant therapy could improve the survival rate compared with surgery alone.

Our study revealed that DFS was worse in patients with G4 lymphopenia during PORT for esophageal cancer. The predictors

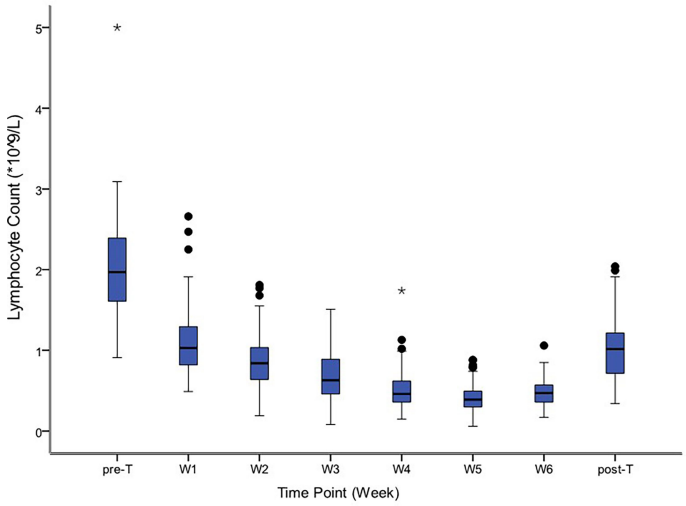

FIGURE 2
Distribution of absolute lymphocyte counts before, during and after treatment. The symbol * means outlier.

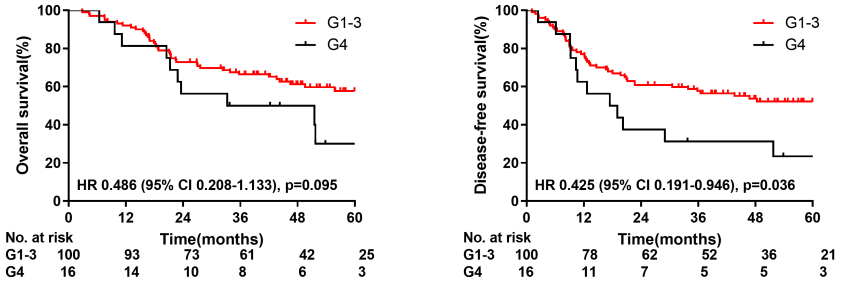

FIGURE 3
Overall survival and disease-free survival for patients with radiation induced lymphopenia.

of G4 RIL include the radiation volume of PTV and the adjacent hematopoietic system, such as sternum, thoracic vertebral body and heart, however it seems to have little relationship with chemotherapy. Lymphopenia is known to be one of the manifestations of immunosuppression. Many clinical studies have shown that it is a predictor of poor prognosis in pancreatic cancer, brain tumor, non-small cell lung cancer, and nasopharyngeal carcinoma (17–20). According to recent studies, patients with lymphopenia during radical or neoadjuvant chemoradiotherapy of esophageal cancer have a poor prognosis and low complete pathologic response rate (12–14). Our study showed that lymphocytes were extremely sensitive to radiation. Lymphocytes decreased at the beginning of radiotherapy and sharply with the accumulation of radiation dose. Radiation doses, as low as 2 Gy, can inactivate about 50% of circulating lymphocytes in the radiation field, resulting in RIL during radiotherapy (21, 22). In a malignant glioma model, 60 Gy prescription dose irradiates the brain at a dose of 2 Gy per fraction, resulting in an average dose of 2 Gy for circulating lymphocytes, and almost all circulating blood is at least irradiated 0.5 Gy (8). T lymphocytes are an important part of cellular immunity. Cytotoxic CD8+ T lymphocytes act as effector cells; they directly kill abnormal cells and secrete proinflammatory cytokines (23). Therefore, radiation-induced reduction of CD8+ T lymphocytes may have a negative effect on cell-mediated immunity, because even if the number of lymphocytes recovers after radiotherapy, the newly produced immature T lymphocytes cannot produce antitumor effects. Regulatory T cells (Tregs),

TABLE 3 Logistic regression analysis of factors associated with grade 4 lymphopenia.

	OR	95% CI	P
Age	1.026	0.942–1.118	0.552
Male vs. Female	1.286	0.255–6.492	0.761
TM Dmean	1.176	1.084–1.275	<0.001
TVB Dmean	1.159	1.078–1.246	<0.001
Sternum Dmean	1.109	1.001–1.228	0.048
TM V5	1.091	1.040–1.144	<0.001
TVB V5	1.075	1.034–1.118	<0.001
Sternum V5	2.421	0.576–10.189	0.228
TM V10	1.087	1.039–1.137	<0.001
TVB V10	1.073	1.034–1.114	<0.001
Sternum V10	1.225	1.040–1.443	0.015
TM V20	1.083	1.040–1.127	<0.001
TVB V20	1.074	1.036–1.113	<0.001
Sternum V20	1.045	1.004–1.088	0.032
TM V30	1.063	1.030–1.097	<0.001
TVB V30	1.061	1.031–1.091	<0.001
Sternum V30	0.979	0.940–1.020	0.307
TM V40	1.057	1.019–1.096	0.003
TVB V40	1.057	1.023–1.092	0.001
Sternum V40	0.995	0.957–1.036	0.815
TM V50	1.100	1.018–1.189	0.016
TVB V50	1.091	1.018–1.170	0.014
Sternum V50	1.037	0.959–1.123	0.363
Heart Dmean	1.152	1.062–1.251	0.001
Heart V15	1.056	1.024–1.090	0.001
Heart V20	1.050	1.023–1.078	<0.001
Heart V30	1.083	1.036–1.133	<0.001
Heart V40	1.122	1.049–1.201	0.001
Heart V50	1.269	1.112–1.449	<0.001
PTV Volume	1.006	1.002–1.011	0.009
PTV Dmean	1.566	1.170–2.095	0.003
IMRT vs. VMAT	0.544	0.164–1.808	0.320

OR, odd ratio; CI, confidence interval; TM, thoracic marrow; TVB, thoracic vertebral body; PTV, planning target volume; Dmean, mean dose; Vx, relative volume of receiving x Gy.

another T cell subtype, are known to be involved in immunosuppression (24). Muroyama et al. (25) found that the phenotypic and functional inhibitory Treg cells number increases in a tumor microenvironment after irradiation of tumor with 10 Gy in mice. According to Oweida et al. (26, 27), the combination of radiotherapy and immunotherapy with Treg targeted inhibitors can inhibit tumor growth. Since Treg is relatively resistant to radiation, surviving Treg cells are usually assumed to have the ability to inhibit the recovery of effector T cells during lymphocyte recovery (28). Clinical study findings also showed that a high proportion of CD8+ T/Treg cells predicted a better therapeutic response (29). Therefore, the effect of lymphopenia on the survival of patients could be mainly due to the extensive effect of radiotherapy on the number and function of effector T lymphocytes in blood circulation. Moreover, Treg cells are radiation-resistant and affect the recovery of effector T lymphocytes after radiotherapy, resulting in the decline of cellular immune function, early recurrence, and worse prognosis.

Lymphopenia is mainly due to the reduction in number of mature lymphocytes in peripheral blood and the production of lymphocytes in hematopoietic organs after radiation. The heart is highly vascularized. The thoracic marrow is the main hematopoietic organ of adults. The heart and sternum are located in front of the esophagus and the thoracic vertebra is located behind the esophagus. In this study, we found that the irradiated volume and dose of thoracic vertebra, heart, and PTV during postoperative radiotherapy of esophageal cancer were the main factors causing G4 lymphopenia. Fang (13, 30) and van Rossum (31) reported that G4 lymphocytes decreased more significantly in patients with larger PTV in radical

TABLE 4 ROC curve cut-off points for prevention of grade 4 lymphopenia.

	Cut-off point	AUC	P
TM Dmean	< 32Gy	0.837	< 0.001
TM V5	< 79%	0.853	< 0.001
TM V10	< 78%	0.847	< 0.001
TM V20	< 75%	0.860	< 0.001
TM V30	< 60%	0.813	< 0.001
TM V40	< 35%	0.758	0.001
TM V50	< 11%	0.698	0.011
TVB Dmean	< 32Gy	0.850	< 0.001
TVB V5	< 74%	0.863	< 0.001
TVB V10	< 74%	0.871	< 0.001
TVB V20	< 71%	0.892	< 0.001
TVB V30	< 62%	0.854	< 0.001
TVB V40	< 35%	0.788	< 0.001
TVB V50	< 17%	0.700	0.010
Heart Dmean	< 14Gy	0.809	< 0.001
Heart V15	< 40%	0.847	< 0.001
Heart V20	< 48%	0.823	< 0.001
Heart V30	< 23%	0.795	< 0.001
Heart V40	< 10%	0.781	< 0.001
Heart V50	< 2%	0.818	< 0.001
PTV Volume	< 507ml	0.742	0.002
PTV Dmean	< 55Gy	0.749	0.001

ROC, receiver operating characteristic; AUC, area under curve; TM, thoracic marrow; TVB, thoracic vertebral body; PTV, planning target volume; Dmean, mean dose; Vx, relative volume of receiving x Gy.

chemoradiotherapy of esophageal cancer, which is consistent with the results of our study. Davuluri (12) reported that the incidence of G4 lymphopenia in patients with lesions in the lower sections of the esophagus is higher than that in patients with lesions in the middle and upper sections of the esophagus. Considering that the lesions in the lower sections of the esophagus are adjacent to the heart and spleen, which are rich in blood, a large number of lymphocytes are irradiated. Saito (32) previously reported that the average irradiation dose of spleen in chemoradiotherapy of esophageal cancer can predict G4 lymphopenia. Besides, the exposure of thoracic vertebra in esophageal cancer radiotherapy has been reported to be related to more grade 3 hematological toxicity (33–35). According to Newman (36), lymphopenia during chemoradiotherapy of esophageal cancer is closely related to the volume of irradiated thoracic vertebral body, which is consistent with our findings.

Proton radiotherapy in malignant tumors has been more widely used than photon radiotherapy for its physical advantages. Mohan (37) reported that proton radiotherapy could better reduce the incidence of G3 lymphopenia in glioblastoma than photon radiotherapy. Nichols (38) also revealed that proton radiotherapy could better reduce the mean radiation dose of the lungs by 33% and bone marrow V10 by 30% than photon radiotherapy. Shiraishi (39) and Liu (40) reported that proton radiation to the heart has lower doses than photon radiation. Several studies have reported that proton radiotherapy has a lower incidence of G4 lymphopenia than photon radiotherapy during chemoradiotherapy in esophageal cancer (30, 41, 42). Our study reveals that a greater volume and dose of PTV has a higher irradiation dose of thoracic marrow and heart, which results in a more obvious decrease in the number of peripheral blood lymphocytes.

Our study reported the cut-off values of PTV, heart, and thoracic marrow necessary to prevent the incidence of G4 lymphopenia. According to the prospective randomized controlled trial by Ni et al. (43), for patients with pathological stage IIB–III esophageal squamous cell carcinoma after radical surgery, POCRT, which reduced the radiation field to 3 cm below the carina and reduced the radiation dose to 50.4 Gy, did not increase the in- or out-of-field recurrence. Additionally, the survival rate was more comparable than with the PORT. POCRT appears to be an effective and safe treatment. Based on findings from the previous and present trials, POCRT can be considered for these patients to ensure a smaller PTV volume and dose to reduce the exposure of the heart and thoracic marrow and prevent severe lymphopenia. In the event where POCRT cannot be performed, attention should be paid to the protection of the heart and thoracic marrow, and corresponding radiation dose constraints should be given to prevent lymphopenia. Therefore, under the condition of reasonably reducing the postoperative irradiation field, synchronous chemotherapy should be strengthened to reduce the impact on lymphocytes and reduce the impact on survival. Of course, the postoperative irradiation field should be designed according to the recurrence sites and rates after esophagectomy, and the irradiation dose of normal tissue should be considered at the same time, so as to reduce the recurrence rate and convert it into the benefit of survival without increasing toxic and side effects.

In addition, actively search for drugs to enhance immunity or promote lymphocyte recovery is the direction of future research. Zheng (44) found that after a single low-dose whole-body irradiation in the mouse lung melanoma model, cinnamon effectively improved the imbalance of T cell subsets and promoted effective antitumor immunity by promoting the proliferation of Th1 and inhibiting the expansion of Th17 and Treg cells. In addition, an experimental study has also shown that exogenous IL-7 delivered to the irradiated animal model can not only restore the lymphocyte count but also enhance the antitumor effect. Exogenous IL-7 is helpful to overcome RIL and improve the therapeutic effect combined with radiotherapy (45). However, these findings need to be verified by future clinical studies.

The limitation of this study is that the sample size is relatively small. We expect to continue accumulating more cases and prolong the follow-up time.

Conclusion

G4 lymphopenia had poor DFS, and the radiation volume of thoracic marrow, heart, and PTV may predict G4 lymphopenia in postoperative esophageal cancer. Radiation dose constraints for these normal tissues may be sufficient to decrease G4 lymphopenia, but further prospective trials are needed to verify the results.

Data availability statement

The original contributions presented in the study are included in the article/Supplementary Material. Further inquiries can be directed to the corresponding author.

Ethics statement

The studies involving human participants were reviewed and approved by Ethics Committee of Cancer Institute and Hospital, Chinese Academy of Medical Sciences, Beijing. The patients/participants provided their written informed consent to participate in this study.

Author contributions

Conceptualization: ZX. Project planning: WN, ZX. Writing: WN. Statistical counseling: WN. Editing: ZX, ZZ, DC, QF, JL, JML. All authors provided review of the manuscript. All authors read and approved the final manuscript.

Funding

This work were supported by the Capital Fund for Health Improvement and Research [grant number 2016-2-4021] and Youth Fund of Beijing Shijitan Hospital (grant number 2020-q12). The manuscript has been peer reviewed by the funding body. The funding source has no role in study design, data collection, analysis, interpretation, the writing of the manuscript, or the decision to submit the current study.

Acknowledgments

We thank all participants of this trial, and all investigators who devote their time and passion in the implementation of this study.

Conflict of interest

The authors declare that the research was conducted in the absence of any commercial or financial relationships that could be construed as a potential conflict of interest.

Publisher's note

Supplementary material

The Supplementary Material for this article can be found online at: https://www.frontiersin.org/articles/10.3389/fonc.2022.936684/full#supplementary-material

References

1. Rice TW, Ishwaran H, Hofstetter WL, Kelsen DP, Apperson-Hansen C, Blackstone EH. Recommendations for pathologic staging (pTNM) of cancer of the esophagus and esophagogastric junction for the 8th edition AJCC/UICC staging manuals. *Dis Esophagus* (2016) 29(8):897–905. doi: 10.1111/dote.12533

2. Xu Y, Liu J, Du X, Sun X, Zheng Y, Chen J, et al. Prognostic impact of postoperative radiation in patients undergoing radical esophagectomy for pathologic lymph node positive esophageal cancer. *Radiat Oncol* (2013) 8:116. doi: 10.1186/1748-717X-8-116

3. Shridhar R, Weber J, Hoffe SE, Almhanna K, Karl R, Meredith K. Adjuvant radiation therapy and lymphadenectomy in esophageal cancer: A SEER database analysis. *J Gastrointest Surg* (2013) 17(8):1339–45. doi: 10.1007/s11605-013-2192-7

4. Zhang W, Liu X, Xiao Z, Zhang H, Chen D, Feng Q, et al. Postoperative intensity-modulated radiotherapy improved survival in lymph node-positive or stage III thoracic esophageal squamous cell carcinoma. *Oncol Res Treat* (2015) 38 (3):97–102. doi: 10.1159/000375391

5. Yu S, Zhang W, Ni W, Xiao Z, Wang Q, Zhou Z, et al. A propensity-score matching analysis comparing long-term survival of surgery alone and postoperative treatment for patients in node positive or stage III esophageal squamous cell carcinoma after R0 esophagectomy. *Radiother Oncol* (2019) 140:159–66. doi: 10.1016/j.radonc.2019.06.020

6. Santin AD, Hermonat PL, Ravaggi A, Bellone S, Roman J, Pecorelli S, et al. Effects of concurrent cisplatinum administration during radiotherapy vs. radiotherapy alone on the immune function of patients with cancer of the uterine cervix. *Int J Radiat Oncol Biol Phys* (2000) 48(4):997–1006. doi: 10.1016/S0360-3016(00)00769-0

7. Grossman SA, Ye X, Lesser G, Sloan A, Carraway H, Desideri S, et al. Immunosuppression in patients with high-grade gliomas treated with radiation and temozolomide. *Clin Cancer Res* (2011) 17(16):5473–80. doi: 10.1158/1078-0432.CCR-11-0774

8. Yovino S, Kleinberg L, Grossman SA, Narayanan M, Ford E. The etiology of treatment-related lymphopenia in patients with malignant gliomas: Modeling radiation

dose to circulating lymphocytes explains clinical observations and suggests methods of modifying the impact of radiation on immune cells. *Cancer Invest* (2013) 31(2):140–4. doi: 10.3109/07357907.2012.762780

9. Grossman SA, Ellsworth S, Campian J, Wild AT, Herman JM, Laheru D, et al. Survival in patients with severe lymphopenia following treatment with radiation and chemotherapy for newly diagnosed solid tumors. *J Natl Compr Canc Netw* (2015) 13(10):1225–31. doi: 10.6004/jnccn.2015.0151

10. Tang CMM, Liao ZM, Gomez DM, Levy LM, Zhuang YM, Gebremichael RAB, et al. Lymphopenia association with gross tumor volume and lung V5 and its effects on non-small cell lung cancer patient outcomes. *Int J Radiat Oncol Biol Phys* (2014) 89(5):1084–91. doi: 10.1016/j.ijrobp.2014.04.025

11. Sun GY, Wang SL, Song YW, Jin J, Wang WH, Liu YP, et al. Radiation-induced lymphopenia predicts poorer prognosis in patients with breast cancer: A *Post hoc* analysis of a randomized controlled trial of postmastectomy hypofractionated radiation therapy. *Int J Radiat Oncol Biol Phys* (2020) 108(1):277–85. doi: 10.1016/j.ijrobp.2020.02.633

12. Davuluri R, Jiang W, Fang P, Xu C, Komaki R, Gomez DR, et al. Lymphocyte nadir and esophageal cancer survival outcomes after chemoradiation therapy. *Int J Radiat Oncol Biol Phys* (2017) 99(1):128–35. doi: 10.1016/j.ijrobp.2017.05.037

13. Fang P, Jiang W, Davuluri R, Xu C, Krishnan S, Mohan R, et al. High lymphocyte count during neoadjuvant chemoradiotherapy is associated with improved pathologic complete response in esophageal cancer. *Radiother Oncol* (2018) 128(3):584–90. doi: 10.1016/j.radonc.2018.02.025

14. Li Q, Zhou S, Liu S, Liu S, Yang H, Zhao L, et al. Treatment-related lymphopenia predicts pathologic complete response and recurrence in esophageal squamous cell carcinoma undergoing neoadjuvant chemoradiotherapy. *Ann Surg Oncol* (2019) 26 (9):2882–9. doi: 10.1245/s10434-019-07334-7

15. Ni W, Yu S, Zhang W, Xiao Z, Zhou Z, Chen D, et al. A phase-II/III randomized controlled trial of adjuvant radiotherapy or concurrent chemoradiotherapy after surgery versus surgery alone in patients with stage-IIB/III esophageal squamous cell carcinoma. *BMC Cancer* (2020) 20(1):130. doi: 10.1186/s12885-020-6592-2

16. Ni W, Yang J, Deng W, Xiao Z, Zhou Z, Zhang H, et al. Patterns of recurrence after surgery and efficacy of salvage therapy after recurrence in patients with thoracic esophageal squamous cell carcinoma. *BMC Cancer* (2020) 20(1):144–52. doi: 10.1186/s12885-020-6622-0

17. Wild AT, Ye X, Ellsworth SG, Smith JA, Narang AK, Garg T, et al. The association between chemoradiation-related lymphopenia and clinical outcomes in patients with locally advanced pancreatic adenocarcinoma. *Am J Clin Oncol* (2015) 38(3):259–65. doi: 10.1097/COC.0b013e3182940ff9

18. Damen P, Kroese TE, van Hillegersberg R, Schuit E, Peters M, Verhoeff J, et al. The influence of severe radiation-induced lymphopenia on overall survival in solid tumors: A systematic review and meta-analysis. *Int J Radiat Oncol Biol Phys* (2021) 111(4):936-948.. doi: 10.1016/S0167-8140(21)07966-4

19. Upadhyay R, Venkatesulu BP, Giridhar P, Kim BK, Sharma A, Elghazawy H, et al. Risk and impact of radiation related lymphopenia in lung cancer: A systematic review and meta-analysis. *Radiother Oncol* (2021) 157:225–33. doi: 10.1016/j.radonc.2021.01.034

20. Xie X, Gong S, Jin H, Yang P, Xu T, Cai Y, et al. Radiation-induced lymphopenia correlates with survival in nasopharyngeal carcinoma: Impact of treatment modality and the baseline lymphocyte count. *Radiat Oncol* (2020) 15(1):65. doi: 10.1186/s13014-020-01494-7

21. Nakamura N, Kusunoki Y, Akiyama M. Radiosensitivity of CD4 or CD8 positive human T-lymphocytes by an *in vitro* colony formation assay. *Radiat Res* (1990) 123(2):224–7. doi: 10.2307/3577549

22. Yovino S, Grossman SA. Severity, etiology and possible consequences of treatment-related lymphopenia in patients with newly diagnosed high-grade gliomas. *CNS Oncol* (2012) 1(2):149–54. doi: 10.2217/cns.12.14

23. Newell EW, Sigal N, Bendall SC, Nolan GP, Davis MM. Cytometry by time-of-Flight shows combinatorial cytokine expression and virus-specific cell niches within a continuum of CD8+ T cell phenotypes. *Immunity* (2012) 36(1):142–52. doi: 10.1016/j.immuni.2012.01.002

24. Fridman WH, Pagès F, Sautès-Fridman C, Galon J. The immune contexture in human tumours: Impact on clinical outcome. *Nat Rev Cancer* (2012) 12(4):298–306. doi: 10.1038/nrc3245

25. Muroyama Y, Nirschl TR, Kochel CM, Lopez-Bujanda Z, Theodros D, Mao W, et al. Stereotactic radiotherapy increases functionally suppressive regulatory T cells in the tumor microenvironment. *Cancer Immunol Res* (2017) 5(11):992–1004. doi: 10.1158/2326-6066.CIR-17-0040

26. Oweida A, Hararah MK, Phan A, Binder D, Bhatia S, Lennon S, et al. Resistance to radiotherapy and PD-L1 blockade is mediated by TIM-3 upregulation and regulatory T-cell infiltration. *Clin Cancer Res* (2018) 24(21):5368–80. doi: 10.1158/1078-0432.CCR-18-1038

27. Oweida AJ, Darragh L, Phan A, Binder D, Bhatia S, Mueller A, et al. STAT3 modulation of regulatory T cells in response to radiation therapy in head and neck cancer. *JNCI: J Natl Cancer Inst* (2019) 111(12):1339–49. doi: 10.1093/jnci/djz036

28. Baba J, Watanabe S, Saida Y, Tanaka T, Miyabayashi T, Koshio J, et al. Depletion of radio-resistant regulatory T cells enhances antitumor immunity during recovery from lymphopenia. *Blood* (2012) 120(12):2417–27. doi: 10.1182/blood-2012-02-411124

29. Shinto E, Hase K, Hashiguchi Y, Sekizawa A, Ueno H, Shikina A, et al. CD8+ and FOXP3+ tumor-infiltrating T cells before and after chemoradiotherapy for rectal cancer. *Ann Surg Oncol* (2014) 21 Suppl 3:S414–21. doi: 10.1245/s10434-014-3584-y

30. Fang P, Shiraishi Y, Verma V, Jiang W, Song J, Hobbs BP, et al. Lymphocyte-sparing effect of proton therapy in patients with esophageal cancer treated with definitive chemoradiation. *Int J Particle Ther* (2018) 4(3):23–32. doi: 10.14338/IJPT-17-00033.1

31. van Rossum P, Deng W, Routman DM, Liu AY, Xu C, Shiraishi Y, et al. Prediction of severe lymphopenia during chemoradiation therapy for esophageal cancer: Development and validation of a pretreatment nomogram. *Pract Radiat Oncol* (2020) 10(1):e16–26. doi: 10.1016/j.prro.2019.07.010

32. Saito T, Toya R, Yoshida N, Shono T, Matsuyama T, Ninomura S, et al. Spleen dose-volume parameters as a predictor of treatment-related lymphopenia during definitive chemoradiotherapy for esophageal cancer. *In Vivo (Athens)* (2018) 32(6):1519–25. doi: 10.21873/invivo.11409

33. Lee J, Lin J, Sun F, Lu K, Lee C, Chen Y, et al. Dosimetric predictors of acute haematological toxicity in oesophageal cancer patients treated with neoadjuvant chemoradiotherapy. *Brit J Radiol* (2016) 89(1066):20160350. doi: 10.1259/bjr.20160350

34. Zhang A, Deek MP, Kim S, Sayan M, Grann A, Wagman RT, et al. Vertebral body irradiation during chemoradiation therapy for esophageal cancer contributes to acute bone marrow toxicity. *J Gastrointest Oncol* (2019) 10(3):513–22. doi: 10.21037/jgo.2019.01.20

35. Fabian D, Ayan A, DiCostanzo D, Barney CL, Aljabban J, Diaz DA, et al. Increasing radiation dose to the thoracic marrow is associated with acute hematologic toxicities in patients receiving chemoradiation for esophageal cancer. *Front Oncol* (2019) 9:147. doi: 10.3389/fonc.2019.00147

36. Newman NB, Anderson JL, Sherry AD, Osmundson EC. Dosimetric analysis of lymphopenia during chemoradiotherapy for esophageal cancer. *J Thorac Dis* (2020) 12(5):2395–405. doi: 10.21037/jtd.2020.03.93

37. Mohan R, Liu AY, Brown PD, Mahajan A, Dinh J, Chung C, et al. Proton therapy reduces the likelihood of high-grade radiation-induced lymphopenia in glioblastoma patients: Phase II randomized study of protons vs photons. *Neuro-oncol (Charlottesville Va.)* (2021) 23(2):284–94. doi: 10.1093/neuonc/noaa182

38. Nichols RC, Huh SN, Henderson RH, Mendenhall NP, Flampouri S, Li Z, et al. Proton radiation therapy offers reduced normal lung and bone marrow exposure for patients receiving dose-escalated radiation therapy for unresectable stage iii non-small-cell lung cancer: A dosimetric study. *Clin Lung Cancer* (2011) 12 (4):252–7. doi: 10.1016/j.cllc.2011.03.027

39. Shiraishi Y, Xu C, Yang J, Komaki R, Lin SH. Dosimetric comparison to the heart and cardiac substructure in a large cohort of esophageal cancer patients treated with proton beam therapy or intensity-modulated radiation therapy. *Radiother Oncol* (2017) 125(1):48–54. doi: 10.1016/j.radonc.2017.07.034

40. Liu C, Bhangoo RS, Sio TT, Yu NY, Shan J, Chiang JS, et al. Dosimetric comparison of distal esophageal carcinoma plans for patients treated with small-spot intensity-modulated proton versus volumetric-modulated arc therapies. *J Appl Clin Med Phys* (2019) 20(7):15–27. doi: 10.1002/acm2.12623

41. Shiraishi Y, Fang P, Xu C, Song J, Krishnan S, Koay EJ, et al. Severe lymphopenia during neoadjuvant chemoradiation for esophageal cancer: A propensity matched analysis of the relative risk of proton versus photon-based radiation therapy. *Radiother Oncol* (2018) 128(1):154–60. doi: 10.1016/j.radonc.2017.11.028

42. Routman DM, Garant A, Lester SC, Day CN, Harmsen WS, Sanheuza CT, et al. A comparison of grade 4 lymphopenia with proton versus photon radiation therapy for esophageal cancer. *Adv Radiat Oncol* (2019) 4(1):63–9. doi: 10.1016/j.adro.2018.09.004

43. Ni W, Yu S, Xiao Z, Zhou Z, Chen D, Feng Q, et al. Postoperative adjuvant therapy versus surgery alone for stage IIB–III esophageal squamous cell carcinoma: A phase III randomized controlled trial. *Oncologist* (2021) 26(12):e2151–60. doi: 10.1002/onco.13914

44. Zheng XM, Guo YM, Wang LM, Zhang HM, Wang SM, Wang LM, et al. Recovery profiles of T-cell subsets following low-dose total body irradiation and improvement with cinnamon. *Int J Radiat Oncol Biol Phys* (2015) 93(5):1118–26. doi: 10.1016/j.ijrobp.2015.08.034

45. Byun HK, Kim KJ, Han SC, Seong J. Effect of interleukin-7 on radiation-induced lymphopenia and its antitumor effects in a mouse model. *Int J Radiat Oncol Biol Phys* (2021) 109(5):1559–69. doi: 10.1016/j.ijrobp.2020.12.004

frontiers | Frontiers in Oncology

TYPE Clinical Trial
PUBLISHED 09 September 2022
DOI 10.3389/fonc.2022.880053

OPEN ACCESS

EDITED BY
Li Jiancheng,
Fujian Medical University, China

REVIEWED BY
Yanyong Yang,
Second Military Medical University, China
Dingde Huang,
Army Medical University, China

*CORRESPONDENCE
Zhichao Fu
fauster1112@126.com
Huachun Luo
luohuachun@hotmail.com

†These authors have contributed equally to this work and share first authorship

SPECIALTY SECTION
This article was submitted to Radiation Oncology, a section of the journal Frontiers in Oncology

RECEIVED 20 February 2022
ACCEPTED 17 August 2022
PUBLISHED 09 September 2022

CITATION
Wang X, Cai L, Wu M, Li G, Zhu Y, Lin X, Yan X, Mo P, Luo H and Fu Z (2022) Real-world experience with anti–programmed cell death protein 1 immunotherapy in patients with esophageal cancer: A retrospective single-center study.
Front. Oncol. 12:880053.
doi: 10.3389/fonc.2022.880053

Real-world experience with anti–programmed cell death protein 1 immunotherapy in patients with esophageal cancer: A retrospective single-center study

Xinpeng Wang[1,2†], Lvjuan Cai[1,2†], Mengjing Wu[1,2†], Guo Li[1,2], Yunyun Zhu[1,2], Xinyue Lin[1,2], Xue Yan[1,2], Peng Mo[1,2], Huachun Luo[1,2*] and Zhichao Fu[1,2*]

[1]Department of Radiotherapy, The 900th Hospital of the Joint Logistics Team, Fujian Medical University, Fuzhou, China, [2]Department of Radiotherapy, Dongfang Hospital of Xiamen University, School of Medicine, Xiamen University, Xiamen, China

The "real-world" data of programmed cell death protein 1 (PD-1) inhibitors in esophageal cancer (EPC) are still an unmet medical need, including the clinical efficacy and safety. Seventy-seven EPC data were studied retrospectively; the progression-free survival (PFS), risk factors (clinical stages larger than stage II, metastatic sites larger than 2, treatment lines larger than the first line, previous surgical treatment, combined positive score [CPS] expression, etc.), and the safety were analyzed. The median PFS for all patients was 7.2 months, clinical stage > stage II; the number of treatment lines > first line was significantly correlated with prognosis (all $P < 0.05$). Subgroup analysis showed that the median PFS of patients with clinical stage ≤ II was better; the results were the same for the patients with ≤2 metastatic sites, first-line PD-1 inhibitors, and not previously received radical surgery (all $P < 0.05$). Meanwhile, the incidence of adverse events (AEs) of varying degrees was 25.97% (20/77) in 20 patients and 6.49% (5/77) of grade 3/4 AEs. The highest AE was myelosuppression (15.58%), followed by liver function injury (7.79%). In addition, ≥2 lines of treatment and >2 metastatic sites predicted poor outcomes for patients with EPC who had failed first-line therapy or progressed with the combined immunotherapy and chemotherapy treatment strategy (all $P < 0.05$).

KEYWORDS

esophageal cancer, immunotherapy, retrospective study, efficiency, safety

Introduction

According to the data of GLOBOCAN 2020, of the 4,568,754 new cancer cases in China in 2020, 38.8% are malignant tumors of the digestive tract, of which the age-standardized incidence rate (ASIR) of esophageal cancer (EPC) ranks the 6th place among all tumors (13.8 cases per 100,000 people). Of the 3,002,899 patients with new cancer-related deaths, the age-standardized death rate (AMSR) of EPC ranked the 4th (12.70 per 100,000 people) (1). EPC has high morbidity and mortality. Although good progress has been made in the traditional treatment model or combination of surgery, radiotherapy, and chemotherapy (2), it is still difficult to meet the expectations of further improving the prognosis of patients.

The emergence of immune checkpoint inhibitors (ICIs) broke this situation. For any patient who responds to the treatment of multiple cancers, ICIs can provide long-term disease control and significantly improve the survival rate and the quality of life of patients (3). The Checkmate-577 study opened a chapter in adjuvant immunotherapy for EPC, suggesting that immunotherapy can significantly improve patients' DFS (4). The studies on ATTRCTION-3 (5), ESCORT (6), and KEYNOTE-181 (7) have shown that immunotherapy, as a treatment for advanced second-line EPC, has significantly better Objective Response Rate (ORR) and Overall Survival rate (OS) than the chemotherapy control group and has good safety. The subgroup analysis data of the KEYNOTE-181 (7) study showed that Asian populations may have more survival benefits from immunotherapy. The data of the interim study of KEYNOTE 590 (8) and ESCORT-1st released at the 2020 ESMO conference suggested that, in the advanced first-line treatment, the OS and progression-free survival (PFS) of the immunotherapy combined with chemotherapy group were significantly better than those of the control group. NCT02743494, CheckMate 648, and Checkmate-649 are expected to further prove that immune-combined chemotherapy and dual immunotherapy have significant benefits in OS and ORR, regardless of PDL1 expression (9). In addition, RATIONALE205 for patients with locally advanced EPC shows that ICI combined with chemotherapy has good efficacy and safety. Studies on KEYNOTE-975, SHR-1210-III-323, and RATIONALE311 (10) further explored the role of concurrent chemoradiotherapy combined with ICI therapy in locally advanced EPC.

More and more evidence supports that immunotherapy and immune-based combined therapy can significantly improve the prognosis of patients with EPC. However, the efficacy and safety of ICI treatment should still be further verified in the real world. Therefore, we retrospectively analyzed the esophagus patients treated in our center for immunotherapy in the past 3 years, evaluated their real safety and efficacy, and further determined relevant factors that significantly affected their prognosis.

Materials and methods

Patients

This retrospective study included a total of 86 patients with EPC who had received ICI treatment in the Radiotherapy Department of the 900th Hospital of the Joint Logistics Support Force between September 2018 and July 2021. Inclusion criteria: (1) age ≥ 18 years; (2) diagnosis of EPC by pathological histology; (3) presence of at least one measurable lesion prior to treatment according to RECIST 1.1 tumor evaluation criteria; (4) patients with no co-infections or other serious systemic diseases before treatment. Exclusion criteria: (1) combination of other malignancies, except cured basal cell carcinoma of the skin or squamous carcinoma of the skin or any other *in situ* carcinoma; (2) presence of any abnormal bone marrow hyperplasia and other hematopoietic disorders prior to treatment; (3) those with active infection requiring treatment, HIV infection, viral hepatitis before treatment; (4) Patients with other serious systemic diseases require pharmacological intervention. Of them, nine patients were excluded: Two patients were excluded due to incompleteness of baseline data, three patients due to having multiple tumors, and four patients due to being lost to follow-up. Finally, 77 patients were included in this study (Figure 1). All patients in the group met the pathological diagnostic criteria for EPC, including one case of adenocarcinoma, one case of neuroendocrine cancer, and the rest cases were esophageal squamous cell carcinoma. The study data were collected through patient electronic medical records and telephone follow-up. The clinical data were collected and analyzed retrospectively, including baseline clinical characteristics of patients, PDL-1 expression, disease progression and the time of death of patients, and treatment-related adverse events (AEs). All patients were informed and accepted the treatment protocol during the previous treatments.

Treatment

ICI includes pembrolizumab, toripalimab, camrelizumab, sintilizumab, and tilelizumab. The doses of pembrolizumab, carrelizumab, sintilizumab, and tilelizumab received by the patients were fixed doses of 200 mg every 3 weeks. The therapeutic dose of toripalimab is a fixed dose of 240 mg every 3 weeks.

The chemotherapy regimen includes adjuvant chemotherapy regimen: cisplatin combined with fluorouracil: cisplatin 60–80 mg/m^2, i.v., d1; fluorouracil 1,000 mg/m^2•d, i.v., d1-5. It is repeated every 3 weeks. Paclitaxel combined with cis-platinum: paclitaxel 150–175mg/m^2, i.v., d1 or 80 mg/m^2, i.v., d1, 8; cisplatin 60–75mg/m^2, d1 or d2. It is repeated every 21 days. Docetaxel combined with platinum: docetaxel 60–75 mg/m^2, i.v., d1 or 30–

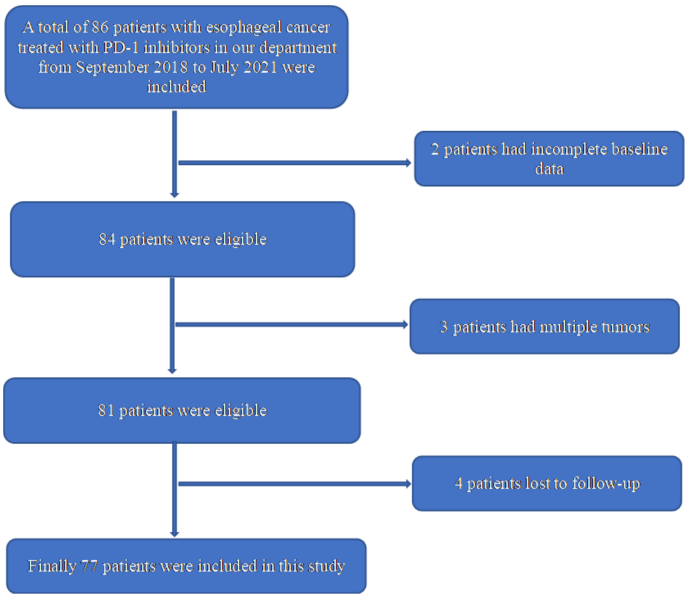

FIGURE 1
Patient selection process for the retrospective cohort.

35 mg/m^2, i.v., d1-2; cisplatin 70 mg/m^2, i.v., d1 or nedaplatin 50 mg/m^2, i.v., d1. It is repeated every 3 weeks. Capecitabine combined with paclitaxel: capecitabine 1,000 mg/m^2, p.o., bid, d1-14; paclitaxel 80 mg/m^2, i.v. d1, 8. It is repeated every 3 weeks. Capecitabine combined with cisplatin: capecitabine 825–1,000 mg/m^2, p.o, bid. d1-14; cisplatin 75 mg/m^2, i.v., d1. It is repeated every 3 weeks. Capecitabine combined with docetaxel: capecitabine 825–1000 mg/m^2, p.o, bid, d1-14, an interval of 7 days; docetaxel 60 mg/m^2, i.v., d1. It is repeated every 3 weeks. Paclitaxel single agent: paclitaxel 60–80 mg/m^2, i.v., d1, 8, 15, and it is repeated every 4 weeks. Docetaxel monotherapy: docetaxel 60–75 mg/m^2, i.v., d1, and it is repeated every 3 weeks. In view of toxic and side effects of combined therapy, no combination of three or more chemotherapy drugs has been used.

Concurrent chemotherapy will include a combination of cisplatin (25 mg/m^2, IV; days 1–3 of each 3-week cycle) and paclitaxel (135 mg/m^2, i.v.; day 1 of each 3-week cycle), and two cycles will be given. Adjuvant or palliative chemotherapy regimens include FP regimen (5-FU 800 mg/m^2 d1-5 Q3W + cisplatin 80 mg/m^2 Q3W) and TP regimen (albumin paclitaxel 260 mg/m^2 i.v. + cisplatin 75 mg/m^2).

The radiotherapy regimen includes radical concurrent chemoradiotherapy with a dose of 50–60 Gy, and postoperative adjuvant radiotherapy with a dose of 45–50.4 Gy (all included patients are R0 resection), and concurrent chemoradiotherapy will be divided into 28 sessions (total dose: 50.4 Gy).

Surgical treatment method: thoracoscopic radical resection of EPC + regional lymph node dissection. The start of the operation is after the confirmation by clinical or biopsy pathological diagnosis, or 6–8 weeks after the end of neoadjuvant chemoradiotherapy, or 3–6 weeks after the end of neoadjuvant chemotherapy.

We used immunotherapy in combination with chemotherapy for stage II (three patients), stage III (nine patients), stage IVA (two patients), stage IVB (20 patients) who received second-line treatment after progression, and for stage IVB patients (12 patients) who received first-line treatment. Two of the stage IVB patients were treated with a combination of anti-vascular targeting agents. Of the remaining patients, six stage I patients underwent surgery and received postoperative immune maintenance therapy. Neoadjuvant immunotherapy in conjunction with chemotherapy was given to four stage II patients and five stage III patients. Induction immunotherapy was given to a further two stage II patients and five stage III patients, along with radical concomitant chemoradiotherapy and immunotherapy. Neoadjuvant chemotherapy and postoperative immune maintenance treatment were used to treat two stage III patients. Postoperative adjuvant immunotherapy combined with chemotherapy was used to treat the remaining stage III patients. Following radical radiation, immune maintenance treatment was given to the remaining three-stage IVA patients.

Ethics statement

The studies involving human participants were reviewed and approved by the ethical review board committee of the 900th Hospital of the Joint Logistics Team. The patients provide their written informed consent to participate in this study.

Evaluation

Tumor staging was based on the 2017 TNM staging standard of the American Joint Committee on Cancer (AJCC). Efficacy was assessed according to RECIST 1.1 tumor evaluation criteria. PFS was defined as the time from the baseline evaluation level of treatment before ICI was used to the imaging (enhanced CT), suggesting the progression of the disease. OS was defined as the time from the baseline evaluation level of treatment before ICI use to death from any cause. CTCAE version 5.0 was used as the standard to evaluate the grade of AEs during the treatment of patients. Statistical criteria for PD-L1 expression: TPS was defined as the percentage of tumor cells stained with PD-L1 membranes at any intensity. CPS was defined as the sum of the number of PDL1-stained tumor cells and tumor-associated immunity per 100 tumor cells.

Statistical analysis

The patient's PFS was estimated using the Kaplan–Meier method. The 95% CI was calculated using the Brookmeyer–Crowley method. The univariate stratified comparison was made through the log-rank test. Then, the covariate ($P < 0.05$ in the univariate analysis) was entered into the regression model of multivariate Cox proportional hazards. The HR for PFS and corresponding 95% CI were calculated with the Cox proportional hazards model. A forest map was plotted for further comparison and analysis. Statistical analysis was performed using SPSS software (version 26.0, IBM Software, Armonk, NY, USA) and R software (version 4.1.0).

Results

Clinical characteristics and treatment

The retrospective study cohort included 77 patients with EPC who had previously received ICI treatment. The median follow-up time was 7.9 ± 1.867 months by the time the data were locked (30 December 2021).

The median age was 60 years (45–74 years), and 37 patients (48.1%) were over 60 years old. Of the 77 patients, 60 (77.9%) were men and 17 (22.1%) were women. The ECOG performance status score (PS) of all included patients was lower than 2 points. Of the 77 patients, according to the staging standard of the 8th edition of the AJCC, T3 patients accounted for the largest proportion (49.3%) of the T stage, and in the lymph node staging, the proportion of N1 and N2 patients accounted for the vast majority, respectively, 33 (42.8%) and 28 (36.4%). The included patients were mainly stages III and VI, 25 (32.5%) and 37 (48.0%), respectively, and six (7.8%) and nine (11.7%) patients were in stages I and II, respectively. Of all stage VI patients, 32 patients were stage VIB, in which 15 had metastases in a single organ, five patients had metastases in two positions, and the rest 12 patients had metastases in more than two organs. Among all the target organs for which metastasis has been observed, lung metastasis has the highest incidence (16 cases), followed by liver metastasis (12 cases), and the rest are bone metastasis (seven cases) and brain metastasis (two cases). Of the 77 patients, 43 (55.8%) patients received neoadjuvant, adjuvant, or first-line immunotherapy, and the rest 34 patients (44.2%) received ICI treatment after the second-line treatment. Thirty-six patients had previously undergone radical EPC ± lymph node dissection; 45 patients received radiotherapy, including preoperative neoadjuvant, postoperative adjuvant, and radical concurrent chemoradiotherapy, and 60 patients joined chemotherapy regimen before or during ICI treatment (including albumin paclitaxel or Tegafur, Gimeracil and Oteracil Potassium monotherapy regimen, and albumin paclitaxel plus platinum or Tegafur, Gimeracil, and Oteracil Potassium plus platinum combined regimen); two patients of second-line treatment were treated with anti-vascular–targeted therapy (apatinib and anlotinib, respectively).

In this study, there are five programmed cell death protein 1 (PD-1) checkpoint inhibitors available: sintilizumab (23.4%), carrelizumab (54.5%), teriprizumab (9.1%), tislelizumab (6.5%), and pembrolizumab (6.5%). According to the PDL1 expression of patients before treatment, 14 patients had PD-L1 CPS lower than 10%, 13 patients had PD-L1 CPS higher than or equal to 10%, and the PD-L1 expression levels of another 50 patients before treatment were not recorded (Table 1).

Treatment outcome and potential predictors

The median PFS for all patients was 7.2 months (Figure 2). The median OS has not yet been reached as of the deadline.

We conducted a univariate analysis of the potential influencing factors of PFS in patients using regression analysis of Cox proportional hazards. According to the results of the analysis, among all the clinical baseline characteristics included in the evaluation, the clinical-stage higher than stage II (HR = 4.778, 95% CI 1.476, 15.469), metastatic sites more than 2 (HR = 2.373, 95% CI 1.193, 4.719), treatment higher than first-line (HR = 2.350, 95% CI 1.300, 2.254), and previous

10.3389/fonc.2022.880053

TABLE 1 Baseline characteristics.

Variables	Number of cases (%)
Age (years)	
Median (range)	60 (45-74)
< 60	37 (48.1)
≥ 60	40 (51.9)
Gender	
Male	60 (77.9)
Female	17 (22.1)
T stage	
1	4 (5.2)
2	22(28.6)
3	38 (49.3)
4	13 (16.9)
N stage	
0	13 (16.9)
1	33 (42.8)
2	28 (36.4)
3	3 (3.9)
M stage	
0	46 (59.7)
1	31 (40.3)
Clinical stage	
I	6 (7.8)
II	9 (11.7)
III	25 (32.5)
IVA	5 (6.5)
IVB	32 (41.5)
≤Ⅱ	15 (19.5)
>Ⅱ	62 (80.5)
Treatment line	
Neoadjuvant, adjuvant, or first-line therapy	43 (55.8)
≥ 2 lines of therapy	34 (44.2)
Tumor involvement site (distant metastasis)	
0	45 (58.4)
1	20 (26.0)
2	8 (10.4)
3	4 (5.2)
Metastasis site	
Lung	16 (20.8)
Liver	12 (15.6)
Brain	2 (2.6)
Bone	7 (9.1)
Previous therapy	
Chemotherapy	60 (77.9)
Radiotherapy	45 (58.4)
Surgery	36 (46.8)
PD-L1 expression (CPS)	
< 10%	14 (18.2)
≥ 10%	13 (16.9)
Unknown	50 (64.9)
Immune checkpoint inhibitors	
Sintilimab	18 (23.4)
Camrelizumab	42 (54.5)
Toripalimab	7 (9.1)
Tislelizumab	5 (6.5)
Pembrolizumab	5 (6.5)

CPS, combined positive score.

surgical treatment (HR = 1.943, 95% CI 1.006, 3.750) were significantly related to the prognosis of patients. However, the age, gender, with/without lung, liver, brain, or bone metastases, whether the patients have received chemoradiotherapy, the type of ICI, and the expression of PD-L1 CPS was not significantly correlated with the patient's PFS (P>0.05) (Table 2). The above conclusions are visually explained by plotting a forest map (Figure 3).

Furthermore, we conducted further multivariate analysis on the four valuable clinical characteristics of the above univariate analysis, and the results showed that the clinical stage higher than stage II (HR = 4.023, 95% CI 1.219, 13.282), and treatment higher than first-line (HR = 2.016, 95% CI: 1.096, 3.708) were still an independent predictor of PFS (Table 2) (Figure 4).

Subgroup analysis

The Kaplan–Meier method was used to analyze the potential influencing factors of patients with PFS, that is, further subgroup analysis on the clinical stage higher than stage II, the metastatic

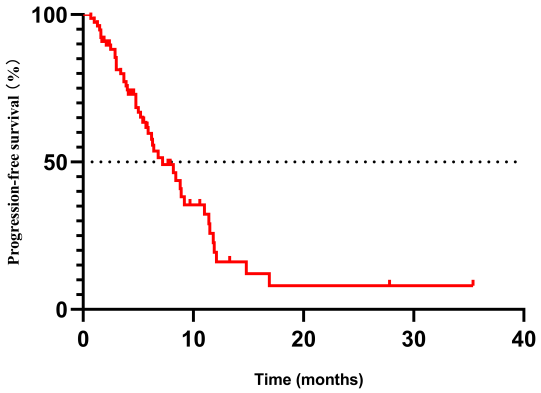

FIGURE 2
Kaplan–Meier plot for the total population (n = 77). PFS, progression-free survival.

TABLE 2 Univariate and multivariate Cox regression models for progression-free survival.

Characteristics (Reference)	Univariate analysis		*P*-value	Multivariate analysis		*P*-value
	HR	95% CI		HR	95% CI	
Age (<60)	0.567	0.316-1.020	0.058			
Gender (male)	0.655	0.319-1.347	0.250			
Stage (≤II)	4.778	1.476-15.469	0.009	4.023	1.219-13.282	0.022
Tumor involvement site(≤2)	2.373	1.193-4.719	0.014	2.001	0.995-4.021	0.052
Treatment line (neoadjuvant,adjuvant, or first-line therapy)	2.350	1.300-2.254	0.005	2.016	1.096-3.708	0.024
Lung metastasis (none)	1.164	0.601-2.217	0.652			
Liver metastasis (none)	1.603	0.767-3.351	0.210			
Brain metastasis (none)	2.104	0.502-8.825	0.309			
Bone metastasis (none)	1.169	0.455-3.002	0.745			
History of chemotherapy (none)	1.553	0.681-3.539	0.295			
History of radiotherapy (none)	1.241	0.681-2.263	0.481			
History of surgery (none)	1.943	1.006-3.750	0.048	1.937	0.971-3.865	0.061
Carrelizumab or others (others)	1.308	0.719-2.381	0.379			

CI, confidence interval; HR, hazard ratio; Carrelizumab or others, Carrelizumab or others immune checkpoint inhibitors.

site more than 2, the treatment higher than the first line, and the previous surgical treatment. As shown in the figure, the median PFS of patients with clinical stage lower than or equal to stage II and higher than stage II was 11.5 months versus 6.2 months, P = 0.004 (Figure 5A). Patients with less than two sites of metastasis may have a longer PFS, with a median PFS of 8.4 months versus 3.9 months for those with more than two sites, P = 0.011 (Figure 5B). The median PFS was 11.0 months versus 4.8 months in neoadjuvant, adjuvant, or first-line immunotherapy groups versus second-line and later immunotherapy groups, P = 0.003 (Figure 5C). The median PFS of patients who had not received surgery (radical radiotherapy or chemotherapy or immunotherapy alone), and those who received surgery was 8.9 months versus 6.2 months, P = 0.044 (Figure 5D). This suggests that patients undergoing surgical treatment may have a worse prognosis than patients undergoing radical chemoradiotherapy.

In addition, we conducted a further subgroup analysis of 27 patients with recorded baseline PD-L1 expression. Of the 27 patients, 16 patients used carrelizumab, seven patients sintilizumab, and the rest patients teriprizumab (three cases), tislelizumab (one case), and pembrolizumab (one case). We found no significant statistical difference in the PFS comparison of each sub-group with PD-L1 CPS higher than 1, 5, and 10%, PD-L1 TPS higher than 1%, and whether PD-L1 is

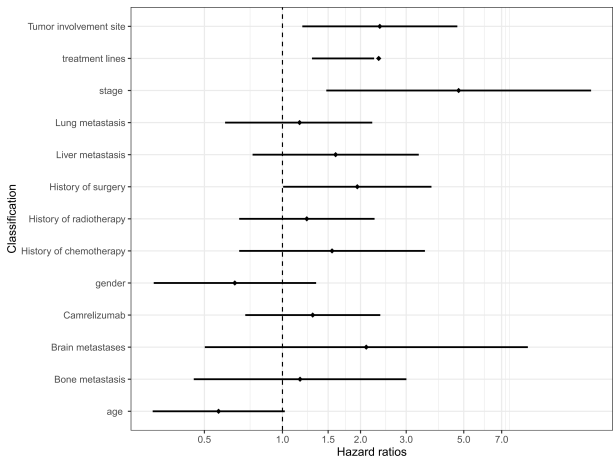

FIGURE 3
Univariate Cox regression models for progression-free survival. CI, confidence interval; HR, hazard ratio; Carrelizumab, Carrelizumab or others immune checkpoint inhibitors.

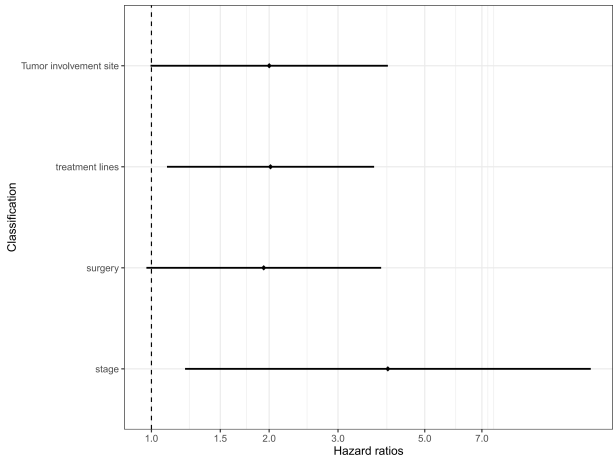

FIGURE 4
Multivariate Cox regression models for progression-free survival. CI, confidence interval; HR, hazard ratio.

simultaneously expressed in tumor cells and immune cells as the sub-group grouping basis (Table 3).

We grouped patients with similar treatment strategies among the included patients and found that 46 of them were treated with immune-combination chemotherapy regimens. This included stages II (three patients), III (nine patients), IVA (two patients), IVB (20 patients) patients who received second or multiple lines of therapy after progression, and 4b patients (12 patients) who received first-line therapy. In this treatment subgroup, the median PFS for all patients was 5.9

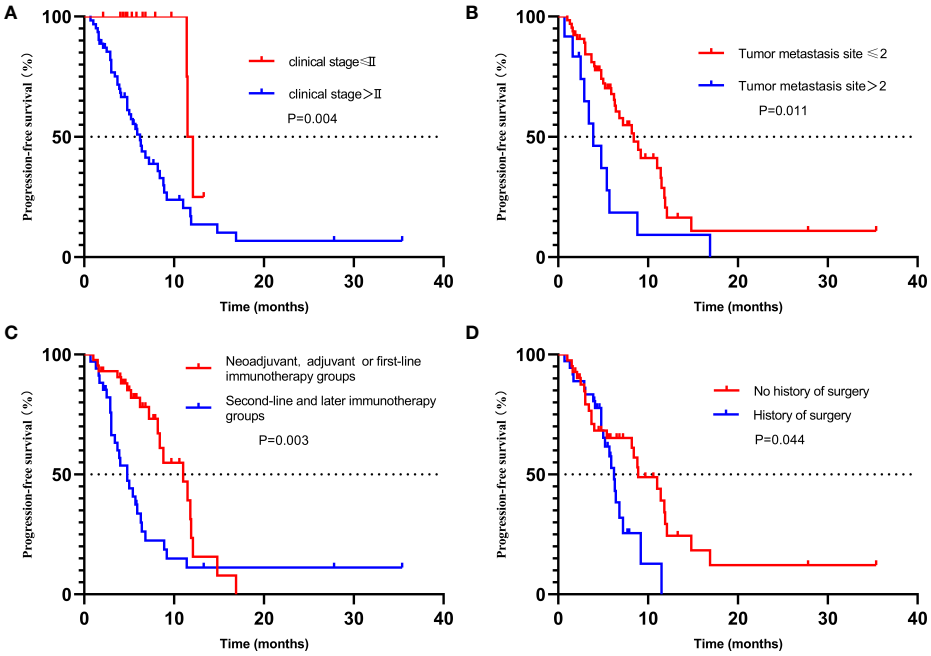

FIGURE 5
Kaplan–Meier plot for progression-free survival stratified by clinical factors, including **(A)** stage, **(B)** Number of metastatic lesions, **(C)** treatment lines, and **(D)** History of surgery. CI, confidence interval; PFS, progression-free survival.

TABLE 3 Subgroup analysis: Univariate Cox regression models for progression-free survival about PD-L1 expression level.

Characteristics	HR	95% CI	*P*-value
PD-L1 CPS≥ 1%	2.384	0.531-10.705	0.257
PD-L1 CPS≥ 5%	0.876	0.337-2.274	0.786
PD-L1 CPS≥ 10%	0.932	0.362-2.398	0.884
PD-L1 TPS≥ 1%	0.886	0.417-2.754	0.886
Simultaneous expression on tumor cells and immune cells	1.241	0.421-3.659	0.695

CPS, combined positive score; TPS, tumor proportion score.

months. Treatment lines ≥2 and metastatic sites >2 were independent risk factors for patients' PFS. In contrast, the staging was no longer critical in affecting prognosis. Suggesting that early intervention remains the key to improving prognosis after the failure of first-line therapy or in immune combination therapy for advanced EPC (Table 4). The median PFS for patients who received neoadjuvant, adjuvant, or first-line therapy was 11.0 months. In contrast, the median PFS of immunotherapy patients after failure of multiple lines of therapy was 4.8 months, which had not been reached in the stage 2 patient group, 4.8, months in the stage 3 patient group, and 4.0 months in the stage 4 patients.

AE analysis

We mainly followed up the patients for thyroid function, bone marrow function, liver function, treatment-related esophagotracheal fistula, and AEs with digestive system diarrhea as the main symptoms and described the occurrence of the abovementioned related AEs during treatment with ICI. Among the 77 patients, 20 patients experienced AEs of varying degrees (25.97%). Of the 20 patients, five patients experienced grade 3/4 AE (6.49%), bone marrow suppression, liver damage (grade 4), diarrhea, and esophagotracheal fistula, respectively. The AE of highest incidence was 12 patients with myelosuppression (15.58%), followed by liver damage (alanine transpeptidase elevation) in six patients (7.79%), of which one patient experienced grade 4 liver functional impairment, and three patients had grade 1 liver damage, and two patients had grade 2 liver damage. Three patients had hypothyroidism (3.90%) (two of grade 1 and one of grade 2), and four patients had diarrhea (5.19%), grades 1, 2, and 3 each. Another patient developed esophagotracheal fistula during treatment. Four patients experienced more than two of the above AEs, and one patient experienced three AEs of liver insufficiency, leukopenia, and diarrhea at the same time (Table 5).

Discussion

ICIs have become one important strategy for the first- and second-line treatment of EPC. In previous clinical studies, ICIs treatment has shown good efficacy and safety in the treatment of

TABLE 4 Univariate and multifactorial analysis of PFS in the immune combination chemotherapy subgroup.

Characteristics (Reference)	Univariate analysis		*P*-value	Multivariate analysis		*P*-value
	HR	95% CI		HR	95% CI	
Age (<60)	0.554	0.276-1.109	0.095			
Gender (Male)	0.616	0.261-1.456	0.270			
Stage (≤II)	4.723	0.637-35.027	0.129			
Stage (≤III)	1.212	0.522-2.814	0.654			
Tumor involvement site(≤2)	2.124	1.021-4.415	0.044	2.784	1.277-6.069	0.010
Treatment line (neoadjuvant,adjuvant, or first-line therapy)	2.545	1.043-6.209	0.040	2.766	1.063-7.201	0.037
Lung metastasis (none)	0.987	0.485-2.009	0.971			
Liver metastasis (none)	1.296	0.598-2.810	0.511			
Brain metastasis (none)	1.707	0.401-7.262	0.469			
Bone metastasis (none)	1.045	0.400-2.726	0.929			
History of chemotherapy (none)	1.374	0.583-3.239	0.468			
History of radiotherapy (none)	1.196	0.579-2.473	0.628			
History of surgery (none)	2.237	1.034-4.839	0.041	1.943	0.875-4.341	0.103
Carrelizumab or others (others)	1.474	0.717-3.027	0.291			

EPC. Our retrospective study aims to study the efficacy and safety of immunotherapy for patients with EPC in the real world. The median PFS in our trial was 7.2 months, with a median mPFS of 11.0 months in patients who received neoadjuvant, adjuvant immunotherapy, or first-line immunotherapy, which was greater than in prior studies (11–13). The early stages and the good physical condition may be the key to a better mPFS. Furthermore, the kind of ICI medication, changes in baseline PDL-1 expression in patients, and disparities in the races included in the study should all be taken into account (14).

Existing studies have proven the efficacy of immunotherapy for EPC, but not all patients can benefit from immunotherapy, which mainly depends on the tumor microenvironment (9). In other words, a suitable biomarker can help us further screen out potential benefit groups for immunotherapy for EPC. Among the common immunotherapy biomarkers, the expression of PD-L1 has been most extensively studied (15). In a meta-analysis involving 4,174 patients with advanced tumors (including lung cancer, kidney cancer, head and neck cancer, melanoma, and urothelial cancer), the patients received nivolumab, pembrolizumab, or atezolizumab treatment, respectively, and the analysis results showed that both PD-L1-positive and PD-L1-negative patients can benefit from PD-1 or PD-L1 blocking therapy, in which the survival benefit of pembrolizumab treatment for PD-L1-negative patients was minimal. In all selected subgroups, PD-1 or PD-L1 inhibitors are more effective in PD-L1-positive patients than in PD-L1-negative patients (16). According to the results of PD-L1 stratified analysis of KEYNOTE-189 (17) and KEYNOTE-407 studies (18), pembrolizumab combined with platinum-containing chemotherapy can bring OS and PFS benefits regardless of the expression status of PD-L1. In the KEYNOTE-180 trial, patients with high PD-L1 expression had a higher 1-year OS than patients with low PD-L1 expression (35% vs. 22%) (19). Quite a lot of existing studies have shown that patients with higher PD-L1 expression seem to get more benefits from ICI treatment. In this study, there was no significant statistical difference between PD-L1 high-expression and low-expression groups. We still found no significant correlation with prognosis after changing the definition of PD-L1 high expression (PD-L1 CPS ≥ 1%, 5%, 10%, CPS is defined as the sum of PD-L1-positive tumor cells, macrophages, and lymphocytes divided by total tumor cells). This may be related to insufficiencies of patients with recorded PD-L1 expression included in the statistics and the resulting bias. The difference in the efficacy of different types of ICI on PD-1 expression also affected our interpretation of the final result. Due to limited data from current clinical studies, the correlation between PD-L1 status and clinical results should be further verified. In addition, due to lack of data, we had not conducted further analysis and comparison of other potential biomarkers for EPC, such as MSI, PD-L2, TMB, and so forth (20) in this study.

TABLE 5 Treatment-related adverse events according to category and grade.

Adverse events	Grand 1	2	3	4	5
Hypothyroidism	2	1	0	0	0
Myelosuppression	3	7	1	1	0
Abnormal liver function	3	2	0	1	0
diarrhea	1	2	1	0	0

A patient has an esophagotracheal fistula.

According to a systematic review published by Sjoerd M. L et al., age was not related to the prognosis of EPC, and most studies do not support gender as a prognostic factor (21). Similar studies by Gregory O'Grady and MARKER S et al. also believed that age was not related to the prognosis of EPC (22, 23). A study by Pierre Bohanes et al. also believed that the female had a better prognosis than the male (24). A study by Yutong He et al. also believed that the female has a better prognosis than the male (25). In another retrospective study by Jiaxin Li et al. on prognosis analysis of non-surgical early stage EPC chemoradiotherapy, in a total of 3,736 patients included, multivariate Cox regression analysis showed that the age, gender, treatment, and cause of surgery are independent predictors of OS (26). In our study, we did not find a significant correlation between the age and gender of patients with EPC with the PFS of the patients in immunotherapy. However, because we did not pay attention to the correlation between OS with the age and gender of patients, further follow-up observation should be conducted on the patients included in the study.

The review by Véronique Vendrely et al. mentioned that the T stage of the tumor was a factor affecting the prognosis of EPC. There are different 5-year survival rates according to different T stage of tumor: 74% for ypT0 lesions, 83% for pTis lesions, 67% for pT1 lesions, 49% for pT2 lesions, and 30% for pT3 lesions (27). The study by Sjoerd M.L et al. believed that lymph node metastasis (N stage) may be a poor prognostic factor for EPC (21). It was reported that the 5-year survival rate for pN0 lesions was 63% and that for pN + lesions was 30% (28). In an analysis of survival of patients after EPC resection by Feng Du et al., a statistical analysis was performed on 4,566 eligible patients in the SEER database. The results showed that AJCC T stage, AJCC N stage, and chemoradiotherapy were independent influencing factors of EPC survival (29). While, in the analysis of the clinical characteristics of 5,283 cases of EPC by Yutong He et al., it was found that pathological stage was an independent predictor of patient prognosis (stage II: HR = 1.80, 95% CI: 1.40, 2.31; stage III: HR = 2.62, 95% CI: 2.06, 3.34; stage IV: HR = 3.90, 95% CI: 2.98, 5.09). Because the patients we included in the study were mainly stages III and VI, we conducted a combined analysis of the stages of the included patients and finally found that patients with clinical stages higher than stage II had worse PFS than patients with stages I and II (11.5 months vs. 6.2 months, $P = 0.004$), and this conclusion was confirmed again by multivariate analysis (HR = 4.778, 95% CI: 1.476, 15.469). Also, due to the limitation of the sample size of grouping, we had not

conducted further analysis on the subgroups of non-surgical patients and surgical patients of different stages. In addition, we did not find a significant difference in PFS in different subgroups of the T stage and N stage during the study process. Because there have been no sample studies on prognostic factors of EPC immunotherapy, this conclusion still should be verified by subsequent further studies.

In a study of immunotherapy for lung cancer by Junlin Yao et al., it was found that liver metastasis (HR = 3.7; 95% CI: 1.6, 8.5; $P < 0.01$) and ≥ 3 line therapy (HR = 3.5; 95% CI: 1.7, 7.4, $P < 0.01$) was a poor predictor of PFS (30). In our statistical process of patients with lung, liver, brain, and bone metastases from EPC in this study, we did not find a significant correlation with the PFS of immunotherapy. In the univariate analysis, we found that patients with less than or equal to two metastasis sites had longer mPFS (8.4 months vs. 3.9 months, $P = 0.011$), but in multivariate analysis, there was no significant difference between the two groups (HR = 2.001; 95% CI: 0.995. 4.021, $P = 0.052$), which may be due to the limited sample size of distant metastases included, so a larger study cohort is needed to better clarify the conclusion. Notably, for the treatment subgroup of immune combination chemotherapy, both univariate and multivariate analyses suggested that the number of metastatic sites was associated with prognosis.

Although we have seen a potential in first-line immunotherapy for EPC from the published interim data of existing phase III clinical studies (14), we still expect the release of final experimental data and further stratified analysis of the treatment lines to further clarify the best timing for immunotherapy intervention. Our study compared the PFS of immunotherapy in different treatment lines of EPC patients and finally found that the prognosis of the first-line immunotherapy patient subgroup was better than that of the latter-line treatment subgroups (11.0 months vs. 4.8 months $P = 0.003$).

In the process of univariate analysis, we found that patients in the group that received surgical treatment previously had worse PFS than those in the group that had not received surgical treatment (received or not received radical chemoradiotherapy), which seems to be different from our previous understanding. Although multivariate analysis ultimately rejected the decisive role of surgical treatment on PFS, what still cannot be ignored is that, for patients with inoperable EPC, immunotherapy and its combination with chemoradiotherapy or anti-vascular–targeted therapy, especially mechanisms of chemotherapy activating tumor immunogenicity and remote effect and the synergistic effect of immunotherapy (31) have long-term prognostic benefits for patients with EPC.

In the treatment subgroup of immunotherapy combined with chemotherapy, the median PFS in patients treated with second-line and multiple lines was 4.8 months, a figure superior to the previously reported 2.5 months (32, 33), thanks to the small number of stage 2 and three patients included in this subgroup. According to Matsubara, Y et al. (34), for the second-line treatment of advanced EPC, the median PFS for CPS ≥ 10 was 4.1 months. We obtained similar results (mPFS = 4.0 months) for patients treated in the advanced second line, although we did not obtain complete PD-L1 expression data. Of course, the difference in the type of immunosuppression remains a potential influence on this outcome. As for stage 2 and three patients, according to Ronan J et al. (4), the median DFS of Nivolumab maintenance therapy was 22.4 months in patients with stage 2 or 3 EPC after surgery after the neoadjuvant radiotherapy. We performed immunotherapy in combination with chemotherapy in patients with stage 3 EPC after a failure of multiple lines of therapy. The median age of this group was 64 years, and the median PFS was 4.8 months. Sample size and the number of lines treated may be the main factors for the poor prognosis of this subgroup of patients. In addition, the overall high age is a factor that should be taken into account. Due to the lack of appropriate genetic testing, we were unable to assess patient resistance to immunotherapy or combination chemotherapy regimens after multiple lines of therapy. In addition, limited by the actual treatment situation in the real world, the included patients were not all examined comprehensively and systematically to exclude actual comorbid conditions.

Because almost all patients that we included were esophageal squamous cell carcinoma, and patients with tumors at the gastroesophageal junction were not included, further analysis of the pathological type and tumor location was not made. In addition, if our research group needs to follow up on the patients for PFS, a longer follow-up period and large sample size are needed to further study relevant data affecting the OS of patients.

In our study, we also evaluated the safety of immunotherapy for EPC. We mainly observed AEs such as thyroid function, bone marrow function, liver function, treatment-related esophagotracheal fistula, and AEs with digestive diarrhea as main symptoms, and immune-related cardiotoxicity was not noted during treatment. We noted that 20 patients who experienced the abovementioned recorded main AEs of varying degrees. Four patients experienced more than two immunotherapy-related AEs, in which one patient experienced three AEs of liver insufficiency, leukopenia, and diarrhea at the same time, but all were grade 1–2 events. Among all observed patients, the incidence of grades 3 and 4 AEs was 6.49%, which were bone marrow suppression, liver damage, diarrhea, and esophagotracheal fistula. Bone marrow suppression was the most frequent AE in this study, with an incidence of 15.58%. The second most frequent AE was liver insufficiency, with an incidence of 7.79%, in which one patient had liver damage of grade 4. The prevalence of hypothyroidism and diarrhea was 3.90 and 5.19%, respectively. Another patient developed esophagotracheal fistula during treatment. The main adverse reactions observed were roughly similar to those in previous reports (35, 36). The difference in the incidence of adverse reactions was mainly due to the fact that the immunotherapy regimen that we included in the study covered five different ICIs, and due to the limitation of observation time, we have limited

records of treatment-related AEs, and some patients may have new or more serious adverse reactions in follow-up treatment. The limit of sample size may also affect the results of the study. In addition, the mixed toxicity caused by combination therapy such as chemoradiotherapy cannot be completely ruled out in about 60% of AEs. One patient with esophagotracheal fistula discontinued the drugs and was given palliative treatment. The other patients with grades 3 and 4 responses were treated with methylprednisolone 1–2 mg/kg after drug withdrawal, and the AE symptoms were all relieved significantly.

In the real world, the strategy selected for patients should not only follow guidance but also consider cost, drug availability, and the patient's willingness. Because of the need for treatment, patients with hypertension, diabetes, coronary heart disease, chronic viral hepatitis (non-replicating period), chronic pneumonia, hyperthyroidism, chronic renal insufficiency, and so forth are not excluded. Corresponding treatment drugs for them such as effects of drugs affecting intestinal flora on immunotherapy cannot be completely excluded from treatment.

Conclusions

In summary, we clarified the efficacy and safety of ICI treatment of EPC in the real world. In addition, a preliminary study has been conducted on potential independent predictors of PFS, and preliminary exploration has been made on the timing of ICI intervention in patients with EPC and the applicable population. However, the above conclusions still need to be further confirmed by larger scale prospective studies in the future.

Data availability statement

The raw data supporting the conclusions of this article will be made available by the authors, without undue reservation.

Ethics statement

The studies involving human participants were reviewed and approved by the ethical review board committee of 900th Hospital of the Joint Logistics Team. The patients/participants provided their written informed consent to participate in this study.

Author contributions

Conception and design: ZF and HL. Administrative support: ZF. Provision of study materials: XW, MW, LC, GL, YZ, XY, PM, and XL. Collection and assembly of data: ZF, XW, MW, LC, and GL. Data analysis and interpretation: HL, YZ, XY, PM, and XL. Manuscript writing: all authors. All authors contributed to the article and approved the submitted version.

Funding

This study was supported by Natural Science Foundation of Fujian Province (grant number: 2021J011259).

Acknowledgments

The authors thank Zhu Z.A. and Ma L. for the collection of data.

Conflict of interest

The authors declare that the research was conducted in the absence of any commercial or financial relationships that could be construed as a potential conflict of interest.

Publisher's note

References

1. Qiu HB, Cao SM, Xu RH. Cancer incidence, mortality, and burden in China: a time-trend analysis and comparison with the united states and united kingdom based on the global epidemiological data released in 2020. *Cancer Commun* (2021) 41(10):1037–48. doi: 10.1002/cac2.12197

2. Gronnier C, Collet D. New trends in esophageal cancer management. *Cancers* (2021) 13(12):7. doi: 10.3390/cancers13123030

3. Das S, Johnson DB. Immune-related adverse events and anti-tumor efficacy of immune checkpoint inhibitors. *J Immunother Cancer* (2019) 7(1):306. doi: 10.1186/s40425-019-0805-8

4. Kelly RJ, Ajani JA, Jaffer A, Kuzdzal J, Zander T, Van Cutsem E, et al. Adjuvant nivolumab in resected esophageal or gastroesophageal junction cancer. *N Engl J Med* (2021) 384(13):1191–203. doi: 10.1056/NEJMoa2032125

5. Takahashi M, Kato K, Okada M, Chin K, Kadowaki S, Hamamoto Y, et al. Nivolumab versus chemotherapy in Japanese patients with advanced esophageal squamous cell carcinoma: a subgroup analysis of a multicenter, randomized, open-label, phase 3 trial (ATTRACTION-3). *Esophagus* (2021) 18(1):90–9. doi: 10.1007/s10388-020-00794-x

6. Huang J, Xu JM, Chen Y, Zhuang W, Zhang YP, Chen ZD, et al. Camrelizumab versus investigator's choice of chemotherapy as second-line therapy for advanced or metastatic oesophageal squamous cell carcinoma (ESCORT): a multicentre, randomised, open-label, phase 3 study. *Lancet Oncol* (2020) 21(6):832–42. doi: 10.1016/S1470-2045(20)30110-8

7. Minami H, Kiyota N, Omori T. Did the randomized phase III KEYNOTE-181 study of pembrolizumab for esophageal cancer yield negative or positive results? *J Clin Oncol* (2021) 39(20):2317–8. doi: 10.1200/JCO.20.03262

8. Kato K, Shah M, Enzinger P, Bennouna J, Shen L, Adenis A, et al. KEYNOTE-590: Phase III study of first-line chemotherapy with or without pembrolizumab for advanced esophageal cancer. *Future Oncol* (2019) 15(10):1057–66. doi: 10.2217/fon-2018-0609

9. Zhao Q, Yu J, Meng X. A good start of immunotherapy in esophageal cancer. *Cancer Med* (2019) 8(10):4519–26. doi: 10.1002/cam4.2336

10. Yu R, Wang WQ, Li T, Li JC, Zhao KL, Wang WH, et al. RATIONALE 311: tislelizumab plus concurrent chemoradiotherapy for localized esophageal squamous cell carcinoma. *Future Oncol* (2021) 17(31):4081–9. doi: 10.2217/fon-2021-0632

11. Kojima T, Shah MIA, Muro K, Francois E, Adenis A, Hsu CH, et al. Randomized phase III KEYNOTE-181 study of pembrolizumab versus chemotherapy in advanced esophageal cancer. *J Clin Oncol* (2020) 38(35):13. doi: 10.1200/JCO.20.01888

12. Kato K, Cho BC, Takahashi M, Okada M, Lin CY, Chin K, et al. Nivolumab versus chemotherapy in patients with advanced oesophageal squamous cell carcinoma refractory or intolerant to previous chemotherapy (ATTRACTION-3): a multicentre, randomised, open-label, phase 3 trial. *Lancet Oncol* (2019) 20 (11):1506–17. doi: 10.1016/S1470-2045(19)30626-6

13. Rodriguez-Abreu D, Powell SF, Hochmair MJ, Gadgeel S, Esteban E, Felipm E, et al. Pemetrexed plus platinum with or without pembrolizumab in patients with previously untreated metastatic nonsquamous NSCLC: protocol-specified final analysis from KEYNOTE-189. *Ann Oncol* (2021) 32(7):881–95. doi: 10.1016/j.annonc.2021.04.008

14. Kato K, Sun JM, Shah MA, Enzinger PC, Adenis A, Doi T, et al. LBA8_PR pembrolizumab plus chemotherapy versus chemotherapy as first-line therapy in patients with advanced esophageal cancer: The phase 3 KEYNOTE-590 study. *Ann Oncol* (2020) 31:S1192–S3. doi: 10.1016/j.annonc.2020.08.2298

15. Lampis A, Ratti M, Ghidini M, Mirchev MB, Okuducu AF, Valeri N, et al. Challenges and perspectives for immunotherapy in oesophageal cancer: A look to the future (Review). *Int J Mol Med* (2021) 47(6):12. doi: 10.3892/ijmm.2021.4930

16. Shen X, Zhao B, Li J, Gu J. Efficacy of PD-1 or PD-L1 inhibitors and PD-L1 expression status in cancer: meta-analysis. *BMJ-British Med J* (2018) 362:9. doi: 10.1136/bmj.k3529

17. Wang YY, Zhao SK, Chen J, Xu S. The KEYNOTE-189 trial as a new paradigm making cure a reality for metastatic non-squamous non-small cell lung cancer. *Transl Lung Cancer Res* (2020) 9(5):2184–7. doi: 10.21037/tlcr-20-874

18. Paz-Ares L, Vicente D, Tafreshi A, Robinson A, Parra HS, Mazieres J, et al. A randomized, placebo-controlled trial of pembrolizumab plus chemotherapy in patients with metastatic squamous NSCLC: Protocol-specified final analysis of KEYNOTE-407. *J Thorac Oncol* (2020) 15(10):1657–69. doi: 10.1016/j.jtho.2020.06.015

19. Shah MA, Kojima T, Hochhauser D, Enzinger P, Raimbourg J, Hollebecque A, et al. Efficacy and safety of pembrolizumab for heavily pretreated patients with advanced, metastatic adenocarcinoma or squamous cell carcinoma of the esophagus: The phase 2 KEYNOTE-180 study. *JAMA Oncol* (2019) 5(4):546–50. doi: 10.1001/jamaoncol.2018.5441

20. Baba Y, Nomoto D, Okadome K, Ishimoto T, Iwatsuki M, Miyamoto Y, et al. Tumor immune microenvironment and immune checkpoint inhibitors in esophageal squamous cell carcinoma. *Cancer Sci* (2020) 111(9):3132–41. doi: 10.1111/cas.14541

21. Lagarde SM, Ten kate FJ, Reitsma JB, Busch ORC, Van lanschot JJB. Prognostic factors in adenocarcinoma of the esophagus or gastroesophageal junction. *J Clin Oncol* (2006) 24(26):4347–55. doi: 10.1200/JCO.2005.04.9445

22. O'Grady G, Hameed AM, Pang TC, Johnston E, Lam VT, Richardson AJ, et al. Patient selection for oesophagectomy: Impact of age and comorbidities on outcome. *World J Surg* (2015) 39(8):1994–9. doi: 10.1007/s00268-015-3072-y

23. Markar S, Low D. Physiology, not chronology, dictates outcomes after esophagectomy for esophageal cancer: outcomes in patients 80 years and older. *Ann Surg Oncol* (2013) 20(3):1020–6. doi: 10.1245/s10434-012-2703-x

24. Bohanes P, Yang D, Chhibar RS, Labonte MJ, Winder T, Ning Y, et al. Influence of sex on the survival of patients with esophageal cancer. *J Clin Oncol* (2012) 30(18):2265–72. doi: 10.1200/JCO.2011.38.8751

25. He Y, Liang D, Du L, Guo TT, Liu YY, Sun XB, et al. Clinical characteristics and survival of 5283 esophageal cancer patients: A multicenter study from eighteen hospitals across six regions in China. *Cancer Commun (Lond)* (2020) 40(10):531–44. doi: 10.1002/cac2.12087

26. Li J, Jia Y, Cheng Y, Wang JB. Chemoradiotherapy vs radiotherapy for nonoperative early stage esophageal cancer: A seer data analysis. *Cancer Med* (2020) 9(14):5025–34. doi: 10.1002/cam4.3132

27. Vendrely V, Launay V, Najah H, Smith D, Collet D, Gronnier C., et al. Prognostic factors in esophageal cancer treated with curative intent. *Dig Liver Dis* (2018) 50(10):991–6. doi: 10.1016/j.dld.2018.08.002

28. Bouvier AM, Binquet C, Gagnaire A, Jouve JL, Faivre J, Bedenne L., et al. Management and prognosis of esophageal cancers: has progress been made? *Eur J Cancer* (2006) 42(2):228–33. doi: 10.1016/j.ejca.2005.08.038

29. Du F, Sun ZW, Jia J, Yang Y, Yu J, Shi YW, et al. Development and validation of an individualized nomogram for predicting survival in patients with esophageal carcinoma after resection. *J Cancer* (2020) 11(14):4023–9. doi: 10.7150/jca.40767

30. Yao JL, Wang ZY, Sheng J, Wang HD, You LK, Zhu XD, et al. Efficacy and safety of combined immunotherapy and antiangiogenic therapy for advanced non-small cell lung cancer: A two-center retrospective study. *Int Immunopharmacol* (2020) 89:8. doi: 10.1016/j.intimp.2020.107033

31. Kodet O, Nemejcova K, Strnadova K, Havlinova A, Dundr P, Krajsova I, et al. The abscopal effect in the era of checkpoint inhibitors. *Int J Mol Sci* (2021) 22 (13):18. doi: 10.3390/ijms22137204

32. Hu ZH, Sun S, Zhao XM, Yu H, Wu XH, Wang JL, et al. Rh-Endostatin plus Irinotecan/Cisplatin as second-line therapy for advanced esophageal squamous cell carcinoma: An open-label, phase II study. *Oncologist* (2022) 27(4):253–+. doi: 10.1093/oncolo/oyab078

33. Chu L, Chen Y, Liu Q, Liang F, Wang SP, Liu Q, et al. A phase II study of apatinib in patients with chemotherapy-refractory esophageal squamous cell carcinoma (ESO-shanghai 11). *Oncologist* (2021) 26(6):E925–E35. doi: 10.1002/onco.13668

34. Matsubara Y, Toriyama K, Kadowaki S, Ogata T, Nakazawa T, Kato K, et al. Impact of PD-L1 combined positive score (CPS) on clinical response to nivolumab in patients with advanced esophageal squamous cell carcinoma. *J Clin Oncol* (2021) 39(15):3. doi: 10.1200/JCO.2021.39.15_suppl.e16045

35. Sullivan R, Weber J. Immune-related toxicities of checkpoint inhibitors: mechanisms and mitigation strategies. *Nat Rev Drug Discov* (2022) 21(7):495–508. doi: 10.1038/s41573-021-00259-5

36. Khan S, Gerber DE. Checkpoint inhibitor therapy and immune-related adverse events: A review. *Semin Cancer Biol* (2020) 64:93–101. doi: 10.1016/j.semcancer.2019.06.012

frontiers | Frontiers in Oncology

TYPE Original Research
PUBLISHED 14 September 2022
DOI 10.3389/fonc.2022.897476

OPEN ACCESS

EDITED BY
Mingqiang Kang,
Fujian Medical University Union Hospital, China

REVIEWED BY
Yongfu Yu,
Fudan University, China
Ahmed Mahmoud Fouad,
Suez Canal University, Egypt

*CORRESPONDENCE
Sheng-Guang Zhao
zsg10935@rjh.com.cn
Jia-Yi Chen
chenjiayi0188@aliyun.com

SPECIALTY SECTION
This article was submitted to Radiation Oncology, a section of the journal Frontiers in Oncology

RECEIVED 16 March 2022
ACCEPTED 23 August 2022
PUBLISHED 14 September 2022

CITATION
Zheng S-Y, Qi W-X, Zhao S-G and Chen J-Y (2022) No survival benefit could be obtained from adjuvant radiotherapy in esophageal cancer treated with neoadjuvant chemotherapy followed by surgery: A SEER-based analysis. *Front. Oncol.* 12:897476. doi: 10.3389/fonc.2022.897476

No survival benefit could be obtained from adjuvant radiotherapy in esophageal cancer treated with neoadjuvant chemotherapy followed by surgery: A SEER-based analysis

Si-Yue Zheng, Wei-Xiang Qi, Sheng-Guang Zhao* and Jia-Yi Chen*

Department of Radiation Oncology, Ruijin Hospital, Shanghai Jiaotong University School of Medicine, Shanghai, China

Background: The aim of this study is to assess the clinical benefit of postoperative radiotherapy (PORT) in patients with esophageal cancer (EC) who treated with neoadjuvant chemotherapy (NAC) and surgery *via* a national population-based database.

Methods: Patients diagnosed with EC between 2004 and 2015 were identified from the Surveillance, Epidemiology, and End Results (SEER) database. Kaplan–Meier survival analysis was used to compare the overall survival (OS) and cause-specific survival (CSS) difference between PORT *vs*. no-radiotherapy (RT) groups before and after propensity score matching (PSM). After PSM for baseline characteristics, Cox proportional hazard regression was performed to investigate the factors associated with OS.

Results: A total of 321 patients were included in the analysis. Of them, 91 patients (28%) received PORT. In the unmatched population, the no-RT group had improved OS compared with PORT (44 *vs*. 25 months, p = 0.002), and CSS was similar in patients undergoing NAC with or without PORT (42 *vs*. 71 months, p = 0.17). After PSM for baseline characteristics, the OS benefit of the no-RT group over the PORT group remained significant with a median OS of 46 *vs*. 27 months (p = 0.02), and CSS remained comparable between groups (83 *vs*. 81 months, p = 0.49). In subgroup analyses, PORT did not improve the OS among patients with adenocarcinoma in the subgroups of cN0, cN1, and cN2–3 (all p > 0.05). In Cox regression, aged ≥71 years old, cT3–4, cN2–3, and receiving PORT were independent predictors of worse OS, whereas cT4 and cN2–3 were independent predictors of worse CSS (all p < 0.05).

Conclusions: The present study demonstrated that no survival benefit could be obtained from the additional use of PORT after NAC and surgery in patients with EC. Well-designed prospective trials are needed to confirm our findings.

KEYWORDS

esophageal cancer, postoperative radiotherapy, neoadjuvant chemotherapy, SEER, prognosis

Introduction

In 2020, around 1 in every 18 cancer deaths is attributed to esophageal cancer (EC), which is now the seventh most common cancer and ranks sixth in mortality worldwide (1). Although esophagectomy is generally accepted as the mainstay treatment for decades, neoadjuvant and adjuvant therapies have been performed to improve the overall survival (OS) among these patients. The benefits of neoadjuvant chemotherapy (NAC) in EC have primarily been proven in the MAGIC trial, in which perioperative chemotherapy was superior to surgery alone for patients with gastroesophageal adenocarcinoma in terms of OS and progression-free survival (2). As demonstrated by the CROSS trial, neoadjuvant chemoradiotherapy (nCRT) could significantly prolong OS and disease-free survival (DFS) in patients with locally advanced EC compared with surgery alone (3). Subsequently, the NEOCRTEC 5010 trial also confirmed that treatment with nCRT plus surgery significantly improved long-term OS and DFS for patients with locally advanced esophageal squamous cell carcinoma (ESCC) (4).

However, the superiority of nCRT over NAC alone has not been evaluated in EC. Although few randomized controlled trials of small sample and meta-analyses have been performed to compare these two treatment modalities, controversy existed because of inconsistent conclusions and limited sample size (5–8). On the other hand, many patients with EC with poor performance status, older age, or comorbidities may be ineligible for nCRT due to expected high toxicity (9).

Meanwhile, the optimal postoperative therapeutic strategy remains undetermined. For those patients who undergo surgery without neoadjuvant therapy, several studies investigated the role of postoperative radiotherapy (PORT) in EC but reached conflicting conclusions (10–13). A prospective randomized study of 495 patients shows that PORT could improve the 5-year survival in patients with EC with positive lymph nodes and those with stage III disease (10). On the other hand, another prospective randomized study of 68 patients found no significant difference between the surgery alone group and the PORT group, and PORT significantly increased the incidence of esophagogastric fibrosis and affected the quality of life (11).

To date, the benefit of PORT in patients with EC undergoing NAC and surgery is not well established. Therefore, we sought to compare the survival benefit of patients with EC treated with and without PORT following NAC and surgery.

Material and methods

Patients

This population-based study was performed by using data from the Surveillance, Epidemiology, and End Results (SEER) database to identify patients with EC who underwent NAC and surgery diagnosed from 2004 to 2015. We obtained permission to access SEER Research Plus Data, Nov 2019 Sub (1975–2017) with reference number 11564-Nov2019. Cases eligible were required to have confirmed diagnosis with the recode as "only malignant in ICD-O-3" and the primary tumor site of the esophagus. Patients who received preoperative therapy without radiation prior to surgery were considered as having received NAC and included for analysis. For the sequence and type of radiation, only external beam radiation after surgery or no radiation was included for analysis. The following covariates were included: year of diagnosis, age, gender, race, chemotherapy, radiotherapy (RT) type and sequence, tumor histology, histological grade, clinical tumor (cT) stage, clinical nodal (cN) stage, clinical metastasis (cM) stage, and vital status, which includes the cause of death and the follow-up duration. cT, cN, and cM stages were categorized on the basis of the sixth edition of the American Joint Committee on Cancer/Union for International Cancer Control staging guidelines, and only cM0-stage patients were eligible. Patients with inadequate information were excluded from the final analysis. A flow diagram for patient inclusion and exclusion is shown in Figure 1.

Statistical analysis

The chi-square test was used to compare the differences for categorical variables in clinicopathologic features between RT

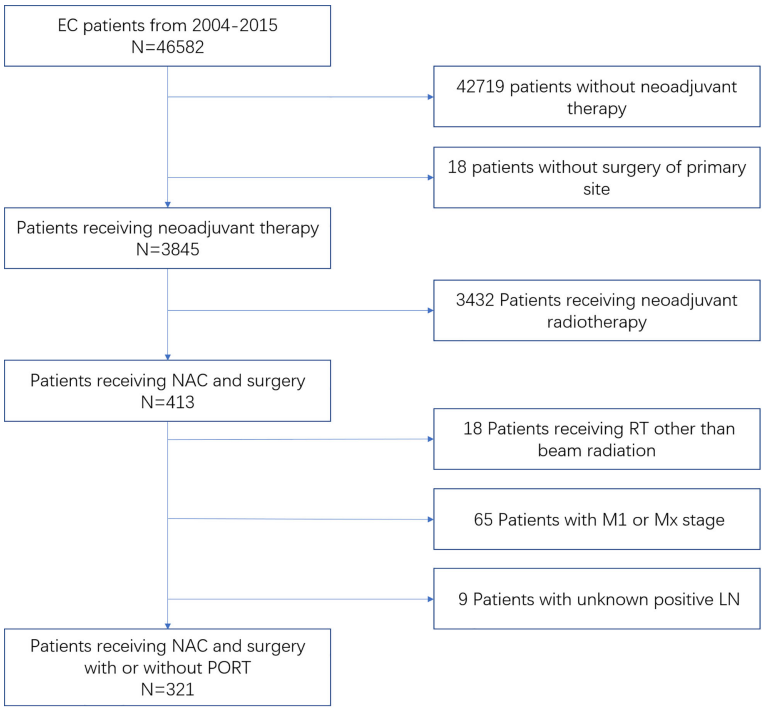

FIGURE 1
Inclusion and exclusion flow diagram for SEER EC patients receiving NAC followed by surgery with or without PORT from 2004 to 2015.

and no-RT groups. A propensity score matching (PSM) analysis (1:2 ratio; method, nearest neighbor matching; caliper, 0.03) was performed to balance the observed characteristics between the two groups. OS and cause-specific survival (CSS) were estimated by the Kaplan–Meier method, and the log-rank test was applied to compare survival curves. Univariate and multivariate Cox regression models were performed to investigate risk factors for OS. The variables with $p \leq 0.10$ in the univariate model were subsequently included in the multivariate analysis. All statistical analyses were performed in IBM SPSS version 23.0 and R statistical software version 4.0.3. Two-sided $p < 0.05$ was considered as statistically significant.

Results

Patient characteristics

From 2004 to 2015, a total of 321 patients registered in the SEER database received NAC alone followed by esophagectomy; the mean age at diagnosis was 62.41 ± 8.99 years. Of these, 230 patients (72%) did not receive adjuvant external beam radiation after surgery, whereas 91 patients (28%) received PORT.

The majority of the patients were of age from 61 to 70 years (43.9%), white (89.7%), and men (86.2%). The most frequent histological type was adenocarcinoma at 81.3% followed by ESCC at 18.7%. Notably, the patients who were treated with PORT tended to have a higher cN classification and a worse differentiated histological grade, whereas there was no statistically significant difference between the two groups in terms of age, sex, race, year of diagnosis, tumor histology, and cT classification. With PSM consisting of the number of positive lymph nodes and histological grade, 79 patients treated with PORT were successfully matched with 140 patients who did not receive postoperative radiation. The baseline clinicopathological characteristics for the study population before and after PSM are demonstrated in Table 1.

Survival prior to PSM

The median follow-up time for the eligible patients was 74 months [interquartile range (IQR), 47–109 months] with the median OS being 37 months (IQR, 18–116 months). Figures 2A, B represent a Kaplan–Meier OS curve and a Kaplan–Meier CSS curve with the number of subjects at risk and 95% confidence

TABLE 1 Baseline characteristics of patients included in the analysis before and after PSM.

Characteristic	Before PSM			After PSM		
	Without PORT (n, %)	With PORT (n, %)	P-value	Without PORT (n, %)	With PORT (n, %)	P-value
Total	n = 230	n = 91		n = 140	n = 79	
Year of diagnosis			0.337			0.728
2004–2007	60 (26.1)	31 (34.1)		43 (30.7)	26 (32.9)	
2008–2011	101 (43.9)	34 (37.4)		59 (42.1)	29 (36.7)	
2012–2015	69 (30.0)	26 (28.6)		38 (27.1)	24 (30.4)	
Gender			0.211			0.07
Male	195 (84.8)	82 (90.1)		115 (82.1)	72 (91.1)	
Female	35 (15.2)	9 (9,9)		25 (17.9)	7 (8.9)	
Age groups (years)			0.838			0.911
≤50	19 (8.3)	10 (11.0)		12 (8.6)	8 (10.1)	
51–60	68 (29.6)	27 (29.7)		38 (27.1)	23 (29.1)	
61–70	101 (43.9)	40 (44.0)		64 (45.7)	36 (45.6)	
≥71	42 (18.3)	14 (15.4)		26 (18.6)	12 (15.2)	
Race			0.337			0.365
White	204 (88.7)	84 (92.3)		124 (88.6)	73 (92.4)	
Black and others	26 (11.3)	7 (7.7)		16 (11.4)	6 (7.6)	
cT classification			0.862			0.606
T1	34 (14.8)	12 (13.2)		18 (12.9)	12 (15.2)	
T2	37 (16.1)	15 (16.5)		22 (15.7)	15 (19.0)	
T3	141 (61.3)	59 (64.8)		89 (63.6)	49 (62.0)	
T4 and Tx	18 (7.8)	5 (5.5)		11 (7.9)	3 (3.8)	
cN classification			0.004			0.832
N0	134 (58.3)	36 (39.6)		66 (47.1)	35 (44.3)	
N1	54 (23.5)	24 (26.4)		46 (32.9)	24 (30.4)	
N2	26 (11.3)	23 (25.3)		23 (16.4)	16 (20.3)	
N3	16 (7.0)	8 (8.8)		5 (3.6)	4 (5.1)	
Tumor histology			0.448			0.896
Adenocarcinoma	195 (84.8)	74 (81.3)		116 (82.9)	66 (83.5)	
SCC	35 (15.2)	17 (18.7)		24 (17.1)	13 (16.5)	
Histological grade			0.041			0.865
Well	6 (2.6)	7 (7.7)		4 (2.9)	4 (5.1)	
Moderate	87 (37.8)	25 (27.5)		43 (30.7)	24 (30.4)	
Poor/Undifferentiated	113 (49.1)	53 (58.2)		83 (59.3)	46 (58.2)	
Unknown	24 (10.4)	6 (6.6)		10 (7.1)	5 (6.3)	

PSM, propensity score matching; PORT, postoperative radiotherapy; T, tumor; N, nodal; SCC, squamous cell carcinoma.

interval (CI) comparing patients who either received or did not receive PORT. The results of the log-rank test are also shown in Figures 2A, B. A significant OS benefit was noted between the no-RT and RT groups (P = 0.002). The median OS rates for patients who received and did not receive PORT were 25 months (95% CI, 18.7–31.3 months) and 44 months (95% CI, 32.6–55.4 months), respectively. The log-rank test did not indicate a significant CSS difference between the two groups (P = 0.17). However, the patients not receiving PORT still had a longer median CSS of 71 months (95% CI, 46.7–95.3 months), followed by the patients receiving RT only with a CSS of 42 months (95% CI, 7.6–76.4 months).

Survival after PSM

In the matched cohort, the OS advantage of the no-RT group over the RT group persisted with a median OS of 46 months (95% CI, 33.3–58.7 months) and 27 months (95% CI, 16.9–37.1 months), respectively (p = 0.02; Figure 3A). CSS remained comparable between the groups (p = 0.49; Figure 3B). The no-RT group still had more favorable median CSS of 83 months (95% CI, 49.2–112.8 months) versus 81 months (95% CI, 22.2–143.8 months) for the RT group.

Moreover, Kaplan–Meier analysis stratified by the cN stage among patients with adenocarcinoma revealed no statistical

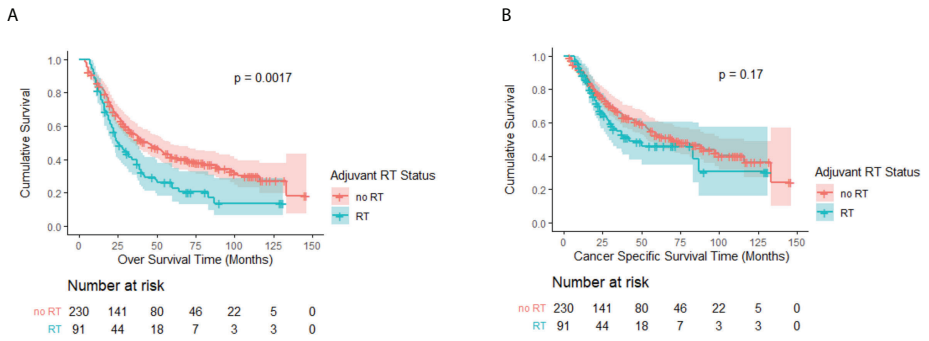

FIGURE 2
(A) Kaplan–Meier OS curve by adjuvant RT status before PSM. A significant difference was noted (P = 0.002). **(B)** Kaplan–Meier CSS curve by adjuvant RT status before PSM. No significant difference was observed (P = 0.17).

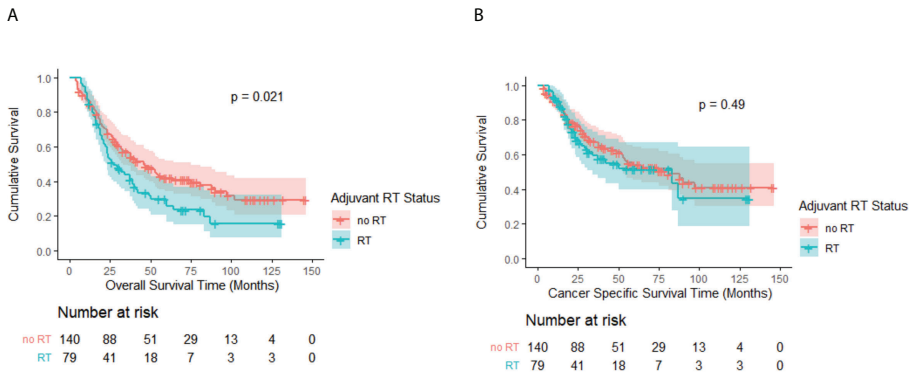

FIGURE 3
(A) Kaplan–Meier OS curve by adjuvant RT status after PSM. A significant difference was noted (P = 0.02). **(B)** Kaplan–Meier CSS curve by adjuvant RT status after PSM. No significant difference was observed (P = 0.49).

significance between the RT and no-RT groups. The median OS rates of the two groups were all not reached in the cN0 and cN1 subgroups, whereas the 3-year OS rates of the RT group were higher than those of the no-RT group but showed no significance (cN0: 69.7% *vs.* 58.9%, p = 0.42, Figure 4A; cN1: 61.9% *vs.* 47.4%, p = 0.22, Figure 4B). There is also no survival benefit of PORT in the cN2–3 subgroup (median OS: 22 months *vs.* 19 months, p = 0.56, Figure 4C).

The prognostic factors associated with OS in univariate and multivariate analyses for the matched cohort are shown in Table 2. Univariate analysis showed that the factors associated with worse OS included age ≥71 years old, cT3–4, cN2–3, and receiving PORT, which remained independent factors significantly decreasing OS in multivariate analysis.

The prognostic factors associated with CSS in univariate and multivariate analyses for the matched cohort are shown in Table 3. On univariate analysis, the factors associated with worse CSS included male sex, cT3–4, cN2–3, and adenocarcinoma. On multivariate analysis, cT4 and cN2–3 were still independently associated with a decreased CSS.

Discussion

According to the National Comprehensive Cancer Network guideline (version 3.2021) recommendation, all patients with EC who have not received nCRT or NAC with R1 or R2 resection should receive PORT. For R0 cases, PORT is only recommended for T3–T4a or N1–3 patients with adenocarcinoma without nCRT or NAC (14). However, the efficacy of adding PORT in patients with EC after NAC alone remains unclear. To the best of our knowledge, this is the first

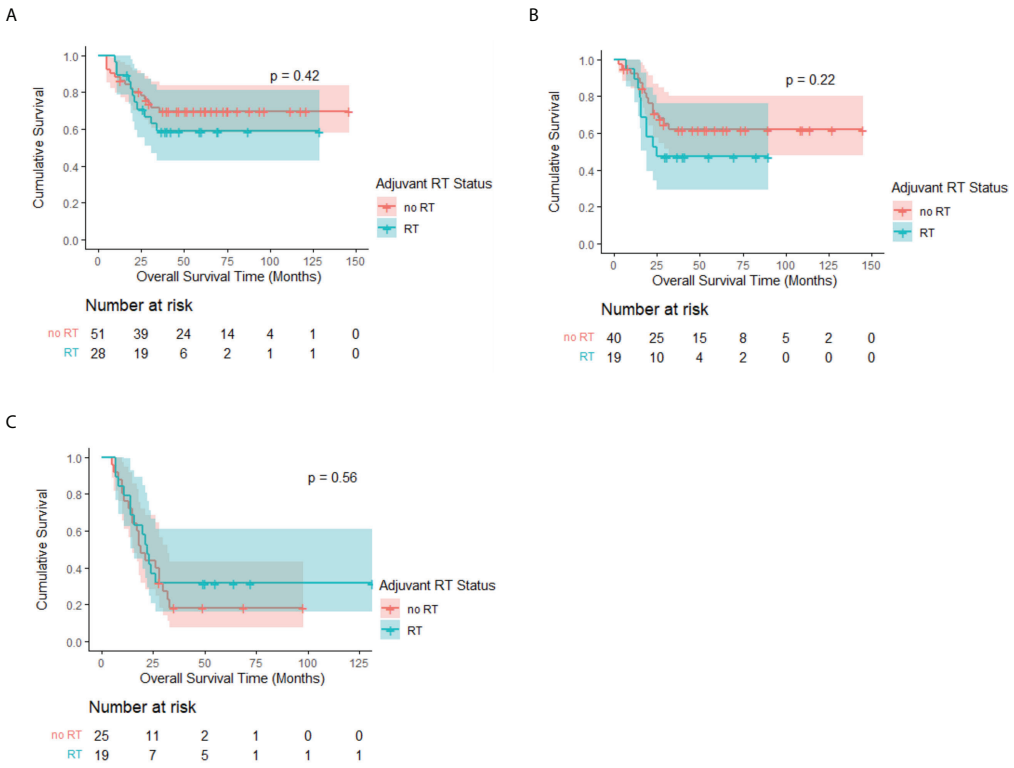

FIGURE 4
Kaplan–Meier OS curve of patients with adenocarcinoma by adjuvant RT status after PSM, stratified by cN stage. Median survival estimates: **(A)** cN0: Both median OS not reached, p = 0.42. **(B)** cN1: Both median OS not reached, p = 0.22. **(C)** cN2–3: RT: 22 months (95% CI, 17.7–26.3 months) *vs*. No RT: 19 months (95% CI, 14.1–23.9 months), p = 0.56.

retrospective study to investigate the role of PORT for patients with EC after NAC and surgery.

We revealed that omitting PORT after NAC and surgery showed a significantly better OS than the PORT group before and after PSM, whereas there were no significant differences in CSS between the two groups. In subgroup analysis according to recurrence risk factors, we also found that no survival benefit could be obtained in those with cT3 stage or positive nodes, which was quite different from previous studies focusing on the effectiveness of PORT in patients with EC without defining the use of NAC (15, 16). This may be attributed to the treatment toxicities caused by PORT, which have already been affected by the chemotherapy and surgery. Wang et al. revealed that 18% of the patients with EC experienced grade 3 or higher cardiac events after RT, which was associated with worse OS (p = 0.041) (17). Pinder-Arabpour et al. demonstrated that ventilation heterogeneities occurred in 30% of the patients with EC undergoing RT (18). Although currently we did not find any research comparing the side effects between NAC + surgery with and without PORT, Zhang et al. reported that NAC caused fewer cardiopulmonary events than nCRT (19). The patients analyzed in our study were diagnosed in the years from 2004 to 2015, and most of them received conventional radiation therapy by using two parallel beams with opposed orientations. Therefore, relatively large volumes of normal tissues adjacent to the treatment field (including the mediastinum, chest wall, and adjacent lung) are irradiated. Further investigations with advanced technology such as intensity-modulated radiation therapy and proton therapy are in progress to confirm the safety of the treatment strategy (NCT01512589).

In our study, adenocarcinoma accounts for 83.8% of all 321 patients, which reflects the high prevalence of adenocarcinoma in Western countries just as most clinical trials conducted in Europe and Northern America (2, 3, 20). Conversely, considering that SCC was the most common histological subtype among Chinese patients with EC, the conclusion might not be directly applied to East Asia people (21). As the 10-year outcome of the CROSS trial demonstrated, nCRT tended to be more beneficial in the SCC group than in the adenocarcinoma group with a 10-year OS in the nCRT-surgery group of 46% and 36%, respectively (22). The conclusion was confirmed by the NEOCRTEC5010 trial, in which the median OS for Chinese patients with ESCC receiving nCRT plus surgery was 100.1 months and the 3-year OS was 69.1%, which is

10.3389/fonc.2022.897476

TABLE 2 Univariate and multivariate analysis of OS for the matched cohort after PSM.

Characteristic	Univariate			Multivariate		
	P-value	OR	95% CI	P-value	OR	95% CI
Year of diagnosis	0.599					
2004–2007	1					
2009–2011	0.731	0.936	0.641–1.367			
2012–2015	0.314	0.783	0.487–1.260			
Gender						
Male	1					
Female	0.135	0.671	0.397–1.132			
Age groups (years)	0.024			0.002		
≤50	1			1		
51–60	0.976	1.01	0.521–1.956	0.511	1.262	0.630–2.526
61–70	0.381	1.318	0.711–2.444	0.068	1.817	0.957–3.451
≥71	0.032	2.098	1.068–4.123	0.002	3.052	1.496–6.228
Race						
White	1					
Black and others	0.293	0.708	0.372–1.348			
cT classification	0.004			0.003		
T1	1			1		
T2	0.45	1.306	0.654–2.609	0.399	1.358	0.667–2.763
T3	0.01	2.153	1.205–3.847	0.013	2.132	1.177–3.862
T4	0.002	4.236	1.684–10.652	0.001	4.91	1.888–12.768
Tx	0.852	0.868	0.196–3.846	0.745	0.777	0.170–3.546
cN classification	< 0.001			< 0.001		
N0	1			1		
N1	0.158	1.332	0.895–1.984	0.159	1.337	0.892–2.002
N2	0.001	2.106	1.349–3.288	0.001	2.177	1.359–3.486
N3	< 0.001	4.597	2.237–9.449	<0.001	4.079	1.965–8.467
Tumor histology						
Adenocarcinoma	1					
SCC	0.934	1.019	0.651–1.596			
Histological grade	0.567					
Well	1					
Moderate	0.251	1.985	0.616–6.393			
Poor/Undifferentiated	0.285	1.876	0.592–5.944			
Unknown	0.169	2.453	0.684–8.800			
PORT						
Yes	1			1		
No	0.024	0.674	0.479–0.948	0.012	0.638	0.448–0.907

T, tumor; N, nodal; SCC, squamous cell carcinoma; PORT, postoperative radiotherapy.

obviously better than that reported in previous trials containing more patients with adenocarcinoma (4, 20). On the other hand, NAC is suggested as the standard treatment for locally advanced ESCC in Japan according to the result of the JCOG9907 trial, in which the 5-year OS of the NAC group was 55% (23, 24). In our study, the 3- and 5-year OS rates of patients with SCC in the PORT group after PSM were 25.6% and 17.1%, respectively, and those in the no-RT group were 56.1% and 44.9%, respectively. Comparing our results with those of the clinical trials mentioned above, the OS of both groups in our study showed a reduction by at least 10% compared with the prognosis in the NEOCRTEC5010 and JCOG9907 trials. Taken together, the present study demonstrated that the addition of PORT to NAC combined with surgery in patients with ESCC may also be associated with a higher mortality and adjuvant RT is also not recommended in patients with ESCC treated with NAC.

It is also worth mentioning that immunotherapy has shown positive impacts on patients with advanced EC from back line to

TABLE 3 Univariate and multivariate analysis of CSS for the matched cohort after PSM.

Characteristic	Univariate			Multivariate		
	P-value	OR	95% CI	P-value	OR	95% CI
Year of diagnosis	0.903					
2004–2007	1					
2009–2011	0.838	0.952	0.592–1.530			
2012–2015	0.651	0.875	0.490–1.562			
Gender						
Male	1			1		
Female	0.056	0.491	0.237–1.018	0.148	0.574	0.270–1.219
Age groups (years)	0.554					
≤50	1					
51–60	0.617	1.223	0.556–2.694			
61–70	0.657	1.188	0.555–2.546			
≥71	0.215	1.715	0.732–4.021			
Race						
White	1					
Black and others	0.177	0.537	0.218–1.325			
cT classification	0.001			0.002		
T1	1			1		
T2	0.650	0.807	0.320–2.034	0.454	0.697	0.270–1.797
T3	0.034	2.127	1.058–4.276	0.083	1.880	0.921–3.838
T4	0.002	5.201	1.843–14.676	0.009	4.107	1.420–11.875
Tx	0.647	0.617	0.078–4.874	0.423	0.424	0.052–3.455
cN classification	0.001			0.004		
N0	1			1		
N1	0.176	1.407	0.857–2.310	0.269	1.330	0.802–2.206
N2	0.003	2.285	1.318–3.962	0.010	2.116	1.195–3.748
N3	< 0.001	4.859	2.003–11.789	0.002	4.134	1.688–10.127
Tumor histology						
Adenocarcinoma	1			1		
SCC	0.031	0.428	0.198–0.926	0.129	0.538	0.242–1.198
Histological grade	0.410					
Well	1					
Moderate	0.380	1.902	0.453–7.989			
Poor/Undifferentiated	0.406	1.821	0.443–7.487			
Unknown	0.156	3.037	0.655–14.071			
PORT						
Yes	1					
No	0.494	1.164	0.754–1.797			

T, tumor; N, nodal; SCC, squamous cell carcinoma; PORT, postoperative radiotherapy.

first line, according to the result of several clinical trials such as KEYNOTE-590 and ESCORT-1st, but little is confirmed about its role in neoadjuvant therapy regimen (25, 26). Some single-armed trials focused on preoperative immuno-chemo-radiotherapy. For example, the PERFECT trial combined Atezolizumab with nCRT, and the pathologic complete response (PCR) rate was 25% (27). PALACE-1 used Pembrolizumab and got a higher PCR rate of 55.6% (28). Meanwhile, some other trials combined chemotherapy alone with immunotherapy. Yang et al. evaluated the efficacy and safety of camrelizumab plus nab-paclitaxel and S1 capsule followed by surgery, and the PCR rate was 33.3% (29). Xing et al. designed a phase II randomized trial, in which both groups received chemotherapy on day 1, then the experimental group received toripalimab on day 3, while the control group received it on day 1. The PCR rates were 36% and 7%, respectively (30). However, none of those neoadjuvant chemoimmunotherapy studies allowed PORT, which may be due to the safety

concern. The studies mentioned above are all with a small sample size, and the value of PORT for patients with EC under the brand new neoadjuvant therapeutic regimen including immunotherapy and chemotherapy needs to be redefined in the future.

However, we acknowledge several important limitations in our study. First, selection bias could not be avoided because of the retrospective nature of our study, although PSM was performed. Second, in the SEER database, it lacks detailed information regarding chemotherapy regimen, radiation dose, surgical margin, and certain risk factors such as smoking and alcohol exposure, which can affect the reliability of our findings.

In summary, our results detect no survival benefit with the use of PORT after NAC and surgery in patients with EC. Furthermore, multivariate analysis indicates that PORT, age ≥71 years old, cT3–4, and cN2–3 are independent predictors of worse OS. Further study is needed to identify an optimal treatment strategy in patients with EC after NAC and surgery.

Data availability statement

The original contributions presented in the study are included in the article. Further inquiries can be directed to the corresponding authors.

Ethics statement

Ethical review and approval was not required for the study on human participants in accordance with the local legislation and institutional requirements. Written informed consent for participation was not required for this study in accordance with the national legislation and the institutional requirements.

Author contributions

S-YZ and W-XQ contributed to the design of the research, to the analysis of the data, and to the writing of the manuscript. S-GZ and J-YC were in charge of overall direction. All authors contributed to the article and approved the submitted version.

Funding

This study was supported in part by the Clinical Research Plan of SHDC (grant numbers SHDC2020CR4070 and SHDC2020CR2052B) and special construction of integrated Chinese and Western medicine in general hospital (numbers ZHYY-ZXYJHZ X-2-201704 and ZHYY-ZXYJHZ X-2-201913).

Conflict of interest

The authors declare that the research was conducted in the absence of any commercial or financial relationships that could be construed as a potential conflict of interest.

Publisher's note

References

1. Sung H, Ferlay J, Siegel RL, Laversanne M, Soerjomataram I, Jemal A, et al. Global cancer statistics 2020: GLOBOCAN estimates of incidence and mortality worldwide for 36 cancers in 185 countries. *CA Cancer J Clin* (2021) 71(3):209–49. doi: 10.3322/caac.21660

2. Cunningham D. Perioperative chemotherapy versus surgery alone for resectable gastroesophageal cancer. *N Engl J Med* (2006) 355(1):11–20. doi: 10.1056/NEJMoa055531

3. Shapiro J, van Lanschot JJB, Hulshof MCCM, van Hagen P, van Berge Henegouwen MI, Wijnhoven BPL, et al. Neoadjuvant chemoradiotherapy plus surgery versus surgery alone for oesophageal or junctional cancer (CROSS): long-term results of a randomised controlled trial. *Lancet Oncol* (2015) 16(9):1090–8. doi: 10.1016/S1470-2045(15)00040-6

4. Yang H, Liu H, Chen Y, Zhu C, Fang W, Yu Z, et al. Neoadjuvant chemoradiotherapy followed by surgery versus surgery alone for locally advanced squamous cell carcinoma of the esophagus (NEOCRTEC5010): A phase III multicenter, randomized, open-label clinical trial. *JCO* (2018) 36 (27):2796–803. doi: 10.1200/JCO.2018.79.1483

5. Stahl M, Walz MK, Riera-Knorrenschild J, Stuschke M, Sandermann A, Bitzer M, et al. Preoperative chemotherapy versus chemoradiotherapy in locally advanced adenocarcinomas of the oesophagogastric junction (POET): Long-term results of a controlled randomised trial. *Eur J Canc* (2017) 81:183–90. doi: 10.1016/j.ejca.2017.04.027

6. von Döbeln GA, Klevebro F, Jacobsen A-B, Johannessen H-O, Nielsen NH, Johnsen G, et al. Neoadjuvant chemotherapy versus neoadjuvant chemoradiotherapy for cancer of the esophagus or gastroesophageal junction: long-term results of a randomized clinical trial. *Dis Esophagus* (2019) 32(2). doi: 10.1093/dote/doy078/5078143

7. Jing S, Qin J, Liu Q, Zhai C, Wu Y, Cheng Y, et al. Comparison of neoadjuvant chemoradiotherapy and neoadjuvant chemotherapy for esophageal cancer: a meta-analysis. *Future Oncol* (2019) 15(20):2413–22. doi: 10.2217/fon-2019-0024

8. Fan M, Lin Y, Pan J, Yan W, Dai L, Shen L, et al. Survival after neoadjuvant chemotherapy versus neoadjuvant chemoradiotherapy for resectable esophageal carcinoma: A meta-analysis. *Thorac Canc* (2016) 7(2):173–81. doi: 10.1111/1759-7714.12299

9. Tougeron D, Hamidou H, Scotté M, Di Fiore F, Antonietti M, Paillot B, et al. Esophageal cancer in the elderly: an analysis of the factors associated with treatment decisions and outcomes. *BMC Canc* (2010) 10(1):510. doi: 10.1186/1471-2407-10-510

10. Xiao ZF, Yang ZY, Liang J, Miao YJ, Wang M, Yin WB, et al. Value of radiotherapy after radical surgery for esophageal carcinoma: a report of 495

patients. *Ann Thorac Surg* (2003) 75(2):331–6. doi: 10.1016/S0003-4975(02)04401-6

11. Zieren HU, Müller JM, Jacobi CA, Pichlmaier H, Müller R-P, Staar S. Adjuvant postoperative radiation therapy after curative resection of squamous cell carcinoma of the thoracic esophagus: A prospective randomized study. *World J Surg* (1995) 19(3):444–9. doi: 10.1007/BF00299187

12. Liu T, Liu W, Zhang H, Ren C, Chen J, Dang J. The role of postoperative radiotherapy for radically resected esophageal squamous cell carcinoma: a systemic review and meta-analysis. *J Thorac Dis* (2018) 10(7):4403–12. doi: 10.21037/jtd.2018.06.65

13. Lin H-N, Chen L-Q, Shang Q-X, Yuan Y, Yang Y-S. A meta-analysis on surgery with or without postoperative radiotherapy to treat squamous cell esophageal carcinoma. *Int J Surg* (2020) 80:184–91. doi: 10.1016/j.ijsu.2020.06.046

14. Ajani JA, Barthel JS, Bentrem DJ, D'Amico TA, Das P, Denlinger CS, et al. Esophageal and esophagogastric junction cancers. *J Natl Compr Canc Netw* (2011) 9(8):830–87. doi: 10.6004/jnccn.2011.0072

15. Chen S, Weng H, Wang G, Liu D, Li H, Zhang H, et al. The impact of adjuvant radiotherapy on radically resected T3 esophageal squamous cell carcinoma. *J Cancer Res Clin Oncol* (2016) 142(1):277–86. doi: 10.1007/s00432-015-2041-z

16. Chen J, Pan J, Zheng X, Zhu K, Li J, Chen M, et al. Number and location of positive nodes, postoperative radiotherapy, and survival after esophagectomy with three-field lymph node dissection for thoracic esophageal squamous cell carcinoma. *Int J Radiat OncologyBiologyPhysics* (2012) 82(1):475–82. doi: 10.1016/j.ijrobp.2010.08.037

17. Wang X, Palaskas NL, Yusuf SW, Abe J, Lopez-Mattei J, Banchs J, et al. Incidence and onset of severe cardiac events after radiotherapy for esophageal cancer. *J Thorac Oncol* (2020) 15(10):1682–90. doi: 10.1016/j.jtho.2020.06.014

18. Pinder-Arabpour A, Jones B, Castillo R, Castillo E, Guerrero T, Goodman K, et al. Characterizing spatial lung function for esophageal cancer patients undergoing radiation therapy. *Int J Radiat OncologyBiologyPhysics* (2019) 103(3):738–46. doi: 10.1016/j.ijrobp.2018.10.024

19. Zhang Z, Zhang H. Impact of neoadjuvant chemotherapy and chemoradiotherapy on postoperative cardiopulmonary complications in patients with esophageal cancer. *Dis Esophagus* (2017) 30(4):1–7. doi: 10.1093/dote/dox002

20. Tepper J, Krasna MJ, Niedzwiecki D, Hollis D, Reed CE, Goldberg R, et al. Phase III trial of trimodality therapy with cisplatin, fluorouracil, radiotherapy, and surgery compared with surgery alone for esophageal cancer: CALGB 9781. *JCO* (2008) 26(7):1086–92. doi: 10.1200/JCO.2007.12.9593

21. Arnold M, Soerjomataram I, Ferlay J, Forman D. Global incidence of oesophageal cancer by histological subtype in 2012. *Gut* (2015) 64(3):381–7. doi: 10.1136/gutjnl-2014-308124

22. Eyck BM, van Lanschot JJB, Hulshof MCCM, van der Wilk BJ, Shapiro J, van Hagen P, et al. Ten-year outcome of neoadjuvant chemoradiotherapy plus surgery for esophageal cancer: The randomized controlled CROSS trial. *JCO* (2021) 39(18):1995–2004. doi: 10.1200/JCO.20.03614

23. Ando N, Kato H, Igaki H, Shinoda M, Ozawa S, Shimizu H, et al. A randomized trial comparing postoperative adjuvant chemotherapy with cisplatin and 5-fluorouracil versus preoperative chemotherapy for localized advanced squamous cell carcinoma of the thoracic esophagus (JCOG9907). *Ann Surg Oncol* (2012) 19(1):68–74. doi: 10.1245/s10434-011-2049-9

24. Kitagawa Y, Uno T, Oyama T, Kato K, Kato H, Kawakubo H, et al. Esophageal cancer practice guidelines 2017 edited by the Japan esophageal society: part 1. *Esophagus* (2019) 16(1):1–24. doi: 10.1007/s10388-018-0641-9

25. Sun J-M, Shen L, Shah MA, Enzinger P, Adenis A, Doi T, et al. Pembrolizumab plus chemotherapy versus chemotherapy alone for first-line treatment of advanced oesophageal cancer (KEYNOTE-590): a randomised, placebo-controlled, phase 3 study. *Lancet* (2021) 398(10302):759–71. doi: 10.1016/S0140-6736(21)01234-4

26. Luo H, Lu J, Bai Y, Mao T, Wang J, Fan Q, et al. Effect of camrelizumab vs placebo added to chemotherapy on survival and progression-free survival in patients with advanced or metastatic esophageal squamous cell carcinoma: The ESCORT-1st randomized clinical trial. *JAMA* (2021) 326(10):916. doi: 10.1001/jama.2021.12836

27. van den Ende T, de Clercq NC, van Berge Henegouwen MI, Gisbertz SS, Geijsen ED, Verhoeven RHA, et al. Neoadjuvant chemoradiotherapy combined with atezolizumab for resectable esophageal adenocarcinoma: A single-arm phase II feasibility trial (PERFECT). *Clin Cancer Res* (2021) 27(12):3351–9. doi: 10.1158/1078-0432.CCR-20-4443

28. Li C, Zhao S, Zheng Y, Han Y, Chen X, Cheng Z, et al. Preoperative pembrolizumab combined with chemoradiotherapy for oesophageal squamous cell carcinoma (PALACE-1). *Eur J Canc* (2021) 144:232–41. doi: 10.1016/j.ejca.2020.11.039

29. Zhang X, Yang G, Su X, Luo G, Cai P, Zheng Y, et al. Neoadjuvant programmed death-1 blockade plus chemotherapy in locally advanced esophageal squamous cell carcinoma. *JCO* (2021) 39(15_suppl):e16076–6. doi: 10.1200/JCO.2021.39.15_suppl.e16076

30. Xing W, Zhao L, Zheng Y, Liu B, Liu X, Li T, et al. The sequence of chemotherapy and toripalimab might influence the efficacy of neoadjuvant chemoimmunotherapy in locally advanced esophageal squamous cell cancer–a phase II study. *Front Immunol* (2021) 12:772450. doi: 10.3389/fimmu.2021.772450

frontiers | Frontiers in Oncology

TYPE Original Research
PUBLISHED 03 October 2022
DOI 10.3389/fonc.2022.954187

OPEN ACCESS

EDITED BY
Li Jiancheng,
Fujian Cancer Hospital, China

REVIEWED BY
Zhiyong Xu,
Shanghai Jiao Tong University, China
Fu Jin,
Chongqing University, China

*CORRESPONDENCE
Yong Yin
yongyinsd@163.com
Changsheng Ma
machangsheng_2000@126.com

SPECIALTY SECTION
This article was submitted to Radiation Oncology, a section of the journal Frontiers in Oncology

RECEIVED 27 May 2022
ACCEPTED 05 September 2022
PUBLISHED 03 October 2022

CITATION
Cui Y, Pan Y, Li Z, Wu Q, Zou J, Han D, Yin Y and Ma C (2022) Dosimetric analysis and biological evaluation between proton radiotherapy and photon radiotherapy for the long target of total esophageal squamous cell carcinoma. *Front. Oncol.* 12:954187. doi: 10.3389/fonc.2022.954187

Dosimetric analysis and biological evaluation between proton radiotherapy and photon radiotherapy for the long target of total esophageal squamous cell carcinoma

Yongbin Cui[1], Yuteng Pan[2], Zhenjiang Li[1], Qiang Wu[3], Jingmin Zou[1], Dali Han[1], Yong Yin[1]* and Changsheng Ma[1]*

[1]Department of Radiation Oncology, Shandong Cancer Hospital and Institute, Shandong First Medical University and Shandong Academy of Medical Sciences, Jinan, China, [2]Medical Science and Technology Innovation Center, Shandong First Medical University and Shandong Academy of Medical Sciences, Jinan, China, [3]Affiliated Hospital of Weifang Medical University, School of Clinical Medicine, Weifang Medical University, Weifang, China

Objective: The purpose of this study is to compare the dosimetric and biological evaluation differences between photon and proton radiation therapy.

Methods: Thirty esophageal squamous cell carcinoma (ESCC) patients were generated for volumetric modulated arc therapy (VMAT) planning and intensity-modulated proton therapy (IMPT) planning to compare with intensity-modulated radiation therapy (IMRT) planning. According to dose–volume histogram (DVH), dose–volume parameters of the plan target volume (PTV) and homogeneity index (HI), conformity index (CI), and gradient index (GI) were used to analyze the differences between the various plans. For the organs at risk (OARS), dosimetric parameters were compared. Tumor control probability (TCP) and normal tissue complication probability (NTCP) was also used to evaluate the biological effectiveness of different plannings.

Results: CI, HI, and GI of IMPT planning were significantly superior in the three types of planning ($p < 0.001$, $p < 0.001$, and $p < 0.001$, respectively). Compared to IMRT and VMAT planning, IMPT planning improved the TCP ($p<0.001$, $p<0.001$, respectively). As for OARs, IMPT reduced the bilateral lung and heart accepted irradiation dose and volume. The dosimetric parameters, such as mean lung dose (MLD), mean heart dose (MHD), V_5, V_{10}, and V_{20}, were significantly lower than IMRT or VMAT. IMPT afforded a lower maximum dose (D_{max}) of the spinal cord than the other two-photon plans. What's more, the radiation pneumonia of the left lung, which was caused by IMPT, was lower than IMRT and VMAT. IMPT achieved the pericarditis probability of heart is only 1.73% $\pm$ 0.24%. For spinal cord myelitis necrosis, there was no significant difference between the three different technologies.

Conclusion: Proton radiotherapy is an effective technology to relieve esophageal cancer, which could improve the TCP and spare the heart, lungs, and spinal cord. Our study provides a prediction of radiotherapy outcomes and further guides the individual treatment.

KEYWORDS

proton radiotherapy, photon radiotherapy, dosimetric analysis, biological evaluation, esophageal squamous cell carcinoma

Introduction

Esophageal cancer is one of the malignant tumors with the highest incidence worldwide (1). In East Asia, the subtype of esophageal cancer (EC) is mainly squamous cell carcinoma, with a poor prognosis and 5-year survival rates of less than 20% (2). As an effective treatment method for esophageal squamous cell carcinoma (ESCC), radiotherapy has been widely used in clinical therapy. Compared to two-dimensional conformal radiotherapy (2D-CRT), three-dimensional conformal radiotherapy (3D-CRT) can significantly improve the dose distribution in the target volume and reduce the accepted dose of normal tissues (3). However, compared to 3D-CRT, intensity-modulated radiotherapy (IMRT) has been used for the radiotherapy of ESCC patients because of its ability to provide superior target volume coverage, conformality, and ability to reduce dose to normal tissues (4). Recently, volume-modulated arc therapy (VMAT) for patients with ESCC has also been widely explored (5). Nonetheless, no matter whether IMRT or VMAT, photon radiotherapy will lead to normal tissue toxicity to some degree.

Hence, it is critical to ensure tumor control probability (TCP) while decreasing dose to normal tissues and normal tissue complication probability (NTCP). In proton beam, there is a deposition characteristic called "Bragg peak," which can be used to create a matchable depth and thickness of the tumor target (6). Previous studies have demonstrated that proton therapy could provide a dose-sparing advantage for organs at risk (OARs) in lung cancer patients (7). Further studies have also proved that proton therapy has therapeutic advantages over conventional external radiotherapy in esophageal cancer (8).

However, whether it is photon therapy or proton therapy, the current research focuses on the dosimetric differences (9, 10). A few studies have looked into the differences in additional biological effects between photon and proton therapy. Wang et al. (11)developed and tested a Lyman–Kutcher–Burman (LKB) model to predict radiation esophagitis (RE) in nonsmall cell lung cancer (NSCLC) cancer. However, those NSCLC patients received passive-scattering proton therapy (PSBT) not modulated scanning.

Therefore, we aimed to compare the dosimetric difference between proton therapy and two-photon therapy in ESCC patients. Thereafter, TCP and NTCP prediction methods are used to predict the radiotherapy outcomes and toxicity. The purpose of this study is to compare the dosimetry advantages of intensity-modulated proton therapy (IMPT) compared with IMRT and VMAT in radiotherapy for patients with ESCC, and then predict the biological effects of TCP and NTCP to guide the individual radiotherapy.

Materials and methods

Patients and imaging acquisition

Thirty ESCC patients were recruited in Shandong Cancer Hospital and Institute, who received radiation therapy with the prescribed dose of 60 Gy between 2015 and 2020. Inclusion criteria were as follows: (1) patients with unresected esophageal cancer; (2) no prior history of radiotherapy and chemotherapy; and (3) no prior cardiac or respiratory diseases. Exclusion criteria were as follows: (1) changed treatment regimens during definitive radiotherapy. (2) a combination of other malignancies. This study was approved by the Ethics Committee of our institute according to the Declaration of Helsinki.

All patients were scanned with Philips Big Core CT (Phillips Medical Systems, 96 Highland Heights, OH). The scanning parameters were as follows: tube voltage: 120 KvP, tube current: 53–400 mA, each scanning period: 2.8 s, interval time: 1.8 s, scanning layer thickness: 5 mm, and a vacuum cushion was used to fix the scanning process. The scanned images were uploaded to the Eclipse15.5 treatment planning system (Varian Medical Systems, Palo Alto, CA, USA) for delineation of the target volume, OARs, and designing radiotherapy plans.

Target volume and organ-at-risk delineation

The target volume and OARs were delineated by the same oncologist with more than 5 years of work experience. The gross

target volume (GTV) was delineated on the target volume of primary esophageal cancer and possible positive lymph node based on diagnostic CT, esophagoscopy, and pathological reports. The clinical target volume (CTV) was based on GTV and the subclinical area of the tumor, taking into account factors such as respiratory movement and esophageal peristalsis. The plan target volume (PTV) was defined as the 6-mm margin of CTV, and the OARs were limited to 5 mm under the skin, including the left and right lungs, heart, and spinal cord.

Designing treatment planning

Three types of plans were designed for each patient: IMRT, VMAT, and IMPT. All patients have been prescribed a dose of 60 Gy in 30 fractions, with a single fraction dose of 2 Gy. The dose limits for OARs were as follows (12): normal lung V_5 (percentage of the normal lung volume irradiated with more than 5 Gy) <65%, V_{20} <25%; cardiac V_{30} <46%, and mean heart dose (MLD) of <26 Gy (the average dose did not exceed 26 Gy). The maximum point dose is less than 48 Gy in the spinal cord (D_{max} <48 Gy).

Among them, two-photon plans were designed based on Varian Eclipse15.5 TPS. The IMPT plan design was based on Varian Eclipse ProBeam proton systems. For the IMRT plan, as shown in Figure 1A, the use of 6 fields was 0°, 35°,150°,185°, 210°, and 325°, respectively. For the VMAT plan, we used 179.9° CCW 181° and 181° CW 179.9°, in order to protect the lungs, setting the angle to avoid 150°–30°, 330°–210°, 210°–330°, and 30°–150°, as shown in Figure 1B.

For the IMPT plan, the Varian Eclipse ProBeam Proton system utilizes the anteroposterior technique (0°/180°), as shown in Figure 1C. The nonlinear general proton optimizer (NUPO) algorithm was used to generate the plan, and the proton convolution superposition algorithm with a grid size of 0.25 cm was used to calculate the dose planning optimization, taking into account the positioning error of 3 mm and the range uncertainty of 3.5%. The beam output was determined using a relative biologic effectiveness (RBE) of 1.1 and is specified in cobalt gray equivalent (CGE) units (13).

Dosimetric analysis

Dose-volume parameters of PTV were obtained from DVH: dose received by 2% of the target volume (D_2), dose received by 98% of the target volume (D_{98}), maximum dose (D_{max}), mean dose (D_{mean}), minimum dose (D_{min}), CI, HI, and GI. The parameters used to evaluate the OAR sparing include the following: MLD, V_5, V_{10}, V_{15}, and V_{20} of the bilateral lung; MHD, V_5, V_{10}, V_{15}, V_{20}, V_{30}, and V_{40} of the heart (V_X represents the volume percentage receiving more than X Gy); and the D_{max} and D_{mean} of the spinal cord.

The CI was calculated according to the following formula:

$$\mathrm{CI} = \left(\frac{V_{\mathrm{TR}}}{V_T}\right) \times \left(\frac{V_{\mathrm{TR}}}{V_T}\right) \quad (1)$$

The CI ranged from 0 to 1, where 1 indicated perfect overlap (identical structures). A value near 0 indicated the total absence of conformation; the target volume was not irradiated.

V_{TR} is the volume of the reference isodose curve coverage of the PTV, V_T is the volume of the PTV, V_R is the volume of the reference isodose curve coverage of the body (including PTV), and 95% of the prescription dose is defined as the reference isodose curve.

The homogeneity index was calculated according to the following formula:

$$\mathrm{HI} = \frac{D_2 - D_{98}}{D_{50}} \quad (2)$$

The HI ranged from 0 to 1, where 0 was the ideal value. A higher HI indicates poorer homogeneity.

D_2 is the dose received by 2% of the target volume, D_{98} is the dose received by 98% of the target volume, and D_{50} is the dose received by 50% of the target volume.

The gradient index was calculated according to the following formula:

$$\mathrm{GI} = \frac{V_{50}}{V_{100}} \quad (3)$$

In particular, V_{50} represents the volume receiving at least 50% of the prescription dose. V_{100} represents the volume receiving at least 100% of the prescription dose.

TCP and NTCP evaluation

The TCP of PTV and NTCP of the left and right lungs, heart, and spinal cord were used to evaluate radiotherapy plans and predict organ's toxicity. The TCP and NTCP were calculated based on MATLAB R2013b (www.mathworks.com, The MathWorks Inc., Natick, MA, USA).

The TCP calculation formula was based on the equivalent uniform dose (EUD) model (14). The TCP formula and EUD model are as follows:

$$\mathrm{TCP} = \frac{1}{1 + \left(\frac{\mathrm{TCD}_{50}}{\mathrm{EUD}}\right)^{4\gamma_{50}}} \quad (4)$$

TCD_{50} is the dose required when the TCP is 50%, and γ_{50} is the slope of the dose–response curve when the tumor target control rate is 50%.

$$\mathrm{EUD} = \left(\sum_{i=1} (\mathrm{ViDi}^a)\right)^{\frac{1}{a}} \quad (5)$$

a is a unit-free parameter describing the volume effect size of the tumor or normal structure; V_i is the relative volume related

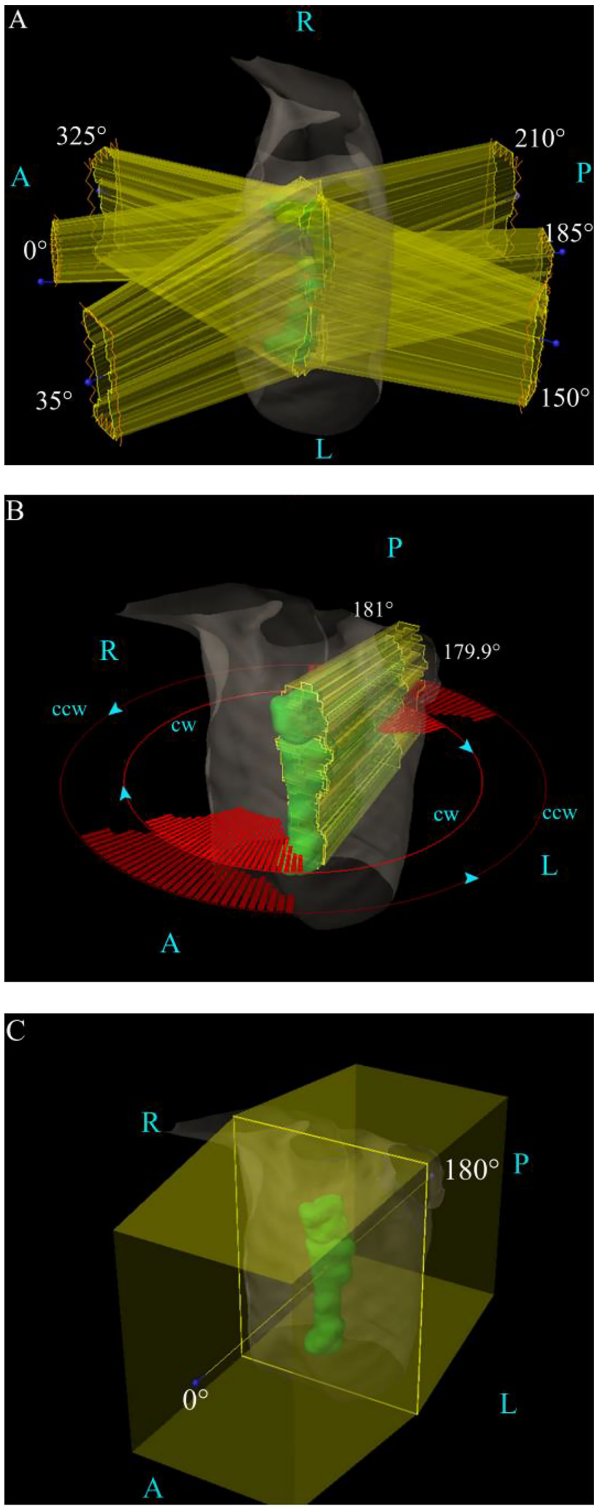

FIGURE 1
The field angle arrangement of the three various plans. **(A)** The IMRT plan's field arrangement. **(B)** The VMAT plan's field arrangement. **(C)** The IMPT plan's field arrangement. A, anterior; L, left; P, posterior; R, right.

to dose-voxel D_i. In patients with esophageal squamous cell carcinoma treated with radiotherapy, TCD_{50} is 51.24 Gy, γ_{50} is 0.83, and a is 0.3.

The calculation of NTCP for the probability of normal tissue complications of OARs is based on the Lyman–Kutcher–Burman (LKB) model (14–17), and the calculation formula is as follows:

$$NTCP = \frac{1}{1+(\frac{TD50}{EUD})^{4\gamma_{50}}} \quad (6)$$

TD_{50} represents the dose to the whole organ (or reference volume), which will result in a 50% probability of complications. γ_{50} is a unitless model parameter that is specific to the normal structure or tumor of interest and describes the slope of the dose–response curve. Parameters a and γ_{50} should be obtained by fitting clinical dose–response data with EUD-based NTCP or EUD-based TCP model (14, 18).

In the calculation of TCP and NTCP, the EQD_2 (19, 20) formula is used for fractional correction based on voxels. EQD_2 is the bioequivalent physical dose, and the unit is 2 Gy/min of partial volume V_i. The formula is as follows:

$$EQD2 = D_i\left(1+\frac{d_i}{\alpha/\beta}\right) \quad (7)$$

D_i is the total absorbed dose in the reference treatment plan, d_i is the dose of each subdose in the treatment process, and α/β is the tissue-specific LQ parameter of exposed organs (19, 21).

The predicted clinical endpoint of the lung is radiation pneumonitis, and pericarditis of any grade is the endpoint of the heart. For the spinal cord, spinal cord myelitis necrosis is the predicted endpoint. For TCP prediction, the parameters published by Niemierko (20) were adopted. For pneumonitis, the parameters published by Seppenwoolde (22) were adopted. For pericarditis of any grade, the parameters published by Gagliardi (23) were adopted. For spinal cord myelitis necrosis, the parameters published by Agren (24, 25) were adopted. All the parameters are shown in Table 1.

Statistical analysis

TCP and NTCP were calculated based on MATLAB2013b (The MathWorks, Natick, MA, USA), and SPSS 25.0 was used for data analysis (IBM Corp, Armonk, NY, USA). All the results were presented in the form of mean ± standard deviation. Univariate ANOVA analysis and Tukey were used to conduct a *post-hoc* *t*-test between the three plans. *p*-values of less than 0.05 were considered statistically different.

Results

Thirty patients with ESCC who underwent radiotherapy achieved the expected clinical dose limits for all types of plans. The detailed values of PTV's dose-volume parameters are shown in Table 2. The parameters include the following: D_2, D_{98}, D_{max}, D_{mean}, D_{min}, CI, HI, and GI all met clinical requirements, but there were significant differences among the three planning methods in D_2, D_{98}, D_{mean}, D_{min}, CI, HI, and GI. The CI of IMPT was 0.89 ± 0.04, which was higher than that of IMRT (0.85 ± 0.03) and VMAT (0.65 ± 0.20). The GI of the IMPT plan was 2.23 ± 0.30, which was significantly lower than IMRT (5.50 ± 1.27) and VMAT (3.60 ± 0.60).

The dose-volume parameters of OARs are summarized in Table 3. As shown in Table 3, the IMPT plan showed significant protection of OARs, such as the lungs and heart. For the left and right lungs, the MLD, V_5, V_{10}, and V_{15} of IMPT were significantly lower than the IMRT and VMAT; there was no significant difference between IMRT and VMAT ($p > 0.05$). For the heart, MHD, V_{10}, and V_{20} of IMPT were significantly lower than IMRT ($p = 0.048$, $p = 0.049$, $p = 0.008$, respectively). MHD, V_{20}, V_{30}, and V_{40} of the IMPT plan were also significantly lower than the VMAT plan ($p = 0.011$, $p = 0.006$, $p = 0.008$, $p = 0.016$, respectively), while there was no significant difference between the IMRT and VMAT plan. For the spinal cord, the D_{max} of the IMPT plan was significantly lower than VMAT ($p = 0.001$), while there was no difference between IMPT and IMRT. Furthermore, the D_{mean} of the spinal cord also showed no significant difference among the three plans.

Table 4 shows the TCP of PTV and the NTCP of OARs. The TCP of the IMPT plan was 73.92% ± 0.01%, which was significantly higher than IMRT (67.28% ± 0.35%) and VMAT (67.92% ± 0.89%) ($p < 0.001$ and $p < 0.001$, respectively). The NTCP for right lung radiation pneumonia and left lung

TABLE 1 The parameters of the formulas.

	TCP	NTCP lung	NTCP heart	NTCP spinal cord
TCD_{50} (Gy)	51.24			
TD_{50} (Gy)		34	50.6	68.6
α/β	10	2	2.5	2
a	0.3	3	2.5	13
γ_{50}	0.83	0.9	1.3	1.9

TCP, tumor control probability; NTCP lung, normal tissue complication probability of the lungs; NTCP heart, normal tissue complication probability of the heart; NTCP spinal cord, normal tissue complication probability of spinal cord.

TABLE 2 The dose-volume parameters of PTV.

Parameters	IMRT	VMAT	IMPT	ANOVA *p*-value	*p*-values		
					IMRT versus VMAT	IMRT versus IMPT	VMAT versus IMPT
D_2 (Gy)	65.25 ± 0.70	66.69 ± 1.23	65.21 ± 0.51	0.001	0.003	0.996	0.002
D_{98} (Gy)	59.93 ± 0.76	57.87 ± 0.88	60.28 ± 0.82	0.000	0.000	0.606	0.000
D_{max} (Gy)	67.57 ± 0.93	69.54 ± 2.24	69.11 ± 2.12	0.061	0.063	0.170	0.866
D_{mean} (Gy)	63.09 ± 0.21	63.66 ± 0.68	63.16 ± 0.01	0.009	0.012	0.928	0.030
D_{min} (Gy)	39.9 ± 10.67	35.80 ± 6.36	47.09 ± 7.23	0.017	0.508	0.153	0.014
CI	0.85 ± 0.03	0.65 ± 0.20	0.89 ± 0.04	0.000	0.003	0.746	0.000
HI	0.08 ± 0.02	0.14 ± 0.03	0.08 ± 0.02	0.000	0.000	0.817	0.000
GI	5.50 ± 1.27	3.60 ± 0.60	2.23 ± 0.30	0.000	0.000	0.000	0.003

All values are shown as mean ± standard deviation.
IMRT, intensity-modulated radiation therapy; VMAT, volumetric-modulated arc therapy; IMPT, intensity-modulated radiation therapy; D_2, dose received by 2% of the target volume; D_{98}, dose received by 98% of the target volume; D_{mean}, the mean dose of PTV; D_{max}, the maximum dose; D_{min}, the minimum dose; CI, conformity index; HI, homogeneity index; GI, gradient index.

radiation pneumonia of IMPT were 12.99% ± 8.43% and 10.23% ± 7.44%, respectively. Although there was no statistical difference, especially in the left lung, the NTCP of the IMPT plan was 3.78% and 3.89% lower than IMRT and VMAT, respectively. As for the NTCP of the spinal cord, VMAT was significantly higher than IMPT ($p = 0.016$).

Discussion

Although photon radiotherapy has been widely used in the clinical treatment of ESCC patients, its late toxicity to normal tissues is still an urgent problem to be solved (26), such as radiation pneumonia, pericarditis, myelitis, etc. In our study, by dosimetric analysis and biological effect evaluation, we conclude that IMPT has the advantage of treating with ESCC. Compared with conventional photon radiotherapy techniques such as IMRT and VMAT, IMPT could significantly reduce the dose and volume of radiation to the heart, lungs, and spinal cord. While improving the TCP, it could provide superior protection for the heart and lungs (especially the left lung).

Some studies have shown that the proton beam has a high response to tumor cells and proton therapy could improve the TCP (6, 27), which is consistent with our research results. Comparing the three treatment technologies, our predicted results show that proton therapy has the highest TCP among the three groups. This might be related to the high linear energy transfer (LET) of the proton beam. LET is a commonly used method to indicate the radiation mass of the ion beam. Generally, high LET is associated with an increase in relative biological effectiveness (RBE) (13, 28). Also, RBE is assumed as 1.1 (13) in our study.

In fact, some studies have investigated the dosimetric and radiobiological differences between photon and proton therapy (29–32). Stokkevag et al. (29) evaluated the differences between proton planning and VMAT planning for children with brain tumors. Based on the LKB model, the NTCP values were compared with the two different plannings. As for the model's parameters, they found that there was no difference between adult and pediatric populations. The parameters were also used in the LKB model for the two different planning comparisons. They found proton therapy planning significantly reduced the auditory complications, xerostomia, and risk of secondary cancers of the brain and salivary glands. As for liver cancer, Prayongrat et al. (30) used the NTCP model to predict the probability of radiation-induced liver toxicity (RILT). They also confirmed the estimated NTCP and ΔNTCP for individual patients along with consideration of uncertainties improving the reliability of the NTCP model-based approach. Feng et al. (31) compared the biological effects of two different beam angle configurations of IMPT. From the prediction of the NTCP model, they concluded that the IMPT planning with superior–inferior oblique posterior beams had a better spare of liver, heart, and lungs at the slight cost of spinal cord maximum dose protection. Recently, Liu et al. (32) investigated the dosimetric and potential clinical benefits for locally advanced pancreatic cancer treated with proton beam therapy. As for the clinical benefits, they also applied the NTCP models and derived the parameters from the previous photon studies. The results demonstrated that two-field IMPT provided lower severe toxicity for the stomach and duodenum than VMAT. Although there were no special models and parameters designed for proton therapy, those studies have proved that the model could provide a reference for radiotherapy (including proton therapy) and further guided radiotherapy planning designing and choosing.

As for the ESCC, there are many important organs around the esophagus, such as the heart, lungs, spinal cone (even ribs), and thymus. Currently, it has been proved that proton therapy can significantly spare the dose of lung and heart, such as MLD, V_5, V_{10}, and V_{20} of the lung (33). This result is consistent with our study. We also found that due to the left physiological laterality of the esophagus, photon therapy would cause the left lung to receive a higher dose. While the protection of the left lung is advantageous in the proton therapy plan. The NTCP of

TABLE 3 The dose-volume parameters of OARs.

OARs	IMRT	VMAT	IMPT	ANOVA *p*-value	*p*-value		
					IMRT versus VMAT	IMRT versus IMPT	VMAT versus IMPT
Right lung							
MLD (Gy)	11.78 ± 3.78	10.79 ± 3.75	4.08 ± 1.94	0.000	0.780	0.000	0.000
V_5 (%)	52.85 ± 19.21	55.29 ± 19.66	13.02 ± 5.64	0.000	0.940	0.000	0.000
V_{10} (%)	35.59 ± 15.36	32.45 ± 18.73	10.79 ± 4.91	0.001	0.876	0.002	0.006
V_{15} (%)	27.08 ± 3.48	21.93 ± 4.01	9.38 ± 1.40	0.002	0.495	0.001	0.025
V_{20} (%)	21.40 ± 7.93	15.77 ± 8.45	8.27 ± 4.04	0.001	0.196	0.001	0.063
Left lung							
MLD (Gy)	13.35 ± 3.68	12.20 ± 3.08	4.31 ± 1.85	0.000	0.668	0.000	0.000
V_5 (%)	57.17 ± 17.63	60.72 ± 15.77	15.41 ± 4.94	0.000	0.837	0.000	0.000
V_{10} (%)	40.98 ± 14.19	38.84 ± 14.92	12.53 ± 4.62	0.000	0.919	0.000	0.000
V_{15} (%)	32.70 ± 10.63	26.86 ± 9.40	10.67 ± 4.42	0.000	0.296	0.000	0.000
V_{20} (%)	26.91 ± 8.09	19.35 ± 7.15	9.16 ± 4.22	0.000	0.045	0.000	0.006
Heart							
MHD (Gy)	21.90 ± 9.58	24.90 ± 14.28	10.35 ± 4.86	0.010	0.793	0.048	0.011
V_5 (%)	75.70 ± 32.09	73.45 ± 33.55	46.22 ± 23.46	0.067	0.985	0.090	0.125
V_{10} (%)	67.23 ± 30.84	64.19 ± 31.73	36.31 ± 18.89	0.036	0.968	0.049	0.082
V_{20} (%)	49.71 ± 25.31	50.89 ± 28.31	16.83 ± 8.68	0.003	0.992	0.008	0.006
V_{30} (%)	30.82 ± 16.73	38.31 ± 28.84	9.97 ± 5.57	0.009	0.671	0.061	0.008
V_{40} (%)	16.80 ± 9.62	28.23 ± 25.63	6.90 ± 4.18	0.021	0.263	0.363	0.016
Spinal cord							
D_{max} (Gy)	44.96 ± 3.31	49.12 ± 6.83	40.2 ± 3.01	0.001	0.139	0.079	0.001
D_{mean} (Gy)	20.95 ± 8.33	23.25 ± 10.09	15.72 ± 6.20	0.138	0.813	0.356	0.128

All data are displayed as mean ± standard deviation.
OARs, organ at risks; MLD, mean lung dose; MHD, mean heart dose; Vx, V_X represents the volume percentage receiving more than X Gy OARs.

TABLE 4 TCP and NTCP.

	IMRT	VMAT	IMPT	ANOVA *p*-values	*p*-values		
					IMRT *vs.* VMAT	IMRT *vs.* IMPT	VMAT *vs* IMPT
TCP_{PTV} (%)	67.28 ± 0.35	67.97 ± 0.89	73.92 ± 0.01	0.000	0.028	0.000	0.000
$NTCP_{Right\ lung}$ (%)	13.28 ± 6.29	12.82 ± 7.47	12.99 ± 8.43	0.990	0.990	0.996	0.999
$NTCP_{Left\ lung}$ (%)	14.01 ± 6.67	14.12 ± 8.94	10.23 ± 7.44	0.451	0.999	0.526	0.507
$NTCP_{heart}$ (%)	4.64 ± 5.07	21.22 ± 24.80	1.73 ± 2.24	0.013	0.045	0.897	0.016
$NTCP_{spinal\ cord}$ (%)	0.07 ± 0.13	0.27 ± 0.29	0.12 ± 0.21	0.015	0.066	0.810	0.016

All data are displayed as mean ± standard deviation.
TCP, tumor control probability; NTCP, normal tissue complication probability.

radiation pneumonia in the left lung is 3.98% and 3.98% lower than IMRT and VMAT, respectively. The incidence of acute cardiac events is thought to be related to the dose received by the heart (26, 34). Keiichi et al. (35) stated in the article that radiation caused cardiotoxicity and increased the incidence of acute cardiac events. Wang et al. (36) also demonstrated that the incidence of cardiac complications after proton radiation therapy was significantly lower than that of photon radiation therapy. This conclusion is in consonance with our study that showed proton therapy can significantly spare the radiation dose and volume of the heart, and the NTCP of cardiac pericarditis is the lowest among the three treatments, achieving the protection of the heart during radiotherapy.

There are several limitations to our study. First, the sample size of the study is not large enough, and the follow-up needs to be demonstrated by a large cohort study. Second, when discussing OARs, the heart is only taken as a whole structure without specific analysis of substructures. However, Shiraishi et al. (37) have discussed and concluded that the radiation exposure of PBT to the whole heart and cardiac substructures was significantly lower than the IMRT plan. Finally, this study does not find a suitable prediction model for other OARs, which may be needed for further study.

Conclusion

This study demonstrated that the IMPT could effectively spare the heart and lungs and reduce the irradiation dose and coverage volume. Furthermore, IMPT is able to improve the TCP of ESCC significantly, which might change the outcome directly. To some degree, the IMPT plan will decrease the NTCP of the heart and left lung. The prediction of TCP and NTCP could also provide a reference and guide future individual treatment.

Data availability statement

The raw data supporting the conclusions of this article will be made available by the authors, without undue reservation.

Ethics statement

This study was reviewed and approved by Shandong Cancer Hospital and Institute Ethics Committee. Written informed consent for participation was not required for this study in accordance with the national legislation and the institutional requirements.

Author contributions

YC drafted the concept and the manuscript. YP, ZL, QW and JZ contributed to acquiring, analyzing, and interpreting data. DH contributed to the target volume delineation and radiotherapy planning examination. YY and CM contributed to acquiring data, designing the study, and enhancing its intellectual content. All authors contributed to the article and approved the submitted version.

Funding

This work is supported by the National Nature Science Foundation of China (81800156, 81974467), Shandong Province Key R&D Program (2018GSF118031), the Natural Science Foundation of Shandong Province (ZR2019MH136), and the Taishan Scholars Project of Shandong Province (ts201712098).

Acknowledgments

The authors would like to thank the editor and reviewers for their insightful suggestions, which helped improve the manuscript.

Conflict of interest

The authors declare that the research was conducted in the absence of any commercial or financial relationships that could be construed as a potential conflict of interest.

Publisher's note

References

1. Sung H, Ferlay J, Siegel RL, Laversanne M, Soerjomataram I, Jemal A, et al. Global cancer statistics 2020: GLOBOCAN estimates of incidence and mortality worldwide for 36 cancers in 185 countries. *CA Cancer J Clin* (2021) 71(3):209–49. doi: 10.3322/caac.21660

2. Luo Y, Mao Q, Wang X, Yu J, Li M. Radiotherapy for esophageal carcinoma: Dose, response and survival. *Cancer Manag Res* (2018) 10:13–21. doi: 10.2147/CMAR.S144687

3. Fan XW, Wu JL, Wang HB, Liang F, Jiang GL, Wu KL. Three-dimensional conformal radiation therapy alone for esophageal squamous cell carcinoma: 10-year survival outcomes. *Thorac Cancer* (2019) 10(3):519–25. doi: 10.1111/1759-7714.12968

4. Fenkell L, Kaminsky I, Breen S, Huang S, Van Prooijen M, Ringash J. Dosimetric comparison of IMRT vs. 3D conformal radiotherapy in the treatment of cancer of the cervical esophagus. *Radiother Oncol* (2008) 89(3):287–91. doi: 10.1016/j.radonc.2008.08.008

5. Takakusagi Y, Kusunoki T, Kano K, Anno W, Tsuchida K, Mizoguchi N, et al. Dosimetric comparison of radiation therapy using hybrid-VMAT technique for stage I esophageal cancer. *Anticancer Res* (2021) 41(4):1951–8. doi: 10.21873/anticanres.14962

6. Ling TC, Slater JM, Nookala P, Mifflin R, Grove R, Ly AM, et al. Analysis of intensity-modulated radiation therapy (IMRT), proton and 3D conformal radiotherapy (3D-CRT) for reducing perioperative cardiopulmonary complications in esophageal cancer patients. *Cancers (Basel)* (2014) 6(4):2356–68. doi: 10.3390/cancers6042356

7. Sha X, Duan J, Lin X, Zhu J, Zhang R, Sun T, et al. A new proton therapy solution provides superior cardiac sparing compared with photon therapy in whole lung irradiation for pediatric tumor patients. *Front Oncol* (2020) 10:611514. doi: 10.3389/fonc.2020.611514

8. Wang X, Hobbs B, Gandhi SJ, Muijs CT, Langendijk JA, Lin SH. Current status and application of proton therapy for esophageal cancer. *Radiother Oncol* (2021) 164:27–36. doi: 10.1016/j.radonc.2021.09.004

9. Allaveisi F, Moghadam AN. Comparison between the four-field box and field-in-field techniques for conformal radiotherapy of the esophagus using dose-volume histograms and normal tissue complication probabilities. *Jpn J Radiol* (2017) 35(6):327–34. doi: 10.1007/s11604-017-0637-8

10. Zhang Y, Jabbour SK, Zhang A, Liu B, Yue NJ, Biswal NC. Proton beam therapy can achieve lower vertebral bone marrow dose than photon beam therapy during chemoradiation therapy of esophageal cancer. *Med Dosim* (2021) 46 (3):229–35. doi: 10.1016/j.meddos.2020.12.003

11. Wang Z, Chen M, Sun J, Jiang S, Wang L, Wang X, et al. Lyman-Kutcher-Burman normal tissue complication probability modeling for radiation-induced esophagitis in non-small cell lung cancer patients receiving proton radiotherapy. *Radiother Oncol* (2020) 146:200–4. doi: 10.1016/j.radonc.2020.03.003

12. Hirano Y, Onozawa M, Hojo H, Motegi A, Zenda S, Hotta K, et al. Dosimetric comparison between proton beam therapy and photon radiation therapy for locally advanced esophageal squamous cell carcinoma. *Radiat Oncol* (2018) 13(1):23. doi: 10.1186/s13014-018-0966-5

13. Paganetti H, Niemierko A, Ancukiewicz M, Gerweck LE, Goitein M, Loeffler JS, et al. Relative biological effectiveness (RBE) values for proton beam therapy. *Int J Radiat Oncol Biol Phys* (2002) 53(2):407–21. doi: 10.1016/S0360-3016(02)02754-2

14. Gay HA, Niemierko A. A free program for calculating EUD-based NTCP and TCP in external beam radiotherapy. *Phys Med* (2007) 23(3-4):115–25. doi: 10.1016/j.ejmp.2007.07.001

15. Semenenko VA, Li XA. Lyman-Kutcher-Burman NTCP model parameters for radiation pneumonitis and xerostomia based on combined analysis of published clinical data. *Phys Med Biol* (2008) 53(3):737–55. doi: 10.1088/0031-9155/53/3/014

16. Mohan R, Mageras GS, Baldwin B, Brewster LJ, Kutcher GJ, Leibel S, et al. Clinically relevant optimization of 3-d conformal treatments. *Med Phys* (1992) 19 (4):933–44. doi: 10.1118/1.596781

17. Burman GJK C, Emami B, Goitein M. Fitting of normal tissue tolerance data to an analytic-function. *Int J Radiat Oncol Biol Phys* (1991) 21(1):123–35. doi: 10.1016/0360-3016(91)90172-Z

18. Emami B, Lyman J, Brown A, Coia L, Goitein M, Munzenrider JE, et al. Tolerance of normal tissue to therapeutic irradiation. *Int J Radiat Oncol Biol Phys* (1991) 21(1):109–22. doi: 10.1016/0360-3016(91)90171-Y

19. Fowler JF. The linear-quadratic formula and progress in fractionated radiotherapy. *Br J Radiol* (1989) 62(740):679–94. doi: 10.1259/0007-1285-62-740-679

20. Niemierko A. Reporting and analyzing dose distributions: A concept of equivalent uniform dose. *Med Phys* (1997) 24(1):103–10. doi: 10.1118/1.598063

21. Chen H, Huang Y, Wang H, Shao Y, Yue NJ, Gu H, et al. Dosimetric comparison and biological evaluation of fixed-jaw intensity-modulated radiation therapy for T-shaped esophageal cancer. *Radiat Oncol* (2021) 16(1):158. doi: 10.1186/s13014-021-01882-7

22. Seppenwoolde Y, Lebesque J, de Jaeger K, Belderbos J, Boersma L, Schilstra C, et al. Comparing different NTCP models that predict the incidence of radiation pneumonitis. normal tissue complication probability. *Int J Radiat Oncol Biol Physics* (2003) 55(3):724–35. doi: 10.1016/S0360-3016(02)03986-X

23. Gagliardi G, Lax I, Ottolenghi A, Rutqvist LE. Long-term cardiac mortality after radiotherapy of breast cancer–application of the relative seriality model. *Br J Radiol* (1996) 69(825):839–46. doi: 10.1259/0007-1285-69-825-839

24. Agren A, Brahme A, Turesson I. Optimization of uncomplicated control for head and neck tumors. *Int J Radiat Oncol Biol Phys* (1990) 19(4):1077–85. doi: 10.1016/0360-3016(90)90037-K

25. Kallman P, Agren A, Brahme A. Tumour and normal tissue responses to fractionated non-uniform dose delivery. *Int J Radiat Biol* (1992) 62(2):249–62. doi: 10.1080/09553009214552071

26. Beukema JC, van Luijk P, Widder J, Langendijk JA, Muijs CT. Is cardiac toxicity a relevant issue in the radiation treatment of esophageal cancer? *Radiother Oncol* (2015) 114(1):85–90. doi: 10.1016/j.radonc.2014.11.037

27. Prayongrat A, Xu C, Li H, Lin SH. Clinical outcomes of intensity modulated proton therapy and concurrent chemotherapy in esophageal carcinoma: A single institutional experience. *Adv Radiat Oncol* (2017) 2(3):301–7. doi: 10.1016/j.adro.2017.06.002

28. Sorensen BS, Overgaard J, Bassler N. *In vitro* RBE-LET dependence for multiple particle types. *Acta Oncol* (2011) 50(6):757–62. doi: 10.3109/0284186X.2011.582518

29. Stokkevag CH, Indelicato DJ, Herfarth K, Magelssen H, Evensen ME, Ugland M, et al. Normal tissue complication probability models in plan evaluation of children with brain tumors referred to proton therapy. *Acta Oncol* (2019) 58(10):1416–22. doi: 10.1080/0284186X.2019.1643496

30. Prayongrat A, Kobashi K, Ito YM, Katoh N, Tamura M, Dekura Y, et al. The normal tissue complication probability model-based approach considering uncertainties for the selective use of radiation modality in primary liver cancer patients. *Radiother Oncol* (2019) 135:100–6. doi: 10.1016/j.radonc.2019.03.003

31. Feng H, Sio TT, Rule WG, Bhangoo RS, Lara P, Patrick CL, et al. Beam angle comparison for distal esophageal carcinoma patients treated with intensity-modulated proton therapy. *J Appl Clin Med Phys* (2020) 21(11):141–52. doi: 10.1002/acm2.13049

32. Liu P, Gao XS, Wang Z, Li X, Xi C, Jia C, et al. Investigate the dosimetric and potential clinical benefits utilizing stereotactic body radiation therapy with simultaneous integrated boost technique for locally advanced pancreatic cancer: A comparison between photon and proton beam therapy. *Front Oncol* (2021) 11:747532. doi: 10.3389/fonc.2021.747532

33. Suh YG, Bayasgalan U, Kim HT, Lee JM, Kim MS, Lee Y, et al. Photon versus proton beam therapy for T1-3 squamous cell carcinoma of the thoracic esophagus without lymph node metastasis. *Front Oncol* (2021) 11:699172. doi: 10.3389/fonc.2021.699172

34. Cai G, Li C, Yu J, Meng X. Heart dosimetric parameters were associated with cardiac events and overall survival for patients with locally advanced esophageal cancer receiving definitive radiotherapy. *Front Oncol* (2020) 10:153. doi: 10.3389/fonc.2020.00153

35. Jingu K, Umezawa R, Fukui K. Radiation-induced heart disease after treatment for esophageal cancer. *Esophagus* (2017) 14(3):215–20. doi: 10.1007/s10388-017-0569-5

36. Wang X, Palaskas NL, Yusuf SW, Abe JI, Lopez-Mattei J, Banchs J, et al. Incidence and onset of severe cardiac events after radiotherapy for esophageal cancer. *J Thorac Oncol* (2020) 15(10):1682–90. doi: 10.1016/j.jtho.2020.06.014

37. Shiraishi Y, Xu C, Yang J, Komaki R, Lin SH. Dosimetric comparison to the heart and cardiac substructure in a large cohort of esophageal cancer patients treated with proton beam therapy or intensity-modulated radiation therapy. *Radiother Oncol* (2017) 125(1):48–54. doi: 10.1016/j.radonc.2017.07.034

frontiers | Frontiers in Oncology

TYPE Systematic Review
PUBLISHED 08 December 2022
DOI 10.3389/fonc.2022.821626

OPEN ACCESS

EDITED BY
Tao Li,
Sichuan Cancer Hospital, China

REVIEWED BY
Chunyan Hua,
Wenzhou Medical University, China
Luigi Cavanna,
Ospedaliera di Piacenza, Italy

*CORRESPONDENCE
Jiancheng Li
jianchengli_jack@126.com
Jianqing Zheng
18060108268@189.cn

†These authors have contributed equally to this work

SPECIALTY SECTION
This article was submitted to Radiation Oncology, a section of the journal Frontiers in Oncology

RECEIVED 24 November 2021
ACCEPTED 14 November 2022
PUBLISHED 08 December 2022

CITATION
Zheng J, Huang B, Xiao L, Wu M and Li J (2022) Treatment- and immune-related adverse events of immune checkpoint inhibitors in esophageal or gastroesophageal junction cancer: A network meta-analysis of randomized controlled trials.
Front. Oncol. 12:821626.
doi: 10.3389/fonc.2022.821626

Treatment- and immune-related adverse events of immune checkpoint inhibitors in esophageal or gastroesophageal junction cancer: A network meta-analysis of randomized controlled trials

Jianqing Zheng[1*†], Bifen Huang[2†], Lihua Xiao[1], Min Wu[1] and Jiancheng Li[3*]

[1]Department of Radiation Oncology, The Second Affiliated Hospital of Fujian Medical University, Quanzhou, China, [2]Department of Obstetrics and Gynecology, Quanzhou Medical College People's Hospital Affiliated, Quanzhou, China, [3]Department of Radiation Oncology, Clinical Oncology School of Fujian Medical University, Fujian Cancer Hospital, Fuzhou, China

Objective: To systematically evaluate the safety and adverse event profiles of immune checkpoint inhibitors (ICIs) in patients with esophageal cancer (EPC) or gastroesophageal junction cancer (GEJC).

Methods: PubMed, Web of Science, Cochrane Library, and major conference proceedings were systematically searched for all phase II or phase III randomized controlled trials (RCTs) in EPC or GEJC using ICIs. Safety outcomes including treatment-related adverse events (trAEs), immune-related adverse events (irAEs), and serious trAEs were evaluated by network meta-analysis or dichotomous meta-analysis based on the random-effects model.

Results: Eleven RCTs involving EPC (five RCTs) and GEJC (six RCTs) were included in the final meta-analysis. NMA showed that placebo was associated with the best safety ranking for grade 3–5 trAEs (SUCRA = 96.0%), followed by avelumab (78.6%), nivolumab (73.9%), ipilimumab (57.0%), and pembrolizumab (56.6%). Conventional pairwise meta-analysis (CPM) showed that ICIs have similar grade 3–5 trAE risk compared with chemotherapy (RR = 0.764, 95% CI: 0.574 to 1.016, I^2 = 95.7%, Z = 1.85, P = 0.065). NMA showed that the general safety of grade 3–5 irAEs ranked from high to low is as follows: ChT (85.1%), placebo (76.5%), ipilimumab (56.0%), nivolumab (48.5%), avelumab (48.4%), camrelizumab (41.8%), pembrolizumab (36.4%), and nivolumab + ipilimumab (21.6%). CPM showed that the rates of grade 3–5 irAEs in the ICI group and the chemotherapy group were 7.35% (154/2,095, 95% CI: [6.23%, 8.47%]) versus 2.25% (42/1,869, 95% CI: [1.58%, 2.92%]), with statistical significance (RR = 3.151, 95% CI = 2.175 to 4.563, Z = 6.07, P = 0.000). The most common irAEs in the ICI group were skin reaction (15.76%, 95% CI: [13.67%, 17.84%]), followed by

hypothyroidism (9.73%, 95% CI: [8.07%, 11.39%]), infusion-related reactions (5.93%, 95% CI: [4.29%, 7.58%]), hepatitis (5.25%, 95% CI: [4.28%, 6.22%]), and pneumonitis (4.45%, 95% CI: [3.5%, 5.4%]).

Conclusion: Different ICIs had different toxicity manifestations and should not be considered as an entity. Compared with chemotherapy, ICIs were more prone to irAEs, but the overall rates remained low and acceptable. For clinicians, it is important to recognize and monitor the adverse events caused by ICIs for patients with EPC or GEJC.

KEYWORDS

immune checkpoint inhibitors, esophageal cancer, gastro-esophageal junction cancer, network meta-analysis, safety assessment

Introduction

Worldwide, esophageal cancer (EPC) still remains one of the most commonly diagnosed cancers and the leading cause of cancer-related death (1), particularly with the highest rates and mortality occurring in China (2). According to the GLOBOCAN report, an estimated 604,100 new cases were diagnosed in 2020 globally, among which Chinese cases accounted for 53.5%, which was up to 324,000 cases (3). An estimated 544,000 new deaths occurred in 2020 globally, while Chinese cases accounted for 55.3%, which was up to 301,000 cases (3). Patients with EPC are most commonly diagnosed with locally advanced cancer stages, and more than 50.4% of cases suffered from distant metastases and irreversible diseases at the time of diagnosis, which led to a frustrating overall 5-year survival rate of less than 20% (4). Generally, fluoropyrimidine and platinum-based regimens are recommended and accepted as standard first-line treatment regimen (5). Although chemotherapy has improved the overall 5-year survival rate to a certain extent, the prognosis of esophageal cancer is still poor (6). In particular, after first-line chemotherapy, there is no accepted and satisfactory standard treatment for advanced or metastatic esophageal cancer (7).

In recent years, cancer immunotherapies based on immune checkpoint inhibitors (ICIs) have become the fifth largest tumor treatment after surgery, chemotherapy, radiotherapy, and small molecules targeted therapy in oncology and have revolutionized the treatment landscape and made major breakthroughs in the treatment of tumors, especially for advanced or metastatic cancer (8). Clinical applications or trials on ICIs had been carried out in the field of various types of tumors, and more and more cancer patients had benefited from this innovative treatment (9). Compared with that of the four existing traditional treatment regimens, the scope of application of cancer immunotherapies is appropriately enlarged, and the number of patients receiving immunotherapies is increasing (10). ICIs directly and selectively killed cancer cells through immunogenic cell death by activating the immune system of cancer patients (11). ICIs had improved the survival rate of many refractory tumors and the quality of life of patients with advanced cancer (12). However, the emergence of a new treatment model and drugs is also accompanied by the emergence of new medication regimens and adverse reactions (11). Although ICIs have shown significant clinical benefits in improving the survival prognosis for most cancer patients, immune-related adverse events (irAEs) that affect body organs are one of the major hindrances when these drugs are applied (13). Although a large number of studies have confirmed the efficacy and safety of ICIs in esophageal cancer, there is a lack of direct head-to-head comparison of evidence for different types of ICIs (9, 14). Therefore, it is not clear if different ICIs have different toxicity profiles in the immunotherapy of esophageal cancer (15). Generally speaking, it is difficult to carry out special randomized controlled trials to compare the differences in the adverse event spectrum of different ICIs, because the occurrence of these adverse events is difficult to predict, and the rates of grade 3–5 adverse events are very low (8). Therefore, meta-analysis is an effective research method for studies focusing on adverse events of ICIs. Network meta-analysis (NMA) may be applied to integrate all available evidence from phase II or phase III RCTs to get direct or indirect comparisons of different ICIs, especially when head-to-head RCTs among regimens are lacking (16). To the best of our knowledge, no NMA of ICI regimens that explored the spectrum of adverse events of immunotherapy is available yet in advanced esophageal or gastroesophageal junction cancer. Therefore, we conducted a systematic review to investigate the safety and adverse event profiles of ICIs for advanced esophageal or gastroesophageal junction cancer using NMA.

Methods

The current study was conducted according to the Preferred Reporting Items for Systematic Reviews and Meta-analyses (PRISMA) (17), and the quality control and quality assurance (QC and QA) of the manuscript were instructed by the corresponding authors (JL and JZ).

Search strategy and inclusion criteria for clinical trials

Relevant clinical trials published in various databases such as PubMed, Web of Science, and Cochrane Library were searched. Major conference proceedings including the Clinicaltrial.gov, American Society of Clinical Oncology (ASCO), and European Society for Medical Oncology (ESMO) databases were also searched for recent conference abstracts.

Relevant search terms relating to the present study were composed of various combinations of the medical subject headings (MeSH) and free-text terms. Search terms were combined by the Boolean operator "AND" or "OR" if necessary. A PubMed search was conducted using the following search terms: 1) search terms related to disease were "esophageal neoplasm," "esophagus cancer," "esophageal cancer," "gastro-oesophageal junction cancer," "gastro-esophageal junction cancer," "cancer of the gastroesophageal junction," "adenocarcinoma of the esophagus and gastroesophageal junction," etc. (2) Search terms related to drugs or immunotherapy were "ipilimumab," "pembrolizumab," "nivolumab," "atezolizumab," "durvalumab," "camrelizumab," and other ICIs. The trade name of the drug includes "Yervoy," "Keytruda," "Opdivo," "Tecentriq," "Imfinzi," etc. 3) Other search terms included "anti-CTLA-4 mab," "anti-PDL1," "anti-PD1," "PD1 receptor," "programmed cell death 1 protein," "PD-1," "PD-L1," etc.

The selection criteria for clinical trials were organized according to the guidelines of the participants, interventions, comparisons, outcomes, and study design (PICOS) recommended by the Cochrane Collaboration. The inclusion criteria were as follows: i) the included patients were all pathologically diagnosed esophageal cancer or gastroesophageal junction cancer (GEJC) patients (P); ii) interventions of concern referred to immunotherapy with ICIs alone or in combination with chemotherapy (I); iii) controlled treatment regimens included chemotherapy alone (ChT) or best supportive treatment (BST), but there were no restrictions related to the chemotherapy regimens and chemotherapy cycles (C); iv) five safety outcomes included rates of treatment-related adverse events (trAEs), immune-related adverse events (irAEs), death, discontinuation of therapy, and grades 3–5 organ-special adverse events (O); and v) all randomized, open-label, controlled clinical trials with efficacy and safety data of ICIs were included. Although priority was given to phase III clinical trials, phase II clinical trials with a control group would be also included.

The exclusion criteria were as follows: i) phase I clinical trials and non-RCT studies, ii) participants with other tumors, iii) case reports and reviews, iv) incomplete data or non-original research, and v) repeated publications.

Articles were only included if they were published in English, but there was no restriction related to publication year. Two researchers (JZ and BH) were assigned to independently review all the data. If there were repeated articles in the selected clinical trials, only the latest published articles will be used for the final analysis. After the discussion according to the inclusion criteria and reaching a consensus, a decision was made to finally include or exclude the eligible articles. If a consensus cannot be reached, the corresponding author (JL) of this article is responsible for the final ruling.

Data extraction and quality assessment

After reading the full text, two researchers (JZ and Tingting Li) extracted and cross-checked the data, including the following: 1) basic information: such as the title of the trial, author's name, year of publication, source of literature, etc.; 2) methodological information of the trial: the sample size of the study included, the basic information of the study population, including the entry time and number of participants, disease stages, etc.; the randomization method of the trial, the evaluation method of important outcome indicators; median follow-up duration, death, and withdrawal, etc.; 3) detailed information on intervention measures: ICI medication, medication in the control group, etc.; and 4) detailed information for safety outcome indicators mentioned above. Disagreements were resolved by consensus.

Two independent researchers evaluated the included RCTs according to the bias risk assessment method recommended by the Cochrane Assistance Network. The evaluation methodological criteria and items were as follows: 1) generation of random allocation sequence, 2) the method of allocation concealment, 3) the method of blinding the patient, 4) the method of blinding the doctor or the therapist, 5) the method of blinding the data collection and analysis personnel, 6) the incomplete data reported, 7) selective reporting bias, and 8) other potential bias affecting authenticity.

We evaluate the risk of bias for each RCT according to the following criteria: "Yes" indicates a low risk of bias, "No" indicates a high risk of bias, and "Unclear" indicates that the literature does not provide sufficient information for bias assessment. The two researchers discussed according to the above standards and methods and, if necessary, reached a consensus according to the opinions of the third researcher.

Statistical analysis

Adverse events including trAEs and irAEs were evaluated from two different perspectives: overview and detail. An overview analysis involved all kinds of AEs observed in ≥ grade 3–5 or all grade of the study population, and a detailed analysis involved some prespecified AEs of interest observed in ≥ grade 3–5 or all grades of the study population. The detailed information of related safety was extracted from the original literature and recorded as the number of events reported and no events for each specific treatment, respectively. If enough data were available to achieve network meta-analysis, a random-effects NMA was conducted in the frequency framework, using the command of "network" in Stata 16.0. Direct or indirect safety effects were combined into some summary statistics, that is, risk ratios (RRs) and 95% credibility intervals, to quantify the effect of adverse events in the network meta-analysis. Risk ratios less than 1 represented a beneficial effect favoring the ICI group. Two-sided P <0.05 indicated that the comparison was statistically significant. If the data were unavailable for the NMA, a conventional pairwise meta-analysis based on the random-effects model or the fixed-effects model was conducted depending on the size of heterogeneity. In this case, the outcome of interest may be grouped by whether ICIs were given. Heterogeneity was assessed using the chi-square test and I^2 statistics. I^2 ≥50% indicated obvious heterogeneity, and a random-effects model should be applied for pooled analysis. The classic half-integer continuity correction, that is adding 0.5 to each cell, was used in the data preprocessing stage if zero adverse events in any arm were reported.

The pooled rates of grade 3–5 or all-grade adverse events for treatments were meta-analyzed by the command of "metan" in STATA 16.0. Subgroup analyses for RRs between the ICI-treated group and the control group were performed based on the panoramic analysis, and prespecified, exploratory stratification factors for subgroup analyses involved the phase of the study (phase II versus phase III), treatment lines (first line, second line, and third line), ICI drug type (anti-PD-1, anti-CTLA-4, anti-PD-L1), treatment mode (ICIs alone versus ICIs combined with ChT), sample size (<500 versus ≥500), etc.

Results

Eligible studies and characteristics

In the literature retrieval stage, a total of 459 articles were obtained through preliminary screening. After reading the titles and abstracts, 422 articles including duplicate reports, irrelevant articles, non-randomized controlled trials, review articles, and phase I trials were excluded. The remaining 20 articles were excluded based on the selection criteria after reading the full text. Finally, a total of 11 trials reported in 17 articles met the inclusion criteria, of which 6 articles were updated or subgroup reports (18–30). Therefore, 11 articles were included in the meta-analysis, all of which were published in English (18, 20–25, 27–30). Updated reports or subgroup reports included three clinical trials, which were ATTRACTION–3 (19), ATTRACTION-4 (26), and ATTRACTION-2 (31–34).

Figure 1 shows the flowchart of the study selection and design procedure. The baseline characteristics of the 11 studies are summarized and shown in Table 1. All 11 studies included 7,089 patients, and the number of analysis population for AEs was 6,992. Most patients included came from an international multicenter. The cancer types included in the study were esophageal carcinoma (18, 20–23) and gastroesophageal junction cancer (24, 25, 27–30). Only one trial was a phase II study (28). First-line ICIs were applied in four clinical trials (22–25), second-line ICIs were applied in five clinical trials (18, 20, 21, 27, 28), and third-line ICIs were applied in two clinical trials (29, 30). Monotherapy with ICIs was found in six clinical trials (18, 20, 21, 27–30). In particular, anti-PD-L1 ICIs were used in only one trial (29), and anti-CTLA-4 ICIs were used in only two trials (23, 28).

Risk of bias

The risk of bias assessment for the included studies involving the 11 articles is summarized and shown in Figures 2A, B. Four clinical trials were judged to be at high risk of bias mainly due to incomplete outcome data for major results of irAEs (18, 23–25). One clinical trial was judged to be at unclear risk of bias because of the lack of total results of grade 3–5 irAEs (21). The remaining studies had a low risk of bias and can be considered high quality.

Network meta-analysis for trAEs

Only one trial had not reported the results of grade 3–5 trAE (25). Therefore, data from the other studies can be successfully applied to implement NMA. A total of 3,005 patients (nine trials) were assigned to ChT therapy, 184 patients (one trial) to avelumab therapy, 228 patients (one trial) to camrelizumab therapy, 57 patients (one trial) to ipilimumab therapy, 539 patients (two trials) to nivolumab therapy, 1,461 patients (three trials) to nivolumab plus ChT therapy, 322 patients (one trial) to nivolumab + ipilimumab + ChT therapy, 314 patients (one trial) to pembrolizumab therapy, 664 patients (one trial) to pembrolizumab plus ChT therapy, and 218 patients (two trials) to placebo therapy. The network plot is shown in Figures 3A, B.

In the consistency model, for the rates of grade 3–5 trAEs, the results with significant benefits for different pairwise comparisons could be found in avelumab versus ChT, nivolumab versus ChT, pembrolizumab versus ChT, placebo

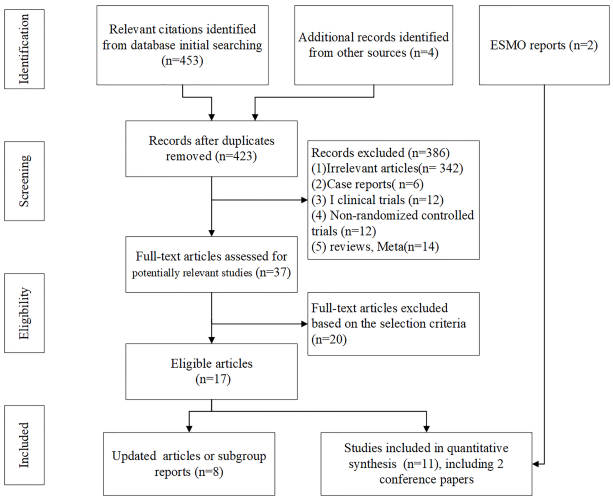

FIGURE 1
Flowchart of the study selection and design.

versus ChT, placebo versus nivolumab + ChT, and placebo versus pembrolizumab + ChT. The results with significant increasing risk could be found in nivolumab + ChT versus avelumab, nivolumab + ipilimumab + ChT versus avelumab, pembrolizumab + ChT versus avelumab, nivolumab + ChT versus camrelizumab, nivolumab + ChT versus nivolumab, and nivolumab + ipilimumab + ChT versus nivolumab.

For the rates of all-grade trAEs, the results with significant benefits for different pairwise comparisons could be found in ipilimumab versus ChT, placebo versus ChT, ipilimumab versus avelumab, placebo versus avelumab, ipilimumab versus camrelizumab, placebo versus camrelizumab, placebo versus nivolumab, placebo versus nivolumab + ChT, placebo versus nivolumab + ipilimumab + ChT, placebo versus pembrolizumab, and placebo versus pembrolizumab + ChT. The results with significant increasing risk could be found in nivolumab versus ipilimumab, nivolumab + ChT versus ipilimumab, nivolumab + ipilimumab + ChT versus ipilimumab, pembrolizumab versus ipilimumab, and pembrolizumab + ChT versus ipilimumab. The details of all comparisons are indicated in Figure 4A. The ranking of benefits for different treatment regimens was assessed by the surface under the cumulative ranking curves (SUCRAs) and is shown in Figure 4B.

As shown in Figure 4B, placebo was associated with the best safety ranking for grade 3–5 trAEs (SUCRA = 96.0%), followed by avelumab (78.6%), nivolumab (73.9%), ipilimumab (57.0%), and pembrolizumab (56.6%); placebo was associated with the best safety ranking for all-grade trAEs (99.5%), followed by ipilimumab (89.3%), nivolumab (60.1%), avelumab (56.8%), and pembrolizumab (53.5%). The relevant SUCRA values for the different treatments are detailed in Supplementary Material Table S1. Forest plots for pairwise comparisons of all individual regimens and their combinations are shown in Figures 5A, B.

For the rates of grade 1–2 trAEs, nivolumab + ChT was associated with the best safety ranking for grade 1–2 trAEs (88.2%), followed by pembrolizumab + ChT (85.1%), nivolumab + ipilimumab + ChT (82.4%), ChT (53.5%), and placebo (53.3%). The results of NMA are indicated in Supplementary Figures S1, S2A, B, and S3 and Table S1.

Subgroup analysis for trAEs

Stratification factors used for subgroup analyses included treatment lines (first line, second line, and third line), ICI drug type (anti-PD-1, anti-CTLA-4, anti-PD-L1), treatment mode (ICIs alone versus ICIs combined with ChT), and sample size (<500 versus ≥500). Based on the panoramic analysis of whether ICI treatment was applied, although the overall rates of grade 3–5 and all-grade trAEs were similar between the two groups, there were statistical differences in the rates of trAEs in some subgroups. For first-line treatment, ICIs were usually applied in combination with chemotherapy; consequently, the additional ICIs had significantly increased the rates of grade 3–5 trAEs (RR = 1.159, 95% CI = 1.012 to 1.327). However, for second-line treatment, ICIs had significantly decreased the rates of grade 3–5 trAEs (RR = 0.395, 95% CI = 0.317 to 0.491). In the case of ICIs alone, compared with chemotherapy, ICIs significantly reduced the rates of grade 3–5 trAEs (RR = 0.584, 95% CI = 0.350 to 0.974). The detailed results for subgroup analyses are listed in Table 2. Forest plots for subgroup analyses are indicated in Supplementary Figures S4A–E and S5A–S5E.

TABLE 1 Characteristics of the included studies.

Study name	References	Trial phase	Treatment line	Cancer type	Treatment	ICI type	Treatment mode	No. of patients	Analysis population for AEs
ATTRACTION-3	32 (18)	III	Second-line	EPC	ChT			209	208
		III	Second-line	EPC	Nivo	PD-1	ICIs	210	209
ESCORT	20 (20)	III	Second-line	EPC	ChT			220	220
		III	Second-line	EPC	Camr	PD-1	ICIs	228	228
KEYNOTE-181	21 (21)	III	Second-line	EPC	ChT			314	296
		III	Second-line	EPC	Pemb	PD-1	ICIs	314	314
KEYNOTE-590	22 (22)	III	First-line	EPC	ChT			376	370
		III	First-line	EPC	Pemb + ChT	PD-1	ICIs + ChT	373	370
CheckMate-648	23 (23)	III	First-line	EPC	ChT			324	304
		III	First-line	EPC	Nivo + ChT	PD-1	ICIs + ChT	321	310
		III	First-line	EPC	Nivo + Ipil + ChT	CTLA-4	ICIs + ChT	325	322
CheckMate-649	Moehler et al., 2020s2202020202020 (24)	III	First-line	GEJC	ChT			792	792
		III	First-line	GEJC	Nivo + ChT	PD-1	ICIs + ChT	789	789
Study name	References	Trial phase	Treatment line	Cancer type	Treatment	ICI type	Treatment mode	No. of patients	Analysis population for AEs
ATTRACTION-4	25 (25)	III	First-line	GEJC	ChT			362	362
		III	First-line	GEJC	Nivo + ChT	PD-1	ICIs + ChT	362	362
KEYNOTE-061	27 (27)	III	Second-line	GEJC	ChT			296	276
		III	Second-line	GEJC	Pemb + ChT	PD-1	ICIs + ChT	296	294
NCT01585987	28 (28)	II	Third-line	GEJC	Placebo			57	57
		II	Third-line	GEJC	Ipil	CTLA-4	ICIs	57	57
JAVELIN Gastric 300	29 (29)	III	Third-line	GEJC	ChT			186	177
		III	Third-line	GEJC	Avel	PD-L1	ICIs	185	184
ATTRACTION-2	30 (30)	III	Third-line	GEJC	Placebo			163	161
		III	Third-line	GEJC	Nivo	PD-1	ICIs	330	330

EPC, esophageal cancer; GEJC, gastroesophageal junction cancer; ChT, chemotherapy; Nivo, nivolumab; Camr, camrelizumab; Pemb, pembrolizumab; Ipil, ipilimumab; Avel, avelumab; ICIs, immune checkpoint inhibitors; PD-1, programmed cell death-1; PD-L1, programmed cell death ligand 1; CTLA-4, cytotoxic T lymphocyte associate protein-4.

Meta-analysis of serious trAEs, events leading to discontinuation, and treatment-related death

Only five clinical trials had provided detailed data comparing the rates of serious trAEs between ICIs and chemotherapy (18, 20, 23, 24, 28). The meta-analysis shows that the rates of serious trAEs in the ICI group and the chemotherapy group were 22.66% (434/1,915) and 11.46% (216/1,885), respectively. However, no significant difference between the two groups was found (RR = 1.786, 95% CI = 0.978 to 3.262, Z = 1.89, P = 0.059). Six clinical trials had provided detailed data comparing the rates of events leading to discontinuation (18, 20–24). The

meta-analysis shows that the rates of events leading to discontinuation in the ICI group and the chemotherapy group were 22.42% (570/2542) and 11.59% (289/2,494), respectively, without statistical significance (RR = 1.447, 95% CI = 0.908 to 2.307, Z = 1.55, P = 0.120). Five clinical trials had provided detailed data comparing the rates of treatment-related death (18, 20–23). The meta-analysis shows that the rates of treatment-related death in the ICI group and the chemotherapy group were 1.88% (33/1,753) and 1.41% (24/1,702), respectively, without statistical significance (RR = 1.335, 95% CI = 0.793 to 2.249, Z = 1.09, P = 0.277). The corresponding forest plots are shown in Supplementary Figures S6A–C.

Meta-analysis based on specific treatment-related adverse events

The meta-analysis for some specific treatment-related adverse events of interest is listed in Figures 6A, B. Compared with

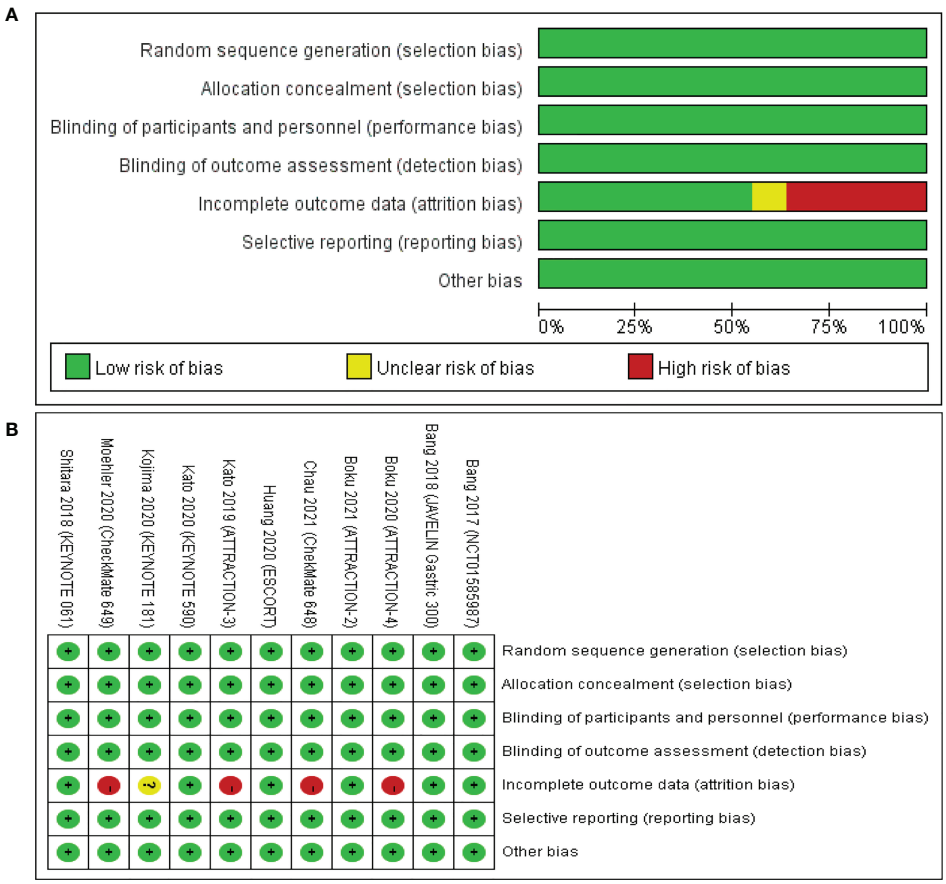

FIGURE 2
Risk of bias assessment for the included studies. Green for low risk of bias, yellow for unclear risk of bias, and red for high risk of bias. **(A)** The risk of bias graph shows an overall risk of bias for each item. **(B)** The risk of bias summary shows the detailed risk of bias of each item for each study.

chemotherapy, in the ICI group, the rates for grade 3–5 trAEs of the following had been significantly reduced: decreased neutrophil count, decreased white blood cell count, neutropenia, anemia, febrile neutropenia, vomiting, and nausea. Moreover, the rates of the following in the ICI group were similar: asthenia, fatigue, decreased appetite, diarrhea, alopecia, peripheral sensory neuropathy, and rash. The highest rates of adverse events in the chemotherapy group were decreased neutrophil count (14.9%), followed by decreased white blood cell count (13.65%), neutropenia (11.75%), anemia (5.88%), and febrile neutropenia (5.45%). However, the most common adverse events in the ICI group were anemia (1.67%), followed by diarrhea (1.42%), fatigue (1.18%), and asthenia (1.11%).

Except for diarrhea and rash, ICIs had significantly reduced the rates of specific treatment-related adverse events. The most common all-grade trAEs were alopecia (33.44%), followed by decreased white blood cell count (27.19%), anemia (23.63%), decreased neutrophil count (23.6%), and nausea (21.31%) in the chemotherapy group and diarrhea (9.84%) in the ICI group, followed by fatigue (9.34%), asthenia (7.26%), rash (6.43%), and decreased appetite (6.25%).

Network meta-analysis for irAEs

Only seven and eight trials had provided data on the rates of grade 3–5 irAEs (20, 22, 23, 27–30) and all-grade irAEs (20–23, 27–30), respectively. The network plot is shown in Figures 3C, D.

The NMA results of the consistency model for the rates of grade 3–5 irAEs and all-grade irAEs are indicated in Figures 7A, B. The general safety of grade 3–5 irAEs assessed by SUCRA for different ICI drugs or ChT ranked from high to low is as follows: ChT (85.1%), placebo (76.5%), ipilimumab (56.0%), nivolumab (48.5%), avelumab (48.4%), camrelizumab (41.8%), pembrolizumab (36.4%), and nivolumab + ipilimumab (21.6%). In terms of all-grade irAEs, the general safety of different ICI drugs or ChT ranked from high to low is as

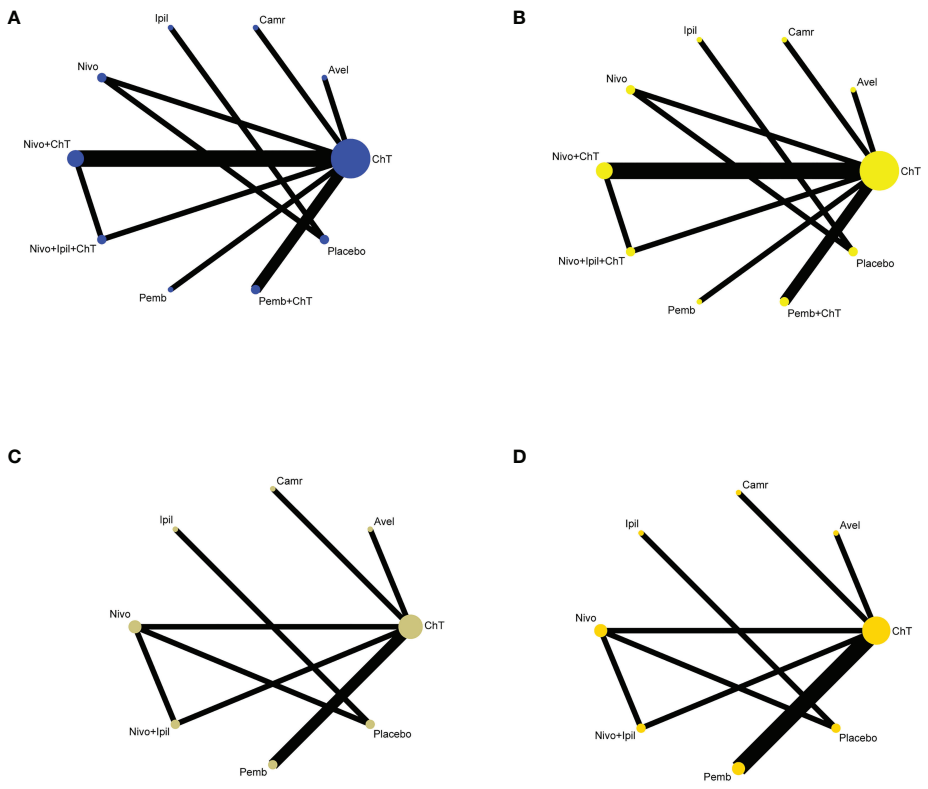

FIGURE 3
Network plots of comparisons with **(A)** grade 3–5 trAEs, **(B)** all-grade trAEs, **(C)** grade 3–5 irAEs, and **(D)** all-grade irAEs based on the network meta-analyses. ChT, chemotherapy; Avel, avelumab; Camr, camrelizumab; Ipil, ipilimumab; Nivo, nivolumab; Pemb, pembrolizumab.

follows: ChT (98.7%), placebo (82.0%), pembrolizumab (73.6%), nivolumab (54.6%), nivolumab + ipilimumab (39.9%), camrelizumab (23.3%), avelumab (17.6%), and ipilimumab (10.3%). The SUCRA values are detailed in Supplementary Table S2.

Conventional pairwise meta-analysis was used to integrate all available data of irAEs. Seven clinical trials had provided detailed data comparing the rates of grade 3–5 irAEs between ICIs and chemotherapy (20, 22, 23, 27–30). The meta-analysis shows that the rates of grade 3–5 irAEs in the ICI group and the chemotherapy group were 7.35% (154/2,095, 95% CI: [6.23%, 8.47%]) and 2.25% (42/1,869, 95% CI: [1.58%, 2.92%]), respectively, with statistical significance (RR = 3.151, 95% CI = 2.175 to 4.563, Z = 6.07, P = 0.000). Eight clinical trials had provided detailed data comparing the rates of all-grade irAEs between ICIs and chemotherapy (20–23, 27–30). The meta-analysis shows that the rates of all-grade irAEs in the ICI group and the chemotherapy group were 44.46% (1,071/2,409) and 11.09% (240/2,165), respectively, with statistical significance (RR = 3.851, 95% CI = 2.767 to 5.359, Z = 8.00, P = 0.000). Therefore, immunotherapy not only increased immune-related adverse events of grades 3–5 but also increased immune-related adverse events of all grades. The corresponding forest plots are shown in Figures 8A, B.

Subgroup analysis for irAEs

The stratification factors of irAEs were the same as those of trAEs. The detailed results for the subgroup analyses are listed in Table 3. Forest plots for subgroup analyses are indicated in Supplementary Figures S7A–E and S8A–E. In terms of grade 3–5 irAEs, except for the second-line treatment subgroup and the PD-L1 subgroup, it can be observed that ICIs had significantly increased the adverse events in almost all of the other subgroups. Moreover, it can be observed that ICIs had significantly increased all-grade irAEs in all subgroups.

Meta-analysis based on specific immune-related adverse events

Some specific immune-related adverse events of interest are listed in Figure 8C and Supplementary Table S3. The most

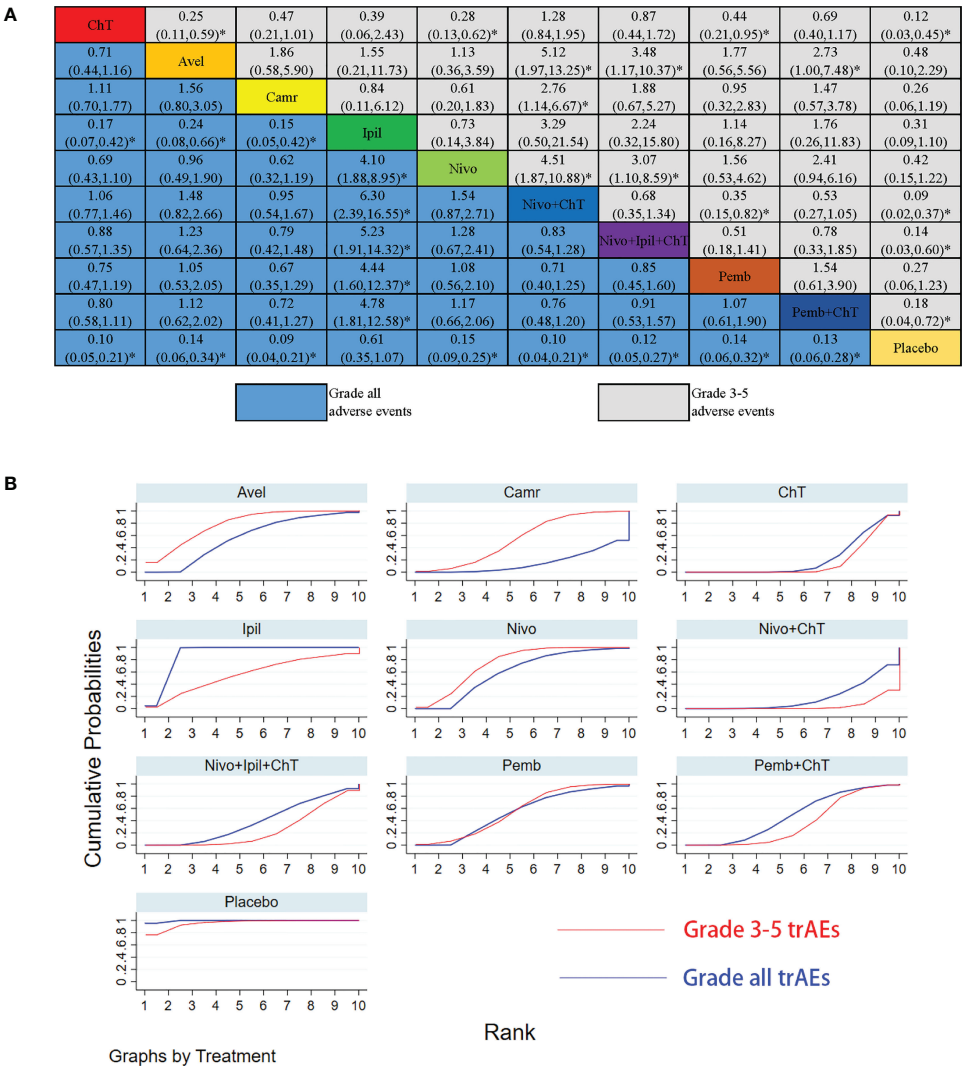

FIGURE 4
Results of the network meta-analysis for 10 treatment regimens in terms of treatment-related adverse events(trAEs) with grade 3–5 trAEs and all-grade trAEs. **(A)** League table for different treatment regimens. Relative effects (RRs) with 95% confidence intervals are shown for different treatment regimens compared with each other. The RR for a given comparison could be read in the intersection of two treatments. All *Z*-tests to compare two treatments were performed two-sided. *$P < 0.05$. ChT, chemotherapy; Avel, avelumab; Camr, camrelizumab; Ipil, ipilimumab; Nivo, nivolumab; Pemb, pembrolizumab. Placebo also involves the best supportive care. **(B)** The surface under the cumulative ranking curves (SUCRAs) for grade 3–5 trAEs and all-grade trAEs.

common irAEs in the ICI group were skin reaction (15.76%, 95% CI: [13.67%, 17.84%]), followed by hypothyroidism (9.73%, 95% CI: [8.07%, 11.39%]), infusion-related reactions (5.93%, 95% CI: [4.29%, 7.58%]), hepatitis (5.25%, 95% CI: [4.28%, 6.22%]), and pneumonitis (4.45%, 95% CI: [3.5%, 5.4%]).

Discussion

Immunotherapy based on ICIs has currently become one of the most promising treatment regimens for cancer, which plays an encouraging role in the treatment of advanced cancer (35). Under normal physiological conditions, immune checkpoints help in maintaining self-tolerance and protecting host tissues from damage by the immune system when the immune system responds to specific physiological and pathological conditions (36). Tumor cells take full advantage of this feature to escape the attack of immune cells (37). Currently, the CTLA-4/B7-1/2 and PD-1/PD-L1 pathways has become the most popular in the field of cancer research on immunotherapy, both of which are the key pathways for immune T-cell activation (38). Most ICIs change the activity of immune checkpoints by targeting the inhibitory

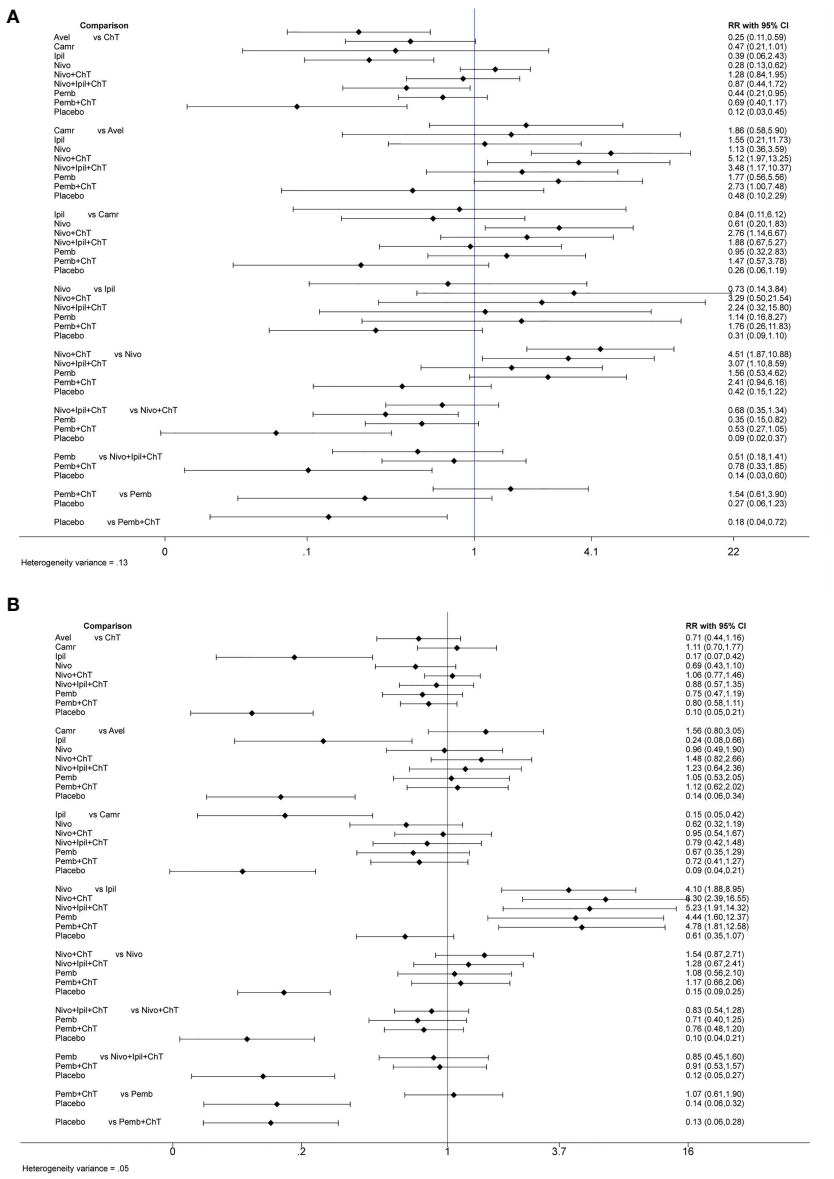

FIGURE 5
Forest plots for pairwise comparisons of all individual regimens with each other with **(A)** forest plots for grade 3–5 trAEs and **(B)** forest plots for all-grade trAEs.

receptors (IRs) CTLA-4, PD-1, or PD-L1 and reactivate the immune response of T cells to tumor cells, thereby achieving antitumor effects (39). As immunotherapeutics have made substantial clinical progress in a variety of solid tumors, many PD-1/PD-L1 and CTLA-4 inhibitors have been approved by the FDA and can be used alone or combined with surgery, chemotherapy, radiotherapy, targeted therapy, and other therapeutic methods for many tumors (40). Due to the lack of effective treatment strategies, patients with advanced esophageal cancer generally have poor long-term survival and quality of life (41). Chemotherapy has been the main treatment strategy for patients with advanced esophageal cancer, but there is a serious lack of effective systemic chemotherapy regimens (42). The ATTRACTION-1 (43), KEYNOTE-028 (44), and KEYNOTE-180 (45) studies confirmed the efficacy and safety of immunotherapy in the second-line and third-line treatment of advanced esophageal cancer. The KEYNOTE-590 and CheckMate-648 studies further established the fundamental status of ICIs in the first-line treatment of advanced or resectable esophageal squamous cell carcinoma (22, 23).

TABLE 2 Subgroup analysis of risk ratios for treatment-related adverse events (trAEs) comparing ICI therapy with chemotherapy.

Subgroup analysis[a]	Grade 3–5 trAEs			All-grade trAEs		
	I^2 (*P*)	RR (95% CI)	*Z* and *P*	I^2 (*P*)	RR (95% CI)	*Z* and *P*
Overall	95.7% (0.000)	0.764 (0.574, 1.016)	$Z = 1.85$, $P = 0.065$	96.7% (0.000)	0.916 (0.831, 1.010)	$Z = 1.77$, $P = 0.077$
Subgroup						
Treatment lines						
Second-line	52.1% (0.100)	0.395 (0.317, 0.491)	$Z = 8.30$, $P = 0.000$	97.6% (0.000)	0.762 (0.570, 1.019)	$Z = 1.83$, $P = 0.067$
First-line	80.1% (0.000)	1.159 (1.012, 1.327)	$Z = 2.13$, $P = 0.033$	89.5% (0.000)	1.006 (0.952, 1.062)	$Z = 0.20$, $P = 0.841$
Third-line	94.2% (0.000)	1.198 (0.199, 7.200)	$Z = 0.20$, $P = 0.843$	95.2% (0.000)	1.190 (0.600, 2.358)	$Z = 0.50$, $P = 0.619$
ICI drug type						
PD-1	96.2% (0.000)	0.773 (0.566, 1.057)	$Z = 1.61$, $P = 0.106$	97% (0.000)	0.919 (0.827, 1.020)	$Z = 1.59$, $P = 0.111$
CTLA-4	82.1% (0.000)	1.531 (0.434, 5.404)	$Z = 0.66$, $P = 0.508$	93.1% (0.000)	1.177 (0.614, 2.258)	$Z = 0.49$, $P = 0.624$
PD-L1	–	0.251 (0.156, 0.404)	$Z = 5.69$, $P = 0.000$	–	0.661 (0.557, 0.785)	$Z = 4.73$, $P = 0.000$
Treatment mode						
ICIs alone	88.7% (0.000)	0.584 (0.350, 0.974)	$Z = 2.06$, $P = 0.039$	95.40% (0.000)	0.952 (0.755, 1.200)	$Z = 0.42$, $P = 0.678$
ICIs + ChT	91.6% (0.000)	1.007 (0.818, 1.239)	$Z = 0.06$, $P = 0.950$	96.80% (0.000)	0.926 (0.836, 1.025)	$Z = 1.49$, $P = 0.136$
Sample size						
<500	90.9% (0.000)	0.663 (0.327, 1.344)	$Z = 1.14$, $P = 0.254$	95.50% (0.000)	1.012 (0.760, 1.348)	$Z = 0.08$, $P = 0.933$
≥500	94.4% (0.000)	0.892 (0.697, 1.142)	$Z = 0.90$, $P = 0.366$	97.60% (0.000)	0.891 (0.795, 0.998)	$Z = 1.99$, $P = 0.047$

[a]Subgroup analyses were conducted based on the pairwise comparisons of all individual trials.

Although immunotherapeutics have special antitumor effects compared with cytotoxic chemotherapy and molecular targeted therapy, treatment- and immune-related adverse events should deserve attention and research (46). Some studies had shown that the toxicity of ICI drugs is generally lower than that of standard chemotherapy, but serious irAEs of ICI drugs will still be reported in clinical trials from time to time (47). In this review, we focused on the rates of trAEs and irAEs for ICIs in different treatment lines for advanced esophageal cancer. Meta-analysis was conducted based on 11 published RCTs to evaluate the safety of ICIs. In this review, we systematically describe the rates and influencing factors of various adverse events caused by ICIs in patients with advanced esophageal cancer or gastroesophageal junction cancer. Now, we discuss the problems discovered during the study process as follows.

In this review, we have included a total of 11 studies, including 7,089 patients, of which 6,992 cases can be used for adverse event analysis. As far as we know, the current meta-analysis may be the study with the largest sample size to explore the possible adverse events of immunotherapy in esophageal cancer and gastroesophageal junction cancer. Based on the results of our NMA analysis of different lines of immunotherapy for esophageal/gastroesophageal junction cancer, we can draw five main conclusions that may affect clinical practice.

First of all, from the point of view of different treatment modalities, different combinations of treatment modalities had obviously distinct safety outcomes in trAEs and irAEs. Similar to the results of practice in lung cancer, ICIs were generally less toxic in monotherapy than in chemotherapy, and the combination of ICIs and chemotherapy would increase the rates of grade 3–5 trAEs and grade 3–5 irAEs (48, 49). Although the overall survival and progression-free survival of combination therapy were significantly longer than those of chemotherapy alone, the treatment- and immuno-related toxicities had also been increased, which should not be underestimated (50). From the results of our network meta-analysis, compared with chemotherapy alone or ICIs alone, almost all combination treatments of ICIs and chemotherapy had increased the rates of treatment-related adverse events. Nivolumab + ChT, ChT, nivolumab + ipilimumab + ChT, and pembrolizumab + ChT had the smallest area under the SUCRA curve (see Supplementary Table S1), which means that these treatment modalities have the highest probability of grade 3–5 trAEs. From the perspective of monotherapy, the general safety of grade 3–5 trAEs for different ICI drugs ranked from high to low is as follows: avelumab, nivolumab, ipilimumab, pembrolizumab, and camrelizumab. However, camrelizumab had the highest rates of all-grade trAEs. Further analysis showed that increased all-grade trAEs are mainly caused by the increased occurrence of reactive capillary endothelial proliferation (RCEP), which was a skin reaction that rarely occurred in other ICIs but commonly manifested in camrelizumab. RCEP mostly appeared within 2 to 4 weeks after medication, most of which were grade 1 to 2 with rare grade 3–4 events occurring. The data showed that the rates of RECP were about 66.8%–70% in solid tumors (51, 52) and 80% in the ESCORT trial (20). In our meta-analysis, as only the ESCORT trial reported the data of RECP, the pooled analysis was not carried out. Our meta-results showed that the risk of all-

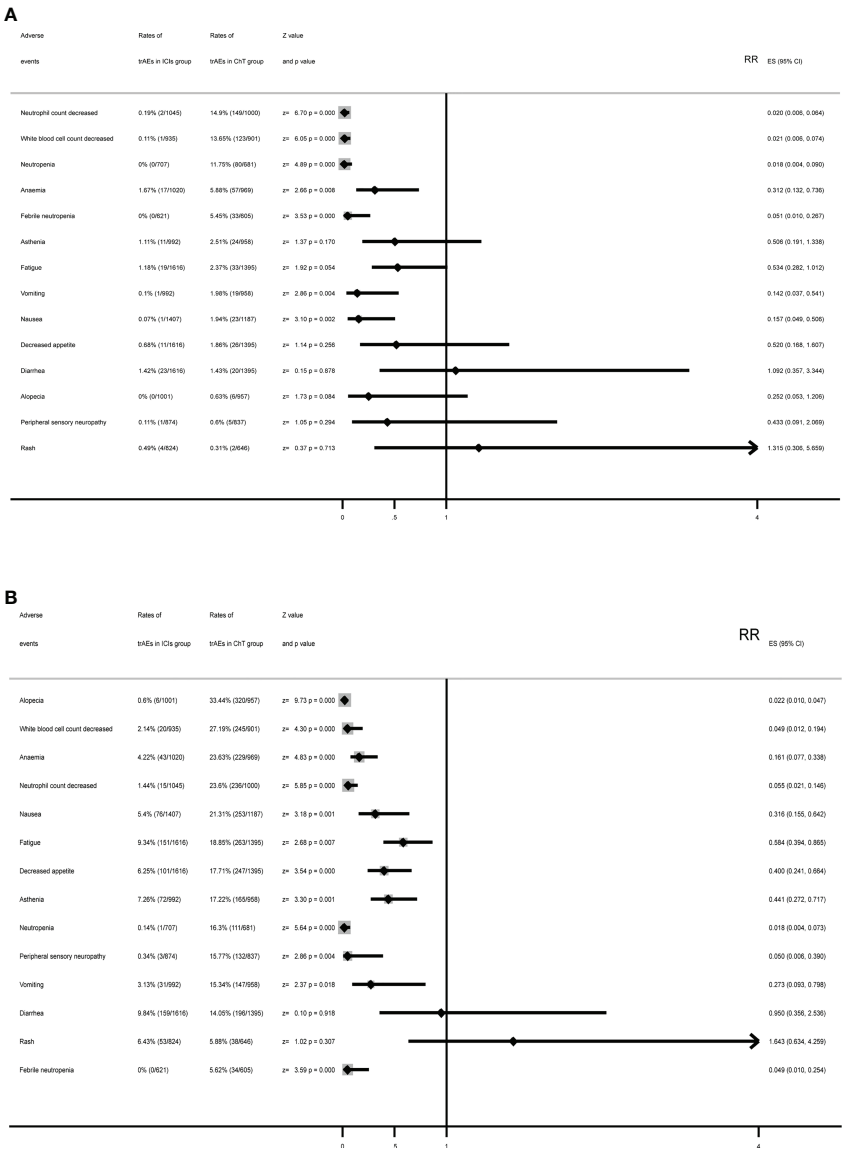

FIGURE 6
Summary forest plots for specific treatment-related adverse events with **(A)** forest plots for grade 3–5 trAEs and **(B)** forest plots for all-grade trAEs.

grade trAEs for different treatment modalities ranked from high to low is as follows: camrelizumab, nivolumab + ChT, ChT, nivolumab + ipilimumab + ChT, and pembrolizumab + ChT. From the perspective of monotherapy, the general safety of all-grade trAEs for different ICI drugs ranked from high to low is as follows: ipilimumab, nivolumab, avelumab, and pembrolizumab (see Supplementary Table S1). Similar to the previous observations reported in related meta-analysis investigating the safety of ICIs, we confirmed that anti-programmed cell death ligand 1 ICI drugs (PD-L1) were safer than ChT in the subgroup analysis (49, 53, 54). A meta-analysis reported that 46% (95% CI 40–53) of patients who received the combination of immunotherapy and chemotherapy encountered grade ≥3 AEs, which was significantly higher than immunotherapy alone or chemotherapy alone (55).

Secondly, the application of ICI drugs in esophageal cancer involved first-line, second-line, third-line, or later-line treatment (56). In most cases, second-line treatment or later-line treatment would be dominated by single-agent therapy, including single-agent chemotherapy or single-agent immunotherapy (56). Monotherapy tended to be better tolerated, especially for patients with advanced tumors with poor ECOG score. In the first-line treatment, ICIs are usually used in combination with chemotherapy in the hope that the efficacy can be further

10.3389/fonc.2022.821626

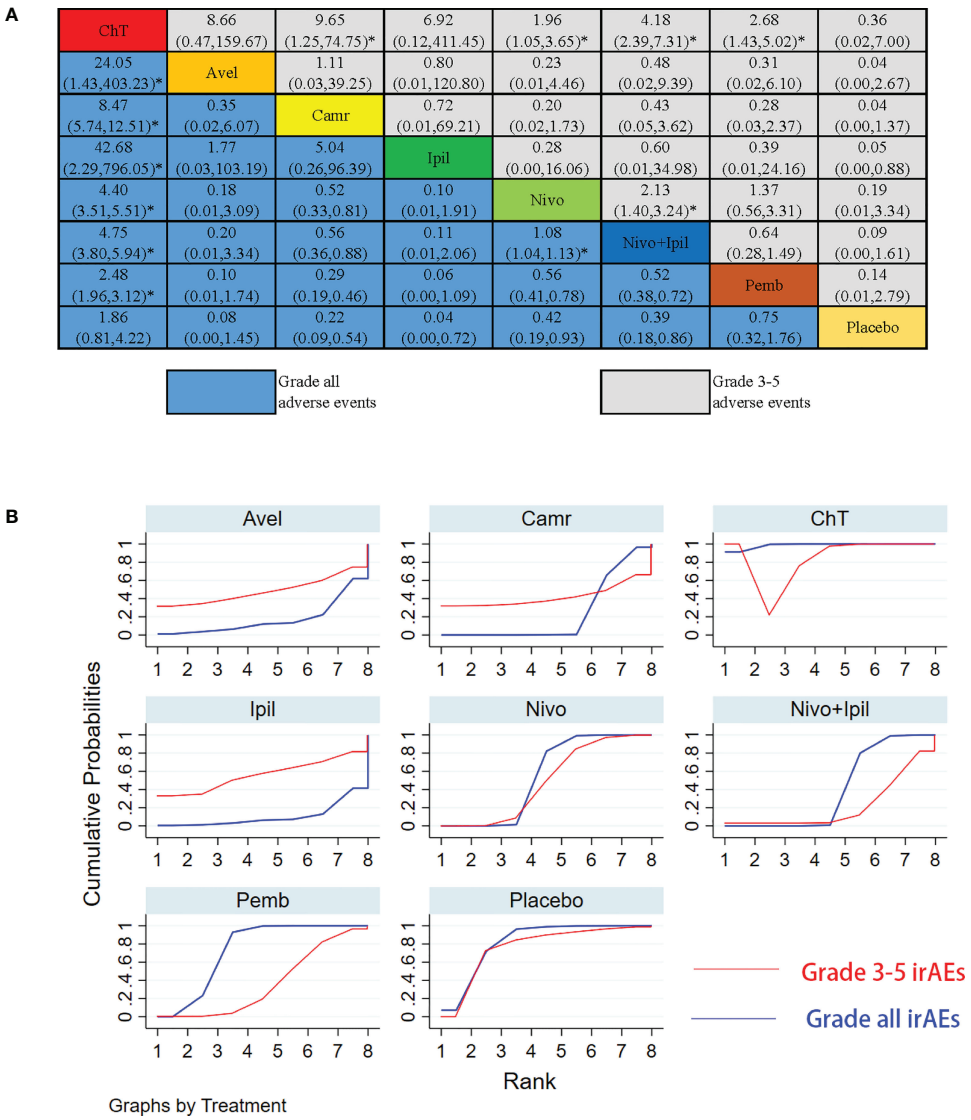

FIGURE 7
Results of the network meta-analysis for 10 treatment regimens in terms of immune-related adverse events (irAEs) with grade 3–5 irAEs and all-grade irAEs. **(A)** League table for different treatment regimens. **(B)** The surface under the cumulative ranking curves (SUCRAs) for grade 3–5 irAEs and all-grade irAEs. *: P<0.05.

improved (22–25). In our subgroup analysis, we found that ICIs applied in second-line treatment significantly reduced the rates of grade 3–4 trAEs, while ICIs applied in first-line treatment had the opposite performance, which further indicated that adding ICIs to chemotherapy will increase the treatment-related adverse events. Although the influence of treatment line on the rates of adverse events was largely due to different treatment combinations, our data showed that ICIs should be avoided as much as possible in combination with chemotherapy in the second- or third-line treatment for esophageal cancer to reduce the risk of adverse events (57).

Third, previous studies had shown that different types of ICIs have different toxicity profiles because of their different mechanisms of action (58). Anti-CTLA-4 drugs work by enhancing T-cell priming, while PD-1/PD-L1 inhibitors are thought to work by reactivating the pre-existing CD8 T-cell response (59). CTLA-4 inhibitors were generally considered to be more toxic, while PD-L1 inhibitors were considered to be more tolerable (60). A previous meta-analysis showed that 34% (95% CI 27–42) of patients treated with CTLA-4 inhibitors encountered grade ≥3 AEs, but only 14% (95% CI 12–16) of patients treated with PD-1/PD-L1 inhibitors suffered grade ≥3 AEs (55). In our

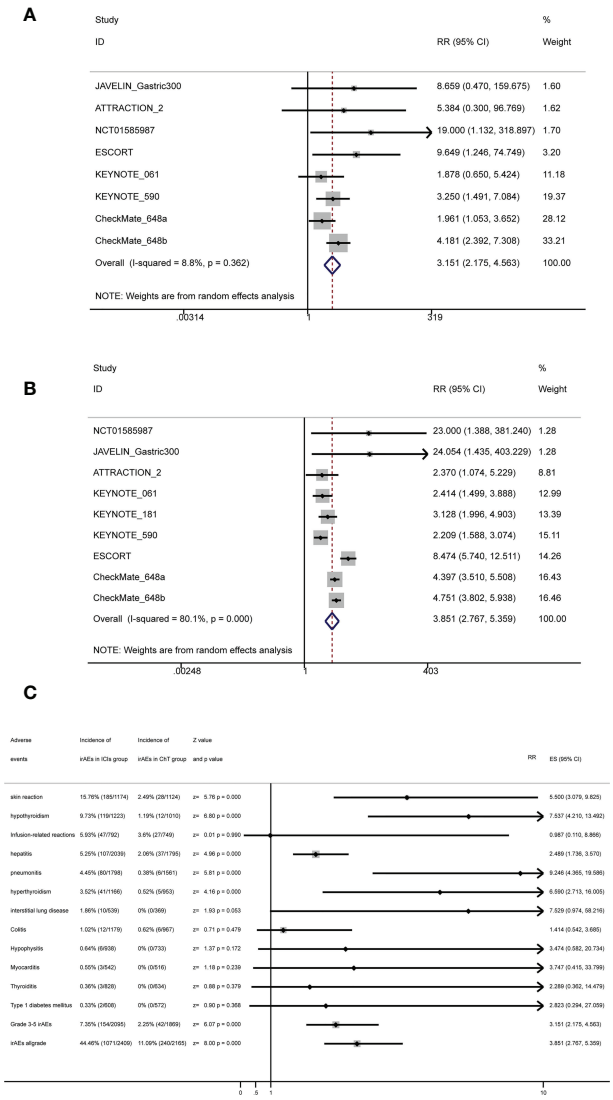

FIGURE 8
Forest plots for irAEs with **(A)** forest plots for grade 3–5 irAEs, **(B)** forest plots for all-grade irAEs, and **(C)** summary forest plots for irAEs.

meta-analysis, only two trials published the safety data on CTLA-4 inhibitors for esophageal cancer (23, 28). In terms of grade 3–4 trAEs, the risk of AEs caused by ipilimumab was lower than that of pembrolizumab and camrelizumab but higher than that of avelumab and nivolumab. This finding is different from previous reports and should be noted. On the other hand, from the perspective of immune-related adverse events, CTLA-4 inhibitors in our NMA had the highest risk of grade 1–5 irAEs, while the risk of grade 3–5 adverse events was relatively low. Compared with monotherapy, combined immunotherapy of nivolumab and ipilimumab had the highest risk of grade 3–5 irAEs. This finding was similar to the previously reported results (55), and the same findings have been found in clithe nical practice of lung cancer (35). Whether using CTLA-4 or PD-1/PD-L1 inhibitors, the application of ICIs significantly increased both the rates of grade 3–5 irAEs and grade 1–5 irAEs in our subgroup analyses. Therefore, a careful balance between toxicity and efficacy should be evaluated when ICIs need to be applied (55).

Fourth, the spectrum of trAEs caused by ICIs was also significantly different from that caused by ChT. Our meta-analysis based on specific treatment-related adverse events showed that ICIs were safer and had a significantly different spectrum of grade 3–5 trAEs and all-grade trAEs from chemotherapy. Hematological toxicity was the main adverse event for chemotherapy, while systemic symptoms such as fatigue, asthenia, and decreased appetite were the main adverse events for ICIs (50). For patients with poor bone

TABLE 3 Subgroup analysis of risk ratios for immune-related adverse events (irAEs) comparing ICI therapy with chemotherapy.

Subgroup analysis[a]	Grade 3–5 irAEs			All-grade irAEs		
	I^2 (*P*)	RR (95% CI)	*Z* and *P*	I^2 (*P*)	RR (95% CI)	*Z* and *P*
Overall	95.7% (0.000)	3.151 (2.175, 4.563)	$Z = 6.07$, $P = 0.000$	80.1% (0.000)	3.851 (2.767, 5.359)	$Z = 8.00$, $P = 0.000$
Subgroup						
Treatment lines						
Second-line	51.6% (0.151)	3.387 (0.690, 16.635)	$Z = 1.50$, $P = 0.133$	89.8% (0.000)	4.036 (1.833, 8.888)	$Z = 3.46$, $P = 0.001$
First-line	37.6% (0.201)	3.011 (1.880, 4.823)	$Z = 4.59$, $P = 0.000$	87.0% (0.000)	3.653 (2.430, 5.493)	$Z = 6.23$, $P = 0.000$
Third-line	0.0% (0.823)	9.716 (1.849, 51.060)	$Z = 2.69$, $P = 0.007$	60.8% (0.078)	7.513 (1.096, 51.516)	$Z = 2.05$, $P = 0.040$
ICI drugs						
PD-1	0.0% (0.504)	2.484 (1.620, 3.807)	$Z = 4.17$, $P = 0.000$	85.3% (0.000)	3.464 (2.280, 5.262)	$Z = 5.82$, $P = 0.000$
CTLA-4	9.4% (0.293)	4.729 (2.071, 10.798)	$Z = 3.69$, $P = 0.000$	19.0% (0.267)	5.562 (2.176, 14.215)	$Z = 3.58$, $P = 0.000$
PD-L1	–	8.659 (0.470, 159.675)	$Z = 1.45$, $P = 0.147$	–	24.054 (1.435, 403.229)	$Z = 2.21$, $P = 0.027$
Treatment mode						
ICIs alone	0.0% (0.943)	9.690 (2.670, 35.166)	$Z = 3.45$, $P = 0.001$	76.9% (0.002)	5.099 (2.396, 10.850)	$Z = 4.23$, $P = 0.000$
ICIs + ChT	23.4% (0.270)	2.839 (1.892, 4.261)	$Z = 5.04$, $P = 0.000$	84.5% (0.000)	3.357 (2.320, 4.858)	$Z = 6.42$, $P = 0.000$
Sample size						
<500	0.0% (0.943)	9.690 (2.670, 35.166)	$Z = 3.45$, $P = 0.001$	68.8% (0.022)	6.573 (2.383, 18.128)	$Z = 3.64$, $P = 0.000$
≥500	23.4% (0.270)	2.839 (1.892, 4.261)	$Z = 5.04$, $P = 0.000$	80.0% (0.000)	3.329 (2.432, 4.559)	$Z = 7.50$, $P = 0.000$

[a]Subgroup analyses were conducted based on the pairwise comparisons of all individual trials.

marrow function, immunotherapy may be a better treatment option (61). For specific immune-related adverse events, our meta-analysis results showed that the most common irAEs in the ICI group were skin reaction (15.76%, 95% CI: [13.67%, 17.84%]), followed by hypothyroidism (9.73%, 95% CI: [8.07%, 11.39%]), infusion-related reactions (5.93%, 95% CI: [4.29%, 7.58%]), hepatitis (5.25%, 95% CI: [4.28%, 6.22%]), and pneumonitis (4.45%, 95% CI: [3.5%, 5.4%]). Due to the limited data obtained, we cannot further analyze the detailed rates of 3–5 grade irAEs and cannot further analyze the difference in the rates of specific trAEs and irAEs between CTLA-4 inhibitors and PD-1/PD-L1 inhibitors. However, the rates of all-grade-specific irAEs were close to the results of the previous meta-analysis reported. More specifically, colitis and hypophysitis seem to be more common with CTLA-4 inhibitors, whereas pneumonitis, hypothyroidism, and arthralgia appear to be more commonly associated with PD-1/PD-L1 inhibitors (55, 62, 63).

Finally, there was no consensus on whether the rates of irAEs were related to the primary site of the tumor. One review found that the rates of several specific AEs of interest varied among different cancer types (64). However, another review found that the overall rates of all-grade and grade 3–5 irAEs did not differ among different tumor sites (62). In our systematic review, both patients with esophageal cancer and gastroesophageal junction cancer were selected as the research subjects. Two reasons for this were the limited number of randomized controlled trials of immunotherapy for esophageal cancer and that some patients with esophageal adenocarcinoma had to be enrolled in some trials on GEJC. We did not further investigate whether specific irAEs differed between EPC and GEJC, which may be a potential focus for future analyses. In our view, the occurrence and severity of adverse events would be influenced by many factors, including the patients' characteristics (disease stage, physical condition, age, gender, basic diseases, etc.). However, the rates were low in some special adverse events, especially for irAEs (47, 65). It is difficult to analyze the impact of these factors on the rates of AEs through the available data extracted from the literature, so we had to ignore the potential impact.

It should be pointed out from the results of our meta-analysis that, although ICIs increased the adverse events, the rates were actually low and acceptable. Although immunotherapy had increased the rates of irAEs, to a certain extent, the occurrence of immune-related events may be positively correlated with the therapy's efficacy and the patient's prognosis (66, 67). When focusing on the anti-tumor effects of ICIs, we should also pay attention to the occurrence of irAEs when ICIs are applied (68). However, we should not stop eating for fear of choking; after all, the current evidence showed that the benefits of ICIs outweigh the potential risks. For clinicians, the task we have to do is to achieve the best balance between the antitumor effects and the related adverse events of ICIs based on the best evidence-based medical practice.

There are some limitations in our review that need to be mentioned. First, the network meta-analysis assumes that the estimates of the study effects between the various trials have commonality, transferability, and exchangeability, which means that the similarities of population characteristics, interventions, chemotherapy regimen, and other features among different trials are required. However, as the conditions of the trials may affect the study results, this assumption is very unrealistic. In our

meta-analysis, heterogeneity was detected in the results of grade 3–5 trAEs and all-grade trAEs. Subgroup meta-analyses revealed that trials with treatment line = second line, treatment line = first line, treatment mode, and a sample size ≥500 patients were potential sources of heterogeneity. Second, some specific irAEs and trAEs may be selectively reported in most trials because the rates of these adverse events were lower than a preset threshold, such as 1% or 5%. In this case, we cannot obtain the pooled estimates of rates for these rare adverse events, so it is inevitable to underestimate the overall mean rates of some adverse events. Third, in order to catch the latest data from newly published trials, some recent conference abstracts were enrolled in our meta-analysis, from which some summary data were extracted. However, this may lead to another selection bias because the comprehensive toxicity data might not be reported in these abstracts. Furthermore, some previous meta-analyses on this topic had shown the influence of different drug doses on the occurrence of adverse events (54). In our study, the related data on the influence of doses were not available. Therefore, we had to ignore this point. Finally, sometimes, serious adverse effects are either rare or not encountered. In this case, the confidence interval of the calculated effect estimate is too wide, which will affect the accuracy of the pooled effect size. This was extremely common in the evaluations of adverse events. In our meta-analysis, the rates of irAEs in arms without ICIs were very low, so a large number of wide-ranging estimates of RR appeared. Therefore, one should be cautious when interpreting the results of the meta-analysis and drawing conclusions.

Conclusion

Monotherapy with immune checkpoint inhibitors displayed better safety profiles in terms of trAEs than chemotherapy alone; however, combinational treatment regimens involving ICIs increased the risk of trAEs. Different ICIs had different toxicity manifestations and should not be considered as an entity. Compared with chemotherapy, ICIs were more prone to irAEs, but the overall rates remained low and acceptable. For clinicians, it is important to recognize and monitor the adverse events caused by ICIs for patients with esophageal cancer or gastroesophageal junction cancer.

Data availability statement

The original contributions presented in the study are included in the article/Supplementary Material. Further inquiries can be directed to the corresponding authors.

Author contributions

JZ and LX collected the data. JZ and MW performed data cleaning and analysis. JZ and BH performed the systematic review. JZ and BH evaluated the data. JL drafted and reviewed the manuscript for scientific soundness. All authors contributed to the article and approved the submitted version.

Funding

This study was supported in part by the National Clinical Key Specialty Construction Program (Grant No. 2021 to JL), the Fujian Provincial Clinical Research Center for Cancer Radiotherapy and Immunotherapy (Grant No. 2020Y2012 to JL), the Fujian Provincial Health Technology Project (Youth Scientific Research Project, 2019-1-50 to JZ), and the Nursery Fund Project of the Second Affiliated Hospital of Fujian Medical University (Grant No. 2021MP05 to JZ).

Conflict of interest

The authors declare that the research was conducted in the absence of any commercial or financial relationships that could be construed as a potential conflict of interest.

Publisher's note

Supplementary material

The Supplementary Material for this article can be found online at: https://www.frontiersin.org/articles/10.3389/fonc.2022.821626/full#supplementary-material

References

1. Siegel RL, Miller KD, Jemal A. Cancer statistics, 2018. *CA Cancer J Clin* (2018) 68(1):7–30. doi: 10.3322/caac.21442

2. Chen W, Zheng R, Baade PD, Zhang S, Zeng H, Bray F, et al. Cancer statistics in China, 2015. *CA Cancer J Clin* (2016) 66(2):115–32. doi: 10.3322/caac.21338

3. Sung H, Ferlay J, Siegel RL, Laversanne M, Soerjomataram I, Jemal A, et al. Global cancer statistics 2020: GLOBOCAN estimates of incidence and mortality worldwide for 36 cancers in 185 countries. *CA Cancer J Clin* (2021) 71(3):209–49. doi: 10.3322/caac.21660

4. Fan J, Liu Z, Mao X, Tong X, Zhang T, Suo C, et al. Global trends in the incidence and mortality of esophageal cancer from 1990 to 2017. *Cancer Med* (2020) 9(18):e03338. doi: 10.1002/cam4.3338

5. Stahl M, Budach W, Meyer HJ, Cervantes A, Group EGW. Esophageal cancer: Clinical practice guidelines for diagnosis, treatment and follow-up. *Ann Oncol* (2010) 21(Suppl 5):v46–9. doi: 10.1093/annonc/mdq163

6. Domper Arnal MJ, Ferrández Arenas Á, Lanas Arbeloa Á. Esophageal cancer: Risk factors, screening and endoscopic treatment in Western and Eastern countries. *World J Gastroenterol* (2015) 21(26):7933–43. doi: 10.3748/wjg.v21.i26.7933

7. Ter Veer E, Haj Mohammad N, van Valkenhoef G, Ngai LL, Mali RMA, Anderegg MC, et al. The efficacy and safety of first-line chemotherapy in advanced esophagogastric cancer: A network meta-analysis. *J Natl Cancer Inst* (2016) 108 (10):1–13. doi: 10.1093/jnci/djw166

8. Kennedy LB, Salama AKS. A review of cancer immunotherapy toxicity. *CA Cancer J Clin* (2020) 70(2):86–104. doi: 10.3322/caac.21596

9. Ku GY. The current status of immunotherapies in esophagogastric cancer. *Hematol Oncol Clin North Am* (2019) 33(2):323–38. doi: 10.1016/j.hoc.2018.12.007

10. Wu DW, Huang HY, Tang Y, Zhao Y, Yang ZM, Wang J, et al. Clinical development of immuno-oncology in China. *Lancet Oncol* (2020) 21(8):1013–6. doi: 10.1016/S1470-2045(20)30329-6

11. Zayac A, Almhanna K. Esophageal, gastric cancer and immunotherapy: small steps in the right direction? *Transl Gastroenterol Hepatol* (2020) 5(2020):9. doi: 10.21037/tgh.2019.09.05

12. Kakeji Y, Oshikiri T, Takiguchi G, Kanaji S, Matsuda T, Nakamura T, et al. Multimodality approaches to control esophageal cancer: development of chemoradiotherapy, chemotherapy, and immunotherapy. *Esophagus* (2021) 18 (1):25–32. doi: 10.1007/s10388-020-00782-1

13. Fan Y, Xie W, Huang H, Wang Y, Li G, Geng Y, et al. Association of immune related adverse events with efficacy of immune checkpoint inhibitors and overall survival in cancers: A systemic review and meta-analysis. *Front Oncol* (2021) 11:633032. doi: 10.3389/fonc.2021.633032

14. Mimura K, Yamada L, Ujiie D, Hayase S, Tada T, Hanayama H, et al. Immunotherapy for esophageal squamous cell carcinoma: a review. *Fukushima J Med Sci* (2018) 64(2):46–53. doi: 10.5387/fms.2018-09

15. Raufi AG, Klempner SJ. Immunotherapy for advanced gastric and esophageal cancer: preclinical rationale and ongoing clinical investigations. *J Gastrointest Oncol* (2015) 6(5):561–9. doi: 10.3978/j.issn.2078-6891.2015.037

16. Cipriani A, Barbui C, Rizzo C, Salanti G. What is a multiple treatments meta-analysis? *Epidemiol Psychiatr Sci* (2012) 21(2):151–3. doi: 10.1017/s2045796011000837

17. Moher D, Liberati A, Tetzlaff J, Altman DG, Group P. Preferred reporting items for systematic reviews and meta-analyses: the PRISMA statement. *J Clin Epidemiol* (2009) 62(10):1006–12. doi: 10.1016/j.jclinepi.2009.06.005

18. Kato K, Cho BC, Takahashi M, Okada M, Lin CY, Chin K, et al. Nivolumab versus chemotherapy in patients with advanced oesophageal squamous cell carcinoma refractory or intolerant to previous chemotherapy (ATTRACTION-3): a multicentre, randomised, open-label, phase 3 trial. *Lancet Oncol* (2019) 20 (11):1506–17. doi: 10.1016/S1470-2045(19)30626-6

19. Takahashi M, Kato K, Okada M, Chin K, Kadowaki S, Hamamoto Y, et al. Nivolumab versus chemotherapy in Japanese patients with advanced esophageal squamous cell carcinoma: a subgroup analysis of a multicenter, randomized, open-label, phase 3 trial (ATTRACTION-3). *Esophagus* (2021) 18(1):90–9. doi: 10.1007/s10388-020-00794-x

20. Huang J, Xu J, Chen Y, Zhuang W, Zhang Y, Chen Z, et al. Camrelizumab versus investigator's choice of chemotherapy as second-line therapy for advanced or metastatic oesophageal squamous cell carcinoma (ESCORT): a multicentre, randomised, open-label, phase 3 study. *Lancet Oncol* (2020) 21(6):832–42. doi: 10.1016/S1470-2045(20)30110-8

21. Kojima T, Shah MA, Muro K, Francois E, Adenis A, Hsu CH, et al. Randomized phase III KEYNOTE-181 study of pembrolizumab versus chemotherapy in advanced esophageal cancer. *J Clin Oncol* (2020) 38(35):4138–48. doi: 10.1200/JCO.20.01888

22. Kato K, Sun JM, Shah MA, Enzinger PC, Shen L. Pembrolizumab plus chemotherapy versus chemotherapy as first-line therapy in patients with advanced esophageal cancer: The phase 3 KEYNOTE-590 study. *Ann Oncol* (2020) 31(2020): S1192–S3. doi: 10.1016/j.annonc.2020.08.2298

23. Chau I, Doki Y, A.Ajani J, Xu J, Wyrwicz L, Motoyama S. Nivolumab plus ipilimumab or nivolumab plus chemotherapy versus chemotherapy as first-line treatment for advanced esophageal squamous cell carcinoma: first results of the ChekMate 648 study. In: *Oncology ASoC, editor. 2021 ASCO annual meeting;* (Alexandria: American society of clinical oncology) (2021).

24. Moehler M, Shitara K, Garrido M, Salman P, Shen L, Wyrwicz L, et al. Nivolumab (nivo) plus chemotherapy (chemo) versus chemo as first-line (1L) treatment for advanced gastric cancer/gastroesophageal junction cancer (GC/GEJC)/esophageal adenocarcinoma (EAC): First results of the CheckMate 649 study. *Ann Oncol* (2020) 31:S1191. doi: 10.1016/j.annonc.2020.08.2296

25. Boku N, Ryu MH, Oh DY, Oh SC, Chung HC, Lee KW, et al. Nivolumab plus chemotherapy versus chemotherapy alone in patients with previously untreated advanced or recurrent gastric/gastroesophageal junction (G/GEJ) cancer: ATTRACTION-4 (ONO-4538-37) study. *Ann Oncol* (2020) 31(2020): S1192. doi: 10.1016/j.annonc.2020.08.2297

26. Boku N, Ryu M, Kato K, Chung H, Minashi K, Lee K, et al. Safety and efficacy of nivolumab in combination with s-1/capecitabine plus oxaliplatin in patients with previously untreated, unresectable, advanced, or recurrent gastric/gastroesophageal junction cancer: interim results of a randomized, phase II trial (ATTRACTION-4). *Ann oncology: Off J Eur Soc Med Oncol* (2019) 30(2):250–8. doi: 10.1093/annonc/mdy540

27. Shitara K, Ozguroglu M, Bang YJ, Di Bartolomeo M, Mandala M, Ryu MH, et al. Pembrolizumab versus paclitaxel for previously treated, advanced gastric or gastro-oesophageal junction cancer (KEYNOTE-061): a randomised, open-label, controlled, phase 3 trial. *Lancet* (2018) 392(10142):123–33. doi: 10.1016/S0140-6736(18)31257-1

28. Bang YJ, Cho JY, Kim YH, Kim JW, Di Bartolomeo M, Ajani JA, et al. Efficacy of sequential ipilimumab monotherapy versus best supportive care for unresectable locally Advanced/Metastatic gastric or gastroesophageal junction cancer. *Clin Cancer Res* (2017) 23(19):5671–8. doi: 10.1158/1078-0432.CCR-17-0025

29. Bang YJ, Ruiz EY, Van Cutsem E, Lee KW, Wyrwicz L, Schenker M, et al. Randomised trial of avelumab versus physician's choice of chemotherapy as third-line treatment of patients with advanced gastric or gastro-oesophageal junction cancer: primary analysis of JAVELIN gastric 300. *Ann Oncol* (2018) 29(10):2052–60. doi: 10.1093/annonc/mdy264

30. Boku N, Satoh T, Ryu MH, Chao Y, Kato K, Chung HC, et al. Nivolumab in previously treated advanced gastric cancer (ATTRACTION-2): 3-year update and outcome of treatment beyond progression with nivolumab. *Gastric Cancer* (2021) 24(1):946–58. doi: 10.1007/s10120-021-01173-w

31. Kang YK, Boku N, Satoh T, Ryu MH, Chao Y, Kato K, et al. Nivolumab in patients with advanced gastric or gastro-oesophageal junction cancer refractory to, or intolerant of, at least two previous chemotherapy regimens (ONO-4538-12, ATTRACTION-2): a randomised, double-blind, placebo-controlled, phase 3 trial. *Lancet* (2017) 390(10111):2461–71. doi: 10.1016/S0140-6736(17)31827-5

32. Kato K, Satoh T, Muro K, Yoshikawa T, Tamura T, Hamamoto Y, et al. A subanalysis of Japanese patients in a randomized, double-blind, placebo-controlled, phase 3 trial of nivolumab for patients with advanced gastric or gastro-esophageal junction cancer refractory to, or intolerant of, at least two previous chemotherapy regimens (ONO-4538-12, ATTRACTION-2). *Gastric Cancer* (2019) 22(2):344–54. doi: 10.1007/s10120-018-0899-6

33. Chen LT, Satoh T, Ryu MH, Chao Y, Kato K, Chung HC, et al. A phase 3 study of nivolumab in previously treated advanced gastric or gastroesophageal junction cancer (ATTRACTION-2): 2-year update data. *Gastric Cancer* (2020) 23 (3):510–9. doi: 10.1007/s10120-019-01034-7

34. Satoh T, Kang YK, Chao Y, Ryu MH, Kato K, Cheol Chung H, et al. Exploratory subgroup analysis of patients with prior trastuzumab use in the ATTRACTION-2 trial: a randomized phase III clinical trial investigating the efficacy and safety of nivolumab in patients with advanced gastric/gastroesophageal junction cancer. *Gastric Cancer* (2020) 23(1):143–53. doi: 10.1007/s10120-019-00970-8

35. Wang M, Liang H, Wang W, Zhao S, Cai X, Zhao Y, et al. Immune-related adverse events of a PD-L1 inhibitor plus chemotherapy versus a PD-L1 inhibitor alone in first-line treatment for advanced non-small cell lung cancer: A meta-analysis of randomized control trials. *Cancer* (2021) 127(5):777–86. doi: 10.1002/cncr.33270

36. De Sousa Linhares A, Leitner J, Grabmeier-Pfistershammer K, Steinberger P. Not all immune checkpoints are created equal. *Front Immunol* (2018) 9:1909 (1909). doi: 10.3389/fimmu.2018.01909

37. Pardoll DM. The blockade of immune checkpoints in cancer immunotherapy. *Nat Rev Cancer* (2012) 12(4):252–64. doi: 10.1038/nrc3239

38. Iwai Y, Hamanishi J, Chamoto K, Honjo T. Cancer immunotherapies targeting the PD-1 signaling pathway. *J BioMed Sci* (2017) 24(1):26. doi: 10.1186/s12929-017-0329-9

39. Parry RV, Chemnitz JM, Frauwirth KA, Lanfranco AR, Braunstein I, Kobayashi SV, et al. CTLA-4 and PD-1 receptors inhibit T-cell activation by distinct mechanisms. *Mol Cell Biol* (2005) 25(21):9543–53. doi: 10.1128/MCB.25.21.9543-9553.2005

40. Sasidharan Nair V, Elkord E. Immune checkpoint inhibitors in cancer therapy: a focus on T-regulatory cells. *Immunol Cell Biol* (2018) 96(1):21–33. doi: 10.1111/imcb.1003

41. Davidson M, Chau I. Immunotherapy for oesophagogastric cancer. *Expert Opin Biol Ther* (2016) 16(10):1197–207. doi: 10.1080/14712598.2016.1213233

42. Shankaran V, Xiao H, Bertwistle D, Zhang Y, You M, Abraham P, et al. A comparison of real-world treatment patterns and clinical outcomes in patients receiving first-line therapy for unresectable advanced gastric or gastroesophageal junction cancer versus esophageal adenocarcinomas. *Adv Ther* (2021) 38(1):707–20. doi: 10.1007/s12325-020-01567-9

43. Kudo T, Hamamoto Y, Kato K, Ura T, Kojima T, Tsushima T, et al. Nivolumab treatment for oesophageal squamous-cell carcinoma: an open-label, multicentre, phase 2 trial. *Lancet Oncol* (2017) 18(5):631–9. doi: 10.1016/S1470-2045(17)30181-X

44. Doi T, Piha-Paul SA, Jalal SI, Saraf S, Lunceford J, Koshiji M, et al. Safety and antitumor activity of the anti-programmed death-1 antibody pembrolizumab in patients with advanced esophageal carcinoma. *J Clin Oncol* (2018) 36(1):61–7. doi: 10.1200/JCO.2017.74.9846

45. Shah MA, Kojima T, Hochhauser D, Enzinger P, Raimbourg J, Hollebecque A, et al. Efficacy and safety of pembrolizumab for heavily pretreated patients with advanced, metastatic adenocarcinoma or squamous cell carcinoma of the esophagus: The phase 2 KEYNOTE-180 study. *JAMA Oncol* (2019) 5(4):546–50. doi: 10.1001/jamaoncol.2018.5441

46. Brahmer JR, Lacchetti C, Thompson JA. Management of immune-related adverse events in patients treated with immune checkpoint inhibitor therapy: American society of clinical oncology clinical practice guideline summary. *J Oncol Pract* (2018) 14(4):247–9. doi: 10.1200/jop.18.00005

47. Stelmachowska-Banaś M, Czajka-Oraniec I. Management of endocrine immune-related adverse events of immune checkpoint inhibitors: an updated review. *Endocrine Connections* (2020) 9(10):R207–R28. doi: 10.1530/ec-20-0342

48. Zhou Y, Chen C, Zhang X, Fu S, Xue C, Ma Y, et al. Immune-checkpoint inhibitor plus chemotherapy versus conventional chemotherapy for first-line treatment in advanced non-small cell lung carcinoma: a systematic review and meta-analysis. *J Immunother Cancer* (2018) 6(1):155. doi: 10.1186/s40425-018-0477-9

49. Wu Y, Shi H, Jiang M, Qiu M, Jia K, Cao T, et al. The clinical value of combination of immune checkpoint inhibitors in cancer patients: A meta-analysis of efficacy and safety. *Int J Cancer* (2017) 141(12):2562–70. doi: 10.1002/ijc.31012

50. Shao J, Wang C, Ren P, Jiang Y, Tian P, Li W. Treatment- and immune-related adverse events of immune checkpoint inhibitors in advanced lung cancer. *Biosci Rep* (2020) 40(5):1–11. doi: 10.1042/BSR20192347

51. Teng Y, Guo R, Sun J, Jiang Y, Liu Y. Reactive capillary hemangiomas induced by camrelizumab (SHR-1210), an anti-PD-1 agent. *Acta Oncol* (2019) 58 (3):388–9. doi: 10.1080/0284186X.2019.1567935

52. Wang F, Qin S, Sun X, Ren Z, Meng Z, Chen Z, et al. Reactive cutaneous capillary endothelial proliferation in advanced hepatocellular carcinoma patients treated with camrelizumab: data derived from a multicenter phase 2 trial. *J Hematol Oncol* (2020) 13(1):47. doi: 10.1186/s13045-020-00886-2

53. Sznol M, Ferrucci PF, Hogg D, Atkins MB, Wolter P, Guidoboni M, et al. Pooled analysis safety profile of nivolumab and ipilimumab combination therapy in patients with advanced melanoma. *J Clin Oncol* (2017) 35(34):3815–22. doi: 10.1200/JCO.2016.72.1167

54. Xu C, Chen YP, Du XJ, Liu JQ, Huang CL, Chen L, et al. Comparative safety of immune checkpoint inhibitors in cancer: systematic review and network meta-analysis. *BMJ* (2018) 363:k4226. doi: 10.1136/bmj.k4226

55. Arnaud-Coffin P, Maillet D, Gan HK, Stelmes JJ, You B, Dalle S, et al. A systematic review of adverse events in randomized trials assessing immune checkpoint inhibitors. *Int J Cancer* (2019) 145(3):639–48. doi: 10.1002/ijc.32132

56. da Silva L, Aguiar P, Park R, Edelman Saul E, Haaland B, de Lima Lopes G. Comparative efficacy and safety of programmed death-1 pathway inhibitors in advanced gastroesophageal cancers: A systematic review and network meta-analysis of phase III clinical trials. *Cancers (Basel)* (2021) 13(11):1–14. doi: 10.3390/cancers13112614

57. Ajani JA, D'Amico TA, Bentrem DJ, Chao J, Corvera C, Das P, et al. Esophageal and esophagogastric junction cancers, version 2.2019, NCCN clinical practice guidelines in oncology. *J Natl Compr Canc Netw* (2019) 17(7):855–83. doi: 10.6004/jnccn.2019.0033

58. Khan Z, Hammer C, Guardino E, Chandler GS, Albert ML. Mechanisms of immune-related adverse events associated with immune checkpoint blockade: using germline genetics to develop a personalized approach. *Genome Med* (2019) 11(1):39. doi: 10.1186/s13073-019-0652-8

59. Chen DS, Mellman I. Elements of cancer immunity and the cancer-immune set point. *Nature* (2017) 541(7637):321–30. doi: 10.1038/nature21349

60. Postow MA, Sidlow R, Hellmann MD. Immune-related adverse events associated with immune checkpoint blockade. *N Engl J Med* (2018) 378(2):158–68. doi: 10.1056/NEJMra1703481

61. Cybulska-Stopa B, Ługowska I, Jagodzińska-Mucha P, Koseła-Paterczyk H, Kozak K, Klimczak A, et al. Immune checkpoint inhibitors therapy in older patients (≥ 70 years) with metastatic melanoma: a multicentre study. *Postepy Dermatol Alergol* (2019) 36(5):566–71. doi: 10.5114/ada.2018.79940

62. Wang Y, Zhou S, Yang F, Qi X, Wang X, Guan X, et al. Treatment-related adverse events of PD-1 and PD-L1 inhibitors in clinical trials: A systematic review and meta-analysis. *JAMA Oncol* (2019) 5(7):1008–19. doi: 10.1001/jamaoncol.2019.0393

63. Khoja L, Day D, Wei-Wu Chen T, Siu LL, Hansen AR. Tumour- and class-specific patterns of immune-related adverse events of immune checkpoint inhibitors: a systematic review. *Ann Oncol* (2017) 28(10):2377–85. doi: 10.1093/annonc/mdx286

64. Si X, Song P, Ni J, Di M, He C, Zhang L, et al. Management of immune checkpoint inhibitor-related adverse events: A review of case reports. *Thorac Cancer* (2020) 11(3):498–504. doi: 10.1111/1759-7714.13315

65. Kottschade LA. Incidence and management of immune-related adverse events in patients undergoing treatment with immune checkpoint inhibitors. *Curr Oncol Rep* (2018) 20(3):24. doi: 10.1007/s11912-018-0671-4

66. Dupont R, Berard E, Puisset F, Comont T, Delord JP, Guimbaud R, et al. The prognostic impact of immune-related adverse events during anti-PD1 treatment in melanoma and non-small-cell lung cancer: a real-life retrospective study. *Oncoimmunology* (2020) 9(1):1682383. doi: 10.1080/2162402X.2019.1682383

67. Kobayashi K, Iikura Y, Hiraide M, Yokokawa T, Aoyama T, Shikibu S, et al. Association between immune-related adverse events and clinical outcome following nivolumab treatment in patients with metastatic renal cell carcinoma. *In Vivo* (2020) 34(5):2647–52. doi: 10.21873/invivo.12083

68. Choi J, Lee SY. Clinical characteristics and treatment of immune-related adverse events of immune checkpoint inhibitors. *Immune Netw* (2020) 20(1):e9. doi: 10.4110/in.2020.20.e9

Frontiers in Oncology

Advances knowledge of carcinogenesis and tumor progression for better treatment and management

The third most-cited oncology journal, which highlights research in carcinogenesis and tumor progression, bridging the gap between basic research and applications to imrpove diagnosis, therapeutics and management strategies.

Discover the latest Research Topics

See more →

Frontiers

Avenue du Tribunal-Fédéral 34
1005 Lausanne, Switzerland
frontiersin.org

Contact us

+41 (0)21 510 17 00
frontiersin.org/about/contact